



Australian Government
Geoscience Australia



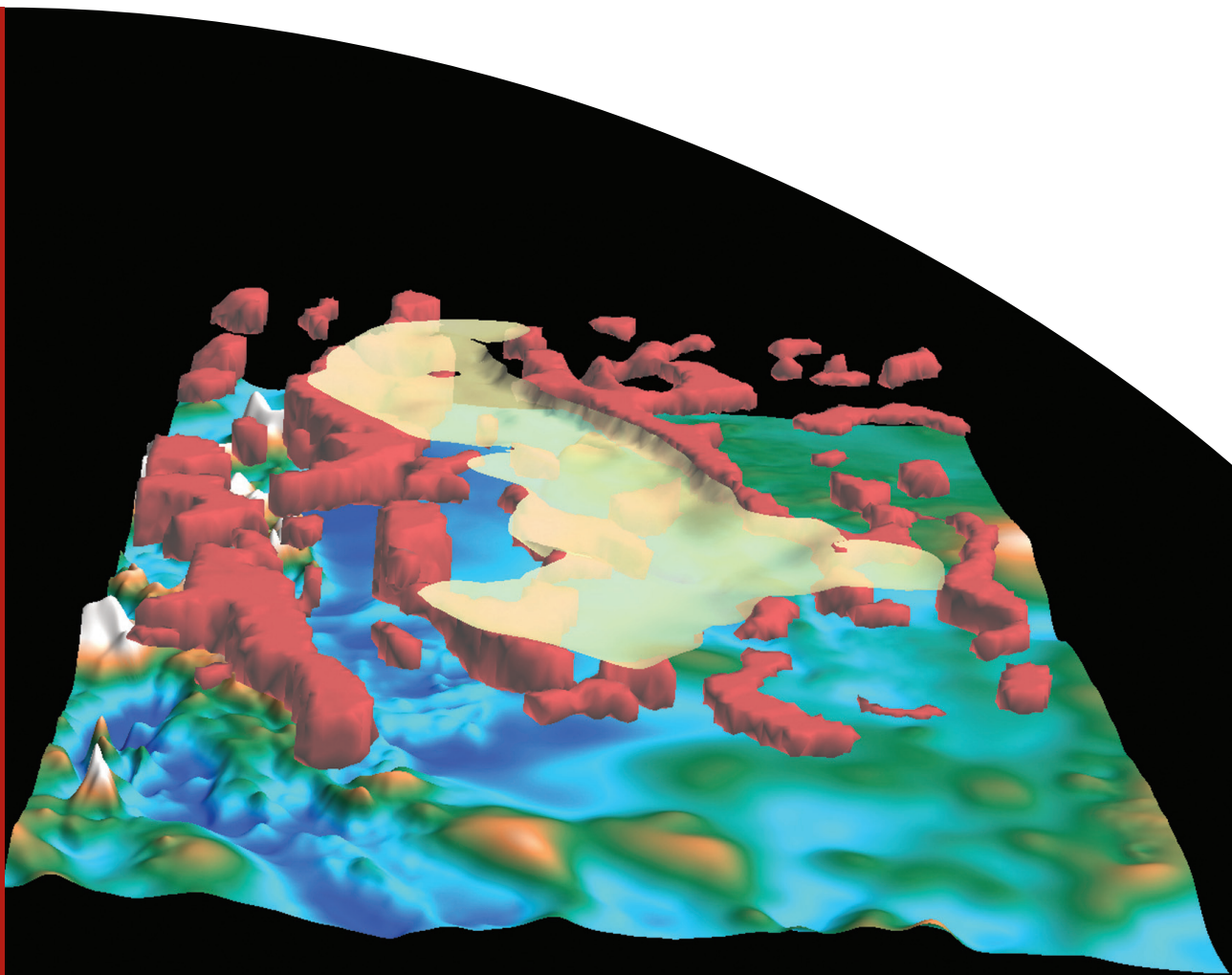
Proceedings of the 2010 Australian Geothermal Energy Conference

Gurgenci, H. and Weber, R. D.

Record

2010/35

**GeoCat #
71204**



Proceedings of the 2010 Australian Geothermal Energy Conference

GEOSCIENCE AUSTRALIA Record 2010/35

Edited by

Hal Gurgenci ¹ and Rikki Weber ²

1 Queensland Geothermal Energy Centre, The University of Queensland, St Lucia 4072

2 Geoscience Australia, GPO Box 378, Canberra, ACT 2601



Australian Government
Geoscience Australia



A horizontal banner for the Australian Geothermal Energy Conference. On the left is a globe showing Australia. The text reads: 'Australian Geothermal Energy Conference' in large white letters, with the website 'www.ausgeothermal.com' below it. To the right, it says '16-19 November Adelaide Convention Centre'. At the bottom right, the slogan 'Tomorrow's energy, today' is written in a cursive font. On the far right, the year '2010' is displayed vertically in white on an orange background. Logos for AGEA and APEG are also present in the center.

Department of Resources, Energy and Tourism

Minister for Resources and Energy: The Hon. Martin Ferguson, AM MP

Secretary: Mr Drew Clarke

Geoscience Australia

Chief Executive Officer: Dr Chris Pigram

© Commonwealth of Australia, 2010

This work is copyright. Apart from any fair dealings for the purpose of study, research, criticism, or review, as permitted under the *Copyright Act 1968*, no part may be reproduced by any process without written permission. Copyright is the responsibility of the Chief Executive Officer, Geoscience Australia. Requests and enquiries should be directed to the **Chief Executive Officer, Geoscience Australia, GPO Box 378 Canberra ACT 2601.**

Geoscience Australia has tried to make the information in this product as accurate as possible. However, it does not guarantee that the information is totally accurate or complete. Therefore, you should not solely rely on this information when making a commercial decision.

ISSN 1448-2177 ISBN 978-1-921781-38-4

GeoCat # 71204

Recommended bibliographic reference: Gurgenci, H. and Weber, R. D. (editors), 2010. Proceedings of the 2010 Australian Geothermal Energy Conference, Geoscience Australia, Record 2010/35.

Recommended bibliographic citation: Glikson, A. and Uysal, T. 2010. Evidence of impact shock metamorphism in basement granitoids, Cooper Basin, South Australia, in: Gurgenci and Weber (editors), Proceedings of the 2010 Australian Geothermal Energy Conference, Geoscience Australia, Record 2010/35.

Cover illustration: 3D image of gravity inversion modelling in the area between Mt Isa and the Georgetown Inlier, Queensland, viewed obliquely from the south. The red bodies enclose regions of low density interpreted as granites located at depth beneath Millungera Basin sediments, the base of which is shown as the yellow surface. The interpreted granites are shown projected above an image of the Bouguer Gravity field, from which the inversion model was generated. Courtesy of Alison Kirkby, Geoscience Australia.

The Convenors would like to thank the following sponsors for their kind support:

Gold Sponsors



Silver Sponsors



Bronze Sponsors



Conference Dinner Sponsor



Happy Hour Sponsors



Introduction

This volume is a compilation of Extended Abstracts presented at the 2010 Australian Geothermal Energy Conference, 17-19 November 2010, Adelaide Convention Centre, Adelaide, organised by the Australian Geothermal Energy Association and the Australian Geothermal Energy Group.

As editors of these proceedings, we first would like to thank the Technical Committee who have been very generous with their time to review the submissions and to work with the authors of the accepted submissions to improve the quality of the Abstracts and the presentations.

We also thank the Conference Chair Tony Hill and the rest of the Organising Committee who were brave enough to take on the job organising this second event on behalf of the Australian Geothermal Energy Association and the Australian Geothermal Energy Group. Rob Bulfield and Sapro Conference Management have done an excellent job in assisting the organisation.

We also thank again the sponsoring companies for their generous support.

We thank Geoscience Australia for publishing the proceedings.

Finally, we thank all delegates without whose participation none of this is worthwhile.

Hal Gurgenci

Rikki Weber

Conference Organising Committee

Susan Jeans, AGEA
Vicki Cleavland, AGEA
Dr Graeme Beardsmore, Hot Dry Rocks Pty Ltd
Dr Betina Bendall, PIRSA
Dr Anthony Budd, Geoscience Australia
Barry Goldstein, PIRSA
Professor Hal Gurgenci, University Queensland
Chris Matthews, AGEA
Jonathan Teubner, Petratherm

Program Technical Panel

Professor Hal Gurgenci (chair), Queensland Geothermal Energy Centre of Excellence,
Dr Anthony Budd, Geoscience Australia,
Delton Chen, Geodynamics Ltd,
Gareth Cooper, Hot Dry Rocks Pty Ltd
Peter Dowd, The University of Adelaide
Des Fitzgerald, Intrepid Geophysics,
Dr Massimo Gasparon, The University of Queensland
Helen Gibson, GeoIntrepid
Alison Kirkby, Geoscience Australia
Alan Knights, Green Rock Pty Ltd
Chris Matthews, AGEA,
Tony Meixner, Geoscience Australia
Professor Behdad Moghtaderi, The University of Newcastle
Professor Klaus Regenauer-Lieb, The University of Western Australia
Peter Reid, Petratherm Ltd
Michel Rosener, Geodynamics Ltd
Dr Catherine Stafford, Granite Power Ltd
Jonathan Teubner, Petratherm
Dr Adrian Williams, Geodynamics Ltd
Doone Wyborn, Geodynamics Ltd
Dr Yung Ngothai, The University of Adelaide

Conference Organisers

Rob Bulfield Sapro Conference Management Ph: 08 8274 6043 Fax: 08 8274 6000
www.sapro.com.au

Stream One

- A.R. Budd, E.J. Gerner, A.M. Kirkby, R.D. Weber, A.J. Meixner and D.C. Champion
Geoscience Australia's Onshore Energy Security Program: progress by the Geothermal Energy Project p1
- Cara Danis and Craig O'Neill
3D thermal modelling VS down-hole temperature extrapolation and the implications for targeting potential geothermal anomalies: a Sydney Basin case stud p4
- M. Hand and Y. Ngothai
South Australian Geothermal Research Centre p9
- Hearst Ghabri Mehran, Robert B. Retallcik, Trent and Killin Kevin
Application of magnetotellurics in geothermal reservoir characterization p11
- David Jenson, Kerry Parker, Ron Palmer and Bertus de Graff
Hutton Sandstone – a viable geothermal development p14
- Ashok A. Kaniyal, Jonathan J. Pincus and Graham J. Nathan
Investment in common-use network infrastructure to trigger incremental expansion in geothermal energy generating capital stock p20
- Ivan Kočiš, Tomáš Krištofič, and Igor Kočiš
Ultra deep drilling technologies for geothermal energy production p21
- Gideon B. Kuncoro, Yung Ngothai, Brian O'Neill, Allan Pring and Joel Brugger
A Preliminary Study on Na-Cl-H₂O-Rock Interactions of the Hot Fractured Rock Geothermal System in Cooper Basin, South Australia p24
- Adrian Larking and Gary Meyer
Geothermal Energy in the Perth Basin, Australia
Comparisons with the Rhine Graben p30
- A.D. Long, A.R. Budd, H. Gurgenci, M. Hand, C. Huddleston-Holmes, B. Moghtaderi and K. Regenauer-Lieb
Australia's Geothermal Research Activities p35
- V. Marshall, J. Van Zyl, S.E. Byron, T. Uysal and M. Gasparon
Comparative petrology & geochemistry of high heat-producing granites in Australia & Europe p41
- Craig McClarren, Massimo Gasparon and I. Tonguç Uysal
Geothermal Prospection Using Existing Groundwater Geochemical and Thermal Datasets: Identifying Regions of Interest in Queensland from Government Well and Bore Data p48
- Malcolm B. McInnes
Genie Impact Drilling: Synopsis of a New Hard Rock Drilling Development p52
- Alexander W. Middleton, I Tonguç Uysal, Massimo Gasparon and Scott Bryan
Hydrothermal alteration aspects of high heat producing granites in Australia & Europe p59
- Thomas Poulet, Soazig Corbel and Michael Stegherr
A Geothermal Web Catalog Service for the Perth Basin p64
- Martin Pujol, Grant Bolton and Fabrice Golfier
Flow and heat modelling of a Hot Sedimentary Aquifer (HSA) for direct-use geothermal heat

Australian Geothermal Conference 2010

production in the Perth urban area, Western Australia (WA)	p69
<u>Sukanta Roy</u> Geothermal Exploration in India	p75
<u>Behnam Talebi</u> , Mark Maxwell, Sarah Sargent and Steven Bowden Queensland Coastal Geothermal Energy Initiative – An Approach to a Regional Assessment	p81
<u>David H. Taylor</u> , Ben Harrison, Michelle Ayling and Kate Bassano Geothermal Exploration in Victoria, Australia	p87
<u>I. Tonguç Uysal</u> , Alexander W. Middleton, Robert Bolhar and Massimo Gasparon Geochemistry of silica rocks in the Drummond Basin as a record of geothermal potential	p91
<u>Gordon Webb</u> and Ben Harrison Estimates of the magnitude of topographical effects on surface heat flow from finite element modelling	p94
<u>Doone Wyborn</u> , Robert Hogarth, Delton Chen and Michel Rosener The next Australian EGS Reservoir – Jolokia 1 stimulation	p97
<u>Chaoshui Xu</u> Optimised Fracture Network Model for Habanero Reservoir	p98
Stream Two	
<u>Aleks D. Atrens</u> , Hal Gurgenci and Victor Rudolph Progress in CO ₂ -based EGS	p104
<u>Peter Barnett</u> and Tim Evans Exploration and assessment of Hot Sedimentary Aquifer (HSA) geothermal resources in the Otway Basin Victoria	p106
<u>J.E. Davey</u> and J.T. Keetley Validation of Geothermal Exploration Techniques for Analysing Hot Sedimentary Aquifer and Enhanced Geothermal Systems	p112
<u>Bertus de Graaf</u> , Ian Reid, Ron Palmer, David Jenson and Kerry Parker Salamander-1 – a geothermal well based on petroleum exploration results	p117
Ben Clennel, <u>Lionel Esteban</u> , Ludovic Ricard, Matthew Josh, Cameron Huddlestone-Holmes, Jie Liu and Klaus Regenauer-Lieb Petrophysical Methods for Characterization of Geothermal Reservoirs	p123
<u>Farizal</u> and Prashanti Amelia Anisa Geothermal Power Plant Competitiveness in Indonesia: Economic and Fiscal Policy Analysis	p130
<u>Desmond Fitzgerald</u> and Raymond Seikel A Method For Calibrating Australian Temperature-Depth Models	p138
<u>Andrew Y. Glikson</u> and I. Tonguç Uysal Evidence of impact shock metamorphism in basement granitoids, Cooper Basin, South Australia	p141
<u>T. Harinarayana</u> Geothermal Energy in India: Past, Present and Future Plans	p148
<u>Peter Leary</u> , Peter Malin, Eylon Shalev and Stephen Onacha	

Australian Geothermal Conference 2010

Aquifer heterogeneity – is it properly assessed by wellbore samples and does it matter for aquifer heat extraction? p149

Yan Liu, Huilin Xing, Zhenqun Guan and Hongwu Zhang
Automatic Meshing and Construction of a 3D Reservoir System: From Visualization towards Simulation p157

Luke Mortimer, Adnan Aydin and Craig T. Simmons
Targeting Faults of Geothermal Fluid Production: Exploring for Zones of Enhanced Permeability p163

Grahame J.H. Oliver
An EGS/HAS concept for Singapore p169

Jared Peacock, Stephan Thiel, Graham Heinson and Louise McAllister
Monitoring EGS Reservoirs Using Magnetotellurics p175

Joshua Koh, Nima Gholizadeh-Doonechaly, Abdul Ravoof and Sheik Rahman
Reservoir characterisation and numerical modelling to reduce project risk and maximise the chance of success. An example of how to design a stimulation program and assess fluid production from the Soultz geothermal field, France p179

P. W. Reid, L. McAllister and M. Messeiller
Status of the Paralana 2 Hydraulic Stimulation Program p203

Alvin I. Remoroza, Behdad Moghtaderi and Elham Doroodchi
Three Dimensional Reservoir Simulations of Supercritical CO₂ EGS p206

Catherine E. Stafford
Measuring the Success of EGS Projects: An Historical to Present Day Perspective p210

J.F. Wellmann, F.G. Horowitz, L.P. Ricard and K. Regenauer-Lieb
Estimates of sustainable pumping in Hot Sedimentary Aquifers: Theoretical considerations, numerical simulations and their application to resource mapping p215

Thomas W. Wideman, Jared M. Potter, Brett O'Leary and Adrian Williams
Hydrothermal Spallation for the Treatment of Hydrothermal and EGS Wells: a Cost-Effective Method for Substantially Increasing Reservoir Production Flow Rates p222

Bisheng Wu, Bailin Wu, Xi Zhang and Rob Jeffrey
Thermal effects on the wellbore stability p226

Matthew Zengerer, Chris Matthews and Jerome Randabel
3D Geological Modelling for Geothermal Exploration in the Torrens Hinge Zone p232

J. Zhang and H.L. Xing
Numerical simulation of geothermal reservoir systems with multiphase fluids p243

Xi Zhang and Robert G. Jeffrey
Development of Hydraulic Fractures and Conductivity near a Wellbore p247

Stream Three

David L. Battye, Peter J. Ashman and GUS J. Nathan
Economics of geothermal feedwater heating for steam Rankine cycles p253

Graeme Beardsmore, Ladislaus Rybach, David Blackwell and Charles Baron
A Protocol for Estimating and Mapping Global EGS Potential p257

Australian Geothermal Conference 2010

G. Beardsmore, A. Budd, B. Goldstein, F. Holgate, G. Jeffress, A. Larking, J. Lawless, J. Libby, M. Middleton, <u>P. Reid</u> , C. Stafford, M. Ward and A. Williams Changes to Geothermal Reporting Code and Guidelines on Company Reporting	p263
<u>Anna Collyer</u> , Nadia Harrison and Natasha McNamara Geothermal Energy's Transition from Resource to Power: Legal Challenges	p269
<u>Barry Goldstein</u> , Betina Bendall, Alexandra Long, Michael Malavazos, David Dockshell and David Love Trusted Regulation for Geothermal Resource Development (Including Induced Seismicity Associated with EGS Operations)	p273
<u>B.A. Goldstein</u> , G. Hiriart, J. Tester, B. Bertani, R. Bromley, L.C.J. Gutierrez-Negrin, E. Huenges, H. Ragnarsson, A. Mongillo, M.A. Muraoka and V.I. Zui Great Expectations For Geothermal Energy – Forecast to 2100	p281
<u>Hal Gurgenci and Zhiqiang Guan</u> New Design Concepts for Natural Draft Cooling Towers	p290
<u>Kamel Hooman</u> QGECE Research on Heat Exchangers and Air-Cooled Condensers	p294
Robert McKibbin, <u>Franklin Horowitz</u> , Neville Fowkes and Brenda Florio Equation-Free Summary of the 2010 Mathematics in Industry Study Group on Geothermal Data Analysis and Optimization	p298
<u>Jim Lawless</u> Status of Compliance With The Geothermal Reporting Code	p302
<u>Jim Lawless</u> Application of the Australian Geothermal Reporting Code to “Conventional” Geothermal Projects	p305
<u>David N. Love</u> , Gary Gibson, Russell Cuthbertson and Wayne Peck Small Australian seismic events and their effects	p306
Steve Kennedy, <u>Chris Matthews</u> , Damia Ettakadoumi and Cynthia Crowe Community Consultation Best Practice Manual	p400
<u>Craig Morgan and David Paul</u> Optimising ORC use in Australian Geothermal Applications	p402
<u>Yung Ngothai</u> , Norio Yanagisawa, Allan Pring, Peter Rose, Brian O'Neill and Joel Brugger Mineral scaling in geothermal fields: A review	p405
<u>Donald J.B. Payne</u> and Dezso Kiraly Direct GeoExchange Cooling for the Australian Square Kilometer Array Pathfinder – Field Trial	p410
<u>Klaus Regenauer-Lieb</u> and the WAGCoE team, Peter Malin and the IESE team, Steve Harvey and the CSIRO CESRE team, Edson Nakagawa and CSIRO's Geothermal & Petroleum Portfolio and Hal Gurgenci and the QGECE team A Research Well for the Pawsey Geothermal Supercomputer Cooling Project	p416
<u>Kyra Reznikov</u> Fracture Stimulation – legal risks and liabilities	p421
<u>Andrew S. Rowlands</u> and Jason Czapla QGECE Mobile Geothermal Test Plant & ORC Cycle Challenges	p422

Australian Geothermal Conference 2010

Jonathan Teubner

Australian geothermal Industry working with Investors – Defining the key parameters contributing to the long run marginal cost of geothermal and providing a comparison benchmark on the key unknowns p426

O. Bouchel, T. Hazou, C. Scott and Roger Winders
COMMUNITY TRUST – Engagement & Communication

p427

Melissa Zillmann and Myria Makras
Geothermal energy legislation and developments in Queensland

p434

Geoscience Australia's Onshore Energy Security Program: progress by the Geothermal Energy Project

A.R. Budd,* E.J. Gerner, A.L. Kirkby, R.D. Weber, A.J. Meixner and D.C. Champion
Geoscience Australia. GPO Box 378, Canberra, ACT 2601.

*Corresponding author: Anthony.Budd@ga.gov.au

Abstract

Geoscience Australia's \$58.9M 5-year Onshore Energy Security Program began in 2006 and includes a new Geothermal Energy Project.

The project aims to assist the development of a geothermal industry in Australia by: providing precompetitive geoscience information, including acquisition of new data; informing the public and government about Australia's geothermal potential; providing technical advice to government; and partnering with industry in international promotional events for the purpose of attracting investment.

This abstract gives a brief summation of activities undertaken by Geoscience Australia within the Onshore Energy Security Program, principally those of the Geothermal Energy Project.

Keywords: data acquisition, modelling, Geothermal Play Systems

The Geothermal Energy Project

Following consultation with industry and State and Northern Territory geological surveys, a number of activities were identified where GA could either fill gaps where no other organisation was able to fulfil, or could complement activities by other partners.

Advice to government

Geoscience Australia (GA) is a prescribed agency within the Department of Resources, Energy and Tourism. GA provides advice to government on geoscience-related matters, including resources. GA participated in the development of the Geothermal Industry Development Framework and Geothermal Industry Technology Roadmap. GA was involved in the program design and subsequent technical assessment of the Geothermal Drilling Program. GA co-authored (with ABARE) the geothermal chapter of the Australian Energy Resource Assessment. GA has been involved in the development of the Australian Code for Reporting of Exploration Results, Geothermal Resources and Geothermal Reserves, and sits on the Joint AGEA-AGEG Code Committee for the purpose of one day compiling and reporting geothermal resource and reserve estimates in the same way as is done for mineral and oil & gas commodities.

OZTEMP

GA has released OZTEMP, an updated dataset and map of predicted temperatures at 5 km depth,

available from the project's webpage (www.ga.gov.au/minerals/research/national/geothermal). Extensive QA/QC was conducted on the dataset of bottom hole temperatures, and where available new data was included. For the map, the OZSeeBase dataset was used (FrOG Tech, 2006), and the Bureau of Meteorology's Mean Annual Average Air Temperature (BoM 2010) was also used with a correction for surface temperature. For the first time, heat flow data was also incorporated into the map.

Data acquisition

There is a paucity of temperature-specific data in Australia, and to address this GA has established a capability for measuring surface heat flow via thermal gradient logging and thermal conductivity measurement.

Thermal gradient logging

Without the possibility of drilling new holes, GA has worked with State geological surveys and minerals exploration companies to access exploration and water bores. Figure 1 shows the distribution of logged bores as of July 2010.

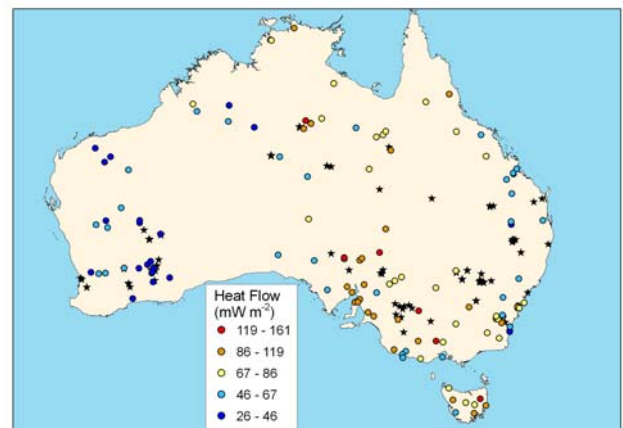


Figure 1. Map showing existing heat flow measurements for the Australian continent, and the distribution of bores logged for temperature by Geoscience Australia (black stars).

Thermal conductivity

GA operates an Anter 2022 Unitherm thermal conductivity meter and associated sample preparation equipment. Project staff have been involved in establishing operating procedures for the instrument, a process which has included inter-lab comparison testing with Torrens Energy, Hot Dry Rocks Pty Ltd, and Southern Methodist University. In addition, GA has engaged Hot Dry

Rocks Pty Ltd to measure two batches of samples.

Samples have been taken from the majority of the bores measured by Geoscience Australia for their thermal gradient, as well as other bores for 'stratigraphic' conductivity values.

Promotion

Undoubtedly the greatest impediment to the development of the Australian geothermal industry since the Global Financial Crisis has been the lack of capital investment. Geoscience Australia has participated in "Team Australia Geothermal" events at the Geothermal Energy Expo, Reno 2009, and the World Geothermal Congress, Bali 2010. The collaboration of industry, government and associations has been aimed at portraying Australia as a favourable investment destination.

Resource assessments

In 2007 GA produced an estimate of the contained heat above 150°C in the top 5 km of the Australian crust. Understandably this produced a very large estimate of energy. To provide a more relevant estimate 1% of the thermal resource was assumed to be accessible and convertible, and this equates to ~26,000 years of energy consumption (Budd et al., 2009).

The production of the Australian Energy Resource Assessment highlighted the need for a better understanding of Australia's geothermal resources potential. This contrasts with other renewable energy resources where the knowledge-base is quite advanced. There is a need for geothermal to be better understood so that it can be compared more directly to other energy sources. With a limitation on the availability of temperature data, other geoscience datasets must be used to inform or derive estimates of geothermal resource potential.

Geothermal Play Systems

As mentioned above, there is a paucity of temperature-specific data publicly available in Australia. There is, however, a wealth of high-quality geoscientific data available throughout the country, much of which can be used to make assessments of geothermal potential from a conceptual view point. Like some companies and other organisations, GA has developed 2.5D and 3D methods for processing geological, geophysical and geochemical data to produce resource potential assessments and estimates. A 'systems' approach has been utilised to enable these data sets to be used as 'mappable proxies' to estimate heat production and thermal insulation at regional scales (Budd et al., 2009). Conceptual and empirical methods of developing the Geothermal Play Systems approach have been pursued, and are still in development.

3D thermal modelling

Through a Primary Industries and Resources South Australia (PIRSA) Australian Geothermal Energy Group (AGEG) Technical Interest Group 9 Tied Grant, a thermal calculation module was built for GeoModeller software by Intrepid Geophysics (Siekel et al., 2009). This has been used to develop thermal models of the Millungerra Basin (unpublished), and the Cooper Basin (such as Gibson et al., 2010).

We have also undertaken synthetic thermal modelling tests. This involved the development of a synthetic grid of granites buried under flat-lying sediments that was used to model the effects of changing thermal and geometric variables (one at a time). Modelled variables include thermal conductivity, heat production and density of the sediments and granite, as well as the thickness, radius and depth extent of the granites and total sediment thickness. This has resulted in 5,400 individual test models, and we are in the process of interpreting these results. These interpretations will then serve as a guide for a first-pass assessment of thermal potential of the whole content based on estimates of granite size, basin geometry and composition (Meixner, 2009).

North Queensland Energy Assessment

A GIS-based approach was used to qualify the Hot Rock and Hot Sedimentary Aquifer geothermal systems of northern Queensland (Huston, 2010).

References

- BoM, 2010, Climate Data Online
<http://www.bom.gov.au/climate/data/>
- Budd, A.R., Barnicoat, A.C., Ayling, B.F., Gerner, E.J., Meixner, A.J. and Kirkby, A.M., 2009, A Geothermal Play Systems approach for exploration Australia, in: Budd and Gurgenci (editors), Proceedings of the 2009 Australian Geothermal Energy Conference, Geoscience Australia, Record 2009/35.
- FrOG Tech, 2006, OZ SEEBASE™ Proterozoic Basins Study. PR107.
- Gibson, H., Seikel, R., and Meixner, T. 2010, Characterising uncertainty when solving for 3D temperature: New tools for the Australian geothermal energy exploration sector. ASEG Extended Abstracts 2010, 1–3. doi:10.1071/ASEG2010ab290.
- Huston, D.L., 2010, An assessment of the uranium and geothermal potential of north Queensland / edited by Huston, D.L. with contributions by Ayling, B., Connolly, D., Huston, D.L., Lewis, B., Mernagh, T.P., Schofield, A., Skirrow, R.S. and van der Wielen, S.E. Geoscience Australia Record 2010/14, Canberra

https://www.ga.gov.au/products/servlet/controller?event=GEOCAT_DETAILS&catno=69711

Meixner, T., Johnston, S., Kirkby, A., Gibson, H., Seikel, R., Stuwe, K., Fitzgerald, D., Horspool, N. Lane, R. and Budd, A., 2009, Establishing hot rock exploration models: from synthetic thermal modelling to the Cooper Basin 3D geological map.

Siekel R., Stuwe K., Gibson H., Bendall B., McAllister L., Reid P., Budd A., 2009, Forward prediction of spatial temperature variation from 3D geology models. ASEG Extended Abstracts 2009, -. doi:10.1071/ASEG2009ab117.

3D thermal modelling VS down-hole temperature extrapolation and the implications for targeting potential geothermal anomalies: a Sydney Basin case study

Cara Danis^{1*} and Craig O'Neill¹

¹ GEMOC Macquarie University, Dept Earth & Planetary Science, NSW 2109, Australia

* Corresponding author: cara.danis@mq.edu.au

Geothermal exploration programs require accurate subsurface temperature information and currently this information primarily comes from temperature maps created from the extrapolation of shallow down-hole temperature measurements. These extrapolations are often taken from measurements made in non-equilibrated boreholes and do not account for variations in geological structure or thermal conductivity. Here we present a case study for the Sydney basin where we explore temperature maps at 5km created from extrapolated equilibrated and non-equilibrated borehole measurements and from modelled basin temperatures and the implications for targeting potential geothermal anomalies. The modelled temperatures are derived from finite element models using 3D basin geology and defined thermal properties.

Keywords: Sydney Basin, 3D thermal modelling, temperature extrapolation, geothermal exploration

Case Study – Sydney Basin

The Sydney Basin, part of the Sydney-Gunnedah-Bowen Basin system, is a major sedimentary basin in the east coast of Australia and an important economic resource. Much attention is given to the coal and coal seam gas prospects but recently the focus has shifted to the basins thermal structure and geothermal potential. Previous work in the Gunnedah Basin (Danis et al., 2010) has shown that basin architecture and insulating sediments have a profound impact on the thermal structure. Heat refracts around insulating coal and sediment layers, into adjacent zones of lower thermal resistance, resulting in large lateral variations in the subsurface temperature.

In order to determine areas for potential geothermal resource exploration an assessment of the temperature at depth is required. Short of drilling deep and expensive boreholes, current methods extrapolate down-hole temperatures from shallow boreholes to 5km using shallow geothermal gradients. This method relies on non-equilibrated temperature information and geothermal gradients, which fails to account for lateral variations in geology and thermal conductivity. Such extrapolations may differ significantly to actual temperatures at depth and

my result in false target anomalies. 3D thermal modelling provides a more representative analysis of the thermal structure, with the ability to set model parameters for lateral geological variation and define thermal characteristics.

The work presented here compares the results of extrapolated equilibrated and non equilibrated temperature information from shallow boreholes to 5km depth and thermal modelling using geological models for target anomaly location. There is a significant difference in temperature structure at depth between equilibrated and non-equilibrated extrapolated temperatures as well as thermal modelled temperatures. These differences have significant implications for targeting resource areas for geothermal exploration.

Methods and Results

Down-hole Temperature Measurements: Equilibrated and Non-equilibrated

Routinely temperature measurements in boreholes are not conducted for the purpose of geothermal exploration, instead they often are designed to assess groundwater aquifer locations and cement setting during construction of groundwater bores. In exploration drillholes temperatures are recorded at the bottom of the hole during airlift tests or geophysical surveys (other than temperature). These results are taken immediately following drilling, generally within 24hrs, and are therefore considered non-equilibrated. On rare occasions temperature information is collected several months or even years after drilling, this is considered equilibrated.

To assess the impact of non-equilibrated and equilibrated temperature maps we collected a large amount of temperature results from both non-equilibrated and equilibrated boreholes. Most equilibrated data is collected in the field using methodology outlined in detail in Danis et al. (2010). As Beardsmore & Cull (2001) recommend equilibrated measurements can be recorded after waiting 3 times the drilling time length, our temperature results were divided accordingly. In general any measurements taken one month or greater after drilling were considered as equilibrated results.

Geothermal gradients were determined for each equilibrated and non-equilibrated borehole using

the 1D two layer extrapolation method (outlined by Chopra & Holgate, 2006) and temperature at 5km depth below surface contour map produced (Figure 1). All temperatures were corrected for climatic variations based on Cull (1979). Where only a bottom hole temperature measurement was recorded a surface temperature average of 15°C was used to calculate the geothermal gradient. Where possible only temperatures from below 100m ground surface were used, to try and avoid diurnal/seasonal temperature influences.

The first layer (sediments) is defined from our Sydney Basin geological model and used the calculated geothermal gradient. The second layer (basement) is also defined from our geological model and uses the uniform geothermal gradient of 25°C/km so as to be comparable to the current temperature at 5km map.

Figure 1 shows a distinctive difference between the extrapolated equilibrated and non-equilibrated measurements for temperature observed at 5km. The equilibrated boreholes (Figure 1a) show low temperatures (60-120°C) in the central part of the Sydney Basin, where sediment thickness is greatest, whilst near the edges of the basin (i.e Ulan and Singleton) temperatures are approaching 200 - 250°C. The non-equilibrated bores also show a similar trend, however on a slightly different scale, with several elevated anomalies in the generally colder parts of the central and southern Sydney Basin.

The position of temperature highs (or in some cases lows) will shift depending on whether equilibrated or non-equilibrated temperatures are used. Three highs appear around the Sydney-Campbelltown-Wollongong region in the non-equilibrated data which are not prominent in the equilibrated map. The high near Singleton is also more localised with the non-equilibrated measurements.

The pattern in temperature distribution of lows over the centre and highs on the edge of the Sydney Basin, were an expected feature. They tie in with the fact that the coal measures provide a thermal insulator, thus temperatures measured above coal measures would be expected to be cooler than those measure in or below coal measures. On the edge of the basin heat refracting around the coal measures produces the elevated temperatures.

Previous thermal modelling of the Gunnedah Basin (Danis et al., 2010) showed basin architecture and the refraction of heat around the coal interval to be major controlling factors in the thermal profile. Therefore to better understand the impact of extrapolating shallow thermal measurements to depth we created 15 thermal model profiles along the lines shown in Figure 1.

Thermal Modelling: Underworld

Thermal models were developed using the finite element code *Underworld*. The code solves the non-steady state heat equation with internal heat sources in two dimensions. Distinct layers from our 3D geological model are imported as different materials into the code, with constant temperature top and bottom boundary conditions. The thermal properties for each material layer are outlined in Table 1, and are aggregates of measurements on each unit/rock type. In addition there is one quasi-

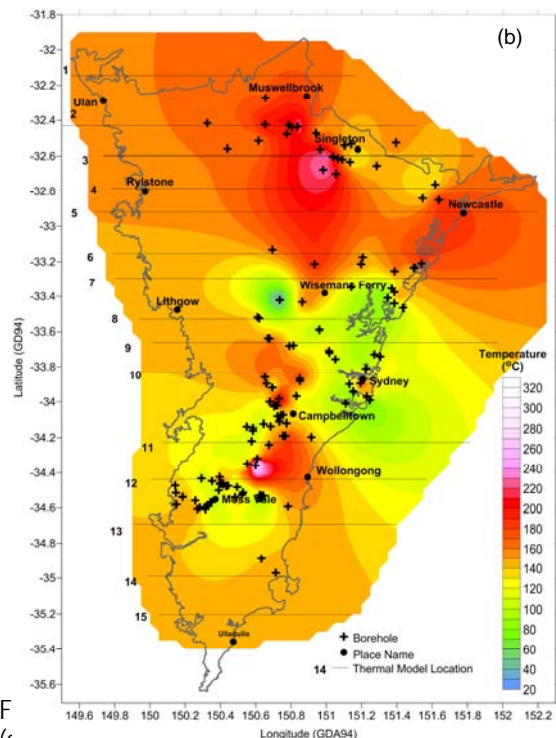
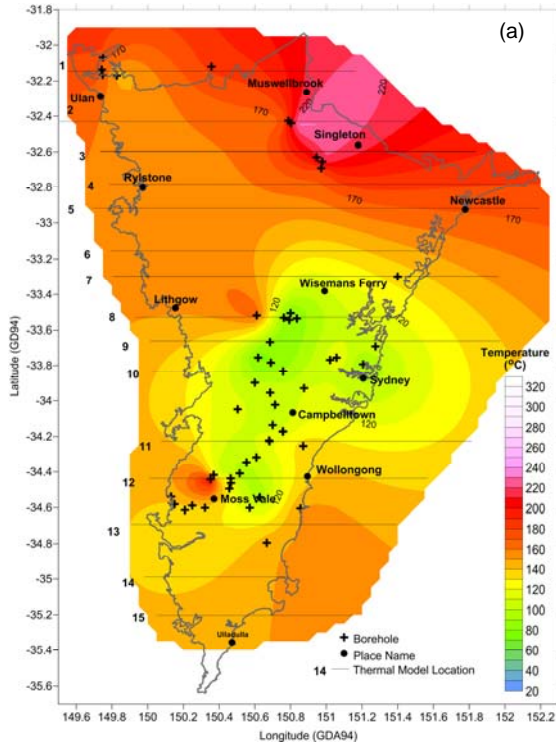


Figure 1 (a) equilibrated and (b) non-equilibrated. Location of boreholes used shown as crosses.

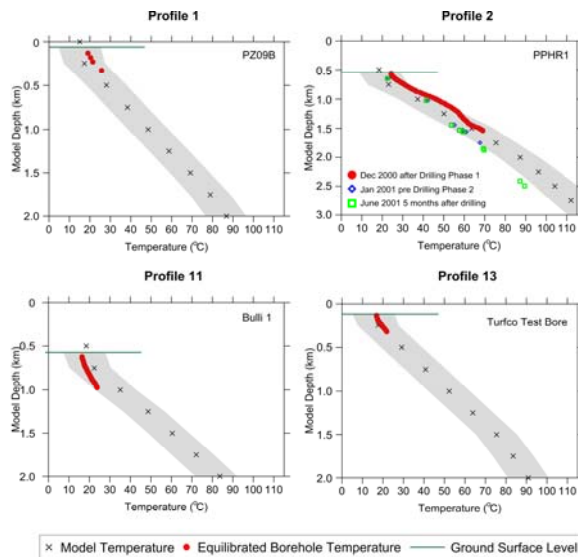
material called 'air'. This top air layer has a large conductivity and its purpose is to allow direct thermal coupling of the varying topographic surface with the top boundary condition. The side boundary conditions are reflecting, and an extra 10km has been added to either side of the model profile to avoid any reflecting edge effects.

Table 1

Rock Type	Density (kg/m ³)	Conductivity (W/m-K)	Heat Production (μW/m ³)
Basement	2700	3	2
Mafics	2950	3	0.5
Sediments	2460	2	1.25
Coal Interval	1900	0.3	1.25

The main free parameter is the bottom temperature condition at 12km, which was extrapolated from the National Temperature at 5km map (e.g Budd, 2007) to be ~350°C. Heat production in the basement is taken from representative Lachlan Fold Belt granites in the OZCHEM database. The model considers thermal conduction only, it doesn't take into account advective effects or the effects of varying surface temperature conditions.

The model boundary conditions were calibrated using limited available equilibrated temperature from shallow boreholes (Figure 2).



equilibrated borehole temperatures for four selected profiles. Ground surface (green line) varies from model depth zero depending on topography. Gray shaded area represents ±10°C of the model geotherm.

The equilibrated borehole temperatures (Figure 2) compare well with the model geotherms and are from boreholes in the Permian sequence. Equilibrated temperatures in profile 1 are from field measurements using Hobo logging

equipment, whilst profiles 2, 11 and 13 have been geophysical logged. The precision of the Hobo logging equipment is 0.37°C at 20°C and the general precision of geophysical temperature logging equipment is 0.1°C (from AUSLOG). The uncertainty of the climate correction applied to the equilibrated measurements is approximately ± 5°C at the surface, ±3°C at 500m and ± 1°C at 1km. We therefore allow an uncertainty buffer of ± 10°C in our measured temperatures when comparing them to the modelled geotherms. It is important to note in profile 2 the green measurements are the equilibrated results and are lower than expected due to cleaning of the borehole before logging. The red and blue measurements represent non-equilibrated temperatures.

In order to compare the results of extrapolated temperature measurements with thermal modelling, a series of temperature profiles were taken along a selected thermal model line. Here the equilibrated and non-equilibrated temperature measurements were extracted at 500m and 5km depth and compared to those of the thermal model profile at the same depths, as shown in Figure 3.

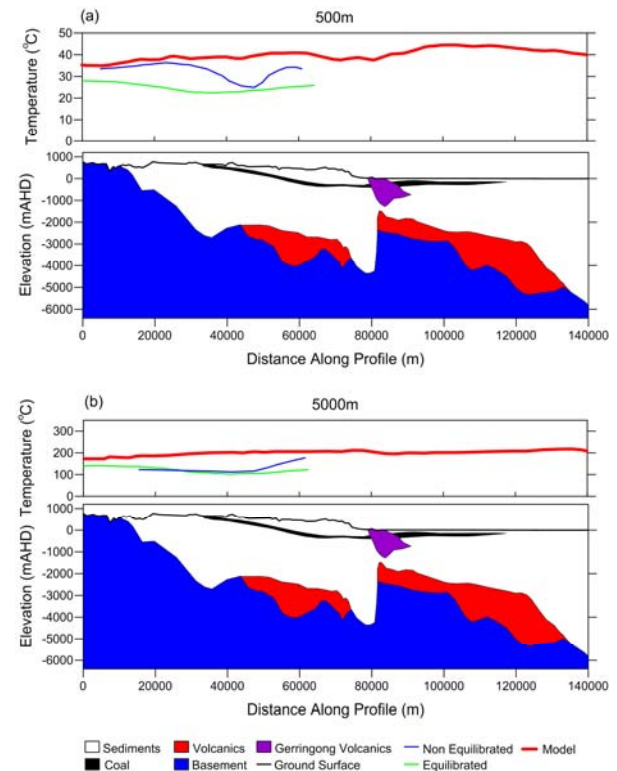


Figure 3: Thermal model Line 12 temperature output with extrapolated temperatures (green = equilibrated, blue = non-equilibrated) at (a) 500m and (b) 5000m below ground surface and showing model geology.

From Figure 3 a distinctive difference in anomaly structure can be seen between the 500m and 5km depths. In both cases the extrapolated

equilibrated and non-equilibrated measurements underestimate the modelled temperatures. Even at 500m, above the influence of the coal measures the extrapolated temperatures are still lower than the modelled temperatures.

At 5km the model temperature also shows very little variation as they are predominately in the Lachlan Fold Belt basement. At 500m shallow surface variations in the modelled temperatures are observed and are most likely related to the geology and/or influences of shallow groundwater aquifers.

In both profiles (Figure 3) the effects of the insulating coal interval on extrapolated equilibrated or non-equilibrated versus modelled temperatures can be seen. It appears that the extrapolation of shallow measurements, without any consideration of the geology and/or thermal conductivity, to depth propagates shallow surface features and produces false anomalies.

To further illustrate the difference between the extrapolated and modelled temperatures Figure 4 is a contour map of modelled temperatures at 5km below ground surface for the Sydney Basin.

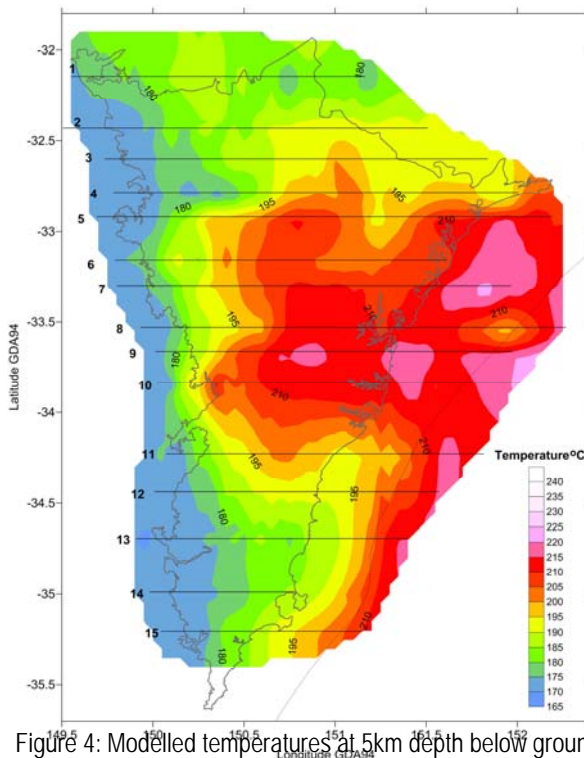


Figure 4: Modelled temperatures at 5km depth below ground surface. Thermal model lines are numbered 1 to 15, outline of the Sydney Basin shown in grey and edge of continental shelf is the offshore black line.

Modelled temperatures (Figure 4) in the Sydney Basin at 5km are hottest where the thickest layers of sediment and coal intervals are. This is most prominent around Sydney and north towards the Hunter/Newcastle Coalfields, where sediment thickness ranges from 3 to 4km, and a thick layer

of basal volcanics are also present. The temperature anomaly observed west of Singleton in the equilibrated extrapolation map appears in a similar location with the modelled temperatures, but is less pronounced. The high on Line 12 north of Mossvale in the equilibrated extrapolation map is not apparent in Figure 4. High basement temperatures offshore of Newcastle in the Newcastle Syncline are a new feature observed with the modelled temperatures. Where basement is shallow, i.e. the southern parts of the Sydney Basin, modelled temperatures at 5km are lower than those further north with greater sediment cover, predominately because the coal interval is generally absent, removing the insulating effect, and sediment thickness is less than 1km.

Modelled temperatures show high (210+°C) temperatures under areas of thick sediment cover, whilst shallow extrapolated temperature measurements often reflect the insulating effect of the coal interval (if above the coal interval) with temperatures ranging from 60°C to 230°C.

Summary

These results show that the temperature variations observed in maps created from extrapolated shallow borehole measurements are likely to be inaccurate. The simple linear extrapolations shown here of both equilibrated and non-equilibrated show shallow temperature measurements propagate near surface features to depth which, when compared to modelled temperatures, are not true anomalies. Therefore given most of the measurements used in the creation of temperature at 5km maps are taken from non-equilibrated boreholes extreme caution should be exercised when considering the temperatures.

However thermal modelling did show that equilibrated measurements are an excellent calibration tool. The modelled geotherms fit well with the shallow equilibrated measurements. A well calibrated thermal model will better account for basin structure and changes in thermal conductivity than extrapolated temperature maps.

Extrapolation doesn't take into account the thermal effects of basin architectural structure and should be avoided as a geothermal exploration tool. Not only is there a risk of the target anomalies being false positives, possible positive targets may be incorrectly located as a result of refracted heat from the basin structure.

References

Beardmore, G.R., Cull, J.P., 2001, Crustal heat flow: a guide to measurement and modelling. Cambridge University Press 324p.
 Budd, A.R., 2007, Australian radiogenic granite and sedimentary basin geothermal hot rock

potential map (preliminary edition), 1:5 000 000 scale. Geoscience Australia, Canberra.

Cull, J.P., 1982, An appraisal of Australian heat flow data. BMR Journal of Australian Geology & Geophysics v.7, p. 11-21.

Danis, C., O'Neill, C., and Lackie, M., 2010, 3D architecture and upper crustal temperatures of the Gunnedah Basin. Australian Journal of Earth Sciences 57, 483-505.

South Australian Geothermal Research Centre

M. Hand and Y. Ngothai
SACGER, IMER, The University of Adelaide, South Australia, 5005.

*Corresponding author: martin.hand@adelaide.edu.au

The emergence of the Australian Geothermal Sector has focussed attention on the potential of the Australia's non volcanic thermal systems to provide both direct and indirect energy. However the challenges are significant, and require a coordinated effort between the private, government and R&D sectors to focus expertise and bring projects to demonstration. The Development Framework and Technology Roadmap (DRET, 2008) outlines a clear plan for project development. A key aspect of this roadmap is consultation between the private sector and research organisations that prioritises research goals that directly aid the sector. In this context there are now a number of research centres within Australia that are seeking to form a cohesive national R&D effort to assist the sector. This paper provides an overview of the South Australian Geothermal Research Centre (SACGER), which is hosted at the University of Adelaide, and provides a compliment to the national overview presented by Long et al (this volume).

Keywords: South Australian Geothermal Research Centre.

South Australian Centre for Geothermal Energy Research - SACGER

The South Australian Centre for Geothermal Energy Research is based at the University of Adelaide within the Institute for Minerals and Energy Resources (IMER), www.adelaide.edu.au/imer. The centre is funded from the South Australian Renewable Energy Fund, established with a grant of AU\$1.6M over two years from 1 July 2009. However initiation of expenditure was delayed until July 2010. The University of Adelaide is providing AU\$400,000 over the same period. Within IMER the South Australian Centre for Geothermal Energy Research forms part of a broader R&D portfolio on energy that includes the Centre for Energy Technologies which has a focus that includes the energy conversion and hybrid technologies whose aim is to optimise the geothermal energy delivered to the surface.

The SACGER research program has three principal foci which compliment the research programs of other centres around the country and build on strengths in subsurface modelling and characterisation to foster reliable estimates and efficient development of geothermal resources.

Program 1: Development of Electromagnetic tools to monitor and assess geothermal reservoir behaviour

This program is designed to the development of technologies and methods to make surface-based magnetotelluric (MT) surveys useful in (1) predicting the presence of fractured reservoirs ahead of the drill bit and (2) monitoring fluid flows in Engineered Geothermal Systems.

Under certain conditions, MT surveys can indicate the presence of naturally occurring hot fractured rock targets that are susceptible to reservoir enhancement with fracture stimulation to create Engineered Geothermal Systems. MT surveys can provide measurements that indicate the nature of changed fracture networks and post reservoir enhancement with hydraulic fracture stimulation. The development of MT technologies and MT interpretation methods is identified as a priority for research in the Australian Government's Geothermal Industry Development Framework and its associated Geothermal Technology Roadmap as requiring immediate attention. The University of Adelaide is internationally recognised for its expertise in the use and development of MT techniques, and is well positioned to become an international leader in the development of electromagnetically based tools for the geothermal industry.

The initiation and propagation of the underground fluid-reservoir is dependent on several parameters, including the stress regime, geometry of pre-existing faults, and reservoir lithologies. Currently, measurements of shear-wave splitting (SWS) is deployed to define EGS stress regimes, while refined measurement of seismicity (natural and induced during EGS field operations) is a standard approach to determine the location of the enhanced extent in the subsurface of EGS reservoirs (by locating seismic events associated with the creation of fractures during EGS operations). Because MT surveys can, under certain conditions, detect fluid flow patterns, advances in MT technologies and interpretation methods hold promise to foster more accurate delineation of EGS reservoirs, and models of fluid flows in EGS reservoirs. Locating MT measurement stations alongside micro-seismic detectors is a way to better understand the relationship between the two datasets and

delineate the location of fracture zones in EGS fields.

The proposed research leverages on knowledge obtained from a pilot project concluded by the University of Adelaide with Petratherm Ltd. Initial studies and field surveys indicate close site spacing of the MT sites and high data quality are crucial for successfully monitoring the reservoir development.

The technologies and approaches developed will be readily transferable to other potential EGS sites in South Australia and more globally.

Program 2: Fluid-rock interactions in geothermal reservoirs

Fracture and flow

Australia's three flagship geothermal projects are all located in South Australia (Geodynamics' Cooper Basin project; Petratherm's Paralana project; and Panax's Salamander (Penola) project. The Geodynamics and Petratherm projects represent two of the world's most significant Engineered Geothermal Systems (EGS) projects. Both projects entail the enhancement of naturally fractured rocks with hydraulic fracture stimulation. Additionally dependent on the reservoir nature, Hot Sedimentary Aquifer systems such as those targeted in Panax's Salamander project may also require stimulation.

Reliably predictive flow modelling of EGS reservoirs is a recognised critical research challenge that is driving a peak international consortia (the International Partnership for Geothermal Technologies; the IPGT) to focus on improving 3-D modelling of reservoir performance through the life of a geothermal field life e.g. models that couple heat exchange, pressure, rock-fluid interaction, fluid flow dynamics, geomechanical properties and other geothermal reservoir and geothermal well parameters over life-cycle production history. The aim of research in SACGER will be to:

- (1) Improve 3D models with new information from the EGS projects, and work in collaboration with the R&D expertise in Australia and internationally. This work will have implications for the risk management of induced seismicity by characterising the geometry of naturally existing fracture patterns, and improving knowledge of the in-situ stresses and potential overpressure regimes.
- (2) Develop laboratory procedures using core flooding under stress aimed at predicting formation damage in production/injection wells and removal of well damage.

Program 3: Chemical reactivity in geothermal systems

Area-specific research to mitigate fouling and geothermal reservoir (pore and fracture) blocking is essential for efficient geothermal energy development projects. This research will build on pilot studies using a hydrothermal cell at representative reservoir temperatures (100-250°C) to study fluid-rock interactions in geothermal reservoirs. However, the pilot study cell operated at pressures (roughly 50 bar, the saturation pressure of fluid) well below pressures (~ 300 bar) typical of EGS reservoirs in South Australia. More realistic reservoir conditions will be simulated by the creation of a high temperature, high pressure flow through cell to experimentally explore the risks of fouling and reservoir blockage at conditions that mimics conditions in the South Australian EGS projects.

The research will also allow the chemical processes in HSA systems to be examined. This will allow prediction of permeability for down-dip (thermally viable) targets HSA targets as well as scaling and fouling.

Development and application of tracers and smart particles to track fluid flow within reservoirs

Tracer technologies are a critical factor in calibrating reservoir performance models in all geothermal projects and can be used to determine the reactive

Conservative tracers for characterizing inter-well reservoir flow processes are:

- Thermally stable to 350°C
- Detectible to low parts per trillion
- Environmentally friendly and non-toxic

Reactive tracers for characterizing fracture surface areas in injection/backflow tests are:

- Thermally decomposing
- Reversibly sorbing
- Possessing contrasting diffusivities

In addition to these research programs is work currently underway within the within the Centre for Energy Technologies that is experimenting verification of underground cooling for efficient thermal cycles and examination of low temperature thermal processing using geothermal energy aimed at optimising geothermal energy investments.

For more information see www.adelaide.edu.au/geothermal/ or contact the centre: imer@adelaide.edu.au or martin.hand@adelaide.edu.au

Application of magnetotellurics in geothermal reservoir characterization

Gharibi¹ Mehran, Hearst^{1*} Robert B. Retallick² Trent and Killin¹ Kevin

¹Quantec Geoscience Ltd., 146 Sparks Ave., Toronto, ON, Canada M2H 2S4

²Quantec Geoscience Pty. Ltd., Unit 2/77 Araluen Street, Kedron, Qld., 4031

*Corresponding author: rhearst@quantecgeoscience.com

In this paper we examine Magnetotelluric (MT) data and analysis from a few different styles of geothermal resource. The geothermal resources examined include both shallow (<1000m depth) and deep (>2000m) scenarios. The implications with respect to survey and limitations imposed by survey design on the interpretation of the results are discussed. The results of 1-D, 2-D and 3-D inversions are compared and discussed in terms of their vertical and spatial resolutions and the reliability of the results in conjunction with the geology of the study areas. The continued improvement in the power and affordability in multi-core PC-platform computing allows for the relatively rapid inversion of MT data in 3-D. In the past it had been necessary to invert in 3-D with only a subset of the original dataset and with a limited number of frequencies (often <10 frequencies) in order to reduce the computational time and cost; this is no longer necessarily the case. The effect of number of frequencies used in the 3-D inversion process is discussed in terms of the choice of the acquisition data density and data distribution for a given dataset.

Keywords: acquisition 1-D, 2-D, 3-D, inversion, magnetotelluric, geothermal.

Magnetotellurics and Geothermal Reservoirs

The Magnetotelluric (MT) method is an EM technique allows one to construct plan maps and depth sections of resistivity variations in the Earth from the surface to depth. The resistivity variations are used to determine and provide insight into the location and character of geothermal reservoirs. Analysis of the resistivity data in terms of the signatures associated with various geologic units and alterations related to a geothermal system can be used to detect and delineate a geothermal reservoir. These resistivity signatures include subsurface resistivity variation associated with different alteration levels and mechanisms that result in a conductive clay reservoir cap which is underlain by a slightly more resistive core. In the case of an "active" geothermal system there is the possibility of the underlying hot water circulation being identified with a low resistivity signature. In the case of a "passive" geothermal system the reverse may be

true. Through the evaluation of MT data in conjunction with other geological, geochemical and geophysical data sets, the definition and characteristics of a particular geothermal reservoir may be determined.

Acquisition Methodologies

The conventional method of MT acquisition involves the establishment of a series of individual MT sites consisting of dipoles for electric field measurements and magnetometers (usually low frequency coils) for magnetic field measurements. An example of such an acquisition system is illustrated by Figure 1.

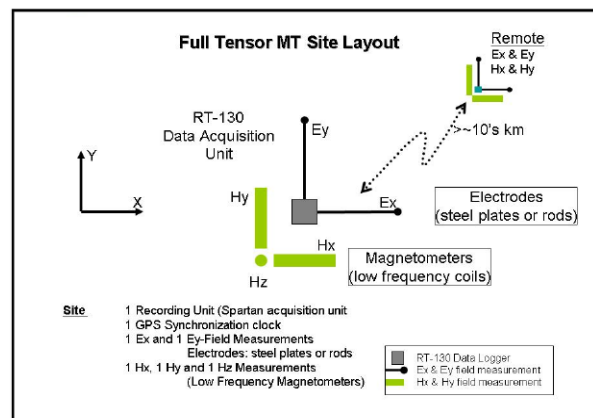


Figure 1: Full Tensor MT Site Layout

This type of system is well suited to investigations in irregular terrain, for deep targets (>2000m) and for reconnaissance type surveys whereby a large amount of ground must be covered in a limited amount of time and hence relatively wide site intervals are required ($\geq 500m$). Detailed profiling can also be accomplished.

The past decade has seen the development of array type systems whereby a large number of MT sites can be deployed in a rapid fashion allowing for a detailed investigation to be completed in a short period time. Often these systems include the ability to acquire other complementary geophysical data sets (e.g. DC resistivity, IP chargeability, TEM). An example of such a system is illustrated by Figure 2. In general, these array type systems can be extremely effective in the delineation of near surface (<1000m deep) geothermal systems and reservoirs.

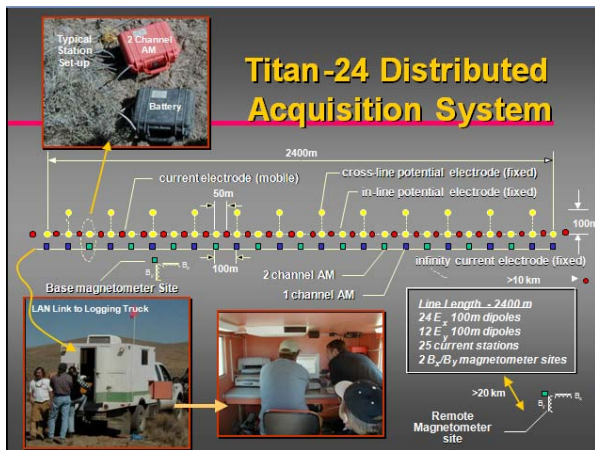


Figure 2: Example of an Array Type MT Acquisition System

Inversion Methodologies

Interpretation of the MT data is performed using the maps of true resistivity of the subsurface. Inversion algorithms in one-dimension (1-D), two-dimension (2-D), and three-dimension (3-D) are used to invert the apparent resistivity and phase data in to the maps of true resistivity of the subsurface. A simple layered subsurface structure generally can adequately be reproduced using the 1-D inversion. In the case of more complex 2-D or 3-D structures, the MT response will be affected by lateral variations in resistivity. Consequently, a 2-D or 3-D inversion algorithm is required to allow the lateral resistivity variations.

In 1-D earth assumption, the 1-D inversion of the MT data produces a resistivity-depth profile for each MT site. The results represent a first order approximation of the resistivity variations with depth using a layered-earth model. Often these inversion results are presented in pseudo-section form as "stitched" 1-D inversion sections.

If there are lateral variations in the resistivity of the subsurface along one direction only (perpendicular to the strike) then a 2-D inversion and interpretation is required. A cross-section of the true resistivity variations perpendicular to the assumed strike direction is created in the 2-D inversion and is used in interpretation.

For more complex geological structures a 3-D inversion is essential to adequately describe the resistivity variation of the subsurface. This is usually the case when mapping the geological settings hosting a geothermal system. In this case no simplifying assumption is made in terms of property of the MT data and dimensionality of the underlying subsurface. In highly heterogeneous environments MT phase data often exhibit an out-of-phase (phase-wrap) behaviour; caused by the complexity of the current paths in the subsurface. Modelling of these data is essential in order to resolve the heterogeneity of the subsurface. This kind of data, however, cannot be modelled using

1-D and 2-D inversions and the data must be mitigated or removed before the inversion. On the contrary, the 3-D inversion uses impedance data and is capable to handle this type of data; making the inversion a robust tool to produce a realistic representation of the subsurface.

In this discussion we contrast the differences between not only the 1-D, 2-D and 3-D inversions but also the effect of variations in MT field sample intervals and spacing on the effectiveness of the various inversion methods on the ability to discern and characterize geothermal reservoirs.

References

- Baars, R.M., Owens, L., Tobin, H., Norman, D., Cumming, W., and Hill, G., 2006, Exploration and targeting of the Socorro, New Mexico direct use geothermal exploration well, a GRED III Project: Proceedings, Thirty-First Workshop on Geothermal Reservoir Engineering, Stanford University, Stanford, California, January 30-February 1, 2006, SGP-TR-179.
- Bahr, K., and Simpson, F., 2005, Practical Magnetotellurics, Cambridge University Press.
- Brophy, P., 2007, A brief classification of geothermal systems: Geophysical Techniques in Geothermal Exploration Workshop, GRC Annual Meeting, 2007, Sparks, Nevada.
- Constable, S.C., Parker, R.L., and Constable, C.G., 1987. Occam's inversion - A practical algorithm for generating smooth models from electromagnetic sounding data. *Geophysics*, 52 (3), 289-300.
- de Lugao, P.P., and Wannamaker, P.E., 1996. Calculating the two-dimensional magnetotelluric Jacobian in finite elements using reciprocity. *Geophysical Journal International*, 127, 806-810.
- Marquardt, D.W., 1963. An algorithm for least-squares estimation of non-linear parameters. *J. Sot. Ind. Appl. Math.*, 11, 431-441.
- Nabighian, M.N., 1987. *Electromagnetic Methods in Applied Geophysics, Volume 2: Application (Parts A and B)*. Society of Exploration Geophysicists (SEG), Tulsa.
- Orange, A.S., 1989. Magnetotelluric exploration for hydrocarbons. *Proceedings of the IEEE*, 77, 287-317.
- Rodi, W., and Mackie, R.L., 2001. Nonlinear conjugate gradients algorithm for 2D magnetotelluric inversions. *Geophysics*, 66, 174-187.
- Siripunvaraporn, W., Egbert, G., Lenbury, Y., and Uyeshima, M., 2005. *Three-Dimensional Magnetotelluric: Data Space Method*. *Physics of the Earth and Planetary Interiors*, 150, 3-14.

Ussher, G., Harvey, C., Johnstone, R., Anderson, E., 2000, Understanding the resistivities observed in geothermal systems: Proceedings World Geothermal Congress 2000, Kyushu-Tohoku, Japan, May 28-June 10, 2000, p.1915-1920.

Vozoff, K., 1972. The Magnetotelluric method in the Exploration of Sedimentary basins. *Geophysics*, 37, 98-141.

Wannamaker, P.E., Stodt, J.A., and Rijo, L., 1987. A stable finite-element solution for two-dimensional magnetotelluric modeling. *Geophysical Journal of the Royal Astronomical Society*, 88, 277-296.

Wight, D.E., 1987. MT/EMAP Data Interchange Standard, Revision 1.0. Society of Exploration Geophysicists (SEG). (Document available at the SEG web site: www.seg.org).

Hutton Sandstone – a viable geothermal development

David Jenson*, Kerry Parker, Ron Palmer, Bertus de Graaf
 Panax Geothermal Ltd. PO Box 2142, Milton, Qld 4064
 *Corresponding author: djenson@panaxgeothermal.com.au

Panax Geothermal Limited (Panax) holds four Geothermal Exploration Licences (GEL's) in the north east of South Australia, namely GEL's 220, 221, 281 and 502. These licences overlap the Great Artesian Basin and in particular the Hutton Sandstone ("Hutton"), a known prolific reservoir. It has been demonstrated in existing wells and extrapolated using seismic data that the Hutton are recognized as a very porous and permeable aquifer and can be found at depths greater than 2,000m and temperatures of up to 145 °C. Reviewing core samples in the region suggests that there is a high likelihood for transmissibility up to 90-100 Dm.

The Hutton Project is based on producing an initial artesian flow of hot water sufficient to generate about 1 MWe. Although greater flows could be produced, either by artesian flow or by pumping, capable of generating up to 5-6 MWe per production well, a smaller development is more appropriate whilst the market evolves. Initially, the focus is on replacing diesel or gas generation in the local oil fields, small settlements and pastoral leases.

This study is based on small scale generation based on multiple (between 2 and 5) proprietary PureCycle 280kW units (580kW – 1400kW gross power output) receiving flows of artesian hot water between 135 and 145 °C from a single 150mm nominal diameter well. The maximum flow that may be required is about 51 kg/s which is less than half of the natural artesian flow that could be expected.

Geothermal potential of Panax's Hutton Sandstone project licences

Panax Geothermal Limited (Panax) holds four Geothermal Exploration Licences (GEL's) in the Cooper Basin region, north east of South Australia, see Figure 1. GEL's 220 and 221 are in the Nappamerri Trough and GEL's 281 and part of 502 are in the Patchawarra Trough. Both areas are covered by the hydrogeological Great Artesian Basin.

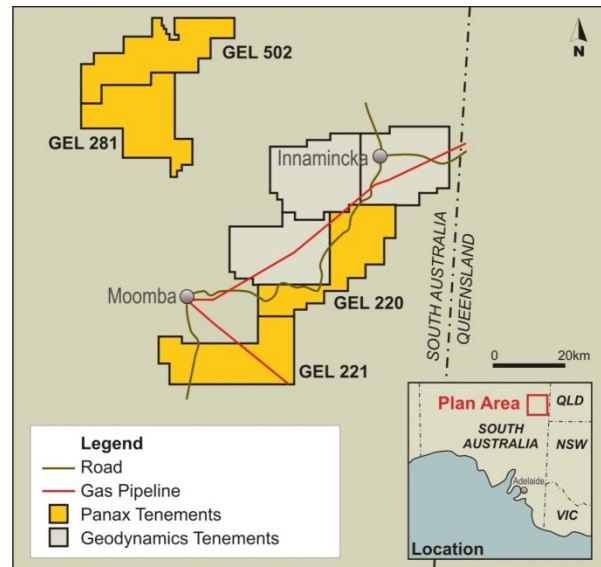


Figure 1. Panax's geothermal licences located in NE South Australia. All four licences are in the hydro-geological Great Artesian Basin

Beardsmore (2009) assessed GEL 281 for its geothermal potential and determined a "Measured Geothermal Resource" of 11,000PJ complemented by an additional 30,000 PJ of "Indicated Geothermal Resource", see table below. This resource classification was in accordance with the Australian Code for Reporting of Exploration Results, Geothermal Resources and Geothermal Reserves, 2008 edition.

The ability to positively assess the significant geothermal resource potential is due to the long history of petroleum exploration with numerous wells and seismic surveys (Figure 2).

This highly encouraging resource classification, the third in Australia and second resource classification of a Hot Sedimentary Aquifer confirmed the high potential of geothermal energy development in sedimentary basins.

Table 1. Geothermal Resource, GEL281

Measured [PJ]	Indicated [PJ]	Inferred [PJ]	Total [PJ]
11,000	30,000	0	41,000

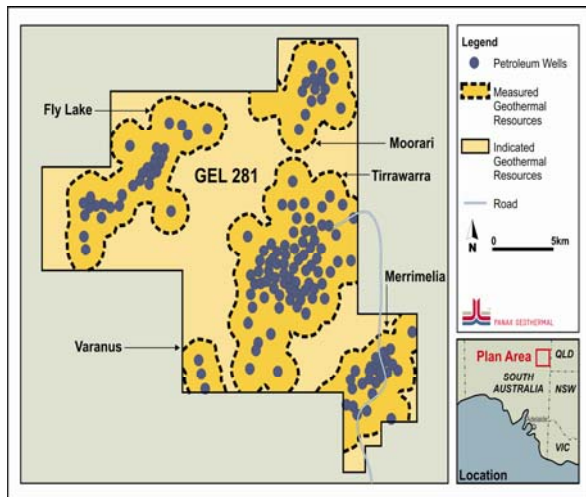


Figure 2. GEL281 - outlines of Measured Geothermal Resources showing existing petroleum wells.

In the following Geothermal Systems Assessment, Cooper et al. (2009) found that the Hutton Sandstone has potential for low enthalpy geothermal energy generation. Cooper points out that the temperature modeling may have been understating the temperature as the data points at this stratigraphic level are sparse and that it is possible that advective (lateral) heat flow may occur that has not been included in the modelling.

Cooper's positive assessment of the Great Artesian Basin in GELs 220 and 221 confirmed together with earlier work over GEL 281 that Panax's GEL's in the region represents a large area with a significant geothermal resource

Panax commissioned Hot Dry Rocks Pty Ltd ("HDRPL") to review depth and temperature potential of GEL's 220, 221 and 281 (GEL 502 was not granted at the time of this review). Walsh (2009A) found in this brief review that preliminary

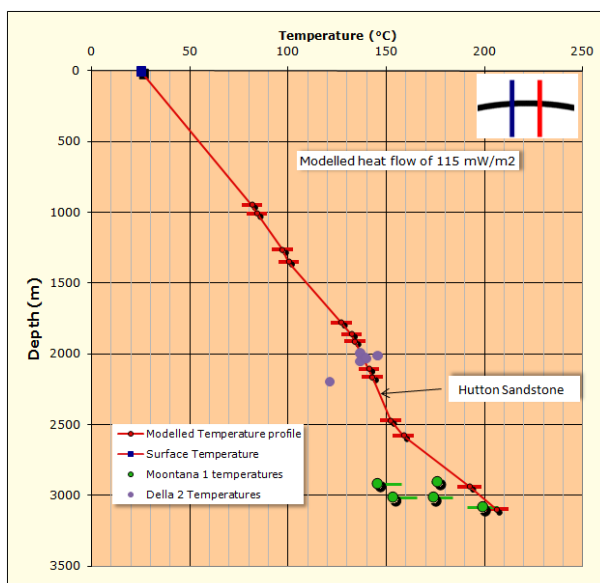


Figure 3. Preliminary 1D temperature prediction for Hutton Sandstone based on temperature data from nearby wells

temperature models using 'best fit' indicated that the temperature at the top of the Hutton where it is at its deepest was estimated to be in the order of 142°C (see Figure ?) and that the top of Hutton Sandstone in the area of maximum thickness is interpreted to lie between 2,150 and 2,200m depth.

Walsh (2009B), finally, also assessed permeability assessments from 246 core samples collected from 12 petroleum wells in a depth range of 1,700m to 2,000m in the area and concluded that the permeability appeared to be high, with the bulk of the values in the encouraging 100 to 2,000 mD region.

Interestingly, though data presented by Walsh showed a wide range of permeabilities, they do indicate that even a less thick horizon of the Hutton Sandstone has the ability to sustain reasonable flow rates.

Concluding, the Hutton sandstone in GEL 220 is modeled at a depth in excess of 2,000m and with a temperature at its top of 142 deg C. Permeability estimates from 12 wells with porosity and permeability estimates of the Hutton Sandstone indicate a bi-modal population with the larger population in the vicinity of 50mD to 2,000mD. If a conservative value of, say, 250mD is chosen assuming not all parts are productive, then at the estimated thickness of Hutton Sandstone of 380m, there is a potential of a reservoir with a transmissivity of 90-100 Dm.

These highly encouraging estimates suggest that the Hutton sandstone represents a strong prospect for developing a low risk hot sedimentary aquifer, geothermal energy.

Great Artesian Basin and Hutton Sandstone

The Eromanga basin was deposited as an un-interrupted sequence from the Early Jurassic to Mid-Late Cretaceous, see Figure below. The basal units are mainly non-marine to marginal marine, however, marine influences dominate the silts and mudstones of the Marree Subgroup. Non-marine sandstones were deposited in the final stages (Winton Formation). Of petroleum and geothermal interest are the terrestrial sandstones of the Hutton, Namur, and Cadna-owie Formations. These units, in particular the Cadna-owie Formation, constitute much of the Great Artesian Basin.

AGE		ROCK UNIT	GROUP		
SYSTEM	SERIES				
QUAT.		Millyera Formation and equivalent	LAKE EYRE BASIN		
TERTIARY		Yandruwantha Sand			
		Namba Formation			
		Eyre Formation			
CRETACEOUS	Late	Mount Howie Sandstone	MAREE SUBGROUP		
		Winton Formation			
	Early			Mackunda Formation	
				Oodnadatta Formation	
				Coorikiana Sst.	
				Buildog Shale	
				Wallumbilla Formation	
	JURASSIC	Late		Cadna-owie Formation	EROMANGA BASIN
				Murta Formation	
		Middle		Namur Sandstone	
Westbourne Formation					
Adori Sandstone					
Early		Hutton Sandstone			
		Poolowanna Formation			

Figure 4. General stratigraphy of the Eromanga and Lake Eyre Basin sequences in the Cooper Basin (Gravestock et al, 1998).

The Jurassic Hutton Sandstone is a sandstone-dominated unit that has been interpreted to have been deposited in a continent-scale, braided-stream environment, and to have been unconfined across a broad alluvial plain extending over much of Queensland and South Australia. The Canterbury Plain in New Zealand is considered as a close modern analogue. The Hutton Sandstone is well-known as a regional aquifer in a number of fields in both South Australia and Queensland.

Habermehl (reference?) notes that the Great Artesian Basin is a well known aquifer with some 4,700 artesian water bores drilled in to it. Most of these artesian wells tap in to the Cadna-owie aquifer, the uppermost artesian aquifer of this multi-layered sequence. Groundwater in the Cadna-owie aquifer is of good quality, containing between 500mg/l to 1,000mg/l total dissolved solids. It is suitable for domestic, town-water

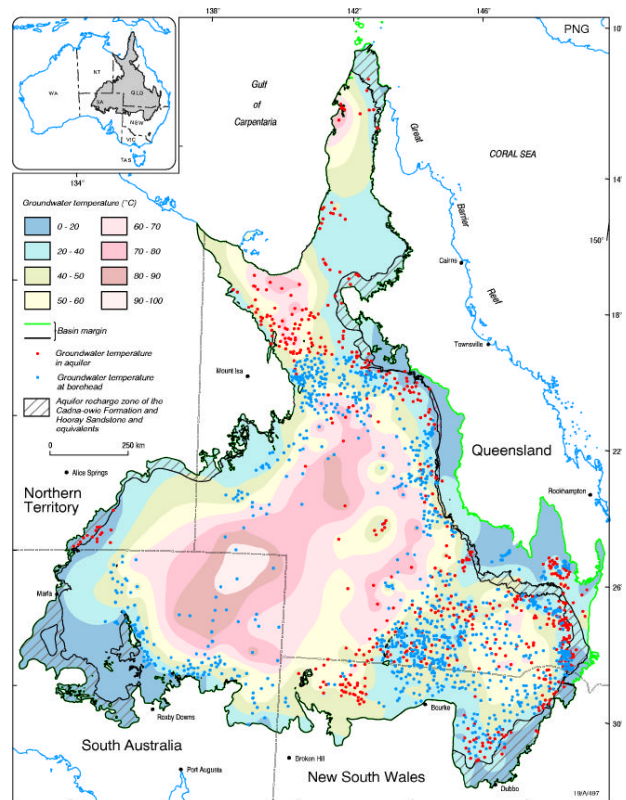


Figure 5. GAB extent and ground water temperatures (after Habermehl, 2001).

supply, as is the case at Birdsville, as well as for stock use. Ground temperatures at the well heads range from 30deg C to 100deg C. Groundwater temperatures from 1,880 water wells tapping in to the Cadna-owie aquifer, above the deeper Hutton Sandstone, from are presented in Figure 5.

Geothermal development

The Hutton Project aims to produce an artesian flow of hot water sufficient to generate about 1 MWe. Although greater flows could be produced, either by artesian flow or by pumping, capable of generating up to 5MWe per production well, sufficient demand to justify such a development does not exist and so the focus is on smaller plants to replace diesel or gas generation in the local oil fields, small settlements and pastoral leases.

Artesian flows at adequate temperature can be produced from the Hutton Sandstone at well depths down to 2,500m. Artesian pressures of at least 10bar are expected which will be easily sufficient for a hot water flow of about 30 kg/s which will be required for 1 MWe Geothermal Power Plant.

It is intended that the cooled exhaust water will be reinjected back into the same formation. For the small flows that are required, it is anticipated that no or minimal reinjection pumping power will be required. ie if pressures can be maintained in a

closed circuit, it is expected that a thermosiphon will be established.

The Hutton Sandstone can be found at suitable depths over relatively wide areas of the GELs and so there is a possibility that a number of stand-alone plants based on a production/reinjection well pair could be developed.

The development scenarios considered are based on the use of two to five PureCycle® units as marketed by Pratt and Whitney Power Systems. These units have a nominal 280 kW gross capacity and are designed to be water cooled. It is believed that water cooling, as opposed to air cooling will be required because of the high ambient dry bulb temperatures encountered in the region.

In order for a small project to be economic, it will be necessary to adopt water well drilling practices as opposed petroleum drilling practices.

A 150mm diameter x 1,500m deep water well drilled at Clifton Hills (outside the license area) flowed at approximately 155 kg/s under artesian pressure and had an overall cost of less than \$1m. It is believed that similar technology could be utilized to drill to depths of 2-2500m for an overall cost of less than \$2m per well.

Location and Infrastructure

GEL 220 has been estimated to be host the hottest Hutton Sandstone in Panax’s geothermal licence portfolio. A strong candidate for the Hutton Sandstone Geothermal Well is the south western part of GEL 220, as indicated in Figure 6. This location is in a large area of deep Hutton, close to a road and outside the Innamincka Regional Reserve. There are Native Title agreements covering this area as is the case for all of Panax’s geothermal licences in Cooper Basin.

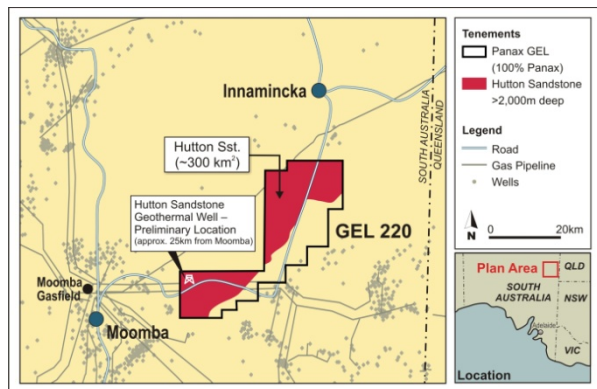


Figure 6: GEL 220 (black outline) with the areas where Hutton Sandstone is interpreted from regional data to be deeper than 2000m (red areas). The estimate of the total area of Hutton Sandstone in excess of 2000 m is about 300 km2. Light purple indicate pipe lines with Moomba gas Plant to the west of GEL 220.

Potential market

Although extensive research has not been completed into available electrical loads that could be satisfied by geothermal electricity produced from the Hutton Sandstone, the project location is about half way between the townships of Moomba and Innamincka, where it is known that there is a significant reliance on diesel and gas fired generation. In addition grazing homesteads are also known to rely on diesel generation. Finally, there are several gas plants and pipeline nodes requiring energy, also representing a small local market

Although the gas plants and pipeline node points are known, maps of these have been removed from public access to prevent them from being targets of a terrorist act. However, studying the pipeline network in Figure 7, one can indirectly

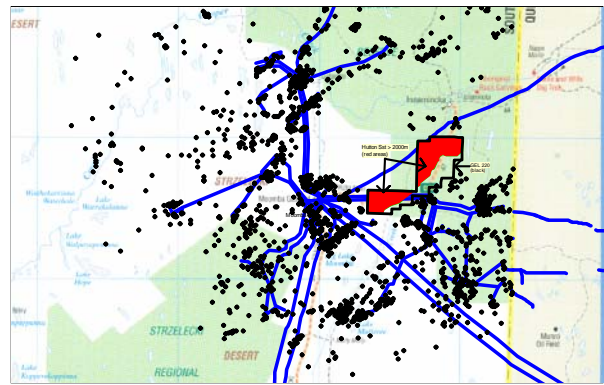


Figure 7. Pipelines in Cooper Basin. Gas production plants are inferred at end points of pipelines (blue) and nodes at intersection of pipelines .

locate gas plants and pipeline nodes, representing small local electricity markets. Innamincka and Moomba townships are also annotated in this figure. It is interesting to note the huge number of wells that have been drilled in to Cooper Basin, represented by black dots on this map. Each of these wells were preceded by intense studies of seismic, 2D and more recently also 3D seismic. These data, available free of charge of PIRSA, represent a huge investment and to Panax, a significant advantage in assessing the Hutton Sandstone, as has been reviewed in previous sections.

It is believed that a mini 3 phase power grid could be established to which users in the vicinity would have access, either with a 3 phase connection or a Single Wire Earth Return(WER)line.

Development Time Frame

It is envisaged that a small scale plant will be able to be brought on line twelve to eighteen months after the spudding of the production well.

Australian Geothermal Conference 2010

PureCycle[®] units are built on a production line in the US and are shipped as a fully assembled skid and therefore a minimum amount of site work is required. A separate cooling system will need to be engineered and installed.

The production and injection wells are each estimated to take about 3 weeks to drill.

The overall project schedule is estimated to be about 24 months.

Cost estimates and assumptions

Capital costs have been estimated from quotations received from plant suppliers and drilling companies and from detailed in-house estimates for balance of plant and other infrastructure requirements.

In respect of operating costs, a small plant of the type initially envisaged will not be permanently manned. Remote or automatic operation will be required with routine maintenance performed on an as required basis. PureCycle plants are very simple with plant overhauls required on a semi-annual or longer interval basis.

Modelling results

The investigation of various engineering scenarios for using the Hutton Sandstones have focused on smaller scale development (500kW – 1.5 MW) which could be used to replace existing diesel or gas fired generation in the adjacent oil fields, small settlements and pastoral leases.

Even smaller sub-optimal developments can still be very attractive as small package plant can be used and parasitic pumping power is much reduced because the artesian pressure together with thermo siphon effects negates the need for production or reinjection pumps.

PureCycle units as marketed by Pratt & Whitney Power Systems could be ideal for this application. These are package units with a nominal rating of 280 kW gross and multiple units could be installed or added to match electricity demand.

Slim (150mm diameter), Deep (1,500m) water wells drilled into the GAB have yielded significant artesian flow rates (155 l/s) at temperatures of about 100 deg C at surface. These wells can be drilled very economically (<\$1m) and so the concept of using similar techniques to drill similar wells to depths of 2,000-2,500m in the Hutton Sandstone have been investigated. It is believed that such wells targeting temperatures from 130 deg C to 145 deg C could be drilled for less than \$2m which would make small scale development economic when compared with diesel generation

that is currently used in the local oilfields, small settlements and pastoral leases.

Results of the modelling indicate that although such wells could produce the order of 5MW if developed to their full potential, smaller scale developments (500kw – 1.5MW) can still be economic. Power costs of \$100 – \$125/MW/hr are feasible which compares very favourably with diesel generation where costs are as high as \$250/MW/hr.

Conclusions

The Hutton Project represents an outstanding opportunity for the development of small scale geothermal plants utilizing hot artesian water flows from the deep areas Hutton Sandstone Aquifer in the Great Artesian Basin.

A larger scale project that utilizes the full potential of this artesian flow, that has not been considered in this Pre-Feasibility Study would probably have the potential to be the most economical geothermal development opportunity available in Australia and would compete with open cycle gas generation.

For small scale developments, the price per MWh compares very favourably with the cost of existing diesel generation.

The key to the success of the project is finding matching “base” loads that are able to fully utilize the generation potential available.

References

Cooper, G., Waining B., Mortimer, L. And Pollington, N., “Geothermal System Assessment of GELs 220 and 221, Cooper Basin, South Australia. HDRPL report, September, 2009.

Beardsmore (2009) Tirrawarra Geothermal Play – Statement of Geothermal Resources prepared for Panax Geothermal Ltd

(A) Walsh, D. “Hutton sandstone potential”, memo, HDRPL, Dec 2009.

(B) Walsh, D., “Additional notes on the Hutton Sandstone”. Note for the record, HDRPL, Dec 2009.

Habermehl, M. A., 2001. Wire-Line Logged Waterbores in the Great Artesian Basin, Australia - Digital Data of Logs and Waterbore Data Acquired by AGSO. Bureau of Rural Sciences publication, Canberra, Australia; also: Australian Geological Survey Organisation, Bulletin 245

Gravestock, D.I., Hibburt, J.E., Drexel, J.F.,

"Petroleum geology of South Australia, Volume 4:
Cooper Basin, Department of Primary Industries
and Resources, South Australia, Report book,
98/9. 1998.

Investment in common-use network infrastructure to trigger incremental expansion in geothermal energy generating capital stock

Ashok A. Kaniyal^{1,3*}, Jonathan J. Pincus², Graham (Gus) J. Nathan^{1,3}

¹ School of Mechanical Engineering, The University of Adelaide SA 5005

² School of Economics, The University of Adelaide SA 5005

³ Centre for Energy Technology, The University of Adelaide SA 5005

*Corresponding Author: Ashok A. Kaniyal, ashok.kaniyal@adelaide.edu.au

This paper analyses the potential of a novel approach to avoid the cost of expensive transmission infrastructure in connecting remote geothermal power suppliers to market through a community of data centres. A strategy for investment in a common-use facility to trigger incremental growth in a complementary commercial alliance is presented. The commercial alliance consists of investors in the 'common-use' fibre-optic cable data network, a community of data centres, and geothermal energy resources.

A real options approach to capital investment decision making is used to define the conditions under which investment in the common-use facility (which in economics is a 'local public good'), will be commercially justifiable. Excess capacity in the fibre-optic network resource is what gives it the attributes of a 'local public good'. A critical assessment shows that investment in such infrastructure could play a significant role in triggering the initial and later additions to installed geothermal energy capital stock, to generate and supply power to a network of data centres in a remote area. The infrastructure needs of data centres are chosen for this assessment because these facilities can be collocated with the geothermal resource, and their energy consumption is well suited to a demonstration-scale plant.

The real options analysis of resource allocation in this hypothetical commercial setting is underpinned by the stochastic representation of the future growth in demand for energy from a network of data centres, in the micro-grid community described. The results from this analysis provide an understanding of the critical conditions under which investment in the fibre optic network resource could take place.

The real options approach is an appropriate tool to assess investment strategy in this context, because it incorporates uncertainty in consumer demand, and analyses the resultant flexibility in the timing of investment decisions. In contrast, the discounted cash flow method suggests that an investment decision is made only once, i.e. at the commencement of the discounting period.

Once a commercially justifiable investment pathway for the local public good is defined, a profile of incremental expansion in the installed

geothermal energy production capacity can be derived. This derivation provides an optimised time series profile of incremental expansion in capital stock, to satisfy the discrete units of stochastic demand for energy in this micro-grid setting. The benefits of this assessment thus lie in the ability to understand the likely time period over which significant economies of scale in generating capacity can be achieved. This henceforth enables a characterisation of the point at which investment in electricity grid infrastructure (or the like) may be justified. The process associated with this stochastic approach to analysing investment decisions enables the consideration of the systematic risks in this much larger but end-goal investment horizon.

Finally the study presents public policy recommendations regarding State involvement in establishing capacity in this network resource, to assist the development of the necessary economies of scale in geothermal energy production over time.

Keywords: Real options theory, network infrastructure, local public good, geothermal energy.

Reference

Dixit, A., Pindyck, R.S., 1994. Investment under uncertainty. Princeton University Press, Princeton NJ.

Ultra deep drilling technologies for geothermal energy production

Dipl. Ing. Ivan Kočiš, PhD., Dipl. Ing. Tomáš Krištofič, Dipl. Ing. Igor Kočiš
Geothermal Anywhere
Bratislava, Slovak republic

Abstract

Substance of the presented research and development is the technology for realization of geothermal boreholes approximately 6 to 10 km deep. In such depths, rock temperature reaches 200°C to 400°C practically all over the world. In this depth, thermal capacity of 1 km³ is about 1017 J (when cooled down by 100°C); this is comparable with annual demand of Slovakia. With real consumption of approximately 20 to 40 MW the capacity of the same borehole would be sufficient for several hundreds of years. Deep geothermal energy is available anywhere, represents the most serious candidate for a base load 24/7 electricity production, there are no CO₂ emissions and is scalable according to the local needs. The main obstacle for utilization of the vast energy reserves is the price rising exponentially per 1 km of a borehole depth in present-day drilling technologies. Costs of such boreholes cannot be considered as a basis of repeated projects in most territories of the world. Thus, intense research and development of new deep drilling technologies is necessary.

There are more than 20 researched new drilling technologies, but none of them gave at present desired economic and technical parameters for 6-10 km depths. The technology must be compatible with extreme conditions at such depth (pressure up to 1000 bar and temperatures more than 400°C) and very hard rock like granite. Presented radically innovative concept of drilling and transport of material is protected by patents and being a basis of a know-how based upon innovative utilization of proven technologies. The method is suitable primarily for extreme pressure and temperature conditions, and has all pre-requisites to meet the basic requirement – linear price growth with borehole depth. The concept was first time publicly presented during Conference of the 6th EU Framework Programme project "Engine", aimed at ultra-deep geothermal energy and related research within future 7th Framework Program projects. The concept aroused considerable attention and interest in participation in future projects.

Keywords: Deep drilling, Bitless drilling, Non-contact drilling, Pulsed plasma drilling, EGS

Introduction

The renowned MIT (USA) study "The Future of Geothermal Energy – Impact of Enhanced Geothermal Systems (EGS) on the United States in the 21st Century" (2006) points out the essential importance of the developing an economical deep geothermal drilling technology. With current drilling technologies, drilling price below 3 km rises exponentially with depth. Thus, finding a drilling technology with which the drilling price rise would be approximately linear with increasing well depth is an important challenge.

In his presentation, Jefferson Tester, a co-author of this study, characterizes the key requirements on new fast and ultra-deep drilling technology as follows:

- the price of drilling rises linearly with depth,
- the possibility to make vertical or inclined boreholes up to 20 km deep,
- casing formed on site in the well.

There are under way more than 20 research efforts solving innovative drilling technology such as: laser, spallation, plasma, electron beam, pellets, enhanced rotary, electric spark and discharge, electric arc, water jet erosion, ultrasonic, chemical, induction, nuclear, forced flame explosive, turbine, high frequency, microwave, heating/cooling stress, electric current and several other.

No one from these until now proved to be effective in severe conditions and no one is solving the problem in complex including the energy and material transport from 6 to 10 km technically and economically. We selected drilling approach based on integration of pulsed electrical plasma with water jet assisted processes.

What is different from current drilling technologies?

Process of rock disintegration is the most important activity when drilling ultra-deep borehole, but not the only one contributing to the exponential price rise. Therefore a completely new approach should be considered. That is also substantial difference between GA's drilling concept and mentioned drilling technologies.

GA drilling approach is based on integration of pulsed electrically generated plasma with water jet assisted processes. Advantages of the GA's technology are as follows:

1. Controllability of the process of disintegration and efficient generation of media for disintegration
2. Pulsed mode of the media towards the disintegrating rock
3. High heat flow
4. Pulsed power technologies - Time compression
5. Optimized cuttings
6. Cuttings washout using thermo lift and water jet interaction
7. Casing while drilling – vitrified rock
8. Dynamic temperature stress on the rock
9. Control and sensoric system in extreme conditions
10. Restart of drilling process in extreme high pressure conditions

We identified nine different physical processes used for disintegration of the rock. Under research is a synergic exploitation of selected processes, also using supercritical fluids.

Total energy costs of drilling represent only a fraction of the total cost and our approach is to melt the rock with a safe temperature tolerance.

What is different compared to spallation technology?

Spallation process is the closest technology, but has several issues and drawbacks. We can mention small temperature interval in which spallation process takes place, dependence of the interval from rocks and non-effective process of spallation in some types of rock.

Total energy costs of drilling represent only a fraction of the total cost. Our approach is to melt the rock and manage cuttings with optimized size. The presented drilling technology is based on a set of research project, development of critical aggregates, proving correctness of the concept and preparation for the industrial development stage which should serve the application aspect. In cooperation with several Universities and Academy of Sciences teams are solved the difficult functional and material problems for extreme in-field conditions. The purpose of the project is to research all critical parts up to the level of functional laboratory samples. Sufficient background data for further industrial development should be provided. On the basis of the results obtained in technological parts of the solution, the project is assumed to give technological proof of the whole concept.

How is that possible?

The innovation concept is able to integrate the proven technologies compatible with high temperatures and pressures using the

combination of electrical energy source for both – producing the needed form of the energy and for enabling the thermal lift buoyancy effect for a cutting transport.

The rock crushing technologies will be used in a synergy of electrical discharge, pulsed plasma and water jet in appropriate alternatives which will be the subject of research and experimental work. This radical innovative method avoids the inherent limitations of conventional rotary drilling and material transport.

Complexity of the problem, harsh environment in which the targeted technology shall work, and the radical innovation concept requires gradual approach to the research, development and realization of the whole system.

Ultra deep drilling technology - geothermal energy revolution enabler

The realization of the Ultra deep drilling technology will open the way to thermal energy resources to be used for production of electric energy without greenhouse gas emissions and with zero operation costs of fuel. The current status of electric energy production is based upon fossil fuel, it is not compatible with reduction of emissions, and, moreover, is not resistant against increase of prices of crude oil and gas in the world, and of those of the nuclear fuel, which are derived from them.

Deep geothermal systems open the way to replacing coal and gas capacities by geothermal capacities within the future 20 years.

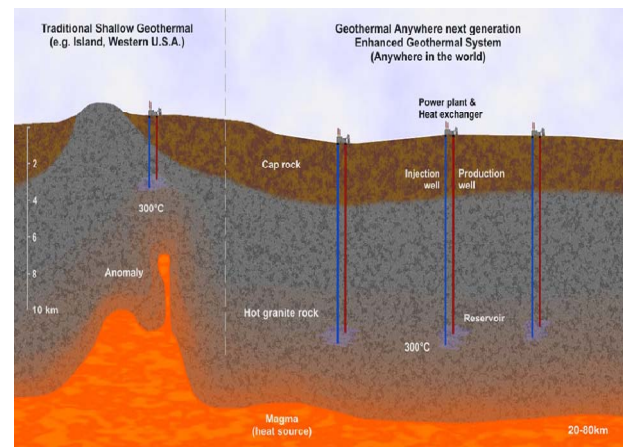


Figure 1: Extra and ordinary geothermal conditions – difference brings the ultra-deep drilling technology.

Such resource of the energy will adequately satisfy the demand of energy, which has the following properties:

- It is local, stable, scalable upon need, with no losses caused by long distance transfer.
- It does not produce any emissions, and is safe.

- No supply of energy carriers is needed, "fuel" costs are zero and unaffected by world prices variation, crisis developments and geopolitical situations.
- Creates numerous secondary applications, primarily for small and medium enterprises; moreover, creation of job opportunities is enhanced.

Conclusion

The revolutionary patented concept of the ultra-deep drilling and transport of crushed rock material upwards leads to new implementation possibilities.

It is a radical abandonment of the classic drilling technologies with connected tubes in long strings with the inefficient energy transport to the drilling site at the bottom of the well and complicated, inefficient pumping of the crushed material to the surface.

This new drilling technology is a result of the long time effort to solve the problem of the exponentially growing price in relation to the borehole depth and thus enabling the real exploitation of the geothermal energy for the electrical power generation.

References

Tester, Jefferson W.; et. al. (2006), The Future of Geothermal Energy, Impact of Enhanced Geothermal Systems (EGS) on the United States in the 21st Century: ISBN 0-615-13438-6, http://geothermal.inel.gov/publications/future_of_geothermal_energy.pdf

Jefferson Tester et al., US Pat 5771984, "Continuous drilling of vertical boreholes by thermal processes: rock spallation and fusion"

Kobayashi et al., US Pat 6870128, "LASER BORING METHOD AND SYSTEM"

Hirotohi et al., 1999, "Pulsed Electric Breakdown and Destruction of Granite", published in Jpn. J. Appl. Phys. Vol.38 (1999), 6502-6505

Dipl. Ing. Ivan Kočíš, PhD., Dipl. Ing. Tomáš Krištofič, Ultra deep drilling technologies for geothermal energy production, International Geothermal Days Conference, May 2009, Casta Papiernicka, Slovakia

A Preliminary Study on Na-Cl-H₂O-Rock Interactions of the Hot Fractured Rock Geothermal System in Cooper Basin, South Australia

Gideon B. Kuncoro¹, Yung Ngothai^{1*}, Brian O'Neill¹, Allan Pring², Joël Brugger²

¹ The University of Adelaide, School of Chemical Engineering, North Terrace, Adelaide, SA, 5000

² South Australian Museum, North Terrace, Adelaide, SA, 5000

*Corresponding author: yung.ngothai@adelaide.edu.au

A preliminary study was undertaken to observe the fluid-rock interaction in Na-Cl-H₂O system. Samples of drill cuttings from a borehole 5 km deep from Habanero 3 well were contacted with 250 ppm sodium chloride solution in a thermosyphon induced loop reactor at 250°C and 40-50 bar. The experiments were carried out in a Titanium flow through cell for 1, 7, and 28 days at 250°C and 40 bars). The fluid was replaced every 24 hours in order to accelerate the dilution rate to observe which minerals are reactive (soluble) and to mimic a condition which uses fresh water or treated water from a precipitation tank that is reinjected to the fracture. Fluid and rock samples were analysed prior to, and after circulation to observe the dissolved minerals and mineralogy.

Water analysis was performed using ICP-MS, and rock analyses were conducted using an optical microscope, SEM and XRD. The experimental results indicated that mineral dissolution was more rapid in the early stages of the experiment. This may be a consequence of the dissolution of finer rock particles. SEM observations showed evidence of etching of the mineral surfaces consistent with partial dissolution. XRD results indicated that the feldspars (NaAlSi₃O₈ and KAlSi₃O₈) in the rock had completely dissolved and small amount of quartz remained. ICP-MS analysis on the water sample confirmed that some mineral dissolution has occurred. The concentrations of the elements increased with time.

Experiment running for 14 days is currently being undertaken and the results will be used to complement this study. Future work will involve reaction path modelling to predict mineral precipitation.

Keywords: hot fractured rock, fluid-rock interaction, Na-Cl-H₂O system, geothermal, Cooper Basin, Habanero, thermosyphon

Introduction

A study of the interactions between rock and circulating fluid is essential to determine the chemical changes and mineral alteration of a geothermal system. This study was undertaken to observe mineral dissolution due to the interaction with Na-Cl-H₂O system. Existing reservoir granites are currently in equilibrium with the surrounding ground water. The injection of fresh water to extract thermal energy from the host rock

will alter the ground water chemistry and thus the fluid-rock equilibrium. While recirculating the brine, partial chemical dissolution or mineral species alteration may occur. This may potentially increase the dissolved solids such as silica and other metals in the water. These dissolution products of the components have different equilibria, which will be a function of temperature and pressure, thus precipitation or scaling of pipe work and closure of fractures in the granite body are possible. The saturation of metals in fluid is volume-dependent, where very small volumes of fluid may require slight under-cooling before precipitation occurs. Clearly, characterization of fluid geochemistry is important in the evaluation of the performance of geothermal systems (Grigsby et al., 1989). Moreover, understanding the chemical interactions due to the injection of fluid into hot granite is crucial for problems concerning clogging by precipitation and heat loss caused by dissolution (Azaroual and Fouillac, 1997).

The study of fluid-rock interaction will allow determination of mineral alteration and dissolution of minerals due to the circulating water. To date, there are a number of geochemical modelling codes therefore thermodynamic data bases are available and improved to predict equilibrium conditions and dissolution-precipitation rates (such as EQ3/6, TOUGH-REACT, SOLVEQ-CHILLER, SOLMINEQ, GWB, etc). However, fundamental processes associated with mineral dissolution and precipitation, pressure-temperature gradient remain poorly understood (Marks et al., 2010). Unfortunately, it is impossible to generalize the actual field experience of mineral deposition in geothermal systems into one consistent theory due to the vast chemical and operational variation between field sites (Robinson, 1982). Therefore, although there have been a number of studies on fluid-rock interactions for different geothermal sites (Rimstidt and Barnes, 1980; Robinson, 1982; Posey-Dowty et al., 1986; Savage et al., 1987; Grigsby et al., 1989; Savage et al., 1992; Azaroual and Fouillac, 1997; Yangisawa et al., 2005; Tarcan et al., 2005; Castro et al., 2006; Marks et al., 2010), and studies of rock-chloride solutions (Ellis, 1968; Dove and Crerar, 1990; Icenhower and Dowe, 2000) these are probably not directly applicable to the hot granite-based geothermal systems in the Cooper Basin.

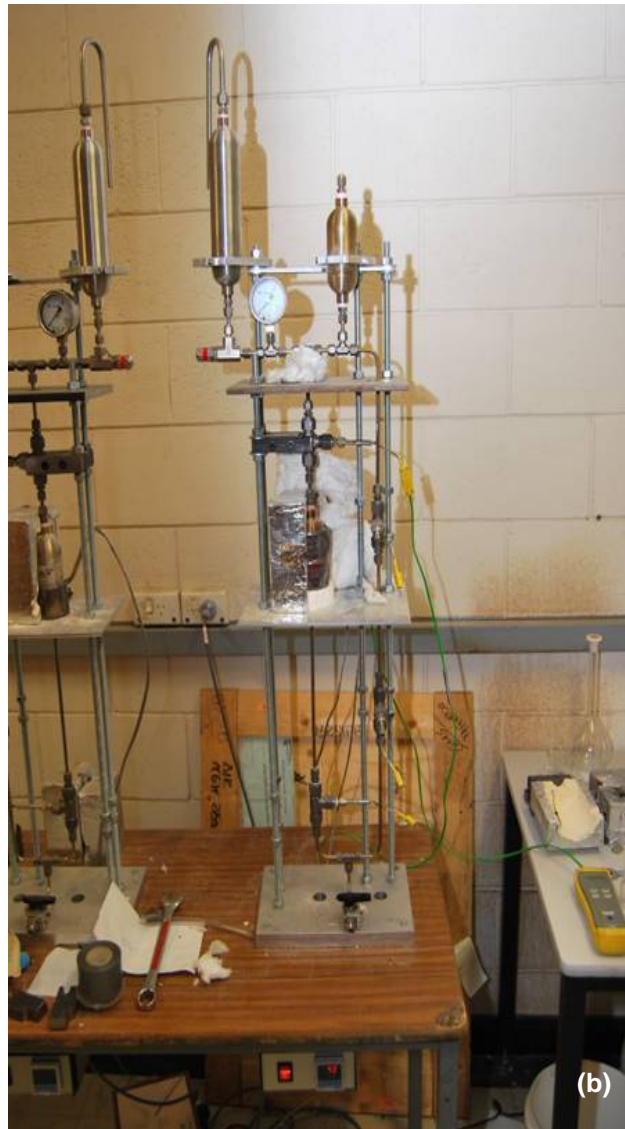
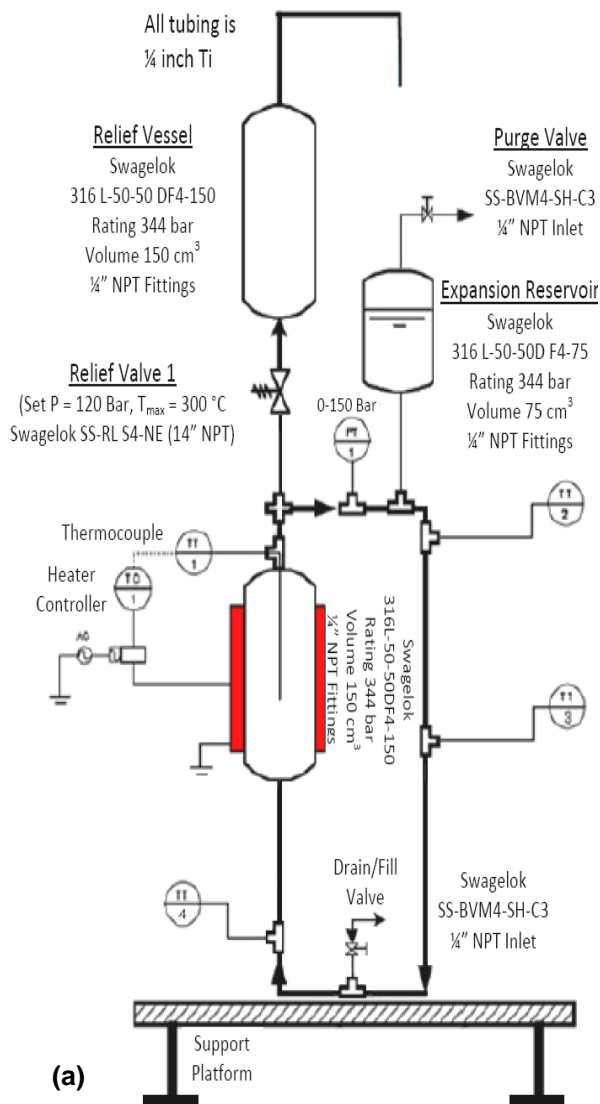


Figure 1: (a) Diagram of the flow through cell (b) Photograph of the geothermal flow through cell

Experimental

Samples of drill cuttings from the Habanero 3 well were provided by Geodynamics. The samples were ultrasonically cleaned and analysed using the scanning electron microscope (SEM) at the Adelaide Microscopy Centre to observe both surface and cross-sectional area. Powder X-ray diffraction (XRD) analysis was carried out by AMDEL to observe the mineralogy. A preliminary set of experiments to observe the fluid-rock interaction were performed in batch mode. The drill cutting was used as the rock sample. The rock sample was crushed and sieved to give 100 – 200 µm size fraction and approximately 0.7 grams of rock were used in each batch. The sample was enclosed in a pre-weighed wire basket (approx. 50 µm mesh size) made from stainless steel and placed in the sample holder of the cell. The cell was filled through a valve in the base of the cell with 250 ppm sodium chloride solution and 90 ml was drained from the cell to

allow for fluid expansion upon heating. The velocity of the thermosyphon circulating fluid is estimated to be approximately 0.1 m/s. The fluid-rock interaction periods were 1, 7, and 21 days. At conclusion of this interaction period, the rock sample was dried (105°C for 48 hours), cooled in a desiccator, and weighed to determine any weight loss.

The rock samples were analysed using SEM and XRD, and the water samples were stored and preserved with 4% w/w of 1M nitric acid until analysis by ICP-MS to identify the dissolved metals. The silica content was quantified using heteropoly blue method (HACH, 2009). Unfortunately, the anions were unable to be analysed since the concentrations of HCO_3^- and SO_4^{2-} in the sample are lower than the detection limit of the current analysis.

Results and Discussion

Preliminary results from the geothermal cell experiment illustrate that the dissolution of the

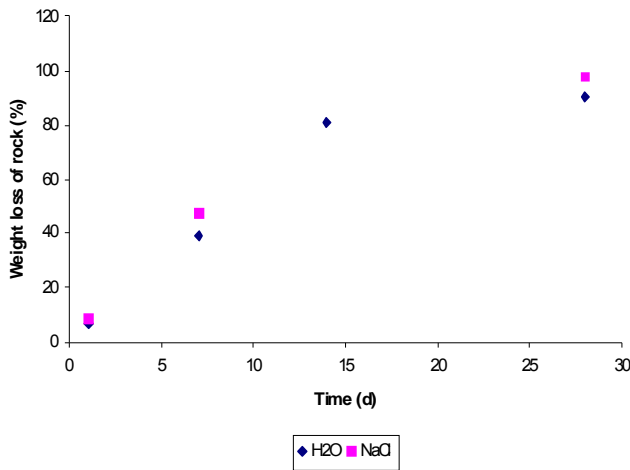


Figure 2: Change in weight loss of rock (% w/w) versus time

rock (% w/w) increases with time (Figure 2). It shows that the dissolution appears more rapid in the early stages of the experiment. This is probably due to the dissolution of the more reactive minerals (feldspars). It is seen that more minerals dissolved in the Na-Cl-H₂O system compared to pure water (reverse osmosis treated water). The presence of higher electrolyte concentration (e.g., Cl⁻) in Na-Cl-H₂O system increases the dissolution rate of some minerals such as quartz (Dove and Crerar, 1990). The latter stage of the experiment approached an equilibrium state. However the fluid is not necessarily saturated with minerals (feldspar), but due to the exhaustion of the soluble phase(s) and slower dissolution rate of the remaining phase(s). Note that the circulating fluid is replaced every 24 hours.

Rock Analysis

Mineralogical analysis was performed on the drill cuttings from Habanero 3 well using x-ray fluorescence (XRF) and x-ray diffraction (XRD). The major elements and their host minerals of the rock are quartz (SiO₂), albite (Na,Ca)AlSi₃O₈, and microcline (KAlSi₃O₈) (Pring, pers. comm. 2009). The XRF analysis was carried out by the School of Earth and Environmental Sciences, Adelaide University (Table 1). The XRD analysis was performed by AMDEL (given in %wt) and converted to mg for better understanding. The results show clearly that rapid dissolution has occurred. Silicon internal standard was added to observe any possible amorphous, unfortunately the amorphous content were unable to be quantified by Amdel. Hematite, magnetite, anatase, chlorite and goethite may be accessory minerals due to corrosion of the stainless steel reservoirs and the stainless steel wire basket used in the experiment.

SEM images of the surface particles were obtained using the secondary electron detector (SE) of the XL30 in Adelaide Microscopy. The

images are presented in Figure 3. The SEM images of the rock sample surfaces of feldspars before and after the experiments are shown in Figure 4. It can be seen that pitting has started to occur in 1 day circulation period. At the conclusion of 7 days circulation, the surface of feldspars experienced severe pitting and breakage. By the end of 28 days circulation, the feldspar has completely dissolved and some quartz and undissolved minerals remain.

Table 1 XRF analysis of the rock sample

Starting Sample	% Weight
SiO ₂	77.27
Al ₂ O ₃	10.62
Fe ₂ O ₃	1.46
MnO	0.08
MgO	0.09
CaO	0.60
Na ₂ O	2.54
K ₂ O	4.45
TiO ₂	0.07
P ₂ O ₅	0.01
SO ₃	0.15
LOI	2.10
Total	99.44

Table 2 XRD analysis of the rock sample

Mineral composition (mg)	Starting sample	After 1 day	After 7 days	After 28 days
Quartz SiO ₂	273.5	252.2	119.6	7.6
Albite (Na,K,Ca)Al _{(1-2)Si₍₃₋₂₎O₈}	206.9	184.0	138.9	0.0
K-Feldspar KAlSi ₃ O ₈	125.6	115.9	57.9	0.0
Muscovite (Na,K,Ca) ₂ (Al,Fe,Mg) ₄ 6(Al,Si) ₈ O ₂₀ (OH,F) ₄	59.1	54.5	34.7	0.0
Pyroxene XY(Si,Al) ₂ O ₆	14.8	13.6	0.0	0.0
Silicon* Si	44.3	47.7	27.0	1.4
Chalcopryrite and or Calcite CuFe ₂ and or CaCO ₃	7.4	6.8	3.9	0.0
Siderite FeCO ₃	7.4	6.8	0.0	0.0
Hematite Fe ₂ O ₃	0.0	0.0	0.0	3.7
Magnetite Fe ₃ O ₄	0.0	0.0	0.0	1.0
Anatase TiO ₂	0.0	0.0	0.0	0.4
Chlorite (Mg,Fe) ₃ (Si,Al) ₄ O ₁₀ (OH) ₂ (Mg,Fe) ₃ (OH) ₆	0.0	0.0	0.0	2.3
Goethite FeO(OH)	0.0	0.0	3.9	0.6
Amorphous	0.0	0.0	0.0	2.5
Total sample	739.1	681.5	385.7	19.4

SEM analyses of the cross section of the rock samples were also conducted. Results are given

in Figure 4. These images were obtained using the backscattered electron detector (BSE) and analysed using the energy dispersive x-ray spectrometer (EDAX). The results suggest that albite feldspar is the most reactive (soluble) mineral, followed by microcline and quartz. The BSE image of the sample from 28 day circulation (Figure 4D) confirms that only quartz and other accessory minerals were observed, and no feldspars were present.

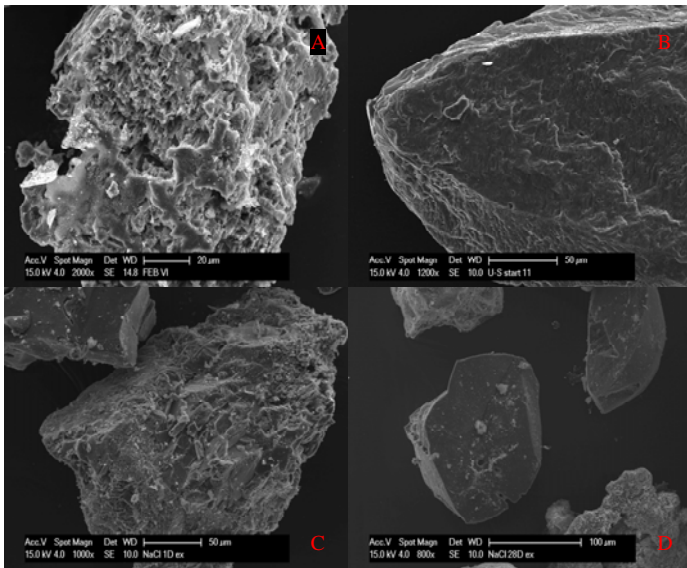
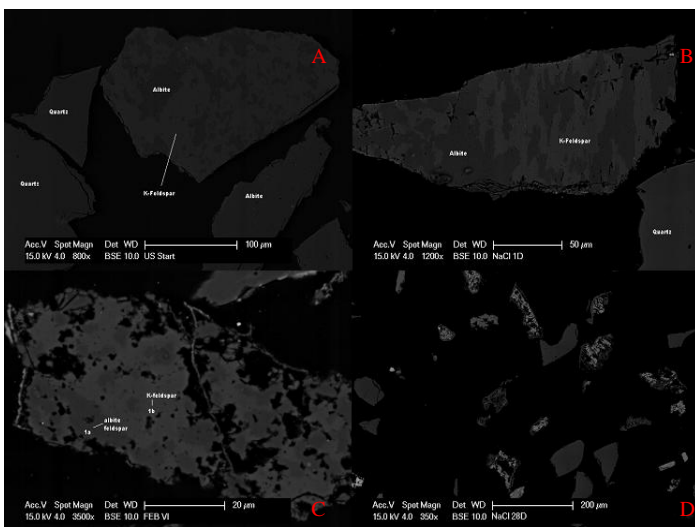


Figure 3: SEM images of the rock sample surface (a) starting rock (b) after 1 day experiment (c) after 7 days experiment (d) after 28 day experiment

Figure 4: BSE images of the rock cross sectional area (a) starting rock (b) after 1 day experiment (c) after 7 days experiment (d) after 28 day experiment



Water Analysis

The initial pH of the water was 5.5. This did not change significantly in all batch experiments.

Figures 5 and 6 show the concentration of elements versus time from the ICP-MS analysis, and Figure 7 show the silica concentration on the circulating water after 1, 7, and 28 days of fluid-rock interactions.

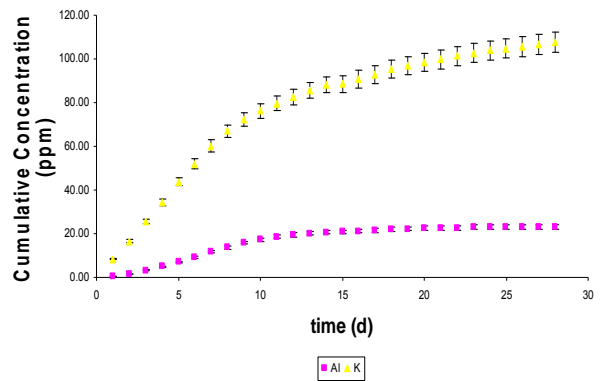


Figure 5: Concentration of Al and K in experimental liquid versus time

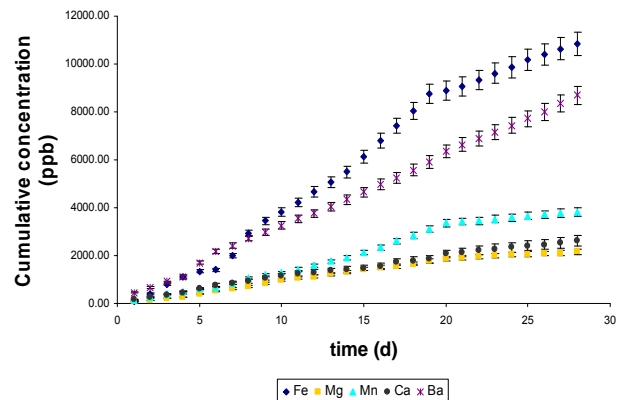


Figure 6: Concentration of Fe, Mg, Mn, Ca and Ba in experimental liquid versus time

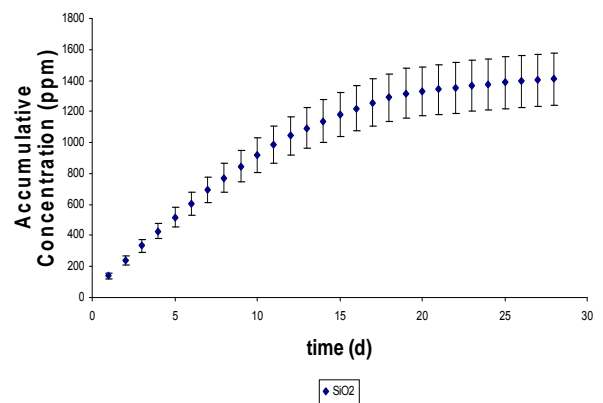


Figure 7: Concentration of SiO₂ in experimental liquid versus time

Water analysis results showed that there was enhanced leaching of the minerals, indicated by the increased element concentration in the liquid phase. The rapid reaction is probably the

consequence to the dissolution of more reactive (soluble) phases in the rock sample. It is seen that high concentration of silica, aluminium and potassium were dissolved in the liquid due to dissolution of albite, microcline and quartz.

Unfortunately the sodium concentration could not be analysed accurately due to the high initial concentration of sodium in the circulating fluid (250 ppm NaCl).

Mass Balance

A simple mass balance was undertaken to observe the sample loss to the circulating fluid. Since the sodium cannot be analysed accurately at this stage, it was assumed that the dissolved concentration would be similar to the dissolution of Albite Feldspars in pure water. Table 3 shows the system mass balance. A short circulating time would result in less sample loss. The sample loss may be due to the replacement of circulating fluid, since at the time of reinjection, the liquid must overflow through the sample and exiting the cell to remove excess air (any air bubble may disrupt the flow in the thermosyphon).

Table 3 System mass balance

time	Initial, mg	Remaining, mg	Dissolved (calc), mg	% wt.	Dissolved, (water analysis),mg	Loss, mg
1	745.2	681.5	63.7	8.55	41.30	22.40
7	734.4	385.7	348.7	47.48	271.00	77.70
28	737.7	19.4	718.3	97.37	427.95	290.35

Not including the concentration of the anions may also be another cause of the unclosed mass balance.

Conclusion

The mineralogical analysis showed that the major composition of the rock is quartz, albite and microcline. The fluid-rock interaction experiment showed that dissolution reactions occur predominantly in the early stages (to 7 days) of the experiment due to the dissolution of reactive minerals (feldspars). The dissolution reaction begins to decrease due to the exhaustion of the reactive mineral and proceeds with the dissolution of the less reactive phase. Results of XRD showed that feldspar experienced a clear reduction with time, followed by quartz.

Liquid analysis showed higher concentrations of Na, K, Si, and Al compared to other analysed elements. These results suggest that the dissolution reaction occurs primarily for the feldspars.

The dissolution of feldspar would suggest the improvement of the permeability (however, not necessarily improving the fracture where mineral

deposits occur) and also suggest of potential silica scaling (if circulating fluid is near neutral pH). The concentration of silica 1400 ppm (from 0.7g rock sample) was released to the liquid phase throughout the experiment.

Future Work

An experiment is currently being conducted for 14 days period to obtain more understanding on the dissolution (Figure 2). Sodium concentration would need to be accurately analysed. The current work has used 250 ppm sodium chloride solution for the fluid-rock interaction and does not quite represent the actual interaction. Experiments with Increased amount of rock sample (increasing the rock/water ratio) are being carried out to observe any changes in equilibrium or saturated condition. A dissolution and precipitation model will be generated using the data from previous experiments (pure water) and the current study. The model will be used to predict the dissolution rate and precipitation rate of the actual fluid-rock interaction.

Acknowledgments

The research described in this paper has been supported by The Department of Primary Industries and Resources of South Australia (PIRSA) and Geodynamics. The author would like to thank Geodynamics for supplying the drill cuttings, and the South Australian Museum and Adelaide Microscopy for the equipment access. The authors would like to thank John Stanley from the School of Earth and Environmental Sciences, Adelaide University, Benjamin Wade and Aoife McFadden for assistance in ICP-MS analysis, Shaun Chan and Kevin Li for their assistance in the experiments.

References

Azaroual, M., and Fouillac, C., 1997, Experimental Study and Modelling of Granite-Distilled Water Interaction at 180°C and 14 Bars: Applied Geochemistry, V. 12, pp. 55-73.

Castro, M. R., Lopez, D. L., Reyes, J. A., Matus, A., Montalvo, F. E., Guerra, C. E., 2006, Expected Silica Scaling from Reinjection Waters After Installation of a Binary Cycle Power Station at Berlin Geothermal Field, El Salvador, Central America: GRC Transactions, V. 30, pp. 487-492

Dove, P. M., and Crerar, D. A., 1990, Kinetics of Quartz Dissolution in Electrolyte Solutions using a Hydrothermal Mixed Flow Reactor: Geochimica et Cosmochimica Acta, V. 54, pp 955-969

Ellis, A. J., 1968, Natural Hydrothermal Systems and Experimental Hot-Water/Rock Interaction: Reactions with NaCl solutions and trace metal extraction: Geochimica et Cosmochimica Acta, V. 32, pp. 1356-1363

Grigsby, C. O., Tester, J. W., Trujillo JR., P. E., and Counce, D. A., 1989, Rock-Water Interactions in the Fenton Hill, New Mexico, Hot Dry Rock Geothermal Systems I, Fluid Mixing and Chemical Geothermometry: *Geothermics*, V. 18, pp. 629-656.

HACH, 2009, DR/2010 Portable Spectrophotometer Procedures Manual. <http://www.hach.com/fmmimghach?/CODE%3A4930022286|1>, p 767 – 772, accessed September 2008

Icenhower, J. P., and Dove, P. M., 2000, The Dissolution Kinetics of Amorphous Silica into Sodium Chloride Solutions: Effects of Temperature and Ionic Strength: *Geochimica et Cosmochimica Acta*, V. 64, pp. 4193-4203

Posey-Dowty, J., Crerar, D., Hellerman, R., and Clarence, D. C., 1986, Kinetics of Mineral-Water Reactions: Theory, Design, and Application of Circulating Hydrothermal Equipment: *American Mineralogist*, V. 71, pp. 85-94.

Pring, A., 2009, personal communication.

Rimstidt, J. D., and Barnes, H. L., 1980, The Kinetics of Silica-Water Reactions: *Geochimica et Cosmochimica Acta*, V. 44, pp. 1683-1700.

Robinson, B. A., 1982, Quartz Dissolution and Silica Deposition in Hot Dry Rock Geothermal Systems, Thesis, Cambridge, Massachusetts Institute of Technology.

Savage, D., Cave, M. R., Milodowski, A. E., and George I., 1987, Hydrothermal Alteration of Granite by Meteoric Fluid: An Example from the Carnmenellis Granite, United Kingdom: *Contributions to Mineralogy and Petrology*, V. 96, pp. 391-405.

Savage, D., Bateman, K., and Richards, H. G., 1992, Granite-Water Interactions in a Flow-through Experimental System with Applications to the Hot Dry Rock Geothermal System at Rosemanowes, Cornwall, U.K.: *Applied Geochemistry*, V. 7, pp. 223-241.

Tarcan, G., 2005, Mineral Saturation and Scaling Tendencies of Waters Discharged from Wells (>150°C) in Geothermal Areas of Turkey: *Journal of Volcanology and Geothermal Research*, V. 142, pp. 263-283

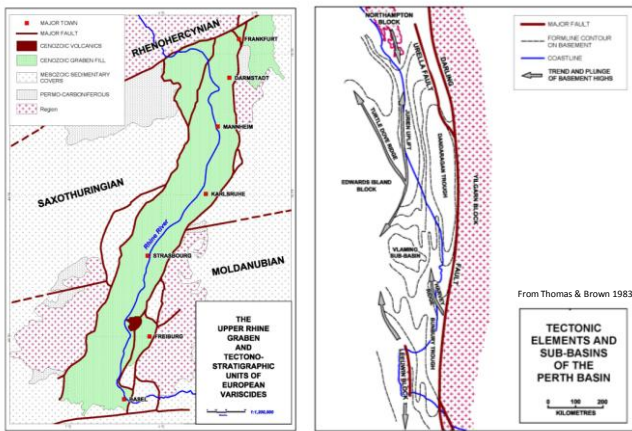
Yangisawa, N. Matsunaga, I., Sugita H., Sato, M., and Okabe T., 2005, Scale Precipitation during Circulation at the Hijiori HDR Test Field, Yamagata, Japan: *Proceedings World Geothermal Congress 2005, Antalya, Turkey, 24-29 April 2005*.

produced the series of deep, north-south trending basins along the western margin of the Yilgarn Craton. Sediment deposition commenced with extension during the Permian (~290 Ma) and continued to the Early Cretaceous (~138 Ma). The Basin was uplifted during the final separation of Western Australia and greater India during the breakup of Gondwana.

Rifting in the 300km long Rhine Graben commenced much later in the Middle Eocene. Graben sinking and shoulder lifting continues to this day with the maximum sediment fill being around 3.4km in the Upper Rhine Graben.

There are substantial geological differences between the Rhine Graben and Perth Basin, in particular the much younger age, shorter graben, thinner sedimentary pile thickness of the former and current tensional and seismically active tectonic stress regime of the Rhine Graben compared to the compressional and relatively seismically inactive regime of the Perth Basin. Even so there are important similarities in their structural setting, extensional tectonic origins, thick sedimentary successions which overlie hot crystalline basements, high heat flows and evidence of the existence of substantial geothermal energy resource potential.

Geological Maps

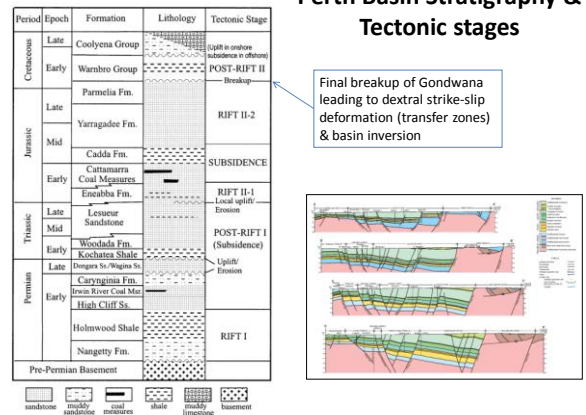


Both basins have vertical structural asymmetry with the sedimentary fill being greater in the eastern flank than the western flank and higher graben shoulders on the east flank in the case of the Rhine. This is considered to have important influences on regional ground water flow in the Rhine. Similarly the hills marking the NS trending Darling Fault forms the eastern boundary fault of the Perth Basin and is also expected to have an influence on ground water flow.

In the Rhine the current stress regime is strike slip with the maximum horizontal stress being oriented approximately NW/SE. In contrast to the Rhine, the early extensional tectonic regime of the Perth Basin is

now overprinted by an essentially compressional setting as the Australian plate migrates NW with a rotational component at the relatively fast geological rate of nearly 7 cm per year. The contemporary stress regime for the Perth Basin has been interpreted to be a transitional reverse to strike-slip faulting stress regime with an approximate east-west maximum horizontal compression direction. Stress field data for the Perth Basin are derived mainly from petroleum well borehole breakouts and drilling-induced tensile fractures from 34 measurements as shown in the World Stress Map. This is important for targetting wells to tap critically stressed faults and fracture directions.

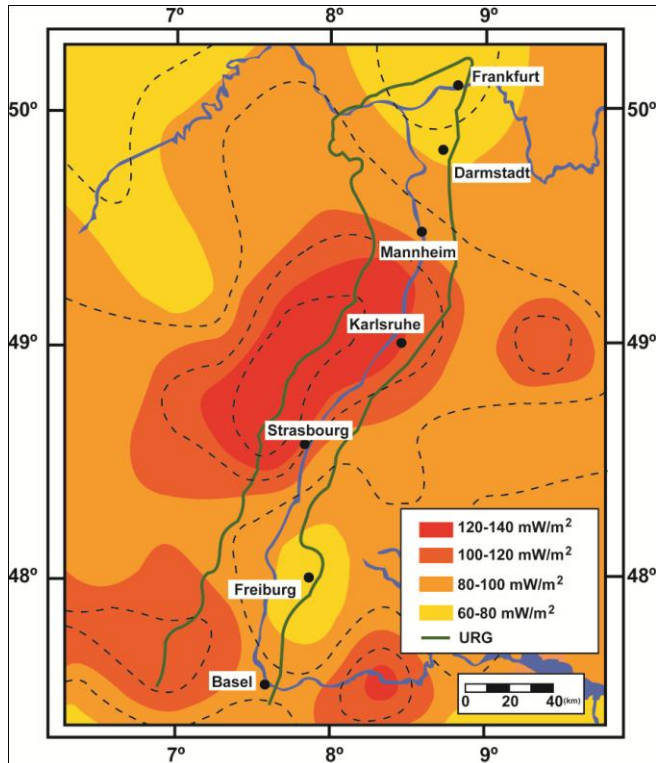
Perth Basin Stratigraphy & Tectonic stages



From Song & Cawood, 1999

Geothermal energy has been recovered to power electricity generation from both sediments and granites in the Rhine Graben at Soultz sous Forêts and Landau. Heat flows of up to 150mW/m² have been recorded in both grabens. Thermal anomalies occur along the western rim of the Rhine Graben. This is has been attributed to enhancement of a conductive basal heat flow of 70-80mW/m² by convection. Some of these sites were mapped as early as 1929 where a temperature of 50°C at depth of 400 metres was known at Soultz.

At Landau convective hot spots have temperatures of 55°C at a depth of 500m & 98°C at a depth of 1,000m. There is considerable evidence for convective water flows in the Rhine Graben, particularly in the western flank where a pattern of adjacent hot and cold spots was found. This is generally considered to be the surface expression of deep convective geothermal systems. At Soultz there is a large reservoir with a similar fluid chemistry. The same geothermal fluid is found in different wells and in different lithologies including sediments and granite basement. Geothermal water at Soultz has salinities of around 100g/l and pH of 5.



Source: From Schwarz 2005 & Lichen 2005

sequences in the Perth Basin. It is not known if this reflects any deeper convection.

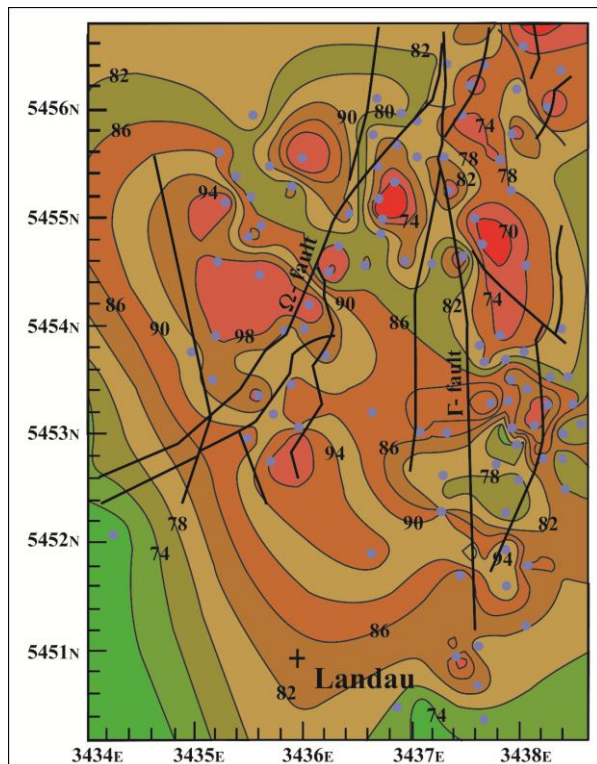
In the Rhine Graben in recent years the emphasis has shifted from targeting temperatures of around 200°C at depths of 5,000 metres where natural flow rates from fracture permeability have proven to be inadequate to targeting shallower depths of 2,500m to 3,500 metres where temperatures of 150°C to 160°C and substantially higher flow rates can be expected from natural faults and fractures.

With its thick sequences of sandstones, the presence of thermal insulating shales and coals and high heat flows the Perth Basin has potential to house geothermal energy resources in the form of hot sedimentary aquifers (HSA) and hot rocks. The source of the heat flows in the Perth Basin may be radioactive basement rocks and radiogenic sedimentary horizons. The Perth Basin contains some of the worlds largest mineral sands deposits many of which are rich in radiogenic thorium minerals at shallow depths.

The highest known heat flows in the Perth Basin have been determined from petroleum wells in or near producing oil and gas fields in the northern Perth Basin. Green Rock holds nine Geothermal Exploration Permits in this region near high voltage power grids connected to Perth's major power markets. Heat flows exceed 100mW/m² within these Permits. Temperatures of around 160°C are expected in hot sedimentary aquifers at depths less than 4,000m which is sufficient to generate electricity commercially at this location provided that sufficient geothermal water flow rates can be achieved.

Unlike Germany, electricity generated from geothermal energy in Australia does not benefit from any feed in tariff arrangement and retail electricity prices in Australia are substantially lower than Gemany's. In general this means that higher recovered temperatures or flow rates are required in Westen Australia to ensure commercial viability. However generators of renewable energy including geothermal energy are entitled under Federal legislation to sell Renewable Energy Certificates (REC's) in addition to selling the electricity they generate. In the absence of feed in tariffs in Western Australia electricity is sold to utilities via power purchase agreements.

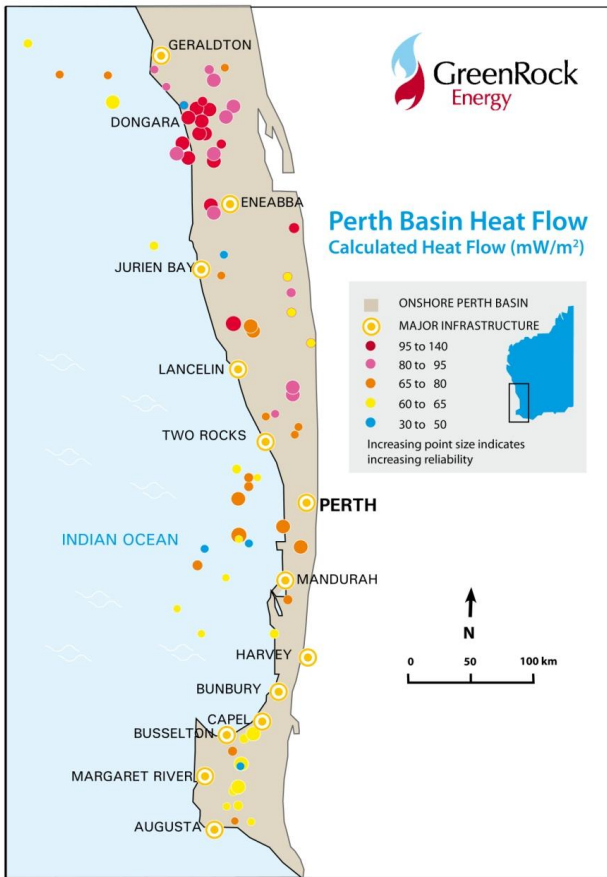
Within Green Rock's permits in the North Perth Basin petroleum wells have proven good primary water permeabilities in sandstone reservoirs down to depths of around 2,700 metres but there is some limited evidence of substantially lower permeabilities at greater depths where temperatures above 150°C would be expected. Much less is known about the potential for good water flows from natural fault or



Landau: Temperatures at 1000m (°C)
Grid in kms (Gauss-Krüger)
Source: Charissé 2007

It is early days yet but evidence is emerging of convective flows in the shallow sedimentary

fracture permeability as this has not been targeted by the petroleum industry there.



Source: Hot Dry Rocks Pty Ltd 2008

In the central Perth Basin near the city of Perth heat flows are lower and temperatures expected at depth are likely to be insufficient for commercial generation of electricity but should be adequate for direct heat uses such as purification of water by distillation and for air-conditioning of buildings. Viability depends on attaining sufficient permeabilities from the aquifers. Within the Perth city area, where petroleum wells and deep seismic data are lacking, most of the useful temperature and permeability data have come from deep water bores, the deepest of which extend to only about 1000 metres but have sufficiently high water flow rates from natural matrix or granular permeability. On the basis of petroleum wells outside the Perth Permit areas good permeabilities are expected in Perth at least down to depths of 2,500 metres.

Geothermal energy has been recovered from aquifers between 750 and 1,000 metres deep in Green Rock's Permit GEP1 in metropolitan Perth. This geothermal water is used to heat a number of major swimming centres including the Challenge Stadium Aquatic Centre where the World Swimming Championships have been held twice in the past decade.



Drilling Water Well in Perth for Heating Aquatic Centres

To develop opportunities in GEP1, Green Rock Energy, plans to carry out a commercial demonstration project to recover geothermal energy from hot sedimentary aquifers beneath the main Perth campus at the University of Western Australia (UWA). This project will be the first stepping stone to larger commercial developments in Perth.

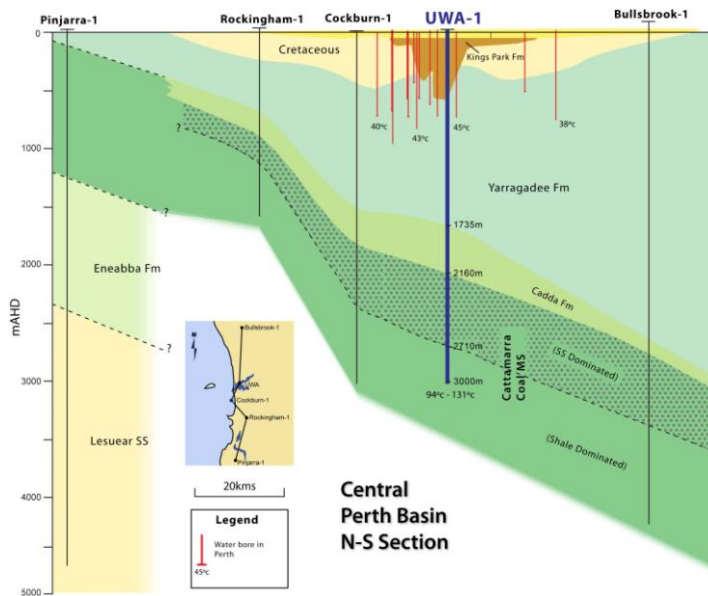
The demonstration project is designed to replace a significant portion of the UWA's electrical powered air-conditioning with geothermal powered absorption chillers for its air-conditioning and heating needs. Absorption chillers, like the one shown below, are commercially available in Australia.

Commercial viability of this project at the UWA campus will depend on obtaining adequate geothermal temperatures and water flow rates from the sandstone aquifers at depth. Geothermal water temperatures of between 80°C and 100°C are required for commercial operation of the absorption chillers which will provide chilled water for the campus. Expected temperatures at the target depths of 2.5km to 3km in Perth should be adequate as indicated by estimated heat flows determined from temperature profiles measured in deep water bores and petroleum wells.



Absorption Chiller

For this first project at the UWA campus, one production and one injection well will be drilled to around 2.5 to 3 kilometres deep to recover geothermal energy from sandstone aquifers in the fluvial Yarragadee Formation and Cattamarra Coal Measures. Drilling wells to these depths should not present any particular difficulty as there is abundant history of petroleum wells drilled without significant problems in the Perth Basin. Preparatory site work and well design is underway to enable this drilling to be carried out in 2011. Seismic acquisition will be completed to optimise well design and orientation prior to drilling.



References

Chopra P.N. and Holgate, F. (Earthinsite Pty Ltd): Geothermal Energy Potential in Selected areas of Western Australia, a Report commissioned by Western Australian Department of Industry and Resources 2007; and also – A GIS Analysis of Temperature in the Australian Crust; Proceedings of World Geothermal Congress, Antalya, Turkey 2005, pp 7.

Clauser, C and Villinger, H, Analysis of conductive and convective heat transfer in a sedimentary basin demonstrated for the Rheingraben, Geophys. J 100, 393-414, 1990

Davidson, W.A... Hydrogeology and groundwater resources of the Perth Region, Western Australia: Western Australia Geological Survey, Bulletin 142, 257 pp, 1995

Freeman, M.J., and Donaldson, M.J.: Geology of the southern Perth Basin and Margaret River wine district, southwestern Western Australia – a field guide: Western Australia Geological Survey, Record 2006/20, 2006

Genter, A., Baumgärtner, J., Cuenot, N., Graff, J J., Kolbel, T., Sanjuan, B. The EGS Sultz Case Study: Lessons Learnt After Two Decades of Geothermal Researches. Second European Geothermal Review, Proceedings, Mainz June 21-23, 2010

Gori, K.A.R.: Perth Basin's Geothermal Resources, Australian Geothermal Energy Conference 2008, Extended Abstract. Geological Survey, Department of Industry and Resources, 2008

Hot Dry Rocks Pty Ltd: Geothermal Energy Potential in Selected Areas of Western Australia, Perth Basin, pp 270, 2008

Hot Dry Rocks Pty Ltd: Western Perth Geothermal project, Geothermal Exploration Stage 2, unpublished report for Green Rock Energy Limited, pp28, 2009,

Mory, A.J., Haig, D.W., Mcloughlin, S., and Hocking, R.M.: Geology of the northern Perth Basin, Western Australia – a field guide: Western Australia Geological Survey, Record 2005/9, 2005

Mory, R.J, and Lasky, R.P.: Stratigraphy and Structure of the Onshore Northern Perth Basin, Report 46, Geological Survey of Western Australia pp 126, 1996

Regenauer-Lieb, Prof. K, Horowitz Dr F, The Perth Basin Geothermal Opportunity, The University of Western Australia & CSIRO, p42-44, April 2007

Schwarz M, Henk, A, Evolution and structure of the Upper Rhine Graben: insights from three-dimensional thermomechanical modeling, Int J Earth Sci (Geol Rundsch), 94: 732-750, 2005.

Australia's Geothermal Research Activities

A.D. Long^{1*}, A.R. Budd², H. Gurgenci³, M. Hand⁴, C. Huddlestone-Holmes⁵, B. Moghtaderi⁶ and Regenauer-Lieb, K.⁷

¹Primary Industries & Resources SA, GPO Box 1671, Adelaide, South Australia, 5001.

²Geoscience Australia, GPO Box 378, Canberra, Australian Capital Territory, 2601.

³QGECE, The University of Queensland, Brisbane, Queensland, 4072.

⁴SACGER, IMER, The University of Adelaide, South Australia, 5005.

⁵CSIRO, PO Box 883, Kenmore, Queensland, 4069.

⁶ATC, The University of Newcastle, Callaghan, NSW, 2308.

⁷WAGCOE, ARRC, 26 Dick Perry Avenue, Kensington, 6151.

*Corresponding author: alexandra.long@sa.gov.au

The challenges and technology needs of Australia's geothermal energy industry are significant yet achievable. The sector is organised and has a clear pathway through the stages of project development defined in the Development Framework and Technology Roadmap (DRET, 2008). Collaboration is facilitated by the Australian Geothermal Energy Group and its Technical Interest Groups, where research needs are prioritised by the industry and researchers. The capacity and capability to undertake the much needed research work will be met by geothermal research centres which work competitively yet collaboratively, with complementary programs, to achieve research outcomes most efficiently. This paper will provide a guide to the research activities in Australia, outlining the programs and areas of expertise of the key research groups working in the geothermal arena; a summary of current projects; and how to find out more information.

Keywords: Geothermal, research, technology development.

Centres of expertise

The desire to develop Australia's geothermal energy resources to supply secure and environmentally sustainable energy has led to the impressive growth of the Australian geothermal sector. The challenges facing the sector are known, and the research and development needs of the industry as they strive to commercialise the resources are being met by a growing capacity at dedicated research centres, universities and research groups.

Centres for geothermal energy research have formed: at the University of Queensland, with the Queensland Geothermal Energy Centre of Excellence (QGECE); in a joint venture of the University of Western Australia, Curtin University and the CSIRO, the Western Australian Geothermal Centre of Excellence (WAGCOE); and at the University of Adelaide, the South Australian Centre for Geothermal Energy Research (SACGER). Geothermal energy research is also being supported at many universities around Australia, Geoscience Australia and at the CSIRO. The following

sections will describe each of these centres and research groups and their capability.

Geoscience Australia

The Australian Government announced the AU\$58.9M Onshore Energy Security Initiative in August 2006, and as part of this, Geoscience Australia established a geothermal energy project. The project aims to improve the existing knowledge about the type and location of geothermal resources in Australia on a national scale. It also aims to encourage investment, exploration and exploitation of this energy source through provision of pre-competitive geoscience datasets relevant to geothermal energy.

To achieve these objectives, the geothermal project:

- collects new heat flow data across Australia to better define and locate geothermal resources;
- uses (heat) source and (thermal) trap modelling to identify potential Hot Rock and Hot Sedimentary Aquifer systems;
- works to compile national datasets which may be useful to the geothermal industry including groundwater temperatures, borehole temperatures, rock thermal conductivities and granite and sediment chemistry;
- uses these new datasets to produce a revised estimate of Australia's total contained geothermal resource; and
- provides advice to government on geothermal resource issues, including the AU\$50M Geothermal Drilling Program.

For more information see www.ga.gov.au or contact the geothermal energy team: geothermal@ga.gov.au.

Queensland Geothermal Energy Centre of Excellence - QGECE

The Queensland Geothermal Energy Centre of Excellence is based at the University of Queensland and was established with an AU\$15M grant from the Queensland Government and AU\$3.3M of in-kind support from the university. The centre commenced operations in

Australian Geothermal Conference 2010

January 2009 with a 5 year program. The centre's research programs were developed to fill gaps in the national and international geothermal research effort and have a focus on above ground technologies with the aim of quickening the pace of large-scale utilisation of hot rocks geothermal energy in Australia. QGECE has four research programs:

- Power Conversion: developing technologies to enable production of 50% more electricity from binary plants using the same subsurface investment;
- Heat Exchangers: development of natural draft dry cooling towers and other cooling solutions to increase by up to 15% the net output of geothermal plants that use air-cooled condensers;
- Reservoir Geology: establish a geochemical/isotopic and geochronological database and improve understanding of geothermal resources in Queensland and develop routine exploration tools for hot rock geothermal systems; and,
- Transmission: research in to electricity grid interaction with an emphasis on remote generation infrastructure.

The current major projects include:

- Design and development of small (5-kWe) supercritical turbines for testing in the QGECE laboratory.
- Construction of a 100-kWe mobile geothermal test plant with high-pressure capability to try supercritical turbines.
- Characterisation of the heat-producing granites in Queensland.
- The effect of ambient dust on air-cooled condenser performance and design against dust.
- Investigation of options for connecting remote geothermal power generation to the Queensland grid.

See also www.uq.edu.au/geothermal or contact the centre Director, Professor Hal Gurgenci: h.gurgenci@uq.edu.au.

Western Australian Geothermal Centre of Excellence - WAGCOE

The Western Australian Geothermal Centre of Excellence is an unincorporated joint venture between the Commonwealth Science and Industry Research Organisation (CSIRO), the University of Western Australia, and Curtin University. The centre was established in February 2009 with an AU\$2.3M grant over three years from the Western Australian government and substantial in-kind and cash contributions from the centres' members. The centre is

providing a scientific focus to the development of the geothermal industry in Western Australia, concentrating on the Perth basin, and building educational programs around geothermal energy. The centre's research focus is on Hot Sedimentary Aquifers and direct use of the heat produced from these resources, as summarised in the centre's vision statement "To provide geothermal zero-emission desalinated water, air-conditioning and power to our cities".

WAGCOE has three research programs:

- Perth Basin Assessment: Develop a rigorous scientific understanding of the geothermal resource in the Perth Basin;
- Above Ground Technologies: Identify and demonstrate innovative applications of HSA geothermal energy; and,
- Deep Resources: Provide a scientific framework for the potential exploitation of deep geothermal resources.

Current major projects include:

- Research and development activities associated with the direct use geothermal powered supercomputer cooling system that is part of CSIRO's Sustainable Energy for SKA project (see below). This system targets hot sedimentary aquifers of the Perth Basin.
- Design of an additional sensor equipped deep research and monitoring well at the same site for research, education, training and long term monitoring.
- Research and development activities associated with the direct geothermally driven MW_{th} scale campus cooling project at UWA run by the leaseholders Green Rock Energy and UWA.
- Development of a novel desalination technology with 30% yield boost from low grade geothermal waters of 65°C and less. A containerised m³/day first generation prototype is sponsored by the Australian Government National Centre of Excellence in Desalination located at Murdoch University.

For more information see www.geothermal.org or contact the centre business manager, Sean Webb: sean.webb@geothermal.org.au.

South Australian Centre for Geothermal Energy Research - SACGER

The South Australian Centre for Geothermal Energy Research is based at the University of Adelaide within the Institute for Minerals and Energy Resources, www.adelaide.edu.au/imer. The centre was announced by the South Australian Government as the first project to be funded from the South Australian Renewable Energy Fund, established with a grant of

Australian Geothermal Conference 2010

AU\$1.6M over two years from 1 July 2009. The University of Adelaide is providing AU\$400,000 over the same period.

The SACGER research program will focus on subsurface factors in Hot Rock and EGS resources such as reservoir characterisation and modelling. This is complementary to the research programs of other centres. The research program is under development and will be designed in consultation with the sector.

Current projects at the centre include those which were funded by tied grants from PIRSA:

- Geophysical mapping and monitoring of an enhanced geothermal system using magnetotellurics.
- Rock fracture characterisation for hot dry rock enhanced geothermal systems.
- Building a regional thermal model for the Adelaide rift complex.
- Experimental verification of underground cooling for efficient thermal cycles.
- Optimisation of geothermal energy investments.
- Investigate low temperature thermal processing using geothermal energy.
- Reconnaissance thermal mapping for uranium and geothermal exploration.

For more information see www.adelaide.edu.au/geothermal/ or contact the centre: imer@adelaide.edu.au.

CSIRO

CSIRO's research capabilities in the geothermal arena are broad, due to the organisation's research diversity and ability to integrate multidisciplinary skills. The primary focus of CSIRO's activities in geothermal has been through its contribution to WAGCOE. CSIRO's contributions to the centre are mainly in the geological, geophysical, ground water, and reservoir engineering aspects of the Perth Basin Assessment research program. CSIRO is also deploying its research expertise in hydraulic fracturing, reservoir engineering, well bore stability, rock petrophysics and microseismic monitoring to geothermal projects

Funding from the Education Investment Fund for CSIRO's Sustainable Energy for SKA project was recently announced. A significant component of this project is a 10 MW_{th} direct use geothermal cooling system for the Pawsey High Performance Computing Centre in Perth. The construction of this system will start with the drilling of a research/monitoring well, followed by a production and injection doublet. The heat produced will be used in an adsorption chiller to provide cooling for the supercomputer. CSIRO will work closely with

WAGCOE during the development of this project. The geothermal component of the project is led by CSIRO Earth Science and Resource Engineering in collaboration with the leaseholder, Geothermal Power Pty Ltd.

Other projects include:

- Development of numerical modelling tools that couple thermal and poro-elastic processes for the assessment of well stability.
- Development of numerical modelling tools and procedures for hydraulic stimulation at high pressures and temperatures.
- Development of numerical modelling tools for fluid flow in fractures.
- Evaluating the application of petrophysical logging techniques to the assessment of thermal conductivity;
- Assessment of waveform characterisation techniques for the interpretation of microseismic monitoring data through laboratory based studies (high pressure high temperature triaxial cell with acoustic emissions monitoring) and the analysis of field data.

For more information see www.csiro.au/org/geothermal or contact the CSIRO: geothermal@csiro.au.

University of Newcastle (Priority Research Centre for Energy – PRCfE)

Located at the University of Newcastle, the Priority Research Centre for Energy has been working on geothermal energy research projects for a number of years through the research program on Renewable Energy Systems. The University of Newcastle has received AU\$30M from the Federal Government through the Education Investment Fund and AU\$30M matching funding from other sources to establish the Newcastle Institute for Energy & Resources (NIER). As part of this initiative, significant funding has been allocated for geothermal research, in particular for the establishment of a state of the art facility for pilot-scale experimental research. The focus of geothermal research at the University of Newcastle is on novel power generation cycles and the concept of a CO₂ thermo siphon for EGS. The study of power cycles is regarded as one of the key areas for major technological improvements since many of the problems associated with power generation from geothermal sources are underpinned by inefficient and often unsuitable heat exchange processes within power cycles. In recognition of these shortcomings, the University of Newcastle initiated a joint R&D program with Granite Power Ltd in 2006 with the goal of establishing alternative and potentially more efficient ways of generating power from geothermal and other low-

grade heat sources, such as industrial waste heat. The result was the creation of the GRANEX Regenerative Supercritical Power Cycle which is now being commercialised.

For more information see www.newcastle.edu.au/research-centre/energy or contact the Renewable Energy Systems Program leader, Professor Behdad Moghtaderi: Behdad.Moghtaderi@newcastle.edu.au.

Melbourne Energy Institute

The Melbourne Energy Institute is located at the University of Melbourne and has a number of geothermal projects including the Victorian Geothermal Assessment Report, which intends to address critical issues for the successful development of geothermal power capability in Victoria.

For more information see energy.unimelb.edu.au or contact the institute: mei-info@unimelb.edu.au

RMIT

A significant project linking geothermal energy and desalination is underway at RMIT in partnership with Greenearth Energy.

The project involves the development of a prototype system that combines fresh water production with electricity generation using entirely renewable sources. The project is supported by an Australian Research Council Linkage grant and Greenearth Energy.

For more information on this project contact Mark Miller, Managing Director of Greenearth Energy, via email markm@greeneearthenergy.com.au or telephone 03 9620 1566.

For the RMIT website see www.rmit.edu.au

AGEG Technical Interest Groups

Collaboration amongst all participants in the sector is enabled through the Australian Geothermal Energy Group (AGEG) and the AGEG Technical Interest Groups (TIGs).

Through linkages to the AGEG and its TIGs, Australia is a member of and contributes to the work of both the International Energy Agency Geothermal Implementing Agreement (IEA-GIA) and the International Partnership for Geothermal Technologies (IPGT). The 105 organisations that are members of the AGEG have nominated research topics of the highest priority to the industry, which are closely aligned with the priorities of both the GIA and the IPGT.

The 12 TIGs are named in Table 1, and described in more detail in the following section. For more information or to join any of the TIGs: see the AGEG website, <www.geothermal.pir.sa.gov.au>, go to AGEG, Technical Interest Groups; or contact the TIG leader. Contact details for all TIG leaders are also provided on the website.

Table 1. AGEG Technical Interest Groups

TIG	Topic
1	Water management & environmental sustainability
2	Reserves and resources
3	Induced seismicity
4	Outreach
5	Economic modelling and novel use
6	Power plants
7	Direct use
8	Information and data
9	Reservoir development and engineering
10	Exploration and well log technologies
11	Drilling and well construction
12	Education

TIG 1 water management and environmental sustainability

Following discussions and a decision made at the AGEG AGM in February, the name and focus of TIG 1 has been redefined as water management and environmental sustainability. The scope of the TIG and definition of outputs from the TIG will be developed by the members and will be available on the TIG webpage. The TIG leader is Steven Kennedy from the Victorian Department of Primary Industries.

TIG 2 reserves and resources

The reserves and resources technical interest group is predominantly to provide a forum for AGEG members to contribute to discussion on the Australian Geothermal Reporting Code. The code is developed and reviewed by the joint AGEG and AGEA Australian Geothermal Reporting Code Committee, chaired by Peter Reid from Petratherm. Peter is also the TIG 2 leader, allowing feedback to the committee. *The Australian Code for Reporting of Exploration Results, Geothermal Resources and Geothermal Reserves, The Geothermal Reporting Code* (AGRCC, 2008), was launched in August 2008 at the AGEG and AGEA Australian Geothermal Energy Conference.

TIG 3 induced seismicity

Highlighting the importance of this topic and the need for research in this area, a new technical interest group has been created to focus on induced seismicity. Led by Michael Malavazos and Barry Goldstein from PIRSA, this TIG will build on the work done under the previous TIG 1, which included the release of two reports, *Cooper Basin HDR hazard evaluation: predictive modelling of local stress changes due to HFR geothermal energy operations in South Australia* (Hunt and Morelli, 2006) and *Analysis and management of seismic risks associated with engineered geothermal system operations in South Australia* (Morelli, 2009).

TIG 4 outreach

The scope of TIG 4 is to assist the development of the Australian geothermal industry through coordinated geothermal training courses (in conjunction with IGA) an annual conference (in conjunction with AGEA), improving communications through provision of a dedicated website that provides linkages to geothermal resource material and informing the public through the provision of accessible information. TIG 4 is led by Betina Bendall from PIRSA.

TIG 5 economic modelling and novel use

TIG 5 has been modified to now cover economic modelling as well as novel use applications for geothermal energy including hybrid systems. Stephen Hinchliffe from SKM is the TIG leader.

TIG 6 power plants

The aim of TIG 6 is to achieve substantial improvements in geothermal power plant efficiency through improvements in, for example, the cycle type, cycle fluids, heat exchanger efficiencies and more efficient cooling processes. Currently the focus is on the following areas:

- New cycles and cycle fluids
- Dry cooling
- Supercritical CO₂ geothermal siphon

The work of this TIG mirrors the IEA Geothermal Research Annex VI. Hal Gurgenci from the QGECE and Behdad Moghtaderi from the University of Newcastle are co-leaders of TIG 6.

TIG 7 direct use

Direct use geothermal applications include both circulating hot water & geothermal heat pumps. Direct use geothermal is being pursued through work in this TIG as a highly desirable substitute for electricity use due to:

- Widespread occurrence
- Shallow depths (i.e. lower cost)
- High efficiency (no energy conversion)
- Utilisation of conventional plant and equipment
- Relatively easy set up
- Can be small to industrial scale

The TIG for direct use is led by Klaus Regenauer-Lieb from the WAGCOE and Donald Payne from the University of Melbourne.

TIG 8 data management

TIG 8, led by Anthony Budd from Geoscience Australia, aims to assist the development of the Australian geothermal industry by simplifying data availability, usefulness and exchange through standards, database design, content, ongoing

enhancements and development of manipulation and interpretive tools. Some initiatives already completed through the TIG include the development of an extension to 3D GeoModeller to enable prediction of 3D temperature and heat flow from inputs of heat production and thermal conductivity. Future projects planned are to populate a heat flow database with new data, liaise with international parties working on geothermal data management for web interoperability standards and to build a data system within the Onshore Energy and Minerals Division of Geoscience Australia.

TIG 9 geothermal reservoir characterisation and engineering

Agreed terms of reference for this TIG are to facilitate collaboration and information exchange on topics including, but not limited to,

- Reservoir characterisation and modelling including 3D stochastic modelling and the simulation of fracture networks
- Fracture stimulation with emphasis on design and modelling
- Geochemistry, corrosion and scaling covering both the geothermal plant and equipment and the rock-fluid interaction in the reservoir.

Some projects planned by the TIG include to compile and evaluate a list of available numerical models (algorithms) for fracture characterisation, scan for pre-existing geothermal data handbooks and build up to include information learnt from overseas projects and to date from Australian projects, promote international collaboration through exchanges and develop 3D stochastic modelling and simulation of fracture networks and fracture propagation in crystalline rocks. Peter Dowd from the University of Adelaide is the leader of this TIG.

TIG 10 exploration technologies

TIG 10 aims to cooperate in studies to advance geothermal methods and technologies: including the indirect detection of subsurface properties to delineate prospective trends; to develop, collect, improve and disseminate geothermal-related information; to identify opportunities to facilitate the efficient advancement of geothermal energy projects; and to disseminate information on geothermal energy in Australia and internationally by way of workshops, and open interchange of experiences and ideas generated within the Australian community. The group have held a number of successful workshops and have been actively defining the research focus of the TIG. A few topics that are the focus of the group include:

- geophysical and geological methods to reduce exploration risks prior to deep drilling

- investigating the possible use of satellite and airborne systems to measure surface radiation to detect high heat producing granites in the sub-surface
- the use of magneto-telluric survey data to identify and locate conductive fluids in fractured rocks
- collection and processing of micro-seismic data around geothermal projects.

Des Fitzgerald from Intrepid Geophysics leads TIG 10.

TIG 11 drilling and well construction

TIG 11 has been very active and has regular meetings to advance the group's objectives. Topics in scope for the TIG include, but are not limited to:

- Lower Cost Drilling: Investigate techniques and new technologies which may lead to a reduction in costs to drill geothermal wells.
- Zonal Isolation and Packers: Isolation techniques and equipment need to be developed to isolate zones of interest, at extremely high temperatures and possibly pressures, to allow both stimulation and production through different zones.
- Temporary Sealing of Fractures: Develop a non-damaging means of isolating fractures where multiple fractures/ loss zones may be encountered.
- Cutting Exploration Drilling Costs: A number of mechanisms can be developed to reduce costs, such as improving ROP, utilising smaller rigs, smaller hole sizes, correct selection of materials.

The two projects that will be the focus for the coming year are to progress the slimhole drilling group and organise a drilling workshop. TIG 11 is led by Dean Hindle and Melanie Vonhethoff from Geodynamics.

TIG 12 education

TIG 12 was recently formed to work on the topics of education for the geothermal sector and encompasses topics such as defining the education needs for the industry, the development of courses either at tertiary or postgraduate level or short courses for industry. The TIG would coordinate with aligned international programs and facilitate the initiation & promotion of occasional society lunches with guest speakers.

For more information about any of the Technical Interest Groups please see: www.geothermal.pir.sa.gov.au/ageg or contact pirsa.ageg@sa.gov.au.

References

Department of Resources, Energy and Tourism (DRET), 2008, Australian Geothermal Industry Development Framework, and, Australian Geothermal Industry Technology Roadmap, Commonwealth of Australia, Canberra.

Australian Geothermal Reporting Code Committee (AGRCC), 2008, The Geothermal Reporting Code. Australian Geothermal Energy Group, Adelaide.

Hunt, S.P. and Morelli C.P, 2006, Cooper Basin HDR hazard evaluation: predictive modelling of local stress changes due to HFR geothermal energy operations in South Australia. Report Book 2006/16. Department of Primary Industries and Resources South Australia, Adelaide.

Morelli, C.P., 2009, Analysis and management of seismic risks associated with engineered geothermal system operations in South Australia. Report Book 2009/11. Department of Primary Industries and Resources South Australia, Adelaide.

Comparative petrology & geochemistry of high heat-producing granites in Australia & Europe

V Marshall^{*1,2}, J Van Zyl^{1,2}, SE Bryan³, T Uysal^{1,2}, M Gasparon^{1,2}

1. Queensland Geothermal Energy Centre of Excellence, The University of Queensland, St Lucia, QLD 4072

2. School of Earth Sciences, The University of Queensland, St Lucia, QLD 4072

3. Queensland University of Technology, Biogeoscience, GPO Box 2434, Brisbane, QLD 4001

To better understand the origin, tectonic setting and generation of high heat-producing granites (HHPG) and provide target criteria for the exploration of granite-hosted Enhanced Geothermal Systems (EGS), Australian examples are being studied and compared with better known European analogues that are being re-examined.

Three areas of long-standing interest for EGS in Europe are Cornwall, UK; Soultz-sous-Forêts, France; and the Erzgebirge, Germany. These areas have higher than average heat flow (at surface and depth), and concentrations of the main heat-producing elements Uranium (U), Thorium (Th) and Potassium (K) in granitic rocks. The Big Lake granite suite of the central Australian Cooper Basin (Gatehouse et al., 1995), is a pre-eminent HHPG target for EGS development in Australia. The Big Lake Suite granites are Australia's hottest with temperatures of >250°C at ~4km depth (Habanero 1, (Baisch et al., 2006). The Soultz-sous-Forêts and Cooper Basin systems have in common an insulating sediment cover of several kilometres.

Keywords: high heat-producing granites (HHPG), Cooper Basin, Cornwall, Soultz-sous-Forêts, Erzgebirge, Uranium, Thorium, Permo-Carboniferous, intraplate.

Background

The development of EGS in the Cooper Basin was started by Geodynamics Ltd in 2002 with the aim to be the first Australian Company producing electricity from EGS sources. Their first geothermal well (Habanero 1) encountered granite at depth. The granite (Big Lake Suite) is situated in the Nappamerrie trough (Meixner et al., 2000; Sun, 1997) and intruded into the Cambrian – Ordovician Warburton Basin (Gatehouse et al., 1995). The Big Lake Suite Granite is covered by a ~3km thick sedimentary package consisting of the Cooper (Late Carboniferous – Middle Triassic), Eromanga (Early Jurassic) and Lake Eyre (Early Tertiary - Holocene) Basins. U/Pb series dating of zircon of granite intersected at depth in two wells established a Permo-Carboniferous age ranging between 323±5 Ma and 298±4 (Gatehouse et al., 1995).

The Cornubian batholith in Cornwall (SW England; Fig. 1) is comprised of six plutons

ranging in age from 293.1±1.3 Ma to 274.5±1.4 Ma, based on U/Pb dating of magmatic monazites (Chen et al., 1993). Two plutons of interest are the Carnmenellis and Land's End granites (Fig. 2) as they contain the highest levels of U and Th (Table 1). During the 1970's and 1980's the Rosemanowes area of the Carnmenellis granite was a test site for the Department of Energy, European Commission and Cambourne School of Mines investigation into EGS technology as it has the highest heat flow in England, over 120 mW/m² (Tenzer, 2001).

Soultz-sous-Forêts (Fig. 1) has been the European test site for EGS since 1987, with temperatures of 200°C at 5 km depth (Antics and Sanner, 2007).

The granites of the Erzgebirge region (Fig. 1), like Cornwall, are associated with Tin (Sn), Tungsten (W), Lead (Pb), Zinc (Zn), Fluorine (F), Barium (Ba) and U mineralisation, with the high U and Th contents and crustal heat flow values giving added prospectivity as a clean energy resource.

Tectonic History

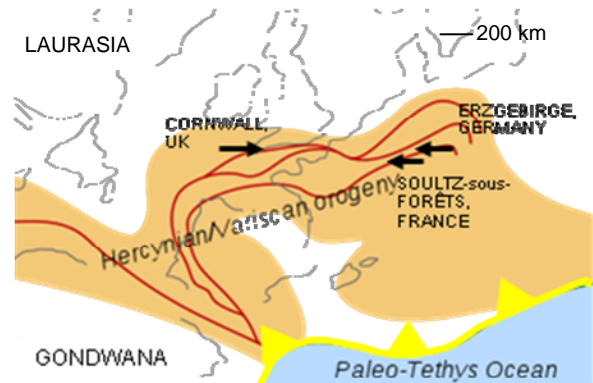


Figure 1: Location of the Hercynian/ Variscan mountain chains in the middle of the Carboniferous period. Red lines are sutures. Yellow line is subduction zone (triangles point in direction of subduction) (Scotese, 2001). Adapted from Matte (2001) and Zeigler (1990).

Regionally, the European granites were emplaced in an extensional environment between 334-270 Ma following collision of Laurasia and Gondwana to form the supercontinent Pangaea (Willis-Richards and Jackson, 1989). This collisional event, known as the Variscan (Hercynian) orogeny, resulted in an extensive rift system within the northern foreland of the Variscan

orogenic belt following termination of orogenic activity (Wilson et al., 2004).

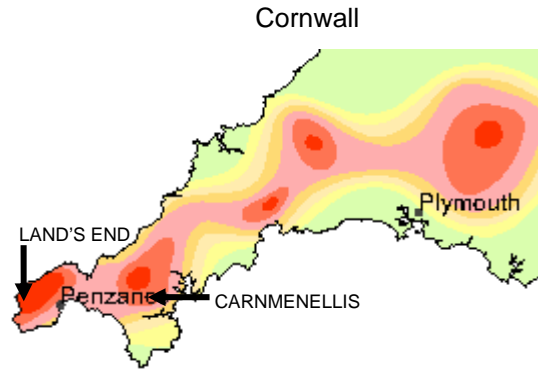


Figure 2: Heat flow map of Cornwall, UK, showing the location of the Carnmenellis and Land's End plutons. Heat flow of >120 mW/m² (deep red), to 60-70 mW/m² (green). Adapted from British Geological Survey GIS heat flow map, 2010.

The Cornubian batholith was emplaced at the end of the Variscan orogeny terminating a period of regional, back-arc continental extension during the Devonian and Early Carboniferous, (Darbyshire and Shepherd, 1985).

This orogenic event caused crustal thickening (Willis-Richards and Jackson, 1989) and has been suspected to have caused anatexic melting (Clark et al., 1993).

Figure 1 shows that at the time of emplacement the Cornubian granites were over 1350 km away from the nearest active plate margin (bounding the Neo-Tethys), suggesting they are not subduction related.

Soultz-sous-Forêts

The Soultz-sous-Forêts granites lie within the Upper Rhine Graben, a tectonically reactivated region associated with Oligocene crustal extension and thinning (Genter et al., 2003). These granites were emplaced slightly prior to those in Cornwall following the Variscan orogeny, from 334 +3.8/-3.5 Ma (U/Pb monzogranite) to 319.8±0.6 Ma (⁴⁰Ar/³⁹Ar), (Cocherie et al., 2004 and Stussi et al., 2002).

Erzgebirge

The Erzgebirge granites were also intruded from the Late Carboniferous to Early Permian during large-scale extension following orogenic collapse (Förster et al., 1999b). In addition, wrenching was associated with granite emplacement (Edel et al., 2007).

Förster and Förster (2000) concluded that peak orogenic metamorphism occurred 350-340 Ma, followed by rapid uplift and cooling between 340 and 326 Ma with the oldest, post-collisional, granites intruded to a depth of 3-6 km at 325 Ma (Förster et al., 1999b).

Table 1 is a summary of relevant information for these areas of HHPG.

Granite Petrography

Cooper Basin

The samples studied from the Big Lake Suite have varying degrees of alteration, with alteration increasing with decreasing depth. Unaltered samples consist of quartz (31%), K-feldspar (31%) and plagioclase (31%), with minor biotite (5%) and accessory phases (2%). Accessory phases identified are magnetite, apatite, thorite/huttonite, zircon, monazite and xenotime with some fluorite.

The altered samples show varying degrees of sericitisation, ranging from minor replacement of the feldspars to complete replacement and the formation of illite. Biotite has altered to chlorite, after which chlorite is replaced by illite. Fresh biotite still exists in the altered samples, but is restricted to small inclusions in quartz. The illite from the Big Lake Suite alteration assemblage occurs as two main textures: 1) pseudomorphic and 2) cryptocrystalline.

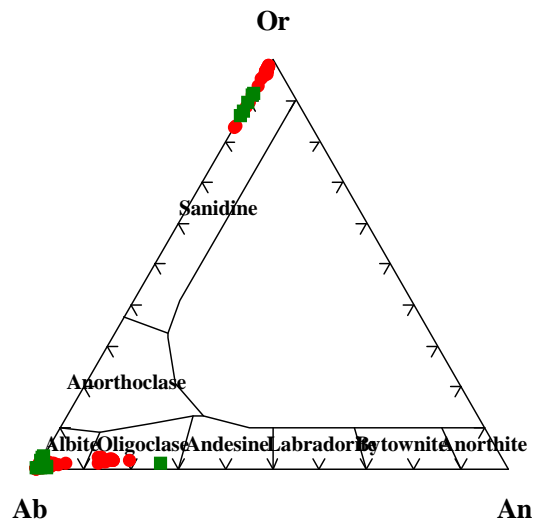


Figure 3: Feldspar classification diagram showing the feldspar composition. Cooper Basin (●) and Soultz-sous-Forêts (■) (Komninou and Yardley, 1997; Stussi et al., 2002).

Electron Probe Microanalysis (EPMA) data shows no compositional differences between the different illite textural types. Although illite does not show compositional differences between the textural types, there are two compositionally distinct illites - the first is a pure illite with low (<1%) to no Fe₂O₃T, and the second is an Fe-bearing illite (up to 7% Fe₂O₃T). The feldspars from the Cooper Basin are mainly partly albitised oligoclase, with the K-feldspar being microcline. Microcline occurs in some instances as graphic intergrowths with quartz indicating eutectic crystallisation of the granite. In some samples, the quartz from the Cooper Basin granites exhibits

Erzgebirge

undulose extinction, with some grains exhibiting planar deformation features.

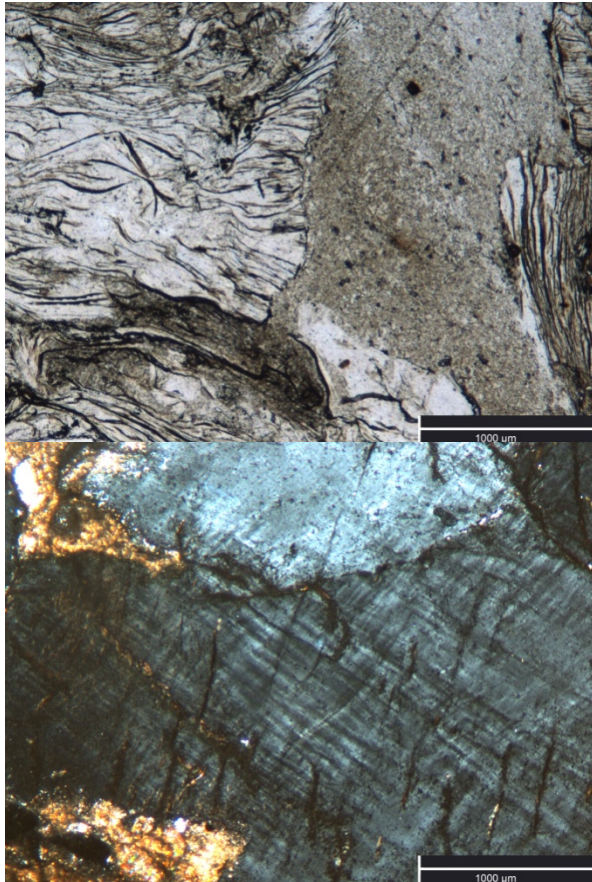


Figure 4: Photomicrographs of two illite textures (top), and planar deformation features in quartz (bottom) in Big Lake Suite granites.

Cornwall

The Carnmenellis granites generally contain around 34% quartz, 32% K-feldspar, 22% plagioclase, 6% biotite, 4% muscovite, 1% tourmaline and 1% accessory phases including andalusite, cordierite, ilmenite, zircon, monazite and uraninite (Charoy, 1985; Chappell and Hine, 2006). The radioactive mineral assemblage important for hosting Th and U are predominantly monazite, apatite, xenotime, zircon and uraninite (hosting ~90% of total U) (Jefferies, 1984; Martel et al., 1990), all of which are commonly associated with apatite and ilmenite (Jefferies, 1984).

Soultz-sous-Forêts

These granites have a normative composition of around 43% plagioclase (37% albite, 6% anorthite), 25% K-feldspar, 22% quartz, 6% biotite, 2% hornblende, and <1% of other minerals including titanite, apatite, magnetite and hematite (Stussi et al., 2002).

The accessory mineral phases important for hosting U and Th are relatively unknown, and will be investigated as part of this study.

The normative composition of the Erzgebirge granite is 36% quartz, 32% plagioclase, 29% K-feldspar, 2% biotite and <1% muscovite, with the remainder in accessory phases including apatite, zircon, monazite, opaques, xenotime and uraninite (Förster et al., 1999b).

Förster and Förster (2000) noted that ~90% of U and Th is bound in accessory minerals; 30-90% of U is fixed in uraninite, with the remainder present in monazite, xenotime, zircon and thorite; monazite hosts 80-90% of the Th budget, followed by allanite and thorite.

Granite Petrology

Cooper Basin

The Cooper Basin granites are peraluminous I-type granites based on mineralogy, but because of alteration it is difficult to distinguish between fractionated I-, A- or S-type (Fig. 5). The occurrence of hornblende, relative abundance of biotite and absence of distinctive aluminosilicate phases, suggests the granite suites are more likely fractionated I- to A-types. The Cooper Basin granites have a wide range in ACNK ($Al_2O_3 / (CaO + Na_2O + K_2O)$ molar) values from weakly (1.04) to strongly (1.98) peraluminous. The range in peraluminosity reflects the high degree of alteration in these samples, with significant leaching of calcium causing some samples to exhibit strongly peraluminous compositions. In contrast to most of the European granite examples, the Cooper Basin granites do show stronger “within plate” tectonomagmatic affinities (Fig. 6). However, Gatehouse et al. (1995) postulated that the Cooper Basin granites may be related to the Alice Springs Orogeny of central Australia, but based on available ages, the granites were emplaced at the end and after the 332–320 Ma climax of uplift in Central Australia (Veevers, 2009). The Cooper Basin granites range from less fractionated with lower total REE and small Eu anomalies to more fractionated with higher total REE and larger Eu anomalies (Figs 7 & 8).

Cornwall

The Cornubian granites have been described as S-type in character (Chappell and Hine, 2006, Fig. 6), reflecting a metasedimentary crustal source. Specifically, the granites are believed to have been derived by partial melting of aluminium-rich pelitic metasedimentary rocks deposited during the Carboniferous and Devonian in a tensional back-arc ensialic setting (Willis-Richards and Jackson, 1989). The Cornubian granites are highly evolved and strongly peraluminous, reflected by the presence of muscovite and cordierite (Charoy, 1995 and Stone, 1995). Recent fieldwork on the Land’s End pluton

confirmed Tammemagi and Smith's (1975) observations of abundant K-feldspar megacrysts in places. Some plutons have subhorizontal flow fabrics (e.g., St Austell granite) suggesting some granitic magma emplacement in sill-like or laccolithic bodies, and mineralogical and age variations indicate the batholith has been incrementally built.

Soultz-sous-Forêts

The Soultz-sous-Forêts granites have been classified as S-type according to tectonic discrimination diagrams (Fig. 6), however they are noted to have hornblende (Stussi et al., 2002) and oxidised K-feldspar, suggesting possible I- or A-type classification. They are also peraluminous and porphyritic, with K-feldspar megacrysts up to 80 mm in diameter. These granites are thought to have originated from either crustal partial melting of enriched metamorphic greywacke, granulite and amphibolite, or meta-igneous rocks of appropriate composition; however, a minor mantle contribution can't be excluded due to the negative

ϵ Nd values (Stussi et al., 2002). Subhorizontal magma fabric oriented to the NE was also noted suggesting either a laccolithic body or the roof of a diapir-like intrusion, in association with post-magmatic fracturing (Stussi et al., 2002).

Erzgebirge

The Erzgebirge granites are more varied, with mildly peraluminous transitional I- to S-types and strongly peraluminous S-types both present (Förster et al., 1999b, Fig. 5).

Förster et al. (1999b) also noted some granites have peraluminous A-type chemical affinities, consistent with the intraplate setting of this magmatism.

Förster and Förster (2000) recognised that the surface heat flow is higher where the granites occur, contributing 70-90 mW/m² to the surface heat flow - two to four times higher than would be estimated from the average composition of the continental bulk crust.

Table 1: Compositions of targeted HHPG for EGS. Sources: Charoy (1985), Chappell and Hine (2006), Jefferies (1984), Martel et al. (1990), Tammemagi and Smith (1975), Willis-Richards and Jackson (1989), Chen et al. (1993), Müller et al. (2006), Förster H.J. (1999), Förster and Förster (2000), Förster et al. (1999a), Förster et al. (1999b), Hooijkaas et al. (2006), Stussi et al. (2002), Uysal and van Zyl (unpubl. data), and Taylor and McLennan, (1985).

EGS TARGETED GRANITES	AGE (Ma)	LITHOLOGY	SiO ₂ (wt%)	K ₂ O (wt%)	U (ppm)	Th (ppm)
Carnmenellis Cornwall, UK	295-270	Megacrystic biotite and two-mica granites	70-76	4-4.3	4.3-35 (12.1 mean)	11-25 (19.3 mean)
Land's End Cornwall, UK	277-274.5	Early megacrystic biotite granites, younger Li-siderophyllite granites	66-73	3.5-6	6.9-38	4.4-46.2
Soultz-sous-Forêts Upper Rhine Graben, France	334-319	Porphyritic monzogranite	67-69	3.8-4	6.2-14.1	23-37
Erzgebirge, Germany	325-315	Transitional I-, S- and A- type biotite granites, two-mica granites and S- and A- type Li-mica granites	67-77 (biotite)	3.8-5.4	9-30.9	10.4-34.3
			71-76 (two-mica)			
			73-76 (Li-mica)			
Cooper Basin, Australia	323-298	Coarse grained two feldspar biotite granite, moderately weathered	-	-	11 - 27	17 - 117
Upper Continental Crust			66	3.4	2.7	10.7

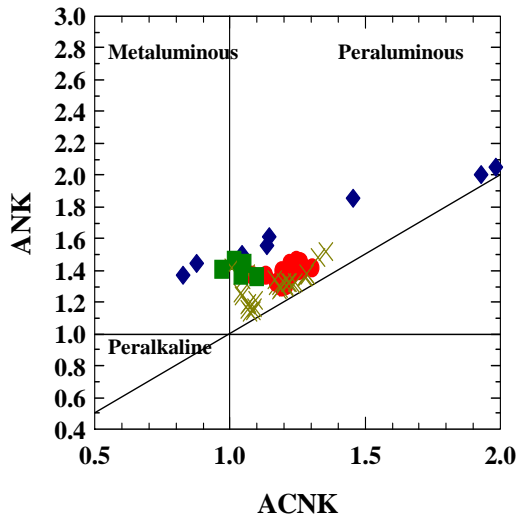


Figure 5: ASI index for granites classification plot according to Shand (1927), Cooper Basin (◆); Cocherie et al. (2004), Soulitz-sous-Forêts (■); Chappell and Hine (2006) and Müller et al. (2006), Cornwall (●); and Förster et al. (1999b) Erzgebirge (×).

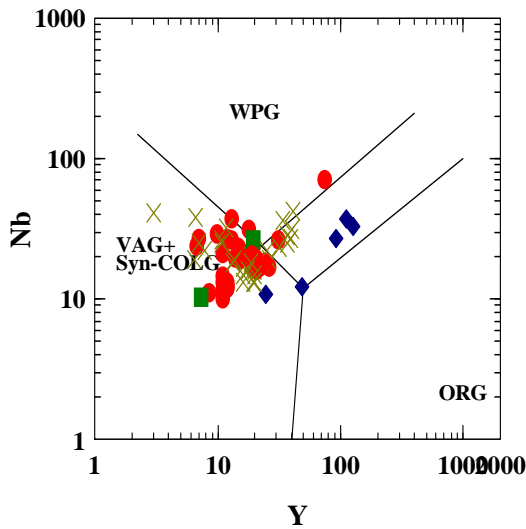


Figure 6: Tectonic discrimination diagram comparing the studied granite suites (Pearce et al., 1984).

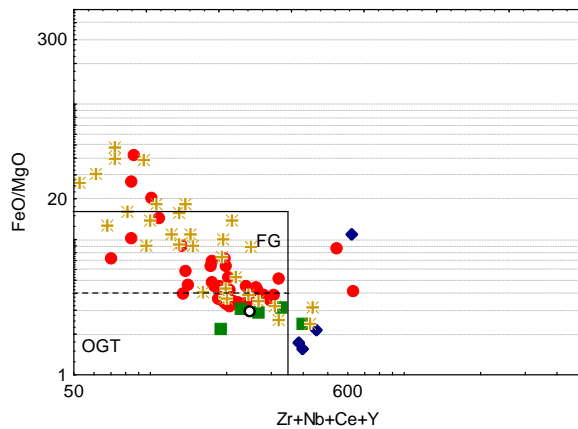


Figure 7: Granite discrimination plot from Whalen et al. (1987) OGT - Other Granite Types (I-, M-, S- type), FG - Fractionated Felsic Granites.

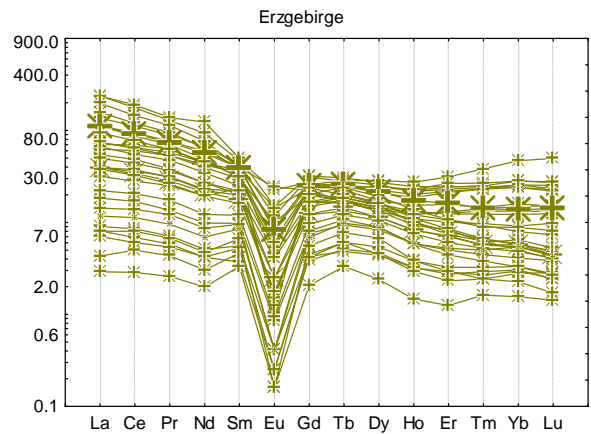
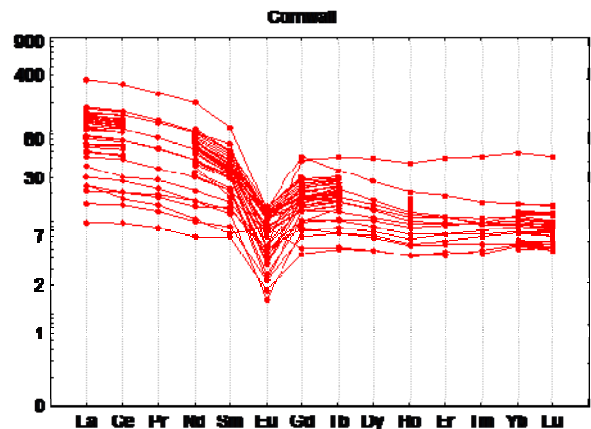
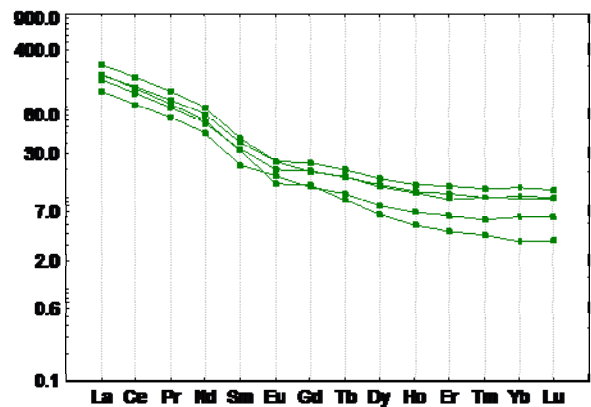
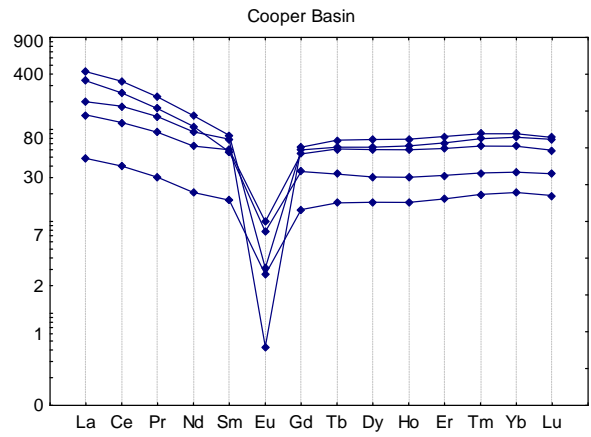


Figure 8: REE Spider plots for the four granite intrusions. Normalisation was performed using McDonough and Sun (1995).

Discussion and Comparison

- Both European and Australian examples of HHPG are Late Carboniferous to Early Permian in age.
- All HHPG in this study were emplaced well in board from active plate margins. The European granites are post-collisional and extension-related, whereas the Cooper Basin granites are also within-plate but may be (temporally) related to intraplate deformation.
- The Cooper Basin, Soultz-sous-Forêts and the Erzgebirge show similar abundances of quartz, plagioclase and K-feldspar, with plagioclase being the more abundant phase in Soultz-sous-Forêts. The Cooper Basin and Erzgebirge are equigranular, whereas Soultz-sous-Forêts and the Carnmenellis are distinctly megacrystic granites.
- It is difficult to use the I- and S- type classification for fractionated granites, but this study suggests all the granites are peraluminous, with the European granites dominantly S-type, but Cooper Basin and Erzgebirge also showing I- and A- type affinities suggesting that crustal source composition may not be a prime control on HHPG generation.
- Literature and field observations indicate that at least part of the Cornubian and Soultz-sous-Forêts granites have sill-like intrusive components but importantly, that all the batholiths discussed here have been incrementally built by a number of intrusions.
- Trace element geochemistry and rare earth element abundances of the Cooper Basin granites show a range from less fractionated to highly fractionated ($Eu/Eu^* = 0.04$ to 0.17), whereas Soultz-sous-Forêts show more uniform REE patterns, and a wide range of REE patterns have been described for the Erzgebirge granites. The Carnmenellis has a narrower range in REE than the Erzgebirge. The Cooper Basin, Carnmenellis and Erzgebirge all show strong Eu anomalies indicating fractional crystallisation was important in the production of these granites (Fig. 7).
- Isotope data suggests that all examples have crustal signatures.
- The Cooper Basin granites are more enriched in Th, but there is similar U enrichment for all examples. Currently, the reason for U and Th enrichment is unknown, except for the normal fractional crystallisation processes.

The current conclusion from this study is that the peraluminous, highly fractionated chemistries have promoted the U and Th enrichment of HHPG.

References

- Antics, M., and Sanner, B., 2007, Status of geothermal energy use and resources in Europe, Proceedings European Geothermal Congress, 2
- Baisch, S., Weidler, R., Vörös, R., Wyborn, D. and de Graaf, L., 2006. Induced Seismicity during the Stimulation of a Geothermal HFR Reservoir in the Cooper Basin, Australia. Bulletin of the Seismological Society of America, 96(6): 15.
- Bartier, D. et al., 2008. Hydrothermal alteration of the Soultz-sous-Forêts granite (Hot Fractured Rock geothermal exchanger) into a tosudite and illite assemblage. European Journal of Mineralogy, 20: 12
- Charoy, B., 1985, The genesis of the Cornubian Batholith (south-west England): the example of the Carnmenellis Pluton, Journal of Petrology, 27, Part 3, 571-604
- Chappel, B.W. and Hine, 2006, The Cornubian Batholith: An Example of Magmatic Fractionation on Crustal Scale, Resource Geology, 56, 203-244
- Chappell, B.W. and White, A.J.R., 2001. Two Contrasting granite types: 25 years later. Australian Journal of Earth Sciences, 48: 12.
- Chen Y., Clark, A.H., Farrar, E., Wasteneys, H.A.H.P., Hodgson, M.J. and Bromley, A.V., 1993, Diachronous and independent histories of plutonism and mineralisation in the Cornubian Batholith, southwest England, Journal of the Geological Society, 150, 1183-1191
- Clark, A.H., Chen, Y., Farrar, E., Wasteneys, H.A.H.P., Stimac, J.A., Hodgson, M.J., Willis-Richards, J., and Bromley, A.V., 1993, The Cornubian Sn-Cu (-As, W) metallogenetic province: product of a 30 M.Y. history of discrete and concomitant anatectic, intrusive and hydrothermal events, Proceedings of the Ussher Society, 8, 112-116
- Cocherie, A., Guerrot, C., Fanning, C.M. and Genter, A., 2004, Datation U-Pb des deux faciès du granite de Soultz (Fossé rhénan, France), Géochimie (Géochronologie), 336, 775-787
- Darbyshire, D.P.F., and Shepherd, T.J., 1985, Chronology of granite magmatism and associated mineralisation, SW England, Journal of the Geological Society, 142, 1159-1177
- Edel, J.B., Schulmann, K. and Rotstein, Y., 2007, The Variscan tectonic inheritance of the Upper Rhine Graben: evidence of reactivations in the Lias, Late Eocene-Oligocene up to the recent, International Journal of Earth Science, 96, 305-325
- Förster H.J., 1999, The chemical composition of uraninite in Variscan granites of the Erzgebirge, Germany, Mineralogical Magazine, 63, 2, 239-252

- Förster, H.J., Davis, J.C., Tischendorf, G., and Seltmann, R., 1999a, Multivariate analyses of Erzgebirge granite and rhyolite composition: implications for classification of granites and their genetic relations, *Computers and Geosciences*, 25, 533-546
- Förster H.J., Tischendorf, R.B., Trumbull, R.B. and Gottesmann, B., 1999b, Late-collisional granites in the Variscan Erzgebirge, Germany, *Journal of Petrology*, 40, 11, 1613-1645
- Förster, A. and Förster H.J., 2000, Crustal composition and mantle heat flow: Implications from surface heat flow and radiogenic heat production in the Variscan Erzgebirge (Germany), *Journal of Geophysical Research*, 105, B12, 27,917-27,938
- Gatehouse, C.G., Fanning, C.M. and Flint, R.B., 1995. Geochronology of the Big Lake Suite, Warburton Basin, northeastern South Australia. . *Quarterly Geological Notes of the Geological Survey of South Australia*, 128: 7.
- Genter, A., Guillou-Frottier, L., Feybesse, J-L., Nicol, N., Dezayes, C. and Schwartz, S., 2003, Typology of potential hot fractured rock resources in Europe, *Geothermics*, 32, 701-710
- Ghosh, P.K., 1934, The Carnmenellis Granite: its petrology, metamorphism and tectonics, *Quarterly Journal of the Geological Society*, 90, 240-273
- Hooijkaas, G.R., Genter, A. and Dezayes, C., 2006, Deep-seated geology of the granite intrusions at the Soultz EGS site based on data from 5 km-deep boreholes, *Geothermics*, 35, 484-506
- Komninou, A. and Yardley, B.W.D., 1997. Fluid-rock interactions in the Rhine Graben: A thermodynamic model of the hydrothermal alteration observed in deep drilling. *Geochimica et Cosmochimica Acta*, 61(3): 17
- Jefferies, N.L., 1984, The radioactive mineral assemblage of the Carnmenellis Granite, Cornwall, *Proceedings of the Ussher Society*, 6, 35-40
- Martel, D.J., O'Nions, R.K., Hilton, D.R. and Oxburgh, E.R., 1990, The role of element distribution in production and release of radiogenic helium: the Carnmenellis Granite, southwest England, *Chemical Geology*, 88, 207-221
- Matte, P., 2001, The Variscan collage and orogeny (480 – 290 Ma) and the tectonic definition of the Armorica microplate; a review, *Terra Nova*, 13, 122-128
- McLaren, S. and Dunlap, W.J., 2006. Use of ⁴⁰Ar/³⁹Ar K-Feldspar thermochronology in the basin thermal history reconstruction: an example from the Big Lake Suite Granites, Warburton Basin, South Australia. *Basin Research*, 18: 15.
- Meixner, T.J. et al., 2000. The Nature of the Basement to the Cooper Basin region, South Australia. *Exploration Geophysics*, 31: 9.
- Müller, A., Seltmann, R., Halls, C., Siebel, W., Dulski, P., Jeffries, T., Spratt, J. and Kronz, A., 2006, The magmatic evolution of the Land's End pluton, Cornwall, and associated pre-enrichment of metals, *Ore Geology Reviews*, 28, 329-367
- Pearce, J.A., Harris, N.B.W. and Tindle, A.G., 1984. Trace Element Discrimination Diagrams for the Tectonic Interpretation of Granitic Rocks. *Journal of Petrology*, 25(4): 28.
- Scotese, C.R., 2001, Late Carboniferous: Atlas of Earth History, 1, *Paleogeography, PALEOMAP Project*, 52
- Stussi, J.M., Cheilletz, A., Royer, J.J., Chevremont, P. and Feraud, G., 2002. The Hidden monzogranite of Soultz-sous-Forêts (Rhine Graben, France). *Géologie de la France*(1): 19.
- Sun, X., 1997. Structural style of the Warburton Basin and control on the Cooper and Eromanga Basins, South Australia. *Exploration Geophysics*, 28: 6
- Tammemagi, H.Y. and Smith, N.L., 1975, A radiogeologic study of the granites of SW. England, *Journal of the Geological Society*, 131. 415-427
- Taylor, S.R. and McLennan, S.M., 1985, *The Continental Crust: its Composition and Evolution*, Blackwell Scientific Publications, 46
- Tenzer, H., 2001, Development of hot dry rock technology, *GHC Bulletin*, 18
- Whalen, J.B., Currie, K.L. and Chappell, B.W., 1987. A-Type granites: Geochemical characteristics, discrimination and petrogenesis. *Contributions to Mineralogy and Petrology*, 95: 13
- Willis-Richards, J. and Jackson, N.J., 1989, Evolution of the Cornubian ore field, southwest England: Part I. Batholith modelling and ore distribution, *Economic Geology*, 84, 1078-1100
- Wilson, M., Neumann, E. R., Davies, G. R., Timmerman, M. J., Heeremans, M., and Larsen, B. T., 2004, Permo-Carboniferous magmatism and rifting in Europe: introduction, *The Geological Society, London, Special Publication*, 223, 1-10
- Veevers, J.J., 2009, Mid-Carboniferous Centralian uplift linked by U-Pb zircon chronology to the onset of Australian glaciation and glacio-eustasy, *Australian Journal of Earth Sciences*, 56, 711–717.
- Zeigler, P.A., 1990, *Geological Atlas of Western and Central Europe*, Shell International Petroleum Maatschappij BV (2nd edition)

Geothermal Prospection Using Existing Groundwater Geochemical and Thermal Datasets: Identifying Regions of Interest in Queensland from Government Well and Bore Data**

Craig McClarren^{1,2}, Massimo Gasparon^{1,2,3}, and I. Tonguç Uysal^{1,2}

¹ School of Earth Sciences, The University of Queensland, Brisbane, QLD. 4072

² Queensland Geothermal Energy Centre of Excellence, The University of Queensland, Brisbane, QLD. 4072

³ National Centre for Groundwater Research and Training, The University of Queensland, Brisbane, QLD. 4072

Geochemical analysis of well and bore waters has the potential to provide valuable clues in identifying regions of high geothermal potential. Chemical and isotopic markers indicative of the presence of high heat producing granites or other heat producing bodies may be mobilized by flowing groundwater and may make their way to deep wells and bores. Though likely highly diluted, these markers may also be detectable in shallow wells and bores in some regions depending on local geological and hydrological conditions. A significant quantity of data of this type already exists in publicly available government databases. These data are often coarse and of frequently unknown quality, but may prove to be a useful tool in first-order large-scale geothermal prospection. We have obtained such a dataset from the Queensland Department of Environment and Resource Management, and have extensively analysed the data with the aim of identifying potential areas of interest in geothermal prospection. This research represents the first stage of a large multi-stage project in groundwater geochemistry aimed at geothermal prospection.

Keywords: Geothermal exploration, bore water, trace element, isotope, Queensland

The Potential for Groundwater Geochemistry in Geothermal Prospecting

Geochemical analysis of groundwater may hold significant potential for identification of unrecognized regions of high geothermal potential. Geothermal source rocks, whether sedimentary, radiogenic igneous, or young igneous, produce mineralogical, chemical, and isotopic markers which can be used to identify them (Marini, L.). Many of these markers are water soluble and can thus be moved from depth toward the surface (Barbier, et. al, 1983). During the process, these markers may suffer significant dilution, but may still be detectable in groundwater samples taken at or near these thermally significant regions (Smedley, P., 1991).

Thousands of ground water samples from across Queensland have already been taken and analysed for a limited range of water quality parameters; this data can be obtained from the State Government for research purposes. By providing chemical analysis results from almost 28,000 water wells and bores across the state, the Queensland Department of Environment and Resource Management (DERM) water borehole database is a locally unparalleled resource for conducting a large-scale first-order type investigation and identification of geothermally prospective regions within the state.

Geochemical tools

While there are dozens of mineralogical, chemical, and isotopic markers that can be used to identify potential geothermal targets, in using the data available from the DERM water borehole database, one is restricted to the limited set of parameters measured. The quality and completeness of the chemical data can be described as highly variable, with results collected and analysed by many different parties using unknown procedures over the course of several decades. Moreover, the results themselves are inconsistent between analyses, with measurements for elements such as boron and phosphorous making occasional appearances while largely remaining absent from the rest of the dataset.

While the quality of measurements may be called into question, the abundance of analyses, as well as their geographic population density in many regions, suggests that the data may still be cautiously used on a large scale (typically a few thousand square kilometres at best) to identify sources of heat at depth. From the database, initially a large number of known indicators of geothermal potential, used extensively internationally, were selected. These include the elements and compounds Na, K, Cl, F, Cu, SO₄, Zn, PO₄, and B. While it was readily acknowledged that many of these elements may be associated to non-geothermally indicative sources, the rationale for this analysis is that where a large number of notably high concentration values for these elements overlapped, these areas would be most worthy of further investigation.

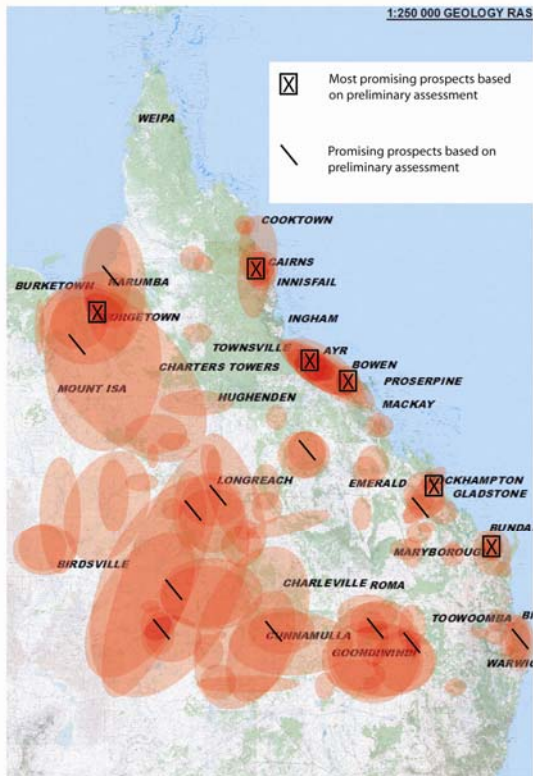


Figure 1: Early map of regions to contain potential geothermal resources based on unfiltered geochemical data. The image was composed by colouring regions with the highest potential for each selected element or compound and then overlaying all of the layers. Diagonal hashes indicate slightly promising regions while boxed X's are the most promising regions based on this early analysis.

Refining the data

With this preliminary analysis of data completed, maps of individual elements were more closely studied to assess their suitability as potential indicators of associated geothermal systems. Na and K were first discarded because of the tremendous abundance of possible alternative sources. Cl was next discarded because of its close relationship with K and Na. PO_4 was next removed as data on this element throughout the dataset was extremely sparse and because the highest values tended to be in wetter, more tropical, parts of Queensland which may simply reflect the infiltration of organic phosphate from the surface into a shallow watertable. Zn was removed both for its scarcity of data as well as for not showing any distinguishable trends or patterns when concentrations were mapped. While Cu concentration showed possibly promising results, again the data was relatively sparse. SO_4 did not show clear trends and has many possible sources, so it was initially removed. One potential source of sulphate, however, are coal measures which are known to be effective cap units to

geothermal reservoirs. Thus, sulphate data may be revisited in the future to analyse the suitability of a geothermally interesting site to future exploitation.

It was finally decided to focus primarily on boron (B) and fluoride (F^-), which are both relatively soluble and abundant in felsic igneous bodies. Boron data, though somewhat sparse, shows easily distinguished trends (non-random geographical and/or geological distributions) when mapped. Fluoride data is abundant and also shows easily distinguished trends when mapped. It was additionally decided that F^- would be most indicative of buried high heat producing granites (HHPGs) at depth, as there are fewer likely alternative sources for F^- than for B.

Filtering the data

The aim of this research is two-fold. First, it is to identify potential regions of geothermal interest and secondly to identify regions on which to focus future sampling work for later stages of this research project (the details of which will be discussed elsewhere). The first filter applied was the most fundamental: many of the bores in the database were no longer existing, but were categorized as "Abandoned and Destroyed." These entries were removed as they were of no practical use to us, in that the results could not be verified by future sampling. Wells that were classified as "Existing" or "Abandoned but Useable" were left in the set. The next filter applied was for F^- concentration; after some consultation and discussion within the group, a value of 1.4 ppm was decided upon as a lower limit for water chemistries we deemed "interesting". The choice of this value significantly reduced the dataset, but left behind more than 3500 values showing easily distinguishable trends and patterns when mapped across Queensland. High values around known igneous regions, such as the Stanthorpe Granite Belt and the more recently active Cairns region, strongly suggests that this could be an extremely valuable tool in identifying igneous bodies at depth elsewhere. High values in regions not already known to contain intrusive bodies will be investigated.

The next filter applied was depth as it is likely that with greater depth comes a lower likelihood of significant dilution of circulating or simply flowing groundwater by local and relatively recent meteoric waters. Entries with bore depths of less than 10 meters were removed; however, because many entries do not have a recorded depth (and thus receive a value of zero through intermediate processing steps), values of zero were left so that wells of unrecorded depth, of which there are many, would remain. Next, because at or near HHPGs we expect to find elevated B concentrations in groundwaters, the sites with the lowest B values were removed from the remaining dataset. A cut-off of 0.3 ppm B was chosen to

remove the sites least likely to show evidence of a nearby HHPG; similar to the filter for depth, values of zero were left as most of the sites sampled for F⁻ content unfortunately do not show B results.

Finally, with purely the aim of sample access in mind the category of “owner” needed to be filtered. Location and ownership information is provided with the data; however access to the monitoring bores is restricted to DERM staff. With these data filtered out, most of the prospective sampling sites along coastal Queensland are removed; the majority of the inland bores, which are usually privately owned, remain, allowing us to extensively investigate most of the geochemically interesting regions within the state. Coastal regions, with close proximity to population centres, however, are thereby restricted.

prove useful when considered together with geochemical data in the future.

In addition to water bore and well data from DERM, there are also publically available data from exploratory coal, oil, and gas drilling in the Queensland Petroleum Exploration Database (QPED) from the Queensland Department of Mines and Energy (DME). These data include temperature results as well as geochemical analyses; because of their extremely limited geographic distribution, however, this dataset is unsuitable to state-wide geothermal prospection. A high concentration of data points in the Great Artesian Basin in Queensland’s Southwest corner may prove useful to individuals or groups investigating this known region of high geothermal potential. In a far more local context, QPED well completion reports may prove valuable as an early investigatory step in areas where such drilling has been conducted.

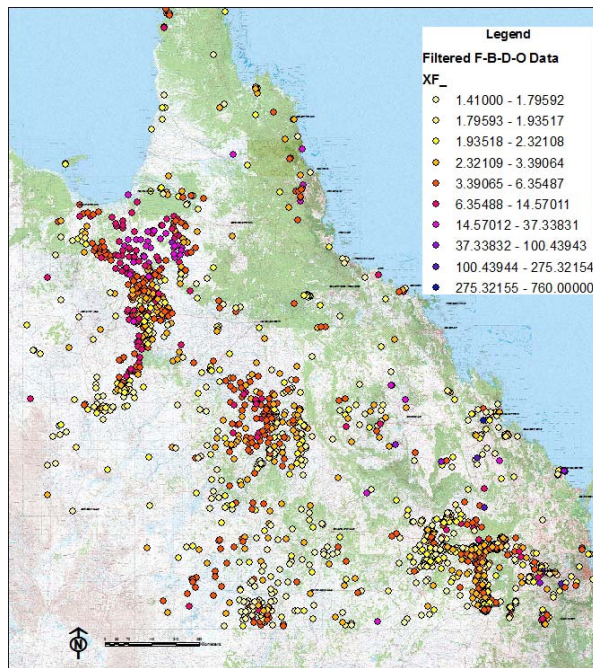


Figure 2: Water well and bore data across Queensland filtered for Fluorine and Boron content, depth, and “owner”. The colour scale is for Fluorine content in ppm.

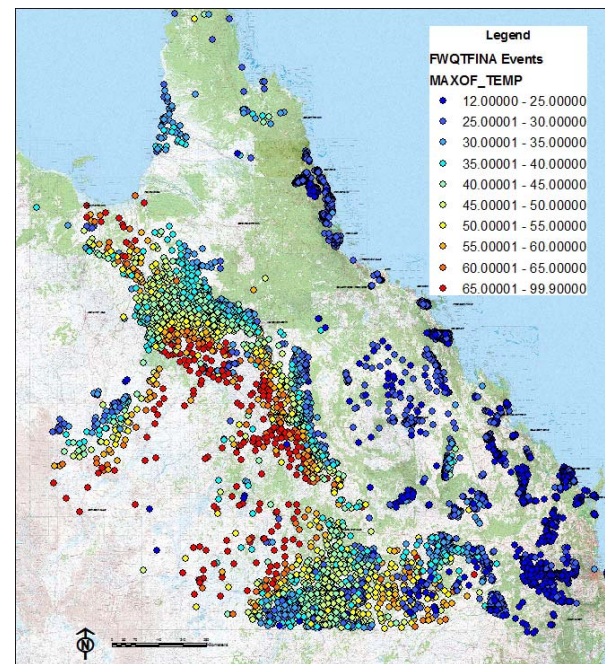


Figure 3: Unfiltered water well and bore thermal data across Queensland. The map shows maximum temperatures recorded at each site; the colour scale is for water temperature in degrees Celsius.

Hydrothermal Data and Results from Other Datasets

As well as geochemical analyses of water bores throughout the state, the DERM dataset also contains water temperature data from many of these same bores. These data, however, are of limited value due to the limitations of bore depth; water temperatures are low throughout coastal Queensland and rise rather predictably with distance inland, likely reflecting the increasing depth to the water table rather than a significant geothermal gradient. These data, however, may

Summary

An extensive dataset comprising thermal and geochemical analyses of public and privately owned water wells and bores from across the state of Queensland is publicly available from the Queensland Department of Environment and Resource Management. While the thermal data have limited potential in geothermal prospection due to the depth-dependent nature of the measurements, the geochemical dataset may be

of tremendous value. Chemical markers indicative of HHPGs or other heat producing bodies may be mobilized by flowing groundwater, making their way to deep wells and bores. Though likely diluted, these markers may also be detectable in shallow wells and bores depending on local geological and hydrological conditions.

We have analysed the available dataset, choosing to focus primarily on fluoride and boron concentrations, as a first-order exploratory tool to identify regions potentially containing geothermal resources and to identify sites and regions for future sampling and geochemical analysis towards that end. Several filters were put in place, reducing the extensive dataset to a more manageable and consistent size and nature.

The Queensland Petroleum and Exploration Database publically available from the Department of Mines and Energy is not suitable for state-wide geothermal prospection due to the geographic distribution of sampling sites, but may be of significant local value in Southwest Queensland.

References

Barbier, E., Fanelli, M., Gouffier, R., 1983, Isotopes in Geothermal Energy Exploration, IAEA Bulletin, v. 25, no. 2, pp. 31-36

Marini, L., Geochemical Techniques for the Exploration and Exploitation of Geothermal Energy, Dipartimento per lo Studio del Territorio e delle sue Risorse, Università degli Studi di Genova, Genova, Italy

Smedley, P., 1991, The Geochemistry of Rare Earth Elements in Groundwater from the Carnmenellis Area, Southwest England, *Geochimica et Cosmochimica Acta*, v. 55, pp. 2767-2779

* Based on or contains data provided by the State of Queensland (Department of Environment and Resource Management) [2009]. In consideration of the State permitting use of this data you acknowledge and agree that the State gives no warranty in relation to the data (including accuracy, reliability, completeness, currency or suitability) and accepts no liability (including without limitation, liability in negligence) for any loss, damage or costs (including consequential damage) relating to any use of the data. Data must not be used for direct marketing or be used in breach of the privacy laws.

+ Based on or contains data provided by the State of Queensland (Department of Employment, Economic Development and Innovation) [2009] which gives no warranty in relation to the data

Genie Impact Drills Synopsis of a New Hard Rock Drilling Development

Malcolm B McInnes FIEAust. CPEng MEng BE ARMIT Mech Eng MAIE SPE
Specialised Drilling Services Australia Pty Ltd
PO BOX 297, Fullarton, South Australia 5063, Australia.

Abstract

In 2004, a lean new Australian company was established to independently focus on the development and commercialisation of new drilling technology for the geothermal, petroleum & scientific industries. It began with assets including know-how, intellectual property, documentation and some equipment retained from pioneering work undertaken in the parent company between 1992 and 2002. It has produced a new commercial product, the Genie 185, a drilling liquid powered impact drill, the first in a range of new, high performance tools which offer higher Rates Of Penetration and simpler, lighter drill strings for hard formation drilling.

Purpose

To build a profitable commercial enterprise based on the development and provision of superior quality drilling services & products to the petroleum, geothermal and scientific industries.

Geothermal power market

Australian geothermal wells are being drilled to depths of around 4,500m but financial viability of hard fractured rock reservoirs is threatened by low Rates Of Penetration and problems associated with traditional rotary drilling systems in these environments.

Technology

High ROP, drilling liquid powered impact drilling systems for harder formations.

Product

Rented, on-site supported, fully serviced & equipped Genie impact drills and bit sales. .

Genie impact drill

Conceived and designed as a flexibly sized tool to create a range rather than a series of successive individually designed tools. The design is disciplined and imbedded in the drawings of the definitive, mid-range Genie 185 (for bits between 8-1/2" & 9-7/8"). See Fig. 1. There are fewer parts than in predecessor tools as well as enhanced bit alignment, new hard surface designs and treatments, corrosion protection, simple and secure jet nozzle mounting, longer tong grip zone and new assembly system for easy, fast and safe maintenance and set-up. A general mathematical model generates hydraulic & dynamic performance simulations which are used with a well model for application checks & set-up.



FIG. 1 – TALISMAN ENERGY INC WITH GENIE 185 ON NABORS RIG – BC, CANADA

General design & manufacturing

Part designs are geometrically and parametrically linked to each other and to a single scaling parameter which sets tool size. This saves repletion and improves drafting quality. The mid-range Genie 185 has a scaling parameter of 1. Each Genie model has an associated range of bit sizes. Bit head design geometry is linked to a second independent scaling parameter, the bit gauge diameter. A custom bit of any size between the specified minimum and maximum size can be produced. Design changes are more easily managed. Manufacturing is more flexible and simpler with improved quality and lead time as the result of feature commonality through the range.

Model selection & model number

The housing diameter in each Genie model is matched to BHA collar sizes whilst keeping the target bit gauge within range. The tool housing diameter in mm (rounded to nearest 5) provides the model number. The model number is not linked to any particular bit size and bit size ranges can overlap between some models.

Size & transport

Genie tools were designed with consideration for carrying in pick-ups and helicopters. They have an integral twin check valve. The Genie 185 is

under 2m long, including the integral jet sub and is half the size and weight of predecessor tools.

Connecting threads

Genie tools have pin down API female top threads for protection during handling and for reduced length & mass. Genie bits are retained in a “pin up”, splined drive sub (chuck) which screws into the Genie tool using a new design thread.

Model range

Current planned models include Genie130 (6” to 6 7/8” bits), 160 (7 1/2” to 8 5/8”), 185, 200 (9 3/8” to 11”), 260 (12” to 14 1/4”) & 320 (14 5/8” to 17 1/2”). The 320 & 260 are next to be made. Smaller tools involve more manufacturing challenges and are expected to follow the bigger tools. A Genie 100 coring tool has been considered.

Hydraulics

The flow rate of fluid to power a new Genie tool over its operating range is generally lower than the flow rate used to clean the hole. The Genie tool therefore has an integral jet sub with a dual check valve. It enables jet nozzles to be fitted as may be required to provide for any additional flow rate at the same differential pressure. As a dynamic mechanism, the tool will be subject to gradual wear through its life at a rate depending on the amount of sand or other abrasive materials in the drilling fluid. It is important for economic reasons to keep the drilling fluid as free of cuttings as practically possible. Wear may be compensated for by increasing the pump rate. It is recommended that a working flow rate range be provided to maximise tool operating flexibility through its life. The Genie tool stops impact cycling when lifted off bottom and additional flow paths open within the tool to provide a more direct and lower flow resistant passage through the exhaust ports in the bit face. This enables higher flow rate bottoms-up circulation at lower differential pressure. It also facilitates passage of LCM. Fluid can become more abrasive under lost circulation control conditions.

Differential pressure & flow rate

The flow rate to run the tool from low to high power, and the resulting differential pressure, depend on the fluid. As an example and using a drilling fluid of 1.05 SG with a Newtonian kinematic viscosity of 5.55 mm²/s (~35 second Marsh funnel), the flow rate is approximately 0.61 to 0.87 m³/min for a new tool and about 0.89 to 1.33 m³/min for a half-worn tool. The corresponding range of differential pressure is about 6.21 to 11.03 MPa. This is much lower than 12.76 to 17.24 MPa of the predecessor tools.

Weight On Bit (WOB)

A low WOB of 1.1 to 4.5 kdaN is required for the Genie 185 with an 8 1/2” (215.9 mm) drill bit. The

WOB for a rotary drilling system of the same size may exceed 20 tonnes for hard formations. WOB outside the Genie limits will cause a reduction in impact energy delivered to the bit face, a loss of ROP and an increase in drill string torque.

Bottom Hole Assembly (BHA)

For ease of control, the lower BHA is isolated from the rest of the drill string by a fully pressure-balanced heave compensator type stroke sub. The applied WOB is thus limited to the weight of the items below it. See Fig. 2 for an example.

TARGET WOB = 1.1 to 4.5 kdaN

Lengths & weights in example estimated only. Detailed drill string & BHA design to achieve target WOB is the responsibility of the client.

Stabilizer

Under gauge, roller reamer recommended. Spiral stabilizer more prone to getting hooked on ledges.

X-Over

Fully pressure balanced stroke sub

Upper part

Telescopic joint (only items below this joint apply WOB)

eg: Smiths HE 6 1/2” Hydra-Stroke AEBB fully pressure balanced, or equivalent NOT A THRUSTER.

Lower part

Pony collar or Collar

Genie 185 integral jet sub & check valve system

Genie 185

Genie 185 bit



FIG. 2 – GENIE 185 BOTTOM HOLE ASSEMBLY

Project status

Approaching sign-off on the Genie 185 tool with its hard surfacing developments.

Relevance to Geothermal projects

- ✓ SUITABLE for HARD formations (metalliferous mining origins)
- ✓ HIGH TEMPERATURE RATING – 204C standard & 260C high temp. version
- ✓ HIGH ROP – up to 3 times offset rotary
- ✓ LOW WOB (1.1 to 4.5 kdaN for 8½” hole)
- ✓ LOW rotational speed (typically 25 rpm)
- ✓ LOW DRILL STRING STRESS
- ✓ LIGHT BHA – faster trips with less rig power
- ✓ API top thread & housing suits collar size
- ✓ LOW VIBRATION
- ✓ NO SEALED BEARINGS
- ✓ SIMPLE – only 3 moving parts plus bit
- ✓ ONE PART CUSTOMISED to mud
- ✓ DIRECTIONALLY STABLE
- ✓ EASY TO USE – manual or auto drill
- ✓ LOWER OFF-BOTTOM CIRCULATION PRESSURE
- ✓ RELIABLE – has always started on bottom
- ✓ RISK MANAGEMENT – no fishing & no bits lost on bottom (since 1993 start)
- ✓ AVAILABLE – designed & manufactured in Australia & based in Adelaide
- ✓ COST EFFECTIVE – cheaper drill string, no mud motor, less string wear, light & compact for transport, integral check valve & jet sub, potential to complete drilling in less than 50% of rotary drilling time for early production.

Abbreviated development chronology

1992 A system was conceived by Fred Moir, founder of S.D.S. Pty Ltd to drill 5¼” blast holes of 20 m depth in hard metalliferous mines using coaxial drill rods and a down-hole hammer powered by clean, high pressure, recirculated water. He sought the benefits of top-hole hydraulic hammers, down-hole air hammers and a

benign, dustless drilling fluid. Used water returned to the surface in drill rods for re-use. A controlled portion was exhausted through the bit for hole cleaning. Malcolm McInnes was contracted to undertake system R&D. Trialled in underground mines with Western Mining and Pasminco with speed and dust suppression advantages.

1993 Performance diminished with depth due to “water hammer” vibration, the result of uneven cyclic flow resistance. Novel down-hole hydraulic accumulator systems had limited success. Managing the effect was replaced with managing the cause. A new concept impact drill (see Fig. 3) with progressive, staged pistons, cyclic flow resistance levelling, anti-cavitation impact faces and a new constant-exhaust bit was invented and designed by Malcolm McInnes who then won a \$500,000 competitive Government R&D grant and completed the project to budget. Extensive mathematical system modelling was undertaken.

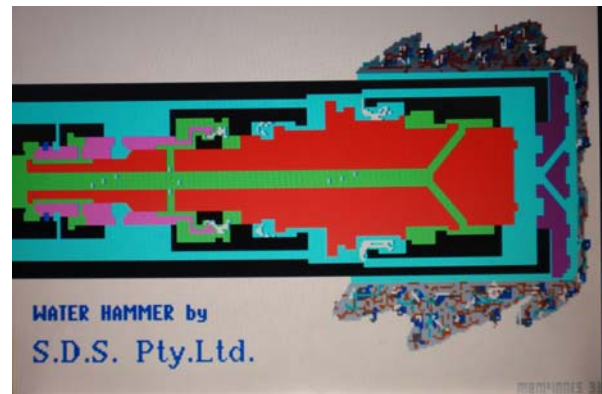


FIG. 3 – 1993 HYDRAULIC PERCUSSIVE DRILL

The compact new, patented design provided smoother, more powerful operation (see Fig 4) independently of depth. Recirculation through drill rods was abandoned for hole cleaning.



FIG. 4 – WATER HAMMER PROTOTYPE TESTING WITH GRANITE & UNDERGROUND

1994 Further underground testing with Mt. Isa Mines. Total distance drilled 1000m.

1995 Attracted to petroleum industry with more suitable pump & fluid infrastructure and more commercial potential. Developed tool coatings for contaminated fluids. Sub project to accommodate

denser drilling fluids put on hold. Mixed results in oil field trial with partner Santos. Partly related to control & instrumentation issues and a packer.

1996 Breakthrough field trial of 6" Water Hammer with Shell in Canadian Rockies foothills with water. Drilled in a pipe stand in an 8½" hole at ~4.5 times ROP of roller cone using manual and automatic drilling.



FIG. 5 – FRED MOIR & MALCOLM McINNES AT WATER HAMMER RUN, CANADA 1996.

Began development of Water Hammer for 12¼" bit to suit same commercial application (water).



FIG. 6 – CLUSTER WATER HAMMER

Developed and successfully trialled 32" hole cluster drilling tool based on 4 water hammers for J C McDermott & Sons. See Fig. 6. Potential for 26" conductors & sub-sea anchorages.

Manufacturing & drafting moved from SDS Pty Ltd in Adelaide to SDS Digger Tools in WA.

1997 New 12¼" hole size water hammer designed & made. Immediately worked in Canada. 30 hour running time with new hard coating technology and flock water. Developed case-while-drilling systems for Ocean Drilling Program. Achieved fast, unsupported spudding on hard, smooth, 30° sloping granite. Quarry tested CWD insertion and retrieval of

casing. Development progressed in offshore trials with the ODP and sea water drilling fluid.



FIG. 7 – FLUID HAMMER 260 WITH ODP

1998 Ran 12¼" tool off shore from jack-up rig through short hard layer with ARCO Indonesia (see Fig. 8). Tool put in at 1,350 m & drilled 11 hours at higher than offset ROP (up to 5 x). This was despite some damage incurred to the bit due to tungsten carbide inserts left in the hole by the preceding roller cone.



FIG. 8 – WATER HAMMER & ARCO INDONESIA

Continued drilling 650 m surface holes with 14¼" bits with Talisman Energy Inc at ROP consistently 2 to 3 times faster than conventional rock bits in hard formations. See Figs. 9 & 10. A major downturn in the international mining industry threatens the internally funded project.



FIG. 9 – WATER HAMMER – CHERT CUTTINGS

Australian Geothermal Conference 2010

SDS Corporation Ltd commissions an independent technical review of the design. The engineering and technology is validated.

2000 Drilled with PDVSA in Venezuela at 4,355 m depth (2 to 3 x offset instantaneous ROP) with SDS water hammer 260 (12-1/4" bit). The fluid was a mineral oil of about 1.03 SG. WOB difficult to control. See Fig. 13.

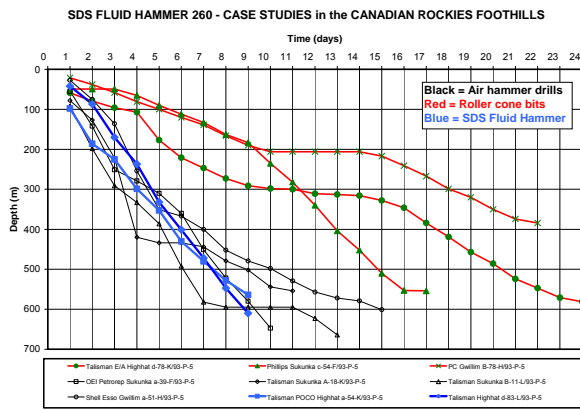


FIG. 10 – COMPARATIVE PERFORMANCE

Shoreline approach hole opening job at Statoil Mongstad refinery, Norway with 12 1/4" hole opening bit on slope rig run by Halliburton. Fig 11.



FIG. 11 – WATER HAMMER 260 & STATOIL

1999 Began development of new 8 1/2" hole tool with fewer parts, new features and for range of drilling fluids (not completed), as new series base model. Performance testing undertaken in Orange Grove quarry, WA. See Fig. 12. Drilling with 12 1/4" tool with Northstar energy - Recorded continuous ROP 4-7 Mt/Hr Vs 2 Mt/Hr tricone. Hammer life increased to 40 hours.



FIG. 12 – QUARRY TEST 8 1/2" PROTOTYPES



FIG. 14 STEERING HYDRA 185. FIG. 13 PDVSA

First steering run using unfinished prototype Hydra 185 (8 1/2") at Sperry-Sun Nisku test facility. The tool built a turn of 5° using a 1° bent sub and 9° using a 1.5° bent sub, in 18.3 m of concrete which it drilled at 100 m/hr (Fig. 14). Successfully demonstrated steering and operation in a well with Measurement While Drilling System (Hydra 185 not developed for fluid SG over about 1.05).

2001 May. Controlled surface benchmark testing of SDS Fluid Hammer 185 at TerraTek testing facility (see Fig. 15) in Salt Lake City, Utah, USA, separately and in conjunction with consortium lead by US Department of Energy. Facility simulates deep, overbalanced drilling with standard rock samples and drilling muds. Despite tool not being designed for 1.2 and 1.8 SG muds, Extensive testing confirmed the soundness of the concept, verified operating characteristics and inspired development to suit denser fluids and expand application versatility.



FIG. 15 – TERRATEK & FLUID HAMMER 185

Fluid Hammer 260 tool (12¼" bit) was trialled with PDVSA in well MCA-2X in Venezuela at 1,498 m. A new drilling technique had been developed in theory and was successfully used to control the tool and Weight On Bit for optimum ROP, a major breakthrough that also protected the bit. Worked despite failure of hook feed indicator. An instantaneous ROP 2 to 3 times off-set roller cone was demonstrated. Project investment and finance options were pursued for the board.



FIG. 17 – FLUID HAMMER 260 & CWD & IODP JOIDES RESOLUTION

2002 June. Verification field tested prototype SDS Fluid Hammer 185 (9¾" bit) with Talisman Energy Inc. & Precision Drilling. See Fig. 16. Used new design Bottom Hole Assembly. BHA provided required low Weight On Bit. Identified torque as a key WOB maximum & minimum indicator. System worked and overcame major hurdles in applying the technology commercially.

2005 Successfully completed IODP job January, 2005. 2 tools ran a total of over 92 hrs in sea water without significant performance loss. The revenue supported the Genie project for the first 18 months. See Fig. 18.



FIG. 16 – PROTOTYPE 185 & BHA. TALISMAN ENERGY INC & PRECISION DRILLING



FIG. 18 – IODP RE-ENTRY CONE ON FLUID HAMMER 260 & CWD INSERTED CASING

Fluid Hammer project suspended.

Designed & built in-house, impact drill dynamometer test rig for new Genie range R&D (see Fig. 19) with mud cooling, mixing, instrumentation, prime pump & twin HT400 pumps. Many components were reclaimed scrap.

2004 Project and its assets moved from SDS Digger Tools into new Adelaide based entity *IMPACT DRILLING INTERNATIONAL Pty Ltd.* to focus on development and commercialisation of the technology for the petroleum & geothermal industries. Genie project announced. New design, engineering, manufacturing and supply, testing, operations, quality systems, branding and funding to develop new range of tools for industry drilling fluids and with lower operating differential pressure to maximise versatility. Managed by Malcolm McInnes. Concurrently with new tool development, the company won a commercial contract with Integrated Ocean Drilling Program to use two 1997 design 260 tools with IODP Hard Rock Re-entry Systems (up to 15" bits) to insert casing with re-entry cones 30m into Atlantic Ocean floor, (1.5 to 2.5 km depth) north of the Azores, without a template. See Figures 17 & 18.



FIG. 19 – IDI GENIE DYNAMOMETER TEST RIG

Successfully tested two different prototypes (see Fig 20) on water and standard muds 1.2 & 1.8 SG (as used in USA benchmark testing), without significant hydraulic vibration and at lower differential pressures. Different valves successfully used for different fluids. The parts supplier was late and the order incomplete. Enough parts provided for 2 complete Genie prototypes and one spare set of internals.



FIG. 20 – A PROTOTYPE GENIE 185

All part drawings parametrically linked and all drawings of the models in the product range linked to simplify and speed-up drafting, improve quality, simplify and standardise manufacturing, reduce lead times & costs. Check valve system redesigned for high solids mud. Safer, easier & faster assembly procedure and tools developed.

2006 SDS Corporation Limited sold to Sandvik Mining & Construction, Adelaide. IMPACT DRILLING INTERNATIONAL Pty Ltd acquired by Fred Moir & minor shareholders.

2007 Prototype Genie 185 design & manufacturing completed. Business name changed to SPECIALISED DRILLING SERVICES AUSTRALIA Pty Ltd.

2008 Prototype Genie 185 tools run with field trial partner Talisman Energy Inc in Canadian Rockies foothills, 5 to 9 January 2008. Fig. 21.

The new Genie 185 system demonstrated:

- Directional stability. Deviation no more than $\frac{3}{4}^{\circ}$
- Low rig mechanical & hydraulic vibration.
- High ROP, average 3 times offset tool ROP.
- Easy auto & manual drilling control.
- Reliable & predictable starting & operation.
- Automatically regulated, low WOB with lightweight BHA.
- Different but easy to learn to use.
- Can pass loss control material.

R&D program to increase durability. Prototypes did not employ hard overlays as used in predecessor tools. Accelerated wear was observed during lost circulation management due to increased sand level in drilling fluid. New design features, materials and pioneering manufacturing processes developed and incorporated into the Genie tools. A new dual check valve system was developed.



FIG. 21 – GENIE 185 TRIAL WELL, CANADA

2009 R&D and prototype manufacture of new hard overlaid tools completed in second half of year. New production systems developed for high volumes and low lead time. Additional field trial partners sought after follow-up drilling program delay in Canada due to financial crisis in USA. Local opportunity provided with contract won in late 2009.

2010 Tools mobilized to rig. Returned unused after anticipated hard formation was not encountered. Tools on stand-by for new project. Contract won for trial managed pressure drilling run in Asian project during last quarter of year. Development of below-the-hook lifting systems, maintenance procedures, manuals, drawings and other documentation continues.

Management

Chairman of the Board of Directors and principal shareholder is Mr Fred Moir. Fred is an international business leader with extensive drilling, service provision and manufacturing experience in the mining industry. Fred was founder of SDS Pty Ltd and instigated the original project to develop a water powered percussion drilling tool in 1992. Impact Drilling International Pty Ltd was established under his Chairmanship. The business is managed by Malcolm McInnes, FIEAust. CPEng MEng BE ARMIT Mech Eng MAIE SPE with over 30 years experience in manufacturing, product development, R&D, marketing, sales & management and has run his own business since 1992. He is the designer and inventor of the Genie tools and inventor of the of the internationally patented SDS water/fluid hammer in 1993. Malcolm has 17 years experience in the drilling industry and became an employee and shareholder of SDSA in 2006.

References

McInnes, M.B. - Internal reports & photographs & company documents & photographs 1992 - 2010.

The Author acknowledges the contributions of all people involved in the project since its inception

Hydrothermal alteration aspects of high heat producing granites in Australia & Europe

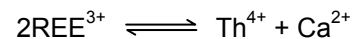
Alexander W. Middleton*¹, I. Tonguç Uysal¹, Massimo Gasparon², and Scott Bryan³

Queensland Geothermal Energy Centre of Excellence, The University of Queensland, Brisbane, QLD. 4072*¹
 School of Earth Sciences, The University of Queensland, Brisbane, QLD. 4072²
 Queensland University of Technology, BiogeoScience, GPO Box 2434, Brisbane, QLD. 4001³

In order to fully understand the relatively unstudied high heat producing granites (HHPG) of the Australian continent, this project has studied the European analogues of Cornwall, (United Kingdom), Soultz-sous-Forêts (France) and the Erzgebirge (Germany). HHPGs are characterised by their anomalous radiogenic element (U, Th and K) contents (Table 1), which is higher than average continental crust values. The Big Lake Suite in the Cooper Basin is the most investigated Australian enhanced geothermal system (EGS); Gatehouse et al., 1995).

Alteration mineralogy is a widely used feature to explore for potential ore deposits; however, this method has not yet been deployed for identifying and characterising EGS. In the current project, we are investigating alteration mineralogy of HHPG, with particular emphasis on trace element and stable isotope geochemistry. If successful, this can offer an additional approach to geothermal exploration and resource characterisation.

phase disequilibrium with the fluid. The alteration assemblage produced depends on factors such as wall-rock and fluid composition, temperature, salinity and water/rock ratio. The variation in alteration assemblage may control the concentration of incompatible elements, including the radiogenic elements as certain alteration reactions are associated with either enrichment or depletion of these elements. A pertinent example of this was noted to have occurred in some Carnmenellis (Cornwall, UK) monazites (Poitrasson et al., 1996), whereby Th was enriched through brabantitic (Förster, 1998) cation exchange during chloritisation of biotites:



Incompatible elements (HFSE, REE, LILE, and B etc., including the radiogenic elements) have a low partition coefficient (K_D) (White, 2007), and hence will preferentially stay in fluid phases during

Table 1: Typical compositions for high heat producing granites for EGS. Sourced from T Uysal, J Van Zyl, S Bryan, unpubl. data; Charoy, 1986; Stussi et al., 2002; Forster et al., 1999; Chappell & Hine, 2006

EGS Target	Composition	Age (Ma)	SiO ₂ (wt%)	K ₂ O (wt%)	U (ppm)	Th (ppm)
Cooper Basin granites	Biotite granites	~Mid-Carb.	-	-	10.0-30	28-144
Carnmenellis granites (Cornwall, UK)	K-feldspar megacrystic biotite granites	293-274	69-76	4.6-5.9	13-20 (4-38)	15-20 (5-45)
Soultz-sous-Forêts (Rhine Graben, France)	K-feldspar porphyritic monzogranite	~330	67-69	~4.5	6.2-14.1	24-37
Erzgebirge (Germany)	Biotite, 2 mica & Li-mica granites	325-318	70-77	4.5-5.3	8.0-30	15-37

Keywords: Geothermal, alteration mineralogy, Cooper Basin, stable isotopes, REE, Soultz-sous-Forêts

Background

During emplacement of granitic bodies, advective heat flow can occur due to hydrothermal circulation of surrounding waters. Several studies have noted that igneous rocks enriched in radioactive elements such as U, Th and K can have a similar effect and promote hydrothermal circulation long after the intrusion has cooled (Allman-Ward, 1985, Pirajno, 2005). On circulation of these hydrothermal fluids, variable alteration products will result from original mineral

crystallisation of melt and hydrothermal fluid movement.

Hydrothermal fluids affecting surrounding wall-rocks can be classified (based on their origin), into meteoric, magmatic, marine or connate. One aspect of this project is to deduce the origin and evolution of the hydrothermal fluids involved in the alteration of HHPG and surrounding sedimentary rocks.

Analytical Work

The project results will be attained via multifaceted petrographic, geochemical and geochronological analyses. The geochronology will use Rb-Sr isochron dating of alteration-related illitic clay minerals, whereas the geochemical techniques will include both stable isotope

analysis ($\delta^{18}\text{O}$ and δD) for hydrothermal fluid evolution and ICP-MS analysis for trace element quantification.

Qualitative and quantitative petrographic analyses will be achieved with transmitted and reflective microscopy, as well as EDS (via JEOL XL 30 SEM) and EPMA. The EPMA will be used to determine quantitatively which mineral phases encompass the elements of interest; such as incompatibles and radiogenics.

Queensland EGS targets and Cooper Basin

Queensland

Following estimated subcrustal temperature mapping and the increasing need for renewable energy sources, Queensland has been targeted by the state government as a prospective area for geothermal energy. The principal areas of interest for EGS are the Galilee Basin, Innot Hot Springs region, Hodgkinson Province, Styx Basin, Maryborough Basin and North d'Aguillar Block, Wandilla Province. These targeted areas have been based on the presence or likely presence of HHPG at depth ranging in age from the Late Devonian to Cretaceous. Many of the granite bodies emplaced within Queensland are linked to an extensional tectonic origin (Glen, 2005). Analysis of the intrusions, overlying sediments and their associated alteration zones will be performed as part of this project.

Cooper Basin

The Carboniferous Big Lake Suite granite in the Cooper Basin' represents one of the world's hottest EGS (Gatehouse et al., 1996). According to our recently acquired ICP-MS trace element data, U and Th contents in these granites reach levels of up to 144ppm, reflecting enrichment levels up to 13 times that of the upper continental crust (UCC(McLennan, 2001)). Cores taken from the granite and overlying sediments show varying degrees of alteration, with a range of incompatible element enrichment, such as U and Th. The highly altered zones have a predominant greisen-style sericite (illite) and re-precipitated quartz assemblage. We believe that this alteration may well have caused the localised enrichment in radiogenic element-bearing minerals such as illite, K-feldspar, and some accessory minerals (e.g., thorite).

The fluid history of the Cooper Basin can be deduced with the use of both crystallinity and stable isotope analyses of the illite. Illite crystallinity is a useful indicator of the temperature gradient in active geothermal systems and for locating fossil hydrothermal systems associated with ore deposition (Ji and Browne, 2000).

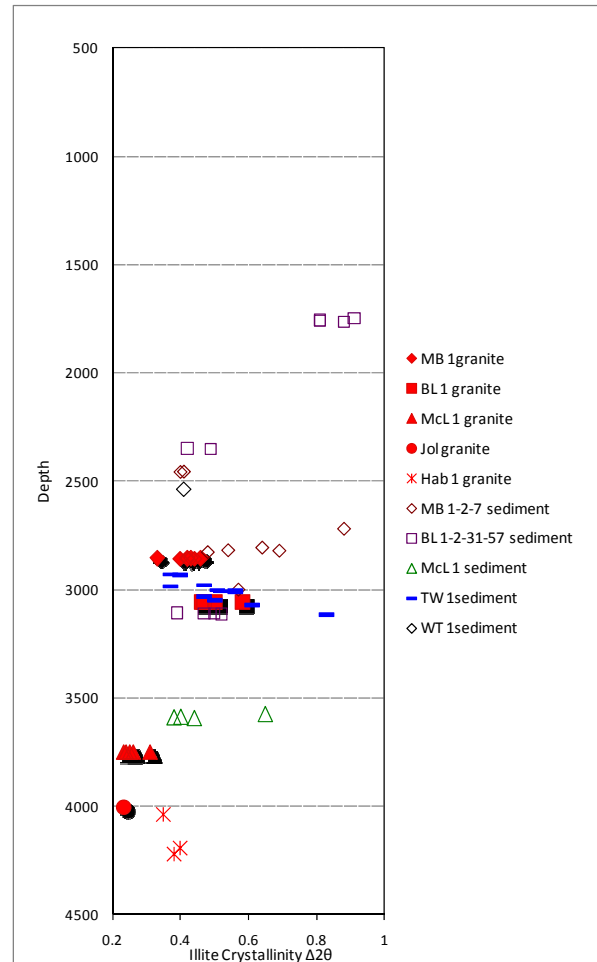


Fig 1: Graph of illite crystallinity against depth from Cooper Basin cores

Illite crystallinity is controlled by crystallisation temperature, water/rock ratio, and time available for crystallization (Arkai, 2002; Ji and Browne, 2000; Merriman and Frey, 1999). Better-developed crystalline illites show narrower 001 basal illite peaks and have lower IC values. Such illites were formed at higher temperatures or during prolonged heating events. Higher IC values (wider peaks), on the other hand, indicate lower crystallisation temperatures and/or rapid precipitation during hydrothermal processes. Illite crystallinities are seen to progressively increase with increasing core depth, suggesting a higher crystallisation temperature and hence hydrothermal fluid temperature at depth. The granite intersected in Jolokia and McLeod 1 seems to have experienced highest reservoir temperatures.

According to our present isotopic studies of alteration-related illite within the granite and sedimentary cover, oxygen and hydrogen isotope compositions range from $\delta^{18}\text{O} = -1.8\text{‰}$ to $+2.7\text{‰}$; $\delta\text{D} = -99\text{‰}$ to -121‰ and $\delta^{18}\text{O} = +2.3\text{‰}$ to $+9.7\text{‰}$, $\delta\text{D} = -78\text{‰}$ to -119‰ , respectively. Such values are much lower than those reported for many deeply buried sedimentary basins (Clauer and Chaudhuri, 1995). The calculated oxygen and hydrogen isotope compositions of

fluids in equilibrium with the illites are depleted in ¹⁸O and deuterium, comparable to those of waters reported for most high-latitude sedimentary basins. Hence, stable isotope data of alteration minerals in the granite and the overlying sedimentary rocks suggest the operation of a hydrothermal system involving high latitude meteoric waters during Permo-Carboniferous extensional tectonism in the Cooper Basin region.

Europe

The European HHPG examples have all been considered to be approximately syn-genetic with extension following the late Palaeozoic Hercynian/Variscan orogeny between Gondwana and Laurasia.

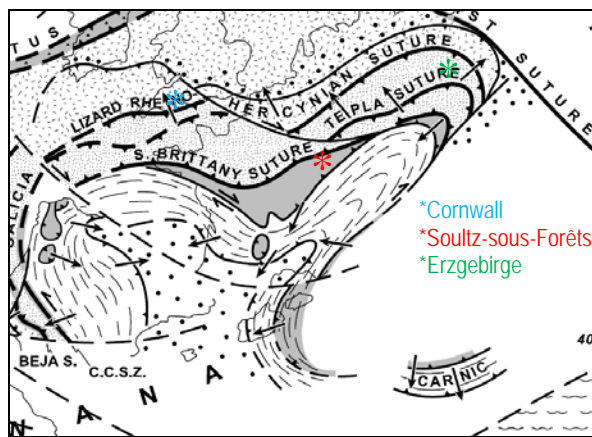


Fig 2: Possible tectonic suture configuration of Hercynian orogeny from Matte (2001)

Erzgebirge, Germany

Located at the north-western edge of the Bohemian Massif (Förster and Förster, 2000), the Erzgebirge consist of highly-evolved voluminous granites intruded into highly crystalline metamorphic rocks (Tischendorf et al., 1965). These granites are highly enriched in U and Th (Table 1) with principal radiogenic mineral phases of uraninite, U-bearing micas, xenotime, monazite-(Ce)-brabantite solid solution series minerals, and thorite (Förster, 1998).

As of yet, our analyses (Rb – Sr dating and stable isotope) have not been undertaken on Erzgebirge samples, but samples will be analysed in collaboration with Dr. Hans-Jurgen Förster (Potsdam, GeoForschungsZentrum).

Saultz-sous-Forêts, France

Located south-west of the Erzgebirge outcrops, Saultz-sous-Forêts was emplaced debatably either as an I-type subduction-related or late-stage extensional granite body (Flötmann and Oncken, 1992). Hydrothermal fluid circulation and alteration was promoted by E-W lithospheric

extension (Schleicher, 1998). Petrographic studies of alteration mineralogy by Bartier et al. (2008) identified intense propylitically altered granite with newly equilibrated mineral assemblages of tosudite (chlorite-smectite), illite, chlorite and carbonates, whilst K-feldspar appears to be largely preserved.

Following further transmitted and scanning-electron microscopy performed at The University of Queensland, we identified several key alteration-related mineral phases. Altered sphene, for example, found in sample K177 (2000m – EPS1), is acting as a principal mineral phase that contains various rare earth elements (REE). Estimations of composition from semi-quantitative EDS have detected Ce, Y, Nd, La, Th and Ca with possible PO₄ or SiO₄ anion complexes.

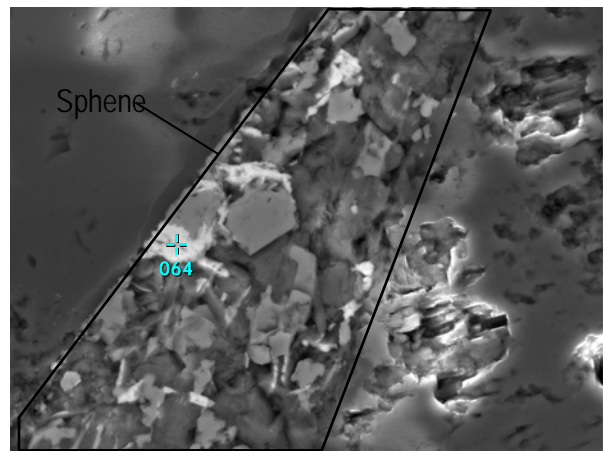


Fig 3: Altered sphene compassing several REE-element-bearing mineral phases

This may indicate a potentially high fluid/rock ratio allowing for incompatible element transport during alteration of the granitic protolith. Monazite has also been found proximal to subhedral hematite grains. A possible mechanism for this mineral association can be traced back to the formation of a redox interface with co-precipitation of U⁴⁺ and Fe³⁺.

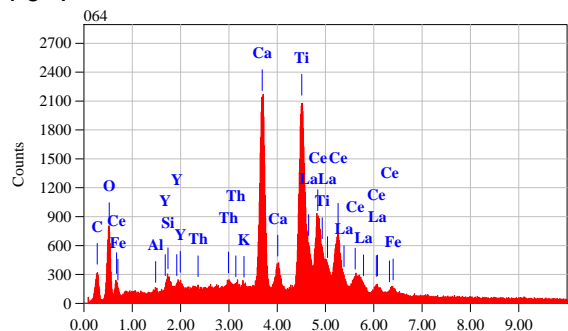


Fig 6: EDS for altered sphene found in sample K177 exhibiting intense propylitic alteration.

Cornwall, United Kingdom

Cornwall marks the far western district of the Euro-Hercynian granites with 5 major outcrops; Dartmoor, Bodmin Moor, St. Austell, Carnmenellis

and Lands End. Multiple studies by Ball et al., (1979) and Charoy (1986) have found the Cornwall granites to be similarly enriched in radiogenic elements (Fig. 1) as the middle-European examples. Alteration systematics are of great importance within this system as they have been directly linked to the leaching and mineralisation of uranium. Allman-Ward (1985) noted 4 predominant alteration styles affecting the St. Austell granite; greisenisation, tourmalinisation, kaolinisation and haematisation. Uranium is likely to be transported in solution during hydrothermal alteration, as oxidising fluids will cause a loss of electrons (U^{4+} to U^{6+}) and hence increase mobility. The most likely location of the displaced uranium will be in a distal alteration zone possibly accompanied by haematite mineralisation. An example of this can be seen in Wheal Remfry where quartz-haematite veins show uranium values of up to 50ppm (Allman-Ward, 1985).

Summary

Highly altered granites in the Cooper Basin are substantially enriched in lithophile elements, particularly in Cs, Rb, Be, Th, U relative to the upper continental crust. U and Th contents are 10 and 13 times higher than those of the UCC. Some enrichment of heat-producing elements was promoted by a regional hydrothermal event leading to the precipitation of U and Th-bearing minerals such as illite, K-feldspar and accessory minerals (other than zircon). Oxygen and hydrogen isotope compositions of fluids are depleted in ^{18}O and deuterium, comparable to those of waters reported for most high-latitude sedimentary basins. European examples of enhanced geothermal systems show similar redistribution and enrichment patterns of rare earth and radiogenic elements as a result of hydrothermal alteration. This can be seen in monazites proximal to chloritised biotites in the Carnmenellis granite of Cornwall. Unlike the Cooper Basin, stable isotope data has not yet been acquired from European samples. However once performed, hydrothermal fluid origin and evolution can be deduced for these EGS. Alteration mineralogy and geochemistry of relatively shallow sedimentary sections is a potentially valuable tool to evaluate the presence of a concealed geothermal heat source in the basement of sedimentary basins.

References

Allman-Ward, P., 1985. Distribution of uranium and thorium in the western lobe of the St. Austell granite and the effects of alteration processes, High heat production granites, hydrothermal circulation and ore genesis conference, The Institute of Mining and Metallurgy, 437-458.

Aquilina, L., Pauwels, H., Genter, A., and Fouillac, C., 1997. Water-Rock interaction processes in the

Triassic sandstone and granitic basement of the Rhine Graben : Geochemical investigation of a geothermal reservoir. *Geochimica et Cosmochimica Acta*, 6, 4281-4295.

Arkai, P., 2002. Phyllosilicates in very low-grade metamorphism: Transformation to micas. *Micas: Crystal Chemistry and Metamorphic Petrology*, 46: 463-478.

Bartier, D. et al., 2008. Hydrothermal alteration of the Soultz-sous-Forêts granite (Hot Fractured Rock geothermal exchanger) into tosudite and illite assemblage. *European Journal of Mineralogy*, 20, 131-142.

Bryan, S. E., Holcombe, R. J. and Fielding, C. R., 2001. Yarrol Terrane of the northern New England Fold Belt: forearc or backarc? *Australian Journal of Earth Sciences*, 48 296-316

Clauer, N. and Chaudhuri, S., 1995. *Clays in Crustal Environments. Isotope Dating and Tracing*. Springer Verlag, Heidelberg, 359.

Flötman, T. and Oncken, O., 1992. Constraints on the evolution of the Mid Crystalline Rise –a study of outcrops west of the river Rhine. *Geologische Rundschau*, 81, 2, 515-543.

Förster, H-J., 1998. The chemical composition of REE-Y-Th-U-rich accessory minerals in peraluminous granites of the Erzgebirge-Fichtelgebirge region, Germany, Part 1: The minazite-(Ce)-brabantite solid solution series. *American Mineralogist*, 83, 259-272.

Förster, H-J., 1998. The chemical composition of REE-Y-Th-U-rich accessory minerals in peraluminous granites of the Erzgebirge-Fichtelgebirge region, Germany, Part 2: Xenotime. *American Mineralogist*, 83, 1302-1315.

Glen, R. A., 2005. The Tasmanides of Eastern Australia, from: Vaughan, A. P. M., Leat, P. T. and Pankhurst, R. J., 2005. *Terrane Processes at the Margins of Gondwana*. Geological Society, London, Special Publications, 246, 23-96.

Ji, J. and Browne, P.R.L., 2000. Relationship between illite crystallinity and temperature in active geothermal systems of New Zealand. *Clays and Clay Minerals*, 48: 139–144.

Ledéser, B. et al., 2009. Fractures, hydrothermal alterations and permeability in the Soultz Enhance Geothermal System. *C. R. Geoscience*

MATTE, P., 2001. The Variscan collage and orogeny (480±290 Ma) and the tectonic definition of the Armorica microplate: a review, *Terra Nova* 13, 122-128.

McLennan, S. M., 2001. Relationships between the trace element composition of sedimentary rocks and upper continental crust. *Geochem. Geophys. Geosyst*, 2.

Merriman, R.J. and Frey, M., 1999. Patterns of very low-grade metamorphism in metapelitic rocks. In: M. Frey and D. Robinson (Editors), *Low Grade Metamorphism*. Blackwell Science, Cambridge, pp. 61-107.

Murray, C. G., 2003. Granites of the New England Orogen., from: Blevin, P. L., Jones, M. and Chappell, B., *Magma to Mineralisation: The Ishihara Symposium*. Geoscience Australia Record, 2003/14, 101-108.

Pirajno, F., 2005. *Hydrothermal Processes and Mineral Systems*. Springer Link, Geological Survey of Australia, 73-157, 990-995.

Schleicher, A. M., Warr, L. N., Kober, B., Laverret, E. and Clauer, N., 2006. Episodic mineralisation of hydrothermal illite in the Soultz-sous-Forêts granite (Upper Rhine Graben, France). *Contrib Mineral Petrol*, 152, 349-364.

Stussi, J-M. et al., 2002. The hidden monzogranite of Soultz-sous-Forêts (Rhine Graben, France): Mineralogy, petrology and genesis. *Géologie de la France*, 1, 45-64.

Taylor, H. P., 1997. Oxygen and Hydrogen Isotope Relationships in Hydrothermal Mineral Deposits, from: Barnes, H. L., 1997. *Geochemistry of Hydrothermal Ore Deposits*. John Wiley and Sons, Inc, 229-288.

White, W. M., 2007. *Geochemistry: Trace Elements in Igneous Process*. John Hopkins University Press, 258-312.

A Geothermal Web Catalog Service for the Perth Basin

Thomas Poulet^{1,2,3}, Soazig Corbel^{1,2}, Michael Stegherr^{1,4}

¹ CSIRO Earth Science and Resource Engineering, P.O. Box 1130, Bentley, WA 6102, Australia.

² Western Australian Geothermal Centre of Excellence, P.O. Box 1130, Bentley, WA 6102, Australia.

³ The School of Earth and Environment, University of Western Australia, WA 6009, Australia.

⁴ School of Science, Curtin University, GPO Box U1987, Perth, WA 6845, Australia

The Western Australian Geothermal Centre of Excellence (WAGCOE) is a science collaboration between Western Australia's leading innovative research institutions – CSIRO, The University of Western Australia and Curtin University of Technology. One of its key research initiatives is to assess geological and geophysical data from the Perth Basin to identify geothermal targets. This geothermal exploration task involves the collection and analysis of all datasets available, which can be a challenging and sometimes daunting exercise. This paper addresses the difficulties encountered in gathering data for geothermal exploration and presents our web catalog service, the application we use to manage our spatially referenced resources.

Keywords: Western Australia, Perth Basin, geothermal exploration, GeoNetwork opensource

Finding and using geo-referenced data

Geothermal exploration is a data intensive activity which requires access to all relevant information available in the region of interest, such as stratigraphic sections and horizons, downhole temperature measurements, rock properties, and hydrogeologic parameters including water quality. Because so many types of sciences are involved (geophysics, geology, geochemistry...), data may be derived from many different potential sources such as seismic surveys, petroleum well logs, mechanical property laboratories, or groundwater mineralogical assays. Data really is an indispensable element for exploration and yet it is still so difficult and expensive to discover, search, access and use; those four simple steps can sometimes represent a real obstacle course for any first-time user. Although most public datasets are nowadays accessible through companies' or governmental agencies' websites, any potential user still needs to know all key data holders in the area in order to access essential information. Once the appropriate data custodian for a particular type of data is identified, the second task is usually to search for data relevant to the location of interest, only to discover that datasets are rarely fully searchable. The third step is then to access this data, which can sometimes involve going physically to an organisation to copy several computer hard drives. The last step is generally to understand the format used, which may be non-standard and can lead to the most significant inefficiencies in a given project. Data manipulation can include for example large amounts of preliminary data conversion,

deciphering any implicit assumption about units of measures and geographical references, or even trying to infer the creation process of the data in order to obtain one piece of missing information. If data is interrelated, this investigative process can loop on itself, creating workflow problems. Any user who has spent a long time going through this process can indeed wonder legitimately if newer data is now available. Our web catalog service is an attempt to eliminate the painful aspects of Perth Basin data discovery.

Using GeoNetwork opensource

GeoNetwork opensource¹ is a discovery service and catalog application, which is useful for managing spatially referenced resources and specially built to facilitate the connection between spatial information communities and their data. It is a Standardised Geospatial Information Management System based on international standards, with a large community of several hundreds of users and developers participating actively to its growth. A more complete description can be found in Ticheler & Hielkema (2007). In collaboration with AuScope Grid (Woodcock 2008) we decided to use GeoNetwork as our catalog application since it addresses most potential problems mentioned above, of data discovery, search, access and usage. GeoNetwork is accessible to users through a web interface and therefore only requires a web browser on any computer platform. Its search functionalities make data easily discoverable and

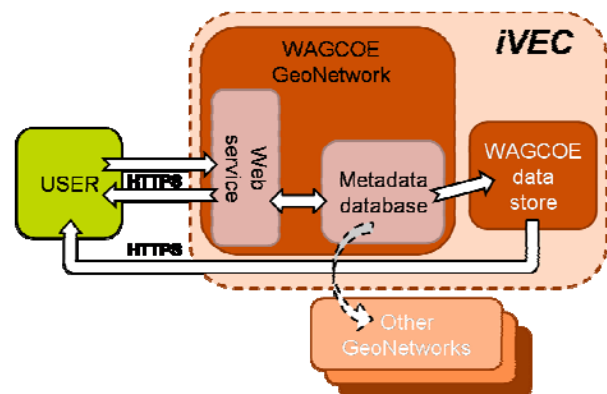


Figure 1: Workflow diagram showing the architecture of WAGCOE's geothermal catalog, using GeoNetwork as the catalog application linking to a petabyte datastore holding the corresponding data. Both components use IVEC's infrastructure and provide an efficient and secure system that can connect to other web services

¹ <http://geonetwork-opensource.org>

searchable. Since we are using GeoNetwork as a cataloguing application, the granularity of the search is limited to the metadata and not the data content itself. This library function is different from a web portal connected to a full database which would make the entire data fully searchable. However, the search facility allows users to find information easily and access the corresponding metadata, including a link to download the associated data itself from a Petabyte store. Figure presents the workflow of any user accessing WAGCOE's web catalog service. Both the web service and Petabyte store are hosted at iVEC², the hub of advanced computing in Western Australia, and all connections are secure. The web catalog service points directly to the data store, and can also be connected to other web catalog services from other institutions.

Using that data is also greatly facilitated as GeoNetwork organises, documents and publishes data collections in a standardised and consistent way, both at the metadata and data levels,

following international standards from the Open Geospatial Consortium³. This fully descriptive metadata in XML format improves accessibility and removes any possibility of data misinterpretation based on assumptions.

As Ticheler & Hielkema (2007) point out, GeoNetwork has also been developed using Web 2.0 techniques to allow for more interactive and intuitive use of the system and to offer building blocks for future web services. This interaction with other web services is a central feature to help reduce duplication and working towards a single point of truth paradigm. It is an essential component of WAGCOE's data strategy to link to all data custodians' databases as defined by the Australian Geothermal Energy Group (AGEG) Technical Interest Group focusing on data management. Such a framework can definitely improve geo-referenced data sharing within and between organisations, hence developing better collaboration. It can also open opportunities for data comparisons which can empower consumers

The screenshot displays the GeoNetwork web interface. At the top, there is a header for the Western Australian Geothermal Centre of Excellence and the GeoNetwork logo with the tagline 'Geographic data sharing for everyone'. Below the header is a navigation bar with links for Home, Administration, Contact us, Links, About, and Help, along with language options (English, Español, Français, Русский, Deutsch, Nederlands) and a user login section for Soazig Corbel (LDAP).

The main content area is titled 'FIND INTERACTIVE MAPS, GIS DATASETS, SATELLITE IMAGERY AND RELATED APPLICATIONS'. It features a search interface on the left with a map of Australia and a search button. The search results are displayed in a list format, showing three items:

- ALTONA 2000 SEISMIC SURVEY**: Abstract: The 2000 Altona Seismic Survey consists of 90,135 km of high fold 2D data. It was acquired to assist in delineating the Whicher Range Gas Field and identify a drilling location for Whicher Range 5. Keywords: Geophysics, Seismic.
- AUSTRALIAN DAY LAND SURFACE TEMPERATURE**: Abstract: Daytime Land Surface Temperature map acquired from standard MODIS data products on a 1km grid spacing. Keywords: Remote Sensing, Thermal Infra-Red.
- AUSTRALIAN APPARENT THERMAL INERTIA**: Abstract: Apparent Thermal Inertia map acquired from standard MODIS data products on a 1km grid spacing. Keywords: Remote Sensing, Thermal Infra-Red.

Each result includes a thumbnail map, a 'Metadata' link, and an 'Owner: admin' label. The interface also shows a sidebar with 'CATEGORIES' (Perth Basin) and 'RECENT CHANGES' (Bouguer Gravity Perth Metro, Cockburn 1 - Petroleum well, etc.).

Figure 2: screenshot of WAGCOE's GeoNetwork web interface. All data are searchable through metadata, including keywords and geographical location. Results are displayed with all corresponding metadata including links for download of the underlying real data.

² <http://www.ivec.org>

³ <http://www.opengeospatial.org>

(Rezabakhsh et al., 2006). In our case the first external web service we are planning to interconnect is the web interface to CSIRO's PressurePlot⁴, a query tool linked to the PressureDB database. That database contains rock properties such as porosity, permeability and thermal conductivity measurements, as well as stratigraphic and downhole pressure data for more than 1700 wells across Australia.

WAGCOE's web catalog service

Figure shows a screenshot of WAGCOE's GeoNetwork web interface⁵ with three entries visible. Each entry is represented by its title and abstract, as well as two small pictures. A thumbnail on the right hand side represents the corresponding data and a logo on the left hand side indicates visually the origin of the data. All current entries appear with WAGCOE's logo as GeoNetwork is not connected to any other external service yet. Part of the data we store was produced by WAGCOE and includes measurements (see Figure) as well as results from numerical models. Most of the underlying data however was not originally created by WAGCOE and comes from other organisations such as the Western Australian Department of Mines and Petroleum, Geoscience Australia, or

other private companies, research and governmental organisations. This local hosting demonstrates the temporary nature of those entries as we are working toward the single point of truth principle enunciated previously. We are only hosting other organisations' data with their permission as they agree for us to do while building their own web services. We are also planning to host data for geothermal companies who choose to use our system to manage part of their data.

As shown on Figure , our infrastructure is deployed at iVEC and benefits therefore from their professional services. All connections to GeoNetwork are encrypted and secure. A custom group management function then provides the granularity required to open some data to the public while restricting the access to protected company data, for example.

The data stored in our catalog covers all major scientific areas relevant to geothermal exploration and GeoNetwork's advanced options allow users to search for entries using the following two levels of categories and sub-categories:

- *remote sensing*: thermal infra-red, landsat, spots, light detection and ranging (LIDAR),

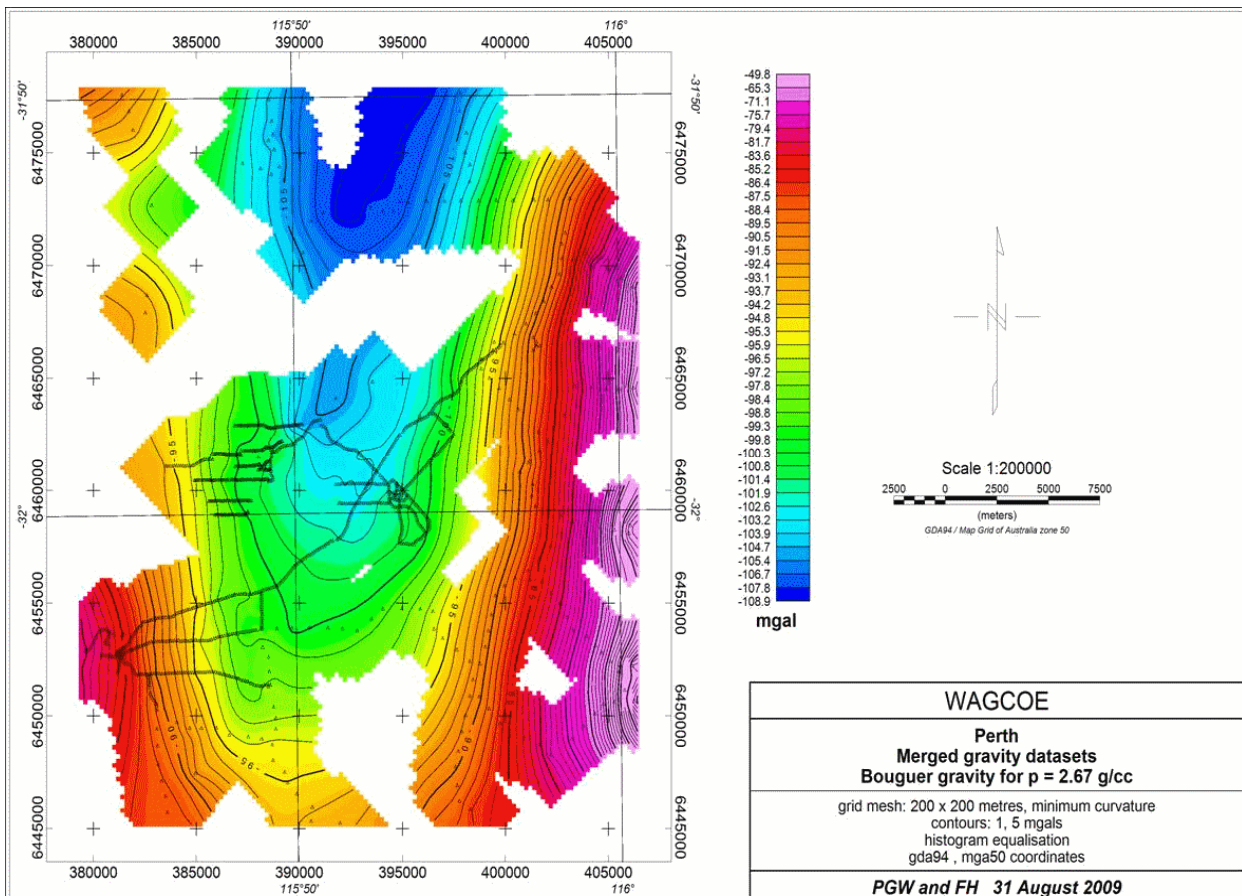


Figure 3: Example of data accessible through our catalog web service. This map shows Bouguer gravity from regional Geoscience Australia data combined with new survey data acquired by WA Geothermal Centre of Excellence.

⁴ <http://www.pressureplot.com>

⁵ <https://wagcoe.ivec.org/geonetwork>

- *geophysics*: seismic, velocities, magnetics, gravity, electromagnetics, radiometrics, geophysical logs, stress measurements, seismology data, magnetotellurics,
- *geology*: geological maps, palynology data, sedimentology data, thin sections, grainsize analysis,
- *hydrogeology*: hydraulic heads, water levels, water flows, rainfall, evapotranspiration data, recharge data, specific yield, storativity,
- *geochemistry*: water quality, rock geochemistry, thermochronology,
- *rock physics*: permeability, porosity, thermal conductivities, heat flux.

While all mechanisms have been implemented for us to manage these data types, populating the catalog with data references is a work in progress; not all sub-categories have data available yet.

WAGCOE’s catalog management tools

We have developed a suite of administrative tools in order to build and manage our system as shown in Figure . We can therefore easily enforce consistency between the metadata on GeoNetwork and the corresponding data on the petabyte store. The user’s group management in both places is also greatly simplified, although not completely automatic. The main feature of our administrative toolbox is a converter between GeoNetworks’ metadata XML file format and an in-house extension of it allowing us to handle specific metadata information which is not supported in GeoNetwork by default and is not part of our customised version yet.

Figure presents a workflow diagram of all conversions occurring, between our WAGCOE metadata XML file format and GeoNetwork’s original one, through an internal Python structure which allows easy data handling and processing, including checking validity, updating time stamps or creating unique identifiers. We can then store our extended metadata along with the original data and still retain the ability to efficiently evolve

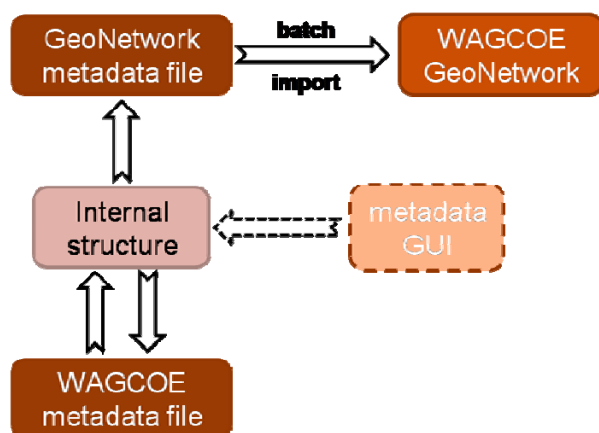


Figure 4: workflow diagram describing WAGCOE’s metadata management

our GeoNetwork implementation through official updates or in-house customisations. All metadata information is stored in the most appropriate format for the particular data type, even though the additional information is displayed currently only as part of a “supplemental information” paragraph for each entry. Any future enhanced display handling in GeoNetwork can be easily accommodated with a script updating all GeoNetwork entries from our original extended metadata files.

Future work

WAGCOE’s geothermal catalog is currently under development and even though nearly all major tools have been developed, some major work still remains to populate the catalog. The last major upgrade to our administrative tools remains a Graphical User Interface (GUI) to enter metadata more easily, as shown on Figure , instead of directly editing metadata files or internal Python structures. There are also several features planned for the future which will come from WAGCOE’s strong collaboration with the AuScope Grid project (Woodcock 2008). The first major enhancement will be to connect our catalog to other web services, starting with CSIRO’s PressurePlot web service. This linkage will provide access to a real pressure and temperature database allowing full content searches (whereas current searches on our catalog are limited to metadata). We are also planning to register our data collection to the Australian National Data Service (ANDS) Register My Data service⁶ which will then automatically harvest all metadata and provide greater exposure to our public entries. Finally, we are monitoring closely the AuScope Grid portal development as it could provide an even more user friendly interface to our catalog. Van Oort (2009) pointed the cost of building such a portal, which only emphasises the importance of AuScope Grid’s generic and open source tools development.

Conclusion

In the last few years, web services such as GeoNetwork have redefined the way users can discover, search, access and use geo-referenced data. This powerful tool is currently seeing a major uptake as it allows a dramatic change of practise for users who can now spend their time using data rather than searching for it. WAGCOE’s GeoNetwork catalog brings this enormous advantage to the geothermal exploration industry and provides an easy, remote, and secure access to various geothermal data sources through an intuitive web interface. It helps to reduce the risk for geothermal exploration in the Perth Basin and could also help some

⁶ <http://ands.org.au/services/register-my-data.html>

companies to store and access their data. We are hoping to connect it as soon as possible to other web services from various geological surveys, companies, research and governmental organisations, thanks to some of the technology developed by the AuScope Grid project

References

van Oort, P.; Kuyper, M.; Bregt, A. & Crompvoets, J. (2009), Geoportals: An Internet Marketing Perspective. *Data Science Journal*, 8, 162-181.

Rezabakhsh, B., Bornemann, D., Hansen, U., & Schrader, U. (2006), Consumer Power: A Comparison of the Old Economy and the Internet Economy. *Journal of Consumer Policy* V29, 3-36.

Ticheler, J. & Hielkema, J. U. (2007), GeoNetwork opensource, *OSGeo Journal* vol. 2, sep 2007.

Woodcock, R., (2008), AuScope: Australian Earth Science Research Information Infrastructure, Geological Society of Australia and the Australian Institute of Geoscientists. Australian Earth Sciences Convention (AESC) 2008. New Generation Advances in Geoscience. Abstracts No 89 of the 19th Australian Geological Convention, Perth Convention and Exhibition Centre, Perth WA, Australia. July 20-24, 276 pages.

Flow and heat modelling of a Hot Sedimentary Aquifer (HSA) for direct-use geothermal heat production in the Perth urban area, Western Australia (WA)

Martin Pujol^{1*}, Grant Bolton¹ and Fabrice Golfier².

¹Rockwater Pty Ltd. 76 Jersey Street, Jolimont WA

²Laboratoire Environnement Géomécanique et Ouvrages. Nancy Universités, Rue du doyen Marcel Roubault, Vandoeuvre-lès-Nancy BP40, 54501FRANCE

* Corresponding author: mpujol@rockwater.com.au

The deep confined aquifers of the Perth basin have been explored for water supply and heat production since the beginning of the 20th century. The availability of warm water was an additional asset and was very popular with laundries and bathing services. Currently, six geothermal bores use warm water from the Yarragadee confined aquifer for heating swimming pools and buildings and several new bores are proposed to be drilled. The cooled formation groundwater is injected into the same aquifer for environmental reasons.

Following the recent success of the release of geothermal acreage for geothermal exploration in WA, HSA direct-use is getting more recognition and support, and the number of projects is likely to increase because the technology is now more advanced, low-risk, and has relatively low CO₂ emissions and at low cost. Typical savings after 20 years of production can be as high as \$6,000,000, with payback in about 5 years and CO₂ savings of up to 800 tonnes/annum.

A key concern for HSA future development in Perth is sustainability and management. This will be achieved through a more comprehensive assessment of HSA geothermal resources. The latter will also require a good estimation of the longevity of existing and future direct-use HSA systems.

In this paper we discuss how simple numerical modelling of temperature and fluid flow using SEAWAT software and the "equivalent solute" approach allows for more accurate evaluations of geothermal resources and sustainability. This is an interesting management tool for existing and future HSA projects in Perth and is an alternative approach compared to the classical interpolation of measured temperatures between bores. Above all, the scope of this paper is to raise questions and discuss the future management of existing geothermal bores in the Perth area and to assist geothermal explorers to develop shallow HSA direct-use projects in the Perth area.

Keywords: Western Australia, Perth, Hot Sedimentary Aquifer, HSA, geothermal, injection, direct-use, heat transport modelling, SEAWAT.

HSA direct-use in the central Perth basin

Geological setting

The Perth urban area is located on the Swan Coastal Plain and is underlain by the Perth sedimentary Basin. The basin is comprised of a series of sub-basins, troughs, shelves and ridges containing predominantly Early Permian to Late Cretaceous sedimentary sequences that are up to 15 km thick.

The central Perth basin comprises a thick sequence of sedimentary rock, of which the upper 3,000 m of Quaternary to Jurassic age are relevant for geothermal projects targeting low temperature HSA systems.

Existing geothermal bores have been drilled to depths up to 1,000 m in Perth; which have targeted aquifers within the Yarragadee Formation and/or the overlying Gage Formation. The Yarragadee Formation consists of laterally discontinuous interbedded sandstones, siltstones and shales and is inferred to be about 1,350 to 1,500 m thick in the Perth urban area.

Hydrogeology

The interbedded sandstones of the Yarragadee Formation form the Yarragadee confined aquifer and are hydraulically connected with interbedded sandstone aquifers of the Gage Formation.

The hydraulic properties of the Yarragadee aquifer vary with location. In the study area, the discontinuous nature of the sandstone beds has lowered the average horizontal hydraulic conductivity to about 3 m/day. Hydraulic conductivity can locally be higher as indicated by pumping tests.

The average rate of groundwater flow through the Yarragadee aquifer is about 0.9 m/year, confirming the very slow rate of flow indicated by the ¹⁴C dating of the groundwater (Thorpe and Davidson, 1991). It is likely that most of the groundwater flow occurs in the top part of the aquifer, in about the top 500 m. Beneath this depth, the groundwater flow is likely to be lower as indicated by higher salinities (Davidson and Yu, 2005).

HSA Resource Assessment: Temperature, Heat in Place, Bore Deliverability and Recoverable Heat

Using a typical “stored heat” method as applied by Beardsmore et al (2009), the HSA geothermal resource for a specific direct-use application can be estimated. However, the authors of this paper emphasize that the Stored Heat calculated below is given as an element of comparison and is not to be used for other purposes.

For the purpose of reservoir volume estimations, we assume a minimum cut-off temperature of 40°C for direct-use projects, and an injection temperature of 30°C. The base of the Yarragadee aquifer is inferred to be at about 70.6°C. This yields a reservoir volume of 126 km³ below the 100km² modelled area where most of the geothermal bores operate. The average reservoir temperature is 55.3°C. Using calculated values of heat capacity for the fluid and solid, an average porosity of 0.15, we estimate 7,926 PetaJoules (PJ=10¹⁵ Joules) of heat in the modelled reservoir. Should other uses be considered, the cut-off temperature, injection temperature and inferred resource may differ.

The deliverable thermal energy for a typical direct-use geothermal bore is a function of source temperature, heat exchanger efficiency, flow-rate and injection temperature. Typical values of 25 L/s and 12°C temperature drop can provide a deliverable thermal power of 1,113 kilowatt (kW_{th}) and recoverable heat energy of 0.04 PJ/annum or 9747 Megawatts hours/annum (MWh_{th}).

Hence, in first estimation, the Yarragadee aquifer appears to be able to sustain a generalised use of HSA for heating buildings and swimming pools among other uses in the Perth urban area for many years. However, this may only be possible if there is no (or very little) thermal contamination between the geothermal and injection bores. This can be predicted using a numerical model of groundwater flow and heat transport. This is the general purpose of this study.

HSA modelling: Initial temperature distribution in the aquifer (Conductive model)

3D structural model of a selected area of the Perth basin

Data from Davidson and Yu (2005), and proprietary data from Rockwater Pty Ltd have been used to create a detailed structural model of an area of about 100 km² of the central Perth Basin where most of the geothermal bores operate. The model comprises seven geological formations: superficial sediments (TQ), Tertiary alluvial (Tk), Cretaceous sediments (Kco, Kwl, Kws and Kwg) and Jurassic sediments (Jy).

Geostatistical methods have been used to infer formation top and bottom surfaces. Additionally, formation coverages specifying the extent of each geological formation (derived from contours in Davidson and Yu (2005) and modified in areas where new data had become available) have been used to constrain the model.

Purely conductive heat flow 1D modelling

A common practice in the geothermal industry, when modelling steady state temperature conditions of HSA geothermal reservoirs, is to assume purely conductive heat transfer and constant heat conductivity within each of the geological layers. This is referred as conductive heat flow 1D modelling and is considered more accurate than the classical approach of average gradient as it accounts for thermal resistance variations within the lithological column. This has been demonstrated in several studies including Cooper and Beardsmore (1998).

The conductive heat flow 1D assumption fails when heat convection occurs such as in areas of high groundwater velocity such as faults, bores or when significant heterogeneity occurs. However, purely conductive models have proven to satisfactorily represent temperature conditions in the Perth Basin and will be used to provide initial temperatures for a more comprehensive conductive and convective numerical model.

In a conductive heat regime the temperature (T) at the bottom of a geological layer, is equal to the temperature at the top of the layer (T₀) plus the product of Heat Flow (Q) and thermal resistance of the geological layer (R) (where the thermal resistance equals the thickness of the layer divided by the average thermal conductivity).

Consequently, the occurrence of prospective geothermally warmed groundwater in sedimentary aquifers results from sufficiently low conductivity (high thermal resistance) of the sedimentary cover combined with high flow of heat from the centre of the Earth. Heat Flow (Q) is a function of the heat generated within the crust by the decay of radiogenic minerals plus heat conducted from the mantle. A commonly accepted value, derived from nearby temperature logs for the modelled area is 74 mW/m².

Conceptual model

In order to represent the temperature distribution in the basin, several physical properties and boundary conditions have to be estimated and a so called conceptual model must be constructed. For each modelled stratigraphic layer, it is assumed that the lithology and physical properties are the same throughout. Measured thermal conductivities are available for the formations of the Perth basin (Chopra and Holgate, 2008) and have been modified for the purpose of the numerical model by a classical trial and error

HSA modelling: Initial temperature distribution in the aquifer (uncoupled Conductive and Convective model)

3D structural model of a selected area of the Perth basin

The same data as before are used but the structural model is limited to the Yarragadee aquifer (Fig. 1).

All layers overlying the Gage Formation are not modelled, apart from the portion of Kings Park Formation that has eroded the Gage and Yarragadee Formations and which is likely to influence groundwater flow and heat transport.

Heat transport modelling using the “equivalent solute” approach and the numerical code SEAWAT

SEAWAT is a standard finite-difference solute code included in the state-of-the-art modelling software Visual Modflow Pro.

Due to the similarities between heat and solute transport, standard solute codes such as SEAWAT can be used to represent heat transport and variables for SEAWAT solute transport simulator can be reinterpreted for heat transport. This has been demonstrated in several studies including Langevin et al (2008). More detailed information on using solute transport simulation for heat transport modelling can be found in Hecht-Mendez et al (2009). Additional information specific to the use of the SEAWAT code for heat transport is available in Ma and Zheng (2010).

In addition, for this study, SEAWAT has been evaluated against analytical results developed for geothermal and injection bores (doublet) and the results were comparable. The analytical solution has been developed by Gringarten and Sauty (1976) to predict the temperature evolution at HSA geothermal production bores used for geothermal urban heating in the Paris basin.

Conceptual model

As groundwater flow needs to be considered when undertaking conductive and convective geothermal modelling, a numerical code had to be used. For the present work, SEAWAT is used. The previously created 3D structural model is imported into SEAWAT and extrapolated to a finite difference 3D grid where the flow and heat transport equations are solved.

Horizontal cell size varies from 140 m to 5 m near the bores and is about 25 m in vertical. Attention has been given to keep aspect ratio (ratio between cell size along x and z and y and z respectively) less than 6.

The calibrated thermal conductivity for Kings Park, Gage and Yarragadee Formations are assigned to the corresponding cells and set constant for each formation.

method during the calibration of the model. For most of the geological formations, the modelled value is close to the calculated value. However, modelled and measured heat conductivity values were found to differ for some geological formations. It is believed that it is due to lithological variations within those formations and variation of the physical properties with depth.

Table 1: Heat conductivity values (W/m°C) of geological formations in the Perth Basin

Geological Formation	Modelled	Measured at 30°C
TQ	1.5	1.42
Tk	2.20	No data
Kco	2.30 to 2.50	No data
Kwl	1.70 to 2.50	2.56
Kws	1.50	1.71 to 1.72
Kwg	2.55 to 2.60	1.71 to 2.20
Jy	3.05 to 3.20	2.30 to 4.31

Method and boundary conditions

The thickness of each geological formation at given coordinates have been extracted and used together with heat conductivity properties for these layers, to calculate thermal resistances. Assuming a constant surface temperature of 19.5°C at the upper boundary (taken as real mean air value measured at the Perth airport plus 1 °C to account for thermal insulation of rocks) and using the thermal resistance values calculated above and the assumed constant heat flow of 74 mW/m², it was possible to predict the temperature distribution within the Yarragadee aquifer.

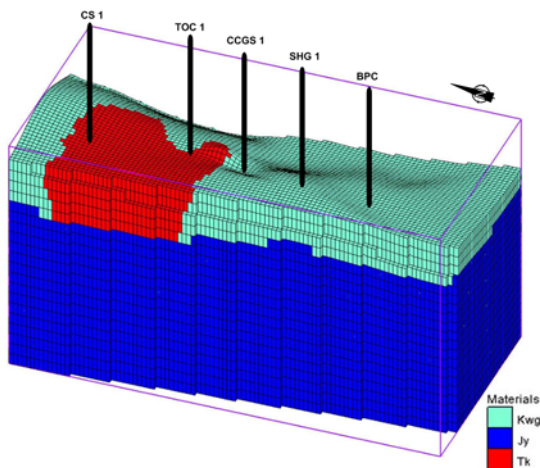


Fig. 1: simplified 3D structural model of the modelled area with geological formations considered in this study and approximate locations of geothermal production bores

CS: Challenge Stadium; TOC:Town Of Claremont; CCGS: ChristChurch Grammar School; SHG: St Hilda Geothermal, BPC: Bicton Polo Club.

Hydrogeological parameters are available for the formations of the Perth basin (Davidson and Yu (2005) and proprietary data from Rockwater Pty Ltd) and have been modified for the purpose of the numerical model by a classical trial and error method during the calibration of the model.

Table 2: Modelled hydrogeological parameters of geological formations in the Perth Basin

Geological Fm.	Kh (m/day)	Kh/Kv (-)	S (-)
Tk	$<1 \times 10^{-4}$	1	2.5×10^{-4}
Kwg	6.5	10	2.5×10^{-5}
Jy	3.5	10	5×10^{-5}

Method and boundary conditions

The conductive and convective model is used to give the present-day temperature distribution of the modelled area of the Perth basin.

In addition to the physical and thermal parameters, aquifer boundaries had to be defined. For the simulation presented here, the temperatures of the upper and lower boundaries are taken from the conductive model and are set constant for all simulations (Dirichlet boundary condition). Monitoring bore heads in the vicinity of the modelled area are gridded (kriging method) and assigned as constant head boundaries. The temperatures of groundwater inflow are taken from results of the conductive model.

Barrier (impermeable) boundaries are set at the top and bottom of the model and are consistent with the hydrogeology of the area. The low permeability South Perth Shale overlies the Yarragadee Formation throughout the modelled area.

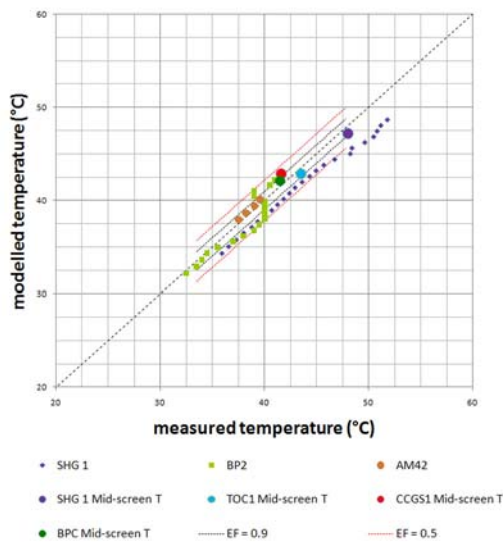


Fig. 2: Calibration plot showing calculated temperatures against measured temperatures

Results

Modelled temperatures were found to agree with measured temperatures and reliable temperature logs from existing geothermal bores (Fig. 2). The evaluation of the model is based on residual errors and follows the method of efficiencies (EF) described by Loague and Green (1991). Overall efficiency values range from 0.91 to 0.95, showing good to very good agreement between measured and modelled temperatures.

Moreover, results from the conductive and convective model were found to be similar, suggesting that regional groundwater flow has little impact on temperature distribution in the Yarragadee aquifer. This may not be true locally in areas where the groundwater flow is more important.

Predictive model (year 2000 to 2050)

Conceptual model

Calculated temperatures from the previous model are taken as initial temperatures (January 2000) and potential heads are considered constant and equal to the potential heads measured in January 2010. Sensitivity analyses have shown that the observed decline of potential heads had little impact on the results. The geothermal installations operating schedule is given in Table 3. For bores screened in several different sections of the aquifer (TOC1, CCGS3), a portion of the total flow-rate (function of the length of the slotted section over the total screened length) is assigned to the corresponding cell of the model (run 1). As geothermal bores operate mostly during winter (April to October) when ambient temperatures are lower than the required temperature (temperature of the pool), modelled flow-rates are reduced to average rates in a second simulation (run 2).

Table 3: Geothermal installations operating schedule

Bore	Operating since	Temperature at the borehead (°C)	Q (L/s)
SHG1	2010	48.0	-25
SHG2	2010	36.0*	25
TOC1	2005	43.5	-14
TOC2	2005	29.0*	14*
CCGS1	2002	41.6*	-17
CCGS3	2002	27.0*	17*
CS1	2003/2004	42.0	-40
CS2	2003/2004	36.0*	20*
CS3	2003/2004	36.0*	20*

*: injection bore

Calibration

CCGS1 temperature and hydraulic head data have been used for calibrating the model as it is the oldest geothermal installation in the area. Little to no increase of the temperature at the

borehead has been recorded since the bore was commissioned. Considering the above assumptions, run 2 (Fig. 3) shows an acceptable agreement with pumped temperature increasing by 0.1°C after 10 years.

Note that a more accurate evolution of temperature at the bore could be obtained using a local model with a higher spatial resolution and an explicit numerical solution for advection.

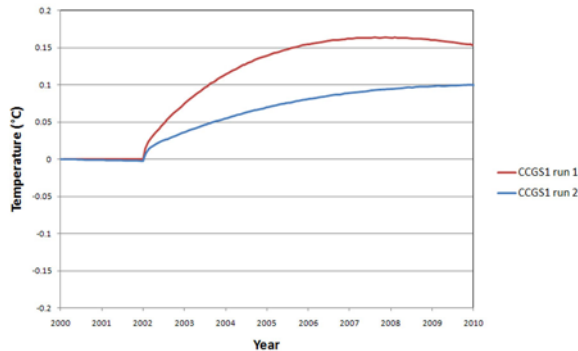


Fig. 3: CCGS1 modelled pumped temperatures

In addition, steady state modelled drawdown is 10.3 m and agrees with the aquifer losses of 8 m measured at the end of the 48 hours constant-rate pumping test.

Results: environmental impact of the injection

Following the calibration, the model was run from January 2000 to January 2050 to predict the evolution of temperatures within the basin.

The model aims are (i) to determine the general evolution of temperature of the Yarragadee aquifer, (ii) to give a first estimation of the lifetime of existing geothermal installations and (iii) to identify areas where there is an impact of injected water on aquifer temperatures.

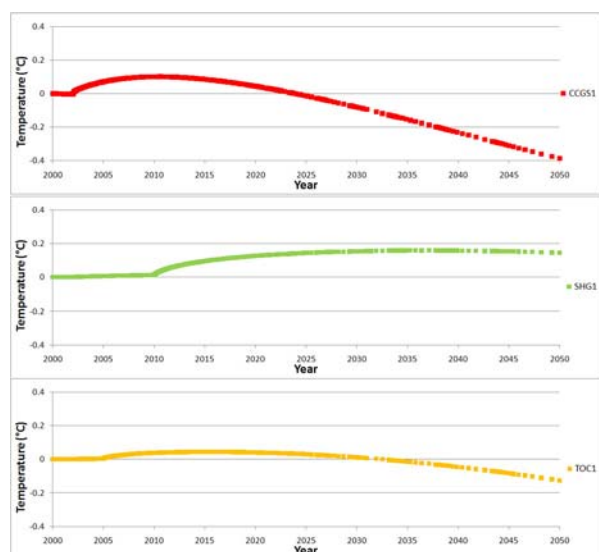


Fig. 4: Predicted evolution of temperature at CCGS1, TOC1 and SHG1

The initial observation is that there is little temperature decline at the production bores after

almost 50 years of continuous operation as shown in Fig. 4.

The modelled temperature decline at CCGS1 in January 2050 is 0.39°C after 48 years, and 0.12°C at TOC 1 after 45 years whereas the temperature at SHG1 has increased by 0.14°C after 40 years. This is likely to have little impact on the geothermal installation efficiencies and subsequently the lifetime of all three geothermal installations; estimated to be more than 40 years.

Discussion

For all three bores, the temperature evolution can be described as follows:

- Stage 1: Increased temperature of the pumped water (increase is higher when flow-rate is higher) provoked by the inflow of deeper and warmer groundwater in the bores. This is further facilitated by the presence of upward heads.
- Stage 2: As the cooled groundwater is injected and travels through the aquifer in the direction of the production bore, the rate of temperature increase diminishes and eventually stabilises (this happens earlier when the vertical distance between injection and production screened section is small).
- Stage 3: Pumped temperatures start declining and eventually decline at a linear rate. It is calculated that bores CCGS1 and TOC1 will reach Stage 3 in year 2050 because of the smaller vertical separation between production and injection screened sections, whereas SHG1 is likely to still be in Stage 2.

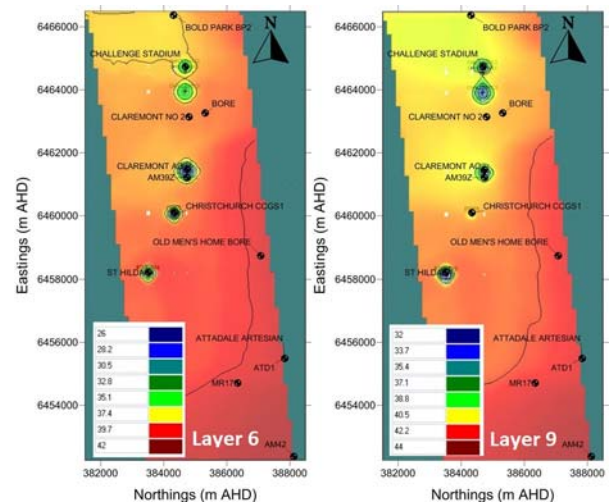


Fig. 5: Calculated temperature distribution (°C) in selected layers: layer 6 from -520 to -676 m AHD and layer 9 from -651 to -767m AHD

The modelled results show that the cooler injected water has a limited impact on the pumped groundwater temperature because of the moderately low vertical hydraulic conductivities, upward heads in the deeper geothermal bores, and the vertical distances between production and injection bore screens.

The cooled groundwater plume is calculated to extend 850 m in a circular pattern from TOC1 (Claremont AC) by 2050 (Fig. 5) indicating that natural groundwater flow has little influence on the shape of the groundwater plume. Conversely, the groundwater plume generated by CS1 (Challenge Stadium) has a very distinctive tear-drop pattern (Fig. 5, layer 9) indicating that a portion of the injected water is recirculated and that thermal contamination is occurring.

Conclusion: HSA direct-use sustainability and future research objectives

Although the presented simulation is decoupled (water density is independent of temperature) and may not be accurate where density effects dominate, the results show that pumped groundwater temperatures are unlikely to change significantly over the next 40 years. This supports the notion that HSA direct-use is a cost-effective solution (payback is about 5 years) for heating buildings or swimming pools for example.

However, temperature depletion seems to extend horizontally and although no visible interference between bores has been recorded, it is advisable to avoid pumping from the same depth as water is injected. Therefore, it is recommended that future production bores should be sited at least 500 m from one another and at different depths (i.e. 100 to 150 m deeper than the nearest injection screens).

To increase the accuracy of the model and to be able to guarantee the sustainability of HSA direct-use projects, additional work could be performed:

- Create local, high resolution models for each geothermal installation.
- Perform temperature logging periodically.
- Model heterogeneity patterns of the Yarragadee aquifer.
- Refine the structural model by considering geological members within the Osborne and Leederville formations.
- Refine the calibration of the model using a transient constant-rate pumping test.
- Perform hydraulic head versus depth measurements.
- Correlate the stratigraphy (siltstone and sandstone beds) between production and injection bores to increase vertical accuracy.
- Monitor geothermal installations periodically to obtain monthly data of injection temperatures, pumped water temperatures, flow-rates and injection pressures.

- Evaluate the impact of density forces (forces driving the formation of convection cells) on initial temperature distribution.
- Consider heat flow variations over the modelled domain.
- Refine the calibration using recent temperature logs of artesian monitoring bores.

References

Beardsmore, G. R., et al, 2009, Statement of estimated Geothermal Resources Metropolitan Perth Geothermal Play, 31/07-8 GEP, 27 July 2009.

Chopra, P.N, and F., Holgate., 2008, Geothermal energy potential in selected areas of Western Australia; a consultancy report by Hot Dry Rocks Pty Ltd for Geological Survey of Western Australia: Geological Survey of Western Australia, G31888 A2.

Cooper, G. T., and Beardsmore, G. R., Geothermal systems assessment: understanding risks in geothermal exploration in Australia: PESA Eastern Australasian Basins Symposium III Sydney, 14–17 September, 2008.

Davidson, W.A., and Yu, X., 2005. Perth regional aquifer modelling system (PRAMS) model development: Hydrogeology and groundwater modelling : Western Australia Department of Water, Hydrogeological record series HG 20.

Gringarten, A.C., and Sauty, J.P., 1976, The effect of reinjection on the temperature of a geothermal reservoir used for urban heating: BRGM, Orleans. 12p.

Hecht-Mendez, J. et al., 2009, Evaluating MT3DMS for Heat Transport Simulation of Closed Geothermal Systems: Wiley-Blackwell. 16p.

Langevin, C.D., Thorne, D.T. Jr., Dausman, A.M., Sukop, M.C, and Guo, Weixing, 2008, SEAWAT Version 4: A Computer Program for Simulation of Multi-Species Solute and Head Transport: U.S. Geological Survey Techniques and Methods Book 6, Chapter A22, 39 p.

Loague, K., and R.E., Green, 1991, Statistical and graphical methods for evaluating solute transport models: Overview and application: Journal of Contaminant Hydrology 7, no. 1–2: 51–73.

Ma, R., and Zheng, C., 2010, Effects of density and viscosity in modelling heat as a groundwater tracer: Groundwater, Volume 48 Issue3, pp. 380-389.

Thorpe, P.M., and Davidson, W.A., 1991, Groundwater age and hydrodynamics of the confined aquifers, Perth, Western Australia: Proceedings of the International Conference on Groundwater in Large Sedimentary Basins, Perth, Western Australia, 1990. Australian Water Resources Council Series, no. 20, p. 420-436.

Geothermal Exploration in India

Sukanta Roy

National Geophysical Research Institute
 (Council of Scientific and Industrial Research)
 Uppal Road, Hyderabad 500 606, India
 Corresponding author: sukantaroy@yahoo.com

In most Precambrian terrains including India, moderate-to-low temperature hot spring systems represent the potential conventional geothermal energy resources. This scenario is in contrast to geothermal fields under production in other parts of the world, which are located in Quaternary volcanic / magmatic settings (Gupta and Roy, 2006). This paper outlines (i) the major hot spring occurrences in India, (ii) the exploration efforts undertaken so far, (iii) possible geothermal models in the light of regional heat flow and heat production datasets, (iv) a few critical information gaps that need to be covered to make realistic assessment of the geothermal energy potential, and (v) perspectives for development and utilisation of geothermal energy in the country, both for electric power generation as well as for direct uses.

Keywords: India, geothermal energy, heat flow, radiogenic heat production

Exploration of Geothermal Energy Resources

The major groups of hot springs in India occur in Manikaran, Puga-Chhumathang valley and Tapoban in the Himalaya, a near N-S trending linear belt in the west coast of Maharashtra, the Son-Narmada-Tapti lineament zone in central India, Tattapani in Chattisgarh, and Rajgir-Monghyr, Surajkund and Bakreshwar in eastern India. The distribution of major groups of hot springs is shown in Figure 1. Rao (1997) provides a brief summary of the historical development of studies on the Indian geothermal resources, starting with the first compilations of 99 hot springs in India and the adjacent countries by Schlagintweit (1865). The locations, geological settings and temperatures of hot springs located in different geologic provinces in India have been compiled by previous workers (for example, Oldham, 1882; Ghosh, 1954; Gupta, 1974; Guha, 1986; GSI, 1991, 2002 and others). A number of those geothermal springs have been used for balneological purposes. However, India is yet to produce electric power from a geothermal field.

Among the most notable achievements during the past five decades have been the assessment of geothermal fields by the Government of India in 1966 and publication of a comprehensive report in 1968 recommending preliminary prospecting of

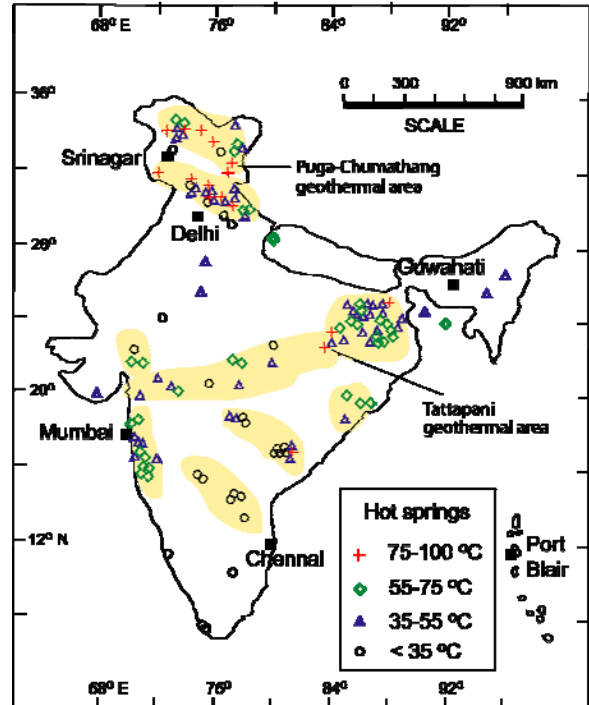


Figure 1. Outline of India showing the distribution of major groups of warm and hot springs (modified after Krishnaswamy, 1975). Temperatures of the hot spring waters are indicated using symbols (see legend). Shaded regions (exaggerated scale) show the major clusters of hot springs.

the Puga and Manikaran geothermal fields in the Himalaya (Hot Springs Committee, 1968). A major, systematic, multi-disciplinary, multi-Institutional programme (including drilling up to 385 m) covering the Puga-Chumathang field in Ladakh was mounted during 1972-74 under the stewardship of V.S. Krishnaswamy of the Geological Survey of India (GSI). The subsurface features were delineated in considerable detail and the results were presented at the Second United Nations Symposium on the Development and Use of Geothermal Resources in 1975. The most significant outcome of the effort was a proposal to set up a 1 MWe binary-cycle power plant on a pilot scale basis, which has not been implemented so far. Attempts to revisit the geothermal exploration in the area include a number of geochemical studies (GSI, 1996) and recent magnetotelluric studies (Abdul Azeez and Harinarayana, 2007). An expert group set up in 2008 by the Ministry of New and Renewable Energy, Government of India made strong recommendations to install pilot-scale plant by

drilling exploration cum demonstration wells in the area (MNRE, 2008). This would be useful not only for monitoring the hot water discharge and temperatures over a period of time but also studying the shallow reservoir characteristics. Another major initiative, directed towards the hot springs of the West Coast belt and the Son-Narmada-Tapti belt was taken up by the GSI with UNDP assistance during 1976-77, and was extended for a few years on its own, including deep drilling up to depth of 500 m. The results were published in the Records of the GSI (1987). The Tattapani hot springs of Chattisgarh district was identified for trials with regard to power production using a 300 KW_e binary-cycle power plant. Summaries of various exploration programmes undertaken in the country during the period 1970-1990 are given in Gupta et al. (1973, 1974); Shanker et al. (1976); Singh et al. (1983); Krishnaswamy and Ravi Shanker (1980); GSI (1983, 1991, 1996, 2002); Thussu et al. (1987); Moon and Dharam (1988) and Gupta (1992). The salient results in the case of the two potential geothermal fields, Puga and Tattapani, are summarized below.

Puga Valley Hot Springs

In the case of Puga valley springs, geothermal evidence gathered so far and geochemical indicators including the occurrence of cesium deposits around the springs have suggested the possibility of high temperature hydrothermal circulation in the subsurface (Absar et al., 1996). A shallow reservoir in the top few hundred meters was inferred from geophysical and geothermal investigations carried out during the 1970s. Recent magnetotelluric studies indicate the presence of an anomalous conductive feature (~5 Ohm m) below a depth of ~2 km in the area of the thermal manifestations (Harinarayana et al., 2006; Abdul Azeez and Harinarayana, 2007). Although broad correlations between high electrical conductivity and high temperatures have been observed in some geothermal areas, the calibration of electrical conductivity anomalies to temperature anomalies at depth is not established. Further efforts are necessary to fill existing gaps in knowledge and verify the hypothesis regarding the occurrence of subsurface magma chambers or young intrusive granites in the region. Such heat sources alone can sustain power generation on a reasonable scale (Rao et al., 2003). Determination of background heat flow outside the hot springs zone, helium-isotopic measurements on the thermal waters, detailed petrographic and geochronological studies on young granite intrusives, and tritium dating of the waters would be useful for testing a magmatic heat source.

Tattapani Hot Springs

In the case of the Tattapani hot springs, the temperatures of the issuing waters is ~110 °C, the

highest recorded so far in the shield. The spring waters are meteoric in origin as indicated by oxygen and helium isotopic data, and the age of these waters indicated by tritium dating is ~40 years (Thussu et al., 1987; Sharma et al., 1996; Minnisale et al., 2000). Repeat well testing carried out by GSI in 1995 and 1999 indicate no significant fall in temperatures and pressures during the intervening period (Sarolkar and Sharma, 2002). Recent magnetotelluric studies in the area have delineated a deep, anomalous conductive zone possibly indicating the subsurface extent of the reservoir (Harinarayana et al., 2004). Lack of evidence for Quaternary magmatism in the region as well as the meteoric nature of the hot spring waters indicate that the hot springs are controlled by forced convection due to peizometric gradient existing between the recharge area and the hot springs, and that the springs could be simply "mining" the normal heat flow (Roy and Rao, 1996; Rao et al., 2003). However, no heat flow measurements outside the localized hot springs zone have been made. There is therefore a clear need to establish the regional thermal conditions by systematic geothermal measurements because they would contain information about subsurface flow and location of recharge area also (Lachenbruch et al., 1976).

Other areas

A large number of warm to hot springs occur in western, central and eastern parts of the Indian shield. The temperatures of these springs are lower than those at Tattapani and vary between 35° and 80 °C. It is likely that a geothermal model similar to that at Tattapani could explain the occurrence of these hot springs.

Heat Flow and Heat Production

Heat flow determinations made through precise temperature measurements in boreholes and thermal conductivity measurements on representative rock formations have been the central theme of the heat flow studies programme at the National Geophysical Research Institute since its inception in 1961. Although boreholes of opportunity have been used for the majority of measurements, a selection has been made on the following criteria to make the heat flow determinations useful for characterization of the thermal state of the lithosphere: (1) depths greater than 150 m in hard rock areas and several hundred metres in sedimentary basins (2) sites away from hot spring manifestations, tectonically active regions, and rugged topography (3) temperature profiles with no characteristic perturbations such as those of heat refraction and groundwater movement. The principal constraint in the data acquisition programme has been the availability of suitable boreholes for making

temperature measurements. This constraint has been addressed, to some extent, through the drilling of 14 dedicated “heat flow” boreholes to depths of up to 500 m at carefully chosen sites in south India. The careful siting of the boreholes in areas of relative lithological homogeneity and low groundwater yields facilitated the acquisition of undisturbed temperature-depth profiles from which gradients could be estimated with a great degree of confidence. In geologic provinces of northern Indian shield, the heat flow coverage is variable and several gaps exist over large segments. In the Himalaya, regional heat flow data are not available. Borehole temperature measurements in close proximity of hot springs exist at a few locations only. However, these measurements are affected by convection due to hydrothermal circulation in the near surface zone and are not representative of deep crustal conditions. Thermal conductivity data for all major rock formations in the southern Indian shield and several rock formations from other parts of India constitute a very extensive database for modelling the thermal structure in the upper few kilometres of the crust.

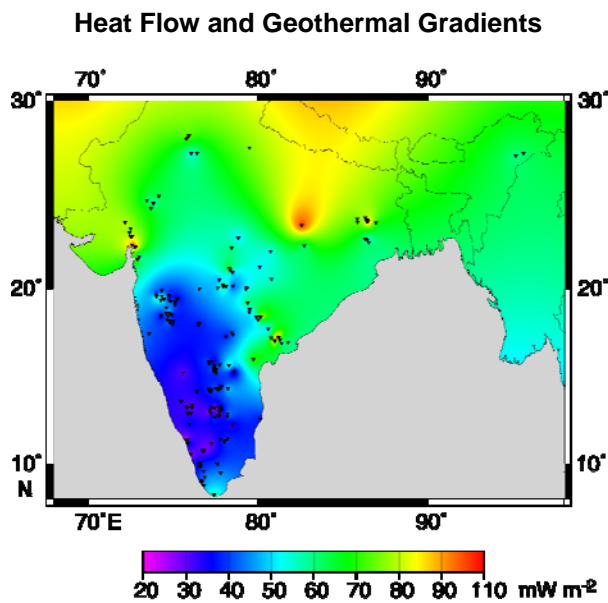


Figure 2. Heat flow map of the Indian Shield. Heat flow sites are shown by filled triangles. Heat flow determinations have been made on the basis of temperature measurements in boreholes and thermal conductivity of rock formations. Over large regions in northern India which are not covered with heat flow measurements, the contours should be treated with caution. [Sources of data: Roy and Rao (2000) and original references therein; Ray et al. (2003); Rao et al. (2003); Roy (2008); Roy et al. (2008)].

A heat flow map for the Indian shield is shown in Figure 2. Heat flow data are now available from measurements made in ~210 boreholes distributed over the major geological provinces in

the shield. The dataset shown here is confined to sites where complete information on geothermal gradient and thermal conductivity are available. Heat flow determined using other techniques such as chemical composition of water, and correlations with P-wave velocity and age, are excluded. A detailed discussion of heat flow characteristics of different provinces is given in the papers by Roy and Rao (2000) and Rao et al. (2003). The salient features of the heat flow spectrum in the Indian shield are briefly mentioned below.

1. The southern Indian shield comprising the Archaean Dharwar greenstone-granite-gneiss province and gneiss-granulite province, is characterized by low heat flow, generally ranging from 25 to 50 mW m^{-2} . Geothermal gradients measured in the top few hundred meters in boreholes and up to 2150 m in a deep mine are in the range 12-15 mK m^{-1} .
2. The low heat flow regime of south India extends northward beneath the Deccan Traps in central India, which indicate the absence of thermal transients related to the ~65 Ma Deccan volcanism in the present-day heat flow. Measurements at several localities distributed in Deccan Traps province indicate an average gradient of ~25 mK m^{-1} . However, beneath the Traps which range from a few meters in the east to 2-3 km in the west, the gradient in the Precambrian granitic basement drops to ~15 mK m^{-1} due to higher thermal conductivity of granitic rocks relative to basalts.
3. The Precambrian provinces in northern Indian shield show a contrasting heat flow regime, with values ranging from 50 to 96 mW m^{-2} . Previous studies have attributed the enhanced heat flow to high levels of radiogenic heat production in the upper crust. Temperature gradients vary between 12 and 30 mK m^{-1} across different rock formations.
4. The Gondwana sedimentary basins (Upper Carboniferous to Lower Cretaceous) have a generally high but variable heat flow in the range 46 to 107 mW m^{-2} . Temperature gradients show large variability, and reach peak values of up to ~50 $^{\circ}\text{C km}^{-1}$ in the Damodar Valley basins and ~40 $^{\circ}\text{C km}^{-1}$ in Godavari Valley basin.
5. The Cambay sedimentary basin of Tertiary age in western India shows consistent high heat flow, 75-96 mW m^{-2} in the northern parts and a lower heat flow, 55-67 mW m^{-2} , in the southern parts. Very high gradients in the range 37 to 56 $^{\circ}\text{C km}^{-1}$ were computed from temperature measurements to depths >1000 m in the northern part.

Radiogenic Heat Production

Heat production due to radioactive decay of long-lived isotopes of U, Th and K (namely, ^{235}U , ^{238}U , ^{232}Th , and ^{40}K) in rock formations constituting the continental crust plays a key role in interpretation of heat flow data. With this primary objective, a low-level counting gamma-ray spectrometric facility using a single-channel analyser was established at the NGRI for analysis of rocks for radioelements U and Th (at ppm levels) and K (Rao, 1974; Rao and Rao, 1979). The facility has been progressively upgraded using a multi-channel analyser and later, a PC-based multi-channel analysing card that provides spectrum stabilization (Roy and Rao, 1999, 2003). Several hundred samples covering major rock types in the Indian shield have been analysed for U, Th and K. The salient features of the dataset are described in Roy (2008).

Over the last two decades, laboratory analyses have been complemented by in-situ gamma-ray spectrometric analysis in several areas in the Indian shield (Roy, 1997; Roy and Rao, 2000, 2003; Ray et al., 2003, 2008). A field-portable, four-channel, spectrum stabilized, gamma-ray spectrometer and a large crystal (6" high and 4" diameter) detector have been used. Analysis for U, Th and K are made by placing the detector directly over fresh rock outcrops. In this case, the detector senses a much larger volume of rock mass, typically a circle of investigation of ~40 cm and a depth of ~12 cm, compared to the laboratory method. In areas abounding with fresh outcrops, this method results in faster coverage.

Significant observations include delineation of pockets of very high heat production in granitic rocks, for example in Tattapani area, and young granite intrusives in northwestern parts of India, detection of granulite facies rocks with lowest heat production reported in literature, and a range of rock formations with intermediate heat production values.

Perspectives for Development of Geothermal Energy

Re-assessment of Energy Potential of Conventional Geothermal Resources

In view of growing energy demands and the emphasis on renewable energy in India, a re-assessment of geothermal energy potential of Puga Valley hot springs in Ladakh and Tattapani hot springs in Chattisgarh should be carried out by covering some critical gaps in information through acquisition of new data, combined interpretation of geothermal datasets and existing geological, hydrological, geochemical and geophysical datasets to throw light on the nature of the heat source of the hot springs and their sustainability for power production, undertaking

drilling and setting up of pilot-scale binary-cycle power plants.

Geothermal resources vary widely from one location to another, depending on the temperature and depth of the resource, the rock chemistry, and the abundance of groundwater. The type of geothermal resource determines the method of its utilization. Variants of binary cycles appropriate to optimum utilization of geothermal heat from hot springs in non-volcanic settings such as those in India need to be developed.

Direct Heat Uses

The heat extracted from warm-to-hot waters emerging from other hot spring systems in the country can be gainfully employed for a number of direct uses such as development of tourist spas for bathing, swimming and balneology, greenhouse cultivation in cold climates, extraction of borax and rare materials such as cesium, and agricultural product processing. The significant economic and environmental benefits of using moderate-to-low enthalpy geothermal waters to replace even small quantities of conventional fuels for direct uses cannot be ignored today in view of the steep increase in costs of fossil fuels and associated greenhouse gas emissions.

Exploration for Enhanced Geothermal Systems

A second category of geothermal resource traditionally referred to as "hot dry rock" and more recently as "enhanced geothermal systems (EGS)", has not yet been explored in India. The primary requirement for such a resource is the occurrence of high temperatures (typically upwards of 150 °C) at economically viable depths (typically the top 1-4 km of the Earth's crust). Areas of anomalous high heat flow, high-heat-producing granites and other silicic igneous intrusives having a depth extent of a few kilometers, could be possible targets of future exploration efforts in the country (Roy, 2008). These considerations reinforce the need for carrying out systematic heat flow as well as radiogenic heat production investigations on a country-wide scale.

Geothermal Heat Pumps

The viability of geothermal heat pumps for heating inside buildings should be explored in the states of Jammu and Kashmir, Himachal Pradesh and parts of Uttarakhand which experience severe winter conditions for long periods. Space cooling requirements in most parts of India have grown several fold in the recent years with the growth in economy. There is enormous scope for developing the capabilities in geothermal cooling of buildings by modifying existing technologies to suit Indian conditions. A proper assessment of the technology for application to different climatic environments existing in the region, and its

exploitation by integrating it with building designs should be encouraged.

Summary

Moderate-to-low enthalpy hot spring systems primarily represent the known geothermal energy resources in India. These resources are distributed in diverse physiographic and tectonic settings, viz., the Himalayan belt and the Precambrian shield. Detailed geological and geochemical exploration followed by limited geophysical exploration and shallow drilling investigations up to a few hundred meters have resulted in first-order geothermal models for the major hot spring zones in the country. However, development of the geothermal resources has remained at a very low level mainly due to inadequate characterization of the deeper thermal regime leading to low confidence in proposed reservoir models and sustainability of the heat source. There is therefore an urgent need to carry out a reassessment of the geothermal energy potential of hot springs by employing new geophysical probing tools and computational techniques available today, both for electric power generation as well as for direct uses. Efficient exploitation technologies appropriate to non-volcanic areas need to be developed. Systematic heat flow and heat production investigations need to be carried out for the identification of areas where high temperatures in the top few kilometers below the ground surface indicate potential for "hot sedimentary aquifers" as well as "enhanced geothermal systems". The vast potential for geothermal heat pumps is yet to be tapped. The existing technology must be made accessible to individuals and small communities as a low-cost alternative for their space heating and cooling needs.

References

- Abdul Azeez, K.K., and Harinarayana, T., 2007, Magnetotelluric evidence of potential geothermal resource in Puga, Ladakh, NW Himalaya : *Curr. Sci.*, v. 93, p. 323-329.
- Absar, A., Jangi, B.L., Sinha, A.K., Rai, V., and Ramteke, R., 1996, Concentration of rare alkalies in the geothermal fluids at Puga, Ladakh, J and K – Significance and possibilities of exploitation, in Pitale U.L. and Padhi R.N., eds., *Geothermal Energy in India : Geological Survey of India, Special Publication 45*, p. 163-167.
- G.S.I., 1983, Status note on geothermal exploration in India by Geological Survey of India and a profile of the exploration strategy: Geological Survey of India, Kolkata.
- G.S.I., 1987, Records of the Geological Survey of India, v. 118, Pt. 6.

- G.S.I., 1991, *Geothermal Atlas of India: Geological Survey of India, Special Publication 19*, 144 p.
- G.S.I., 1993, *Geological Map of India, scale 1:5,00,000 : Geological Survey of India.*
- G.S.I., 1996, *Geothermal Energy in India*, U.L. Pitale and R.N. Padhi, eds., Geological Survey of India, Special Publication 45.
- G.S.I., 1998, *Geological Map of India, 7th Edition, scale 1:2,000,000. Geological Survey of India.*
- G.S.I., 2002, *Geothermal Energy Resources of India. Geological Survey of India, Special Publication 69*, p. 12-29.
- Ghosh, P.K., 1954, *Mineral springs of India : Records, Geological Survey of India, v.80*, p. 541–558.
- Guha, S.K., 1986, *Status of geothermal exploration for geothermal resources in India : Geothermics, v. 15*, p. 665–675.
- Gupta, H.K., and Roy, S., 2006, *Geothermal Energy: An alternative resource for the 21st Century : Elsevier, Amsterdam*, 292 p.
- Gupta, M.L., 1974, *Geothermal resources of some Himalayan hot spring areas : Himalayan Geology, v.4*, p. 492–515.
- Gupta, M.L., 1981, *Surface heat flow and igneous intrusion in the Cambay basin, India : J. Volcanol. Geotherm. Res., v.10*, p.279-292.
- Gupta, M.L., 1992, *Geothermal resources of India: geotectonic associations, present status and perspectives*, in Gupta, M.L., Yamano, M., eds., *Terrestrial Heat Flow and Geothermal Energy in Asia : Oxford and IBH, Delhi*, p. 311–329.
- Gupta, M.L., Rao, G.V., and Hari Narain, 1974, *Geothermal investigations in the Puga Valley hot spring region, Ladakh, India : Geophysical Research Bulletin, v.12*, p.119–136.
- Gupta, M.L., Rao, G.V., Singh, S.B., and Rao, K.M.L., 1973, *Report on thermal studies and resistivity surveys in the Puga Valley geothermal field, Ladakh district, J&K. NGRI Technical Report 73–79, National Geophysical Research Institute, Hyderabad, India.*
- Harinarayana, T., Abdul Azeez, K.K., Murthy, D.N., Veeraswamy, K., Rao, S.P.E., Manoj, C., and Naganjaneyulu, K., 2006, *Exploration of geothermal structure in Puga geothermal field, Ladakh Himalayas, India by magnetotelluric studies : J. App. Geophys., v.58*, p. 280-295.
- Harinarayana, T., Someswara Rao, M., Sarma, M.V.C., Veeraswamy, K., Lingaiah, A., Rao, S.P.E., Virupakshi, G., Murthy, D.N. and Sarma, S.V.S., 2004, *Delineation of a deep geothermal zone in Tattapani region, Surguja district, M.P.: EM-INDIA Seminar, Hyderabad, India, Abstracts.*

- Hot Springs Committee, 1968, Report of Hot Springs Committee: Government of India, unpublished.
- Krishnaswamy, V.S., 1975, Geothermal energy resources of India: Symposium on Energy Resources in India, Indian Science Congress, Abstracts.
- Krishnaswamy, V.S., Ravi Shanker, 1980, Scope of development, exploration and preliminary assessment of the geothermal resource potentials of India : Records, Geological Survey of India, 111, Pt. II, p. 17-40.
- Lachenbruch, A.H., Sorey, M.L., Lewis, R.E., and Sass, J.H., 1976, The near-surface hydrothermal regime of Long Valley Caldera : J. Geophys. Res., v.81, p. 763-768.
- Minnisale A., Vaselli O., Chandrasekharam D., Magro G., Tassi F., and Casiglia, A., 2000, Origin and evolution of intracratonic thermal fluids from central-western peninsular India : Earth Plan. Sci. Lett., v.181, p. 377-394.
- Moon, B.R. and Dharam, P., 1988, Geothermal energy in India – Present status and future prospects : Geothermics, v.17, 2/3, p. 439-449.
- MNRE, 2008, Report of Expert Group on Power Generation from Geothermal Energy at Puga, Jammu and Kashmir, India : Ministry of New and Renewable Energy, Govt. of India.
- Oldham, R.D., 1882, The Thermal Springs of India : Geological Survey of India, Memoir, vol. 19.
- Rao R.U.M., Roy, S., and Srinivasan, R., 2003, Heat Flow Researches in India – Results and Perspectives : Geol. Soc. India Memoir, v. 53, p. 347-391.
- Rao, R.U.M., 1974, Gamma-ray spectrometric set-up at NGRI for analysis of U, Th and K in rocks : Geophys. Res. Bull., v.12, p.91-101.
- Rao, R.U.M., and Rao, G.V., 1979, Radiogeologic studies at NGRI – A Review : Geophys. Res. Bull., v. 17, p. 163-173.
- Rao, R.U.M., 1997, Book review – Geothermal energy in India, Pitale, U.L. and Padhi, R.N., eds. : J. Geol. Soc. India, v.49, p.746-748
- Roy, S., 2008, Heat Flow Studies in India during the past five decades: Geological Society of India Memoir 68, p. 89-122. .
- Roy, S. and Rao, R.U.M., 1996, Regional heat flow and the perspective for the origin of hot springs in the Indian shield, in Pitale, U.L., Padhi, R.N., eds., Geothermal Energy in India: Geological Survey of India, Special Publication 45, p. 39-40.
- Roy, S. and Rao, R.U.M., 2000, Heat flow in the Indian shield: J. Geophys. Res., v.105, p.25,587-25,604.
- Roy, S. and Rao, R.U.M., 2003, Towards a crustal thermal model for the Archaean Dharwar Craton, southern India: Physics and Chemistry of the Earth, v.28, p.361-373.
- Roy, S., Ray L., Kumar, P.S., Reddy, G.K., and Srinivasan, R., 2003, Heat Flow and Heat Production in the Precambrian Gneiss-Granulite Province of Southern India, in M. Ramakrishnan, ed., Tectonics of Southern Granulite Terrain – Kuppam-Palani Geotranssect: Geological Society of India, Memoir 50, p.177-191.
- Roy, S., Ray, L., Bhattacharya, and Srinivasan, R., 2008, Heat flow and crustal thermal structure in the Late Archaean Closepet Granite batholith, south India : Int. J. Earth Sci., v.97, doi: 10.1007/s00531-007-0239-2, p.245-256.
- Sarolkar, P.B., and Sharma, S.K., 2002, Geothermal well testing at Tattapani geothermal field, district Surguja, India: 27th Workshop on Geothermal Reservoir Engineering, Stanford University, Stanford, California, Abstracts, SGP-TR-171
- Schlagintweit, R. de., 1865, Enumeration of Hot Springs of India and High Asia : Journal of the Asiatic Society of Bengal, v. 33 (2), p. 51-73.
- Shanker R., Padhi, R.N., Arora, C.L., Prakash, G., Thussu, J.L., and Dua, K.J.S., 1976, Geothermal exploration of Puga and Chumathang geothermal fields, Ladakh, India : Second U.N. Symposium on the development and use of geothermal resources, San Francisco, Abstracts, p. 245-258.
- Sharma S., Nair, A.R., Kulkarni, U., Navada, S.V., and Pitale, U.L., 1996, Isotope and geochemical studies in Tattapani geothermal area, district Surguja, Madhya Pradesh, in Pitale UL and Padhi RN, eds, Geothermal Energy in India: Geological Survey of India , Special Publication 45, p. 233-242.
- Singh, S.B., Drolia, R.K., Sharma, S.R., and Gupta, M.L., 1983, Application of resistivity surveying to geothermal exploration in the Puga valley, India: Geoexploration, v. 21, p. 1-11.
- Thussu, J.L., Rao, S.M., Prasad, J.M., Navada, S.V., and Kulkarni, U., 1987, Isotope composition of thermal and non-thermal waters of Tattapani hot spring area, district Surguja, Madhya Pradesh: Geological Survey of India, Records, v.115, Pt.6, p. 56-65.

Queensland Coastal Geothermal Energy Initiative – An Approach to a Regional Assessment

Behnam Talebi^{1*}, Mark Maxwell¹, Sarah Sargent¹ and Steven Bowden¹

¹Mines and Energy, 80 Meiers Road, Indooroopilly QLD 4068.

*Corresponding author: behnam.talebi@deedi.qld.gov.au

The best-known potential geothermal resources in Queensland are located beneath the Cooper-Eromanga Basins in the south-west of the state. The depth to the resources, and their distance from potential markets and the existing national electricity grid, are the main challenges for their development for power generation in the near term. The \$5 million Coastal Geothermal Energy Initiative (CGEI) is the Queensland Government’s program to implement the commitment made in the ClimateSmart 2050 strategy through the Queensland Renewable Energy Fund to investigate additional sources of hot rocks for geothermal energy close to existing transmission lines and potential markets. The initiative is a cooperative project between Office of Clean Energy and Geological Survey of Queensland (GSQ) and comprises a structured drilling program of shallow boreholes for the collection of new datasets to identify heat-flow anomalies along the east coast of Queensland. Target areas have been identified based on geological and geophysical characteristics and have been ranked based on their potential for a geothermal resource. The CGEI will reduce exploration risks and assist potential explorers to explore for and develop this source of clean energy in Queensland.

Keywords: Queensland, geothermal exploration, drilling, heat flow, inversion modelling.

Objectives

The main objectives of the CGEI are to identify prospective areas along the east coast of Queensland and collect additional datasets through a shallow drilling program. The purpose of this is firstly to increase knowledge of the crustal temperatures along the coast and secondly to provide an enhanced assessment of geothermal resource potential by generating basic datasets. This new data should assist geothermal exploration and development programs in Queensland.

Heat Flow Investigation

A precise crustal heat-flow determination is the preferred method of identifying the geothermal prospectivity of a target area. Heat flow is the product of the temperature gradient and the thermal conductivity of rocks in the earth’s crust, and can be determined through the sampling and logging of cored drill holes. A heat-flow investigation program has been planned as part of

the CGEI to evaluate the geothermal prospectivity of selected geological provinces along the east coast of Queensland.

Drill Target Selection

The potential occurrence of suitable heat sources within basement was evaluated, based on available geophysical datasets and regional geological knowledge for each area. The main geothermal source/reservoir targets are felsic crystalline basement rocks such as granitoids and rhyolite with high thermal conductivity values (generally greater than 4 Watt per meter Kelvin (W/mK)) and high radiogenic heat production ability (greater than 5 micro Watt per cubic meter ($\mu\text{W}/\text{m}^3$)).

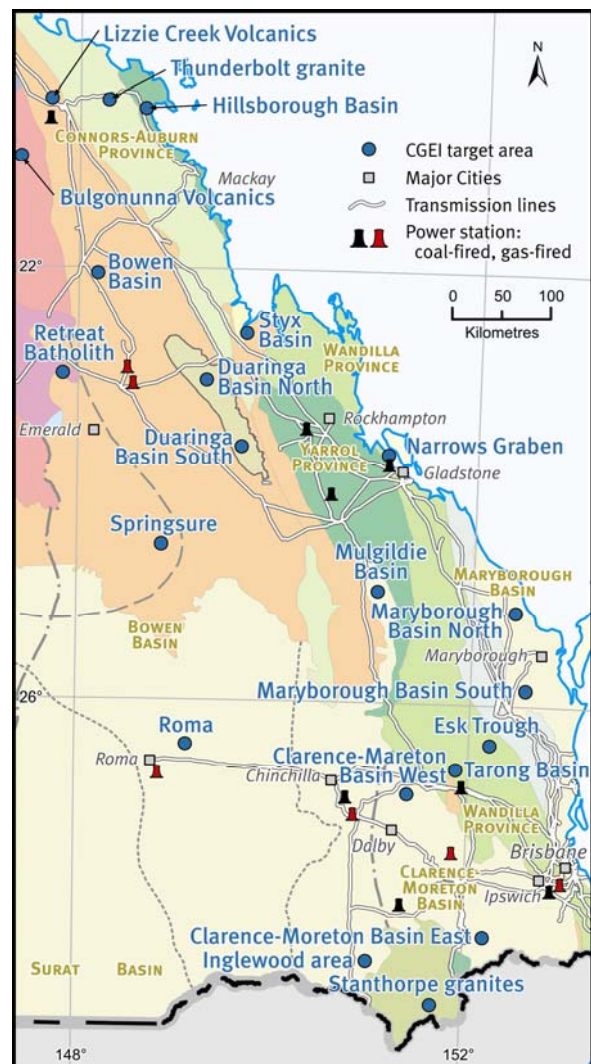


Figure 1a: Location of CGEI drill targets in Central and Southern Queensland

Priority in the CGEI was given to geological provinces where geothermal source/reservoir units are overlain by a thick succession of thermal blanketing sediments with harmonic mean thermal conductivity values generally less than 3 W/mK. The assessment process involved a desktop analysis of each geological province. The provinces were selected as they were considered likely to have a high heat-flow or evidence of previous elevated temperatures. Existing temperature data from available petroleum wells in or adjacent to each geological province were considered to infer subsurface temperature gradients. The main obstacle to this approach has been the variable data quality and availability in eastern Queensland where petroleum drilling is relatively rare. The temperature gradients were integrated with the available geological and geophysical data with the aim of identifying possible sources of heat at depth. Specific targets were then identified that would test the interpretation that this part of the geological province has geothermal potential.

To date, forty-seven targets generally within 100km of the existing national electricity grid have been identified with thirty-two being selected for drilling. These targets are located from near Cairns in the north to the border of New South Wales (Figures 1a, b).

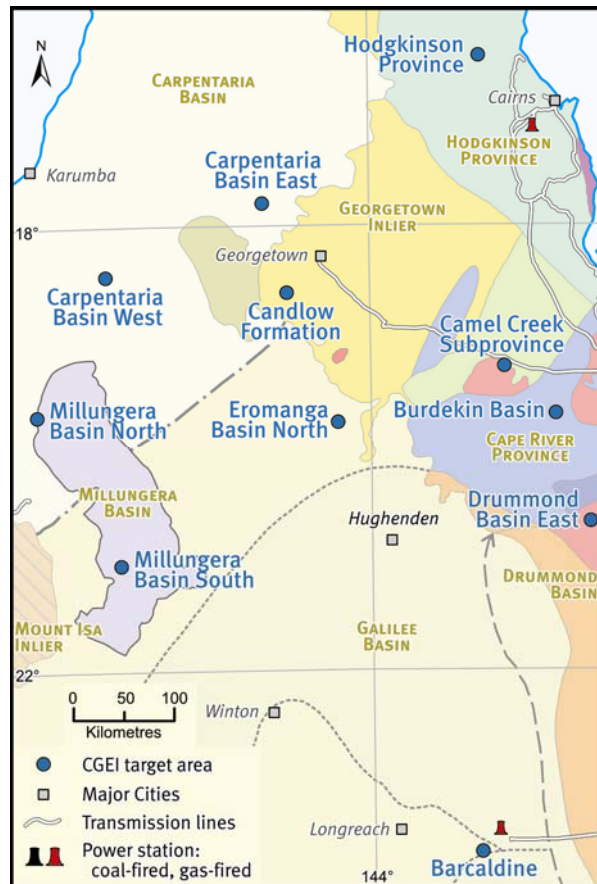


Figure 1b: Location of CGEI drill targets in Northern Queensland

Technical criteria were used to rank targets in order of likelihood of the identification of a geothermal resource. The criteria were based on the nature of the basement and the thermal blanketing sedimentary cover. All targets were ranked against these criteria in order to establish a drilling priority. The final location of each drill hole was determined after consultation with landholders and consideration of terrain condition, environmental and cultural heritage issues. The spatial distribution of the holes effectively requires each site to be considered as a drilling project in its own entity. Consequently, a substantial amount of extra work has been required to obtain the necessary clearances. Phase 1 drilling of the 10 highest priority targets is scheduled to commence in late 2010 (pending contract confirmation).

Geological Setting

Traditionally, rifting margins have been identified as more prospective for geothermal energy exploitation. However, preliminary geological assessment of the geothermal potential of coastal Queensland shows a variety of tectonic settings may host high heat producing (HHP) granites under insulating cover sequences. The assessment process resulted in the identification of five different geological settings which are summarised in Table 1.

Table 1: Geological Setting of CGEI Targets

AGE	Geological Setting	No. of CGEI Targets
Proterozoic	Intercontinental rifting	5
Ordovician-Silurian	Thomson Orogen	4
Early Carboniferous–Early Permian	Tasman Orogenic Zone	13
Late Permian – Mid Triassic	Hunter Bowen Orogen	7
Late Cretaceous - Tertiary	Cretaceous Rifting	3

Intercontinental Rifting: The Proterozoic was a time of elevated heat flow causing the emplacement of voluminous granites and associated volcanics in northern Queensland (McLaren et al, 2003). These granites were emplaced during multi-stage intracratonic rifting events and in some areas they are overlain by sedimentary basins which include the Millungera Basin (no younger than Triassic, Figure 2) and the Jurassic - Late Cretaceous Carpentaria Basin. The heat production values of 5-9 $\mu\text{W}/\text{m}^3$ (GSQ Geochemistry database, 2010) from intrusives of the Croydon Province and the Georgetown and Mt Isa Inliers (including the Esmeralda, Forsayth and Williams Supersuites) delineate a prospective heat source at depth in these areas. A number of geophysical tools including gravity, magnetic, magnetotelluric and radiometric ternary images as well as sporadic drilling data were used to identify

five targets which are considered worthy of further investigation. These targets are found beneath the insulating units of the Karumba, Carpentaria and Millungera Basins and the Georgetown Inlier (Figure 1b).

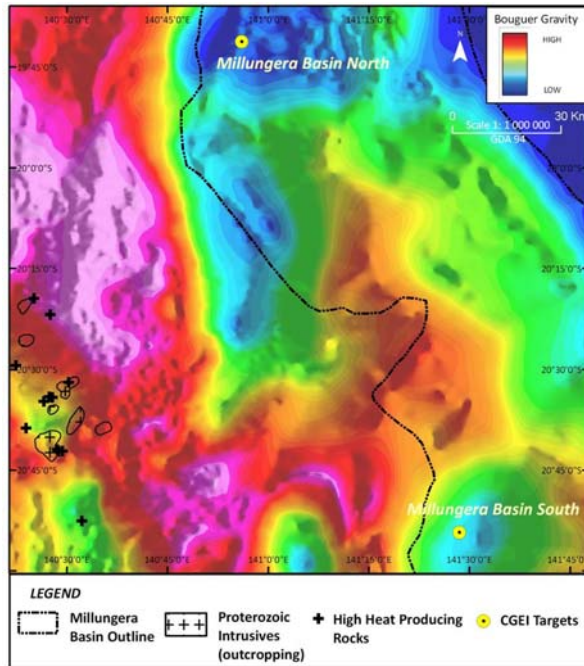


Figure 2: Millungera Basin CGEI rationale, showing gravity response (Bouguer), location and extent of outcropping Proterozoic intrusives and high heat producing rocks

Thomson Orogen: Another region of outcropping potentially HHP granites is located within the basement packages of the Ordovician-Silurian Thomson Orogen. The heat production values of I-type and S-type granites are generally greater than $5 \mu\text{W}/\text{m}^3$. If properly insulated, these granites would provide a geothermal heat source at depth. A geophysical and geological assessment identified the western and southern Bowen Basin, eastern Drummond Basin, and the Burdekin Basin, as target areas, as inferred HHP granites are present in the basement complexes of these basins with Tertiary volcanics, which could indicate an additional, younger contributing heat source.

Tasman Orogenic Zone: The Carboniferous-Permian intrusions of the Tasman Orogenic Zone (which encompasses the Northern Tasman Orogenic Zone and the New England Orogen) contain medium to high concentrations of the radiogenic elements uranium, thorium and potassium and should be prospective for geothermal energy potential. Within the Northern Tasman Orogenic Zone, the Carboniferous-Permian Wypalla Supersuite and the Purkin Granite have heat production values between $3.5\text{--}8.55 \mu\text{W}/\text{m}^3$ (GSQ Geochemistry database, 2010). The heat production potential of these intrusive units at depth in conjunction with a good insulating capacity and thickness of overlying

cover sequences have identified three targets within the Hodgkinson Province, northern Eromanga Basin and Camel Creek Province. The existence of anomalous heat flow within the Hodgkinson Province in particular can be inferred by the Innot hot spring which has a surface temperature of 71°C (Lottermoser & Cleverley, 2007). This spring is located in the southern part of the province.

The New England Orogen contains numerous I-type and S-type intrusions and associated felsic volcanics. Whole rock geochemical analyses of these units indicate medium concentrations of potassium, thorium and uranium. As a result the geological and geophysical assessments undertaken delineated where these intrusives extend at depth underneath insulating basins. The overlying insulating sedimentary packages include oil shale units of the Duaringa Basin and extensive coal measures of the Bowen, Clarence-Moreton and Styx Basins. Nine sites were selected for heat flow determinations including the Bulgonnuna Volcanics, Lizzie Creek Volcanics, Bowen Basin, Roma Granite, Styx Basin, Duaringa Basin, western Clarence Moreton Basin (Jandowae) and Inglewood (Figure 1a).

Hunter Bowen Orogen: The onset of the Permian-Triassic Hunter Bowen Orogen initiated the widespread emplacement of granites along the New England Fold Belt. Elevated heat is likely as the granitic outcrops generally have heat production values greater than $5 \mu\text{W}/\text{m}^3$. Gravity, seismic and magnetotelluric datasets suggest these potentially HHP granites extend at depth underneath the cover of the Tarong, Mulgildie, Clarence-Moreton, Galilee and Maryborough Basins, which all contain coal measures. A more detailed geological and geophysical assessment of these basins identified seven target sites as prospective for elevated heat flow namely the Thunderbolt Granite, Tarong Basin, eastern Clarence-Moreton Basin, Mulgildie Basin, Stanthorpe Granite, Barcaldine and northern Maryborough Basin (Figures 1a and 3).

Cretaceous Rifting: The Cretaceous saw the cessation of the active convergent margin along the east of the Australian continent and the initiation of rifting of the Tasman and Coral Seas. Cretaceous granites lining the western edge of the Maryborough Basin (Figure 3) may be a prospective geothermal target. The sediment thickness of the overlying Maryborough Basin is up to 3400m with two significant coal sequences, Tiaro Coal Measures and Burrum Coal Measures, forming an excellent insulator to any potential heat producing intrusive at depth.

The Hillsborough Basin (Figure 4) and Narrows Graben sites primarily target the more northern Cretaceous intrusions. These two sites may also benefit from additional heat sources associated with intrusions and related volcanics of the Late

Cretaceous Whitsunday Large Igneous Province. In addition, volcanics resulting from Tertiary rifting and intraplate volcanism suggest that there still may be significant heat production in this area. The insulating capacity of the Hillsborough Basin and Narrows Graben sequences is considered to be good due to the presence of significant intervals of oil shale.

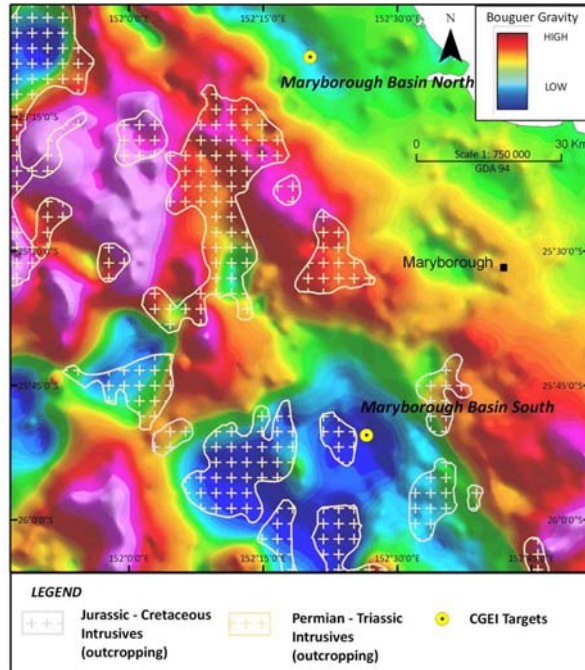


Figure 3: Maryborough Basin CGEI rationale, showing gravity response (Bouguer), location and extent of Jurassic-Cretaceous and Permian-Triassic outcropping intrusives

Drilling Program and Data Collection

An effective heat-flow determination process requires a shallow (300–500m) drill hole, suitably completed to enable a temperature log to be acquired that accurately records the temperature in lithological units intersected. In order to get an accurate temperature log the hole needs to remain undisturbed for sufficient time (typically 5–8 weeks) to minimise any remaining drilling-induced temperature disturbances and essentially ensure that the downhole temperature is adequately re-equilibrated. Each well is then thermally logged from the surface to the bottom of the hole by measuring a temperature at specific intervals (typically every 1 meter). From these measurements, temperature gradients can be calculated for the corresponding intervals down the hole.

The hole should also be continuously cored from the base of unconsolidated units to total depth (~320m) to recover at least 200-250 meters of continuous core enabling samples to be taken and analysed for thermal conductivity properties in order to establish a thermal conductivity profile for the hole. Core samples are usually taken at regular intervals, typically every 10 metres.

Sampling is to be undertaken at the drill site immediately after the core has been logged. Each sample is enclosed in plastic wrap to preserve their *in-situ* fluid saturation levels prior to dispatch to a laboratory. Visual assessment of the downhole geology (lithological log) against the temperature log will also be used as a tool for further sampling in case additional thermal conductivity analyses are required at a later stage (Figure 5).

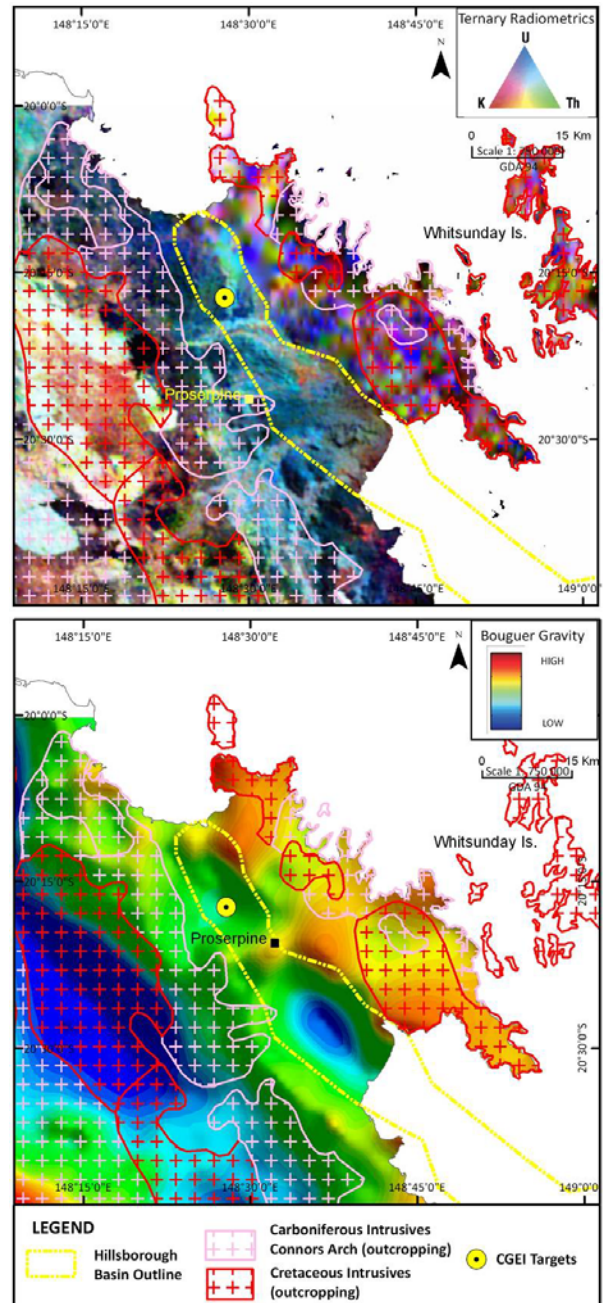


Figure 4: Hillsborough Basin CGEI rationale, showing gravity response (Bouguer), ternary radiometric image, location and extent of outcropping Carboniferous and Cretaceous intrusives

The CGEI drilling program is likely to consist of up to 32 HQ size shallow boreholes to a nominal depth of ~320 metres cased with continuous PVC. The hole design and completion have been

optimised to ensure that a high quality data collection process is attained throughout the program (Figure 6). A call for tender was released in June 2010 for the selection of drilling contractors. Geophysical downhole logs such as Resistivity, Spontaneous Potential (SP) and Gamma Ray are being run on an “as–required” basis with the aim of determining possible aquifer leakage into the hole that may interfere with the temperature profile and also for data quality checking purposes.

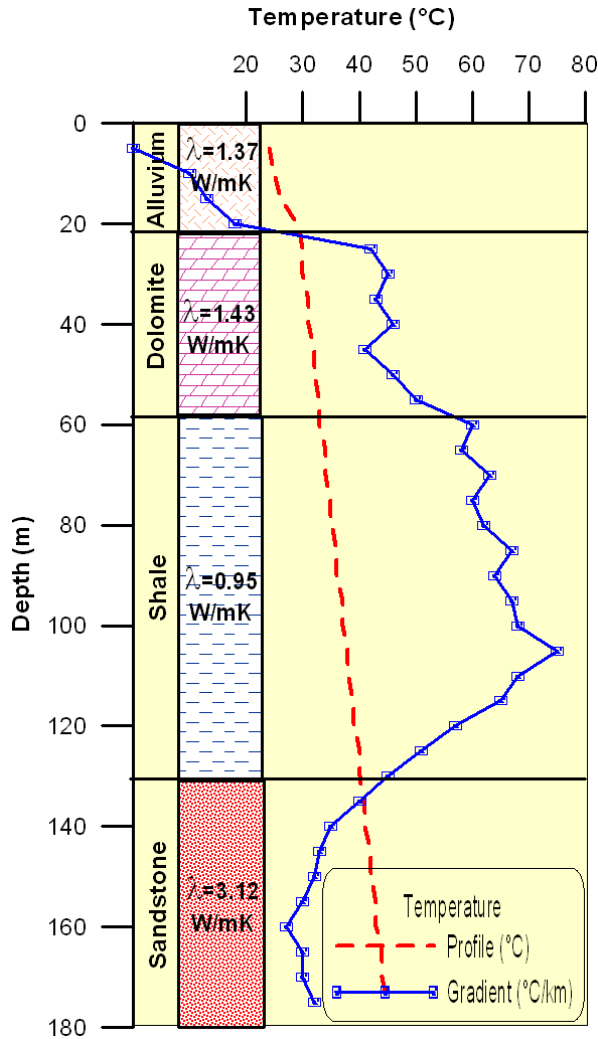


Figure 5: Example of a temperature log versus lithological log

Heat-Flow Modelling

Mathematically, the average vertical conductive heat flow at the earth’s surface, q (in W/m^2), can be calculated using the Fourier expression:

$$q = k \cdot \frac{dT}{dz}$$

Where (k) is the rock thermal conductivity (in W/mK) at depth z , and (dT/dz) is the corresponding vertical temperature gradient (in K/m) over the same interval. As shown by the equation, the temperature gradient has an inverse relationship with thermal conductivity (one decreases as the other increases). This assumes

a purely conductive regime and therefore a constant heat flow across all lithological units intersected. From the global heat-flow database, the mean surface heat flow of the Australian continent is approximately 65 mW/m^2 , so areas with heat-flow values greater than this may indicate promising areas for further geothermal investigation and exploration activities provided that the thermal resistance of the overlying lithological units is sufficient to support presence of economical temperature at depth.

Considering the spatial coverage of the CGEI, one dimensional inversion modelling of the conductive heat-flow regime in the vicinity of each borehole is to be undertaken using the new temperature and thermal conductivity datasets collected (Figure 7). Modelled data will then be extrapolated to 5 km, the economic drilling depth for most geothermal resources, to predict temperatures at this depth range. Generally, temperatures of greater than 200°C are expected at such depths for Engineered Geothermal System (EGS) to be commercially viable for electricity generation.

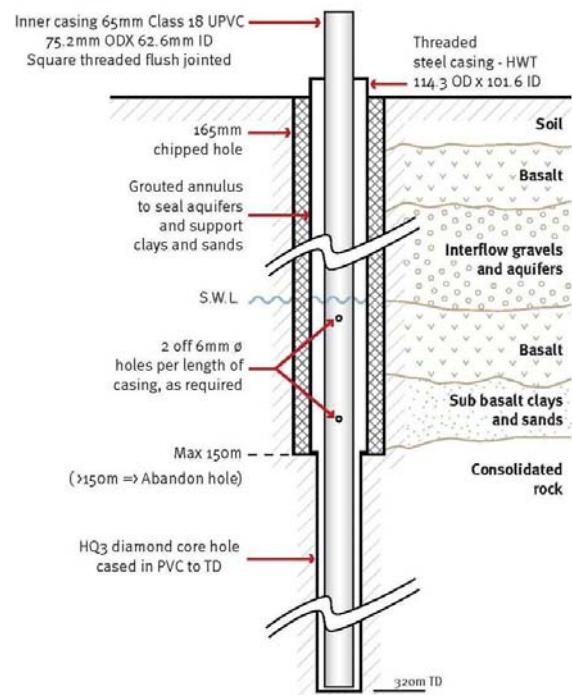


Figure 6: Schematic borehole design

In addition, depth predictions of the 100, 150 and 200°C isotherms may be approached depending on data availability for estimating the formations intersected at those isotherm depths. This will assist in the assessment of the prospectivity of each target area for either Hot Sedimentary Aquifer (HSA) or Engineered Geothermal System (EGS) development in the future.

Collaboration

Collaboration with other government agencies, research centres and industry is an important part

of this initiative. In this respect, Geoscience Australia will provide technical support to the CGEI by providing down-hole temperature logging and laboratory analysis services through an agreement under the National Geoscience Accord. Furthermore, additional research over the CGEI target areas has been discussed through collaboration with the Queensland Geothermal Energy Centre of Excellence (QGECE) based at the University of Queensland through post-graduate research studies.

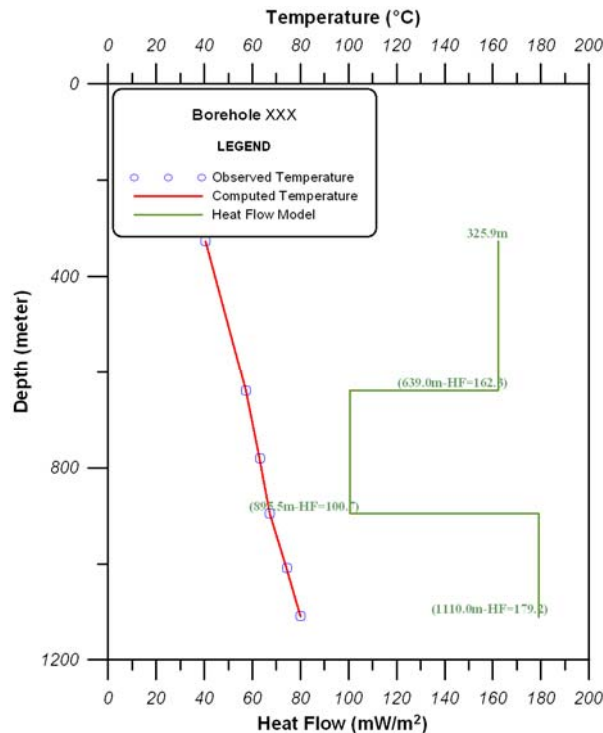


Figure 7: Example of 1D inversion heat flow modelling

Future Work

Future work that would contribute to a better understanding of geothermal prospectivity in eastern Queensland would include the collection of new heat-flow data at a closer spacing for prospective areas identified from the CGEI. An assessment of current regional and local *in-situ* stress fields in those areas could also be undertaken to evaluate the susceptibility of potential reservoir rock to the artificial permeability enhancement process.

Summary

The Coastal Geothermal Energy Initiative is the Queensland Government's program for identifying sources of hot rocks for geothermal energy close to existing national electricity grid and potential markets along the east coast of Queensland. The initiative will be implemented through a structured drilling program of up to 32 shallow boreholes with a nominal depth of ~320 metres to collect new temperature and heat-flow datasets. The major aim of the initiative will be to increase knowledge

of the crustal temperatures in selected geological settings along the coast and provide background data for industry that would consequently stimulate exploration activities for geothermal energy in Queensland. It is anticipated that final results of the initiative will be publically available by the middle of year 2012.

Acknowledgements

The authors wish to acknowledge staff from other GSQ units who are strongly supporting the implementation of the Coastal Geothermal Energy Initiative by any means and in every aspect.

References

Beardmore, G. R., and Cull, J. P., 2001, *Crustal Heat Flow: A Guide to Measurement and Modelling*, Cambridge University Press, 324pp.

Cull, J. P. and Beardmore, G. R., 1992, Statistical methods for estimates of heat flow in Australia, *Journal of Exploration Geophysics* 23, p. 83-86.

Denaro, T. and Dhnaram, C. (Compilers), 2009, *Queensland Minerals 2009. A Summary of major mineral resources, mines and projects*. Department of Mines and Energy, 87pp.

Fitzell, M., Hamilton, S., Beeston, J., Cranfield, L., Nelson, K., Xavier, C. and Green P., 2009, Approaches for identifying geothermal energy resources in coastal Queensland, *Proceedings of the 2009 Australian Geothermal Energy Conference*, 6pp.

McLaren, S., Sandiford, M., hand, M., Neumann, N., Wyborn, L. and Bastrakova, I., 2003, The hot southern continent: heat flow and heat production in Australian Proterozoic terranes, In: Hillis R.R. & Müller R.D. eds. *Evolution and Dynamics of the Australian Plate*, Geological Society of Australia Special Publication 22.

Murray, C., 2003. Granites of the northern New England Orogen, in BLEVIN, P., JONES, M., & CHAPPELL, B., editors, *Magma to Mineralisation: The Ishihara Symposium*, Geoscience Australia, Record 2003/14, 19-24.

Rybach, L., 1989, Heat flow techniques in geothermal exploration, *First Break* Vol. 7, No.1, p. 9-16.

Somerville, M., Wyborn, D., Chopra, P., Rahman, S., Estrella, D. and Van der Meulen, T., 1994, *Hot Dry Rocks Feasibility Study*, Energy Research and Development Corporation, Report 243, 133pp.

Webb, A. W. and McDougall, Ian, 1968, The geochronology of the igneous rocks of Eastern Queensland, *Australian Journal of Earth Sciences*, 15: 2, 313 — 346.

Geothermal Exploration in Victoria, Australia

David H Taylor, Ben Harrison, Michelle Ayling, Kate Bassano
GeoScience Victoria, GPO Box 4440, Melbourne, Victoria, Australia

Corresponding author: david.taylor@dpi.vic.gov.au

Geothermal energy is keenly sought as a sustainable, low emissions energy source for Victoria. Exploration companies have been active since 2006 looking for geothermal systems where temperatures of greater than 150 C would allow electricity generation. Initial exploration was largely guided by legacy temperature data in groundwater and petroleum bores but lots of dedicated heat flow data is now being acquired, including a State-wide program by the government. Active volcanic systems are not present but there is good potential for hot sedimentary aquifers already known from the legacy data. Other heat sources such as Palaeozoic radioactive granites or residual magmatic heat from recent basaltic volcanism are possible but data is very limited. As exploration progresses, a number of different geothermal play types across the various heat sources are being investigated. A number of inferred resources have already been declared, in preparation for deep appraisal drilling.

Keywords: Hot Sedimentary Aquifer, Heat Flow, geothermal

Victorian geothermal background

The oil shocks of the 1970's piqued interest into alternate energy sources. Town water supplies being drawn from thick Cretaceous-Tertiary basins along the Victorian coast at that time, showed temperatures of about 50-90 C at 1-2 km depth. The potential of direct use of this hot water was investigated (King et al., 1987). Petroleum exploration in the same area also occasionally intersected deeper basin aquifers with temperatures of about 130-150 C at 3.5-4 km depth (Woollands and Wong, 2001).

Low oil prices throughout the 1990's suppressed interest in alternate energy sources but the return of higher prices and concerns around greenhouse gas emissions have again sparked interest in geothermal energy. Dedicated legislation was put in place in 2005 and a grid of large exploration permit blocks was established across the State. Exploration companies took up many of the permits in two rounds of tenders over 2006 and 2008. About two thirds of the State is now under exploration for the next 3-4 years by seven companies with work plan commitments of approximately \$365M.

Victorian Geothermal Data

To support the tender bidding process for permits, a preliminary review of geothermal prospectivity was published by the State government geology organisation (Driscoll, 2006). This report included a compilation of about 300 temperature data points from pre-existing groundwater and petroleum bores but the accuracy and precision of much of the petroleum temperature data for geothermal assessments is questionable.

A handful of heat flow calculations from precision temperature logging and rock conductivity analysis already existed as a result of academic studies since the 1970s. Many of the geothermal exploration companies have started collecting much more of this dedicated type of geothermal data. To accelerate this type of work the State government has undertaken a data collection program for heat flow.

The Victorian Heat Flow Map

In 2009-10 the State government commissioned a one year \$500,000 project to generate a State-wide heat flow map. Over the year, this project has compiled the existing academic and company data, plus collected new data, to generate over 100 heat flow measurements that give good coverage over much of the State. Data points are generally close enough together (ideally closer together than the crust is thick: about 40 km) so that interpolation of the point data into a map should still have regional scale meaning.

GeoScience Victoria directly collected borehole temperature profiles in the southern Murray Basin and across the Otway Basin using its own temperature logging unit. As part of the National Geothermal Energy Project (Budd et al., 2009) GeoScience Australia collected temperature data from the northern Murray Basin using their temperature logging unit. GeoScience Victoria is also working collaboratively with Melbourne University who have collect data from the Gippsland basin. The exploration companies in the Gippsland Basin have also collected a fair amount of new temperature data in that region and made it available. Several recent unpublished honours thesis and some additional temperature logging for GeoScience Victoria undertaken by Hot Dry Rocks add further data to the previous handful of heatflow measurements that was all that was available several years ago.

About 200 conductivity analyses have been performed by Hot Dry Rocks on samples from the boreholes measured for temperature. This data allows reasonably precise heat flow calculations to be generated. Heat flow modelling for data from completely new holes was undertaken by Hot Dry Rocks. The various pre-existing honours thesis and company work was remodelled by GeoScience Victoria using consistently applied methodology and better informed conductivities stemming from the new sampling.

This regional scale appraisal of heat flow, when combined with analysis of thickness of basin cover, will help show 'where it is hot and where it is not'. The map will help companies direct their permit scale efforts, as well as informing government policy on geothermal resource potential.

This work is still in progress and thus current assessments of Victoria's geothermal potential still rely on looking at geological factors.

Geological Framework for geothermal potential

Geothermal potential depends on the interaction of a number of geological factors. The best resources are likely to exist in regions where high heat flow passes through rocks of low conductivity (good insulation) to create high temperature at shallow depth (Duffield & Sass, 2003).

The recent publication of a more complete geothermal systems assessment framework (Cooper & Beardsmore, 2008) outlines that in addition to (1) the heat producing basement (2) an insulating blanket; there needs to be (3) a fluid available to extract and move the heat; and (4) a reservoir to accommodate the fluid.

Applying this four factor analysis to the major geological provinces of Victoria gives some idea of their relative geothermal prospectivity. The broad diversity in the age and types of rocks across Victoria (Figure 1) gives some potential for all three types of geothermal systems: Hot Rock; Hot Sedimentary Aquifer; and Magmatic.

Victorian Geology/Geothermal Province Map

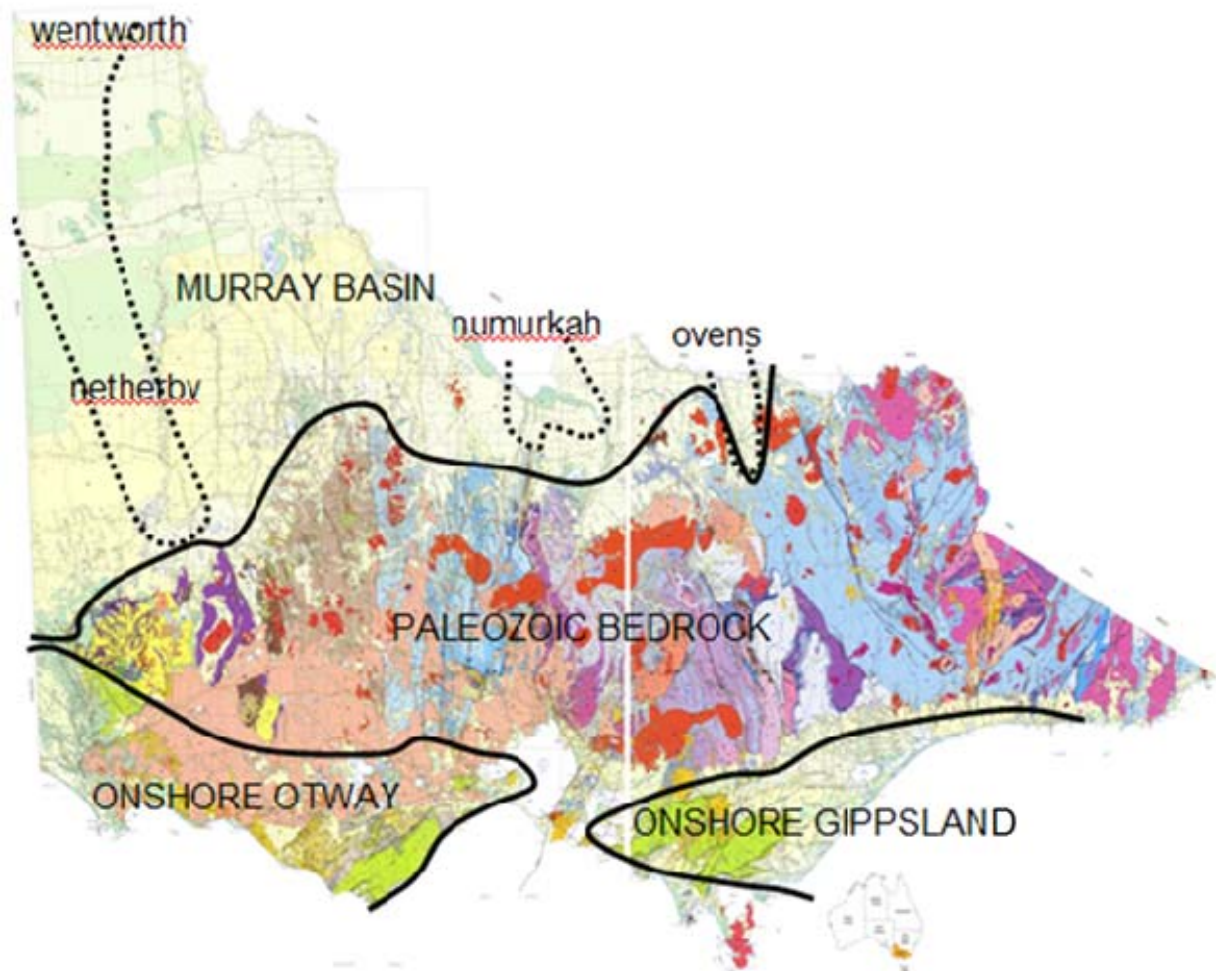


Figure 1: Geological geothermal province map

Pathways to Resource Development

Three broad geological/geothermal provinces can be delineated across Victoria: (1) The Palaeozoic bedrock (2) the onshore Otway and Gippsland Basins and (3) the Murray Basin.

The Palaeozoic bedrock consists predominantly of Cambrian to Devonian deep marine muddy siliciclastics that have been tightly folded and cleaved at various times in the Palaeozoic (blues, browns and purples of Figure 1). This bedrock also underlies the other provinces and thus gives good insight into the potential of their heat producing basement. Numerous granites intrude this bedrock (red blobs on Figure 1). In west and central Victoria some of them have felsic, fractionated geochemistry with mild enrichment in heat producing elements, so Hot Rock plays may be possible where granites lie buried within the bedrock or beneath the adjacent basins. In the southwest, an extensive province of young basalts has erupted onto the bedrock in the last few million to tens of thousands of years (the light pink in Figure 1). Teleseismic data suggests a mantle hot spot still underlies this recent volcanism (Graeber et al., 2002). In addition to an increased mantle heat flow contribution across this region, there may be some residual magmatic heat in the crust from the volcanic activity to allow Magmatic geothermal plays.

The Onshore Otway and Gippsland Basins are Cretaceous rift basins associated with Gondwana break-up (greens and yellow along coast in Figure 1). These basins are well characterised thanks to a long history of petroleum exploration with many deep wells. They contain several kilometres of muddy sediments overlying a coarser grained basal unit. This basal unit provides a natural reservoir already charged with hot water beneath an insulating blanket to create an attractive fairway for Hot Sedimentary Aquifer plays. In the Otways this basal unit has been intersected upon the basin floor but in the Gippsland basin this unit has yet to be tested away from the margins, at the depths necessary for a geothermal play. Beneath these basins there is also potential for Hot Rock plays in places where they are floored by granites.

The Murray Basin is a Tertiary intracratonic sag basin (light greens and yellow inland in Figure 1). It generally contains only a few hundred metres of sandy marly cover. This is insufficient cover to act as a heat blanket but in some places deeper troughs – such as the Wentworth, Netherby, Numurkah and Ovens - exist and can contain up to a couple of kilometres of sediment that is poorly known since there has been limited petroleum exploration here. Alignment of favourable factors over the deeper troughs may allow Hot Rock or Hot Sedimentary Aquifer plays but the favourability of the geothermal factors in this province has yet to be validated.

In the absence of detailed, dedicated geothermal data, most of Victoria can be viewed as 'blue sky' or perhaps 'green fields' at best, in those areas where some legacy petroleum data exists. The new heat flow map and better characterisation of rock thermal insulation (conductivities) will provide a new level of interpretation on prospectivity.

Most of the Victorian geothermal explorers are small companies with limited amounts of capital and cash-flow to fund their 5 year exploration programs. Ideally, as these companies collect information and decrease risks and unknowns, they could call for more capital through either debt or equity raisings until it becomes probable that a major backer would farm-in for development. The Global Financial Crisis has badly affected this traditional venture capital pathway through to resource development.

At the national level the Federal government has committed a significant amount of funds into a geoscience investigation program and also put up money for co-funding deep appraisal drilling. If these drilling appraisals lead to early success, then perceived risks around geothermal energy may be reduced and allow easier funding for the whole industry from the more traditional pathway. The State government has also offered substantial funds towards industry assistance for shallow and deep drilling plus contingent money for demonstration power plants.

Company announcements around Inferred Resources and/or conceptual targets suggest that several thousand MW of electricity generation may be possible but it is still early days for the geothermal industry in Victoria.

References

- Budd, A.R., Holgate, F.L., Gerner, E.J., Ayling, B.F. & Barnicoat, A.C., 2009, Pre-competitive geoscience for geothermal exploration and development in Australia: Geoscience Australia's Onshore Energy Security Program. Proceedings, Australian Geothermal Energy Conference, Brisbane, Australia.
- Cooper, G.T. & Beardsmore, G.R., 2008, Geothermal systems assessment: understanding the risks in geothermal exploration in Australia. Proceedings, Eastern Australian Basins Symposium III, Sydney, Australia.
- Driscoll, J., 2006, Geothermal prospectivity of onshore Victoria, Australia. VIMP Report 85. GeoScience Victoria.
- Duffield, W.A. & Sass, J.H., 2003, Geothermal energy: Clean power from the earth's heat. Circular, U. S. Geological Survey 1249.
- Graeber, F.M., Houseman, G.A. & Greenhalgh, S.A., 2002, Regional teleseismic tomography of the western Lachlan Orogen and the Newer

Volcanic Province, southeast Australia.
Geophysical Journal International, v. 149,
249-266.

King, R.L., Ford A.J., Stanley, D.R., Kenley, P.R.,
& Cecil, M.K., 1987, Geothermal Resources of
Victoria, Department of Industry, Technology
and Resources and Victorian Solar Energy
Council, Melbourne.

Wollands, M.A., & Wong, D., (eds.) 2001,
Petroleum Atlas of Victoria, Australia,
Department of Natural Resources and
Environment.

Geochemistry of silica rocks in the Drummond Basin as a record of geothermal potential

I. Tonguç Uysal*¹, Alexander W. Middleton¹, Robert Bolhar², and Massimo Gasparon²

Queensland Geothermal Energy Centre of Excellence, The University of Queensland, Brisbane, QLD. 4072*¹
Department of Earth Sciences, The University of Queensland, Brisbane, QLD. 4072²

Silica is the most abundant mineral in the Earth's upper crust; yet its trace element composition has not been utilised routinely in the exploration of natural resources. Siliceous sinters are pristine rocks that precipitate at the surface from spring waters heated by deep-seated magma chambers. They can be useful indicators of hot radioactive magmatic basements in sedimentary basins. However, distinguishing silica sinters from other siliceous lithologies is often ambiguous because siliceous lithologies of various origins occur ubiquitously on the ground surface as rock chips or soil material eroded from deeper geological units. In this study, we characterise trace element compositions of silica sinters to provide geochemical criteria for exploration of geothermal energy sources. We investigated silica sinters and the associated hydrothermal quartz veins, volcanic rocks, silicified hydrothermal breccias, alteration minerals, and some soil samples from the Paleozoic Drummond Basin, Australia by ICP-MS trace element analysis.

Keywords: Sinter, quartz, geochemistry, geothermal, Drummond Basin, Galilee Basin

Sampling

Samples for this study were collected from the Twin Hills area hosting high-grade epithermal gold resource, 309 and Lone Sister (BMA company report). Location 309 mine is a fault-bounded area characterised by the occurrence of a silicified breccia system capped by sinter deposits, whereas Lone Sister represents a rhyolite dome. The textural features of the sinters at 309 are very similar to those of sinters from other locations in the Drummond Basin (Cunneen and Sillitoe, 1989; White et al., 1989). They are well-laminated (from white through gray to orange-brown), consisting of dense and vitreous chalcedony.

Results and implications

The Drummond Basin sinters and quartz veins are unique in having anomalously enriched incompatible element (Cs, Li, Be, W, U, Th and rare earth elements) concentrations in comparison to hydrothermal quartz veins from various granitic-pegmatitic systems elsewhere in the world (Figure 1). Bonding factors such as ionic size and charge are the main factors controlling the distribution of elements in precipitating

crystals. Large-ion lithophile elements (LILE, e.g. Rb, Cs), large highly charged cations (e.g. W^{6+} , U^{4+}) and small variable charged cations (e.g. Be, Li) are usually prevented from being incorporated into crystalline phases during early magmatic processes (Strong, 1981). Hence these incompatible elements tend to concentrate in residual melts with high concentrations of fluids and volatiles, which commonly occurs during pegmatitic stages of granite magmatism. It has long been recognised that Cs, Li, Rb, Be (the alkali and alkaline earth elements) can be quite mobile during water/rock interaction (Nesbitt and Markovics, 1997; Nesbitt and Young, 1989). Tracing such elements can thus be used as a geochemical tool for locating areas of hydrothermal convection cells interacting with deep heat-producing granitic rocks. Alkali mobile element concentrations are divided by concentration of most immobile elements such as Lu to compare alkali element mobility (Fig. 2). The majority of sinter and quartz samples within or near the highly mineralised area (309 mine) are significantly more mobile for Cs, Li, Rb and Be than the sinters and silica deposits from areas distal to 309 (except the quartz vein from Off Limits) and the volcanic rocks (Fig. 2). Plotting all data set, a good correlation ($R^2 = 0.70$, power regression) is evident between Cs/Lu and Be/Lu, with the highest ratios being for sinter samples from 309 (Fig. 2A). Considering only silica deposits in Fig. 8A (black filled symbols) a significantly better correlation ($R^2 = 0.79$, power regression) would be obtained. Sinter and quartz samples from 309 have also high Rb/Lu and Li/Lu ratios, (Fig. 2B). A well-developed correlation ($R^2 = 0.77$) between Rb/Lu and Li/Lu is evident among silica samples from the entire Twin Hills area (Fig. 2B). The interaction of hydrothermal waters with the late Carboniferous alkaline igneous rocks resulted in the breakdown of K-Feldspar releasing alkali elements, which were subsequently mobilised in these fluids. This process led to the generation of an evolved, fertile hydrothermal fluid system that carried precious metals (Au, Ag) as was the case at 309 and Lone Sister in the Twin Hills area.

U and Th content of silica and clay samples from the surface can also be used in evaluating hot dry rock geothermal potential of the igneous rock association buried by heat-insulating sediments in adjacent sedimentary basins. Compared to pegmatite quartz compiled from the literature (Götze et al., 2004), U and Th concentrations in

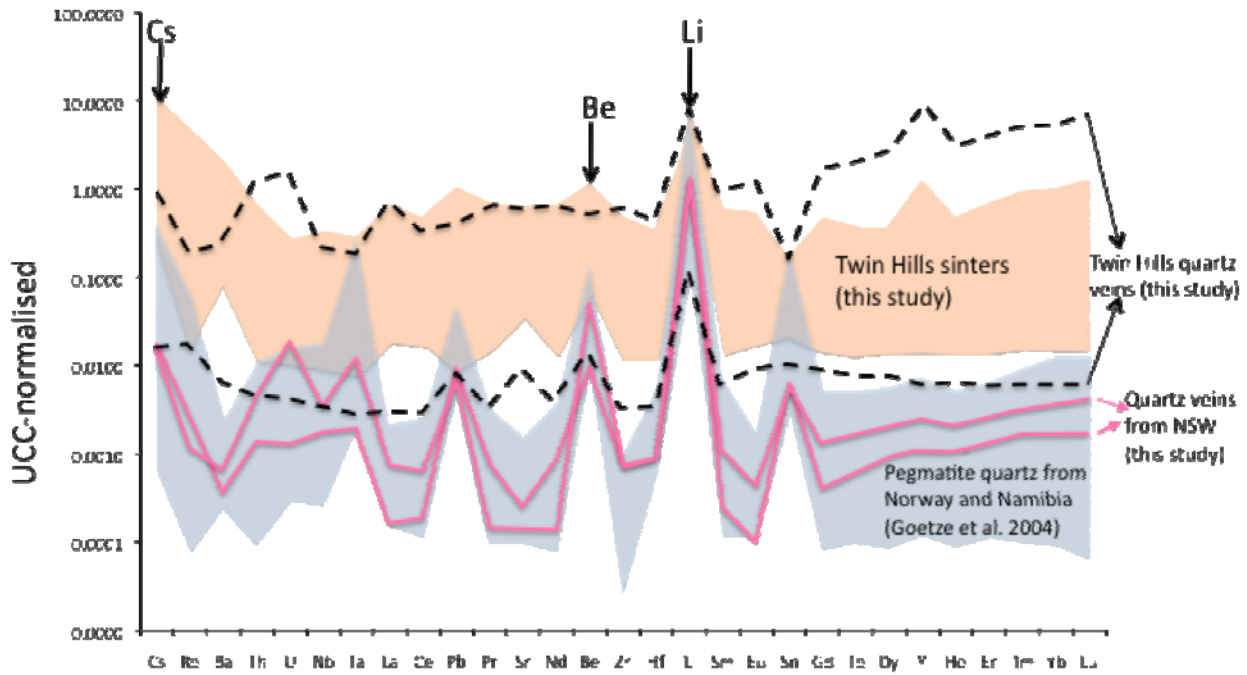


Figure 1: Upper continental crust (UCC) –normalised trace element concentration of the silica deposits from the Drummond Basin (Twin Hills area) in comparison to quartz from various granitic/pegmatitic environments.

sinter and quartz deposits from the Drummond Basin are significantly elevated (Fig. 3A-B). U and Th contents of the illitic clay minerals that formed in response to the interaction of hydrothermal fluids with host rocks are similarly high as those from the Cooper Basin. The latter represent a radiometric heat production from the basement granite (Middleton, 1979), whereas the clay concentrations for the Bowen Basin in Queensland and Paris Basin in Europe are similar to those of the upper continental crust (Fig. 6A-B).

Geothermal potential in the Galilee Basin

Igneous rocks of the Drummond Basin occur as the basement of the adjacent Galilee Basin of Upper Carboniferous to Middle Triassic age (Evans, 1980). The late Permian coal deposits and carbonaceous pelitic rocks in the Galilee Basin are ideal heat insulating sediments (Nun and Li, 2002) that would store the radioactive heat generation in the basement. Indeed, temperatures of about 80°C at 1000 m were measured in coal seam gas drilling boreholes in the Galilee Basin (pers. commun. with several coal seam gas companies) that indicate high heat flux from the basement. Furthermore, the vitrinite reflectance values measured on the coal cores throughout most of the Galilee Basin range between 0.63 and 0.73 %R_omax (Holland and Applegate, 2008), translating into reservoir temperatures of about 95°C - 110°C (Barker and Pawlewicz, 1986).

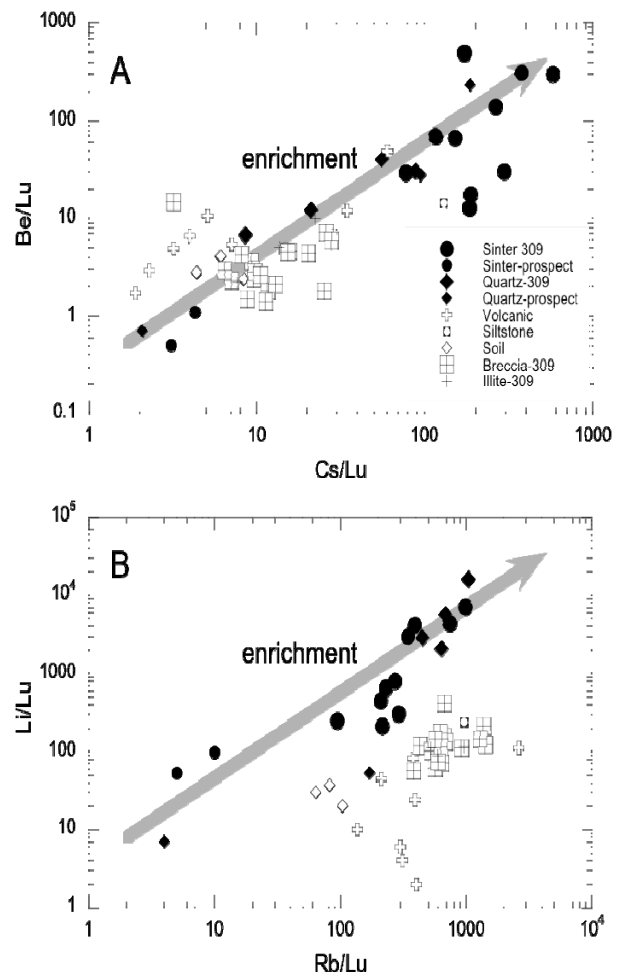


Figure 2. Alkali element mobility in the Twin Hills area.

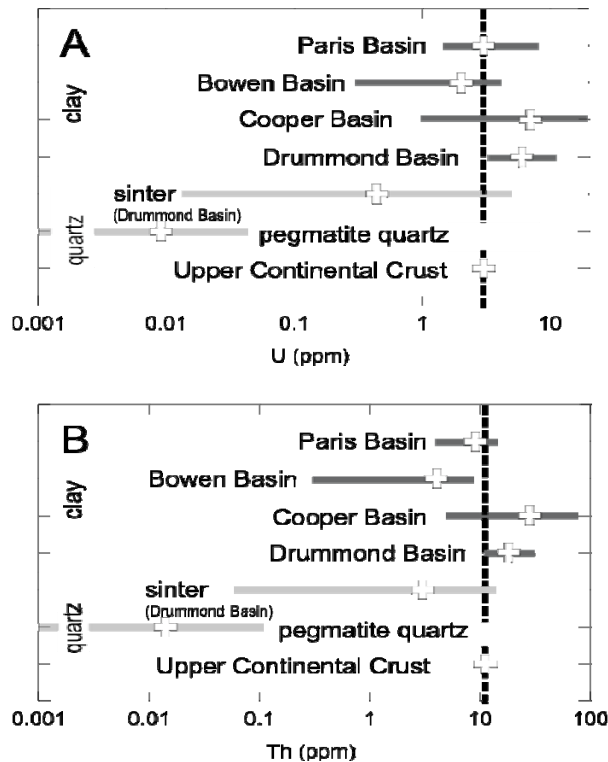


Figure 3. U – Th abundances of sinter and clay deposits from the Drummond Basin in comparison to those of other sedimentary basins. Pegmatite quartz from Götze et al. (2004).

Conclusion

The results of the pilot study suggest that trace element geochemistry of silica samples and the associated clay alteration can serve as a powerful tool in 1) discriminating between sinter and quartz veins from hydrothermal systems driven by granitic heat sources and other siliceous rock types (barren quartz/silica deposits) and 2) to be used in reconnaissance soil sampling to identify hydrothermal alteration zones associated with heat-producing granite plutons. Further work aimed at investigating similar samples from various settings with different ages will expand existing knowledge of how these techniques can be used to effectively discriminate areas with high geothermal potential from barren systems on a routine basis.

References

Barker, C.E., Pawlewicz, 1986. The correlation of vitrinite reflectance with maximum temperature in humic organic matter. In: Buntebarth, G. and Stegena, L. (Eds.), *Paleogeothermics*, New York, Springer-Verlag, p. 79-83.

Cunneen, R. and Sillitoe, R.H., 1989. Paleozoic hot-spring sinter in the Drummond Basin, Queensland, Australia. *Economic Geology*, 84(1): 135-142.

Evans, P.R., 1980. Geology of the Galilee Basin. In: R.A. Henderson and P.J. Stephensen (Editors), *Geology and Geophysics of Northeastern Australia*. Geological Society of Australia, Queensland Division, pp. 299–305.

Götze, J., Plotze, M., Graupner, T., Hallbauer, D.K. and Bray, C.J., 2004. Trace element incorporation into quartz: A combined study by ICP-MS, electron spin resonance, cathodoluminescence, capillary ion analysis, and gas chromatography. *Geochimica Et Cosmochimica Acta*, 68(18): 3741-3759

Holland, J.R. and Applegate, J.K., 2008. Recent Coalbed Methane Exploration in the Galilee Basin, Queensland, Australia. 2008 International Coalbed & Shale Gas Symposium.

Middleton, M.F., 1979. Heat flow in the Moomba, Big lake gas fields of the Cooper Basin and implications for hydrocarbon maturation. *Bulletin of the Australian Society of Exploration Geophysics*, 10: 149-155.

Nesbitt, H.W. and Markovics, G., 1997. Weathering of granodioritic crust, long-term storage of elements in weathering profiles, and petrogenesis of siliciclastic sediments. *Geochimica Et Cosmochimica Acta*, 61(8): 1653-1670.

Nesbitt, H.W. and Young, G.M., 1989. Formation and diagenesis of weathering profiles. *Journal of Geology*, 97(2): 129-147.

Nunn, J.A. and Lin, G., 2002. Insulating effect of coals and organic rich shales: implications for topography-driven fluid flow, heat transport, and genesis of ore deposits in the Arkoma Basin and Ozark Plateau. *Basin Research*(14): 129-145.

Strong, D.F., 1981. Ore deposit models – 5. A model for Granophile mineral deposits. *Geoscience Canada*, 8: 155–161

White, N.C., Wood, D.G. and Lee, M.C., 1989. Epithermal sinters of Paleozoic age in north Queensland, Australia. *Geology*, 17(8): 718-722.

Estimates of the magnitude of topographical effects on surface heat flow from finite element modelling

Gordon Webb^{1*} and Ben Harrison²

¹ Northern Territory Geological Survey, PO Box 8760, Alice Springs NT 0871, Australia

² School of Earth Sciences, The University of Melbourne, Victoria 3010, Australia

* Corresponding author: gordon.webb@nt.gov.au

Introduction

Surface heat flow calculations are employed by geothermal exploration companies to estimate the geothermal gradient down to depths of 3 km to 6 km. Surface heat flow is typically calculated from coincident thermal conductivity data or estimates, and temperatures obtained by drilling a slim-line hole down to depths of 300 m to 1000 m. At such shallow depths the effect of a variable surface topography needs to be considered when performing temperature extrapolations to greater depth. This is because, for a given crustal volume with an undulating surface, heat will tend to flow towards topographic lows and away from topographic highs as it migrates from the base to the ground surface. A linear approximation method was developed by Lees (1910) to correct for topography under idealised geometric mountain ranges.

This study presents results from a series of finite element method (FEM) models that predict the magnitude of variation of surface heat flow at the surface of a homogenous two-dimensional slice of crust with a uniformly curved surface. The results from this simple geometry are then compared to irregular topographic surfaces derived from real world examples.

The main advantage of using the FEM method, described in this study, - rather than the method described by Lees (1910) - is that any regular or irregular surface topography may be used.

Keywords: surface heat flow, temperature, numerical modelling, topography.

Model Parameters

A series of two-dimensional model geometries were constructed with a flat base and sides and a sinusoidal top edge representing the topographic surface (Figure 1). The models were all 10 km deep (measured from the midway point of the surface curvature to the base) to minimise near-field effects in fixed boundary conditions. The surface topography has a sinusoidal form with a wavelength denoted by λ and maximum elevation difference denoted Δh .

The width of the models was scaled with respect to the x-axis to generate different values for the ratio $\Delta h/\lambda$. Fifteen model geometries were constructed with values of $\Delta h/\lambda$ varying between

0.01 (representing subdued, long wavelength topography) and 0.9 (representing steep, short wavelength topography). Δh had a constant value of 412 m for each of the models. The lower $\Delta h/\lambda$ values might represent the gently undulating terrains encountered in areas such as the Darling Ranges near Perth, while $\Delta h/\lambda$ values of about 0.07 might represent areas of moderate topographic expression, such as the Flinders Ranges and Mt Lofty Ranges in South Australia.

The model volume was defined as "non-radiogenic granite" with an isotropic thermal conductivity (k) of $3.2 \text{ W.m}^{-1}.\text{K}^{-1}$, a heat capacity (C) of $8500 \text{ J.kg}^{-1}.\text{K}^{-1}$ and a density (ρ) of 2600 kg.m^{-3} .

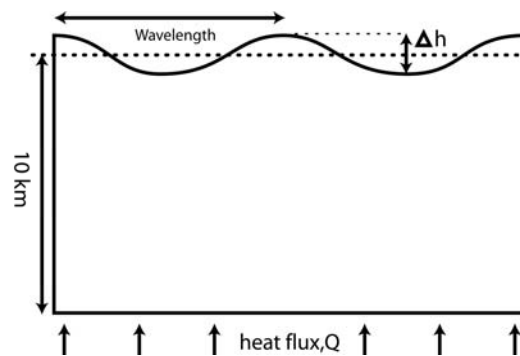


Figure 1: Diagram showing the generic geometry of the models.

A constant temperature of 20 degrees Celsius was maintained at the top surface of the models. The sides of the model were defined to be symmetrical and reflective to remove edge effects.

A uniform heat flux (Q) was applied to the bottom surface of each model. A basal heat flux of 60 mW.m^{-2} was applied to each of the 15 models. Ten additional models were run with a basal heat flux of 80 mW.m^{-2} for comparison. The models were meshed with a uniform Lagrange linear mesh with greater than 10,000 nodes per model space. The models were solved iteratively using the time-varying relationship,

$$\rho C \frac{\partial T}{\partial t} - \nabla \cdot (k \nabla T) = Q,$$

until the model residuals approach zero and a steady-state solution was attained.

Results

Figure 2 shows the percentage decrease or increase in the modelled surface heat flow with

respect to basal heat flux at the highest and lowest topographic points, respectively. For relatively short wavelength topography ($\Delta h/\lambda > 0.2$) the modelled surface heat flow differs from the basal heat flux by greater than 50%. The modelled surface heat flow is within 5% of the basal heat flux value for very long wavelength, subdued topography ($\Delta h/\lambda < 0.02$).

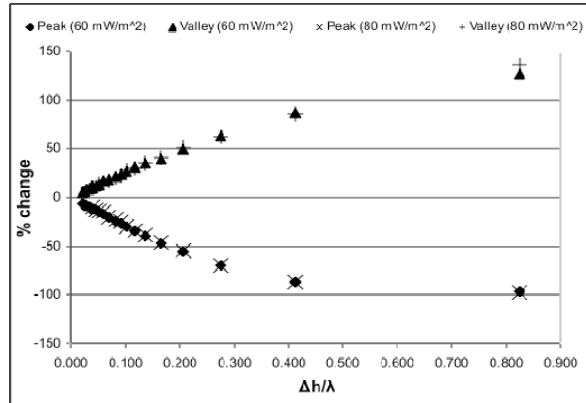


Figure 2: Plot of the percentage difference between the modelled surface heat flow with respect to the basal heat flux measured at the highest (peak; negative change) and lowest (valley; positive change) points on the surface topography.

Curves were generated below the highest and lowest topographic points that describe the vertical variation between the modelled surface heat flow and the basal heat flux (figure 3). Each pair of curves is a characteristic of the specific geometry of the model surface. An arbitrary point at which the curves have decayed to within 5% of the basal heat flux value can be usefully compared in each model to assess the depth at which the thermal perturbation is significantly diminished (figure 4). The depth of the thermal perturbation gradually increases with increasing wavelength (decreasing $\Delta h/\lambda$) until a maximum penetration is reached at a $\Delta h/\lambda$ value of ~ 0.04 (figure 4).

Discussion

The model solutions presented here represent an initial attempt to assess the magnitude of the variation of surface heat flow measurements with respect to regional heat flux due to the effect of topography using the finite element method. A number of other factors also affect surface heat flow measurement including (but not limited to) internal heat production, ground water flux, altitude/climate effects, and lateral thermal conductivity contrasts (Beardsmore and Cull, 2001 and references therein). The approach taken in this study deliberately ignores these other effects to specifically investigate the effect of topography in isolation.

These models predict that, for relatively short wavelength - high relief topography, surface heat flow measurements, will be significantly different from the regional, “deep” heat flux. For longer

wavelength - low relief topography the observed difference will be less but may still be significant. These models also predict that the depth of thermal perturbation is related to the ratio of the relief height and the wavelength of surface topography and that this relationship is not linear.

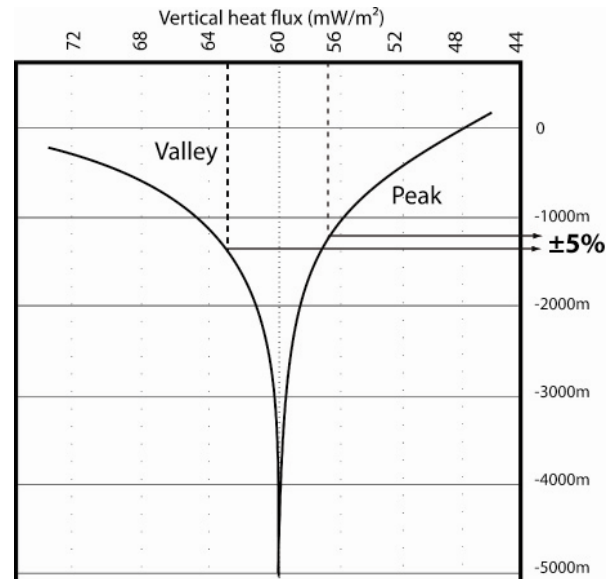


Figure 3: Profile of the modelled vertical heat flux below the peak (highest surface elevation) and the valley (lowest surface elevation) for model hft010 ($\Delta h/\lambda = 0.082$, $\lambda = 5$ km, $\Delta h = 412$ m). The decay of the thermal perturbation increases with depth until the basal heat flux value is reached. The 5% cut-off values used to generate figure 4 are shown.

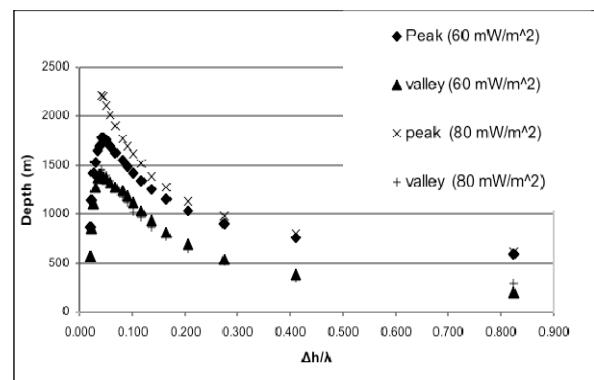


Figure 4: Plot of the depth at which the model heat flow is within 5% of the basal heat flux measured below the highest (peak) and lowest (valley) points on the surface topography. Note that the depth of perturbation attains a maximum value and then diminishes as a function of $\Delta h/\lambda$.

This study highlights a potentially significant source of uncertainty that must be factored in/corrected for when extrapolating heat flow data to depths of 3 km to 6 km. Furthermore, the results of this study suggest that the practice of estimating resource temperatures by calculating one-dimensional thermal models may only be valid for areas where surface topography is relatively subdued. In most other cases it is preferable to construct well parameterised two- and/or three dimensional thermal models.

References

Beardsmore, G. R. & Cull, J. P. 2001 Crustal heat flow: a guide to measurement and modelling. Cambridge University Press.

Lees, C. H. (1910) On the Shapes of the Isotherms under Mountain Ranges in Radio-Active Districts. *Proceedings of the Royal Society of London*. Vol. 83, No. 563, pp. 339-346

The next Australian EGS Reservoir – Jolokia 1 stimulation

Doone Wyborn*, Robert Hogarth, Delton Chen and Michel Rosener
Geodynamics Limited.
PO Box 2046, Milton, Queensland, 4064

Abstract

Geodynamics drilled the Jolokia 1 well in 2008 to a depth of 4,911m in the Innamincka granite at a location 9.5km west of the Habanero EGS field in north eastern South Australia. The reservoir stimulation program was delayed until 2010. Initially the delay was related to the need to undertake further evaluation of the well and implementation of a technical solution to allow multi-fracture stimulation. The stimulation was further delayed when the casing in Habanero 3 well failed in April 2009.

The aims of the stimulation are to:

- (i) Confirm the capacity to create heat exchange reservoirs at locations spread across the Innamincka granite resource.
- (ii) Develop two separate reservoirs in the one well, both deeper and hotter than the reservoir operated at the Habanero field
- (iii) Demonstrate injectivity increases compared to the Habanero field.

Prior to the stimulation the well is to be logged with a high temperature imaging tool and completed with a liner, tubing and packer. The stimulation consists of injecting more than 20,000 cubic metres of clean water into the well at pressures up to 69MPa. A conservative benign chemical tracer is included in the injected water. It is expected that a single reservoir will be created at a depth below the liner set to 4,350m. The reservoir development is monitored by a microseismic network of seven triaxial geophone stations up to 5 km from the well and 100 to 200m deep. The stimulation will be carried out over a period of 10 days. A pumping regime has been determined based on (i) the understanding that has come from the stimulations of the Habanero field, and (ii) the best information from international experts who have carried out such operations in other projects. Currently the operation is due to take place in August 2010. A comprehensive site-specific microseismic risk analysis was needed before the South Australian regulators could give approval to proceed.

Existing understanding of the stimulation process indicates that once a fracture zone begins to stimulate its transmissibility increases by orders of magnitude so that that zone dominates the continuance of reservoir growth with time. At the Habanero field the reservoir grew outwards at a relatively constant rate of 1 km² for every 12,000 m³ of water pumped after an initially more rapid growth within 200m radius of the wellbore. Based

on transient well-test analyses the transmissibility of the Habanero reservoir increased from a pre-stimulated 50 milliDarcy metres to a post stimulation 2000 milliDarcy metres. This increase is less than has been observed in the lower stress conditions of other projects. The increase is considered permanent because the roughness of the fracture surface gives rise to self-propping of the fracture once it has slipped by an amount in the order of the dimensions of the grain size of the rock. This permanency was vindicated at Habanero since stimulation in 2005 proceeded aurally beyond what had been achieved by the first stimulation in 2003, with virtually no overlap in development within 1 km of the injection well.

Only one reservoir can be developed at a time. Given the stress conditions of the Innamincka granite determined at the Habanero field there is ample potential for the stacking of multiple reservoirs in a vertical interval of well-bore provided these can be grown separately. The Jolokia reservoir program envisages one reservoir built from Jolokia 1 and a second built from a later well Jolokia 2 at a different depth interval. Future use of open hole high temperature packers should allow for such multiple reservoir development to be achieved in a single well.

The Jolokia 1 stimulation is to be carried out in August 2010 and measurement of injectivity and mapping of reservoir growth based on microseismic returns will allow comparisons with the Habanero reservoir. The stimulation program includes pressure transient fall-off analysis using down-hole gauges and pressure-temperature-spinner logs to evaluate the distribution of permeable fractures.

This paper reports on the results of the Jolokia 1 stimulation and the implications for further development of the vast Innamincka granite geothermal resource. The Jolokia stimulation is the key to proving that EGS development can be effected at virtually any location in granite bodies. The prize of large scale economic production of zero-emission EGS electricity will then depend on achieving increased heat extraction rates and reduced development costs.

Keywords:

Stimulation, EGS, microseismic monitoring, multi-fracture reservoir

Optimised Fracture Network Model for Habanero Reservoir

Chaoshui Xu*, School of Civil, Environmental and Mining Engineering, University of Adelaide
 Peter Dowd, Faculty of Engineering, Computer and Mathematical Sciences, University of Adelaide
 Doone Wyborn, Geodynamics Limited

Abstract:

Fracture networks and their connectivity are the principal factors affecting fluid flow in hot dry rock (HDR) geothermal reservoirs. Largely because of the complexity of the problem models of HDR reservoirs tend to be over-simplified using either a very limited number of fractures or an equivalent porous media approach. This paper describes a Markov Chain Monte Carlo (MCMC) conditioning technique for reservoir fracture modelling by taking into account the seismic events collected during the fracture stimulation process. Using the technique, the fracture model "evolves" during the simulation process and eventually converges to a predefined optimal criterion. The proposed method is tested using seismic data collected during the hydraulic fracture stimulation processes of the Habanero wells in Geodynamics' Cooper Basin project.

Keywords: Fracture network, seismic events, Markov chain Monte Carlo.

Introduction

The technical and commercial viability of HDR geothermal energy depends on the creation of artificial reservoirs, or Enhanced Geothermal Systems (EGS), in the rock mass by stimulating and creating fractures (generally by hydro-fracturing) to enable geothermal flow. The artificial reservoir forms the critical component in an EGS: the fracture network that connects the injection and production wells and acts as the heat exchange chamber for the system. HDR productivity depends crucially on the connectivity/permeability of the reservoir fracture network and a realistic fracture model, such as that described in this paper, is the key to assessing reservoir performance and designing a suitable heat exchange chamber for the EGS.

The characterisation of rock fracture networks is a very difficult problem not least because accurate field measurement of a single fracture is difficult and measurement of all fractures is impossible. Thus, in practice, the whole fracture system is not observable on any meaningful scale and the only realistic approach is via a stochastic model informed by sparse data and/or by analogues. In HDR applications, a realistic solution is even more difficult as the only reference data related to the fracture system are either from geophysical borehole logs and/or sparse seismic events kilometres beneath the surface and detected during the hydraulic stimulation process. For

these reasons current models of fracture systems used for HDR flow modelling are oversimplified representations of reality. They either use an equivalent porous media approach (e.g., Xing et al. 2009), single fracture representation (e.g., Zhang et al., 2009) or a combination of both.

Stochastic fracture modelling is the general approach in which locations, size, orientation and other properties of fractures are treated as random variables with inferred probability distributions. In the simplest case, once the parameters of the distributions are inferred, the rock fracture model is constructed by Monte Carlo simulation. First, the fracture locations are generated, usually by a Poisson distribution in which fracture intensity for a particular area is either assumed to be constant or is derived from geostatistical estimation or simulation. Secondly, the orientation of each fracture is generated, most commonly from a Fisher distribution. Finally, the size of each fracture is generated from a specified distribution, the most common being exponential, lognormal or gamma. Other fracture properties, such as aperture width and fracture strength, can then be added into the network by additional Monte Carlo steps. Options for fracture intersections and fracture termination can also be incorporated. Simulated fracture models are usually validated by sampling the model (using scan lines or areas) and assessing the extent to which the sampled values conform to the statistical models specified (Kulatilake et al. 2003). Such models are certainly very useful in describing the statistical behaviours of the fracture system. However, in order to make the generated models more realistic, some forms of data conditioning must be built into the fracture generation process. Data conditioning in two-dimensional fracture trace simulation is generally considered a simple matter but, probably because of the complexity involved, there are very few publications of algorithms and methods for data conditioning in three-dimensional stochastic fracture modelling. Mardia et. al (2007) described an attempt to condition a fracture model by borehole intersection data using Markov Chain Monte Carlo (MCMC) simulation. In this paper, however, the conditioning data are the seismic events observed during the fracture stimulation process of the HDR reservoir and they are not, therefore, confined to any known order (e.g., boreholes).

During hydraulic stimulation, fracture slips/initiations/propagations produce micro-

seismic events that can be monitored by a network of geophones and analysed to obtain the event locations. To date, these “point cloud” data have been used to estimate the volume of a reservoir that is connected by wells. We believe these micro-seismic events not only identify the locations of fracture slip, initiation and/or propagation but also contain vital information about the structure of existing fractures and fracture networks. Successful extraction of this information will significantly improve the reliability of fracture models so that a more realistic fracture representation of the HDR reservoir can be obtained. Moriya et al. (2002) use microseismic multiplet analysis to derive the fracture plane on the assumption that seismic events from the same fracture will produce similar microseismicities. This approach, however, only accounts for a small proportion of the total seismic events (17% in Moriya et al. 2002) and the fundamental assumption behind the approach is questionable.

Assumption

It is generally acknowledged that during the hydraulic fracture stimulation process, the effective normal compressive stress acting across two fracture planes of a fracture is reduced due to the hydraulic pressure and that will cause the two planes to slip against each other. This is generally considered to be the key mechanism in creating a permeable HDR reservoir as shear-slips will result in mis-alignment of fracture surface topographies which will cause a lateral dilation and thereby enhance fracture apertures and significantly increase the permeability of the fracture network. The shear slips between fracture planes will produce small-scale seismicity whose seismic waves can be captured and analysed by a network of geophones to derive the location of the event (Baisch et al. 2006). The effect of hydraulic pressure also makes it possible for existing fractures to propagate in the reservoir and new fractures to be initiated. The final outcome of the process will be a permeable reservoir connected to the wells through a complex fracture network.

Based on this conceptual description of the fracture stimulation process, it is reasonable to assume that seismic events only occur on fracture planes. The criterion of a realistic fracture model is then directly related to the overall closeness of the seismic events to fracture planes fitted in the model. In this context, fracture simulation essentially becomes a stochastic geometry reconstruction problem given a set of point clouds. Reconstruction of a surface from random point clouds is computationally and algorithmically challenging and is an active research area in computer and mathematical sciences (Bercovier et al. 2002). The success of current practice, however, depends critically on close sampling

points on the surface, which is usually not an issue as the point clouds are generally obtained from laser scanning or some form of digitizing. For seismic point clouds in geothermal applications, however, samples are very sparse. For a given fracture, only a few points are available, which indicate either the propagation front of the fracture or a point on the fracture surface where shear slip occurs at the time the events are detected. Current methodology is thus not directly applicable to fracture modelling.

The most common approach in stochastic fracture modelling is to use a 3D plane to represent a fracture, which could be bounded (e.g., elliptical plane, polygonal plane) or unbounded (e.g., Poisson plane). The fracture model (network) then becomes a series of connected fracture planes, $F_i, i=1,2,...n$, where n is the total number of fractures. A seismic event point, $P_j, j=1,2..m$ (m is the total number of seismic event points) can then be associated with a fracture F_i with distance

$d_{ji} = \sum_{j=1}^m d_{ji}^2$ can then be used as a simple criterion to quantify the goodness of fit of the fitted fracture model.

MCMC model

Planar polygons are used to represent fractures in this research. For each fracture polygon F_i , the location is described by the coordinates of its centre point (x_i, y_i, z_i) , the orientations are described by three angles: dip direction α_i , dip angle β_i and rotation angle γ_i and the sizes of the fractures are described by a major axis a_i and a minor axis b_i of an ellipse containing the polygon (Xu & Dowd, 2010). In other words, we parameterize fracture planes with parameters $(x_i, y_i, z_i, \alpha_i, \beta_i, \gamma_i, a_i, b_i), i=1,2...n$. Fracture plane F_i can also be expressed in functional form as $\lambda_x^{(i)} x + \lambda_y^{(i)} y + \lambda_z^{(i)} z = \omega^{(i)}$ where

$(\lambda_x^{(i)}, \lambda_y^{(i)}, \lambda_z^{(i)})$ is the unit vector normal to the fracture plane and can be calculated from $(\alpha_i, \beta_i, \gamma_i)$. Given a point $P_j (x_j, y_j, z_j)$, not necessarily lying on the plane, the signed orthogonal distance to fracture F_i is defined by:

$$d_{ji} = \begin{cases} \lambda_x^{(i)} x_j + \lambda_y^{(i)} y_j + \lambda_z^{(i)} z_j - \omega^{(i)} & \text{if } P_j^{(F_i)} \in F_i \\ \infty & \text{otherwise} \end{cases} \quad (1)$$

where $P_j^{(F_i)}$ is the projection point of P_j on fracture plane F_i . A matching function $\xi(j) \in \{1,2,...,n\}$ is used to associate each point P_j with one and only one fracture polygon. We shall

impose a simple criterion of minimum distance for this association and therefore by writing $d_{f,i}$ we mean point P_j is associated with fracture polygon F_i as its distance calculated by Equation (1) is the minimum when compared with distances to any other fracture plane.

$d=\{d_{f,i}\} \forall j$ is then the complete set of projection distances. Since seismic event points that lie on the same fracture will not be exactly co-planar, we must allow for statistical variation and treat a fracture as a distorted version of an idealized plane. A simple Gaussian noise model can then be adopted:

$$d_{j,i} \sim N(0, \sigma^2) \quad (2)$$

to represent the distortion in the data from the idealized plane. In other words, the orthogonal distances are identically and independently normally distributed with mean zero and variance σ^2 . Therefore, the likelihood function for the set of seismic event points $P=\{P_j\}$ can be defined as:

$$L(P; F, \xi) = \left(\frac{1}{\sqrt{2\pi\sigma}} \right)^m \prod_{j=1}^m e^{-\frac{(d_{ji})^2}{2\sigma^2}} \quad (3)$$

given a set of fractures $F=\{F_i\}$ and the matching function $\xi(\cdot)$. The product of this likelihood with priors of F gives the posterior distribution for F and the attention now is to estimate the posterior distributions of F and hence the parameters of the fracture set. A Markov chain can be used to generate samples from the posterior distribution which is commonly constructed by the Metropolis-Hastings algorithm using the Monte Carlo acceptance/rejection technique imposed by the Hastings' ratio:

$$\varepsilon(F^{(t)}, P) = \min \left\{ 1, \frac{\delta(P)q(F^{(t)} | P)}{\delta(F^{(t)})q(P | F^{(t)})} \right\} \quad (4)$$

where $\delta(\cdot)$ is the posterior (target) distribution and $q(\cdot)$ is a transition kernel which is usually chosen so that it is easy to sample from.

A more detailed description of this model can be found in Mardia et al (2007) where a similar model was developed to generate fracture models conditional on intersection points between fractures and boreholes drilled on a regular grid.

The Habanero Point Cloud

The point cloud used in this study is the Q-Con processed dataset of locations of seismic events recorded during the hydraulic fracture stimulation of Habanero 1 between November 6 and December 22, 2003 (Weidler, 2005). A total of 23,232 seismic events are recorded in this dataset which covers an area roughly of 2.5 km².

Figure 1 shows the absolute hypocentre locations of these events.

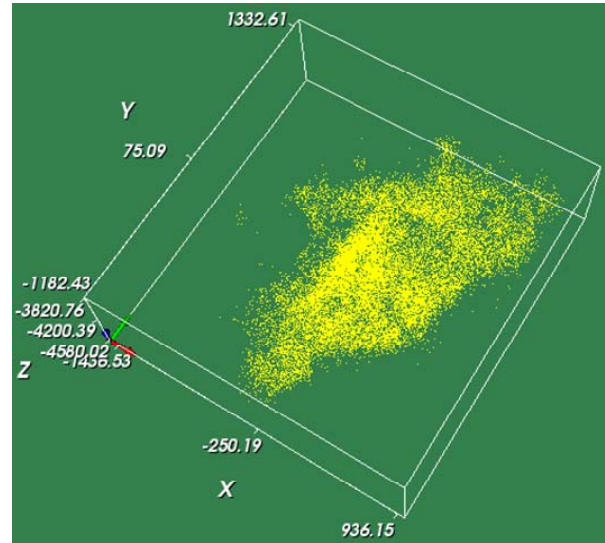


Figure 1 Absolute hypocenter locations of the seismic events

Clearly an ideal sub-horizontal reservoir has been formed by the stimulation process which is gently dipping in the South-west direction. Early analysis has revealed that the major part of the reservoir is confined within a sub-horizontal layer of approximately 30m (Baisch et al. 2006). Figure 2 shows ratios of increments in the volume of the reservoir, the geographical extents in the horizontal, East-west and North-south vertical planes covered by the seismic events during the stimulation period. Note that the increments are plotted on a relative scale where the ordinate represents the ratios against the volume or geographical extents of the reservoir covered by seismic events on November 6, 2003.

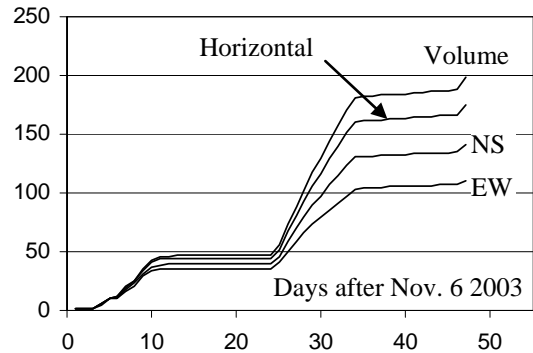


Figure 2 Increments in volume and geographical extents covered by seismic events

Habanero Fracture Model

A total of 20052 fractures were initially generated based on a non-homogeneous point process with a non-parametric density model estimated by the point cloud shown in Figure 1. Fracture locations (x_i, y_i, z_i) , $i=1, \dots, 20052$, are generated. The following parameters are used for initial fracture generation:

- Fracture orientation: Fisher distribution with $\kappa=1$. Orientation parameters ($\alpha_i, \beta_i, \gamma_i$) are then calculated.
- Fracture size: lognormal distribution with mean = 80m and variance = 12,000 m².

MCMC method described was then applied to update the fracture network. The following transition kernels are used in the MCMC process:

- Fracture orientation ($\alpha_i, \beta_i, \gamma_i$): normal proposal with standard deviation of 0.1 (in radian).
- Fracture location (x_i, y_i, z_i): normal proposal with standard deviation of 1.0.

Fracture size is not optimised in the current trial. Fractures without any association with any point after 100,000 iterations were removed from the system. After 2M iterations, the fracture model obtained is shown in Figure 3.

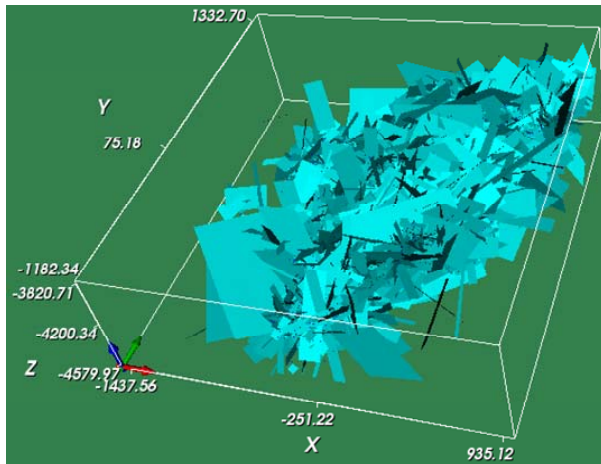
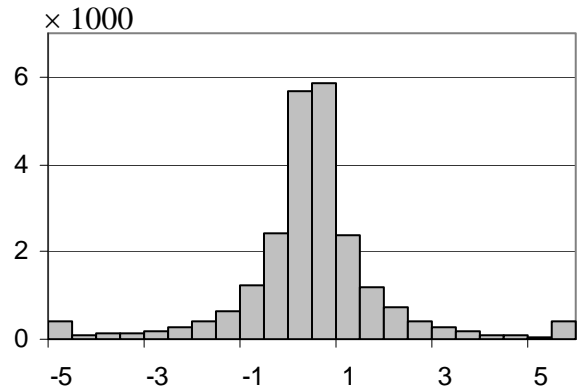
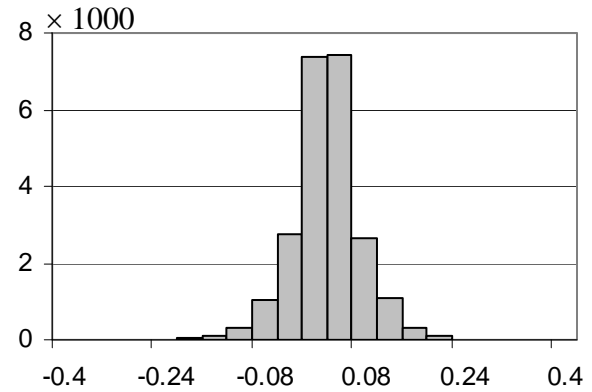


Figure 3 Habanero fracture model after 2M MCMC steps

This fracture model includes 10,995 fractures. Figure 4 shows the distribution of $d_{j,i}$ before and after the application of the MCMC updating process. Comparison of statistics is given in Table 1. Clearly the reliability of the model has been significantly improved.



(a) initial model



(b) optimised model

Figure 4 Histogram of $d_{j,i}$ for initial and optimised fracture models

Orientations of fractures have also changed significantly. There is no clear indication of orientation preference in the original fracture model (see the lower hemispherical projections of poles of fracture planes in Figure 5a). The fracture pole plot after optimisation (Figure 5b) clearly demonstrates a great proportion of sub-horizontal fractures. This is encouraging as it agrees well with the propagation pattern of the seismic event point cloud observed during stimulation (Baisch et al. 2006).

Table 1 Comparison of statistics of $d_{j,i}$ before and after MCMC optimisation

	Initial model	Optimised model
Number of fractures	20052	10995
Minimum $d_{j,i}$	-116	-0.35
Maximum $d_{j,i}$	303	0.39
Mean value of $d_{j,i}$	0	0
Variance of $d_{j,i}$	12.5	0.0028
$\sum d_{j,i}^2$	291437	66
99% of $d_{j,i}$ within range	[-11, 34]	[-0.17, 0.17]

signals (Baisch et al. 2009). The hydraulic conductance between wells can then be estimated.

References

Baisch S., Weidler, R., Vörös R., Wyborn D. And de Graaf, L. (2006) Induced seismicity during the stimulation of a geothermal HFR reservoir in the Cooper Basin, Australia, *Bulletin of the Seismological Society of America*, 96, No. 6, 2242–2256.

Baisch S., Vörös R., Weidler R. and Wyborn D. (2009) Investigation of fault mechanisms during geothermal reservoir stimulation experiments in the Cooper Basin, Australia, *Bulletin of the Seismological Society of America*, 99, No. 1, 148–158.

Bercovier, M., Luzon, M., Pavlov, E. (2002) Detecting planar patches in an unorganized set of points in space, *Advances in Computational Mathematics*, 17, 153 – 166.

Dowd, P.A., Martin, J.A., Xu, C., Fowell, R.J. and Mardia, K.V. (2009) A three-dimensional data set of the fracture network of a granite. *International Journal of Rock Mechanics and Mining Sciences*, 46, 5, pp.811-818.

Dowd, P. A., Xu, C., Mardia, K. V. and Fowell, R. J. (2007) A comparison of methods for the simulation of rock fractures, *Mathematical Geology*, 39, 697 – 714.

Kulatilake, P. H. S. W., Um, J., Wang, M., Escandon, R. F. and Narvaiz, J. (2003), Stochastic fracture geometry modelling in 3D including validations for part of Arrowhead East Tunnel, California, USA, *Engineering Geology*, 70, 131-155.

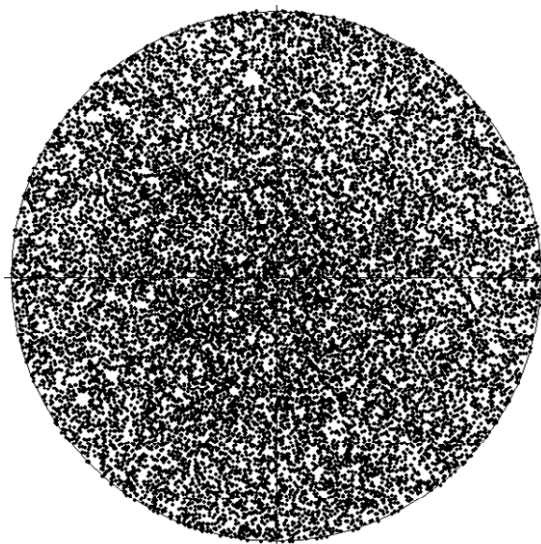
Mardia, K. V., Nyirongo, V. B., Walder, A. N., Xu, C., Dowd, P. A., Fowell, R. J., Kent, J. T. (2007) Markov Chain Monte Carlo implementation of rock fracture modelling, *Mathematical Geology*, 39, 355 – 381.

Mardia, K. V., Walder, A. N., Xu, C., Dowd, P.A., Fowell, R. J., Nyirongo, V.B., Kent, J. T. (2007a), A line finding assignment problem and rock fracture modelling. Bayesian Statistics and its Applications, Eds. Upadhaya, S.K., Singh, U., Dey, D.K. Anamaya Pubs, New Delhi; ISBN 10 81-88342-63-7; ISBN 13 978-81-88342-63-1. 319-330.

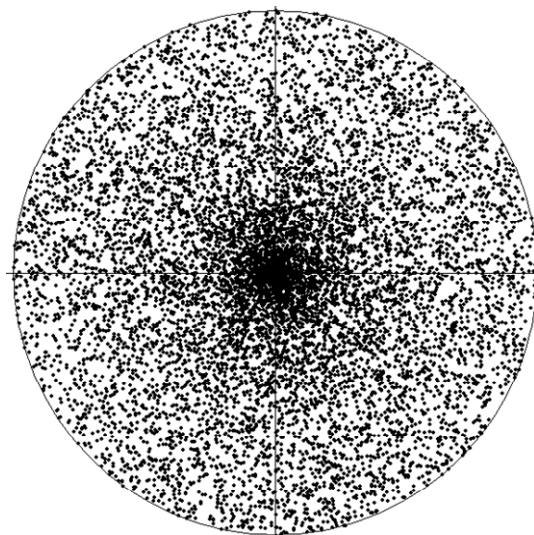
Moriya, H., Nakazato, K., Niitsuma, H. And Baria, R. (2002) Detailed fracture system of the Soultz-sous-Forêts HDR field evaluated using microseismic multiplet analysis, *Pure and Applied Geophysics*, 159, 17-541.

Weidler, R. (2005), The Cooper Basin HFR project 2003/2004: findings, achievements and implications, Technical report, Geodynamics Ltd.

Xing, H., Zhang, J., Liu, Y. and Mulhaus, H. (University of Queensland, 2009) Enhanced geothermal reservoir simulation, *Proceedings of the Australian Geothermal Energy Conference 2009*, Brisbane.



(a) initial model



(b) optimised model

Figure 5 Hemispherical projections of poles of fracture planes

Conclusions

This is a preliminary trial to demonstrate the application of MCMC in fitting a fracture model using a point cloud dataset. Clearly the method is effective, however there are still many remaining challenging issues. Fracture join/split (Mardia et al. 2007) is not yet considered in this work. The effect of the initial point process model has not been assessed and this will affect the total number of fractures retained in the final fracture network. The illustrated fracture model is by no means the ultimate optimal model for the Habanero fractured reservoir and further investigation is needed to achieve such a model.

The next stage of the process is to assess the connectivity of the fracture network between wells (e.g., between Habanero 1 and 3). Hydraulic apertures of fractures can be estimated from the degree of seismicity recorded in the seismic

Xu, C. and Dowd, P. A. (2010), A new computer code for discrete fracture network modelling, *Comps & Geosc.*, 36, 292-301.

Zhang, X. Jeffrey, R. and Wu, B. (CSIRO, 2009) Two basic problems for hot dry rock reservoir stimulation and production, *Proceedings of the Australian Geothermal Energy Conference 2009*, Brisbane.

Progress in CO₂-based EGS

Aleks D. Atrens^{1*}, Hal Gurgenci¹, Victor Rudolph¹

¹ The Queensland Geothermal Energy centre of Excellence.

Mansergh Shaw Building (#45),

The School of Mechanical & Mining Engineering, The University of Queensland, QLD 4072

The concept of Engineering Geothermal Systems (EGS) using CO₂ as a heat extraction fluid has been expanded since it was first proposed. A better theoretical understanding is available for the behaviour in the reservoir, process design, corrosion & condensation issues, and rock geochemistry, although knowledge of some of these systems is incomplete. Sufficient understanding is now available to provide a power plant design given site and reservoir parameters, and viability can be estimated. A number of challenges remain, however, and these must be addressed for the concept to be realisable. Those challenges are contextualised here to provide focus for the most urgent issues to be addressed.

Keywords: Carbon dioxide, CO₂, EGS, enhanced geothermal systems, thermosiphon, hot dry rock, hot wet rock

Introduction

CO₂-based EGS have been discussed previously (Brown 2000; Pruess 2006; Pruess and Azaroual 2006; Gurgenci et al. 2008; Pruess 2008; Atrens et al. 2009a; Atrens et al. 2009b; Atrens et al. 2010). A full discussion of the technical and economic issues related to CO₂-based EGS have been reported (Gurgenci 2009). Many of those issues are broadly applicable to all EGS; those will not be discussed here. There are a number of issues that are unique to CO₂-based EGS. These have primarily been lack of understanding of the process design, performance in the reservoir, CO₂-H₂O interactions, CO₂-H₂O-rock interactions, thermodynamic performance, etc. Some of these issues have been addressed in varying levels of detail.

Many technical challenges for the concept to overcome remain. These can be grouped under two broad categories: general challenges, which are overarching and apply to any use of CO₂ in EGS, and reservoir challenges, which are specific to the reservoir type.

General Challenges

There are a number of challenges that must be addressed to make CO₂-based EGS viable. Each of these is effectively show-stopping if the associated issues are unresolvable.

The overarching challenges that must be addressed are:

- CO₂ Sourcing

- CO₂ turbomachinery
- Solubility and reactivity of rock compounds and elements in pure or near-pure CO₂
- Legal/regulatory issues with subsurface CO₂.

Reservoir Challenges

Beyond the overarching issues, the remaining number of issues that depend on the type of reservoir being examined. The individual challenges for the different reservoir types are discussed below.

Un-dryable Reservoirs

This term is used to group reservoirs that are well hydraulically connected, and initially saturated or oversaturated with water. This grouping would include hot sedimentary aquifer systems (HSA), and EGS projects such as in the Cooper Basin where high pressure implies long-distance connectivity. These type of systems have an associated challenge of extreme difficulty in creating a dry CO₂-rich operating zone within the reservoir, either due to the large energy input necessary to displace water, or the difficulty in containing CO₂ within the desired region.

Dryable Reservoirs

Dryable reservoirs signify a reservoir grouping of those which are under-saturated with water at the outset, or have a limited initial volume of water that is easily displaceable. Examples of this category are the Fenton Hill reservoir, which was acknowledged as being unconnected and relatively lacking in water content, or the Hijori reservoir system, which experienced significant losses of injected fluid into the reservoir formation (implying an ease in displacing existing reservoir fluids). The challenges associated with systems of this type are the time period required to dry the reservoir, and the profile over time of fluid loss into the reservoir formation.

Wet Reservoir

This category is used for systems that have a liquid water phase coexisting with CO₂-rich fluid near the reservoir operating zone. CO₂-rich fluid may be produced in this case, allowing a single-loop, but there are important issues of both water and carbon dioxide being present in the reservoir. The challenges associated with this type of

system are related to the water-CO₂ relationships: time required until sufficiently pure CO₂ can be recovered, CO₂-H₂O dynamics in the reservoir (horizontally and vertically), rock-water-CO₂ interactions including mineral transformation / dissolution / deposition (permeability change) and geo-sequestration, and the thermodynamic effects of high water content in the CO₂-rich phase.

CO₂-Rich Reservoir

There is also the possibility of operating a CO₂-based EGS system in a reservoir that is already CO₂-rich. This could be a naturally occurring reservoir, or artificial as the result of artificial CO₂ injection for reasons other than CO₂-based geothermal power generation. The challenge associated with this reservoir type is identifying a reservoir that contains or may in the future contain CO₂, and is also suitable for geothermal power generation.

Discussion

There is a continuum between the three former reservoir types, and so some of the challenges relating to CO₂-H₂O interactions overlap. Separating reservoirs into the categories discussed above clarifies the range of these interactions that are vital to consider for different situations. The implication of this is that there is an opportunity to target the proposed CO₂-based EGS technology towards situations where the challenges are more readily overcome. This may be useful where there are particular issues related to certain systems that may not be feasibly answered in the foreseeable future, or that may be most suitably resolved by field trials in a reservoir of a different type.

It is recommended that current goals towards implementation of a CO₂-based EGS power system focus on reservoirs that can feasibly be dried, as these have a smaller number of associated challenges. Reservoirs of this type are also less likely to be targeted for use for water-based EGS, so the relative risk of competitively disadvantaging one technology over another.

References

- Atrens, A. D., H. Gurgenci, et al., 2009a., "CO₂ thermosiphon for competitive power generation." *Energy & Fuels* **23**(1): 553-557.
- Atrens, A. D., H. Gurgenci, et al., 2009b., Exergy analysis of a CO₂ thermosiphon. Thirty-fourth workshop on geothermal reservoir engineering. Stanford University, Stanford, California.
- Atrens, A. D., H. Gurgenci, et al., 2010., "Electricity generation using a carbon-dioxide thermosiphon." *Geothermics*.
- Brown, D. W., 2000., A hot dry rock geothermal energy concept utilizing supercritical CO₂ instead of water. Twenty-Fifth Workshop on Geothermal Reservoir Engineering, Stanford University, Stanford, California.
- Gurgenci, H., 2009., Electricity generation using a supercritical CO₂ geothermal siphon. Thirty-fourth workshop on geothermal reservoir engineering. Stanford University, Stanford, California.
- Gurgenci, H., V. Rudolph, et al., 2008., Challenges for geothermal energy utilisation. Thirty-Third Workshop on Geothermal Reservoir Engineering. Stanford University, Stanford, California.
- Pruess, K. 2006. "Enhanced geothermal systems (EGS) using CO₂ as working fluid — A novel approach for generating renewable energy with simultaneous sequestration of carbon." *Geothermics* **35**: 351–367.
- Pruess, K., 2008., "On production behaviour of enhanced geothermal systems with CO₂ as working fluid." *Energy Conversion and Management* **49**: 1446-1454.
- Pruess, K. and M. A. Zaroual, 2006., On the feasibility of using supercritical CO₂ as heat transmission fluid in an engineered hot dry rock geothermal system. Thirty-first workshop on geothermal reservoir engineering. Stanford University, Stanford, California.

Exploration and assessment of Hot Sedimentary Aquifer (HSA) geothermal resources in the Otway Basin Victoria

Peter Barnett and Tim Evans
 Hot Rock Limited, GPO Box 216, Brisbane QLD 4001
peter.barnett@hotrockltd.com and tim.evans@hotrockltd.com

The Otway Basin contains a number of Hot Sedimentary Aquifer (HSA) geothermal resources with potential for commercial development. The methodology Hot Rock Limited has used to assess these resources is detailed in this paper. The resulting stored heat estimates for the HSA resources of the Otway Basin is large, even by world geothermal standards. A total of 550,000 PJ of HSA resources have been so far estimated and declared by three companies.

While there is confidence in the estimation of in-place heat in the Otway Basin HSA resources and the rate that heat in geothermal water recovered to surface can be converted to electricity, there is less certainty as yet on the amount of heat that can be recovered and the rate it can be recovered. Both of these variables are determined by permeability in the geothermal reservoir.

By comparison with both HSA and volcanic geothermal systems elsewhere, and a detailed assessment of the structural geology at the Otway Basin tenements, HRL considers that the HSA resources in the Otway Basin are dominated by secondary fracture permeability, with primary permeability being subordinate. HRL is proceeding to drill in early 2010 two proof of concept wells in to its flagship HSA project at Koroit. These wells are specifically targeted on both primary and secondary permeability, with the firm expectation that secondary permeability will prove to be dominant and that commercial grade temperatures and well flow rates will be obtained.

Keywords:

Geothermal, Otway Basin, Hot Sedimentary Aquifer, HSA, resource assessment, Monte Carlo, proof of concept, generation potential, well targeting.

Introduction

Hot Rock Limited (HRL) holds a large geothermal tenement position in Victoria of 27,500km² in five permits. Some 15,000km² of this holding contains rocks of the Crayfish Subgroup in the onshore portion of the Otway Basin within Victoria. These are predominantly sandstones of Cretaceous age and have known geothermal potential.

They occur in a series of individual depositional centres (shown coloured in both light and dark green in Figure 1), deposited onto the tops of

subsiding basement fault blocks developed along the northern margin of the rift zone which led to Australia separating from Antarctica during the breakup of Gondwanaland in late Cretaceous times.

The crustal thinning produced in this extensional tectonic environment allows for elevated heat flow through the Palaeozoic basement into the overlying sediments over most of the Otway Basin where geothermal gradients of 35 to 45°C/km are measured. This combination of regional shallow heat and large areal extent, thickness and hence volume of geothermal reservoir rock make the Otway Basin a significant terrain for potential HSA geothermal development, even by world standards.

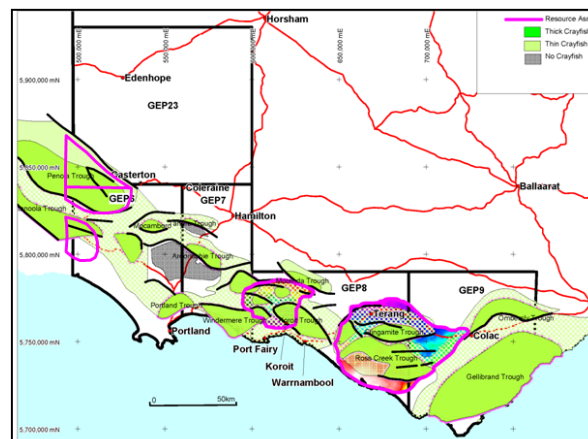


Figure 1: Series of fault bound rift basins containing thick accumulations of Crayfish subgroup rocks developed along the northern margin of the onshore Otway Basin.

Exploration of HSA resources

Although the HSA geothermal plays in the Otway Basins are essentially blind – i.e. without observable discharge of heat or mass at surface, HRL has been able to define these resources at depth from the extensive geoscientific data that have been acquired over the past 40 to 50 years by particularly the petroleum and groundwater industries in Victoria. These data have been systematically archived by State and Federal government agencies such as the Department of Primary Industries and Geosciences Australia and are readily accessible

Existing data include gravity, magnetics and stratigraphy which are applicable at relatively coarse scale to regional scale studies. More

detailed data, of value for prospect scale studies, include seismic reflection data, geological logs and cores from existing petroleum and ground water wells, and measurements of temperatures and other data in these wells.

In addition to use of existing data, HRL has applied to its HSA exploration studies in the Otway Basin a number of exploration methods that are routinely used in the exploration and delineation of volcanic geothermal systems. The most significant of these has been the use of magneto-telluric (MT) resistivity surveying and the application of geothermal geochemistry interpretative methods to ground water and petroleum well fluids analyses.

Key deliverables from the HRL exploration studies include the following:

Starting Point: An initial review of geothermal gradients as a tool for prioritizing areas for detailed geothermal assessment.

End Point: A range of 3-D models gridded at typically 100 m centers over geothermal resource areas of typically 300 to 500 km² areal extent which include:

- Stratigraphic models defining formation tops, bottoms, vertical (cross sections) and horizontal sections (slices in plan)
- Structural geological models
- Thermal models showing distribution of isotherms in 3-D, isothermal sections in 2-D combined with geology, estimates of temperature in each grid block at any depth
- Multi discipline, integrated, conceptual hydrogeological models which form the basis for subsequent resource assessment, and formulation of exploration drilling and development strategy.

Assessment of HSA Resources

The Otway Basin HSA resources have been assessed in terms of in-place stored heat contained in the Crayfish subgroup reservoir rocks between assigned upper and lower depth limits. This involves initially considerations of resource thickness, lateral extent and hence volume, followed by considerations of porosity and temperature from which heat contained in both the rocks in the resource volume and hot water contained in pores and fractures in the reservoir rocks can be estimated.

The upper depth limit to the resource is referred to as the resource temperature cut off (or abandonment temperature) and the lower depth limit is an assumed depth limit to which geothermal fluids can be reasonably recovered

from the resource, and is taken to be a practical drilling depth limitation.

Estimates of temperature values throughout the resource volume have been obtained from 3D thermal modelling. Porosity has been assessed conservatively at 10% throughout and although this is an important parameter in considering the amount and rate at which hot water can be recovered from the geothermal resource, the amount of heat stored in the rock and the water is relatively insensitive to porosity.

The values used for the above parameters in HRL’s assessment of HSA resources are given in Table 1 where they are compared with a range of values used by other developers working in the HSA environment. Relative to these other values, those used by HRL are conservative.

Table 1: Comparison of parameters used by HRL for estimating the thickness, volume and in-place heat of HSA geothermal resources.

Parameter	Values used by HRL	Values used by others in OB
Minimum resource temperature	130°C (GEP6 and 23) 140°C (GEP-8)	125°C
Power plant rejection temperature	70°C	70°C
Resource base: i.e. practical depth limit for recovery of geothermal fluids	4500m	5000m
Porosity	10%	5 % to 15%
Minimum reservoir thickness	500m	Nil to 250 m

The computation of in-place heat has been undertaken by HRL on a probabilistic basis using a purpose developed Monte Carlo simulation model in which probability distributions are used to characterise the key resource assessment parameters. The stored heat is summed over individual resource blocks for which formation tops, top and bottom resource limits and modelled temperature distribution have been gridded at 1000m intervals. The Monte Carlo model is run 2,000 times to obtain the frequency distributions and cumulative probability distributions for the stored heat contained in the geothermal resource volume.

The results of the resource assessments are reported in accordance with the Australia Geothermal Reserve Reporting Code (1st edition, 2008) in terms of in-place stored heat. At this stage in the exploration of HRL’s Otway Basin HSA resources, two types of geothermal resources have been determined:

- “Inferred resource” – where temperatures are not directly measured, and

• “Indicated resource” where temperatures are measured in-situ within the geothermal resource. Typically the former is declared where temperatures are measured in petroleum and / or deep ground water wells that have not penetrated as deep as the geothermal reservoir in the Crayfish Subgroup and the latter is where existing wells have been drilled into the Crayfish thus allowing for temperatures to be measured directly within the geothermal resource. If a new well drilled into the geothermal resource successfully flow tested then the “Inferred resource” estimate can be upgraded to “Measured resource”.

Results of Resource Assessments

HRL has completed resource assessments at the following Crayfish Subgroup depository centres in the Victorian portion of the Otway Basin. These centres are shown outlined in pink in Figure 1 and include (from west to east):

- GEP-23: Penola Trough
- GEP-6: Penola Trough
- GEP-6: Tantanoola Trough
- GEP-8: Koroit Trough
- GEP-8: Ross Creek Trough
- GEP-8/9: Elingamite Trough

From these assessments a number of geothermal resources have been declared, as summarised in Table 2.

Table 2: Results of estimations of Inferred and Indicated HSA geothermal resources identified and declared by HRL within GEP-6, GEP-8 and GEP-23 in the Otway Basin.

Resource	Tenement	Resource Area	Resource Volume	Indicated Resource	Inferred Resource	Report Date
		km ²	km ³	PJ	PJ	
Koroit	GEP-8	50	47	7,600		
Koroit	GEP-8	400	340		59,000	
Koroit	GEP-8	450	387	7,600	59,000	1-Oct-09
Penola	GEP-23	20	24	5,000		
Penola	GEP-23	120	150		29,000	
Penola	GEP-6	8	9	1,700		
Penola	GEP-6	290	306		55,000	
Penola	GEP23 & 6	440	490	6,700	84,000	27-Jul-10
Tantanoola	GEP-6	180	130		22,000	27-Jul-10
Totals		1,070	1,010	14,300	165,000	180,000

Power Generation Potential

The estimated geothermal resources declared today by HRL in the Otway Basin total 15,000 PJ for indicated resources and 165,000 PJ for inferred resources, at the P50 level. These figures represent very large store of geothermal heat, however, not all of this heat is available for conversion to electricity. Only a small amount of the geothermal heat will be recoverable from the resource and only a small amount of the heat recovered to surface will be converted to electricity in a power plant due to thermal to mechanical energy losses.

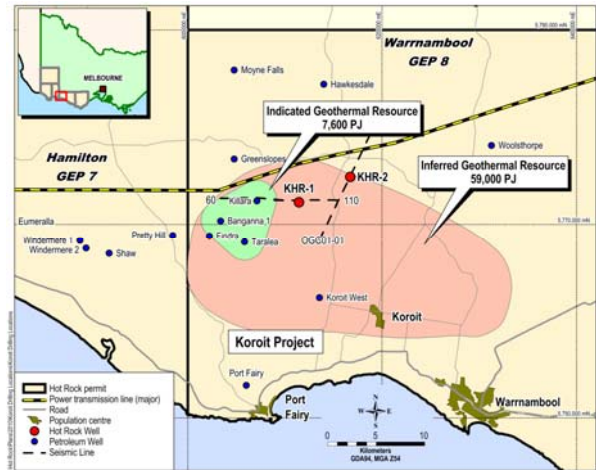


Figure 2: “Inferred” and “Indicated” geothermal resources declared in the Koroit area, GEP-8 (Source: HRL, 2009).

Representative values for HSA geothermal resources are 5% and 12%, respectively, which means that only about 1% of the in-place heat in the geothermal reservoir will be converted to electricity. On this basis, only some 1,000 PJ of the total value of 180,000 PJ of heat contained in the Koroit geothermal resource, would be able to be extracted and converted to electricity. Nonetheless, 1000 PJ of energy in electrical energy terms is still a large value, equivalent to about 300,000GWh. To achieve generation at this level a power plant with a generation capacity of about 1300MWe would be required to operate at a capacity factor of 90% for a period of 30 years.

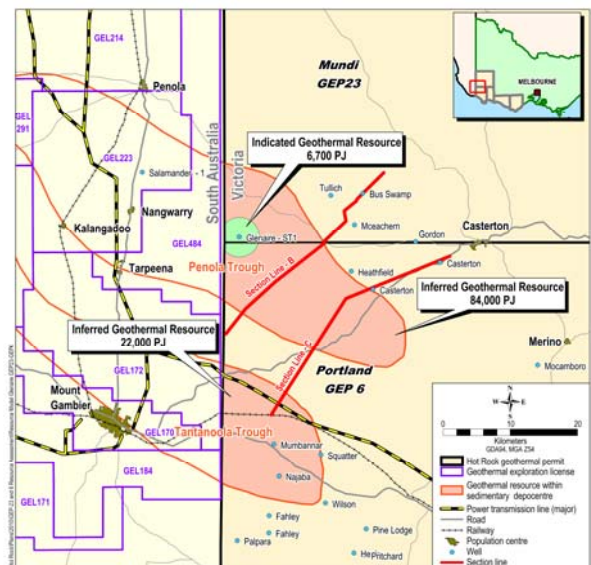


Figure 3: “Inferred” and “Indicated” geothermal resources declared in the Penola and Tantanoola Troughs in GEP-23 and GEP-6 (Source: HRL, 2010)

In addition to the 180,000 PJ geothermal resources estimated by HRL, two other geothermal developers have also delineated,

assessed and declared HSA geothermal resources in the western and eastern ends of the Otway Basin, on either side of HRL's tenements. The total declaration of geothermal resources to date from the three companies for the onshore Otway Basin in both Victoria and South Australia totals some 550,000 PJ (Table 3). On the same basis as the calculations above for Koroit, this amount of thermal energy has the potential to generate some 9 000,000 GWh of electricity and this would require a power plant generating capacity of some 3,500 MWe for 30 years.

Table 3: Summary of all declared HSA geothermal resource assessments over the greater Otway Basin

Trough in Otway Basin	Tenement	Developer	HSA Inferred Resource PJ	HSA Indicated Resource PJ	HSA Measured Resource PJ	HSA Estimated Total PJ
Tantanoola	GEP-6	HRL	77,000	1,700		78,700
Koroit	GEP-8	HRL	59,000	7,600		66,600
Penola	GEP-23	HRL	29,000	5,000		34,000
Anglesea	GEP10	Green Earth	40,000			40,000
Tantanoola	GEL-170, 171, 172	Panax	130,000			130,000
Rendelsham	GEL-170, 184, 212	Panax	17,000			17,000
Rivoli St Clair	GEL-173	Panax	53,000			53,000
Penola	GEL-223	Panax	89,000	32,000	11,000	132,000
Totals			494,000	46,300	11,000	551,300

The in-place heat stored in the HSA resources in the Otway Basin and the potential generating capacity of these are large, even by world geothermal standards considering that the geothermal industry has a global installed capacity of 11,000 MWe.

The confidence in the estimation of heat in-place in the Otway Basin HSA resources is relatively high, as is the rate at which the heat in geothermal water recovered to surface can be converted to electricity. Of lesser certainty is the amount of heat that can be recovered from the HSA resource and the rate at which it can be recovered - both of these are determined by permeability in the geothermal reservoir.

Permeability

Permeability in Otway Basin HSA reservoirs can be of two types (1) primary permeability, associated with natural porosity in the Crayfish Subgroup sandstone reservoir rocks, and/or (2) secondary permeability associated with faults and fractures in the reservoir rocks.

Primary permeability

The petroleum industry has generated considerable data on porosity and permeability throughout the Otway Basin from geological and electrical logging and analysis of cores and cuttings from petroleum wells. Poro-perm data for the Pretty Hill sandstone from petroleum wells in both Victoria and South Australia (but predominantly from the latter) are shown in Figure

4. The pink line is a regression fit for channel sands in the Pretty Hill and the red line is the same for bar sands in the Pretty Hill. Clean channel sands are the prime target for geothermal development being more coarse grained and with both higher porosity and permeability at any depth.

As well as variation in primary permeability in the Otway Basin with depth there is also significant variation in the character and quality of the Crayfish Subgroup reservoir facies, depending on provenance of source material and environment of deposition.

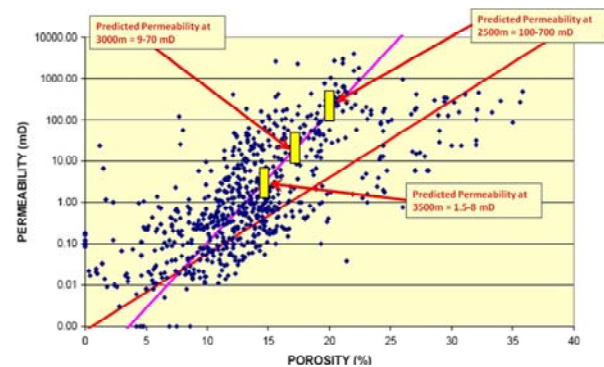


Figure 4: Summary of declared geothermal resource assessments in the greater Otway Basin with HSA geothermal development potential. Source: 3DGeo (2009)

From a detailed analysis of seismic data and petroleum well data, the Koroit geothermal resource is assessed to have particularly good reservoir facies characteristics having thick accumulations of clean coarse grained sands, with minimal lithic material, especially in the Lower Pretty Hill Formation (3DGeo 2009). Based on statistical analysis of the poro-perm data in Figure 3, estimates have been of porosity and permeability potential with depth in the Koroit geothermal resource (3D Geo, 2009). The estimates are for better than average poro perm values than occur for the Otway Basin.

The variation in poro perm with depth in Figure 4 is instructive as it confirms:

- porosity in the Pretty Hill Formation to be reducing with depth, from 20% at 2500 m to 14% at 3500m, and
- permeability decreasing by two orders of magnitude between 2500 and 3500m.

In spite of these reductions in poro-perm with depth, the evidence is that permeability within the Pretty Hill at Koroit will still be sufficient to give commercial geothermal well flows from primary reservoir permeability alone. For example, assuming, as a conservative case, that the lower value in the range of the permeabilities predicted at each the 3 depth ranges in Figure 4 apply, and a net to gross ratio of 50%, then a transmissivity

of 13 Dm would be expected over the depth range of 2500 to 3500m, with an expected temperature range of 130 to 170°C. For this transmissivity value, a standard size geothermal well completion (with a 9-5/8 inch diameter open production hole) can be expected to yield a flow rate of 90 kg/sec, and for a large diameter well completion (with 12-1/2 inch diameter production hole) to yield a flow rate of 160 kg/sec (SKM, 2009).

Secondary permeability

The importance of secondary permeability in HSA geothermal systems seems not to be well appreciated in the Australian geothermal community. Few if any geothermal systems in the world, of any type, produce from only primary permeability. For example, for the following two key overseas analogues for HSA geothermal resources in Australia:

- Heber and East Mesa fields in Southern California: secondary permeability controls an upflow of hot geothermal fluids from basement into overlying fluvial sediments where primary permeability is high. Geothermal wells produce from both fractures around the upflow and primary permeability in the sediments
- Southern Germany: high flow rates (up to 140 kg/sec) are obtained from deep intersections (at depths of up to 4500m) of well bores with fractures in Malm limestone with little if any evidence of primary permeability

In conventional volcanic geothermal systems developed in sedimentary reservoir rocks, fracture permeability is also the major control on geothermal fluid hydrology and well productivity. For example:

- The large and very well documented Geysers geothermal field in California produces steam from fractured greywacke basement rocks which have low primary porosities and permeabilities.
- The Ohaki geothermal field in New Zealand has good production well flows from fractured greywacke basement rocks which underlie lavas and volcanoclastics.

In the Otway Basin there are well developed faults and structures at both large and small scale which affect both the Palaeozoic basement rocks and the overlying sedimentary successions, particularly the Crayfish Subgroup. The present-day stress regime in the Otway Basin is on the boundary between oblique-slip and reverse faulting. The NW-SE maximum horizontal stress orientation is calculated at ~140 degrees N. Analysis of structural geologic data has been interpreted to show that faults and fractures orientated approximately WNW-ESE to NE-SW are consistent with the present day stress regime and structures on these orientations are considered to be mechanically open, with good

potential for providing secondary permeability channels for geothermal fluid flow (3D-Geo, 2009). The potential for secondary fracture permeability is therefore considered to be good in the HSA resources of the Otway Basin.

HRL is proceeding in early 2010 to drill two proof of concept wells at its flagship Koroit geothermal project. These two wells are specifically targeting major faults at depth as primary well targets. A subordinate target is porosity in the upper levels in the open production hole where porosity and permeability prospects are best. Having the highest geothermal gradient in the Otway Basin (of up to 46 °C/km) at the Koroit resource, a minimum production temperature of 130°C can be targeted at the top of the geothermal reservoir within the Crayfish Formation at depths of only 2500m. At this comparatively shallow depth, poro-perm prospects are much better than at greater depth, particularly below 3500m as evident from Figure 4.

HRL's "Proof of Concept wells" are therefore designed to intersect an optimum combination of primary and secondary permeability and HRL is optimistic of successful outcomes in terms of good permeability and transmissivity results and commercial grade temperatures and well flow rates.

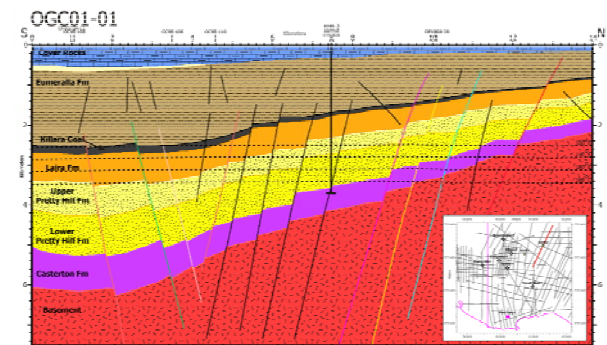


Figure 5: Geological section, Koroit HSA resource, showing proof of concept well targeted on (1) deep intercept with major fault target and (2) primary porosity target (upper and lower Pretty Hill Formations from 2500m) Source: 3DGeo (2009)

Summary and Conclusions

The Otway Basin contains a number of HSA geothermal resources with good potential for commercial development.

These resources exist as a result of the favourable combination of:

- elevated geothermal gradients of typically around 40°C/km, but as high as 46°C/km in prime resource areas such as Koroit in GEP-8.
- Thermal gradients in this range are sufficient to obtain commercial grade geothermal temperatures within practical drilling depths

- The fortuitous occurrence of thick stratigraphic sequences of quartz rich sandstones in the Crayfish Subgroup reservoir rock within the same depths that commercial temperatures occur and within practical drilling reach

The stored heat contained in the HSA resources of the Otway Basin are large, even by world geothermal standards. A total of 550,000 PJ of HSA resources have been so far estimated and declared by three companies. Although current expectations are that only some 0.5% of this in-place heat can be recovered from the geothermal resources and converted to electricity, the generation potential on even this basis is large, requiring some 3,500MWe of generation capacity for 30 years.

There is confidence in the estimation of heat in-place in the Otway Basin HSA resources and the rate that heat in geothermal water recovered to surface can be converted to electricity. However, there is less certainty yet on the amount of heat that can be recovered from the HSA resources and the rate at which this can be recovered - both of these variables are determined by permeability in the geothermal reservoir.

HSA resources seem to be viewed by the Australian geothermal community as having only primary permeability. By comparison with both HSA and volcanic geothermal systems elsewhere, and a detailed assessment of the structural geology of its Otway Basin tenements, HRL views the Otway Basin resources to be dominated by secondary fracture permeability, with primary permeability being subordinate to this.

HRL is proceeding in early 2010 to drill two proof of concept wells at the Koroit HSA resource, specifically targeting both primary and secondary permeability with the firm expectation that secondary permeability will prove to be dominant and that commercial grade temperatures and well flow rates will be obtained.

Statement of Competent Person

The information in this paper that relates to Exploration Results, Geothermal Resources or Geothermal Reserves is based on information compiled by Peter Barnett who is a full time employee of Hot Rock Limited. He has sufficient experience which is relevant to the style and type of geothermal play under consideration and to the activity which he is undertaking to qualify as a Competent Person as defined in the Code. In this work he has drawn freely from reports on HSA geothermal resources in the Otway Basin prepared under his supervision, by both staff of Hot Rock Limited and by external consultants, notably 3D-Geo of Melbourne. The assessment of stored heat and levels of Indicated and Inferred Resources and the reporting of these have been

undertaken solely by Peter Barnett. Peter Barnett consents in writing to the inclusion in the report of the matters based on his information in the form and context in which it appears.

Acknowledgments

This paper draws freely on graphical material prepared by 3D Geo of Melbourne under contract to HRL, particularly the power point presentation for this paper to be given at the conference.

References

3D Geo Pty Limited, 2009, Otway Basin Project. Koroit Area WP2 Report. Unpublished report prepared under contract to Hot Rock Limited 2009.

AGEA and AGEG, 2008, Australian Code for Reporting of Exploration Results, Geothermal Resource and Geothermal Reserves, 2008 Edition. Prepared by the Australian Geothermal Code Committee, AGEA and AGEG,

Hot Rock Limited, 2009, Statement of Estimated Geothermal Resources for the Koroit Geothermal Power Project, Victoria, Geothermal Exploration Permit GEP- 8. Hot Rock Internal report, prepared by Peter Barnett, 30 September, 2009. A full copy is available at:

<http://www.hotrockltd.com/IRM/Company/ShowPage.aspx?CPID=1224&EID=16267720>

Hot Rock Limited, 2010, Characterization and Assessment of Geothermal Resources in GEP-23 & GEP-6, Hot Rock Internal report, prepared by Peter Barnett, June 2010. A full copy available at: <http://www.hotrockltd.com/IRM/Company/ShowPage.aspx?CPID=1227&EID=77703804>

Sinclair Knight Merz (SKM), 2009, several well bore flow modelling studies. Unpublished report prepared under contract to Hot Rock Limited 2009.

Validation of Geothermal Exploration Techniques for Analysing Hot Sedimentary Aquifer and Enhanced Geothermal Systems.

J.E. Davey & J.T. Keetley
3D-GEO

Level 5 / 114 Flinders Street, Melbourne, 3000.

Validated geothermal resource estimates are based on geological models that combine the geology from the surface to basement incorporating properties such as lithology, structure, fluids, compaction, porosity and permeability with thermal models consisting of heat flow, conductivity and thermal gradients. These models must extend beyond single point well analysis, and provide a balanced and geologically reasonable estimate of the size, structure, accessibility and maturity of a subsurface thermal system. To achieve a geologically reasonable model, all available geological and geophysical data must be considered. However, datasets and measurements must be analysed, interpreted and weighted in a manner that reduces error for thermal models.

This paper focuses on building validated geothermal resource evaluations from geological and geophysical interpretations for Hot Sedimentary Aquifer (HSA) and Enhanced Geothermal Systems (EGS). This paper also focuses on limitations of some datasets, and this can be realized when modeling.

Limitations in Thermal Modeling

For any given geological dataset (field, well, seismic, remote sensing, temperature) virtually an infinite number of 2D and/or 3D interpretations can be made. However, the set of physically possible geological interpretations are far more limited. The tests for such physical plausibility derive from our knowledge of the processes which control sediment deposition, structural evolution, and geothermal systems. Interpretations which can pass these tests may

not be correct, but they are more likely to be so, and can be labeled with that highly sought appellation: Validated.

Limitations occur with thermal modeling that are not as prevalent in other forms of subsurface modeling. The main limitation is the abundance and representation of temperature throughout the system. Temperature measurements are typically limited to single point measurements obtained from wells and bores previously drilled.

While heat is the basis of all geothermal systems, temperature is only ever measured from a single point. This provides the vertical component of a temperature gradient at that point source making it an isotropic analysis of temperature. While this is an ideal measurement for volcanic and plutonic rocks where heatflow is primarily in the vertical domain, it does not account for the anisotropic 'radial' heat distribution that occurs in sedimentary and metamorphic rocks (Clauer & Huenges 1995). The temperature-depth profile from a well can therefore be thought of as the vertical summing of the geothermal gradients established within the individual layers within the sediment pile at that location. Such a profile is rarely linear with depth.

However, when extrapolating temperature from the well profiles, the anisotropic component of heat distribution within a sedimentary basin must be accounted for. Because of this, the thermal component of the model is highly dependent on incorporating other factors such as structure, lithological distribution, fluids, porosity and permeability, hydrocarbons and fracturing to control the distribution of heat throughout the model. Because of this, a geological model must be created first. This will help to generate the

properties needed to consider for the anisotropic extrapolation of temperature. The thermal modeling will be revisited later in this paper.

Subsurface Geothermal Modeling

Utilizing all the available data to construct a geological model will aid in validating a geothermal resource. In terrains currently being explored with Australia, available data includes: wells, 2D-3D remotely sensed imagery, 2D-3D seismic, potential field data sets (namely gravity and magnetics), petrophysical logs and occasionally magnetotelluric data sets.

Wells

Wells provide geological truthing to any subsurface model. Basic information such as lithology, formation depth, fluid presence and temperature are recorded.

Because temperature is currently only measurable in situ, wells provide the basis of the thermal modeling. Down hole tools deployed during drilling and after drilling are used to record temperature at different stages within the well. This information is combined with estimates or measurements of conductivity to generate information on heatflow. This is in turn used as the basis for extrapolating a temperature model across the area.

Wells often have vital information collected from down hole logging tools employed during drilling or just after. These tools collect information on temperature, pressure, flow rates, densities and even fracturing. A seldom used, but highly beneficial technique for EGS and HSA is down hole vertical conductivity and horizontal resistivity measurements. These techniques are designed to identify fracture orientation as well as what orientation of fracture is open (that is, a potential fluid conduit) in the well. Both measurements are obtained while drilling. Horizontal resistivity measures the resistivity of a formation by dispersing a current flowing in a horizontal plane. Vertical conductivity is measured in a similar manner, however in the vertical plane. These measurements are

obtained by using wireline logging tools such as laterologs and propagation logs. Two survey types are used, a single orientation plane surveys (i.e. vertical or horizontal) cannot take measurements in the plane parallel to the plane where the electromagnetic current is flowing. Vertical conductivity is used for imaging high angle fracturing (fractures with dip $20-70^\circ$) and sub-horizontal fracturing (dip $<20^\circ$). Horizontal resistivity is better at imaging sub-vertical fracturing (dip $>70^\circ$). The surveys are analysed and plotted as frequency diagrams indicating the primary orientation of the open fracturing.

Information about the contemporary stress fields in the area can be obtained from well data. Borehole breakouts reflect a measurement of the orientation of disintegration of the well during drilling as a result of compressive stress failure. The orientation of the breakout is parallel to the orientation of the minimum horizontal stress. This orientation is perpendicular to the orientation of the drilling induced tensile fractures, the orientation in which the tangential stress is below tensile rock strength. This orientation is parallel to the maximum horizontal stress. Information about contemporary stress can assist with drilling and also with determining the nature and orientation of any structure that may be active or 'open' within the system.

Surficial Geology and Remotely Sensed Imagery

Geothermal exploration is greatly aided from surficial geology and remotely sensed imagery as it provides approximate ground truths to structure and morphology interpreted in the subsurface. Not all subsurface geology has a surficial representation, a significant portion does. Actual exposure of these features helps to understand the magnitude and style of structure and the physical properties of rocks at depth. An important component of this is developing a n understanding of the cover rocks and how they may aid in assisting or impeding the success of the geothermal resource. Regolith mapping and remotely sensed imagery such as radiometrics are being used to find areas of surface fluid

leakages and potential conduit faulting in seal analysis and reservoir integrity studies.

Magnetotellurics and Potential Field Surveys

Magnetotellurics (MT) and potential field surveys can be used to define the basic limits of a reservoir. MT has been an industry standard for over 20 years for defining geothermal reservoir limits and boundaries. The 'fuzzy' imaging produced by MT can pick up resistivity anomalies typically associated with fluid bodies, large scale structures, and cap rocks. This technique has been used within Australia with varying success, which is often a product of survey design as opposed to the reliability of the technique. MT modeling requires trial and error of forward modeling (Arango et al. 2009). This process generates different models that could fit the data, and tries to assign the most likely model. Reliability of the MT is compromised as a result of this. Accessory data refines this error; such the technique is better used in conjunction with other modeling techniques. The most important result from MT models is the ability to identify the presence of geothermal fluids. This is particularly useful in the identification of HSA reservoir systems. However, the recognition of the fluid is still limited to the errors defined above.

MT is commonly being combined with potential field modeling. Magnetic and gravity surveys have been used with geothermal projects to define large scale structures and also as the basis for deterministic lithological variance identification subsurface. Potential field inversions are often coupled with petrophysical logs such as sonic and density logs to create 'layer cake' models that accumulate to the potential field signatures produced by the surveys. These techniques provide approximately the same resolution of data as the MT techniques do; however can be cheaper, and manipulated in different ways to account for different geological scenarios.

Seismic Interpretations

Seismic interpretation is not commonly used as a tool for EGS and HSA resource model evaluation. Seismic is typically used as a tool in the petroleum industry to extrapolate lithological boundaries across large areas with the assistance of wells. Features included on seismic are: formation and stratigraphic boundaries, sedimentary features such as onlap and downlap patterns, facies and sequence stratigraphy, structure, and tectono stratigraphic relationships. These features are all essential for creating balanced geological models.

A benefit of seismic interpretation is that 2D and 3D seismic surveys are available from most basin and foldbelt terrains in Australia as a result of previous petroleum or academic work conducted.

Basic interpretations can create the basis of a geological model, and can be tethered to other aspects such as wells and potential field surveys.

Advanced seismic interpretations can be conducted by procession of the seismic data such that the mechanical signatures of the seismic traces are transformed in particular ways to highlight specific features (Nourollah et al. 2010). An example of this technique that is beneficial in HSA systems is a process called Neural Network Inversion Modeling (NNIM). NNIM attempts to build relationships between data sets similar to the way the human brain perceives and analyzes data. The mechanical signature of a seismic wavelet is compared to a known source, such as a well log, and particular features characterized in the log are matched to their corresponding seismic signature. Once relationships are built between well logs and seismic traces using well defined data sets, this model can be applied to other seismic traces away from the known well locations to generate target logs from seismic sections. This process can be used to define sand bodies in a potential reservoir, fluids such as gas and water and associated migration pathways, potential seals and different lithological patterns that were not

obvious in the initial seismic interpretation and to highlight structures. Other forms of seismic processing can produce similar results.

Integration of Geological Interpretations

The integration of interpretations in geothermal systems is rare. Exploration techniques are often considered to be unique sources of information, rather than part of a dynamic system. However, this is far from the truth.

The integrating of the full suite of available data constraints, including 2D/3D remote sensing, field, 2D-3D seismic, and well logs/picks/production validates geological models and provides the basis for a constrained HSA and EGS model.

Techniques such as gravity and magnetic inversion which are considered to be low resolution interpretations can have their resolution increased by using petrophysical logs, seismic interpretations, and surface data to better constrain the layers in the model. Seismic can also be tied to surface features, particularly structure to help define attitudes and confirm structure. The combination of these techniques increases the validation of the model.

Revisiting Temperature modeling

Thermal Conductivity

Thermal conductivity of a rock determines the efficiency (or otherwise) with which heat is propagated through it. It is controlled by lithology and state of the rock (that is compaction, fracturing and metamorphic attributes). Accessory factors such as the presence of fluids such as water and gas also play a big role in this (Clauser & Huenges 1995; Vasseur et al. 1995; Beardsmore 2004).

Two primary methods are employed with respect to measuring conductivity: *in situ* measurements conducted within the subsurface using logging tools; and, laboratory measurements performed on small sections of rock. *In situ* measurements are considered to be the best form of measuring conductivity as they are done so within the

actual surroundings that the rock exists within. This incorporates factors such as fluids, fracturing, pressure and compaction better than a sample done in a lab. *In situ* measurements also represent an average over a large area of rock (Clauser & Huenges 1995).

Lab measured samples have a higher precision, because factors inhibiting to the *in situ* measurements such as equipment difficulties, drilling interference and general control issues are negated. This makes the measurement more precise, however, not more accurate.

In places where there is no data available for this modeling, default thermal conductivities for end-member lithologies that can be mathematically averaged to reflect lithological mixtures as necessary, and so do not rely on the laboratory measurement of conductivities on down-hole samples can be used. This has been recognized as a useful and reasonably accurate tool as it does not have the large extrapolation and errors that are associated with the precise laboratory measurements (Clauser & Huenges 1995). Estimating the conductivity of a rock can occasionally miss factors such as minor lithological changes, small fracture zones and pressure changes (Vasseur et al. 1995). However these tend to have minimal impact when averaged over the system, especially when used within a detailed geological model.

Temperature Modeling

Modeling temperature across a large area requires the measured temperatures to be fed into a constructed geological model and propagated according to the physical constraints interpreted. Commercially available software can then be used to construct a more anisotropic thermal model. Burial history modeling software that is routinely used in petroleum exploration for the prediction of the degree and timing of source rock maturation, reservoir temperature is favored as it can incorporate the physical properties of rocks as well as structure. Lithostratigraphic data from a well, or from seismic interpretation, can be input to the burial-history modeling software package and modeled

across larger areas with geological and thermal reason. Such packages also take into account burial-compaction effects (in particular, increase in conductivity with increasing compaction), permitting the calculation of a temperature-depth profile from which predictions of depths to key isotherms can be made. This process also accounts for structure, fracturing and fluids.

Conclusions

By creating a validated set of interpretations a constrained geothermal model can be created. These thermal models can be used to better constrain geothermal targets, reservoirs and production and can be used to monitor the progression of the resource throughout the life of the project.

Temperature, when projected amongst a validated model is no longer a source data set, but an accurately extrapolated potential field.

References

- Arango C., Marcuello A., Ledo J. & Queralt P. 2009. 3D magnetotelluric characterization of the geothermal anomaly in the LIU major aquifer system (Majorca, Spain). *Journal of Applied Geophysics*, 68, pp. 479-488.
- Beardsmore G. 2004. The influence of basement on surface heatflow in the Cooper Basin. *Exploration Geophysics*, 35, pp. 223 - 235.
- Clauser C. & Huenges E. 1995. Thermal Conductivity of Rocks and Minerals. *Rock Physics and Phase Relations: a Handbook of Physical Constants*, Vol. 3, pp. 105-126.
- Nourollah H., Keetley J. & O'Brien G. 2010. Gas chimney identification through seismic attribute analysis in the Gippsland Basin, Australia. *The Leading Edge*, 29.
- Vasseur G., Brigaud F. & Demogodin L. 1995. Thermal conductivity estimation in sedimentary basins. *Tectonophysics*, 244, pp. 167-174.

Salamander-1 – a geothermal well based on petroleum exploration results

Bertus de Graaf*, Ian Reid, Ron Palmer, David Jenson, Kerry Parker
 Panax Geothermal Ltd, PO Box 2142, Milton, Qld 4064, Australia.
 Corresponding author: bdegraaf@panaxgeothermal.com.au

Salamander-1 and the Penola Geothermal Project

Panax Geothermal Ltd (“Panax”) has secured several Geothermal Exploration Licences (GELs), within troughs or grabens in the Otway Basin in southeast South Australia (Fig 1). Together the licences cover an area of more than 3,000 km². The initial development of the Limestone Coast Geothermal Project is focused on the Penola Trough (GEL 223 and GEL 484; Fig. 2) - promoted by an existing comprehensive database of historical information from extensive oil and gas exploration and production.

The Penola Trough has been subjected to intensive oil and gas exploration, including 27 deep petroleum wells with wireline logging and conventional core measurements of reservoir porosity and permeability. In addition, 321 km² of 3D seismic and a significant amount of 2D seismic data have been acquired in this area. All of this data is available as part of a public open file database.

Geological setting

The Penola Geothermal Project lies within the Penola Trough, which is a Cretaceous-aged extensional basin formed on top of Palaeozoic basement. It is covered in South Australia by GEL 223 and GEL 484. The Penola Trough forms part of the Otway Basin, a rift basin initiated during the Cretaceous, on what is now the southern margin of the Australian mainland. The trough contains a thick accumulation of Cretaceous sediments and is bounded to the northeast by the Padthaway Ridge, and to the southwest by the Kalangadoo High. Well and seismic data indicate that the sediment pile is six kilometres thick or more, in the deepest sections of the trough, including over 1,000m thick sections of cretaceous Pretty Hill Formation (sandstones).

The Penola Trough area of the Limestone Coast Project bears many similarities with the Imperial Valley area of California which includes the East Mesa and Heber geothermal areas (Bergosh et al., 1982). The East Mesa reservoir sandstones are similar to the Pretty Hill Formation sandstone, which is the target reservoir of the proposed Hot

Sedimentary Aquifer (HSA) system of the Limestone Coast Geothermal Project.

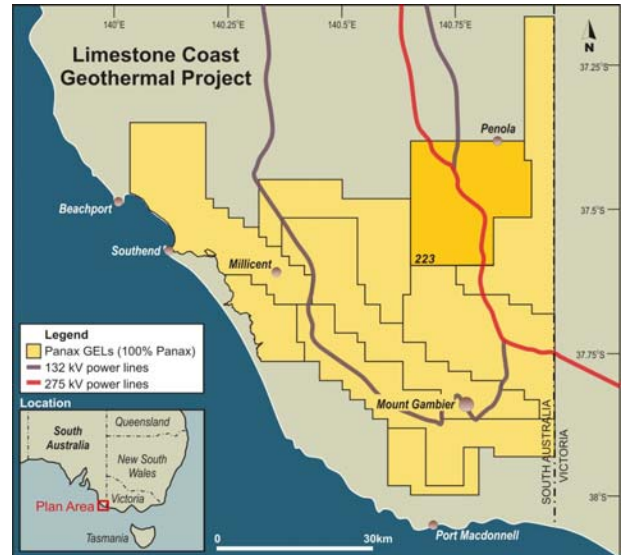


Figure 1. Panax's geothermal licences in the Limestone Coast Geothermal Project – demonstrating proximity to infrastructure

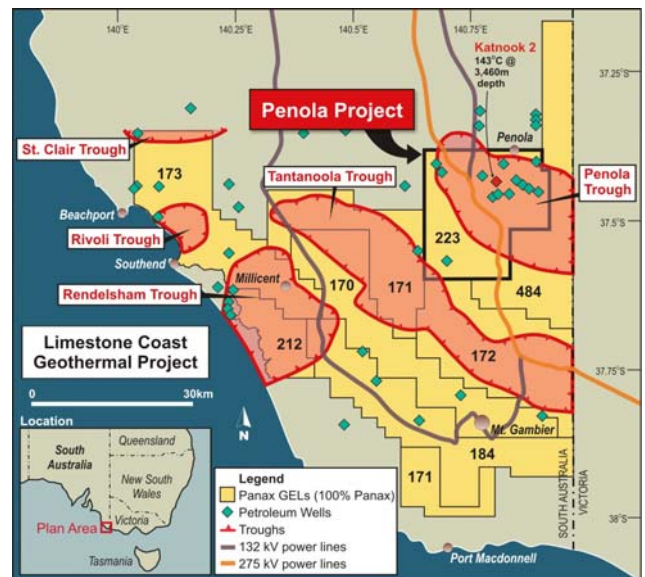


Figure 2. Panax's geothermal licences in the Limestone Coast Geothermal Project – outlining four major trough zones, including the Penola Trough and the Penola Geothermal Project

The Pretty Hill Sandstone was deposited by a low sinuosity, high energy, sand-rich river system (Scholefield et al, 1996). Its good reservoir quality has been known from petroleum activities for

some time. Significant permeability is preserved in the formation at depths of up to 3,500m.

3D seismic data has been particularly useful in mapping the distribution of the porous sandstones of the Pretty Hill Formation. The seismic response evident on 3D data represents to some extent the porosity distribution within the Pretty Hill Formation (Boult & Donley, 2001). The lower acoustic impedance of the more porous sandstones can be identified on the basis of the data (with varying degrees of success), and has been used to map the distribution of individual sandstone bodies.

Temperature data, and rationale for Salamander-1

A numerical model was generated for the Penola Trough to compute, in three dimensions, the distribution of temperature which best matches the observed surface heat flow distribution, while respecting the laws of conductive heat transfer, and the thermal properties of the geological strata. The model predicted that the temperature is relatively constant around 160°C at 4,000 m within most of the Penola Trough. This temperature modeling and a knowledge of the reservoir quality provided the rationale for the drilling of the first geothermal well, Salamander-1, in the Penola Trough in the first quarter of 2010.

Additionally, Beardsmore (2009), assessed the Limestone Coast Geothermal Project for its geothermal potential and determined a “Measured Geothermal Resource” of 11,000PJ complemented by an additional 32,000 PJ of “Indicated Geothermal Resource”, see Table 1 below. This resource classification was in accordance with the Australian Code for Reporting of Exploration Results, Geothermal Resources and Geothermal Reserves, 2008 edition.

This highly encouraging resource classification, the third in Australia and second-ever resource classification of a HSA, confirmed the high potential of geothermal energy development in sedimentary basins.

The ability to directly assess this significant geothermal resource potential is courtesy of the long history of petroleum exploration with numerous wells and seismic surveys, see figure 3 below.

Limestone Coast Geothermal Resources ¹ .					
Trough	Measured (PJ)	Indicated (PJ)	Inferred (PJ)	Total (PJ)	Report Date
Penola 11	,000	32,000	89,000	132,000	18/02/2009
Rivoli & St. Clair			53,000	53,000	28/01/2009
Rendelsham 17			,000	17,000	28/01/2009
Tantanoola			130,000	130,000	31/03/2009
Total	11,000	32,000	289,000	332,000	

Table 1 - Reproduced from the 2008 Penola Trough Report by Dr. Graeme Beardsmore (Hot Dry Rocks Pty Ltd)

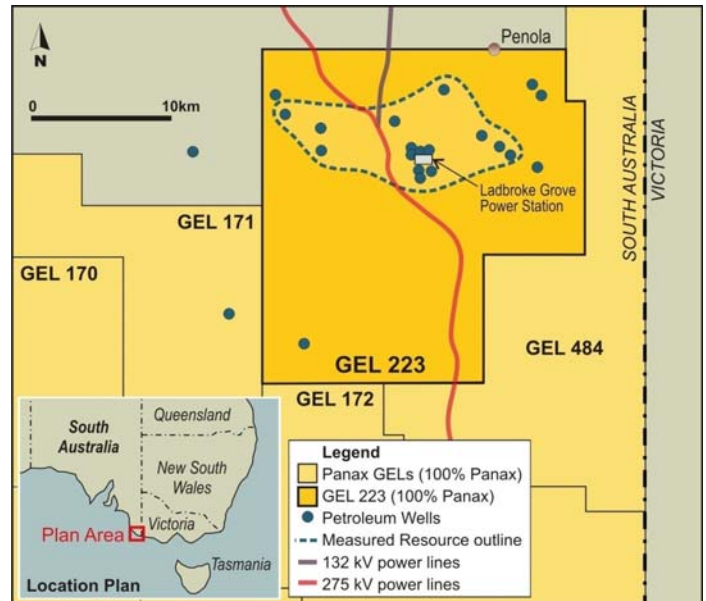


Figure 3. GEL 223 – Penola Geothermal Project showing outline of the Measured Geothermal Resource, and information relating to prior petroleum wells drilled in the area.

Salamander-1 drilling objectives

Salamander-1 is the first geothermal well in the project area. It was drilled in Panax’s Geothermal Exploration Licence 223 (GEL223), in the first quarter of 2010.

The drilling objective for Salamander 1 was to intersect the Pretty Hill Formation (reservoir) at a depth of 3,000m and continue to 4,000m to secure an intersection of 1,000m of the reservoir. To minimise the risk of intersecting gas, the well was sited 5km away from the closest gas producing well (now depleted) and at least 500m vertically down dip of any gas producing well. Also, a further drilling requirement was that no significant faults should exist between the closest gas producing well, and Salamander 1 - that could potentially be a gas seal.

To minimise friction losses in a future production environment, the casing scheme was designed as wide as possible, although standard casing

dimensions and safety issues took precedence. Figure 4 below presents the casing scheme for Salamander 1.

Drilling

Salamander was drilled with Weatherford's Rig 828 and the design and management of the well was contracted to AGR.

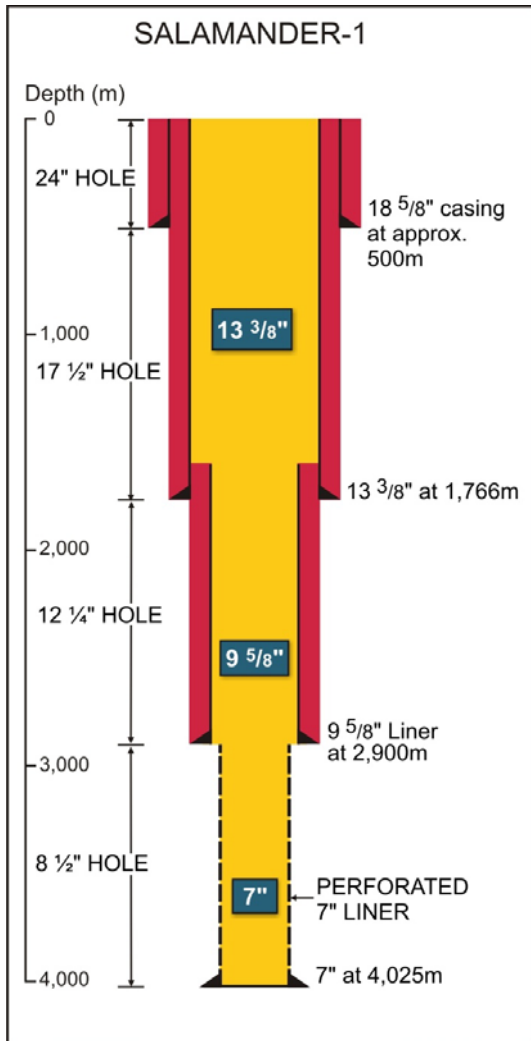


Figure 4. Schematic illustration of the well design and well casing design – Salamander-1

WDI Rig 828 was handed over to Panax at the rig's previous engagement at 20:00 on 12 December, 2009. The rig move to Salamander 1 was disrupted due to poor weather restricting truck access to the rig, in particular the larger transporters. Salamander-1 was spudded at 23:45 on 31 January 2010.

The 24" hole was drilled from the base of the 26" conductor to 503m, and 18-5/8" casing was run and cemented at 499m (Figure 4).

The 17-1/2" hole was drilled from the 24" casing shoe to 1,766m. Due to lower Rates of

Penetration (ROP), Panax elected to set 13-3/8" casing at this depth. The 13-3/8" casing was run and cemented at 1764m.

The 12 1/4" hole was drilled using Schlumberger's Power V system, an auto-vertical seeking directional drilling tool, to maintain verticality. The ROP in the 12-1/4" section was extremely good and intersected the top of Pretty Hill Formation at 2,900m, some 150m shallower than the original prognosis.

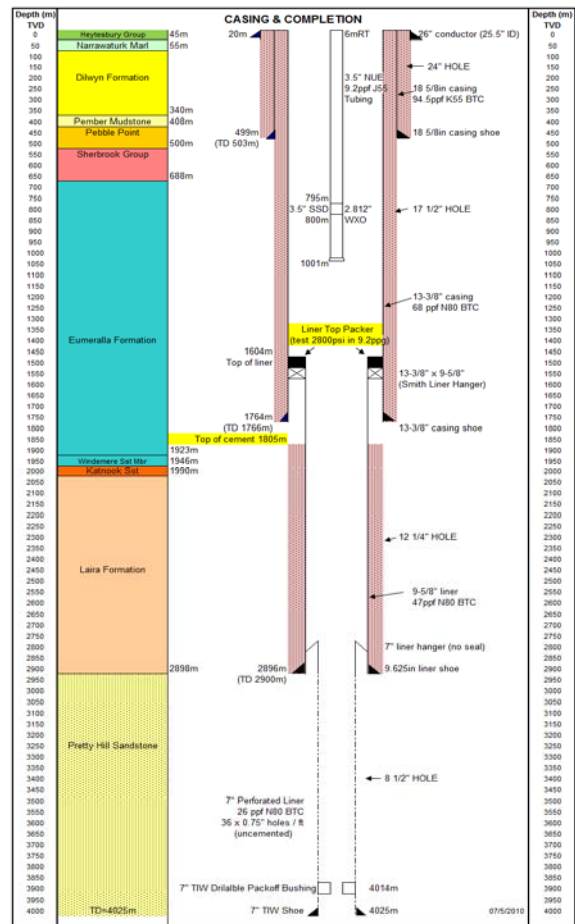


Figure 5. Salamander-1 Well Completion Schematic

A cement plug was set from 2,800 – 2,900m to stabilise this zone, and the 9 5/8" liner was run and cemented at 2,896m.

The 8-1/2" hole section was drilled to 4,025m with a bit change made at 3,670m. An EMS directional survey was recorded at TD and Open Hole logs were run. A 7" perforated liner was run and set to bottom.

Following displacement of the drilling fluid with brine, and with the wellhead and Christmas tree installed, the rig was released at 1500 hrs 26 March, 2010.

The well was drilled to a total depth of 4,025 metres in 45 days (inclusive of 3 rig repair days)

using only 6 drilling bits, setting a new drilling record for the Australian geothermal sector.

Importantly, the Salamander-1 drilling programme was concluded with zero Lost Time Incidents

Wireline logging

The wire-line logging services were provided by Schlumberger, and four trips were planned. The main objectives of the wire-line logging were to: i) determine formation acoustic velocities to tie in the well with 3D surveys, ii) observe pressure regimes to determine the absence of any hydrocarbons, and iii) collect information about formation density and porosity. The wire-line programme is presented in Table 2 below.

Log	Interval
XY Cal-GR	2890 – 1750m
DLL MSFL LDT CNL-GR	4021.5 – 2898m
HNGS	3738 – 2898
Sonic Scanner	4025 – 2989
	2900 – surface. Sonic scanner switch modes to Cement Bond Log
MDT-GR	37 points (could not pass 3845m)
VSI-4	3810 to 99m

Table 2 – Wireline Logs Obtained

Salamander-1 Well Results

The recently announced 15.4°C increase in the measured bottom hole temperature (“BHT”) of the Salamander-1 well, from 156°C to 171.4°C, which is likely to have been caused by breakthrough from the well bore to the reservoir, has confirmed predictions of the regional 3D temperature modelling by Hot Dry Rocks Pty Ltd (HDR Report, 2008). Figure 6 below shows that the 3D modelled temperature at 4,025m for the Salamander-1 well of 172°C is very close to the recently measured BHT at 4,000m of 171.4°C. This figure also shows that projected temperatures at 4,000m increase to the south and south-east into Panax’s GEL484, reaching 180°C within 4km of Salamander-1.

The new BHT of Salamander-1 combined with the new 3D temperature modelling is likely to

increase the geothermal resources of GEL223. More importantly, it upgrades the overall regional potential of the Penola Geothermal Project, with higher temperatures allowing the proposed power outputs to be achieved with lower flow rates.

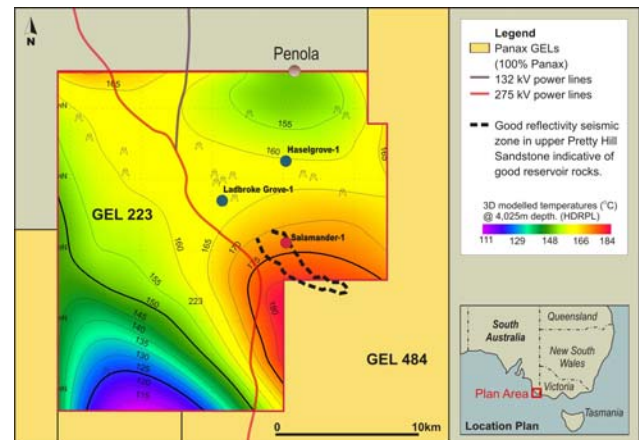


Figure 6 - Penola Trough, 3D conductive heat flow modelling (HDR, 2008) - predicted 172°C @ 4,025m, while the actual measured temperature at Salamander-1 for this depth was 171.4°C – recently measured.

A borehole seismic survey (vertical seismic profile or VSP) was recorded by Schlumberger in the near vertical Salamander-1, on 19 March 2010. This VSP allowed a good correlation of the Salamander-1 penetrated geology with the 3D seismic data. Examination of the seismic data correlated to Salamander-1 located towards the southeast of the GEL, shows an excellent correlation, with a more reflective seismic package in the upper section of the Pretty Hill Formation. Seismic attributes of reflection strength, and volume attributes of RMS reflection strength were used to determine the areal distribution of these more porous sandstones. A single reservoir body is interpreted extending from the Ladbrooke Grove gasfield area, through the Salamander-1 well, and 6.5km to the south east - covering an area of approximately 22.5km². This zone is interpreted as having similar reservoir properties to those in the well.

Full analysis of the petrophysical review are currently in progress and will be available at the time that the paper is presented in November 2010.

A review of the wireline logging data of the open hole section of the Salamander-1 well (from 2,900m to 4,025m) for estimating the reservoir quality of the target reservoir rocks (the Pretty Hill Sandstone) has been completed by Down Under Geosolutions (“DUGEO”) based in Perth. We have been advised that the combination of the “Lin-Log and MDT methods” are the most appropriate to estimate the “transmissivities” (≈

reservoir quality) of the intersected target reservoir rocks.

DUGEO has advised that the transmissivities in Darcy metres (Dm) of the Pretty Hill Sandstone in the open hole section of Salamander-1 well range from 6.7 Dm to 13.5 Dm, as set out in Table 3 below:

	Method	Transmissivity (Dm)
Most Likely Case	Average Lin-Log relationship	6.7
Maximum Case	Optimistic Lin-Log relationship	13.5

Table 3. Transmissivity Range

Transmissivity is loosely described as the capacity of the reservoir to flow water. The “Most Likely Case” of 6.7 Dm is lower than the minimum requirements of 10 Dm for a flow rate of 175 l/sec @ 145°C. However, with higher geothermal temperatures now apparent (from the most BHT measurement in Salamander-1, and consistent with the 3D temperature modelling), flow rates could be reduced as these two inputs are inversely proportional. Also, the “Maximum Case” estimate provides the upside.

Salamander-1 Well Testing

Salamander-1 was discharged using air lift to a 10,000m³ capacity HDPE lined pond. Steam was vented to atmosphere from a flash tank and water flow was measured using a weir plate.

The reservoir fluids collected in the pond will be used for the injection test which is the last test to be carried out on the well.

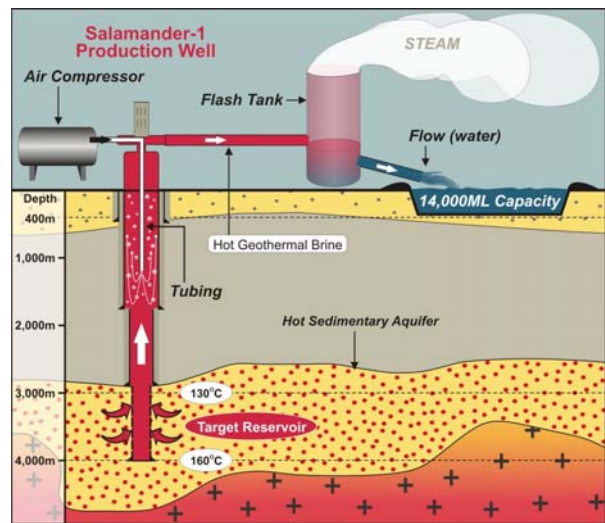
Analysis of downhole pressure and temperature data obtained during short cleanup flows, although indicating higher than expected temperatures, up to 171 deg C also indicated initial mud damage that arose during drilling.

The well was acidized using 15% acetic acid in order to remove the skin damage caused by calcium carbonate and flowed again using nitrogen gas lift. Results of this operation are awaited.

Results of production and injection testing are pending. Based on the results of these tests, the feasibility of installing a pilot plant will be investigated.

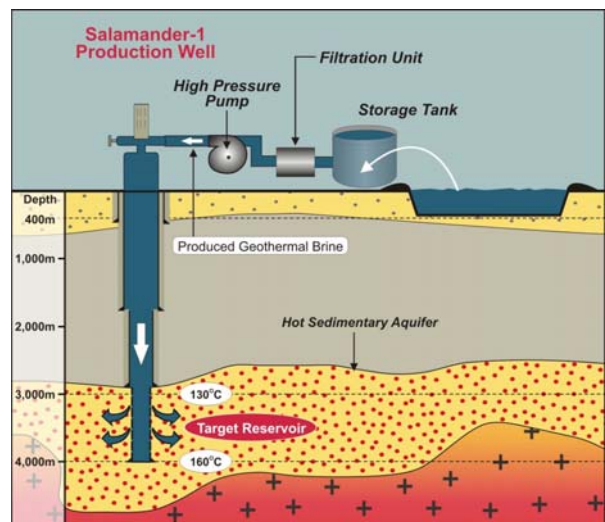
A number of depleted gas wells within approximately a 5km radius of Salamander-1 were checked for injection potential. It is estimated that 4 of these wells could accept more than 100 l/s in their current configuration and more than 200 l/s after workover, with further improvement possible with additional perforation. The costs of working over these wells are in the range \$2-3m each, which is a much more economic proposition than drilling a purpose built reinjection well.

Salamander-1 Reservoir Testing Program – Step 1 :



- a. Flow well using air lift;
- b. Measure pressure, temperature and flow (surface), down hole logging tools in the target reservoir measure pressure, temperature and flow.

Salamander-1 Reservoir Testing Program – Step 2 :



Australian Geothermal Conference 2010

- c. Re-inject produced geothermal brine using filtration unit and high pressure pump;
- d. Down hole logging tools in the target reservoir measure pressure, temperature and flow.



Figure 7. Salamander-1 Well clean-up flow test, May 2010.

Sand81-7008, Terra Tec Inc under contract to Sandia National Laboratories.

Boult, P.J., and Donley, J., 2001, Volumetric Calculations Using 3D Seismic Calibrated Against Porosity Logs — Pretty Hill Formation Reservoirs, Onshore Otway Basin. Eastern Australian Basins Symposium, 2001

Scholefield, T., North, C.P., and Parvar, H.L., 1996, Reservoir characterisation of a low resistivity gas field – Otway Basin, South Australia, APPEA Journal 1996.

Salamander-1 – Interpretation And Analysis Of Well Testing Results

At the time of writing this Abstract, this work is currently being undertaken.

This will be available for presentation at the time that the paper is presented in November 2010.

References

Beardsmore, G. R., 2008, Limestone Coast Project: Penola Geothermal Play. Statement of Geothermal Resources. Hot Dry Rocks Pty Ltd, 2008.

Bergosh et al 1982, Mechanisms of Formation Damage in Matrix Permeability Geothermal Wells,

Petrophysical Methods for Characterization of Geothermal Reservoirs

Ben Clennell¹, Lionel Esteban^{*1}, Ludovic Ricard^{1,3}, Matthew Josh¹, Cameron Huddlestne-Holmes¹, Jie Liu², Klaus Regenauer-Lieb^{1,2,3}

¹ CSIRO Earth Science & Resources Engineering, ARRC, 26 Dick Perry Avenue, Kensington

² University of Western Australia, M004, 35 Stirling Av., 6009 Crawley

³ Western Australian Geothermal Centre of Excellence, ARRC, 26 Dick Perry Avenue, Kensington

Abstract: Australia has a unique wealth of non-volcanic geothermal resources. To tap these for local and distributed energy needs, optimal targeting and development strategies for the reservoirs are needed. In the case of Hot Sedimentary Aquifers (HSA), many tools for formation evaluation developed in the oil and gas industry for High Pressure/ High Temperature environments could be applied directly; this applies both to downhole tools and laboratory characterization methods. The standard suite of petrophysical methods is adequate for determining basic matrix and fluid characteristics, but for full characterization of flow and geomechanical parameters advanced acoustic and nuclear magnetic resonance tools could find a place, at least for high value resources. In both crystalline rock and HSA plays, image logs are a vital tool, not least for enabling improved core-to-log workflows. Understanding of the thermal properties of rock and how that relates to field scale thermal structure is another challenge unfamiliar to most petrophysicists. Modelling from pore/grain through to formations scale is vital for assessing both thermal and flow performance. CSIRO and the Western Australian Geothermal Centre of Excellence have brought together experience and capabilities in rock physical and thermal properties and in this paper review what petrophysical tools and methods are available to the geothermal industry and illustrate some of the research currently underway.

Keywords: Petrophysics, Reservoir Characterization Thermal Conductivity, Heat Capacity, Porosity, Permeability, HP/HT.

Introduction

Australia's immense geothermal energy resources have the potential to contribute significantly to our nation's demand for affordable and sustainable clean energy. However, for the efficient exploitation of geothermal energy a good characterization of the reservoir is a prerequisite.

Petrophysics is the systematic investigation of rock and fluid physical properties to understand the rock type and fluid flow performance of underground formations. Petrophysical techniques measure the physical and chemical properties of the rock either in situ (well logging) or in a lab (core and chips). The data generated from these analyses can be used to characterize

the reservoir rock's composition, structure, porosity and permeability, temperature, pressure and mechanical properties, leading to a better overall understanding of the resource.

Petrophysical methods for the characterization of geothermal reservoirs have progressed significantly overseas particularly for the extreme environments such as HR and volcanic sources. In this paper we describe CSIRO's expertise in the Petroleum sector, which is directly applicable to HSA. It is our intention to grow this expertise further into the HR domain.

Our petrophysical characterization of geothermal reservoirs forms part of a larger collaborative initiative of CSIRO and Universities working with industry and government with the aim to reduce the risks of implementing geothermal technology through computationally assisted guidance of drilling programs to target locations and depths. The core of the required scientific innovation will be to develop new data assimilation inversion tools, which ensure that all available information, including geologic, geophysical, geomechanics, fluid dynamics, rock physics, geochemistry and economic data is integrated into the subsurface and above-ground geothermal design. In this contribution we focus on the petrophysical methods for characterization of geothermal reservoirs. These comprise the characterization of rock mechanical, thermal, geochemical and fluid permeability properties.

Standard petrophysical tools and characterization workflows

Since the Schlumberger brothers invented the first downhole electric log in the 1920s, the oil and gas industry has provided the platform to develop a wide range of petrophysical logging tools, (see Ellis and Singer 2007). The range of physical properties that can be sensed today is impressive (Table 1). While the uptake of down-hole technologies in water, mining and environmental sectors has largely been limited by cost to a basic suite, certain slim-hole and extreme environment tools have been developed outside of oil and gas, most notably for borehole imaging.

Petrophysical characterization serves three main purposes, each with its own workflow to: (1) define the lithostratigraphy, and therefore help in geological correlation between wells and definition of reservoir structure; (2) quantify matrix, fluid and

Table 1

Type of tool	Physics employed-what is measured	Geothermal application
Resistivity-galvanic	Direct current injected into the formation, usually focused electrode array.	Relations between porosity, water saturation and water salinity.
Resistivity-induction	Coil magnetic field transmitter induces ground loops in formation, measures conductivity of formation	Relations between porosity, water saturation and water salinity.
Gamma ray-standard	Scintillator detects total radioactivity of formation	Shaliness, heat production
Spontaneous potential (SP)	Electrochemically and electrokinetically induced potentials	Pore water salinity. Indicator of clay layers vs sand layers, permeability of the latter.
Density log	Uses backscattered gamma rays from a radioactive source, typical ¹³⁷ Cs.	Sensitive to formation bulk density, based on atomic number contrasts.
Photoelectric effect	Measured from relative energy absorption from the density source	Indicates mineral electron density
Neutron log	Detects neutron absorption from hydrogen nuclei	Sensitive to water content including clay bound water
Sonic Log	Compressional wave velocity	Porosity and strength (stiffness) of formation
Gamma ray-spectral	Energy sensitivity detectors distinguish U, Th and K	Shaliness, rock geochemistry heat production
Magnetic susceptibility	Measures magnetic permeability of the formation by inductive coupling or other means.	Can provide good lithological discrimination, even of very thin layers, and in crystalline rocks
Geochemical Logging Tool	Measures spectra of gamma absorption-re-emission	Identifies a wide range of specific elements, especially heavy ones
Elemental Capture Spectroscopy	Measures gamma spectra from nuclei activated by neutron capture	Identifies a narrow range of specific elements, especially heavy ones
Dielectric log	Permittivity from attenuation and phase of propagating electromagnetic wave	Porosity/saturation independent of salinity. Shale and texture indicator
Nuclear magnetic resonance	Transverse relaxation time of hydrogen nuclei	Fluids content, pore size and permeability estimate
Waveform sonic	Compressional and shear waves	Geomechanics

flow properties of the reservoir and (3) assess stresses and geomechanical properties *in situ*.

1. For definition of lithology and structure one is looking to use tools, such as gamma ray, resistivity and sonic, which show substantial contrasts between different lithologies. At this stage, quantitative relationships are less important than the signatures that mark boundaries between correlated rock units. In crystalline rock situations magnetic susceptibility (not generally used in oil and gas exploration) is valuable to identify certain geological markers. At the next level of detail we require identification of features such as tilted beds, coal seams, igneous dykes, faults and fractures. Dip logs and image logs are most useful here. The best type of imaging tool for a geothermal hole (borehole televiewer for air or clean water filled holes, ultrasonic scanning tool) may be different from that used mostly in oil and gas (formation resistivity array imager). In crystalline rocks, flow properties begin and end with fractures, so image logs are especially vital. Resistivity images have the advantage that open and flowing fractures may have different contrast to closed or non-flowing ones.

In the laboratory we gain complimentary lithological information from petrographic analysis of cores and cuttings samples, usually aided by optical and electron microscopy. Structural logging of core can define fault and fracture sets, determine relative timing, and differentiate natural from drilling-induced fractures, which is not always possible from borehole images alone.

2. For quantitative formation evaluation for a HSA target reservoir, combining the basic "oilfield" tools performs a vital function. Density and neutron tools enable porosity to be delineated, along with some understanding of matrix mineralogy and especially clay content. Neutron-porosity to density porosity ratio can indicate zones not completely saturated with water, and with gamma ray, indicates clay content. Clay fraction has a first order effect on permeability, even if porosity is constant. Sonic logs can reinforce the interpretation of porosity, and indicate zones that are more or less fractured. Resistivity and spontaneous potential can be analysed together with an understanding of the clay content and porosity, to deduce pore water content, saturation and salinity. This information also helps integrate downhole observations with surface electromagnetic geophysical surveys such as deep resistivity or magnetotellurics (MT).

Wireline-conveyed formation testing (e.g. MDT*) is the final technology used in a standard "oilfield" petrophysical evaluation. Drawdown and build-up tests define permeability and can also be combined with fluid sampling. Wireline testers offer a much more versatile solution than larger scale packer tests or drill stem tests, though the

latter are required in crystalline rocks or otherwise low-matrix-permeability settings.

Laboratory measurements on core substantially reduce the uncertainty in formation evaluation. At the CSIRO petrophysics laboratory for example, we routinely measure porosity and permeability of core samples under overburden conditions, electrical properties at a wide range of frequencies corresponding to different logging tools, and sonic compressional and shear wave velocities under conditions of (P , T) *in situ* stress.

3. Stresses in the Earth are complex, and defining stress conditions in a borehole can be a difficult process. Generally it is based on the analysis of break-out and fracture patterns observed in image logs, complimented by formation pressure tests designed to open natural fractures and/or induce new fractures. To interpret these results and make predictions of reservoir performance, "fracture-ability", well stability in the reservoir and overburden, it is desirable to have core suitable for geo-mechanical testing. From core tests unconfined compressive stress, cohesive strength and frictional strength parameters can be determined directly and used to construct a Mechanical Earth Model. At CSIRO we conduct such tests routinely, and have recently obtained a High Pressure (to 150 MPa confining, >500 MPa axial) High Temperature (to 200 C) triaxial rig and with 20 channel acoustic emission to monitor in 3D the development and coalescence of fractures. Sonic logs are used widely for geomechanical interpretation, and core measurement of P and S velocities and their anisotropy is very helpful for defining rock physics and mechanical property models. This also closes the loop for seismic-to-log-to-core workflows.

Smarter petrophysics: geothermal applications of non-standard tools.

The limited scope of standard tools has led to more exotic physics being applied to formation evaluation in oil and gas. Some special tools have obvious HSA applications but require cost/benefit to be proven. Extreme condition versions of some advanced oilfield tools do not even exist yet.

An obvious "upgrade" is to use a spectral gamma ray tool that quantifies the U, Th and K content of the formation. This enables quantification of *in situ* heat production, and is also useful for rock typing. Natural gamma tools can be cross-calibrated with laboratory spectral gamma ray detection instruments used for recovered cores or chips.

Geochemical Logging Tool (GLT**) and neutron activation (e.g. ECS* or FLEX*) logs can be employed to quantify a subset of the chemical elements in the formation. The GLT has been

used in both sedimentary and crystalline rocks, including hydrothermal zones, in the Ocean Drilling Program, with excellent results. The GLT is complex, having active neutron and gamma sources coupled with filtered detectors and a passive natural gamma ray spectroscopy module. Hot sources raise obvious issues of HSE permitting. The ECS approach can be engineered to use a non-chemical neutron source called a minitron, essentially a small particle accelerator in the tool. However, the number of elements detected by ECS is limited, as is its track record for hard rock situations.

Another oilfield technology of potential value in hot sedimentary aquifers is Nuclear Magnetic Resonance (NMR) spectroscopy. NMR tools measure the magnetic spin relaxation of hydrogen nuclei, and offer the only way to determine rock pore size distribution and thereby estimate formation permeability in a continuous way. This is an excellent way to interpolate point measurements from permeability tests on core, and compare with formation tests from MDT. NMR also provides a salinity-independent total porosity and an estimate of clay content. CSIRO is currently commissioning an elevated P/T NMR core testing capability which will help to assess the value proposition of NMR petrophysics for HSA geothermal applications.

Temperature limits on measurements

Some technologies such as NMR, which depends on magnets, and some spectroscopic tools with crystal detectors have inherent temperature limitation making their application to hotter geothermal settings unlikely. On the other hand, various logging tools have been developed specifically for geothermal boreholes: the extreme environment televiewer for example. The exploitation of ultra-deep (>5000 m) and High Pressure High Temperature (HPHT, or >150 C > 70 MPa) oil fields has also driven the development of sophisticated petrophysical tools that can perform in extreme environments, leading to a convergence of technology towards the needs of the burgeoning geothermal market. Major players like Schlumberger, Baker Hughes and Weatherford compete in this market with small and specialised tool suppliers, including a growing number from Australia. Standard tools are available up to at least 260 C and 200 MPa. We therefore see expanding options to deploy such oilfield tools—or cheaper versions of them—into the geothermal marketplace.

In the laboratory also, standard oilfield analysis equipment for porosity, permeability, resistivity etc. is not designed for the extremes of geothermal conditions. A typical operating range is 70 MPa and 100C. At least in a research context, systems have been engineered enabling all of these parameters to be obtained under *in*

* MDT, GLT and ECS are marks of Schlumberger. FLEX is a mark of Baker Hughes

situ formation conditions and throughout prolonged experiments (e.g. Milsch et al. 2008).

Understanding the thermal structure

Whether it is a Hot Sedimentary Aquifer (HSA) or Enhanced Geothermal System (EGS), appraisal and exploitation of a geothermal reservoir requires a detailed characterization of thermal properties and heat flows. The temperature distribution on the underground is driven by the surface climate, the characteristics of the rocks to conduct, produce and accumulate the heat and also the fluid circulation into the rocks and the basal (or mantle) heat flow. When estimating the temperature at depth, we have to consider the main mechanism driving the thermal flow and temperature distribution according to the controlling equation.

$$\rho C \frac{\partial T}{\partial t} + \vec{V} \cdot \overrightarrow{\text{grad}}(T) + \text{div}(\overrightarrow{\lambda \cdot \text{grad}}(T)) + A(z) = 0$$

Here ρ is mass density, C the specific heat capacity, T the temperature, V the fluid velocity vector, λ the thermal conductivity, and A the specific heat production per unit rock volume. In the absence of fluid flow, rock thermal conductivity estimation is adequate for the characterization of the thermal conduction regime. An estimation of the specific heat of the rock will provide direct insights on the stored heat. This parameter will also play an important role during the production of the reservoir as the rock releases the stored energy to the working fluid. The radiogenic heat production rate of the rocks in combination with stratigraphic information will enable us to estimate the local heat flow value. If advection is significant, in the system, then permeabilities, porosity and fracture characterization are needed to quantify V and thus the contribution of the advective flow to the temperature distribution.

In terms of fluid transport characterization, the key parameters to identify are the permeabilities (absolute for water only and relative, when steam and liquid are both present in the reservoir), porosity and the thickness of the targeted reservoir. Initial and time lapse values from repeat logging passes will be of interest to design and assess any well stimulation processes and to quantify the contribution of the local hydrogeology to the temperature distribution.

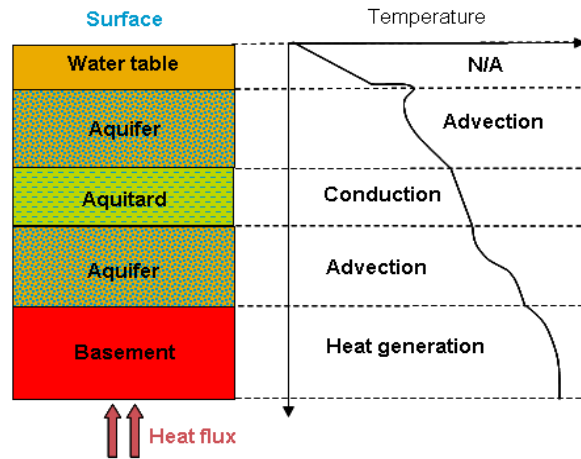


Figure 1. Isotherms and formation temperature/ depth profile in a hypothetical rock sequence (adapted Jorden and Campbell, 1984).

These parameter estimations are important at the exploration stage to evaluate the geothermal potential and must be refined at the production stage where the underground geothermal system will be significantly affected by the production and re-injection of a working fluid.

Determining thermal properties

Most of the research on thermal properties has focused on modeling of the thermal propagation in geological reservoirs. But the needs in petrophysical data, particularly in geothermal reservoirs, have never been so important to verify and validate models. Two main approaches are available to provide hard data on thermal structure and properties downhole logging and laboratory measurements. Both methods have their advantages and disadvantages:

- Logging data give access to a continuous records with depth but with high uncertainties because of some chemico-physical processes that actively occurs during the data recording (heat flow, fluid flow, mudcakes, fracturations...) or simply because of the limited sensitivity and depth resolution of the tools (Beck et al., 1971). Three general logging methods are available: (1) relaxation methods (Wilhelm, 1990), (2) direct thermal measurements downhole with no control at all on chemico-physical influences and (3) the classical correlation methods which combine logging parameters such as sonic traveltime, hydrogen index, density, porosity, lithology and temperature (Brigaud et al., 1989; Demongodin et al., 1991; Griffiths et al., 1992). All of these methods use empirical models and some form of averaging or effective medium theory to predict the thermal properties. To calculate the thermal conductivity and diffusivity accurately from such methods, the tools being employed must be capable of distinguishing the different minerals and fluids sensitively.

• Lab measurements enable control of all the parameters (mineralogy, porosity, water content, fractures) but the sampling (except for drill-cuttings) is never continuous and the *in-situ* reservoir conditions are difficult to reproduce in the lab. Moreover, lab equipment and protocols are not infallible. Poor sample quality, representativeness, coupling, effects of fractures etc., limit typical accuracy to around 5% or so. It is rare that specific information is gathered on anisotropy: this requires measurement of the tensor components of thermal conductivity and diffusivity. At the highest temperatures, non-linear properties and especially thermal expansion make good measurements a challenge.

One new technology that can help overcome some of these issues is Optical Thermal Scanning (Fig. 2). OTS is a non-destructive non-contact measurement of the thermal conductivity and thermal diffusivity on rocks and minerals at room conditions (Popov et al., 1999). OTS is able to scan a sample surface with 3 temperature sensors in combination with a focused mobile and continuously operated constant heat source. The heat source and sensors move at the same speed relative to the sample and are calibrated before and after each measurement with rock standards, which leads to high accuracy quoted as 1.5%, a sampling size from 1 cm to 70 cm long having any

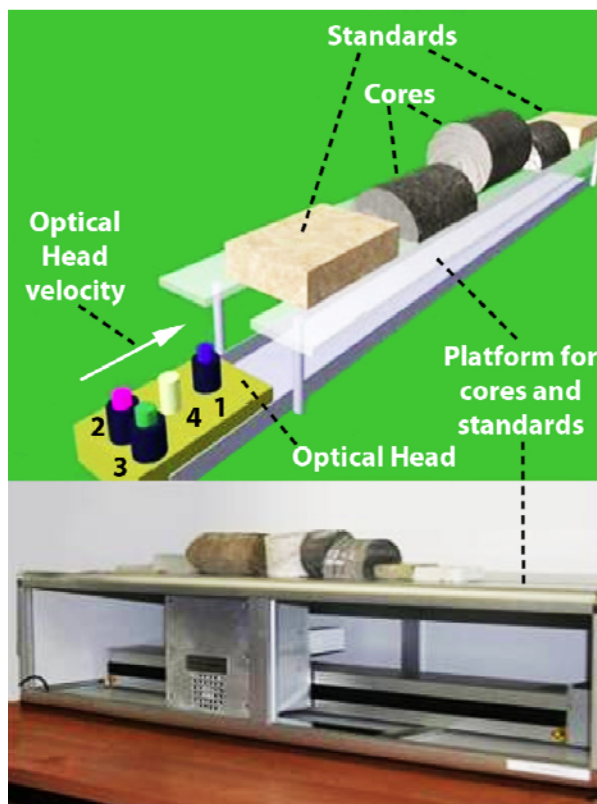


Fig. 2. Optical Thermal Scanner instrument for rock thermal property measurements on full cores (modified from Popov et al., 2010). Optical Head: sensor (1) measure the rock temperature at room condition and sensors (2 and 3) measure the rock temperature after heating from the heat source (4).

shape, short time measurements (10-30s), contactless tool and without time and cost of special sample preparation. Hence the OTS offers the opportunity to investigate direct thermal conductivity, diffusivity, pore space and geometry on full cores and anisotropic thermal properties of samples under various conditions, and with a wide range of form factor, size, and prevailing conditions (wet/dry, elevated temperature, etc).

The combination of the two petrophysical approaches (lab and downhole) can be very powerful and removes most of their respective disadvantages. Lab measurements allow parameter calibrations and better control on the logging interpretations. Proper integration of petrophysical data from lab and downhole sources enables us to test, correct and enhance the existing theoretical models used to predict steady state and dynamic thermal behaviour.

Petrophysical property modelling

The characterisation of geothermal reservoirs is a typical multi-scale problem. CSIRO and WACOGS have developed a number of workflows to model and upscale rock physical properties appropriate for geothermal problems. An exciting recent advance with wide uptake in the petroleum industry is the incorporation of so-called Digital Rock or Digital Core methods whereby high resolution 3D images of real rocks form the basis for physical property calculations. In the example workflow presented here we analyse small scale rock properties in 3D based on micro-computed tomography (micro-CT), and scale up for hydraulic properties by using percolation theory.

Firstly, the original images of microtomography are converted to binary images, and 3-D binary models are built up from the tomography slices. Image processing and segmentation is crucial which recognises target phases (pores, different minerals) according to their greyscale values in the images. Fig. 3 shows the pore-structure of a synthetic sandstone sample of size $1.3 \times 1.3 \times 1.17 \text{ mm}^3$ after segmentation in which the pore interiors are "painted" light blue. Micro-scale characterisations are analysed based on 3-D binary models, including volume fraction (porosity for pores of porous media), percolation (or connectivity), specific surface area (SSA), tortuosity, and anisotropy.

Stochastic analyses of all phases are the second step of this multi-scale characterisation. It conducts scale-dependent probabilities and the size of representative volume element (RVE). Our stochastic analysis uses the moving window method, in which a cubic sub-volume with variable side-length L moves all over the model. In this way, the probabilities of volume fraction, percolation and anisotropy of different scales are obtained. The size of the RVE is determined when these probabilities are convergent with the increasing sub-volume-size L (Liu et al. 2009).

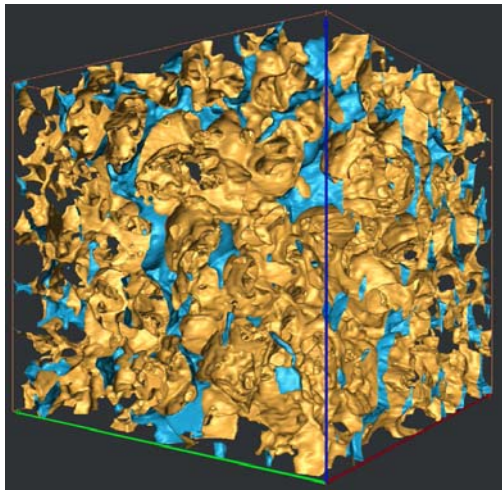


Fig. 3. Pore-structure of a synthetic sandstone sample, light blue denotes inside of pores. Model size is 1000*1000*900 voxels, resolution of voxels is 1.3 μm .

Once at the RVE size or larger, the estimated properties are reliable for application to that particular rock type. Meanwhile, the probability distribution functions can be used to create “digital rocks” at any size which have certain common characteristics, but vary in their details. For example, one may vary porosity, connectivity, or fracture density and see the effects.

Physical properties of geothermal reservoirs, in particular, permeability, elastic parameters, and thermal expansion coefficient are calculated on the digital rock elements using numerical simulations. Permeability can be simulated by using the finite difference Stokes equation solver Permsolver and based on micro-scale pore structures. Fig. 4 is a RVE of size 1 mm³ of a synthetic sandstone sample. The simulated permeability is 1763 millidarcy. Thermo-mechanical properties are computed by using a finite element method based on the mineral properties and structure. Fig. 5(a) is a RVE of a digital rock which includes two weak minerals of different shapes. Fig. 5(b) gives the relationships of stress and strain components of the RVE and matrix, respectively. Although matrix and weak inclusive minerals are all isotropic, the microstructure makes the upscaled properties of the RVE remarkably anisotropic, see Fig.5(b), in which red and black lines correspond to x and z-directions, respectively. As stress and strain values in Fig. 5(b) are volumetric means on element sets, the relationships for the matrix show a slight anisotropy over all elements in the RVE (see blue and green lines in Fig.5b), which is reasonable. With these simulated results, thermo-mechanical properties of the representative volume element can be computed.

To extrapolate properties from microscale to macroscale it is necessary to combine micro-scale properties with scaling laws. We use percolation theory to extract the main critical parameters including fractal dimension, critical

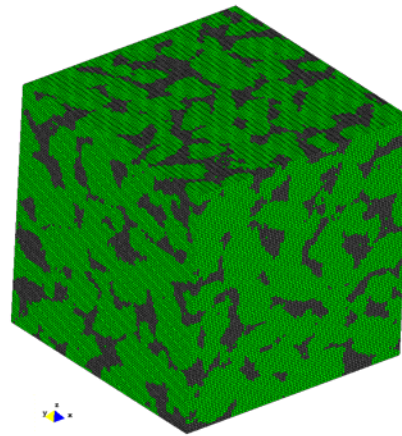
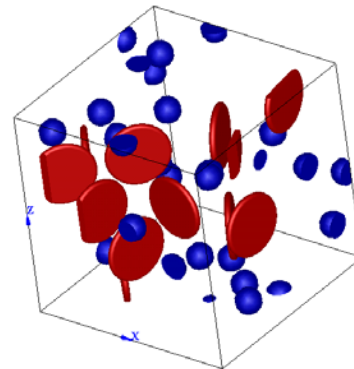
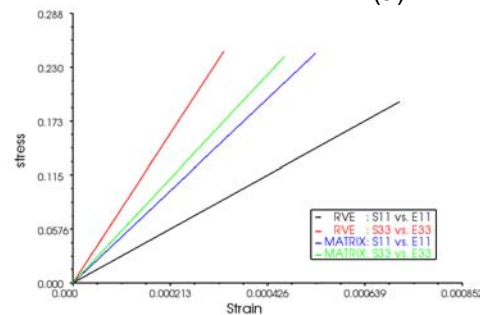


Fig.4 A RVE of a synthetic sandstone sample for permeability simulation.



(a)



(b)

Fig.5 (a) RVE of a digital rock with two weak minerals of different shapes, matrix is not shown; (b) relationships of stress and strain in x and z-directions for matrix and RVE, respectively. Oriented microstructure makes the RVE be remarkably anisotropic, although minerals of matrix and inclusions are all isotropic.

exponent of correlation length, percolation threshold, and crossover length, for the purpose of upscaling.

For the synthetic sandstone sample shown in Fig. 4, the critical exponent of correlation length and the fractal dimension extracted from micro-tomography are close to the theoretical values. The percolation threshold of this structured medium is 3.94%, while the sample has a porosity of 24.4%, which is far above the percolation threshold. In addition, the crossover length of the critical model is smaller than 50 μm . Based upon these observations, we can directly use the transport properties obtained from the micro-scale analysis for upscale modelling in the macro-scale.

The simulated permeability of 1763 md in 1 mm scale is close to the experimental test permeability on a plug sample of 2567 md. Results show that the detection of the scale dependence of permeability is accurate from the crossover length of 50 micron to the cm laboratory scale (Liu et al. 2010).

These upscaling methods based on statistical physics on small rock samples (potentially even cuttings) can be combined with more geologically informed methods of geostatistics, based on core- and log based lithofacies or flow units, to populate reservoir models at the larger scale.

Summary

The characterization of geothermal reservoirs requires the integration of field, laboratory and computational petrophysical methods. The formulation and parameterization of rock property models is based on proper combination of remotely sensed (e.g. seismic) downhole and core measurements. These methods combining interpretation and modelling provide critical inputs to the understanding of the geothermal reservoir.

From early exploration, hard petrophysical data and good physical understanding will help to constrain and develop regional and reservoir models of the geothermal resources not only to evaluate the resources but also to plan its production. At the development stage, these data contribute to reduce the risk on the well design, well stimulation, hydraulic fracturing but also the field sustainability during production.

CSIRO, with WAGCOE and other partners around Australia, is investing in applied R&D and critical infrastructure to improve the application of petrophysics to the geothermal energy sector. Demonstration projects now underway in WA will provide an excellent testbed for several of the methods described here.

References

Baker Hughes 2010. Logging services web page <http://www.bakerhughes.com/products-and-services/drilling-and-evaluation/formation-evaluation-wireline-services/petrophysics/nautilus-ultra-hpht>

Beck, A.E., Anglin, F.M. and Sass, J.H., 1971. Analysis of heat flow data-in situ thermal conductivity measurements. *Canadian J. Earth Sc.*, 8, 1-19.

Brigaud, F., Vasseur, G. and Caillet, G., 1989. Use of well log data for predicting detailed in situ thermal conductivity profiles at well sites and

estimation of lateral changes in main sedimentary units at basin scale. Rock at great depth, Eds. Maury and Fourmaintraux, Rotterdam, A.A. Balkema. ISBN 90 6191 975 4, Vol.1, 403-409.

Demongodin, L., Pinoteau, B., Vasseur, G. and Gable, R., 1991. Thermal conductivity and well logs: a case study in the Paris basin. *Geophys. J. Int.*, 105, 675-691.

Ellis, D.V. & Singer, J.M., 2007. *Well Logging for Earth Scientists*. Second Edition, Springer, 2007.

Griffiths, C.M., Brereton, N.R., Beausillon, R. and Castillo, D., 1992. Thermal conductivity prediction from petrophysical data: a case study. *Geological Applications of Wireline Logs II*. Geological Society Special Publication, 65, 299-315.

Jorden, J.R. and Campbell, F.L., 1984. *Well Logging I – Rock Properties, Borehole Environment, Mud and Temperature logging*. SPE of AIME, N.Y., Dallas, 131-146.

Liu J., Regenauer-Lieb K., Hines C., Liu K., Gaede O., and Squelch A., 2009. Improved estimates of percolation and anisotropic permeability from 3-D X-ray microtomographic model using stochastic analyses and visualization. *Geochem., Geophys. Geosyst.*, 10, Q05010, doi: 10.1029/2008GC002358.

Liu J. and Regenauer-Lieb K., 2010. Application of percolation theory to microtomography of structured media: percolation threshold, critical exponents and upscaling, submitted to *Physics Review E*.

Ocean Drilling Program Downhole Logging Guide. <http://www.ideo.columbia.edu/BRG/ODP/LOGGIN G/TOOLS/geochem.html>

Popov, Y., Pribnow, D.F.C., Sass, J.H., Williams, C.F. and Burkhardt, H., 1999. Characterization of rock thermal conductivity by high-resolution optical scanning. *Geothermics*, 28, 253-276.

Popov, Y., Miklashevskiy, D., Romushkevich, R., Safonov, S. and Novikov, S., 2010. Advanced technique for reservoir thermal properties determination and pore space characterization. *Proceedings World Geothermal Congress, Bali, Indonesia, 25-29 April 2010*.

Schlumberger 2010. Logging services web page <http://www.slb.com/en/services/additional/geothermal.asp>

Wilhelm, H., 1990. A new approach to the borehole temperature relaxation method, *Geophysical Journal International*, 103, 469-481.

net present value, internal rate of return, and payback period are used on this study.

Net present value (NPV) of a project is the total cash flow per each unit of time that has been charged to the present value of the investment that have been cashed. NPV is calculated by adding up all the cash flows occur from period of zero, so-called as investment, to the last period of the project.

$$NPV = I + \sum_{n=1}^n \left(\frac{An}{L(1+r)^n} + \frac{Vn}{L(1+r)^n} \right)$$

where:

I: investment

r: rate of return

An: cash flow / proceed

n: economic value of investments

Vn: salvage value of investments at the end of economic period

If NPV turns out to be positive, then the project is feasible to run. Positive NPV indicates the investment has achieved favourable condition.

Internal rate of return (IRR) is a percent increase in the value of money contained in the current cash flow. IRR can be interpreted also as the discount rate that produces zero NPV.

$$IRR = \frac{An}{(1+r)^n}$$

In general, investment decision based on NPV and IRR will give a consistent result which mean if an investment proposal is considered feasible based on the NPV, the proposal assessed based on IRR is also feasible.

Payback period (PBP) is the time needed to fully recover the costs and liabilities incurred in a project.

$$PBP = m + \frac{0 - CCF_m}{CCF_{m+1} - CCF_m}$$

Where:

PBP: Payback Period, years

m: Year of the CCF negative after a positive CCF

m+1: Year of the CCF positive after a negative CCF

CCF_m: Cumulative Cash Flow in *m* (<0)

CCF_{m+1}: Cumulative Cash Flow in *m+1* (>0)

Although PBP does not reflect profitability indicator of an investment proposal and the calculation does not consider time value of money, but it is often used to complement the

feasibility analysis of investment proposals. PBP may reflect the liquidity of an investment proposal.

Profitability indicators also consider investor required rate of return (RRR). RRR is influenced by two main factors, risk free rate and risk premium project with relationship as RRR = risk free rate + risk premium project. RRR is defined by the investor. The higher the risk of a project, the higher the RRR is. Geothermal electric prices are considered feasible if they can generate an IRR more than RRR. In this study, RRR is set as 16%. In Indonesia, government regulations limit the sale price of geothermal electricity not exceeding US 9.7 ¢/KWh. Geothermal electricity price is considered competitive if the price does not exceed 9.7 ¢/KWh.

Input Factors

Government policy on tax and incentives influence the competitiveness of GPP. In Indonesia, government policy on tax includes investment tax credit, duty-free import, free value added tax, and government initial survey. While incentives include clean development mechanism and carbon tax.

Investment tax credit

Business tax rate for GPP is 30%. Investment tax credit is assumed to reduce the basic tax rate to a certain extent, up to 5%, over six year period.

Duty-Free Import

Through import duty policy, the government frees the import duty that used to be 5 percent to 0 percent.

Free Value Added Tax (VAT)

PMK 24/PMK.011/2010 policy states that geothermal exploration activities are borne by the government. With his policy, the government bears the VAT payable on the importation of goods that are used for geothermal exploration activities.

Government Initial survey

Preliminary survey conducted by the government in the early stages of GPP development is an effective way to reduce the risk of developing geothermal resources. The survey includes surface surveys and drilling of two test wells. All survey results are transferred to private developers at no cost.

Implementation of Clean Development Mechanism

Clean development mechanism (CDM) scheme is a scheme in which developed countries are able to use the amount of carbon dioxide (CO₂) reduction as a result of joint project between developed and developing countries. Certified

Emission Reduction Credit (CER) is issued depending on the amount of greenhouse gases reduction. CER credit can be traded on market thus can be used to improve the profitability of the project. CER value is assumed to be US\$ 10 per ton CO₂ and the emission factor is 0.819 ton CO₂ per MWh.

Application of Carbon Tax

Carbon tax applied to fossil fuel plants will make some changes in the structure of energy prices thus will make geothermal more attractive (Table 1).

Table 1 Average price impact of Rp 80.000 carbon price, projected revenue, and possible revenue uses

	Price increase	Tax/levy revenue	Possible use of revenues
Electricity	Rp 60 per kWh	Revenue would rise to around Rp 95 trillion by 2020 per year.	Government free to decide on revenue use.
Diesel/kerosene	Rp 235 per liter		Proposed strategy: Offset the impact of price rises on households and on businesses; reduce other taxes; support additional abatement initiatives.
Gasoline	Rp 190 per liter	Additional permit export revenue of several billion dollars per year may be available	

Project Capital	
Exploration	
Initial Survey	\$1,200,000
Access Roads, Pads, Land	\$4,000,000
Logistic Support and Facilities	\$1,000,000
Rig Mobilization incl. Upgrade Roads	\$1,300,000
Exploration Well Drilling	\$6,360,000/well
Well Testing	\$680,000
FS (NORC, Env. Permits)	\$1,300,000
Steam Field Development	
Production Well Drilling	\$5,861,250/well
Well Testing	\$1,750,000
Injection Well Drilling-Brine	\$3,300,000/well
Injection Well Drilling-Condensate	\$3,313,000/well
Steam Field Facilities	
Access Roads and Well Pads	\$4,819,000
Piping and Production Facilities	\$3,647,000
General facilities	\$4,518,000
Permits, Land, etc.	\$4,217,000
Power Generation Facilities	\$143,000,000
Operation and Maintenance Cost	
Steam Field (cent/kWh)	0.53
Power Generation Facilities (cent/kWh)	0.63
Overhead Cost	0.03
Work Over sumur (well/3 yrs)	\$1,200
Major Overhaul PP (per 3 yrs)	\$1,300
Make Up Well	\$5,023,000/well

Figure 3. Geothermal Power Plant costs

Assumptions on GPP project used in this study:

- Type of project: The total project (project downstream + upstream)
- Scale of project: 110 MW which consisted of two units of 55 MW
- Period of contract: 35 years (5 years for pre production and the rest for production)
- Capacity Factor: 90%
- Success Ratio:
 - exploration wells: 50%, production wells: 80%
- Decline Rate 3% per year
- Steam Production
 - exploration wells: 8 MW, production wells: 12 MW
- Income Tax Rate: 30%
- Depreciation Method: Declining Balance with 8 years
- Investment Tax Credit 5% per year for 6 Years
- Free Value Added Tax: 10%
- Duty-Free Import

Summary of GPP costs is shown in Figure 3:

The number of wells drilled in the pre production is 20 wells. Among them nine make up wells for a 30-year production periods (year of production 2, 5, 9, 12, 15, 18, 21, 24, 27).

Result and Discussion

The calculation result for 110 MW GPP found that using the price of US 9.70 ¢/KWh, the IRR, NPV, and PBP are 15.16%, US\$ 17,570, and 10 years, respectively. The IRR is slightly less than developer's RRR, which is 16%. Meanwhile, when using developer's RRR the electricity price will be a bit higher than 9.70 ¢/KWh, i.e. 10.07 ¢/KWh. the NPV is US\$ 30,578 and nine years PBP.

A 10% reduction on capacity factor and electricity price causes a decrease in IRR of 1.68%, while on the other side a 10% addition of capacity factor and the price of electricity increases 1.22% of IRR. Reduction of investment costs by 10% leads to an increase of IRR by 1.51%, while the addition cost of investment with the same amount causes a decrease in 1.28% IRR (Figure 4)

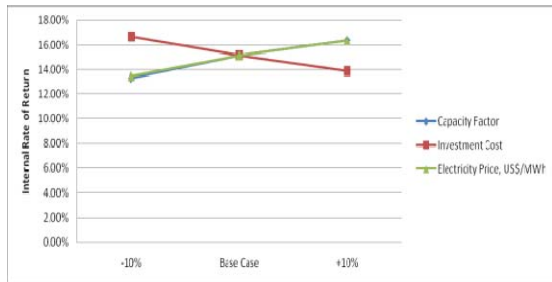


Figure 4. Capacity Factor, Investment Costs and Price of Electricity; Sensitivity Analysis on IRR

Toward the NPV, a 10% reduction of capacity factor and electricity price causes the NPV decreases of \$27.83, while the 10% addition causes an increase of \$19.32. Reduction of investment costs by 10% leads to an increase NPV of \$19.63, while the addition decreases NPV of \$19.59 (Figure 5).

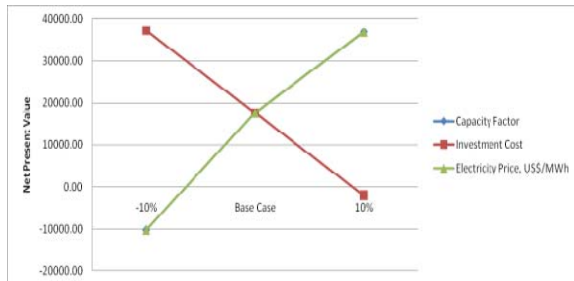


Figure 5. Capacity Factor, Investment Cost and Price of Electricity; Sensitivity Analysis on NPV

For the PBP, a 10% reduction in capacity factor and electricity price causes a slower PBP with one year, while the 10% addition causes the payback period a year earlier. Reduction of investment costs by 10% causes PBP a year earlier, while the addition causes a slower PBP by one year (Figure 6).

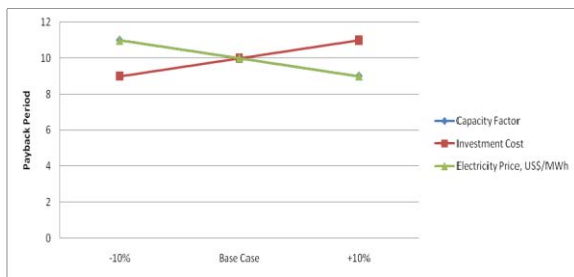


Figure 6. Capacity Factor, Investment Cost and Price of Electricity; Sensitivity Analysis on PBP

With the governments' geothermal electricity price of US 9.70 ¢/KWh, with a capacity factor of 90% (base case, CF 90%), the IRR will be less than 16%. If the capacity factor reduces to 80%, with geothermal electricity prices of US 7 ¢/KWh, 9.70 ¢/KWh and 12 ¢/KWh, the IRR will fall by 1.55%, 1.87% and 2.13%, respectively. In the base case (CF 90%) with IRR 16%, geothermal electricity price is feasible if it is above 10.2 ¢/KWh (Figure 7).

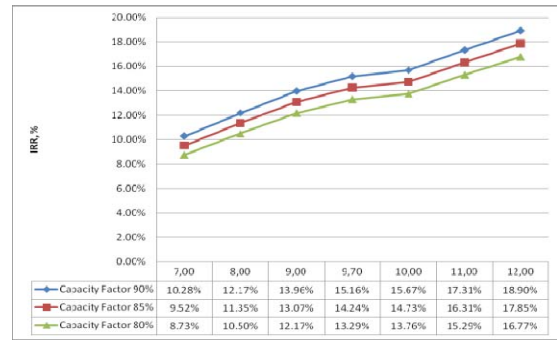


Figure 7. IRR Profile at Different Capacity Factor

At government electricity price of US 9.70 ¢/KWh, the IRR may be more than 16% if the investment cost can be pressed not less than 10%. If the investment cost reduces by 10%, the IRR would increase by 1.18%, 1.51% and 1.76% on the geothermal electricity prices of US 7 ¢/KWh, 9.70 ¢/KWh and 12 ¢/KWh, respectively. On the contrary, if the investment costs increase by 10%, the IRR will drop by 1%, 1.28% and 1.51% on the geothermal prices of 7 ¢/KWh, 9.70 ¢/KWh and 12 ¢/KWh, respectively. If the investment costs decrease by 10%, then the feasible geothermal electricity price at 16% IRR will not be less than \$ 9.5 ¢/KWh (Figure 8).

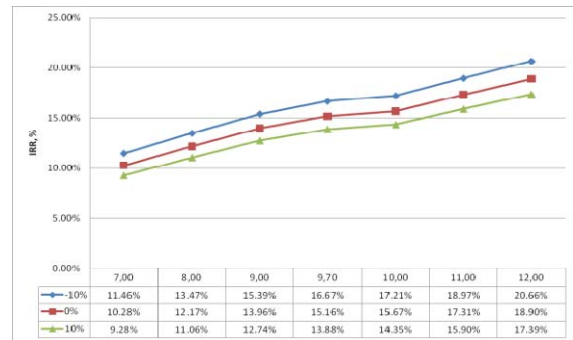


Figure 8. Profile of IRR at Different Investment Costs

The most influential incentive improving the project IRR is the 10% VAT-Free incentive followed by import duty-free incentive, government preliminary survey, and investment tax credit (Figure 9).

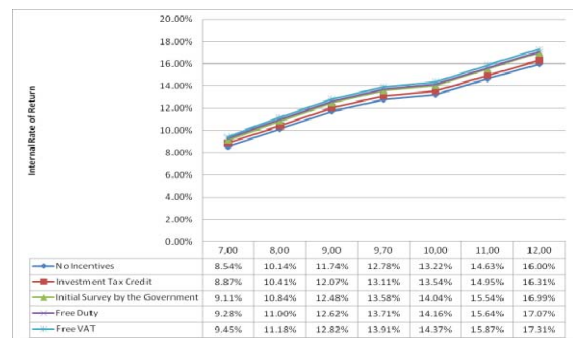


Figure 9. Analysis of the effect of Government Incentives on IRR and Electricity Prices

Australian Geothermal Conference 2010

The effect of free duty, free VAT, the implementation of investment tax credit, and the preliminary survey incentive reduces the geothermal electricity price by \$ 0.75 ¢/KWh, 0.91 ¢/KWh, \$ 0.23 ¢/KWh and \$ 0.69 ¢/KWh, respectively (Table 2).

Table 2. Effect of Government Incentives on Electricity Prices

Incentives	Electricity Price At IRR=16%
No Incentives	12
Investment Tax Credit	11.77
Initial Survey by the Government	11.25
Free Duty	11.31
Free VAT	11.09

The effect of the implementation of CDM reduces the electricity price by 0.82 ¢/KWh and increases the IRR to 16.53% which is a bit above the desired RRR (Figure 10).

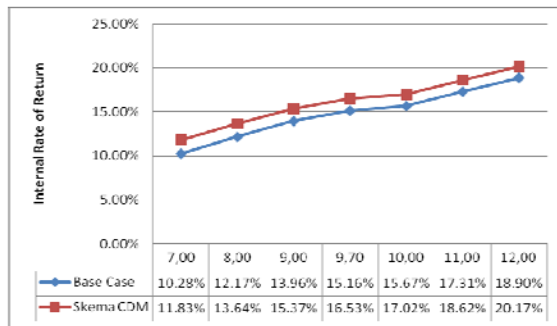


Figure 10. Analysis of the effect of CDM on IRR and Electricity Price

Table 3 below lists 6 scenarios of implementing combination of government tax and incentives.

Table 3. List of Scenarios

Scenario	Fiscal Policy
1	Duty Free
	VAT Free
	ITC 5% for 3 years
	No Survey Incentives
	No CDM Scheme
2	Duty Free
	VAT Free
	ITC 5% for 8 years
	No Survey Incentives
	No CDM Scheme
3	Duty Free
	VAT Free
	ITC 5% for 5 years
	Survey Incentives
	No CDM Scheme
4	Duty Free
	VAT Free
	ITC 5% for 5 years
	No Survey Incentives
	CDM Scheme
5	Duty Free
	VAT Free
	ITC 5% for 5 years
	Survey Incentives
	CDM Scheme
6	Duty 5%
	VAT 10%
	No ITC 5% for 5 years
	No Survey Incentives
	No CDM Scheme

In scenario 1, at the electricity price of 9.70 ¢/KWh, the IRR only reaches 14.66%. Electricity prices that feasible at IRR 16% is 10.54 ¢/KWh (Figure 11).

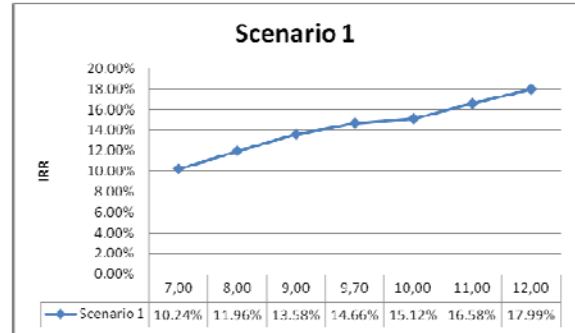


Figure 11. Analysis of the effect of Scenario 1 on IRR and Price

Results of scenarios 1 to 6 are summarized at Table 4 below:

Table 4. IRR and Geothermal Electricity Price

Scenario	IRR (%)	Electricity Price (cents/KWh)
	when electricity price is set as 9.70 cents/KWh	when IRR is set by 16%
1	14.66	10.54
2	15.29	10.23
3	16.02	9.6
4	16.53	9.26
5	18.72	8.68
6	14.53	10.5

According to National Energy Mix 2025, coal will still play as primary energy source, but its role will be reduced. As a substitution, geothermal will contribute 5% of total energy source (Figure 2). It is imperative to check GPP competitiveness toward coal power plant.

The assumptions used in calculating the cost of coal-fired power plant are as follows:

- Capacity: 300 MW
- Capital Cost: US\$ 2,500/MW
- O & M Cost: US\$ 88/KW
- Operation time: 7000 hours a year
- Carbon Tax: Rp 60/KWh
- Fuel Consumption: 0.439 Kg/KWh

The fact that geothermal fuel cost is quite stable during the life time of GPP, while on the contrary coal fuel cost is increasing by time. Using US\$ 24.76/MWh for geothermal energy cost for 30 years, geothermal cost will be less than coal in year 14. At the time coal fuel cost is US\$ 24.78 (Figure 12).

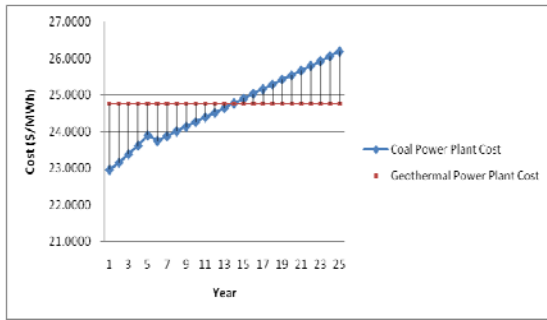


Figure 12. Levelized Cost Comparison Between Geothermal and Coal

Meanwhile, when applying carbon tax, geothermal will outperform even earlier, i.e. in fourth year, where the cost of coal is \$ 24.88. Application of carbon tax adds to the cost of coal Power Plant to \$ 1.26/MWh (Figure 13).

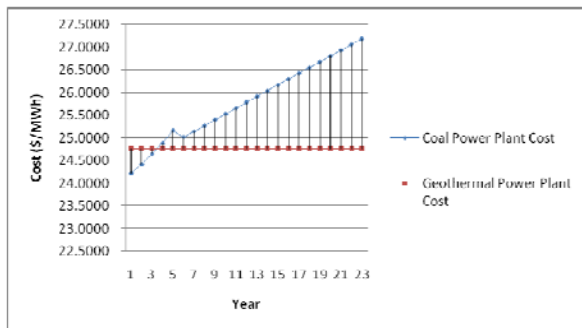


Figure 13. Levelized Cost Comparison Between Geothermal and Coal with Carbon Tax

Conclusion

The current policy, refers to PM K No. 21/PMK.011/2010 with the highest geothermal price US 9.70 cent/KWh, is not able to provide the investor desired IRR, i.e. 16%. To fulfil the investor IRR with the government electricity price, the investment costs must be reduced to at least 10% or increase the capacity factor by 10%.

Free VAT apparently has the most significant influence on the IRR and the geothermal electricity price followed by free import duty, initial survey by government incentive, and investment tax credit. The effect of those policies can lower the selling price by US 0.91 cent/KWh, 0.75 cent/KWh, 0.69 cent/KWh, and 0.23 cent/KWh, respectively. The effect and the implementation of CDM reduces the price by US 0.82 cent/KWh and increases the IRR to 16.53%.

From the six scenarios studied, only scenario 3 (combination of Duty-Free, Free of VAT, the ITC is 5%, and government pre survey), scenario 4 (Duty-Free, Free of VAT, the ITC is 5%, application of the CDM) and scenario 5 that can enhance GPP competitiveness. Among these three scenarios, scenario 5 (Duty Free, free of VAT, ITC is 5%, government survey and the application of the CDM) is the best scenario to

promote GPP. Without implementation of carbon tax, the cost of geothermal electricity can compete with coal in the year 14. The implementation of carbon tax to coal plant improves the competitiveness of GPP. Geothermal can compete with coal in the year 4.

References

Akmal, F, H. Darnell, and P. Sugiharto (2000). The geothermal power business in Java Bali: trading mechanism, competitiveness with fossil fuel and challenges to its development. Proceedings World Geothermal Congress pp 777-783. Kyushu-Tohoku, Japan, May 28 – June 10, 2000.

Ministry of Energy and Mineral Resources (2006). Blueprint National Energy Policy 2006-2025, The Republic of Indonesia. Jakarta, Indonesia

Canada, J.R., W.G. Sullivan, and J.A. White (1996). Capital Investment Analysis for Engineering and Management, 2nd ed., Prentice Hall, Inc. Upper Saddle River.

Danar, A.S. (2010). Geothermal electricity price determination based on investment decision. World Geothermal Congress. Nusa Dua, Indonesia (in Indonesia language)

Dardak, E (2007). Incorporating energy commodity price volatility in economic cost of supply analysis for electricity expansion plan. The 10th International Conference on QIR (Quality in Research). Jakarta, Indonesia, 4 – 6 December 2007.

Darnell, H. and A.R.T. Artono (2001). An analysis on the geothermal electricity competitiveness. the Annual Scientific Conference of Indonesian Geothermal Association. Yogyakarta, Indonesia, February 2001.

A METHOD FOR CALIBRATING AUSTRALIAN TEMPERATURE-DEPTH MODELS

Desmond Fitzgerald^{1*} and Raymond Seikel¹

¹Intrepid Geophysics Unit 2, 1 Male Street, Brighton Victoria, Australia 3186.

*Corresponding author: des@intrepid-geophysics.com

The Australian geothermal industry is moving rapidly, and in that process requires a lot from geophysics to aid in characterising regional prospectivity for exploitable heat resources.

Various groups are using hybrid methods to estimate 'Curie point' temperatures at depth, or alternatively, the temperature at 5 kilometres below the surface. Deep drilling observations and airborne magnetic compilations are the key components, together with a basement geology interpretation. Several generations of this work are already published with more to come.

A method to test the se maps and also help characterise uncertainty is proposed based upon a deep 3D continental model scale, extending to the lithosphere. Variable surface temperature and heat flow grids, based upon remote sensing are used, together with a simple lithosphere boundary condition. The heat diffusion is then employed to test the temperature-depth maps. Progress on applying this method to Australia is reported.

Key words: Sensing Heat Flow Anomalies, EM spectrum, High Energy photons, Continental scale 3d Geology models

Introduction

Not enough attention is paid to the influences of heat, both on-going and its history, in the field of exploration geoscience. Scant regard is paid to heat alteration mineral products, unless it is obviously a primary indicator of an economically viable resource. A more holistic approach to creating 3D earth models that embrace all aspects of heat and its influence on rocks is required. The challenge (Stein) is the classical one of using the measured temperature and temperature gradient at an object's surface to infer the temperature field at depth, $T(x,t)$, a function of position x and time t . Near the earth's surface, the temperature gradient is essentially vertical, so the outward heat flow q is the product of the vertical gradient of the temperature $T(z)$, which is most everywhere positive downwards (temperature increases with depth z), and the measured or estimated thermal conductivity of the material, k .

Australian developments

The systematic gathering of borehole observations of downhole temperatures, rock

heat conductivities and temperature gradients with depth below surface were the basis of producing the first generations of predicted temperatures 5km below the surface for the Australian continent (Chopra & Holgate, 2005), see figure 1.

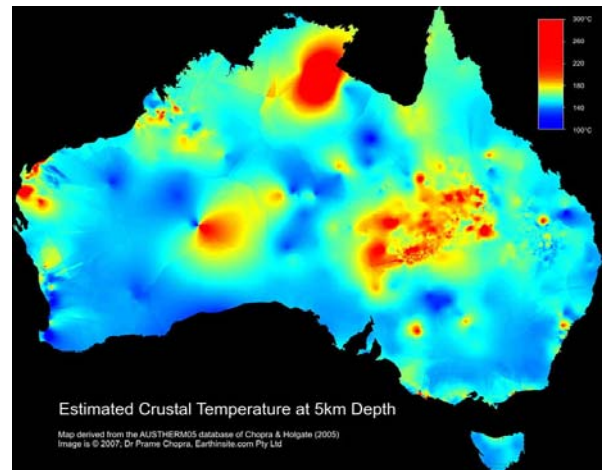


Figure 1: Map of estimated crustal temperatures at a depth of five kilometres.

Maus, 1997 developed the idea that compilations of the magnetic anomaly map could form the basis for estimating the depth to the Curie point. This requires a technique to find the bottoms of causative bodies. A moving window method using a modified Spector-Grant type algorithm was initially proposed for this task.

In recent times, Geoscience Australia has produced the 5th generation magnetic anomaly grid and with this edition there is much greater confidence that the longer wavelength anomalies (greater than 50 km) are faithfully reproduced. This follows from the AWAGS survey, funded by the "Securing Australia's Energy" initiative. Also, more theoretical work has been done on automatic depth to basement techniques, such that the ability to separate top/bottom and centres of causative bodies. (see Stavrev and Reid 2007).

Several groups have formed to tackle this problem and the recently reported progress from the USGS team (Bouligand et al 2009) is encouraging. In this work, a variety of approaches were applied to the California/Utah/Nevada region where over 25% of all geothermal power station capacity for the

world is located. These heat sources are labelled "conventional" as they follow from near surface volcanic sources associated with the Rocky Mountains and Yellowstone.

In Australia, a significant initiative is being mounted around the so-called South Australia Heat Flow anomaly. This was first recognized by Sandiford 1998, as the burial of a basement sequence enriched in heat producing elements during thermal subsidence following rifting. This major rift in the Australian continent from Adelaide north to the Cooper Basin, has a massive granitic intrusion which is Uranium rich. Naturally occurring low grade thermo-nuclear heating of this granite peaks at around 4 km deep. This type of play is termed an Enhanced Geothermal System.

Geochemistry

It is mainly the oil industry that has come to realise just how important the heat history of rocks and sedimentary packages is, in the prospectively of basins for oil or gas finds. Observationally, the key technique is defining the mineral alteration products and from experiment, just what must have been the heat history to have left this legacy. Diamond exploration has also traditionally looked for indicator minerals that imply the necessary heat history.

Structural geology

Most structural geology phenomena have an underlying genesis where heat has played a major role.

1. A deep pipe from the mantle to the surface can form as nature "vents" heat in explosive events. Kimberlite pipes retain a record of heat altered minerals that can be interpreted for temperatures during formation.
2. Granite intrusions in general.
3. All tectonic and plate scale movements are thought to be manifestations of heat circulation effects in the mantle.
4. Volcanic activity is mostly associated with crustal faulting, often on a plate boundary. Basalt flows and flood plains, and sills are remnants of this activity.
5. Rifting or failed rifts.

Observational geophysics

All the measurable geophysical phenomena such as gravity, magnetics, deep crustal seismic and radiometrics can indirectly be used to help interpret structural geology and define heat province boundaries.

Missing from these lower cost, bulk observational methods, is a viable methodology

to either directly or indirectly observe heat or temperature. This would lead to near surface temperature and/or heat flow maps that significantly improve upon Figure 1. So what is the physics and why do we struggle with this challenge?

Electro-magnetic spectrum

Thermal radiation is emitted by all substances above absolute zero and includes visible and infrared radiation and some ultra-violet radiation. Thermal radiation occurs in solids, liquids, and gases, at the speed of light and has no attenuation in a vacuum. Thermal radiation can occur between two bodies with a colder medium in between. Actually, the electromagnetic spectrum can be expressed in terms of energy, wavelength, or frequency. Each way of thinking about the EM spectrum is related to the others in a precise mathematical way.

	Wavelength (m)	Frequency (Hz)	Energy (J)
Radio	$> 1 \times 10^{-1}$	$< 3 \times 10^9$	$< 2 \times 10^{-24}$
Microwave	$1 \times 10^{-3} - 1 \times 10^{-1}$	$3 \times 10^9 - 3 \times 10^{11}$	$2 \times 10^{-24} - 2 \times 10^{-22}$
Infrared	$7 \times 10^{-7} - 1 \times 10^{-3}$	$3 \times 10^{11} - 4 \times 10^{14}$	$2 \times 10^{-22} - 3 \times 10^{-19}$
Optical	$4 \times 10^{-7} - 7 \times 10^{-7}$	$4 \times 10^{14} - 7.5 \times 10^{14}$	$3 \times 10^{-19} - 5 \times 10^{-19}$
UV	$1 \times 10^{-8} - 4 \times 10^{-7}$	$7.5 \times 10^{14} - 3 \times 10^{16}$	$5 \times 10^{-19} - 2 \times 10^{-17}$
X-ray	$1 \times 10^{-11} - 1 \times 10^{-8}$	$3 \times 10^{16} - 3 \times 10^{19}$	$2 \times 10^{-17} - 2 \times 10^{-14}$
Gamma-ray	$< 1 \times 10^{-11}$	$> 3 \times 10^{19}$	$> 2 \times 10^{-14}$

Table 1 : shows these relationships..

So why do we have three ways of describing things, each with a different set of physical units? After all, frequency is measured in cycles per second, wavelength is measured in meters, and energy is measured in electron volts and is inversely proportional to the wavelength.

By convention, gamma-rays are reported in electron volts, with the highest energy going to the right hand side. Figure 2 below has the order reversed, and shows the EM spectrum wavelengths increasing to the right, in what is the conventional manner for visible light, heat etc.

This traditional view also includes some what misleading with the label "thermal radiation". This type of heat is arguably the least well understood. While at the same time, most people are very familiar with the weather and sensing radiant heat. The body is receptive, largely due to the interaction of parts of the EM spectrum with water and to a lesser extent, other organic molecules. With this in mind, it is normal to associate heat with infra-red band, terra-hertz band and the ultra-violet bands (sun-burn). We have evolved to sense visible light which radiates from the sun due to thermal black body radiation at 5800K. What this is really showing is the range of Planck's law (see Figure 3) and how parts of the spectrum relate to "black body" radiation from the Earth. As can be seen, microwaves are not considered to be thermal radiation, yet clearly that have a very effective capacity to "heat". At the high end of the energy scale, gamma rays are part of the mix in nuclear power plants that, of course, generate heat prior to conversion to electricity.

From a geophysical point of view, any EM emission from the Earth could be harnessed to extract heat. The challenge of how to do this is largely an engineering problem.

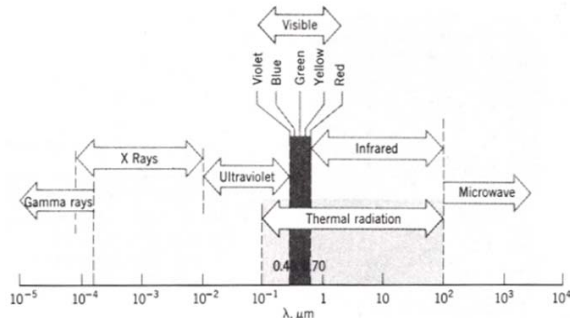


Figure 2. Radiation Spectrum, showing wavelengths. Note, it is not usual to think of thermal radiation extending into the higher energy parts of the spectrum e.g. X Rays.

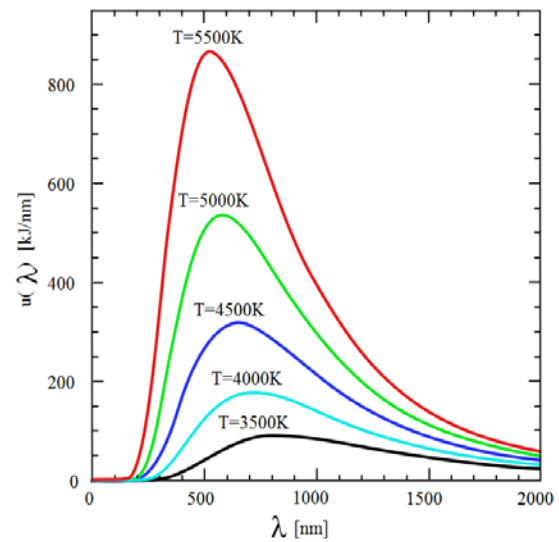


Figure 3 Planck's law and Black Body radiation. At normal surface temperatures of the Earth, the range of wavelengths still emitting radiation is large, while the overall energy (the area under the curve), falls off dramatically.

There are two types of radiation categories

- Volumetric phenomenon – radiation emitted or absorbed throughout gases, transparent solids, some fluids
- Surface phenomenon – radiation into/from solid or liquid surface.

Initially, heat is emitted from the surface of the earth and then it is "attenuated" and absorbed in the atmosphere.

The magnitude of the radiation varies with wavelength – it's spectral. The wavelength of the radiation is a major factor in what its effects will be. This is illustrated in Figure 4.

Radiation is made up of a continuous, non-uniform distribution of monochromatic (single-wavelength) components.

The magnitude and spectral distribution (how the radiation varies with wavelength) varies with temperature and type of emitting surface. We are interested in the continental crust and regional variations due to the age and composition of the rocks.

Attenuation of signal

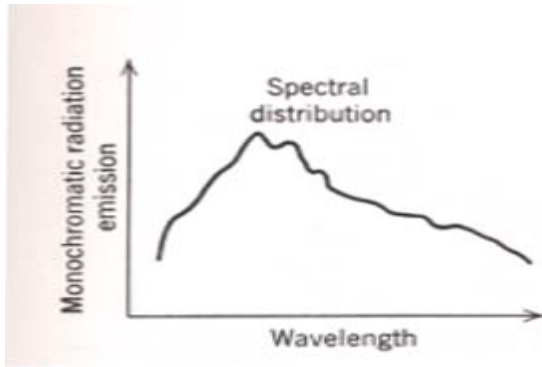


Figure 4. Shows varying emissivity with wavelengths

Radioactive (crustal) heat production

The continental crust contains a relatively high density of radioactive isotopes, primarily those of uranium, thorium, and potassium.

Hence, within a region the heat flow depends on

- (1) radioactivity in the crust,
- (2) tectonic setting, and
- (3) heat flux from the mantle below.

For a given area, termed a heat -flow province, the measured heat flow "q" varies linearly with the near surface radioactive heat production.

The technology to observe radiometrics emissions from the earth or gamma-rays has traditionally always ignored the "low channels", due to high counts and diurnal effects, often labelled "skyshine". Very few observations using these instruments have ever been done at night, when these diurnal effects are minimized. With the newer hardware now available and the sensitivities and counting capacities increased, a 66 litre system, designed for 1 024 channels and/or a Ge Li purpose built system, would be able to observe a considerable portion of the "thermal radiation" tail. The first channel of a radiometrics instrument covers most of the conventional EM spectrum, covering from 0 to 12 keV. Figure 5 recasts the EM spectra into the form favoured for measuring gamma rays.

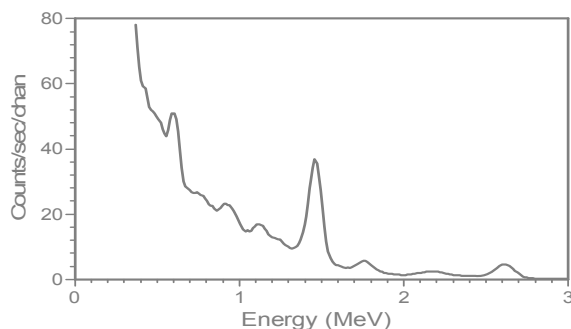


Figure 5 Typical Gamma Ray spectrum view, observed remotely within 100 m. of ground.

Radiant energy from the earth is readily absorbed and attenuated in the lower atmosphere. At lower energies, the photoelectric effect is mostly responsible for this. Radiometric airborne surveys are conducted at flying heights of around 100m, to ensure emissions characteristic of particular minerals can be observed before this attenuation smooths the characteristic spectral peaks. This required observation distance reduces as the energy of the photons reduces, if individual characteristics are to be seen. If one re-examines the generalized "Black Body" diffuse curve at 3 00 degrees Kelvin, it is very smooth and covers a broad range of energies, with no possibility of peaks from good emitting minerals.

This appears to be an area that requires either more research, or practical observations in differing terrains and natural light conditions. Towards the classic heat portion of the spectrum, bolometers exist that have been deployed at large distances, to observe that portion of the spectrum. (TIMS, ASTER etc.) The reason these show any signal, is that wavelengths are chosen that minimize absorption with water vapour.

Modelling construts

The oceanic lithosphere is relatively uniform in composition, and little heat is generated within it by radioactivity, oceanic heat flow is essentially a simple function of age. In contrast, a continental crust is heterogeneous in composition, due to its much longer tectonic history. Moreover, the heat flow depends critically on radioactive heat production in the crust. The two primary effects are thus that continental heat flow is proportional to the surface crustal radio activity in a given region, and decreases with the time since the last major tectonic event.

A rational way to construct a 3 D continental scale earth model that is to serve the purpose of constraining the complexity while still honouring the important factors is to use the new radiometrics map of Australia, to define tectonic and cratonic provinces characterised by the radiogenic rock content. The big unknown is the depth extent of each of these units. It is also here that geophysics is needed to play a part. To date, see Figure 1, no geological influences are taken into account when interpolating the temperatures away from observation points.

At the same time, great strides are being made to construct large scale 3D solid geology models that are consistent with structural geology observations and all the geophysical datasets.

In Australia, we have 3D models for Tasmania, most of Victoria, and about one third of South Australia. (Preliminary 3D geological models of the Curnamona basin and Gawler craton). In addition, some purpose built 3D heat/geology models for the Cooper basin have been constructed with a view to characterising the heat flow domains and defining uncertainties on this resource.

Numerical/computational complexities

A current challenge is thus to deal with all these complexities, deciding on the 4 or 5 most important aspects of the geoscience, and construct more realistic and therefore useful models. It turns out there is a barrier with the numerical methods used to solve the heat diffusion equation. The methods do not scale well. For simple situations, all is well, but when the requirements of 3D, structural geology, material inhomogeneity and continental scale are stated, no really viable techniques present themselves. For this reason, leading edge numerical methods, using Fast Fourier transforms etc., are being followed up. Two significant recent publications point the way here. Caratori 2009, elegantly shows how gravity and magnetic forward modelling in 3D can be rapidly achieved using 3D FFT methods. Li, 2007, looks at faster methods for the heat diffusion equation, but just the homogeneous case.

Conclusions

Craton scale and larger 3D numerical models, with structural geology constraints, properties and boundary conditions of measured surface heat flows, and more fuzzy "Curie Point" depths, can be integrated to create heat flow anomaly maps that will be a vast improvement on the existing practise.

The EM spectra and its measurement continue to provide challenges and insights into whole earth processes. The ability to interpret the EM spectra from the standpoint of extracting information about crustal heat deserves more thought and development.

A better understanding of how Planck's Law and the physics implied by it would be important in interpreting non-solar influenced earth heat emissions.

References

Bouligand C., Glen J., Blakely R., 2009, Mapping Curie temperature depth in the western United States

with a fractal model for crustal magnetization, J. OF Geophysical Research, VOL. 114.

Caratori Tontini F., Cocchi L., Carmisciano C., 2009, Rapid 3-D forward model of potential fields with application to the Palinaro Seamount magnetic anomaly (south ern Tyrrhenian Sea, Italy) J. OF Geophysical Research, VOL. 114.

Chopra, P., and Holgate, F., (2005) A GIS analysis of temperature in the Australian crust, Proceedings of the World Geothermal Congress 2005, Antalya, Turkey, 24-29 April 2005.

Li J-R., Greengard L., 2007, On the numerical solution of the heat equation I: Fast solvers in free space. Journal of Computational Physics 226.

Maus S., Gordon D., Fairhead D. 1997, Curie-temperature depth estimation using a self-similar magnetization model, Geophysics J. Int 129, 163-168.

Sandiford M., Hand M., McLaren S., 1998, High geothermal gradient metamorphism during thermal subsidence, Earth and Planetary Science Letters 163, 149-165.

Stavrev P., Reid A., 2007, Degrees of homogeneity of Potential fields and structural indices of Euler deconvolution, Geophysics, Vol. 72, NO. 1.

Stein, C.A. 1995, Global Earth Physics A Handbook of Physical Constants AGU Reference Shelf 1.

Evidence of impact shock metamorphism in basement granitoids, Cooper Basin, South Australia

Andrew Y. Glikson^{1*} and I.Tonguç Uysal²

¹Australian National University

²Queensland Geothermal Energy Centre of Excellence, The University of Queensland

*Corresponding author: Andrew.Glikson@anu.edu.au

The original observation of parallel closely spaced (microns to tens of microns) planar features in quartz grains from basement granitoid samples of Cooper Basin drill holes by I.T. Uysal, followed by Universal stage, scanning electron microscope (SEM) and energy dispersive spectrometry (EDS) tests by A.Y. Glikson, identify intracrystalline planar deformation features (PDF) in quartz which correspond to unique Miller indices diagnostic of shock metamorphism. U-Stage measurements of angles between the C-optic axis of quartz (C_{qz}) and poles to planar deformation features (P_{pdf}) in the same quartz grains (87 planar sets in quartz 54 grains) define intracrystalline planar orientations dominated by $\{10\bar{1}3\}$ and $\{10\bar{1}2\}$ Miller indices, correlated with shock pressures above 10 Gpa and above 20 Gpa, respectively (Engelhard and Stoffler, 1968; French, 1968; Stoffler, 1974; Stoffler and Langenhorst, 1994; Grieve et al., 1996; French, 1998). These Miller indices are characteristic of large impact structures, including Chesapeake Bay (D~85 km), Woodlough (D~120 km) and other impact structures. SEM/EDS studies of core samples indicate features consistent with shock metamorphism, including recrystallized pseudotachylite veins and micro breccia veins injected into resorbed quartz grains. Extensive alteration of feldspar to sericite and illite represent hydrothermal effects. Negative Bouguer anomalies of c. $-20 \mu\text{m/s}^2$ below parts of the Cooper Basin reflect low density basement sectors ($2.64\text{-}2.76 \text{ gr/cm}^3$) as compared to adjacent high density basement terrains ($2.9\text{-}2.99 \text{ gr/cm}^3$), consistent with impact fracturing of target rocks. Low magnetic anomalies of c. -200 nT associated with the Moomba structural dome and similar structures to the northeast may represent reset magnetisation such as is commonly associated with impact structures. An extension of the

Bouguer and magnetic anomalies over a >80 km-long belt defines the minimum extent of the shock metamorphosed basement, consistent with measured shock pressures of above 20 GPa. A regional altered zone at the top of the basement approximately $10,000 \text{ km}^2$ large and up to 524 meters deep (Boucher, 2001) may correspond to the impact aureole. Domal seismic structural elements and overlying unconformities in overlying sedimentary sequence of the Cooper Basin may be related to post-impact isostatic uplift of impact-fractured low-density basement sectors. The evidence for impact bears potential implications for the origin of K-U-Th enrichment in the basement in terms of an impact-triggered hydrothermal cell, mobilization and re-concentration of radiogenic elements.

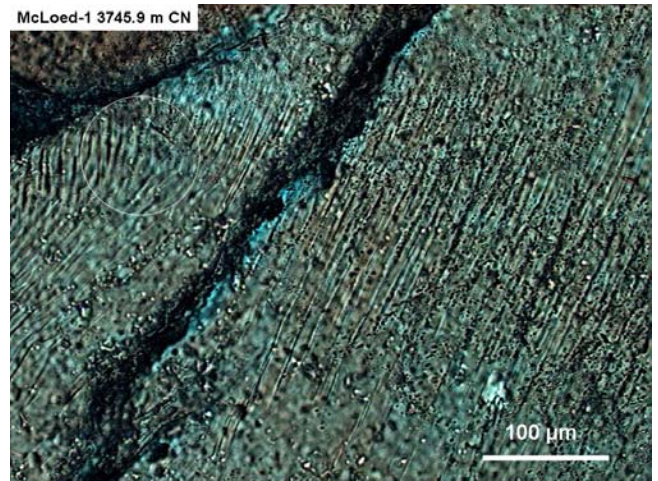


Fig. 1. Planar deformation features (PDF) in quartz deflected along a post-impact fracture, McLoed-1 3745 m.

Identification of planar deformation features (PDF)

Penetrative intracrystalline planar deformation features (PDF) in quartz possess specific crystallographic Miller indices with orientations diagnostic of shock metamorphism at pressures in excess of levels associated with endogenic processes such as seismic shock, volcanic explosions and shear processes which produce metamorphic deformation lamella (MDL) in quartz (Engelhard and Stoffer, 1968; French, 1968; Stoffer, 1974; Stoffer and Langenhorst, 1994; Grieve et al., 1996; French, 1998; French and Koeberl, 2010) (Figs 1 - 5). PDFs are (1) restricted to individual grains, i.e. they do not cross grain boundaries; (2) are often multiple, with N sets per grain; (3) have a strict planar character though they can be deflected along shear zones and fractures and in some instances fan out; (4) are typically 2-4 micron wide; (5) are closely spaced, typically 10-20 micron; (6) consist of glassy or recrystallized quartz mosaic lamellae, or are marked by arrays of fluid inclusions; (7) possess unique crystallographic orientations.

Shock metamorphic features are classified in the following terms (French, 1998):

1. Mineral fracturing {0001} and {10⁻¹¹} in quartz: 5-7 GPa
2. Basal Brazil twins {0001}: 8-10 GPa
3. PDF in quartz {10⁻¹³}: >10 GPa
4. Transformation of quartz to stishovite: 12-15 GPa
5. PDF in quartz {10⁻¹²}: >20 GPa
6. Transformation of quartz to coesite - >30 GPa

The results of universal stage measurements are presented in Figs 4 and 5. U-stage analysis of PDF orientations is complicated by a number of factors, arising from differential deformation related to the attenuation of shock of quartz grains by enveloping hydrous phases, as well as post-shock deformation (Figs 1, 2) and recrystallization of quartz grains. This includes superposition of multiple sets of planar features, including well defined parallel micro-n-scale to tens of micron-scale PDF sets (Fig. 3) and less well-defined to poorly defined parallel or undulating planar features, including deformed PDF and planar features (PF) formed by pre-impact and/or post-impact deformation (Figs 1, 2). By contrast to PDFs planar features may show degrees of undulation and waviness and may be accompanied by fluid inclusions and cryptocrystalline clou ding (Fig. 3). Rarely are

PDFs completely expressed and a high proportion of grains display only one or two PDFs.

Planar features displayed by quartz grains of the Moomba-1 and McLoed-1 samples include genuine PDFs defined by:

1. Penetrative planar parallel sets with spacings on the scale of few microns to few tens of microns (Figs 1 - 3).
2. Differential development of PDFs between grains and within grains.
3. Common association of PDFs with less-well defined inclusion-marked somewhat curved fracture sets (Fig. 3).
4. Post-impact deformation indicated by drag-fold features along younger microfractures (Fig. 1) and wavy deformation of PDFs within grains (Fig. 2).

In the present study PDFs were measured on planar sets displaying high degree of parallel orientation at a few microns to few tens of micron intervals. PDFs measured in quartz grains of the Moomba-1 and McLoed-1 samples are plotted in Figs 4 and 5 in terms of percent frequency of PDFs which correspond within measurement accuracy of $\pm 3^\circ$ to specific Miller indices of {10⁻¹³}, {10⁻¹²}, {11⁻²²}, {11⁻²¹}, {10⁻¹¹} and {51⁻⁶¹}.

The plots demonstrate a prevalence of PDFs with Miller indices of {10⁻¹³} and {10⁻¹²} in Moomba-1 core samples and of Miller index of {10⁻¹²} in the McLoed-1 core samples (Figs 4, 5), suggesting shock pressures of >20 GPa in both cores in accord with criteria indicated in studies of shock deformation of quartz (Engelhard and Stoffer, 1968; French, 1968; Robertson et al., 1968; Stoffer, 1974; Stoffer and Langenhorst, 1994; Grieve et al., 1996; French, 1998; French and Koeberl, 2010). Other measured Miller indices diagnostic of shock metamorphic effects include {11⁻²¹}, {11⁻²²}, {10⁻¹⁰}, {10⁻¹¹} and {51⁻⁶¹}.

PDF indices correlated with shock pressures of >20 GPa are found in large to very large impact structures, including Yarrabubba impact structure, Western Australia (Macdonald et al., 2003), Woodleigh impact structure, Western Australia (D=120 km; age ~359 Ma) (Glikson et al., 2005A, B), Chesapeake Bay impact structure (D=85 km; age ~35 Ma) and large Canadian impact structures (Type D) (French and Koeberl, 2010).

Moomba-1 2857.4 m PPL

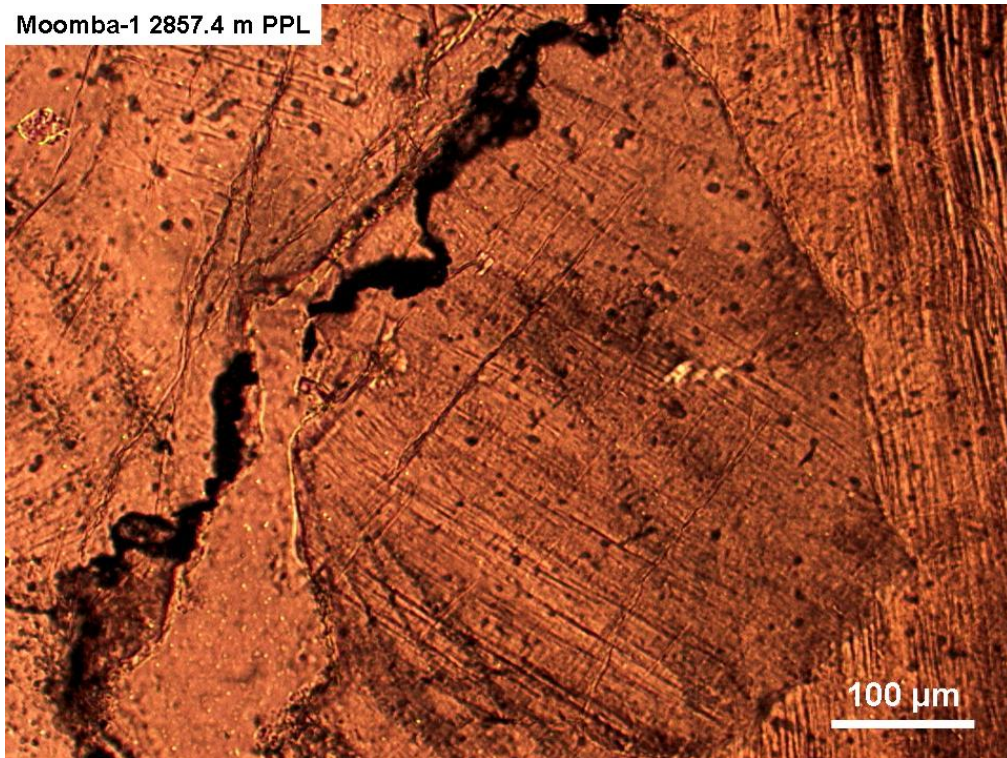


Fig. 2. Three quartz grains bearing planar deformation features (PDF): Note the wavy planar structure of the right-hand grain, representing post-impact plastic deformation of the quartz grain. Moomba-1 2857.4 m PPL.

Moomba-1 2857.4 m CN

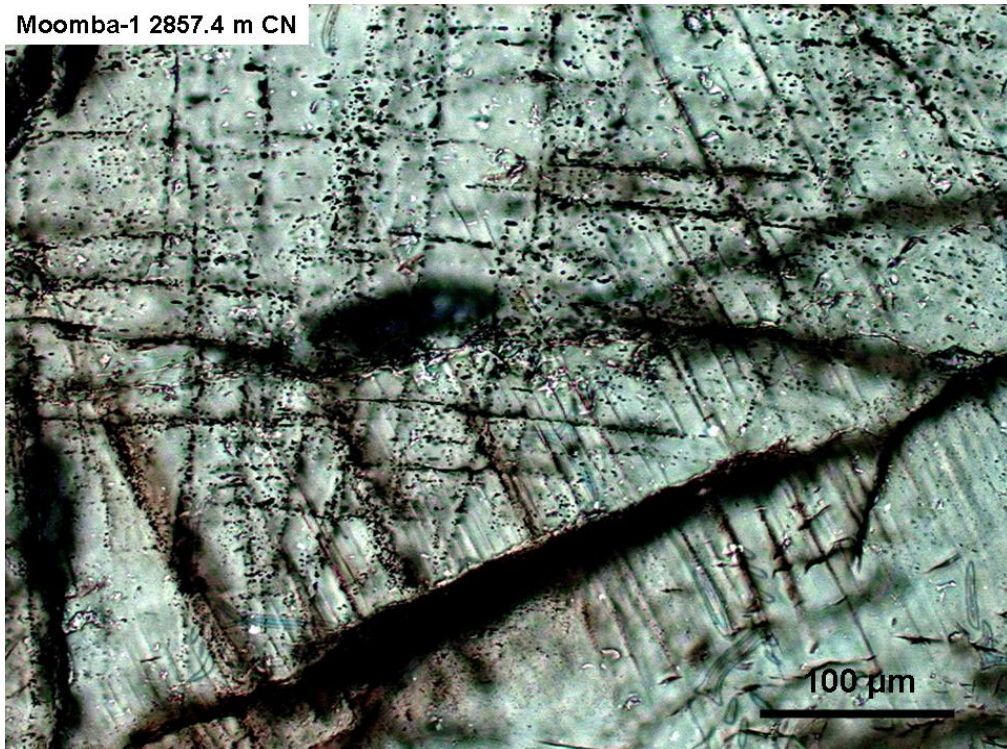


Fig. 3. Planar deformation features (PDF) (NNW-trending at lower and right-hand part of image) and inclusion-dotted planar fractures (at left side of image). Moomba-1 2857.4 m, PPL.

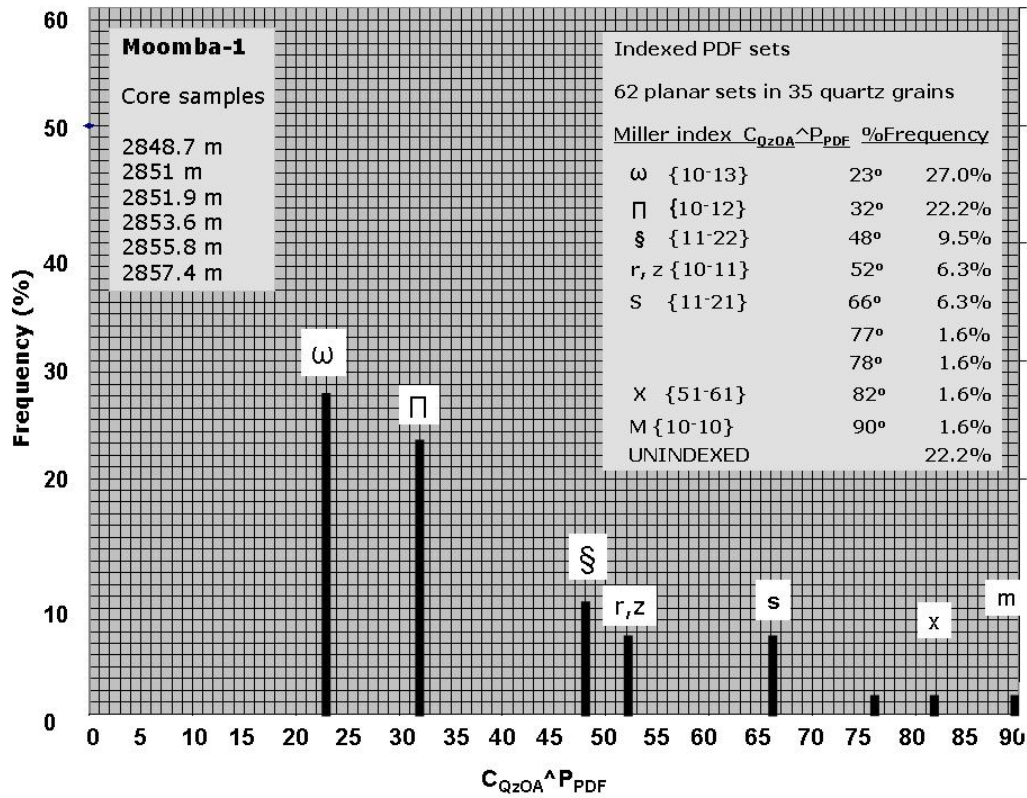


Fig. 4. Percent frequency distribution of the Miller-indexed angles between C-optic axis of quartz grains (C_{QzOA}) and the pole to planar deformation features (P_{PDF}) in 62 planar sets in 35 quartz grains from Moomba-1 granitoid core samples. Planes are indexed within measurement accuracy of $\pm 3\%$ of Miller indices.

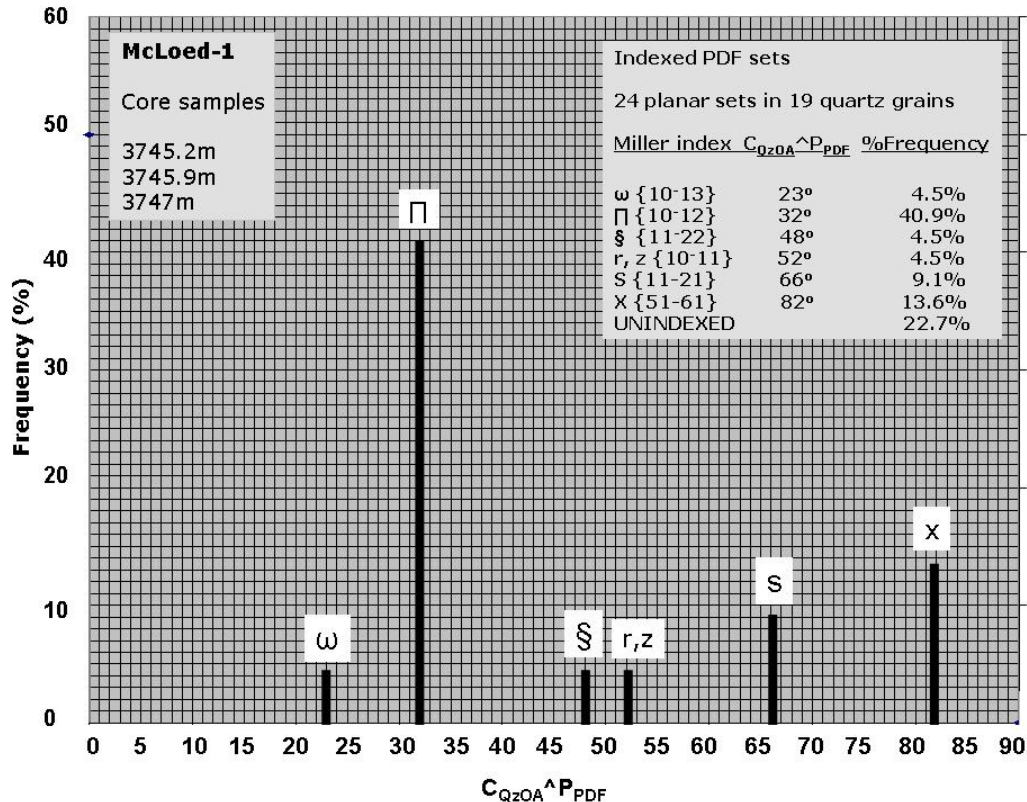


Fig. 5. Percent frequency distribution of Miller-indexed angles between C-optic axis of quartz grains (C_{QzOA}) and the pole to planar deformation features (P_{PDF}) in 22 planar sets in 19 quartz grains from McLoed-1 granitoid core samples. Planes are indexed within measurement accuracy of $\pm 3\%$ of Miller indices.

Scanning electron microscopy and energy dispersive spectrometry

Three samples were analysed by scanning electron microscopy (SEM) and Energy Dispersive Spectrometry (EDS) on a Jeol-6400 electron microscope at the Research School of Biological Studies, Australian National University (analyst: A. Glikson; supervisors: F. Brink, H. Chen). SEM/EDS analytical procedures included point analyses of element abundances at detection levels of >2000 ppm. Using a 15 KeV accelerating voltage, spot analyses were carried with a 1 micron-size beam, with a spectrum collection time of 80 seconds (120 seconds real time) at 8 000 cps. Accuracy and precision are based on reference standards by Astimex Scientific Limited MINM 25-53 (Serial Number 95-050) using standard olivine, diopside, almandine garnet, albite and barite.

Studied samples include:

Moomba-1 2857.4 m (Fig. 6): Altered coarse-grained granitoid consisting of quartz with resorbed grain boundaries injected by microbreccia veins which consist of micron to tens of micro-scale quartz, sericite/illite, sulphide and minor magnetite.

McLoed-1 3745.9 m: Altered coarse-grained granitoid containing K-feldspar, albite and sericite/illite, injected by microbreccia veins. Hydrothermal alteration is manifested by partly corroded/resorbed quartz grains and magnetite grains.

Big Lake -1 3057m : K-feldspar-albite-quartz granitoid consisting of resorbed quartz fragments injected by microbreccia.

EDS analyses indicate an abundance of sericite and occasional preservation of K-feldspar and albite. Observations relevant to the search for shock metamorphic features include:

1. Planar deformation features identified by optical microscopy do not display on either electron backscatter mode or secondary electron (SE1) scanning mode. This indicates PDF lamina consist of cryptocrystalline quartz of similar electron density as the host quartz.
2. The injection of microbreccia veins into quartz grains is consistent with, although does not prove, shock effects.
3. The corroded boundaries of quartz and magnetite grains (Fig. 6) and the abundance of sericite and illite are consistent with hydrothermal alteration of the granitoids.

The extremely fine grained texture of the microbreccia veins suggests their possible derivation by recrystallization of pseudotachylite veins consisting of impact-generated comminuted and fluidized material similar to veins found around exposed impact structures (Spray, 1995; Spray and Thompson, 1995; Reimold, 1995, 1998).

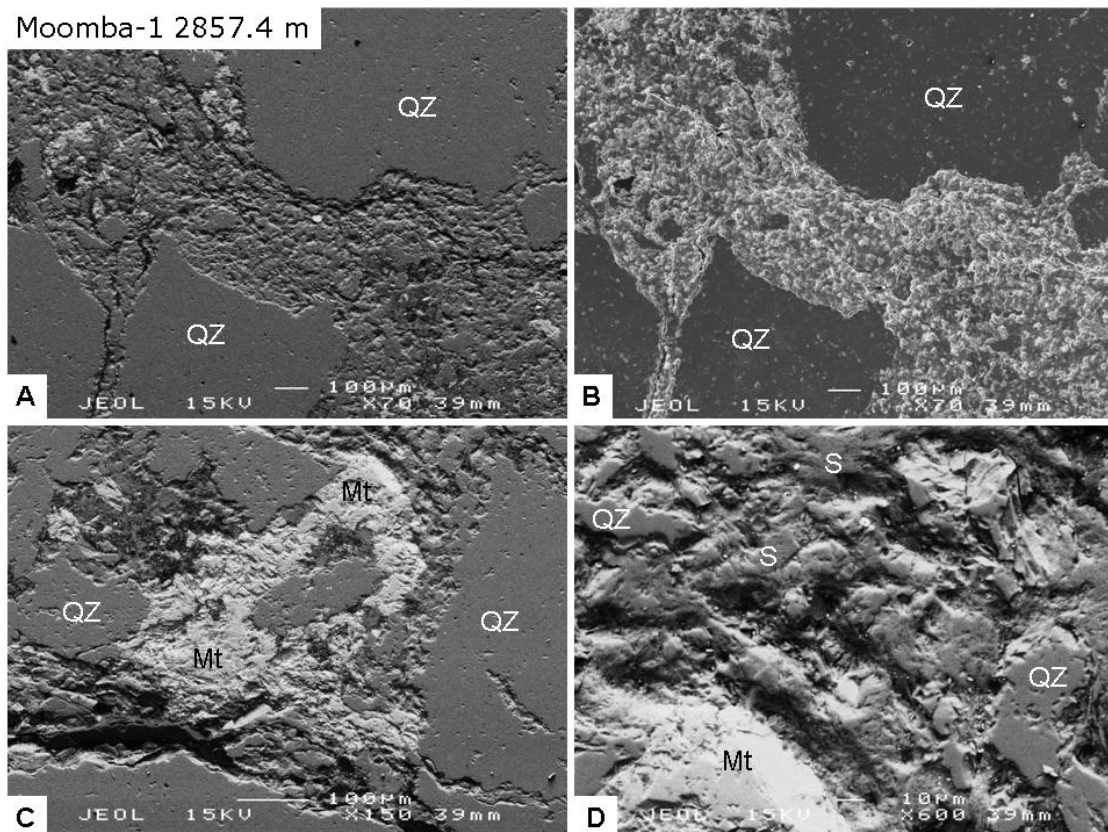


Fig. 6. Moomba-1 2857.4 m: SEM image of hydrothermally altered microbreccia-injected granitoid. (A) backscatter image of microbreccia veins injected into quartz grains; (B) SE1 image of frame A; (C) secondary magnetite within microbreccia veins; (D) magnified view of microbreccia vein consisting of quartz, sericite and magnetite.

Implications for structure and the origin of geothermal anomalies

Boucher (1996, 2001), on the basis of wireline log signatures and drill core logs, reported an altered zone up to 524 meters-thick at the top of the top of early to mid Palaeozoic basement underlying the Cooper Basin. Boucher (2001) considered the origin of this zone in terms of either weathering or hydrothermal alteration, or merely as a wireline logging anomaly.

The presence of signatures of shock metamorphism within the altered top basement zone may suggest extensive hydrothermal activity triggered by a large asteroid impact, as has been documented in large impact structures (Allen et al., 1982; Naumov, 2002; Pirajno, 2005; Glikson et al., 2005; French, 1998; Uysal et al., 2001, 2002; French and Koeberl, 2010). Based on an association of hydrothermal alteration with impact effects, the extent of the impact aureole may be outlined by the altered zone, which covers an area larger than 10,000 km² in the Cooper Basin (Boucher, 2001; Fig. A8).

Shock metamorphism of basement sectors is consistent with geophysical and structural

evidence for low density (2.64 – 2.76 g/cm³) basement sectors underlying the Moomba-1 and McLoed-1 holes, as compared to higher density bodies (2.8 – 3.0 g/cm³) in adjacent terrain (Meixner et al., 2000). The low-density basement sectors likely represent intense hydration and fracturing related to the impact, as is the case with the Woodleigh impact structure (Glikson et al., 2005a, 2005b), Gnarnoo probable impact structure (Lasky and Glikson, 2005) and Mount Ashmore probable impact structure (Glikson et al., 2010). The low magnetic anomalies associated with the gravity lows (Meixner et al., 2000) are consistent with demagnetisation of impacted basement zones, observed in a number of impact structures (Grieve and Pilkington, 1996).

The evidence for impact bears potential implications for the origin of K-U-Th enrichment in the Cooper Basin in terms of an impact-triggered hydrothermal cell and associated mobilization and reconcentration of radiogenic elements. Temperatures over 225°C at 5 km depth (T_{5km}) occur over an area about 79,000 km² large under an insulating sedimentary cover about 3.5 – 4.5 km-thick at the Napamerri Trough between Moomba dome and Innamincka where geothermal gradients as high as 55–60°C/km are measured (Middleton, 1979; Wyborn et al., 2004; Radke, 2009). The highest

temperatures occur near Innamincka in the proximity of McLeod-1, where maximum shock pressures of > 20 Gpa are measured (Fig. 5). Extreme total heat flow of 7.5-10.3 mWm⁻² originate from enrichment of the Big Lake Suite granites in radiogenic heat-producing elements, including Uranium (13.7, 16.5 ppm), Thorium (46, 74 ppm) and Potassium (5.2, 6.0 % K₂O) (Middleton, 1979; Sandiford and McLaren, 2002; Chopra, 2003; McLaren and Dunlap, 2006). The presence of a highly radiogenic basement within 3-4 km of the surface may in part reflect upward migration and re-concentration of large ion lithophile elements associated with an impact-generated hydrothermal cell, as is the case in some impact structures, including Woodleigh (Glikson et al. 2005), Shoemaker impact structure and Yarrabubba impact structure (Pirajno, 2005).

References

- Allen, C. C., Gooding, J. L., Keil, K. 1982. *Journal of Geophysical Research* **82**, 10083 – 10101.
- Boucher, R.K., 1996. *MESA Journal*, 21, 30-32.
- Boucher, R.K., 2001. Nature and origin of the altered zone at the base Cooper Basin unconformity, South Australia. *South Australia. Department of Primary Industries and Resources, Report Book 2001/012*.
- Chopra, P., 2003. *Preview Australian Society of Exploration Geophysics*, **107**, 34-36.
- Engelhard, W.V., Stöffler, D., 1968. in: *Shock Metamorphism of Natural Materials*. Mono Book Corp, Baltimore, MD, 159-168.
- French, B.M., 1968. In: *Shock Metamorphism of Natural Materials*. Mono Book Corp, Baltimore, MD, 1-17.
- French, B.M., 1998. Traces of catastrophe: a handbook of shock-metamorphic effects in terrestrial meteorite impact craters. *Lunar and Planetary Institute, Houston, TX, Contribution CB-954*. 120 pp.
- French, B.M., Koeberl, C., 2010. The convincing identification of terrestrial meteorite impact structures: What works, what doesn't, and why. *Earth-Science Reviews*, **98**, 123-170.
- Glikson, A. Y., Eggins, S., Golding, S., Haines, P. W., Iasky, R. P., Mernagh, T. P., Mory, A. J., Pirajno, F., Uysal, I. T., 2005. *Australian Journal of Earth Sciences*, **52**, 555-573.
- Glikson, A. Y., Mory, A. J., Iasky, R. P., Pirajno, F., Golding, S. D., Uysal, I. T. 2005. *Australian Journal of Earth Sciences*, **52**, 545-553.
- Glikson, A. Y., Jablonsky, D., Westlake, S., 2010. *Australian Journal of Earth Sciences*, **57**, 411-430.
- Grieve, R.A.F., Pilkington, M., 1996. *Australian Geological Survey Organisation Journal of Australian Geology and Geophysics*, **16**, No. 4, 399-420.
- Grieve, R.A.F., Langenhorst, F., Stöffler, D., 1996. *Meteoritics and Planetary Science*, **31**, 6-35.
- Iasky, R. P., Glikson, A. Y. 2005. *Australian Journal of Earth Sciences*, **52**. 575-586
- Macdonald, F.A., Bunting, J.A., Cina, S., 2003. *Earth and Planetary Science Letters*, **213**, 235-247
- McLaren, S., Dunlap, W.J., 2006. *Basin Research*, **18**, 189-203.
- Meixner, T.J., Gunn, P.J., Boucher, R.K., Yeats, A.N., Murray, L., Yeats, T.N., Richardson, L.M., Freares, R.A., 2000. *South Australia Exploration Geophysics*, **31**, 024-032
- Middleton, M.F. (1979) *Bulletin of the Australian Society of Exploration Geophysics*.
- Naumov, M. V. 2002. In: *Impacts in Precambrian Shields*, pp. 117 – 173. Springer Verlag, Berlin.
- Pirajno, F., 2005. *Australian Journal Earth Science*, **52**, 4/5, 587-606.
- Radke, B., 2009. *Geoscience Australia Record* 2009/25.
- Reimold, W.U., 1995. *Earth Science Reviews*, **39**, 247-265.
- Reimold, W.U., 1998. *Earth Science Reviews*, **43**, 45-47.
- Robertson, P.B., Dence, M.R., Vos, M.A., 1968. *Shock Metamorphism of Natural Materials*. Mono Book Corp, Baltimore, MD, pp. 433-452.
- Sandiford, M., McLaren, S., 2002. *Earth Planetary Science Letters*, **204**, 133-150.
- Spray, J.S., 1995. *Geology*, **23**, 1119-1122.
- Spray, J.G., Thompson, L.M., 1995. *Nature*, **373**, 130-132.
- Stoffler, D., 1974. *Fortschritte der Mineralogie*, **51**, 256-289.
- Stoffler, D., Langenhorst, F., 1994. *Meteoritics*, **29**, 155-181.
- Uysal, T., Golding, S. D., Glikson A. Y., Mory A. J., Glikson, M., 2001. *Earth and Planetary Science Letters*, **192**, 281 – 289.
- Uysal, T., Golding, S. D., Glikson, A. Y., Mory, A. J., Glikson, M., Iasky, R. P., Pirajno, 2002. *Earth and Planetary Science Letters*, **201**, 253-260.
- Wyborn, D., de Graaf, L., Davidson, S. and Hann, S., 2004. *Eastern Australian Basins Symposium II, PESA Special Publication*, 423-430.

Geothermal Energy in India: Past, Present and Future Plans

Harinarayana, T., National Geophysical Research Institute, Hyderabad (Council of scientific and industrial research)

Abstract

It is well known that among the various new and renewable energy sources, geothermal energy is known to be one of the clean energy without smoke and also without environmental hazards. Although its importance is realized long back in other countries, its exploitation is still far away in India, mainly due to lack of knowledge on the deep sub surface structure and lack of dedicated program on deep drilling in high pressure, high temperature conditions. Geological Survey of India (GSI) and National Geophysical Research Institute (NGRI) have made concerted efforts in identifying these resources in different parts of our country for possible exploitation. In this direction, different geothermal regions have been investigated in recent years

using deep electromagnetic geophysical technique, namely the Magnetotellurics. The geothermal regions investigated include Puga in higher Himalayas of Jammu and Kashmir, Tattapani of Surguja district in Chattisgarh, Surajkund of Jharkhand, Tapovan-Vishnugad, Lohari-Nag-Pala, Badrinath regions of Uttarakhand, Kullu-Manali regions of Himachal Pradesh. These investigations have provided the quantitative dimensions of the anomalous subsurface structures related to geothermal heat source. In this talk, an overview of the details of present day knowledge of geothermal energy at different locations with estimated potential based on the geophysical studies and shallow boreholes temperature logs are discussed. Concrete plans and future directions are also provided to develop this untapped resource.

Aquifer heterogeneity – is it properly assessed by wellbore samples and does it matter for aquifer heat extraction?

Peter Leary*, Peter Malin, Eylon Shalev & Stephen Onacha
Institute of Earth Sciences and Engineering, University of Auckland
58 Symonds Street, Auckland 1142, New Zealand
p.leary@auckland.ac.nz

Abstract

Oil field reservoir formations are sampled for porosity and permeability on the tacit assumption that small scale well-log and well-core data are representative of the formation flow properties at arbitrary distances from the wellbore. In formal terms, this statistical assumption is valid only if the formation properties are adequately characterised by a mean and standard deviation, or, equivalently, if variations in formation properties are spatially uncorrelated on all scale lengths. This statistical validity condition is, however, violated by crustal rock; well-log and well-core data are spatially correlated over a wide range of scale lengths. It is, therefore, formally wrong to assume that small scale sample means and standard deviations adequately represent large-scale variation of aquifer reservoir/formation properties.

As a practical matter, the formal failure of oil field well-log and well-core sampling to adequately estimate large-scale formation flow property variation is buffered by (i) the high energy density of hydrocarbons, (ii) lack of need for large drainage flow rates, (iii) ability to drill infill wells if *de facto* well drainage volumes are too small, and (iv) ability of time-lapse seismic imaging to detect fluid substitution volumes to determine large-scale formation flow structures that are not inferred from small-scale formation sampling strategies.

As an equally practical matter, however, the above caveats do not apply to producing hot aquifer fluids: (i) geothermal energy density is far smaller than hydrocarbon energy content; (ii) high flow rates are essential to geothermal power production; (iii) infill wells are at high risk to not intersect large drainage volumes unless guided by reliable auxiliary information; (iv) time-lapse hot aquifer imaging has no fluid-substitution signal.

An alternative strategy to aquifer production well-siting based on small-scale wellbore sampling of the aquifer focuses on measuring large-scale aquifer fracture-structures. Experience with magnetotelluric (MT) detection of *in situ* fracture volumes in geothermal fields suggests that MT surveys can form the basis for physically accurate sampling of large-scale aquifer fracture/flow structure.

Keywords: fractures, faults, porosity, permeability

Introduction – Treating aquifers as oil field reservoir formations

The following statement, made at the Bali 2010 World Geothermal Congress, succinctly describes an approach to hot aquifer energy production based on oil/gas reservoir formation characterisation using wellbore samples.

As part of the drilling of the petroleum wells, a significant amount of wireline logging, core sampling and resulting petrophysical evaluation were undertaken..... The porosity of the targetsection was determined...based on wireline logs calibrated to porosity samples from conventional cores and sidewall cores. The core porosities were calibrated to measured permeabilities using all the cores from a larger database..... Several studies.....provide insights into the petrophysical evaluation....and its calibration of porosity to permeability. Using the calibration of porosity to permeability, and the calibrated porosity derived from wireline logging and cores, it is thus possible to determine the permeability....sandstone section and integrate this across the borehole to get the transmissivity or permeability metres. (de Graaf et al 2010).

Parallel statements were made at the WGC2010 by Clauser et al (2010) and Vogt et al (2010). The working assumption is that formation wellbore data recorded by geophysical logging tools and/or recovered in well core adequately samples the formation properties at all relevant scales. While indisputably the wellbore data sample specific geological formations, it does not follow that within a geological formation any or all important geophysical properties conform to a small-scale sample mean throughout the formation, or that important geophysical property variations within the formation are confined to the formation. Rather the evidence from well-log data systematics is precisely the opposite: variation of geophysical properties within a formation can be substantial and these variations can be connected to the enclosing crustal volumes outside the formation. Well-log systematics thus indicate that near-wellbore samples do not accurately assess the degree of large-scale spatial variation expected for *in situ* formation properties, and that the spatial distributions of formation variations cannot be adequately estimated from small-scale sampling.

These general statements are illustrated by well-log and well-core data for Perth Basin formations encountered by the 3km-deep Cockburn1 well.

Well-log and well-core sample data for Perth Basin sedimentary formations

Perth Basin formations were drilled, logged and core-sampled by the 3km-deep Cockburn1 oil exploration well on the coast 18km southwest of Perth (Smith 1967). Well-log data in general, and for the 1200m thick Yarragadee aquifer in particular, conform to well-log *in situ* geophysical property variations observed worldwide. Figure 1 shows the well-log systematics for specific aquifer formations in the Cockburn1 well sequence.

Well-log power-law scaling systematics

The Fourier power-spectra of *in situ* spatial variations of rock properties measured by well logs worldwide closely conform to a specific power-law scaling form (Leary 2002):

$$S(k) \propto 1/k^1, \quad (1)$$

where k is spatial frequency and S is the well-log fluctuation power at scale length k . Depending upon the well log, the spectral scale-length range k tends to ~3 decades in the overall 5-decade scale range ~1cycle/cm to ~1cycle/km. High spatial frequency data at ~1cycle/cm are recorded by formation microscanner tools measuring electric resistivity with mm-scale electrodes. Km-long well logs of gamma activity, acoustic velocity, neutron density, electron density and electrical resistivity logs routinely return low spatial fluctuation power data at ~1cycle/km.

Well-log spectral form (1) is important for three reasons:

- It is power-law over all scale lengths relevant to reservoir performance and crustal deformation processes;
- The power-law exponent is the same for essentially all *in situ* properties, rock types, and geological settings;
- The non-zero power-law exponent destroys the basis for standard statistical inferences from standard sampling.

Power-law scaling of well-log spatial fluctuations over the five-decade cm-km scale range is indisputable evidence that something beyond geology is at work in the brittle crust. A power-law scaling exponent that is essentially the same for a range of geologic media and settings is evidence that power-law scaling derives from fundamental physical properties of rock with secondary regard to geological details at all scale lengths. Spatially fluctuating grain-scale fracture density is a likely candidate for the fundamental parameter controlling how *in situ* physical properties of rock vary both vertically and horizontally (Leary 2002).

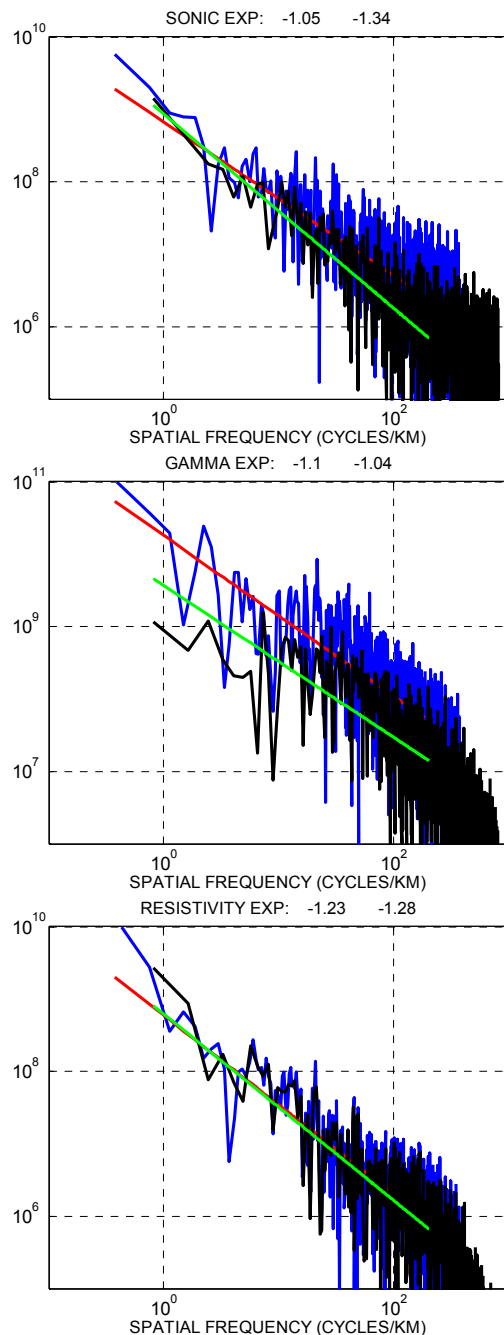


Figure 1: Well-log fluctuation power-spectra for Cockburn1 geological section (blue) and Yarragadee formation (black) fit to power-law trends for sonic velocity, gamma activity and resistivity data. Red line fit to entire section, green line to Yarragadee section. Spectral exponent -1.17 ± 0.13 is non-zero, showing that fluctuations of *in situ* rock physical properties of the Cockburn1 drill site and the Yarragadee aquifer in particular are spatially correlated rather than spatially uncorrelated over the m-km scale range.

The non-zero power-law scaling exponent in (1) means that *in situ* spatial fluctuations in geophysical properties are spatially correlated at all scale lengths and hence systematically violate the necessary condition of the central-limit theorem upon which standard geostatistical inferences are commonly based.

The general idea that small-scale sample means and standard deviations reasonably represent large-scale property variations within an ensemble is valid only if the ensemble property variations are spatially uncorrelated. Fluctuations are, in turn, uncorrelated only if the associated fluctuation power-law spectrum is ‘white’,

$$S(k) \propto 1/k^0 \sim \text{constant}, \quad (2)$$

at all relevant scale lengths. Figure 1 tests fluctuation power condition (2) for well-log acoustic velocity, gamma activity, and electrical resistivity data over the entire Cockburn1 section (blue) and the Yarragadee formation (black). Since the power-law exponent of each spectrum is ~ 1 instead of 0 over the 3 decade m-km scale range, condition (2) for spatially uncorrelated fluctuations in the Cockburn1 well geological section is mathematically untenable. Whatever properties of *in situ* rock are responsible for the variations in well-log readings, it cannot be logically maintained that the mean and standard deviation of small-scale sample data accurately predicts the scale of variations in those properties at arbitrary distances from the wellbore.

Well-core poroperm fluctuation systematics – percolation via grain-scale fractures

An underlying connection between *in situ* fractures and $S(k) \propto 1/k$ power-spectra is plausible since spatial variations in gamma activity of soluble radiogenic minerals, acoustic velocity and electrical resistivity are naturally related to spatial variations in fracture density. That is, crustal volumes with a greater number of fractures tend to have greater gamma activity, lower resistivity and lower seismic velocity. However, physically more immediate evidence for spatially variable fracture density is available through the systematics of well-core porosity-permeability (poroperm) spatial fluctuations measured in numerous oil/gas field reservoir formations (Leary & Walter 2008).

Figure 2 graphically illustrates the systematics of poroperm spatial fluctuations for well-core data from tight gas reservoir formations in the Cooper Basin, South Australia. The blue trace tracks variations in well-core porosity ϕ and the red trace tracks variations in the logarithm of well-core permeability κ as the core sequence moves along the well. The Figure 2 spatial fluctuation relation between porosity ϕ and logarithm of permeability κ can be written,

$$\delta\phi \sim \delta\log(\kappa), \quad (3)$$

where $\delta\phi$ and $\delta\log(\kappa)$ denote respectively normalised spatial variations in well-core values of porosity and $\log(\text{permeability})$ over a well-core sequence.

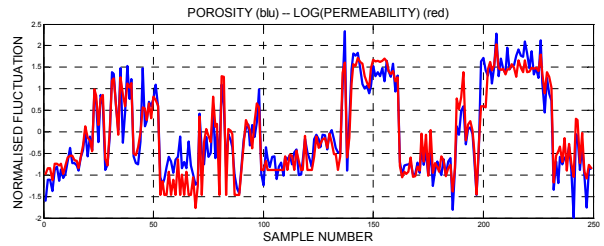


Figure 2: Overlay of poroperm fluctuation data for tight sandstone formations in the Cooper Basin, South Australia. The blue and red traces denote zero-mean/unit-variance fluctuations in, respectively, well-core porosity and the logarithm of well-core permeability. Cross-correlation of the two traces is 85% at zero-lag.

High degrees of spatial cross-correlation (3) are common in the abundant well-core poroperm sequences acquired for clastic reservoir sections. The cross-correlations have a natural explanation in terms of fluid percolation at grain-scale fractures. Consider a core-sized rock volume of N grain-grain contacts with intact cement bonding and no fluid percolation. Within the core, however, a number $n \ll N$ grain-grain contacts will have cement bonds ruptured by tectonic finite strain deformation, with geofluids able to percolate through the ruptured grain-grain contact. Neighbouring core volumes of N intact grain-grain contacts will vary in their number $n+\delta n$ of ruptured contacts, $\delta n \ll n$.

We know that, say, aquifer rock is permeable to fluids, and (1) tells us that grain-scale fractures probably influence rock properties on scales from cm to km, so it is reasonable to expect that percolation pathways exist across this scale range. We might thus expect that sample rock volumes have porosity variations in proportion to grain-scale density fluctuations, $\delta\phi \sim \delta n$, while variations in core permeability κ are related to the variation in combinatorial terms $n!$ and $(n+\delta n)!$ that measure the number of ways n and $n+\delta n$ percolation defects can be connected in percolation pathways, $\delta\log(\kappa) \sim \delta\log(n!)$. With this logic, the permeability variation terms evaluate as

$$\begin{aligned} \delta\log(\kappa) &\sim \delta\log(n!) = \log((n+\delta n)!) - \log(n!) \\ &= \log\left[\frac{(n+\delta n)!}{(n)!}\right] \\ &= \log[(n+\delta n)(n+\delta n-1)(n+\delta n-2)\dots(n+1)] \\ &\sim \delta n \log(n). \end{aligned}$$

If the defect density n doesn't vary much between well-core samples, and with $\log(n)$ varying much more slowly than n , we can normalise the factor $\log(n)$ out of the above expression to recover the empirical poroperm fluctuation relation (3) in form

$$\delta\log(n!) \sim \delta n. \quad (4)$$

Thus, if n is the number of percolating defects in a unit volume of rock and $n!$ is proportional to the percolation permeability of the rock sample with n percolation defects, then empirical relation (3) is effectively a mathematical identity, $\log(n!) = n(\log(n) - 1)$. The close equivalence of (3) and (4) argues that *in situ* permeability is a percolation process in rock volumes whose physical properties on all scale lengths are internally defined by spatially fluctuating populations of grain-scale defects consistent with power-law scaling of well-log spectra (1).

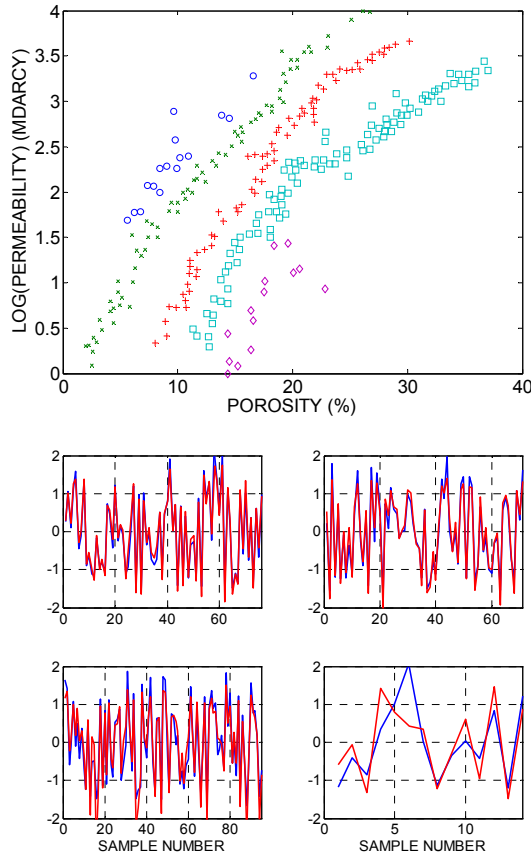


Figure 3: (Upper) Composite poroperm data as traditionally presented in oil and gas literature; a sequence of poroperm traces are sorted by grain size from coarser on left to finer on right. (Lower) Same poroperm data rendered in Figure 2 format; spatial fluctuation correlations between porosity and log(permeability) masked in upper display emerge in agreement with spatial fluctuation relations (3) and (4).

It may be useful at this point to contrast the multi-scale-length spatially-correlated fracture phenomenology of well-log fluctuations (1) and well-core empirical fluctuations (3) and fracture-fluctuation percolation interpretation (4) with the standard treatment of poroperm data in the oil/gas industry literature. With reference to empirical relation (3), the upper plot in Figure 3 shows standard industry presentation of poroperm data for a sequence of size-graded well-core (coarser grain samples on the left grade into finer grain

samples on the right). Inherent in this poroperm data presentation is the expectation that each sample is integral into itself, with no reason to suppose that the sample could be systematically related to neighbouring samples on any particular scale length (except, of course, by 'random' happenstance). The lower subplots of Figure 3 show, however, that latent in the poroperm data is the empirical poroperm spatial correlation (3). The subplots render four of the five upper-plot grain-size-graded poroperm data trends in the zero-mean/unit-variance sequence normalisation format of Figure 2. Spatial correlation (3) between porosity and log(permeability) emerges directly from the obscurity of the standard poroperm data presentation.

Again in line with the industry assumption that rock samples are only 'randomly' related to their neighbours, common oil industry practice uses a generic permeability dependence on porosity such as the Carman-Kozeny cubic expression (e.g., Dvorkin 2009; Cox et al 2001; Mavko & Nur 1997),

$$\kappa \sim \phi^3 \quad (5)$$

Poroperm dependency (5) is derived from estimates of tubular flow through clusters of pore space without reference to grain-scale fractures or fracture connectivity at any scale. Such formulations with reference only to the smallest scale lengths are consistent with spatially uncorrelated rock property heterogeneity (2) but, of course, make no contact with the essentially universal well-log observation (1) that *in situ* rock property heterogeneity is spatially correlated over five decades of scale length.

Well-log and well-core data thus provide clear lines of evidence that

1. small-scale (wellbore) sampling of permeability does not accurately assess large scale *in situ* permeability variability;
2. *in situ* fractures and fracture-controlled permeability on all scale lengths are an essential ingredient of crustal rock heterogeneity;
3. large amplitude *in situ* permeability heterogeneity is expected at large scale lengths.

Yarragadee well-core poroperm fluctuations

Applying the above argument to the Cockburn1 well data, Figure 4 shows the poroperm spatial fluctuation data for the complete Cockburn1 well-core suite in the Figure 2 format. Dotted data points in Figure 4 mark poroperm data for the Yarragadee aquifer within the Cockburn1 well sequence. In contrast with typical oil field reservoir well-core sample data tightly confined to short intervals of oil-bearing sands, many of the Cockburn1 well-core samples were taken at 100m to 200m intervals over which formation properties change significantly.

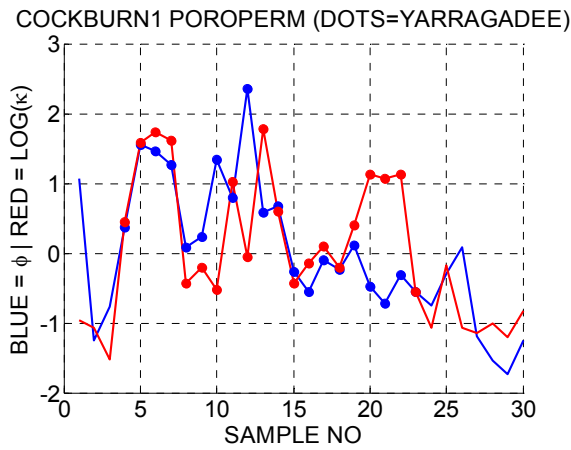


Figure 4: Cockburn1 well-core poroperm data sequence in Figure 2 format (blue = porosity, red = log(permeability) normalised to zero-mean/unit-variance). Compared with standard oil field reservoir poroperm fluctuations in, say, Figure 2, departures from close spatial correlation are due to well-core samples being taken at 100m intervals in varying formations.

Despite the far more variable nature of the Cockburn1 well rock-type and formation-type poroperm sampling, Figure 5 shows 60% zero-lag spatial correlation (red trace) between variations in Cockburn1-well sample porosity and sample log(permeability). The blue trace indicates the typical 20% level of cross-correlation excursion of spatially-uncorrelated fluctuation sequences with spectral content of the Cockburn1 poroperm data. The 60% Cockburn1 data cross-correlation peak at zero-lag is statistically significant.

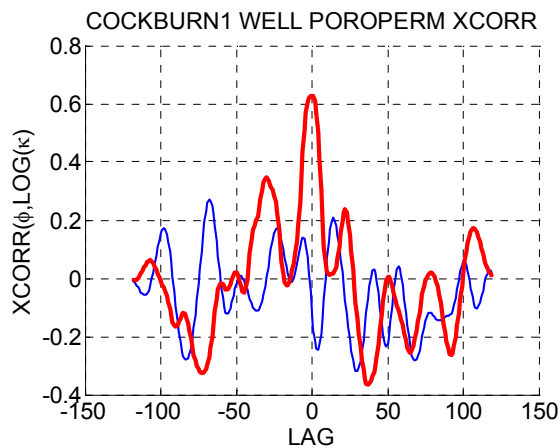


Figure 5: (Red) Cross-correlation of resampled Cockburn1 well-core poroperm data sequences. (Blue) Cross-correlation of uncorrelated random sequences with frequency content of well-core poroperm data; 60% correlation between poroperm sequences at a specific lag (here zero) is seen to be statistically significant.

Fracture heterogeneity and hot aquifer energy production

The foregoing discussion challenges the oil/gas industry reservoir characterisation assumption that spatially sparse wellbore samples more or less represent geological formation properties at all larger scale lengths. Plentiful well-log and well-core data instead point to *in situ* percolation flow processes controlled by spatially-correlated random fracture networks on all scale lengths. Such random fracture networks are spatially erratic and effectively unpredictable from small-scale sparse sampling, leading to a degree of geofluid flow spatial heterogeneity consistent with the statistics of production well drilling success. The following quote assesses the success rate of drilling geothermal wells at one half the success rate of drilling oil/gas wildcat wells:

Given the extremely high degree of uncertainty involved in well siting and design, hydrothermal exploration success rates are around 25%, estimates the GEA. That compares with a worldwide oil wildcat success rate of 45% in 2003, according to IHS Energy, a consultancy. (Petroleum Economist 2009),

While a number of factors affect both production well success/failure rates, two factors stand out:

- oil and gas are far more energy rich than hot water;
- to be profitable oil and gas do not have to come of out the ground at high flow rates but hot water does.

With the chemical energy of oil about 50MJ per litre, and long-term oil field production average rate ~1 litre per 4 seconds (~15 barrels of oil per day for ~5x10⁵ US wells for years 1954-2006, www.eia.doe.gov/aer/txt/ptb0502.html), wellhead power production for a typical oil well is of order 12MW. In contrast, a geothermal well discharging N litres per second of water with ΔT°C excess temperature produces about 4xNxΔT/1000 MW of thermal power. For ΔT = 100°C, it requires N ~ 25 litre/s to produce 10MW of thermal power. For equal wellhead power production, a geothermal well flow rate must thus be of order 100 greater than an oil well.

Translating geofluid flow rate into dollar-rate to cover drilling costs, and taking into account the different efficiencies of electrical power production, a geothermal well must flow on order 300 times greater rate to produce an income equivalent to pure oil recovery. Allowing for production of water as well as oil, 90% water cut requires a geothermal well to flow effectively 30 times the rate of its oil equivalent for comparable income to cover drilling costs.

These contrasting order-of-magnitude well-flow-rate numbers for hydrocarbon and geothermal power production make it clear that effective geothermal production well siting demands understanding the potential for flow heterogeneity of the target formation. It is not surprising that the global success rate for geothermal production well success is one half that of hydrocarbon wildcat wells. Within a developed hydrocarbon reservoir, the rate of infill drilling success is probably substantially higher than wildcat well success, giving all the more reason to be cautious about adopting oil field practices regarding aquifer permeability distributions.

To make aquifer energy production commercially viable, physical logic and practical experience indicate that close attention needs to be paid to finding aquifer volumes of sufficient size and fracture density that production wells can cover their cost. To that end, we discuss several surveys of producing geothermal fields in which:

- MT data identified reservoir volumes of significant aligned fracture density;
- production wells drilled in the MT-identified aligned-fracture reservoir volumes had flow rates far exceeding the field average.

An MT approach to sounding for large-scale aquifer fracture structures

Magnetotellurics (MT) is the practice of measuring the natural magnetic field fluctuations of the earth's atmosphere as they reach the earth's surface, and at the same time and place measuring electric (telluric) currents induced by the travelling magnetic fields. By measuring the natural magnetic and induced electric fields over a wide range of temporal frequencies (as high as 1-10kHz to as low as 0.1mHz), the electrical conductivity of the earth at a specific site can be inferred as a function of electromagnetic wave depth penetration.

An important aspect of MT data is that the measurements can register systematic amplitude differences in electrical currents running along fracture trends versus electrical currents running across fracture trends. Since currents move more easily along fracture trends, the earth appears more conductive (less resistive) along fracture trends, and less conductive (more resistive) across fracture trends. MT surveys, thus, are sensitive to a dual phenomenology closely relevant to fluids and fractures:

- over a range of (x,y) coordinates a sequences of MT stations can seek out zones in which electrical currents flow better in one direction than they do in the orthogonal direction;
- the same MT data can reveal the approximate depth to the current-flow directional anomalies by noting at which

MT field frequencies the anomalies first occur.

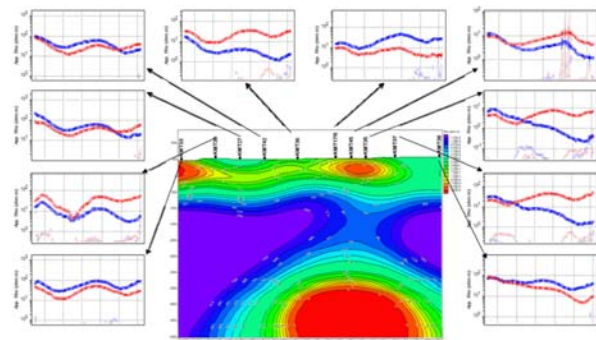


Figure 6: Summary of 5km MT traverse of Krafla, Iceland, geothermal field. Central figure is deduced resistivity profile beneath the survey traverse. Peripheral plots are resistivity depth profile data in the form of measured MT field resistivity versus MT field wavelength. Red curves denote data for electric currents along the traverse, blue curves data for electric currents across the traverse. Left ends of resistivity curves are for shorter wavelengths (shallower depths), right ends for longer wavelengths (deeper depths). Divergence of blue/red curves interpreted as evidence that current-carrying aligned fractures run in/out of the section plane, with fractures concentrated in the volume denoted by the red oval at the base of the crustal section.

Figures 6-7 illustrate the dual phenomenology of fracture-related MT surveys over a 5km crustal volume enclosing the Krafla geothermal field of central Iceland (Malin et al 2009; Onacha et al 2010). The Krafla field sits astride the NE-SW-trending mid-Atlantic rift system as it passes through central Iceland. Figures 6-7 show that the geothermal activity along the rift system is greatest where a shallow NW-SE trending tectonic fault system intersects the NE-SW rift trend.

The MT surveyed Krafla crustal volume partitions into more resistive rock represented as cold colours and more conductive rock represented as warm colours. MT surveys across the volume return paired sequences of resistivity versus depth profile displayed as blue and red curves for each MT station. The red curve measures the resistivity profile parallel to the MT traverse; the blue curve measures resistivity normal to the traverse.

Figure 6 summarises a rift-parallel SW-NW (left-right) MT traverse of the Krafla crustal volume. The leftmost survey station resistivity profile is shown in the lower-left panel. The blue and red MT profile curves do not diverge significantly as MT wavelength increases from left to right (shallow data register at left end of curve, deep data register at right end of curve). A lack of systematic divergence between blue and red resistivity profile curves persists over the next three MT stations moving clockwise from the

lower-left panel. When, however, the MT survey moves to the vicinity of the deep conductivity anomaly represented as the red oval at depth in the crustal section, the red and blue resistivity curves begin to diverge with increasing MT signal wavelength. Relative to the electrical current flowing in the plane of the traverse (red curve), the current flow in/out of the traverse plane increases, hence the effective resistivity drops (blue curve). Except for the next station (presumably affected by the near-surface low resistivity red zone), the blue-curve-lower-than-red-curve resistivity profile relation persists through the succeeding four survey stations, thus establishing the existence of the buried red oval high conductivity structure. This structure, given by the blue resistivity profiles, defines a NE-SW trending fracture/fault system intersecting the rift-oriented NE-SW traverse plane.

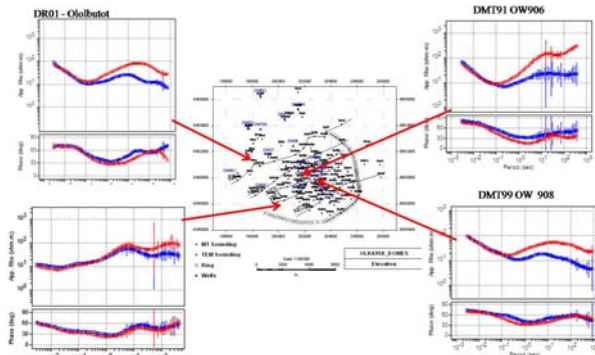


Figure 7: Map MT station resistivity depth profile distribution for the Krafla, Iceland, geothermal field as in Figure 6. The upper-left and right-hand resistivity profiles show that electrical currents travelling NW-SW are strong along the MT station sequence line, while the lower-left resistivity profile shows that away from the NW-SE line the NW-SE electrical currents are reduced. By inference, the 3-station line locates a local fracture/fault trend; in the Krafla geothermal field this line collocates with a known tectonic fracture trend.

Figure 7 displays the Figure 6 resistivity phenomenology for a map distribution of MT stations. The NW-SE trend of 3 upper-left + right-hand resistivity profile panels defines the fracture trend seen as the red high-conductivity feature at depth in Figure 6. For each of the 3 MT stations, the blue resistivity curve diverges strongly from the red curve, indicating enhanced ability to carry current along the NW-SE trend. In contrast, the lower-left MT station sees significantly smaller resistivity profile divergence, implying that at depth at this location there is much reduced fracture alignment to carry electrical currents at depth. Geologically, the 3-station NW-SE MT station trend in Figure 7 collocates with a known regional fault system normal to the NE-SW trending rift system.

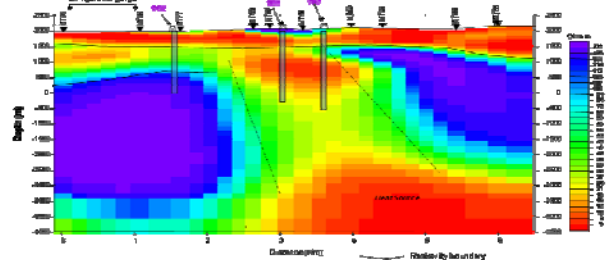
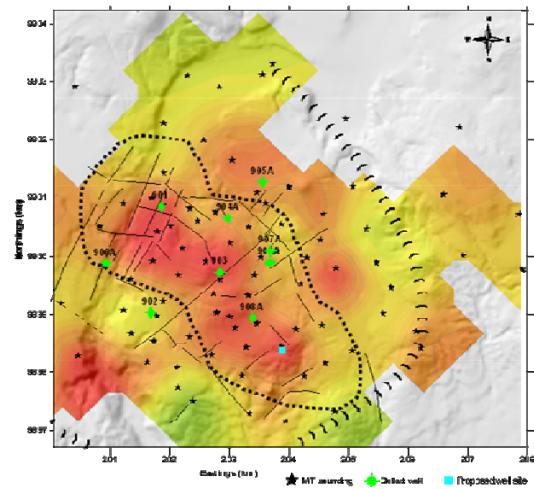
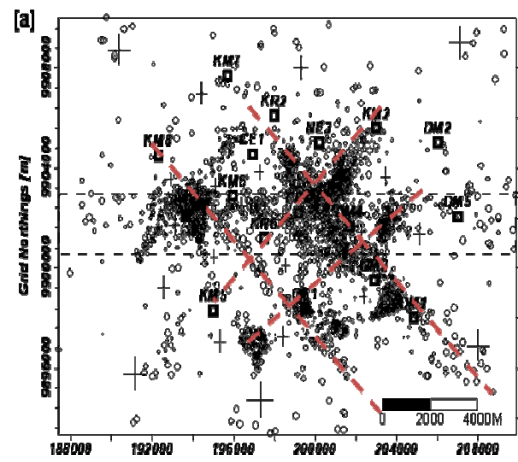


Figure 8: (Upper) Seismicity at the Olkaria, Kenya, geothermal field; the NE-SW trends lie along the East Africa Rift; the NW-SE trends lie along a local tectonic fault feature; (centre) MT resistivity distribution summary in which red/yellow tints denote areas of high/low electrical conductivity for the NW-SE aligned fractures; (lower) production well history along NE-SW rift trend, with lefthand well in yellow tint zone a poor producer and righthand wells in red tint zone well above average producers.

The three parts of Figure 8 summarise a similar fault-intersection phenomenology observed in the Olkaria, Kenya, East Africa rift system geothermal field (Simiyu & Malin 2000; Onacha et al 2009). The upper plot of Figure 8 seismically defines two fault trends, the NE-SW trend along the rift, and the NW-SE trend along a locally defined tectonic fault. The centre plot is a

composite rendering of MT survey data in which red tints mark MT sites for which NW-SE rift-normal electrical currents are strong while yellow tints mark MT sites where such electrical currents are weak. The lower plot summarises the production well history: the lefthand well drilled in the yellow-tinted MT zone is a poor producer, while the two righthand wells drilled in the red-tinted MT zone produce at double to triple the field average production rate.

Summary/Conclusions

We argue:

- well-log and well-core systematics show that fracture systems are important, perhaps (probably?) crucial, conduits for geofluid flow on all scales in all rock, with particular reference to aquifer rock currently targeted for heat extraction;
- power-law scaling well-log spectra indicate that small-scale rock samples fundamentally do not represent the range of rock property fluctuations likely to occur at large scale lengths;
- in absence of utility from small-scale sampling of rock properties, and in light of essentially unlimited fluctuations in rock properties on large scales, it is logical to consider large scale sampling of rock formations for information on *in situ* permeability;
- large scale measurements of fracture distributions are particularly relevant where geofluid flow rates are essential to drill hole success;
- in geothermal fields, where fractures are almost universally acknowledged to control geofluid flow, MT resistivity profiles indicate that geofluid flow is greatest where known fracture/fault trends intersect; enhanced production well flow has validated MT data as a geophysical guide to well siting.

We conclude from these arguments that MT surveys of potentially exploitable hot aquifers are a plausible investment in advance of costly drilling.

References

Clauser C, Marquart G, Rath V & MeProRisk Working Group (2010) MeProRisk – a Tool Box for Evaluating and Reducing Risks in Exploration, Development, and Operation of Geothermal Reservoirs, World Geothermal Congress, Bali April25-30 2010.

Crude Oil Production and Crude Oil Well Productivity, 1954-2008
www.eia.doe.gov/aer/txt/ptb0502.html

de Graaf L, Palmer R & Reid I (2010) The Limestone Coast Geothermal Project, South

Australia: a Unique Hot Sedimentary Aquifer Development, World Geothermal Congress, Bali April25-30 2010.

Dvorkin J (2009) Kozeny-Carman equation revisited, pangea.stanford.edu/~jack/KC_2009_JD.pdf

Leary P (2002) Fractures and physical heterogeneity in crustal rock, in Heterogeneity of the Crust and Upper Mantle – Nature, Scaling and Seismic Properties, J. A. Goff, & K. Holliger (eds.), Kluwer Academic/Plenum Publishers, New York, 155-186.

Leary PC & Walter LA (2008) Crosswell seismic applications to highly heterogeneous tight-gas reservoirs, Special Topic on Tight Gas, First Break 26, 33-39.

Malin P, Leary P, Shalev E & Onacha S (2009) Joint Geophysical Imaging of Poroperm Distributions in Fractured Reservoirs, GRC Transactions, Vol. 33, 4-7October 2009

Mavko, G., and Nur, A., 1997, The effect of a percolation threshold in the Kozeny-Carman relation, Geophysics 62, 1480-1482.

Onacha S, Shalev E, Malin P, & Leary P (2009) Joint Geophysical Imaging of Fluid-Filled Fracture Zones in Geothermal Fields in the Kenya Rift Valley, GRC Transactions Vol. 33, 4-7October 2009

Onacha S, Shalev E, Malin P, Leary P & Bookman L (2010) Interpreted Fracture Anomalies: Joint Imaging of Geophysical Signals from Fluid-Filled Fracture Zones in Geothermal Fields, Proceedings World Geothermal Congress, Bali, Indonesia, 25-29April 2010

Petroleum Economist (2009) Unlocking the value of the world's geothermal resources, www.petroleum-economist.com

Simiyu S & Malin P (2000) A "volcano seismic" approach to geothermal exploration and reservoir monitoring: Olkaria, Kenya and Casa Diablo, U.S.A. World Geothermal Congress 2000, Kyoto-Tohoku Japan, 1759-1763.

Smith DN (1967) Well Completion Report Cockburn No. 1 Well, Western Australia, West Australian Petroleum Pty. Ltd

Vogt C, Mottaghy D, Rath V, Wolf A, Pechinig R & Clauser C (2010) Quantifying Uncertainty in Geothermal Reservoir Modeling, World Geothermal Congress, Bali April25-30 2010.

Automatic Meshing and Construction of a 3D Reservoir System: From Visualization towards Simulation

Yan Liu¹, Huilin Xing^{1,*}, Zhenqun Guan² and Hongwu Zhang²

¹ Earth Systems Science Computational Centre (ESSCC), The University of Queensland, St. Lucia, QLD 4072, Australia;

² Department of Engineering Mechanics, State Key Laboratory of Structural Analysis of Industrial Equipment, Dalian University of Technology, Dalian, China

*Corresponding author: xing@esscc.uq.edu.au

Finite Element Method (FEM) Geocomputing is increasingly important in analysing and evaluating enhanced geothermal reservoirs. Due to the complexity of geological objects, it is difficult to build a reasonable mesh for FEM. The development of digital 3D geological modelling tools and applications (such as GeoModeller and GoCad) makes it possible to establish geometric models for 3D geological objects. Our work focuses on constructing a geothermal reservoir system which transforms geometric models used in 3D geological visualization into FEM models. A 3D Geological model for visualization is used as input here, and the transformation processes are implemented following: (1) generating a tetrahedral mesh by 3D Delaunay triangulation methods; (2) abstracting boundaries of different geological objects; (3) building a well model by tetrahedral mesh refinement, which will be used in future FEM-based simulations.

Keywords: GeoModels; Delaunay Triangulation; 3D geological modelling; FEM

1. Introduction

In the field of geoscience, modelling of geological objects is of great interest in visualization and simulation. With the development of digital 3D geological modelling applications (such as GeoModeller and GoCad), 3D geological objects including geological units, faults and ore deposits can be easily built into GeoModels. However, these GeoModels are mainly used for visualization, and lack topological relations which are crucial in simulation. Topological query [1-3] is a common issue which depends on topological relations between different geological objects. Furthermore, in the field of analysing, topological models which are suitable for simulating are urgently requested. The Finite Element Method (FEM), which is based on the FEM mesh, is an effective means of geocomputing. Whenever 3D geological objects are transformed into an FEM mesh such as a tetrahedral or hexahedral grid, FEM can be employed to present simulations for future analysing and evaluating. 3D Delaunay triangulation (DT) [4, 5] is one well studied 3D tetrahedral mesh generation method, which can be utilized to transform geometric geological

models into FEM ones. Recently, regarding to DT, scientists [1, 6, 7] have worked on modelling geological objects innovatively. Ledoux [6] used the dual of DT named Voronoi Diagram (VD) to represent and analyze oceanographic datasets. Ledoux [7] also compared the VD-based method with geographical information systems (GIS) and outlined shortcomings of GIS and merits of the VD approach. Pouliot [1] used DT to build topological relationships between geological objects.

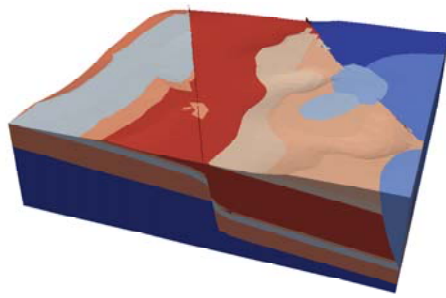
Our work focuses on constructing a geothermal reservoir system by transforming geometric geological models into a FEM mesh which will be utilized in simulation by FEM. Generally speaking, the output of geological modelling tools can be formed into a set of triangles which respect the geometric profiles of geological objects. Taking these triangular surfaces as input, our transformation process is outlined as below: In section 2, automatic DT mesh generation based on 3D geological modelling data, including boundary abstraction of different geological objects. In section 3, one of the geological objects is chosen to illustrate how to build a well model based on tetrahedral mesh refinement, and a boundary condition will be introduced for FEM in future analysing. Finally, conclusion and further work are discussed in section 4.

2. Topological modelling for 3D geological objects

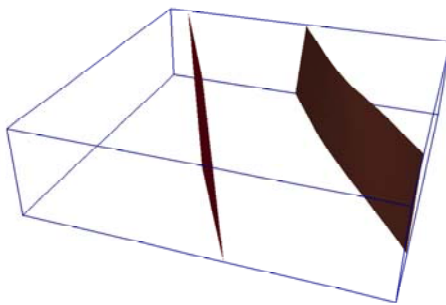
2.1 3D geological objects data input and refinement

In this paper, we choose outputs of software such as GeoModeller and GoCad as input data. It is a set of geological objects, including two faults through different geological units, as illustrated in figure 1. The model data are in the format of a set of triangular facets which respect boundaries of different geological objects. At the beginning of this file, node coordinates are provided. And then boundary triangular facets are presented by the indexes of nodes.

To demonstrate the effectiveness of refining boundaries of the geological model, a geological unit with large area but small thickness from our geological model is chosen to present our approach, as illustrated in figure 3 (a). After performing boundary refinement on it, large triangular facets are broken into small pieces; meanwhile, nodes on its boundaries are dense enough to represent its geometric feature in 3D geological space, as shown in figure 3 (b).



(a)



(b)

Figure 1: Geological model from Geomodeller: (a) the whole model; (b) two faults in geological space

As our approach to extracting boundaries between different geological objects is based on density of boundary nodes, the geological model should have a set of reasonable discretized nodes on its boundaries. In other words, nodes used to represent boundaries of the geological model should have a specified distance ϵ between each other. This distance ϵ is defined as the precision of our transforming process.

The Edge-splitting method, which breaks a triangular edge into two subordinate ones, is employed to refine the initial geological model boundaries. It is simple but effective, as illustrated in figure 2. The middle point P of Edge AB is introduced to split AB into two edges AP and PB. And then triangles linked with AB are separated into two triangles respectively.

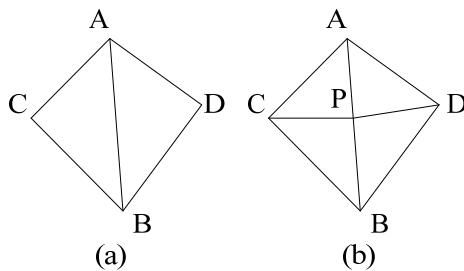
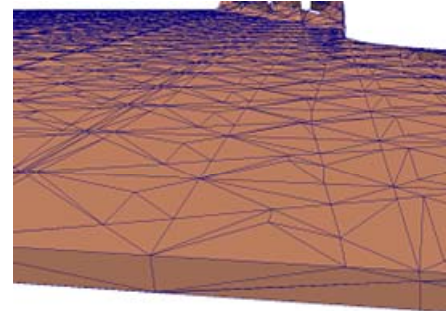
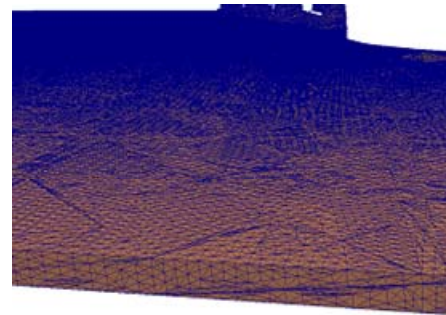


Figure 2: Edge-splitting method: (a) before splitting; (b) after splitting



(a)



(b)

Figure 3: Refinement of geological object boundaries: (a) before refining; (b) after refining.

2.2 3D Delaunay triangulation

After refining the boundaries of the geological model, nodes on boundaries appear with a reasonable density due to a specified ϵ . In order to distinguish different parts of the geological model and construct a topological model for FEM, a tetrahedral generation method should be presented on the current boundary nodes of the geological model. Because nodes that are close to each other (which respect model boundaries) are expected to construct tetrahedrons, then the Delaunay triangulation method is adopted to generate the tetrahedral mesh for the geological model.

First of all, the definition of Delaunay triangulation is introduced below:

Let $\{P_k\}$ be a set of points in R^d . The Voronoi cell of P_k is V_k defined by

$$V_k = \{p : \|p - P_k\| \leq \|p - P_j\|, j \neq k\}$$

$\{V_k\}$ forms the well-known Voronoi Tessellation of the entire domain concerning $\{P_k\}$. The Delaunay triangulation of $\{P_k\}$ is defined as the dual of the Voronoi Tessellation; it was presented in 1930 by Delaunay, who found the property of empty circumsphere criterion. In the 3D domain, the empty circumsphere criterion can be presented as below: for every tetrahedron there are no vertices in its circumsphere except for the four vertices of its own. Then in 1981, Bowyer[4] and Watson [5] proposed a method of this algorithm, which is simple and efficient. The kernel of this method is inserting points step by step. In order to keep the empty circumsphere criterion, correct the topology of the mesh after inserting a point. Algorithm 1 shows the basic procedures of this method used in this paper.

Algorithm 1: Classical 3D Delaunay triangulation

- Step 1: Construct a super tetrahedron, which contains all points prepared to be inserted. This super tetrahedron bounds a convex domain.*
- Step 2: Insert a point into this convex domain, and extract all the tetrahedrons violating the empty circumsphere criterion.*
- Step 3: Delete tetrahedrons extracted in Step 2, which leads to construction of a convex cavity. Use the inserted point to generate tetrahedrons with the surface of this cavity.*
- Step 4: Repeat Steps 2-3 until all the points are inserted.*

2.3 Abstraction boundaries from different geological objects

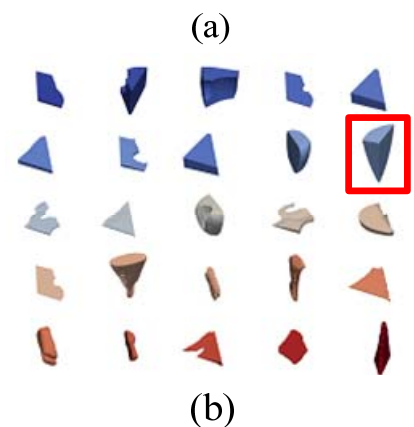
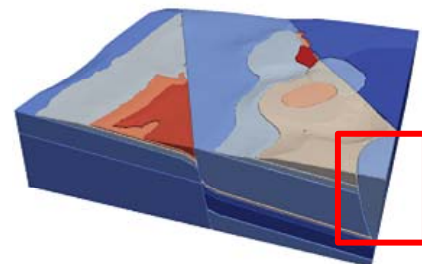
As 3D DT tends to generate tetrahedrons by nodes close to each other, most of the triangular geological surfaces will construct naturally during the process of DT. Mark facets which do not have any edges longer than ϵ (which is specified in section 2.1) boundaries. And then use Algorithm 2 to abstract boundaries of different geological objects.

Algorithm 2: Abstraction of geological object boundaries

- Step 1: Roughly abstract geological objects in the form of tetrahedrons by facets which are marked as boundaries.*

- Step 2: Allocate each geological object a universal 'colour', and calculate its volume by its components (tetrahedral elements).*
- Step 3: Sort geological objects by their volumes in an increasing order.*
- Step 4: Extend geological objects to their neighbours one by one, merging the gap generated by boundary facets.*
- Step 5: Abstract facets shared by tetrahedrons with different colours.*

In our geological sample, due to two faults, after abstraction the whole model (as illustrated in figure 4 (a)) is separated into 25 components (in figure 4 (b)), and colours of geological objects are updated, so they appear with colours different from original ones. Boundaries between different components have a abstracted in the form of triangular facets which contain topological relationship information. Because the number of boundary triangular elements is too huge to visualize clearly, only one of the 25 components which is a corner of the geological model is illustrated in the format of triangular boundary, as shown in figure 4 (c). Furthermore, two faults break the geological model into three blocks, as shown in figure 4 (d) (e) and (f), which is useful for further simulation and analysing. With the help of the topological model generated above, different geological objects can be easily identified and the generated tetrahedral mesh is an ideal model for FEM-based simulation.



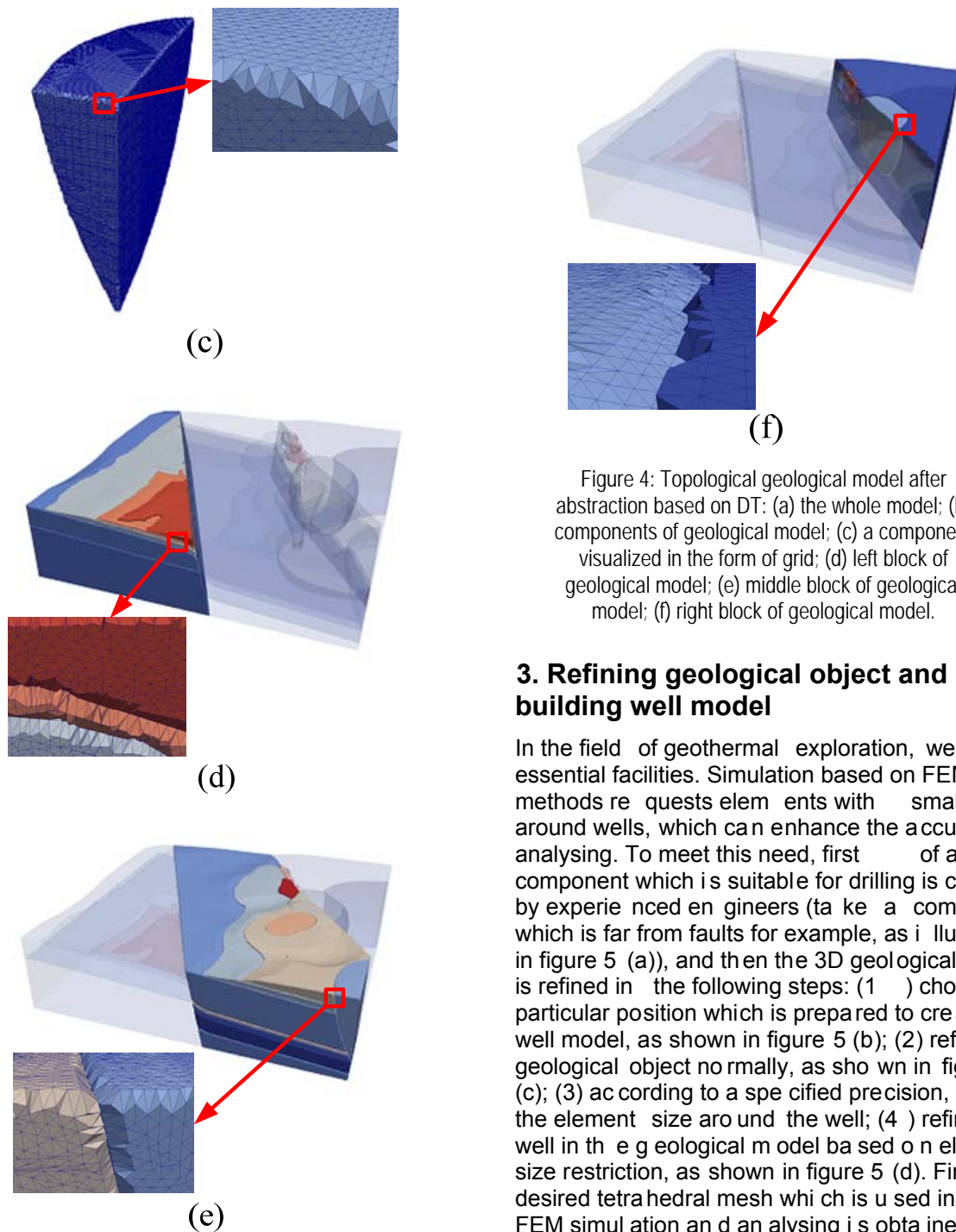
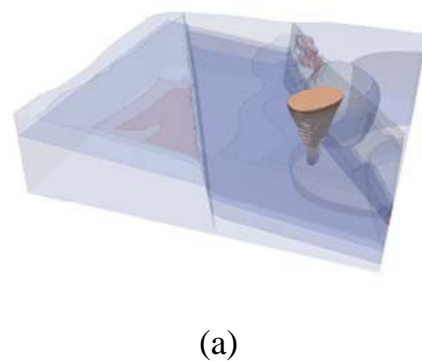


Figure 4: Topological geological model after abstraction based on DT: (a) the whole model; (b) components of geological model; (c) a component visualized in the form of grid; (d) left block of geological model; (e) middle block of geological model; (f) right block of geological model.

3. Refining geological object and building well model

In the field of geothermal exploration, wells are essential facilities. Simulation based on FEM methods requests elements with small size around wells, which can enhance the accuracy of analysing. To meet this need, first of all, a component which is suitable for drilling is chosen by experienced engineers (take a component which is far from faults for example, as illustrated in figure 5 (a)), and then the 3D geological model is refined in the following steps: (1) choose a particular position which is prepared to create the well model, as shown in figure 5 (b); (2) refine the geological object normally, as shown in figure 5 (c); (3) according to a specified precision, restrict the element size around the well; (4) refine the well in the geological model based on element size restriction, as shown in figure 5 (d). Finally, a desired tetrahedral mesh which is used in future FEM simulation and analysing is obtained, and the local tetrahedral mesh is illustrated in figure 5 (e)



4. Conclusion and future work

In this paper, automatic meshing and construction of a geothermal reservoir system is proposed, which focuses on transforming geometric models into an FEM mesh. In order to make a general interface between geological softwares (such as Geomodeler and GoCad) and the geothermal reservoir system, the input data are designed in the form of a set of triangles which presents the geometric features of the geological model. Then in the process of transforming, input data refinement, tetrahedral mesh generation and geological objects boundaries abstraction are performed step by step, which focuses on generating a reasonable FEM mesh. Finally, the well model used in geothermal exploration is introduced; automatic mesh generation for it is demonstrated in detail. Our approach presents a way of using geological data for visualization to construct an FEM mesh for geothermal simulation.

Further works should be done to enhance the approach proposed in this paper: in the first place, instead of a specified precision ϵ , boundary abstraction should be improved to adaptively detect small features on geological models; in the second place, as geological models have been divided into several parts, both parallel mesh generation and FEM analysis should be considered.

Acknowledgements

Support is gratefully acknowledged by Australian Research Council through ARC Discovery project DP0666203, ARC Linkage International LX0989423 and ARC Linkage project LP0560932 with collaboration of Geodynamics Limited. The authors are grateful to Helen Gibson of Intrepid Geoscience for creating the 3D geological model with Geomodeler which used as the input data in this paper.

References

Pouliot, J., et al., Reasoning about geological space: Coupling 3D GeoModels and topological queries as an aid to spatial data selection. Computers & Geosciences, 2008. 34(5): p. 529-541.

Apel, M., From 3d geomodelling systems towards 3d geoscience information systems: Data model, query functionality, and data management. Computers & Geosciences, 2006. 32(2): p. 222-229.

James, W., et al., ADVISER: Immersive Scientific Visualization Applied to Mars Research and Exploration. Photogrammetric Engineering & Remote Sensing, 2005. 71(10): p. 1219-1225.

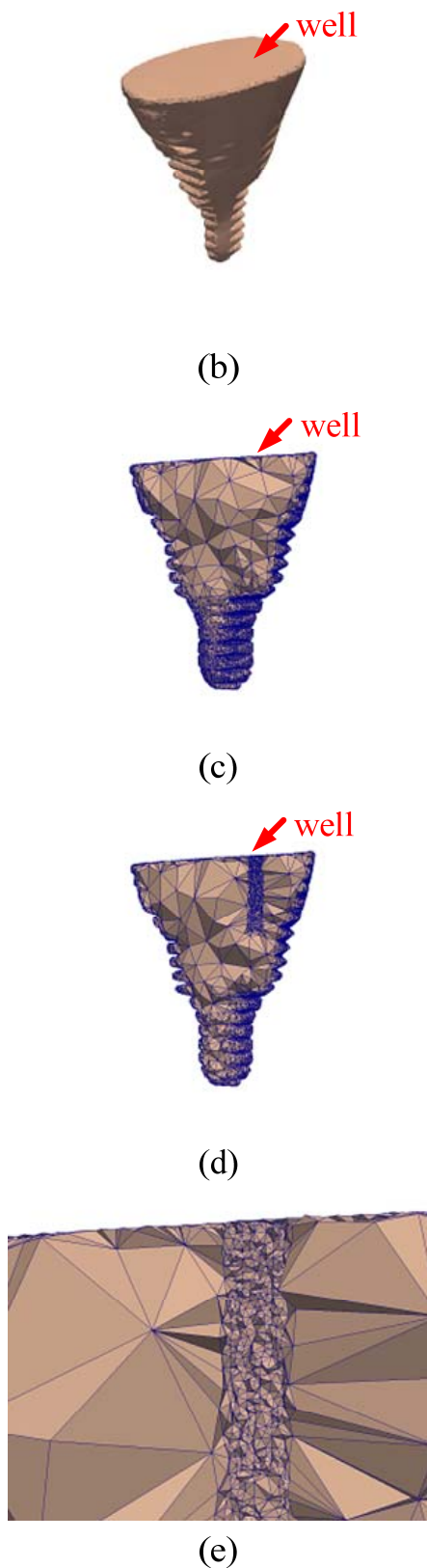


Figure 5: Building well model on particular geological object for FEM analysing: (a) choosing geological object; (b) well location; (c) refining geological object; (d) building well model; (e) local tetrahedral elements for well.

Bowyer, A., Computing Dirichlet tessellations. *The Computer Journal*, 1981. 24(2): p. 162-166.

Watson, D. F., Computing the n-dimensional Delaunay tessellation with application to Voronoi polytopes. *The Computer Journal*, 1981. 24(2): p. 167-172.

Ledoux, H. and C.M. Gold. A Voronoi-based map algebra. in *Spatial Data Handling—12th International Symposium on Spatial Data Handling*. 2006: Springer.

Ledoux, H. and C.M. Gold, Modelling three-dimensional geoscientific fields with the Voronoi diagram and its dual. *International Journal of Geographical Information Science*, 2008. 22(4-5): p. 547-574.

Targeting Faults for Geothermal Fluid Production: Exploring for Zones of Enhanced Permeability

Luke Mortimer^{1,2}, Adnan Aydin³ and Craig T. Simmons²

¹Hot Dry Rocks Pty Ltd, PO Box 251, South Yarra, Victoria 3141

²National Centre for Groundwater Research and Training, Flinders University, GPO Box 251, Adelaide, South Australia 5100

³Department of Geology and Geological Engineering, University of Mississippi, PO Box 1848, MS 38677, USA
luke.mortimer@hotdryrocks.com

Fault structures can potentially deliver increased geothermal fluid production by boosting the bulk permeability and fluid storage of a production zone. However, the hydromechanical properties of faults are inherently heterogeneous and anisotropic, thereby, making it challenging to distinguish between permeable and impermeable faults. This discussion paper outlines the key features that determine fault permeability and how the probability of locating zones of enhanced fault permeability can be derived from preliminary fault stress state modelling. It is proposed that preliminary fault stress state modelling for early stage exploration projects or in areas of unknown or complex geology can reduce the uncertainty and risk of exploring for fault-related geothermal targets.

Keywords: geothermal, exploration, fault, permeability, *in situ* stress, hydromechanical modelling.

Introduction

Permeable fault structures present an attractive geothermal exploration target as faults have been proven to boost substantially reservoir permeability and fluid production at some existing geothermal energy operations (e.g. Dixie Valley, USA; Landau, Germany). However, not all faults are permeable. Their hydraulic properties are inherently heterogeneous and difficult to characterize, making it challenging to distinguish between faults acting as fluid conduits and fluid barriers. This challenge is compounded when a fault has no surface expression because to achieve sufficiently high production fluid temperatures a fault typically must be intersected at some depth where the exact hydraulic character of the fault is unknown prior to drilling. Therefore, if exploring for permeable fault structures the key questions are: (1) which fault or fault segment has the highest probability of being permeable?; and (2) what information is required to reduce the uncertainty and exploration risk prior to drill testing? To help answer these questions the main objectives of this discussion paper are to describe the key features that determine fault permeability and how the probability of locating zones of enhanced fault permeability may be derived from preliminary fault stress state

modelling. For illustrative purposes, hypothetical examples of preliminary fault stress state models are provided.

Targeting fault structures involves exploring at depth for zones of enhanced natural *in situ* fracture porosity and permeability to maximise geothermal fluid production from a prospective area. A permeable fault target can be viewed as either: (1) having sufficient natural *in situ* porosity and permeability with natural fluid recharge occurring at the optimal fluid temperature (e.g. Dixie Valley, USA); or (2) as a zone of enhanced porosity and permeability that may still require some degree of reservoir stimulation (e.g. Landau, Germany).

Two critical elements considered positive for fault permeability targets are:

- (1) Favourable fault orientation with respect to the *in situ* stress field (i.e. 'critically stressed'); and
- (2) Hydraulic contact with a significant volume of porous/fractured and permeable reservoir (i.e. fluid mass storage).

For the latter, the fluid mass storage may be provided by the fault structure itself or an adjoining and hydraulically connected rock unit such as thick, porous sandstone. Fluid overpressures associated with the fault may also be beneficial for fluid advection along the structure from a connected, deeper and potentially hotter reservoir and for lowering the effective stress state of the fault.

Fault Architecture and Hydrogeology

The architecture of a fault structure can vary greatly in form from simple faults where strain is accommodated along a narrow plane to more complex structures where strain is distributed over a composite zone that may include numerous faults, small fractures, veins, breccias and cataclastic gouge. Generally, fault structures are subdivided into two simple components being the fault core and the fault damage zone both of which may vary over widths ranging from centimetres to hundreds of metres (Figure 1; Caine and Forster, 1999; Gudmundsson *et al.*, 2009). These two components are distinguishable by their distinct mechanical and hydrogeological properties although these are inherently heterogeneous and can vary significantly along a fault. The fault core refers to the main fault plane that takes up most of the displacement and where

the original lithology has been altered through fault-related processes such as grain size reduction, hydrothermal alteration and mineral precipitation in response to mechanical and fluid flow processes (Caine and Forster, 1999). The character of the fault core zone is strongly dependent on its protolithology (Caine and Forster, 1999). Fault damage zones are defined as the adjacent network of subsidiary structures including small faults, fractures, veins, cleavage, pressure solution seams and folds that laterally decrease in density away from the fault core zone (Figure 1; Caine and Forster, 1999; Gudmundsson *et al.*, 2009)

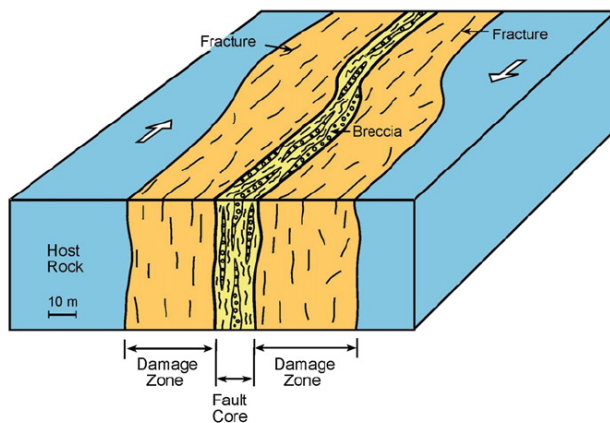


Figure 1. Illustrative schematic diagram of a fault including its fault core and damage zone. From Gudmundsson *et al.* (2009).

The permeability of faults can vary considerably ranging from impermeable flow barriers to significant flow conduits with a high degree of spatial heterogeneity and anisotropy. Generally, faulting in low porosity, competent rock is expected to result in an increase in fault zone permeability whilst faulting in high porosity sedimentary rocks may lead to a general decrease in fault zone permeability through comminution and porosity reduction processes such as grain-size reduction and the formation of clay-rich fault gouge and deformation bands (Zoback, 2007; Wong and Zhu, 1999). Commonly, fault cores are of a relatively lower permeability than their associated damage zones, which is attributed to porosity reducing processes occurring within the cores (Caine *et al.*, 2010). For example, at the Mirrors site, Dixie Valley geothermal field, measured core plug permeabilities ranged from 10^{-8} m^2 (10^7 mD) in fault damage zones to 10^{-20} m^2 (10^{-8} mD) in fault cores, however, the bulk permeability of the fault zone is on the order of 10^{-12} m^2 (1000 mD) (Caine and Forster, 1997; Seront *et al.*, 1998). In terms of anisotropy, the permeability tensor is expected to be at a maximum parallel to the fault, intermediate down dip of the fault plane and at a minimum

perpendicular to the fault, which allows for both vertical and lateral flow but may limit cross-fault flow (Ferrill *et al.*, 2004). Faults of sufficiently high permeability can also contribute significantly to both local and regional scale coupled groundwater flow and heat transport via advection/convection processes (e.g. Bachler *et al.*, 2003).

Stress-Dependent Fault Permeability

Stress acting on a fault plane can be resolved into normal and shear stresses, which are the components of stress that act normal and parallel to a plane, respectively. In nature, these stresses are highly coupled and can cause faults to undergo reactivation and deform. The link between stress, fracture deformation and permeability is such that as fracture void geometries and the connectivity of a flow network change in response to changing *in situ* stress, the storage, permeability and flow pattern is also expected to change in magnitude, heterogeneity and/or anisotropy. Fracture deformation can result in significant changes in permeability and storage because the ability of a fracture to transmit a fluid is extremely sensitive to its aperture. For example, the transmissivity of an individual fracture (T_f) idealised as an equivalent parallel plate opening can be expressed as:

$$T_f = \frac{(2b)^3 \rho g}{12\mu} \quad (1)$$

Where $2b$ is the fracture aperture width (m), ρ is the fluid density (kg.m^{-3}), g is gravitational acceleration (m.s^{-2}) and μ is the dynamic viscosity of the fluid ($\text{kg.m}^{-2}.\text{s}$).

One key aspect of exploring for permeable faults is the theory of stress-dependant fracture permeability in deep-seated, fractured rocks. This theory is supported by studies relating to hydrocarbon and geothermal reservoirs and potential nuclear waste repository sites (e.g. Finkbeiner *et al.*, 1997; Gentier *et al.*, 2000; Hudson *et al.*, 2005). The theory is that *in situ* stress fields exert a significant control on fluid flow patterns in fractured rocks, particularly, for rocks of low matrix permeability. For example, in a key study of deep ($>1.7 \text{ km}$) boreholes, Barton *et al.* (1995) found that permeability manifests itself as fluid flow focused along fractures favourably aligned within the *in situ* stress field, and that if fractures are critically stressed this can impart a significant anisotropy to the permeability of a fractured rock mass. Critically stressed fractures are defined as fractures that are close to frictional failure within the *in situ* stress field (Barton *et al.*, 1995). Specifically, the theory of stress-dependent fracture permeability predicts preferential flow occurring along fractures that are oriented orthogonal to the minimum principal stress (σ_3) direction (due to low normal stress), or inclined

~30° to the maximum principal stress (σ_1) direction (due to shear dilation).

Frictional sliding along a plane of weakness such as a fault occurs when the ratio of shear (τ) to the effective normal stress (σ'_n) equals or exceeds the frictional sliding resistance. It is based upon Amonton's Law, which governs fault reactivation:

$$\tau = \mu \cdot \sigma'_n \quad (2)$$

Where μ is the coefficient of friction (a rock material property) and σ'_n is equal to the total applied normal stress resolved onto the plane minus the pore fluid pressure (i.e. $\sigma_n - P_p$). The value of μ has been found to typically range between 0.6 and 1.0 (Byerlee, 1978; Zoback, 2007). This relationship also shows that pore fluid pressure can have a significant impact as it determines the effective stress acting on a plane and that increasing pore pressures can destabilise a fault surface by increasing the ratio of shear to normal stress. The coupling of these hydromechanical (HM) processes means that fluid pressure and flow within faults is linked to tectonic stress and deformation through changes in permeability and storage whilst tectonic stress and deformation is linked to fluid flow through changes in fluid pressure and effective stress (NRC, 1996).

How exactly a fault will behave under an applied stress regime depends upon many factors, however, investigating stress-dependent fault permeability based solely on fault alignment with respect to the *in situ* stress field is an oversimplification. Just as important are the geomechanical properties of the host rock and its contained faults. Important intact rock material properties include parameters such as density, bulk moduli, uniaxial compressive strength, tensile strength, cohesion and friction angle that are typically estimated from laboratory tests. Fracture stiffness is a function of both fracture wall surface contact (i.e. fracture roughness profile) and the elastic properties of the intact rock material (i.e. bulk rock moduli) where for the same given alignment within an *in situ* stress field relatively stiff fractures deform less than weaker fractures. Fracture normal and shear stiffness are measures of resistance to deformation perpendicular and parallel to fracture walls, respectively, and both increase with increasing effective normal stress. In general, faults tend to exhibit high stiffness if formed within hard, competent rocks or if they become locked open by earlier deformation episodes (e.g. shear dislocation) or mineral infill and cementation, and may even become stress insensitive even if subjected to high effective normal stresses (Hillis, 1998; Laubach et al., 2004). In contrast, low stiffness faults can exhibit a wide range of shear and closure behaviour as their alignment with respect to σ_1 changes (Hillis, 1998). Ultimately, estimates of fracture stiffness

attempt to account for more realistic fracture heterogeneity, asperity contact, deformation and tortuous fluid flow. Equations 3 & 4 below describe the simplified relationship between fracture stiffness and fracture deformation (Rutqvist and Stephansson, 2002):

$$\Delta\mu_n = jk_n \Delta\sigma'_n \quad (3)$$

$$\Delta\mu_s = jk_s \Delta\sigma_s \quad (4)$$

Which states (a) that fracture normal deformation ($\Delta\mu_n$) occurs in response to changes in effective normal stress ($\Delta\sigma'_n$) with the magnitude of opening or closure dependent upon fracture normal stiffness (jk_n); and (b) that the magnitude of shear mode displacement ($\Delta\mu_s$) depends upon the shear stiffness (jk_s) and changes in shear stress ($\Delta\sigma_s$).

Structural permeability within faults is likely to be a transient effect as faults often become modified by porosity reducing processes such as hydrothermal mineralisation, hence, fault deformation processes compete with permeability reduction caused by fluid flow (Sibson, 1996; Zoback, 2007). Active fault slip is typically episodic and can temporarily increase the permeability of a fault zone by as much as many orders of magnitude (Gudmundsson, 2000). Therefore, for faults to remain effective permeable structural conduits fault deformation processes must be at least intermittent to continual. For example, in the Dixie Valley geothermal field fluid production is sourced from high permeability faults and fractures that are favourably aligned and critically stressed whilst it is inferred that the formation of fault permeability associated with active deformation out competes permeability destroying hydrothermal quartz precipitation processes (Zoback, 2007).

Preliminary Modelling of Fault Stress States

The numerical modelling of fault stress states has previously been employed by several researchers to identify zones of potential fault enhanced permeability and fluid flux (e.g. Ferrill *et al.*, 2004; Gudmundsson, 2000; Moeck *et al.*, 2009; Zhang and Sanderson, 1996). In a similar methodology, this study uses the Universal Distinct Element Code (UDEC) to simulate the coupled HM response of deformable faulted rock masses under an applied *in situ* stress field to derive preliminary indications of fault stress states and, by corollary, their potential permeability. UDEC represents a rock mass as an assembly of discrete rigid or deformable, impermeable blocks separated by discontinuities (faults, joints etc) and can reproduce fully coupled HM behaviour (Itasca, 2004). Fluid pressure and fracture conductivity is dependent upon mechanical deformation whilst simultaneously fluid pressures

modify the mechanical behaviour of the fractures (for a comprehensive review of the UDEC governing equations see Itasca, 2004). The 2.5D UDEC models describe a geometrical reconstruction that consist of 2D horizontal planar or vertical slices of the conceptual faulted rock mass model and incorporates the effects of the 3D stress field (i.e. σ_v , σ_H , and σ_h). That is, the models perform plane strain analyses, which assumes that the model continues indefinitely (and uniformly) out of the plane of analysis with computations performed for a slice that is one unit thick (Itasca, 2004). The ultimate aim of this type of modelling is to distinguish which fault or fault segments in a specified area are critically stressed and, therefore, a potential exploration drill target. These models are designed to assist explorers in areas of unknown or complex geology prior to drilling, however, large model parameter uncertainties means that the results are preliminary indications only i.e. a 'probabilistic' representation of potential fault stress states.

To illustrate this methodology, three hypothetical geological models are presented based upon the northern Perth Basin as an example setting. This involves a strike-slip faulting stress regime, stress tensor $\sigma_H > \sigma_v > \sigma_h$ equivalent to 1.25 : 1.0 : 0.75 and an east-west principle horizontal stress (σ_H) orientation (King et al., 2008; van Ruth, 2006). For the purposes of this illustrative exercise, rock mass parameters (e.g. density, bulk modulus etc) were sourced from the UDEC rock property database although, where possible, these should be based upon measured representative field samples or at the very least global average values. The most difficult part of this process is assigning fault stiffness values, particularly, as they are expected to vary with host lithology. As fracture stiffness is a function of wall contact area, the jk_n for smooth planar surfaces can approximate the value of the Young's Modulus (E) whereas the jk_s , for perfectly matching rough surfaces, can approximate the value of the Shear Modulus (G). At shallow depths, estimates can be derived based upon jk_n ranging from 1/2 (smooth) to 1/10 (rough) the value of E and jk_s ranging from 1/2 (rough) to 1/10 (smooth) the value of G , which are compatible with published data and those derived from empirical relationships (Kulhawy, 1978; Norlund et al., 1995). However, prior to drill testing the true nature of the fault at depth is unknown. As the aim is to attempt to evaluate relative fault stress states, possibly across multiple faults and lithologies, a 'smooth' fault stiffness for each respective lithology was chosen along with zero tensile strength, cohesion and dilation angle values. In theory, these geomechanical properties replicate the behaviour of a 'weak' fault plane, which allows each fault segment to potentially deform. This is a reasonable approach as most active fault zones are inferred to be weak (Gudmundsson et al. 2001; Gudmundsson et al. 2009).

The three hypothetical geological model examples are:

Model 1: 4km x 4km horizontal planar model set at -3.5 km depth below the surface comprising of a single fault with jog hosted within sandstone (Figure 2).

Model 2: 5km x 5km cross-section of a listric fault hosted with a sedimentary sequence comprising of limestone (surface-1km depth), siltstone (1km-2.5km depth), shale (2.5km-3.5km depth), sandstone (3.5km-4km depth) and granite (4km-5km depth) (Figure 3).

Model 3: 4km x 4km horizontal planar model set at -3.5 km depth below the surface comprising of a central, circular, granite batholith of 1km radius hosted within a weak shale unit plus three cross-cutting faults of differing orientation (Figure 4).

In these models, rock mass deformation was defined by the Mohr-Coulomb model, which is the conventional model used to represent shear failure in rocks and soils whilst fracture behaviour was defined by the Coulomb-Slip criterion, which assigns elastic stiffness, tensile strength, frictional, cohesive and dilational characteristics to a fracture (Itasca, 2004). Mechanical boundaries were defined as fixed velocity (displacement) boundaries and initial *in situ* and boundary fluid pore pressures are assumed hydrostatic.

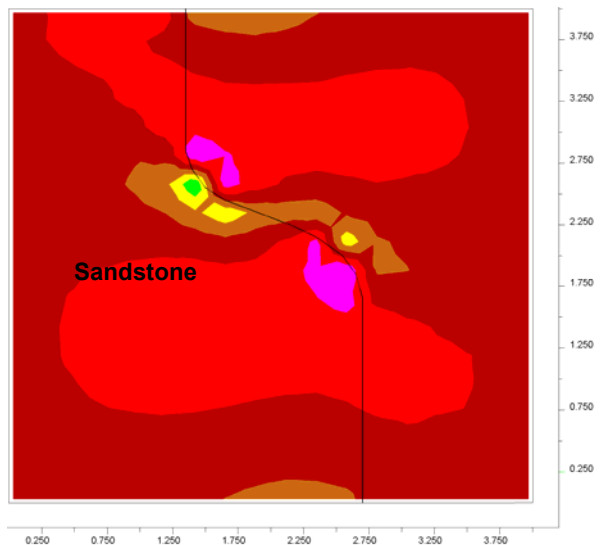


Figure 2. Model 1: 4km x 4km horizontal planar contour map of x-direction stress magnitudes highlighting the concentration of high and low stress zones into quadrants along the fault jog. This highlights that although fault alignment maybe favourable stress-dependent fault permeability can be segmented and localised. Note that the principle stress (σ_H) direction is east-west (right-left). Legend: purple, red, brown, green and yellow colours represent a decreasing range of high to low stress magnitudes, respectively.

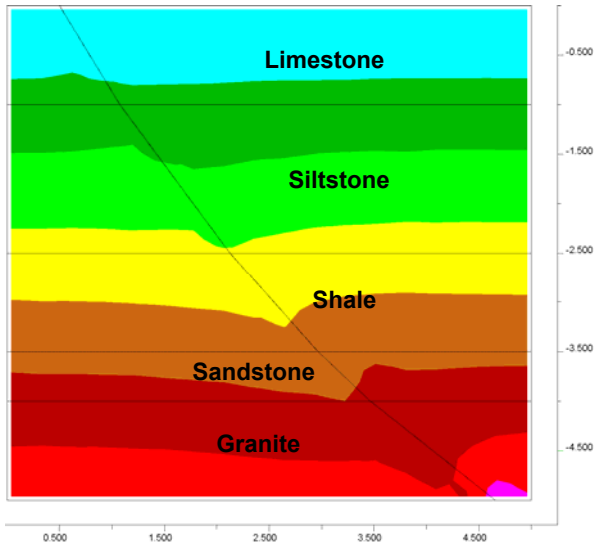


Figure 3. Model 2: 5km x 5km vertical cross-section profile of contoured y-direction stress magnitudes highlighting a localised low stress field perturbation closely associated with the trace of the listric fault. This indicates low fault plane stress and potentially enhanced fault permeability. Note that the principle stress (σ_H) direction is east-west (right-left). Legend: purple, red, brown, green and yellow colours represent a decreasing range of high to low stress magnitudes, respectively.

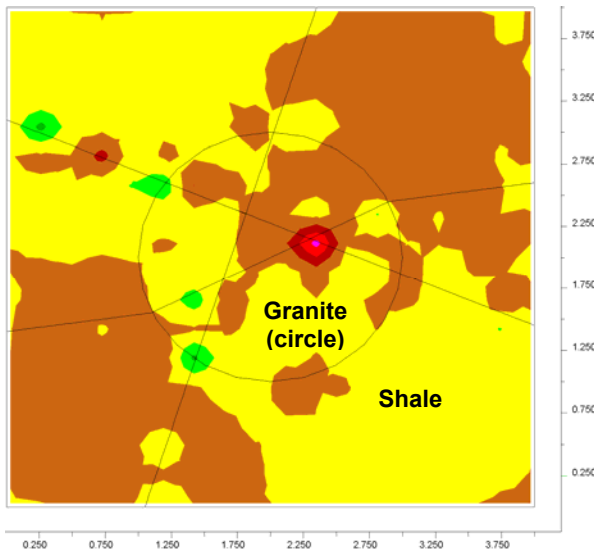


Figure 4. Model 3: 4km x 4km horizontal planar contour map of x,y-direction stress magnitudes highlighting a critically stressed fault intersection (red) which potentially represents the location of enhanced fault permeability. This intersection is also coincident with a low stress anomaly in the x- and y-direction. Note that the principle stress (σ_H) direction is east-west (right-left). Legend: purple, red, brown, green and yellow colours represent a decreasing range of high to low stress magnitudes, respectively.

Conclusion

The risks of targeting permeable faults as geothermal reservoirs include: (1) a relatively high permeability structure may result in fluid pathway short-circuiting and accelerated rates of reservoir thermal drawdown; (2) multiple fault structures with varying amounts of displacement may truncate and compartmentalise a reservoir thereby reducing accessible reservoir volume; and (3) the targeted fault structure may still be hydraulically sealed and/or stress insensitive as a result of other competing natural processes. These risks can be partially mitigated through interpretation of good quality seismic reflection data and with direct drill testing. The fault stress state models shown in this discussion paper are deliberately simplistic but specifically designed to demonstrate how this method can be used to identify zones of potentially enhanced fault permeability prior to any drill testing in areas of unknown or complex geology. This method may be of benefit to the Australian geothermal exploration sector as target depths are typically in excess of 3 km depth below the surface where natural *in situ* porosity and permeability are typically low and there is a general paucity of data.

Nevertheless, it is important to note that the results of such preliminary models can only indicate the probability of encountering enhanced fault permeability and that these 2D models simplify the 3D reality. It could be argued that simply evaluating targets on structural alignment relationships within the *in situ* stress field alone might be sufficient, however, in complex areas this would neglect the influence of features such as multiple rock competency and fault stiffness contrasts and fault intersections on perturbing the local stress field. The results of these numerical models are only as accurate as the quality of the input data and this particular methodology can include a significant amount of model parameter uncertainty (e.g. fault stiffness, estimated or inferred stress field etc). Therefore, this methodology should be viewed as just one tool that can form part of a broader exploration risk management strategy.

References

Bachler, D., Kohl, T., and Rybach, L., 2003, Impact of graben-parallel faults on hydrothermal convection-Rhine Graben case study: *Physics and Chemistry of the Earth*, 28, 431-441.
 Barton, C.A., Zoback, M.D. and Moos, D., 1995, Fluid flow along potentially active faults in crystalline rock: *Geology*, 23, 683-683.
 Byerlee, J.D., 1978, Friction of rocks: *Pure and Applied Geophysics*, 116, 615-626.

- Caine, J.S. and Forster, C.B., 1997, Fault zone architecture and fluid flow. An example from Dixie Valley, Nevada: Proceedings 22nd Workshop on Geothermal Reservoir Engineering, Stanford University, Stanford, California.
- Caine, J.S. and Forster, C.B., 1999, Fault zone architecture and fluid flow: insights from field data and numerical modelling, Faults and Subsurface Fluid Flow in the Shallow Crust: American Geophysical Union, Geophysical Monograph 113, 101-127.
- Caine, J.S., Bruhn, R.L. and Forster, C.B., 2010, Internal structure, fault rocks and inferences regarding deformation, fluid flow, and mineralisation in the seismogenic Stillwater normal fault, Dixie Valley, Nevada: Journal of Structural Geology. In Press.
- Ferrill, D.A., Sims, D.W., Waiting, J.W. Morris, A.P., Franklin, N.M. and Schultz, A.L., 2004, Structural framework of the Edwards Aquifer recharge zone in south-central Texas: GSA Bulletin, 116 (3/4), 407-418.
- Finkbeiner, T., Barton, C.A. and Zoback, M.D., 1997, Relationships among in-situ stress, fractures and faults, and fluid flow: Monterey Formation, Santa Maria Basin, California: AAPG Bulletin, 81 (12), 1975-1999.
- Gentier, S., Hopkins, D., and Riss, J., 2000. Role of Fracture Geometry in the Evolution of Flow Paths under Stress: *In* Faybishenko, B., Witherspoon, P.A and Benson, S.M. (eds), Dynamics of Fluids in Fractured Rocks. AGU Geophysical Monograph 122, 169-184.
- Gudmundsson, A., 2000, Active faults and groundwater flow: Geophysical Research Letters, 27 (18), 2993-2996.
- Gudmundsson, A., Berg, S.S, Lyslo, K.B. and Skurtveit, E., 2001, Fracture networks and fluid transport in active fault zones: Journal of Structural Geology, 23, 343-353.
- Gudmundsson, A., Simmenes, T.H., Larsen, B. and Philipp, S.L., 2009, Effects of internal structure and local stresses on fracture propagation, deflection and arrest in fault zones: Journal of Structural Geology, In Press.
- Hillis, R.R., 1998. The influence of fracture stiffness and the *in situ* stress field on the closure of natural fractures: Petroleum Geoscience, 4, 57-65.
- Hudson, J. A., Stephansson, O., and Anderson, J., 2005. Guidance on numerical modelling of thermo-hydro-mechanical coupled processes for performance assessment of radioactive waste repositories: International Journal of Rock Mechanics and Mining Sciences, 42, 850-870.
- Itasca, 2004. UDEC 4.0 Theory and Background. Itasca Consulting Group Inc., Minnesota.
- King, R.C., Hillis, R.R., and Reynolds, S.D., 2008, In situ stresses and natural fractures in the Northern Perth Basin, Australia: Australian Journal of Earth Sciences, 55 (5), 685-701.
- Kulhawy, F. H. and Goodman, R. E., 1980, Design of Foundations on Discontinuous Rock: Proceedings of the International Conference on Structural Foundations on Rock. International Society for Rock Mechanics, 1, 209-220.
- Laubach, S. E., Olsen, J. E., and Gale, J. F. W., 2004. Are open fractures necessarily aligned with the maximum horizontal stress?: Earth and Planetary Science Letters, 222, 191-195.
- Moeck, I., Kwiatek, G. and Zimmermann, G., 2009, Slip tendency analysis, fault reactivation potential and induced seismicity in a deep geothermal reservoir: Journal of Structural Geology, 31, 1174-1182.
- National Research Council (NRC), 1996. Rock Fractures and Fluid Flow. Contemporary Understanding and Applications. National Academy of Sciences, Washington D.C.
- Nordlund E, Radberg G, Jing L., 1995, Determination of failure modes in jointed pillars by numerical modelling: *In* Fractured and jointed rock masses. Balkema, Rotterdam, pp 345-350
- Rutqvist, J. and Stephansson, O., 2003. The role of hydromechanical coupling in fractured rock engineering: Hydrogeology Journal, 11, 7-40.
- Seront, B., Wong, T-F., Caine, J.S., Forster, C.B, Bruhn, R.L., and Fredrich, J.T., 1998, Laboratory characterisation of hydromechanical properties of a seismogenic normal fault system: Journal of Structural Geology, 20, 865-881.
- Sibson, R.H., 1996, Structural permeability of fluid-driven fault-fracture meshes: Journal of Structural Geology, 18 (8), 1031-1042.
- van Ruth PJ, 2006, Geomechanics: Vlaming Sub-Basin, Western Australia: CO2CRC Report Number RPT06-0043.
- Wong, T-f. and Zhu, W., 1999, Brittle faulting and permeability evolution: hydromechanical measurement, microstructural observation, and network modeling, Faults and Subsurface Fluid Flow in the Shallow Crust: American Geophysical Union, Geophysical Monograph 113, 83-99.
- Zoback, M. D., 2007. Reservoir Geomechanics. Cambridge University Press, New York, pp.449.
- Zhang, X. and Sanderson, D.J., 1996, Numerical modelling of the effects of fault slip on fluid flow around extensional faults: Journal of Structural Geology, 18 (1), 109-119.

Acknowledgements

The authors gratefully acknowledge the funding and logistical support received for this research from the National Centre for Groundwater Research and Training, the Department of Water, Land and Biodiversity Conservation South Australia and the University of Hong Kong.

An EGS/HSA concept for Singapore

Grahame J.H. Oliver

Department of Civil Engineering, National University of Singapore. cvegjho@nus.edu.sg

Abstract

Hot springs are a good indicator for geothermal resources in Singapore. An Engineered Geothermal System (EGS) for commercial power generation would require 3 km deep directional wells in hot sedimentary aquifers (HSA) or in hot, wet, fractured granite and the generation of electricity from +150 °C hot water through binary cycle turbines with the 'waste' water being recycled down injection wells. Proof of concept for a 50 MW power station might cost US\$ 19 million. Development costs (US\$ 200 million) could be written off in 6.4 years after production started. Large corporations and the military could benefit from autonomous geothermal power sources (e.g. electricity, heat processing, district cooling). Several neighbourhood 50 MW geothermal power stations could provide part of the national base load with 'renewable', clean, green power generation of strategic importance for a country that is viewed as having no natural resources.

Keywords: Concept, EGS, Singapore.

Introduction

Sixty million people living on plate boundaries around the world already obtain their electricity from hydrothermal sources in young magmatic rocks. Many commentators see the return of the US\$100-plus barrel of crude oil with future gas prices tracking that rise. Eighty percent of Singapore's electricity is generated from imported natural gas. Geothermal exploration of buried hot granite terrains in continental interiors is now attractive: in Australia and Alaska, EGS exploration has now passed into the development phase. Australian State Governments have committed US\$ 90 million for research and demonstration and another US\$ 750 million has been allocated to works programs for the period 2002 and 2013⁽¹⁾. In May 2009, the US Government announced a US\$ 350 million stimulus boost for US geothermal energy⁽²⁾.

The main heat releasing isotopes in rocks are ²³⁵U, ²³⁸U, ²³²Th and ⁴⁰K. Granites usually

have more of these elements than most other rocks. Granites with more than 10 ppm U can be classified as "hot" and provided the granite has been allowed to heat itself up under a thermal blanket of overlying rocks, significantly high temperatures can build up over millions of years. New technology means that at boiling geothermal water or steam is not required. The commercial binary cycle Chena Power Station in Alaska boils R-134a refrigerant with 74°C geothermal water extracted from Mesozoic hot granite, and produces 2-300 kWh at US 5 cents/kWh⁽³⁾. This is in contrast to the US 30 cents/kWh cost of diesel generators previously used at Chena⁽³⁾. The Geysers region in California generates electricity at 5 cents/kWh⁽⁴⁾. US 5 cents/kWh is competitive against all forms of power generation except for coal.

Geology and hot springs of Singapore

Singapore lies inside the stable Asian continental plate called Sundaland. The island is composed mainly of Middle Triassic I-Type granite and minor gabbro, intruded into a km thick blanket of contemporary and partly covered by Upper Triassic and Lower Jurassic sediments (Fig. 1). There are three confirmed hot springs situated at or near the coasts (although the precise locality of the one on the SW side of Pulau Tekong is uncertain because of land reclamation). Seeping "steam" (*sic*) has been reported to me but not confirmed from another location on Sembawang Singapore Air Force base (Fig. 1). The best known hot spring at Sembawang has been drilled down to 100 m into a 50 m wide fault zone in granite: temperatures of 70.2 °C were measured (Zhao et al. 2002). Chemical analyses classify it as a typical neutral chloride spring with total dissolved solids (TDS) measured at 914 mg/l and a Cl content of 431 mg/l (Zhao et al. 2002). I have applied various geochemical thermometers (listed in Bowen 1986) using Si, Na, K, Ca concentrations listed

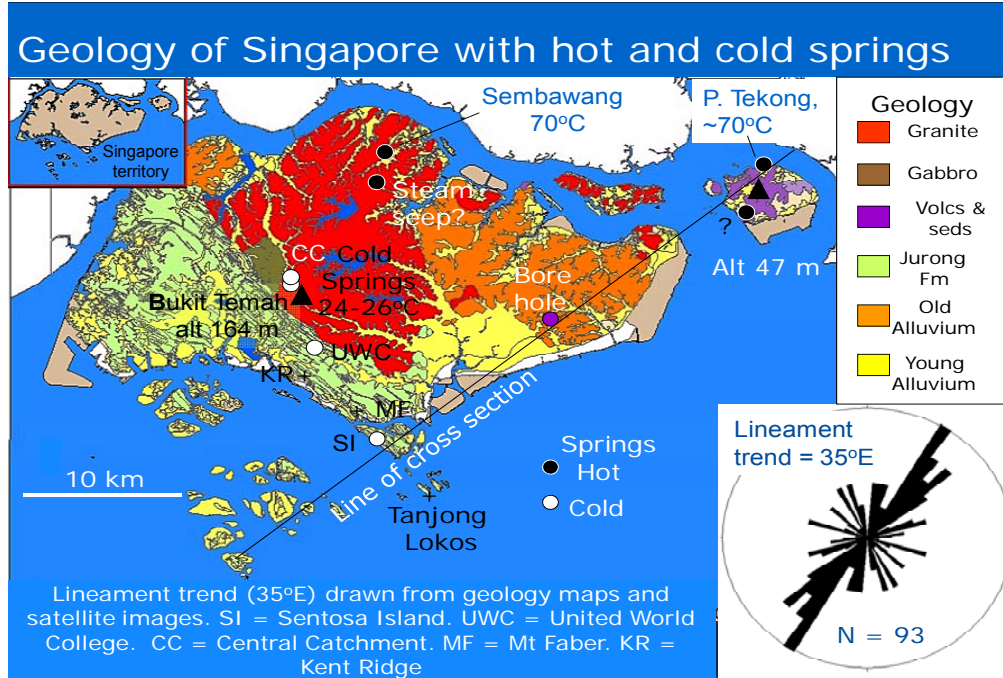


Figure 1: Geology map of Singapore (after Lee and Zhou 2009)

in Zhao et al. (2002) which indicate underground reservoir temperatures between 122 and 209 °C: Na/K thermometers give temperatures of ~160 °C. Granite bedrock is not normally considered to be permeable unless it is well fractured, jointed and faulted. I have investigated the granite quarries around Bukit Temah and Pulau Ubin and close spaced jointing is common. Cold springs occur around Bukit Tema, United World College and Sentosa Island (Fig. 2).

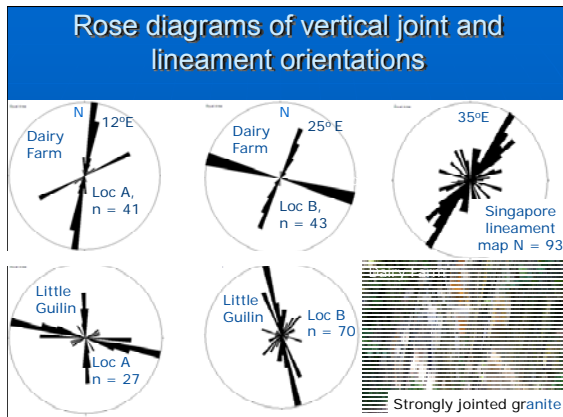


Figure 2: Structural data from quarries

The average maximum horizontal stress (sigma

1) in ~100 m boreholes in central Singapore has a 13°E orientation (Zhou 2001). My analysis of the stress vectors in the Sumatra section of the Australian Plate collision in the Sumatra-Java trench and subduction zone to the SW of Singapore, suggests that the maximum horizontal stress in the hanging wall of the subduction zone is orientated 40°E. The present day stress map of SE Asia⁽⁵⁾, based on earthquake fault solutions and borehole breakouts and fractures, shows that the maximum horizontal stress is orientated 40°E in neighbouring Sumatra. Furthermore, my lineament map of Singapore, based on topography, geological map and satellite data shows a very strong NE/SW trend (35°E, see Figs. 1 and 2). The important implication is that any joints (of whatever age) that are orientated NE/SW could be open in this stress regime and would be the first to open at depth during an HF-acid fracture stimulation.

I have measured joints and fault orientations in various Singaporean granite and gabbro quarries and there is a NE/SW correlation with the lineament map (see Fig. 2). The prediction is that granite with a strong NE/SW orientation of open joint sets will preferentially channel ground water in a NE/SW direction away from the watersheds. Figure 1 shows that the confirmed hot springs in Singapore are indeed

NE of their associated watershed maxima.

Heat flow and geothermal gradient

There are no direct measurements of heat flow, thermal conductivity of rocks or geothermal gradient from Singapore territory. Hall & Morely (2003) estimate that based on an extrapolation of oil and gas well data from central Sumatra, the Malaysian Peninsular and the Malay Basin, the heat flow values for Singapore are between 110 mW/m² in the east and 130 mW/m² in the west of the island (Fig. 3).

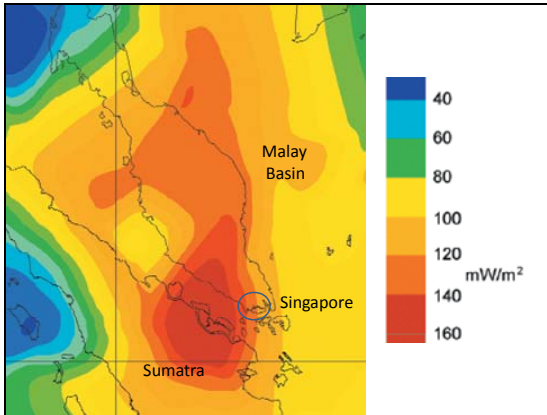


Figure 3: Contoured heat flow map of part of SE Asia. After Hall and Morley (2003).

Applying the Fourier Law of thermal conduction and assuming an average heat flow value of 120 mW/m² and an average thermal conductivity for granite of 3.48 W/mK gives a geothermal gradient of 34.5 °C/km. This assumes that the earth's crust below Singapore is made from granite.

There is a permanent spring at an altitude of 120 m at Jungle Falls on the N side Bukit Temah, the highest hill in Singapore (164m) in the Central Catchment Area, indicating a high water table (Fig. 1). The temperature of this spring is 24.0 °C (D. Higgitt pers. comm.). At 60 m along the NE side of Bukit Temah, another spring issues out of the granite along the Wallace Trail. The temperature is 26.0 °C, an increase of 2.0 °C over a 60 m drop in altitude from Jungle Falls, which could be interpreted as being caused by a geothermal gradient of 3.3 °C per 100 m (or 33 °C / km).

Ground water model for Singapore

The USGS groundwater model⁽⁶⁾ for islands with an unconfined aquifer surrounded by seawater can be applied to Singapore (Barlow 2005). Assuming seawater has a density (P_s) of 1.025 g/cc compared with fresh water (P_f) of 1.0 g/cc, then according to the Ghyben-Heerberg relation:

$$z = \frac{P_f}{P_s - P_f} \cdot h$$

a head (h) of 120m above sea level in the centre of the island will drive cold fresh water down 4.8 km below sea level (z). The permanent (24 °C) spring at an altitude of 120 m on Bukit Temah, (164m), indicates that such a high water table is present. Assuming that the average geothermal gradient for the Singapore region is 35 °C/km (Mazlan et al. 1999, and see discussion above), ground water at 4.8 km depth will reach 168 + 24 = 192 °C. Because of the high rainfall (2.4 m/year) and the 120 m head, the hot groundwater will be driven along the fresh water/seawater transition and up to the surface at the coast (Fig. 4). As described before, this hot water is likely to be preferentially channeled along NE/SW orientated joints and fractures.

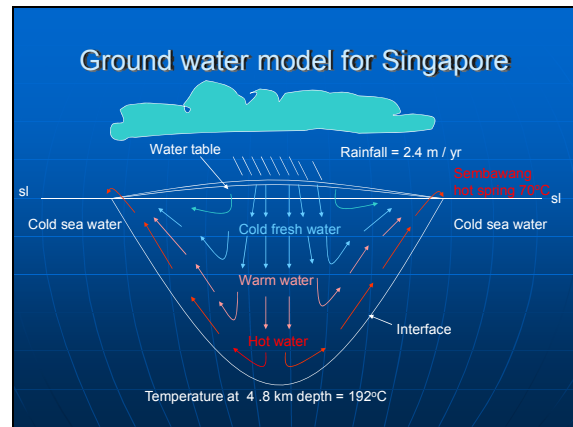


Figure 4: Ground water model predicts 192 °C water at 4.8 km depth.

The Sembawang hot spring is 3.7 m above sea level which was at sea level during the warm interglacial periods at ~80 ka and ~125 ka (Kopp 2009). The Pulau Tekong hot spring is at 0.5 m above sea level, and from photographs, it looks to be in the mangrove transition, which explains the high Cl and Mg contents (Lee and Zhou 2009).

Exploration of geothermal prospects

Figure 5 illustrates the three prospects in the Singapore geothermal play: Pump testing of 100 m deep wells into a fault zone in the Bukit Temah granite at the Sembawang hot spring prospect produced up to 400 l/min at a constant 70 °C for many days (Zhao et al. 2002). However, this rate is not high enough to support a commercial power plant. Deeper production wells are required to intercept hotter water and these need to be coupled with injection wells to supplement the artesian flow.

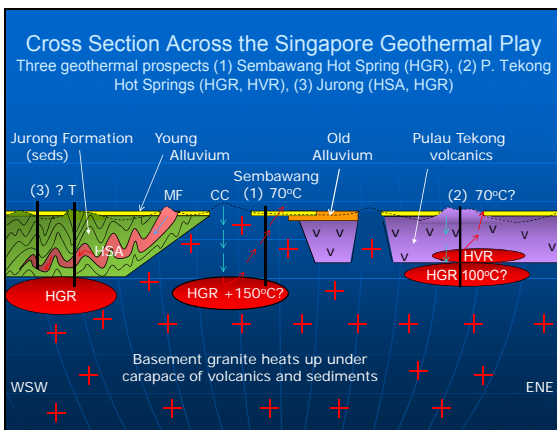


Figure 5: Geothermal prospects in Singapore. Arrows indicate a model for groundwater flow. CC = Central Catchment Area, MF = Mount Faber recharge area, HGR = hot granite rock, HVR = hot volcanic rock, HAS = hot sedimentary aquifer.

The Pulau Tekong prospect has two hot springs, one of which is estimated to be 70 °C, the other which has been lost due to land reclamation. The heat source is unlikely to be in the Triassic volcanic/sedimentary carapace but rather in the fractured granite underneath. The Jurong Formation prospect is composed of conglomerates, sandstones, mudstones, limestones and mineral measures, unconformably lying on top of the granite basement (Lee and Zhou 2009). If the Jurong is thick enough (3 – 4 km?) then it could have acted as a thermal insulator to the 'hot' granite basement. If the Jurong is permeable enough, then any aquifers in contact with the 'hot' granite basement could have been heated to form a hot sedimentary aquifer. Cold springs on Santosa Island and from near United World College might be recharged from the high

ground of Mount Faber and Kent Ridge. Strong jointing in open folded conglomerates at

Tanjong Lokos (Fig. 1) indicates good permeability.

Geophysical surveys: e.g. gravity, MT, TEM, 3D seismics, and heat flow surveys (i.e. a grid of 10 km spaced 300 m deep bore holes) are required to locate 2 - 3 km deep exploration wells that will test for high heat flow, geothermal gradients and stress orientation. These deep wells might intercept significantly hot artesian water (HSA) or hot dry rock suitable for EGS. Age dating of spring waters would be useful to model artesian flow rate: i.e. $^3\text{H}/^3\text{He}$, SF_6 and CFC's.

Proof of Concept

For the purpose of this study, it is assumed that 150°C geothermal water will be used in a binary generation system. Obviously, viability will be increased with a hotter source but that would require drilling deeper, more expensive wells.

Proof of concept for an EGS 50 MW power station, providing power for 50,000 homes by tapping +150°C water at 2 km depth might cost US\$ 19 million: i.e. two 3 km long L-shaped wells at US\$ 3 million/km, plus US\$ 1 million for a 1 km HF acid-fracture job. The horizontal part of the wells should be 1 km long and orientated NW/SE so as to maximize intersections of NE/SW trending vertical joint and fracture sets (Fig.6).

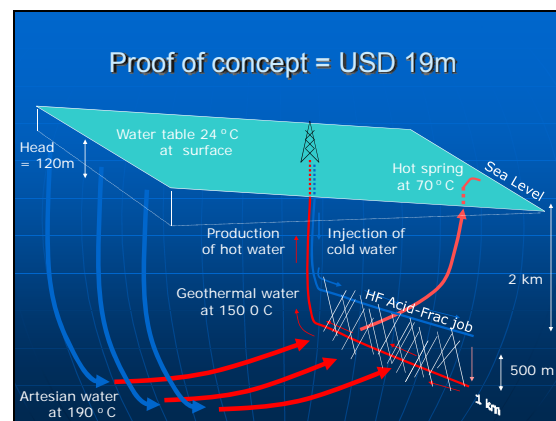


Figure 6: Proof of concept requires sufficient connectivity between injector and production wells.

If this was proved to be successful, then other pairs of L-shaped wells could be drilled from

the same drilling pad until the requisite flow rates were acquired.

Development Costs

Development costs for a 1 MW demonstration power station can be estimated by comparison with the 400 kW binary geothermal system constructed at Chena, Alaska. This uses 74 °C hot spring water from shallow wells (~200 m deep) in granite and generates electricity using mass-produced refrigeration components. Development costs were US\$1300/kW⁽³⁾, i.e. US\$ 1.3 million/MW. Production costs at 5 US cents/kWh and selling at a domestic rate of 12 US cents/kWh would generate a profit of 7 cents/kWh, i.e. US\$70/MWh. Based on these 2007 figures, and adding a notional US\$ 1 million for deeper drilling than Alaska, in one year a proof of concept 1 MW power station (for 1000 homes) might make 70 x 1 x 365 x 24 = US\$ 0.613 million "profit" before tax. The development costs could be written off in 2.3 / 0.613 = 3.75 years and save the equivalent of 10,000 barrels of oil/year (with crude oil at US\$100 oil/barrel this is a saving of US\$ 1 million/year in carbon credits).

The cost of actually drilling 3 km deep directional wells in granite in Singapore is unknown therefore it is difficult to estimate costs and times to break even for a commercial EGS 50 MW power station. According to the U.S. DoE (2006) the initial cost for larger field and power plants was around US\$ 2.5 million per installed MW in the U.S. At 5% inflation per year, this is US\$ 3.0 million per MW at 2010 prices. Sanyo et al. (2007) estimate that EGS would be US\$ 4.0 million per MW at 2007 prices, i.e. US\$ 4.6 million at 2010 prices. Estimates for Australia are equivalent to US\$ 4.2 per MW at 2010 prices (see Appendix 1 in Cooper et al. 2010). An average of these estimates is US\$ 3.93 million per MW.

A 50 MW EGS geothermal power station might therefore cost 50 x 3.93 = US\$ 197 million. Assuming production costs at 5 cents/kWh and selling at a domestic rate of 12 cents/kWh generates a profit of 7 cents/kWh, i.e. US\$70/MWh. In one year a 50 MW power station might make 70 x 50 x 365 x 24 = US\$ 30.6m "profit" excluding taxes and interest payments. Write off would take 197/30.6 = 6.4 years: an EGS is assumed to last 30 years. 50 MW saves the equivalent of 0.25 million barrels of oil/year which at US\$100/bbl = US\$ 25 million/year worth of carbon credits.

Markets

There is a domestic market of 5 million people and a sophisticated infrastructure of transport (electric Mass Rapid Transport system, airports), industrial (coal and biomass fired power stations, oil refineries, ship and oil rig construction), and military installations. Each of these could benefit from an autonomous supply of electricity. Alternatively, hot water could be used directly in process industries or to power district cooling projects using absorption chiller technology. Neighbourhood 50 MW geothermal power stations (costing US\$ 200 million each) could be distributed around Singapore on reclaimed or Government land or concentrated on Pulau Tekong, to provide base load electricity. The generating costs would remain static whilst the cost of imported natural gas varies.

Environmental Impact

An environmental impact and risk assessment would be a high priority. Geothermal energy is viewed as renewable, clean and green with a small carbon footprint during the construction phase. No doubt, a rig capable of drilling 3 km long directional wells would be disruptive in Singapore's mainly urban environment. All the drilling for a power station could be conducted from one noise-proofed drilling pad.

The surface geology indicates that there is ample permeability in the strongly jointed granite and Jurong Formation and it might be that permeability stimulation at depth is not required. However, any HF acid-fracture job would create micro-seismicity. Singapore experiences micro-seismicity from the Java/Sumatra subduction zone and the population is seismically aware. Consequently, any frac-job would require monitoring with a seismic array.

The infrastructure for a 1 MW 'proof of concept' power station would fit into 2 or 3 tennis courts. A 50 MW commercial power station could perhaps be located underground on an area the size of three or four football fields. Pipe work and high tension transmission lines would also be placed underground. Water supply in Singapore is an issue and there would be an initial requirement to augment the working hydrothermal fracture system with fresh or storm water, but not sea

water which could cause scaling. Once the system was pressured up and if the injector/production well connections were efficient, the requirement for augmented water would drop. Air rather than water cooling might be installed in tower blocks on top of the underground generating halls to condense turbine vapour for recycling. Sembawang hot spring has virtually no smell but Pulau Tekong hot spring is reported to be H₂S-rich (Lee and Zhou 2009); however, binary generating systems do not release fluids or gases to the atmosphere.

Summary

Hot springs in Singapore are good indicators for a geothermal power resource. A 1 MW demonstration geothermal power station in a hot spring area of Singapore could be commissioned for US\$ 2.3 million. Construction of a commercial geothermal power generation would involve the drilling of 3 km deep directional boreholes and the generation of electricity from +150 °C hot water through binary cycle turbines with the cooled 'waste' water being recycled down injection wells. Proof of concept for an EGS 50 MW power station might cost US\$ 19 million. Development costs (US\$ 200 million) could be written off in 6.4 years after production started. Several neighbourhood EGS 50 MW geothermal power stations could supply base load electricity to the national grid. This is 'renewable', clean, green power generation of strategic importance for a country that is viewed as having no natural resources.

Acknowledgements

This research was funded by an internal NUS grant to Professor A. Palmer, Department of Civil Engineering, National University of Singapore, who is thanked for many insightful discussions.

References

Barlow P.M., 2005, Ground water in fresh water - salt water environments of the Atlantic coast, United States Geological Survey Circular, 1262, 26 pp.
Bowen, R., 1986, Groundwater, 2nd edition, Elsevier, 427 pp.

Cooper, G.T., Beardmore, G. R., Wainwright, B.S., Pollington, N. and Driscoll, J.P., 2010, The Relative Costs of Engineered Geothermal System Exploration and Development in Australia. Proceedings of the World Geothermal Congress 2010, Bali Indonesia, 25-29 April 2010.
Hall, R. and Morley C.K., 2003. Sundaland basins. In: Clift, P. D., Wang, P., Kuhnt, W., Hall, R. and Tadai R. (eds.) Continental-Ocean Interaction within East Asian Marginal Seas. Geophysical Monograph Series 1949, 55 – 85.
Kopp, R.E., Simons, F.J., Mitrovica, J.X., Maloof, A.C. and Oppenheimer, M., 2009, Probabilistic assessment of sea level during the last interglacial stage. Nature, 462, 863-867.
Lee, K.W. and Zhou, Y., 2009, Geology of Singapore, 2nd Edition, Defence Science and Technology Agency, Singapore, 90pp.
Mazlan, M., Abolins, P., Mohammad Jamaal and Mansar, A., 1999, In: PETRONAS. The Petroleum Geology and Resources of Malaysia. Kuala Lumpur 171-217.
Sanyal, S.K., Morrow, J.W., Butler, S.J., Robertson-Tait, A., 2007, Cost of electricity from enhanced geothermal systems. Proceedings Thirty-Second Workshop on Geothermal Reservoir Engineering, Stanford.
U.S. Department of Energy. (2006). <http://www1.eere.energy.gov/geothermal/m/faqs.html>
Zhao, J., Chen, C.N. and Cai, J.G., 2002, A hydrological study of the Sembawang hot spring. Bulletin Engineering Geology Environment, 61, 59-71.
Zhou, Y., 2001, Engineering Geology and Rock Mass Properties of the Bukit Timah Granite. Underground Singapore, 29-30 Proceedings, 308-314.

Web sources were accessed in May, 2010.

- (1) <http://www.searchanddiscovery.com/documents/2008/08181goldstein/index.html>.
- (2) http://useconomy.about.com/od/candidatesandtheeconomy/a/Obama_
- (3) <http://www.chenahotsprings.com/geothermal-power/>.
- (4) www.geyser.com.
- (5) http://wwwsm.physik.unikarlsruhe.de/pub/stress_data_frame.html
- (6) <http://pubs.usgs.gov/circ/2003/circ1262/#heading156057192>.

Monitoring EGS Reservoirs Using Magnetotellurics

Jared Peacock^{1*}, Stephan Thiel¹, Graham Heinson¹, Louise McAllister²

¹ TRaX, School of Earth and Environmental Sciences, University of Adelaide, SA 5005, Australia

² Petrathem Ltd, Adelaide, Unley, SA 5061, Australia

*Corresponding author: jared.peacock@adelaide.edu.au

A novel time-lapse magnetotellurics (MT) method is proposed to monitor and estimate a real extent of enhanced geothermal systems (EGS). Being directly sensitive to subsurface electrical conductivity, MT has the capability to measure fluids at depth which are both thermally and electrically conductive. MT measurements before, during and after fluid injection are compared to estimate the lateral extent of the induced reservoir at Paralana, South Australia. 3D forward modelling shows the residual MT response between a system with and without conductive fluids to be small, of the order of a few degrees in MT phase. It is crucial to obtain accurate and precise MT responses throughout the surveys in order to produce a reliable model of the changing subsurface. Presented are MT responses before fluid injection and after the first fluid injection. Furthermore, time series measurement of the electric and magnetic fields during the fracturing process may allow studies of EM disturbances generated by the seismic waves, also known as the seismoelectric effect, which can provide information about pore fluid inclusion.

Keywords: Magnetotelluric, EGS, Monitoring

Introduction

EGS has the potential to supplement energy production as the world slowly and resistantly shifts towards renewable energy. One important constraint of EGS is monitoring where the fluids go once injected into the hot lithology. Traditionally, reservoirs are monitored with microseismometer arrays, which measure seismic events generated by fractures (Phillips et al., 2002). Tomography can be applied to estimate location of the fracture (House, 1987), and shear-wave splitting can be used to estimate size and orientation of the fracture (Elkibbi and Rial, 2005). Unfortunately, these measurements do not provide information about fluid inclusion.

Magnetotellurics (MT)

MT is a passive volumetric measurement that exploits Faraday's law of magnetic induction by measuring orthogonal components of the Earth's natural magnetic field and its subsequent electrical response. MT is a diffusive method, which means source energy spreads as a function of time and resolution is proportional to source period, as defined by the skin depth equation. It is sensitive to variations in electrical conductivity of

the subsurface, which makes it a prime technique to monitor changes as electrically conductive fluids are introduced. The fluids are assumed to be conductive due to thermal and dissolved ion enhancement and will provide a large contrast with resistive host rocks (Spichak and Manzella, 2009).

Test site: Paralana, South Australia

The test site is in the northern part of South Australia, about 60 km due north of Adelaide, near the edge of the Flinders Ranges and Paralana hot springs. Here, the thermal activity is generated by an innately large density of radiogenic elements, where residual heat is a by-product of millions years of decay (Brugger, 2005). The 1590M crystalline lithology of the uplifted Flinders Ranges has an estimated heat flow on the order of 60mW/m² (Neumann, 2000), compared to a typical basement rock heat flow of about 10mW/m². To the East of the Flinders Ranges, the hot crystalline rocks are unconformably overlaid by about 4-500m of Adaladian sediments, which acts as a lithologic blanket keeping heat from escaping. As a result the heat flow is estimated to be 1-12mW/m², making the area a prime location for EGS.

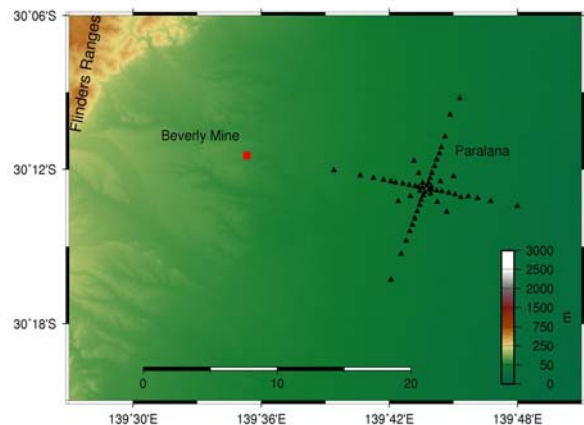


Figure 1: Survey design centred on Paralana 2 drill hole, overlying elevation (m). Two orthogonal lines parallel to assumed principle stress directions provide dense 2D estimation with 22 stations per line. Spacing varies from 200m near the centre to 1.5km near the extremities. Two off diagonal lines with variable spacing of 250m, 500m, 1km provide dimensionality constraints with 6 stations each. One survey encompasses a total of 58 stations, 56 plus two remote reference stations.

Petratherm and joint venture partners Beach Energy Ltd and True Energy Geothermal Pty Ltd lease a 500km² tenement where Paralana 2 has been drilled to a depth of 4012m and cased to 3725m. The bottom hole temperature has been estimated at 190 C and fluids were encountered at a depth of 3860m. Note the proposed EGS will not be located in the basement rock, but in the sediment package directly above, which has a dominant horizontal stress field. It is proposed that inducing permeability and porosity in this sediment package via mechanical fracturing will be achieved more easily than in the crystalline basement without losing much in reservoir temperature. The proposed reservoir size will be about 1 km in the east-west direction and about 2km in the north-south direction and about 400m thick at around 3600m depth. Perforation of the well casing is proposed to commence in August, 2010, followed by two separate fracturing periods occurring in September, 2010 and January, 2011.

Procedure

A preliminary survey was collected to compare any changes in other surveys collected during and after the two fracturing periods. For all surveys, the basic layout, centred on Paralana 2, contains an orthogonal pair of NNE-SSW and WNW-ESE lines employing 22 stations each, Figure 1. The lines have variable spacing of ~20 0m near the centre increasing to 1.5km near the extremities to get maximal coverage at depths of investigation. Two off diagonal lines containing 6 stations each, again centred on Paralana 2, with variable spacing of 250m, 500m, 1 km, aid in estimating 3-dimensionality. Each survey will employ 56 stations in total plus 2 remote reference stations 60km and 80 km south of Paralana. The survey design is based on forward modelling and logistics. The goal is to estimate reservoir extent as a function of time by measuring changes in the MT responses.

Survey 1: Base survey

A base survey was collected in March, 2010 with AuScope instruments run by the University of Adelaide. The sampling rate was 500Hz, with 50m dipole lengths, measuring horizontal magnetic fields Bx and By, along with horizontal electric fields Ex and Ey, where the x component measuring the field relative to magnetic north and y measuring the field relative to magnetic east. The vertical magnetic component Bz was measured for 6 stations. Stainless steel stakes were used as dipoles for 51 sites, the other 5 sites employed Cu-CuSO₄ pots. Induction coils were used as magnetometers. The average data collection time was 22 hours. MT responses were calculated using BIRRP (Chave, 2004) and an in house interface written in Python. It was found that 30 sites were not precise enough due to an unknown source of noise resembling a non-

periodic charge-recharge pattern in the electric channels, Figure 2. The noise does not appear to correlate between stations and does not appear to have any location objectivity. Different filtering techniques were employed with little effect on transfer function accuracy. Therefore, those 30 sites have been redone using Cu-CuSO₄ electrodes, which seem to produce more stable and reliable electric field measurements. Most data have low coherence and larger error bars around 1-10 seconds, Figure 5 which is a well known dead band. Also, the apparent resistivity and phase polarizations suggest a dominant 1D geoelectric structure to a period of a few seconds, then a multidimensional structure after periods of a few seconds. The sites are near a large working uranium mine, Beverly in Figure 1, which produces 50Hz (and harmonics) EM signal. This signal is observed in the time-frequency spectrogram, and in estimated apparent resistivities and phases below periods of .1 seconds, where the estimations are less smooth.

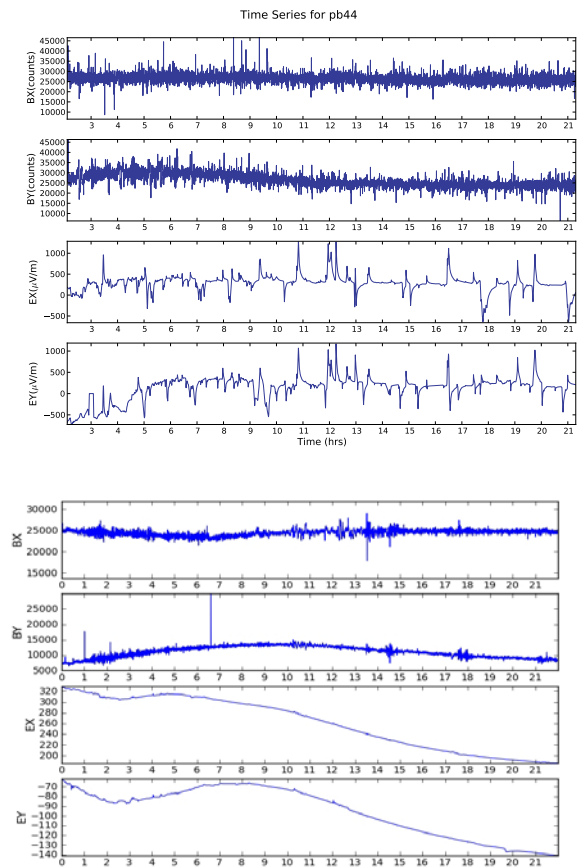


Figure 2: Plots of time series data for two stations plotting, Bx (counts), By (counts), Ex (mV/m), and Ey (mV/m). Bottom axis is time in hours. Top: station pb44, 5km west of Paralana 2, showing a sporadic charge-recharge pattern in the electric channels giving irregular estimates of the MT response. Bottom: station pb 24, 500m east of Paralana 2, showing smooth response in electric channels giving smooth estimates of the MT response.

A second base survey was collected in May, 2010 to redo the stations from the first survey that were not precise enough. The same parameters and locations were used, but Cu-CuSO₄ electrodes were used for all stations and no B_z signals were recorded due to instrument constraints. Unfortunately, at the same time this survey was being collected the Epic Pipeline, which runs parallel to the NNE-SSW line about 2 km west of Paralana 2, was being tested for corrosion. To do this an electric 3 second square wave is sent down the pipeline every 12 seconds, Figure 3.

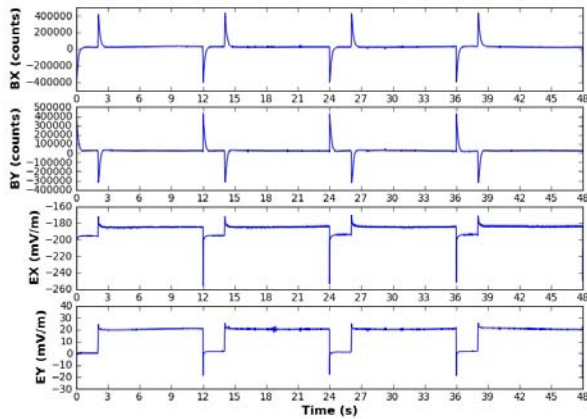


Figure 3: Left: time series of Bx (counts), By (counts), Ex (mV/m), Ey(mV/m) for station pb37 from second survey, 200m near the pipeline. Notice the dominating 3 second square wave in the electric channels and the corresponding magnetic response.

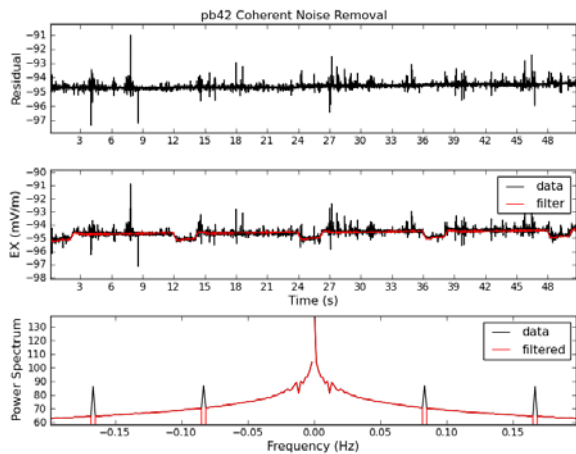


Figure 4: Plot demonstrating a method to remove periodic noise by subtracting the average wave form for a 12 second window from the data for pb42 Ex channel. Top: E_x (mV/m) with periodic noise removed plotted against time (s). Middle: filter in red compared to the raw data plotted against time(s). Bottom: Plot of the power spectrum of the raw data in black and the filtered data in red. Notice the large notches at 12 seconds and its harmonics are removed.

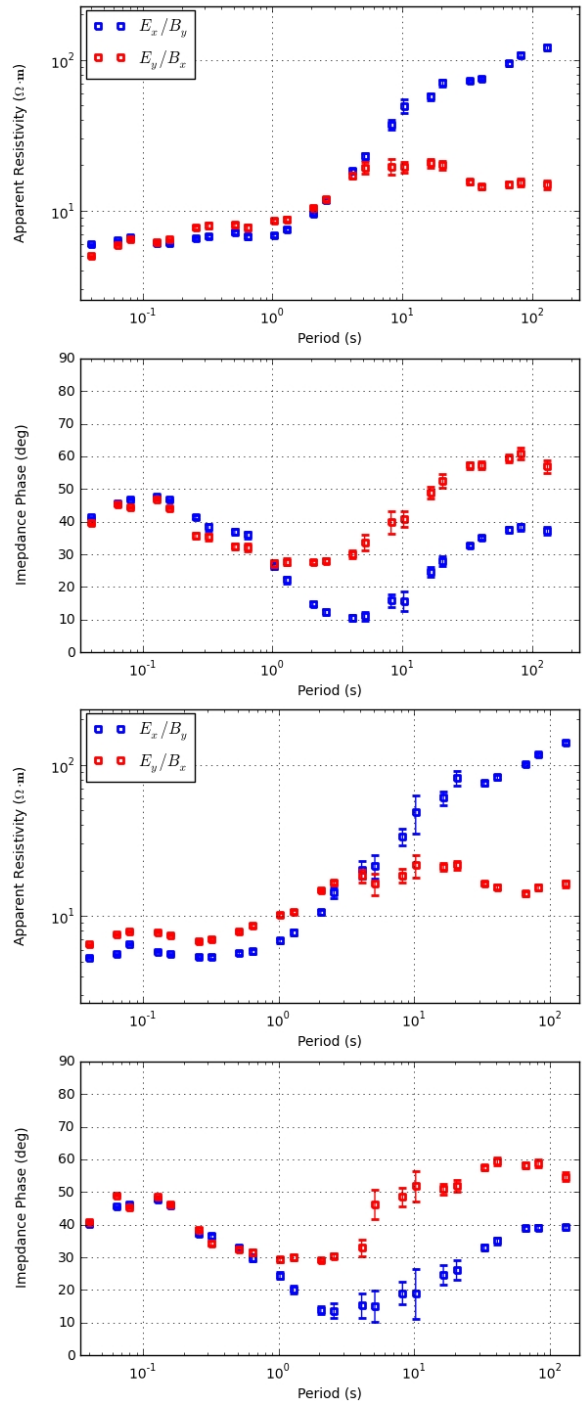


Figure 5: MT responses of two orthogonal modes Ex/By and Ey/Bx. Top are log-log plots of apparent resistivity versus period. Bottom plots are phase in degrees versus log period. Top: pb24 from first base survey displaying a relative smooth MT response with minimal error bars. Bottom: pb42 from second survey with periodic noise removed. Again notice the plots display relative smooth MT responses with minimal error bars, but still have a coherent biased in periods of 1-10 sec. Notice in all plots the error bars are larger around 10 seconds which is where a change in the MT response is expected to occur when fluids are injected. This is also the known dead band where there is naturally low signal power.

Because this signal is distinctly periodic and regular, simple time series analysis can remove this from the data. By taking an average of a 12 second window the average wave form can be

calculated. That waveform is convolved with a series of delta functions every 12 seconds. A linear trend calculated from the data is added to the filter time series to fit the data better. The filter is then subtracted from the raw data, Figure 4. This method works fine for stations at least 1 km away from the Epic Pipeline, but breaks down closer due to the large amplitudes of the periodic signal. Along with this method, remote referencing is used to constrain the transfer functions, Figure 5. Unfortunately, with the periodic noise removal some of the signal is also removed which adds to larger error bars around 3-12 seconds. It was decided to redo the inner 30 stations to get the best estimate of the MT response as possible and reduce error bars. This survey will be collected at the end of August, 2010 in conjunction with the perforation test.

Analysis

The MT responses commonly suffer from near-surface galvanic heterogeneities that distort the calculated impedance tensor Z . Given the existence of a subset with 1D characteristics in the data it is possible to fully calculate the distortion-free regional impedance tensor (Bibby et al., 2005). In the current case, the presence of the 1D resistivity distribution of the sediment strata allows a reliable estimate of the regional impedance tensor. Knowledge of the distortion-free regional impedance tensor ensures a more accurate estimation of the subsurface resistivity. The regional impedance tensor is inverted in a 2D sense to obtain the resistivity distribution underneath the profiles (Rodi and Mackie, 2001). This has been applied to

Conclusions

A novel method of monitoring enhanced geothermal systems using the magnetotelluric method has been proposed because MT is sensitive to the bulk electrical conductivity of the subsurface and therefore directly to the high conductivity of the injected fluids. The EGS system at Paralana will be induced in the sediment package above the hot basement rocks. The relatively high conductivity of the sedimentary basin near the surface requires high quality MT responses to ensure detection of small changes in the MT responses before and after the injection of fluids. Keep in mind the base survey to which all changes are going to be compared to needs to be precise and accurate. Therefore it is important to collect the best data possible even if it means

repeating surveys. Learning is about making mistakes, therefore the more you make the more you learn.

Acknowledgments

The authors would like to thank Petrat herd and joint venture partners Beach Petroleum and TruEnergy for support of this project. Goren Boren, Jonathan Ross, Hamish Adam, Tristram Wurst, and Kiat Low for field work assistance. IMER and PirSa for financial support.

References

- Bibby, H.M., Caldwell, T.G. and Brown, C., Determinable and non-determinable parameters of galvanic distortion in magnetotellurics, *Geophysical Journal International*, 163, pp 915-930.
- Brugger, J.; Long, N.; McPhail, D. C. & Plimer, I., An active magmatic hydrothermal system: the Paralana hot springs, Northern Flinders Ranges, South Australia, *Chemical Geology*, 2005, 222, 35-64
- Chave, A. D. & Thomson, D. J., Bound ed influence magnetotelluric response function estimation, *Geophysical Journal International*, 2004, 157, 988-1006
- Elkibbi, M. & Rial, J. A., The Geysers geothermal field: results from shear-wave splitting analysis in a fractured reservoir, *Geophysical Journal International*, 2005, 162, 1024-1035
- House, L. S., Locating microearthquakes induced by hydraulic fracturing in crystal line rock *Geophysical Research Letters*, 1987, 14, 919-92
- Neumann, N.; Sandiford, M. & Foden, J. Regional geochemistry and continental heat flow: implications for the origin of the South Australian heat flow anomaly, *Earth and Planetary Science Letters*, 2000, 183, 107-120
- Phillips, W. S.; Rutledge, J. T.; House, L. S. & Fehler, M. C., Induced microearthquake patterns in hydrocarbon and geothermal reservoirs: six case studies, *Pure and Applied Geophysics, Seismic Research Center, Los Alamos National Laboratory*, 2002, 159, 345-369
- Rodi, W. and Mackie, R. L. Nonlinear conjugate gradients algorithm for 2-D magnetotelluric inversion, *Geophysics*, 66, pp 174-187.
- Spichak, V. V., and Manzella, A., 2009, Electromagnetic Soundings of Geothermal Zones, *Journal of Applied Geophysics*, 68, pp459-478

Reservoir characterisation and numerical modelling to reduce project risk and maximise the chance of success. An example of how to design a stimulation program and assess fluid production from the Soultz geothermal field, France

Joshua Koh¹, Nima Gholizadeh-Doonechaly¹, Abdul Ravoof¹ and Sheik S Rahman*¹, Luke Mortimer²

¹School of Petroleum Engineering, University of New South Wales, Sydney

²Hot Dry Rocks Pty Ltd, 1A Yarra Street, South Yarra, Victoria

This paper describes a predictive, fully coupled poro-thermo-elastic numerical model that is specifically developed to evaluate and optimise geothermal reservoir development strategies. This paper illustrates this via an investigation into the role of stimulation to enhance the permeability for economic hot water production from the deep geothermal site at Soultz-sous-Forêts (France). This study integrates four key elements: a natural fracture characterization model, a fluid flow simulation model, a heat transfer model and a stimulation model. Fluid flow is simulated using a finite element based model wherein stresses and temperature are fully coupled to the fluid flow equations. The heat transfer model is based on conductive heat transfer within the reservoir rock, convective (including conduction) heat transfer through the reservoir fluid and time dependent thermal equilibrium between the rock and fluid. The stimulation model integrates shear dilation mechanisms and stress dependent permeabilities. Effective permeability tensors (based on discrete fracture network) are estimated dynamically and are iteratively used to determine the pore pressure, stress and thermal state within the reservoir.

A numerical reservoir model of the Soultz-sous-Forêts field was constructed based on the data available in the open literature. The reservoir was subjected to different pressure cycles to determine the degree of permeability enhancement that could be achieved. Flow rate and corresponding pressure losses between injector and producers as well as heat recovery of the produced water were calculated to assess the geothermal potential of the reservoir. Results of this study show that effective tensile normal stresses from the injected cold fluid tend to increase fracture apertures, and hence, increase fracture permeability within the zone of cooling. It was also shown that for a nominal stimulation bottomhole pressure of 10,000 psi, a maximum number of shear dilation events is observed after a stimulation period of 42 weeks for the generated Soultz fracture system and this level of stimulation was sufficient to obtain an economic flow rate of 100 L/s (at an acceptable pressure loss of 2000psi). Our experience also shows that prior to stimulation, flow rates at an acceptable pressure loss between the injector and producers are not sufficient for economic heat extraction. Hence these reservoirs require either stimulation to enhance reservoir permeability or installation of down-hole pumps to lift hot water.

In addition, it has been observed that a major factor responsible for heat recovery as well as thermal drawdown is the degree of interconnection of the fractured reservoir. The produced fluid temperature for the more weakly connected well GPK4 remains very high (~195⁰ C) after a production period of 14 years. During the same period the average matrix temperature drawdown is in the order of 20⁰ C for an initial reservoir temperature of 200⁰C. For the case of a highly interconnected GPK2 well, the

temperature of the produced fluid falls from an initial temperature of 200°C to about 130°C after 14 years of production.

Introduction

Understanding of the hydraulic flow and heat transfer within crystalline rocks is of significant importance in the utilization of deep earth (at least 4 km) hot rock (HR) for geothermal reservoir systems (Baria et al. 1999; O'Sullivan et al. 2001). The characteristics of fluid flow and heat transfer in crystalline rocks are dominated by the fracture systems found within them and in-situ stress which affect the properties of the fracture system significantly. Modelling of coupled hydraulic, thermal and mechanical processes can help in the understanding of the effects of *in-situ* stresses, induced fluid pressure and heat transfer on fluid flow and thermal drawdown of naturally fractured geothermal systems. The long-term response of fracture systems to changes in effective stresses has been investigated by several authors (McDermott and Kolditz, 2006). The change in effective stresses can be induced by hydraulic and thermo-elastic stress alterations resulting from heat extraction from the fractured geothermal systems (rocks). Circulation of cold fluid induces temperature differences within the rock matrix due to heat transfer which leads to large amounts of stress energy release. In an experimental study, O'Sullivan et al (2001) observed some degree of geo-mechanical effects of thermal stresses on geothermal reservoir characteristics (fracture apertures and fracture permeability) and suggested a need for a long term investigation of the thermal stress effect. In particular, the mechanisms that cause phenomena, such as variation of injectivity/productivity with thermal drawdown and occurrence of seismicity need to be understood.

The response of a fracture network to stimulation by injection of cool fluid is time dependent and is a function of discrete fracture behaviour (McDermott et al. 2006; Beeler and Hickman 2003). The individual response of the discrete fractures within the fracture system are determined by interaction of the injected fluid and its physical characteristics such as viscosity, heat capacity and temperature. Other factors, such as the elastic response of the rock matrix and pervasive *in-situ* conditions, including pore pressure and rock temperature have a significant bearing on the closure and shear state of a fracture. The effective stress profiles along fracture surfaces are functions of the far field tectonic stresses, induced hydraulic stresses and thermal stress release (McDermott et al. 2006) during heat extraction. Induced tensile stresses normal to the fracture surfaces from cold water injection can increase fracture aperture and induce new fractures (Zhou et al., 2009). Therefore, alterations of fracture system parameters, such as effective permeability need to be coupled to changes in the pervasive conditions.

Recently, Rutqvist and Stephanson (2003) provided a generic overview of models used for hydromechanical coupling at an aquifer depth and a number of well-known empirical approaches to changes in the normal stress across fractured medium. Most notable, is the study by Beeler et al (2000) who applied elastic solutions for elliptical cracks to define the deformation responses of elliptical fractures under tectonic loading. The effect on the surrounding rock mass however, was not included.

Few authors have investigated the effects of induced fluid pressure on naturally fractured rock on a reservoir scale. Rahman et al. (2002) developed a steady state fluid flow model to study the shear dilation effect due to fluid pressure on permeability enhancement. Shaik et al. (2009) considered poroelastic stresses in the stimulation of a discrete fracture network by induced fluid pressure. In the aforementioned studies, however, thermal stresses were not considered.

Kumar and Ghassemi (2005) developed a numerical model to study fluid pressure and permeability changes in a rock mass by taking into account the effects of thermal stresses and silica precipitation/dissolution. The numerical model incorporated a single planar fracture connecting an injection well and a production well as an idealized reservoir-matrix system. The temporal variation of fracture aperture in response to the individual and combined effects of thermo-elastic stress and silica dissolution/precipitation were examined, however, changes in fracture aperture and pressure in response to non-uniform cooling were not addressed.

Poroelastic and thermoelastic effects of cold-water injection into a single pre-existing fracture in a hot rock matrix was investigated by Ghassemi et al. (2007). Assumptions of plane fracture geometry were used to derive expressions for changes in fracture aperture caused by cooling and fluid leak-off into the matrix. The variations in aperture and pressure occurring under non-isothermal flow conditions when the fracture is subject to injection and heat extraction were examined. The problem was analytically solved for the cases pertaining to a constant fluid injection rate with a constant leak-off rate using a partially coupled formulation.

As part of this study, four computationally efficient models are presented in an effort to evaluate and optimise reservoir development strategies: a natural fracture characterization model, a fluid flow simulation model, a heat transfer model and a stimulation model. The fully coupled thermo-poroelastic numerical model is applied to the Soultz geothermal reservoir, France, where several deep wells have been drilled and stimulated in the Rhine graben (Soultz, France) to evaluate the geothermal Hot Dry Rock potential of the deep fractured granite reservoir. Three main boreholes, GPK2, GPK3 and GPK4 which reach 5080, 5100 and 5270m depth respectively, intersect a crystalline basement overlain by 1400m of Cenozoic and Mesozoic sediments. The layout of the Soultz-sous-Forets EGS site and the well traces and locations are presented in **Fig. 1**. The novelty of this approach lies in its dynamic treatment of the characteristic properties of individual fractures in simulating fluid flow and the pervasive response of the natural fracture system to cold fluid injection. The coupled numerical algorithm is presented in **Fig. 2**.

Modelling of the Soultz fracture network

Variably oriented and intersected fractures with different sizes and irregular patterns (i.e. all fracture complexities) are characterized with the use of two integrated methodologies (Tran, Chen et al. 2007). In the hybrid neuro stochastic methodology, fracture properties are generated based on their characterized statistical distributions. A selective random sampling scheme is used for this purpose. Continuum maps of fracture density and multifractal dimensions are integrated in the discrete model. Hierarchical simulation technique is used to deal with different degrees of heterogeneity in the

reservoir. In the second methodology, hybrid neuro stochastic methodology is upgraded to handle more complex measurements. In this methodology, an object based conditional global optimization concept is applied. It combines continuum distributions with statistical distributions and correlations of discrete fracture properties, thus representing a great improvement over other object based stochastic simulation as well as grid based fracture models.

Based on the observed data recorded, a specified number (say 1000 fractures) of unbiased data specimens are generated by re-sampling the weighting field using a normalized probability method for different fracture classes. Once at least 1000 fractures are created, then the fractures are sorted with respect to their radii. The sorting is performed based on the input value for the smallest and the largest fractures to be modeled. Once the fracture network with specific characteristics is generated, the next step is to define the fracture density in a square volume of rock of interest. The fracture density is the representation of the fracture area per unit volume of rock mass observed in the field. The fracture network is stochastically realized within this volume using a pseudo-random number generator. This is accomplished by repeated re-sampling of earlier fracture records and placing the fractures randomly in the volume of interest until the required fracture density is reached.

In this study, the statistical analysis of the fracture networks in the Soultz geothermal reservoir as performed by Gentier et al. (2010) was used. **Table 1** presents the four main fracture sets F1, F2, F3 and F4, with a fifth set F5 defined for fractures not falling within the initial four main sets as “background noise” (Gentier et al., 2010). Two ~N-S striking sets are distinctly recognised, respectively W-dipping (F1) and ENE-dipping (F2). In addition, two NE-SW and NW-SE striking sets are also observed, respectively NW-dipping (F3) and SW-dipping (F4).

The fracture data was used to stochastically resample the fracture network around the wells GPK2, GPK3 and GPK4 in the abovementioned manner. The generated fracture network is presented in **Fig. 3** for a parallelepiped volume of 2.5 km (east west) by 3.0 km (north south) by 3.5 km (vertical, 2500m – 6000m).

Numerical flow simulation

A finite element based poro-thermo-elastic reservoir model is developed for evaluating hot water production. This model fully couples fluid flow, temperature and geomechanics. The governing equations of non-isothermal thermo-poroelasticity is expressed as follows (Kurashige, 1989; Ghassemi et al., 2002):

$$\left(K + \frac{G}{3} \right) \nabla(\nabla \cdot u) + G \nabla^2 u - \alpha \nabla p - \gamma_1 \nabla T_R = 0 \quad (0.1)$$

$$\frac{\partial \zeta}{\partial t} = \frac{k}{\mu} \nabla^2 p \quad (0.2)$$

$$\dot{\zeta} = \alpha \dot{\varepsilon}_{ii} + Q' \dot{p} - \gamma_2 \dot{T} \quad (1.3)$$

$$\dot{T}_f + \nabla(J_f T_f) - c_f^T \nabla^2 T_f = 0 \quad (1.4)$$

$$\dot{T}_R - c_R^T \nabla^2 T_R = 0 \quad (1.5)$$

where, K is the bulk modulus (MPa), G is the shear modulus (MPa), u is the displacement vector, (ux, uy) (m), α is Biot's coefficient, γ_1 is the thermal expansion coefficient of solid (K^{-1}), γ_2 is the thermal expansion coefficient of fluid (K^{-1}), T_R and T_f are the rock and fluid temperatures respectively (K), p is the pore pressure (Pa). Superconvergent patch recovery (Zienkiewicz et al. 1992) is used to evaluate nodal stress tensors from the numerical results of nodal displacement, u.

Fracture response to stimulation

The naturally fractured medium is pressurised by injecting fluid with a view to stimulate the reservoir. In practice, the fluid pressure develops gradually and some of the fractures may start propagating before the fluid pressure reaches a threshold level at which shear slippage may takes place for a large number of fractures.

The shear slippage criterion similar to Rahman et.al (2000) is applied to identify fractures that are favorable for shear slippage and dilation. When the fracture pressure becomes higher than the given in-situ stress effective normal stress becomes negative and fractures open and surfaces no longer remain in contact. The shear displacement, U_s in such condition can be expressed as:

$$U_s = \frac{\tau_n}{K_s} \quad (1.6)$$

where K_s is the fracture shear stiffness and τ_n is the access shear stress.

The increase in fracture aperture due to shear dilation, a_s can be expressed as (Willis-Richards, Watanabe et al. 1996):

$$a_s = U_s \tan(\varphi_{dil}^{eff}) \quad (1.7)$$

The total stimulated aperture can be expressed as (Muskat 1937):

$$a = \frac{a_0}{1 + 9\sigma_{eff}/\sigma_{nref}} + a_s + a_{res} \quad (1.8)$$

where a_{res} is the residual aperture that usually exists at high effective stress and is considered to be zero in this study. The normal effective stress, σ_{eff} , is the resultant normal stress arising from the effects of induced pressure and thermal contraction at the fracture surface. The total stimulated aperture, a can finally be expressed by mathematical manipulation as:

$$a = \frac{a_0 + U_s \tan(\varphi_{dil})}{1 + 9\sigma_{eff}/\sigma_{nref}} \quad (1.9)$$

The above equation is used in the evaluation of permeability enhancement by numerical simulation of fluid flow within the stimulated fractured network.

Numerical algorithm

The algorithm of the design methodology is shown in Fig. 2. Initially, real field data, such as the fracture orientation, size and other fracture parameters that influence reservoir performance are acquired from the open literature.

An analysis of hot water productivity in terms of well placement is performed for three well configurations. Well location and distance between wells are chosen based on the Soultz EGS system and used to investigate common problems associated with development of EGS, such as short circuiting and high pressure loss between injector and producer wells, and at the same time a perform a hydraulic stimulation program to provide sufficient permeability enhancement.

For the configuration, the reservoir permeability is calculated based on the discrete fracture network data and fluid flow simulation. Then the injector is pressurised and the pore pressure, temperature and stress tensor across the reservoir at each time step are evaluated. Shear slippage and dilation that may occur as a result of change in local stress and pore pressure are determined and evaluated.

Numerical results of stress and pore pressure are used to calculate current total aperture (accounting for the contributions of fracture opening (mode I), shear dilation (mode II)) for every individual natural fracture and update the permeability of the reservoir.

Using these results, reservoir simulation is carried out to calculate flow rates at the producers for discrete values of injector-producer pressure drops as well as temperature profiles of both the rock and fluid within the reservoir.

Results and Discussion

In the current thermo-poroelastic numerical model, flow between the injection well and production wells are assumed to be planar and is approximated through the open hole interval (3500m to 5100m) through a statistically representative trace. This is achieved by alteration of the fractal dimension, which is used to spatially distribute the fractures within a defined volume. A statistically representative trace of the Soultz fracture network between a depth of 2500 m and 6000 m is presented in **Fig. 4**. The well placements on the plane are taken as their separation at a depth of 4430m, which is midway through their depth-averaged open hole sections. The reservoir is pressurized by injecting fluid through the injection well (GPK2). To increase the injectivity, a pair of coplanar fractures of half length of 30m, is placed at the injection well. The pressurization was carried out over a period of one year and the results recorded at different stages (8 weeks, 24 weeks, 40 weeks and 52 weeks). During the pressurization, the change in fracture width for each individual natural fracture and the resulting permeability tensor were calculated. Following stimulation of the reservoir, a flow test was carried out over a period of 14 years. During the flow test, changes in fracture apertures due to thermo-poro-elastic stresses and the consequent changes in permeabilities were determined. Also estimated was the thermal drawdown of the Soultz EGS.

Effect of stimulation time on shear dilation

Results of shear dilation are presented as average percentage increase in fracture aperture and dilation events with time (see **Figs. 5** and **6a-6d**). From Fig. 5, it can be seen that there exists three distinct aperture histories: 0-28 weeks, 28-42 weeks and greater than 42 weeks. Until about 28 weeks, the rate of occurrence of dilation events due to induced fluid pressure of 10,000 psi (bottomhole) remains fairly constant. Following this time, the rate of occurrence increases sharply until about 42 weeks, after which, no significant dilation events can be observed (a plateau of events is reached). This infers that for every set of reservoir and stress parameters as well as injection schedule, a maximum level of shear dilation can be achieved.

In Figs. 6a, 6b, 6c and 6d, the events of shear dilation at different stimulation times are presented. From these figures, it can be seen that by 8 weeks, distribution of shear dilation events is relatively non-uniform. This can be attributed to rapid propagation of pressure through well interconnected fractures.

As pressure continues to build up, more fractures are dilated in the vicinity of the active shear dilation front (see Figs. 6c and 6d). In **Fig. 7**, permeability enhancement in the form of the root mean square (RMS) permeability tensor, at the end of 16 weeks and 42 weeks of stimulation, respectively, are presented. The low initial permeabilities can be attributed to high *in situ* closure stresses in the reservoir. After 42 weeks of stimulation, reservoir permeability has been significantly increased, both due to pressure induced inflation (temporary) and shear dilation (retainable) of the fracture network. The RMS permeabilities local to the major fractures are roughly an order of magnitude greater after 42 weeks of stimulation than after 16 weeks.

Effect of well placement on reservoir stimulation and hot water production

As shown in Fig. 4, the two production wells, GPK2 and GPK4 are separated from the injection well, GPK3, by roughly 480m and 440m respectively. During stimulation, the production wells are kept closed. Once a desired stimulation is achieved at the end of the stimulation period (42 weeks) the fluid was circulated over a period of 14 years. During this circulation period, production rates from each well, fluid velocities throughout the reservoir produced fluid temperatures and average matrix temperature drawdown were estimated. The production parameters are listed in Table 2. Results of hot water production over the 14 year circulation period after an initial 42 weeks of stimulation are presented in **Figs. 8** through **13**.

In Fig. 8, the RMS fluid velocities after 10 years of production are presented. It can be observed from this figure that there exists distinct fluid flow paths connecting the injector and the producers. The flow paths connecting the injector and GPK4 however, are not as prominent (not well connected) as that of GPK2. In addition, it can be observed that the fluid velocities are much greater for the 42 week stimulation case than the 16 week stimulation case. Fluid velocities up to 1×10^{-3} m/s through the major connected pathways is reached after 42 weeks which is three times higher than that after 16 weeks of stimulation. In **Fig. 9**, the reservoir temperature profile after 10 years of production is presented. It is apparent from the figure that the high flow rates experienced between the injector and

producers (see Fig. 8) resulted in significant cooling of the reservoir rock along these flow paths. Once thermal breakthrough has taken place through to GPK2, the temperature of the produced fluid begins to decline steadily. This thermal breakthrough takes place at about 8 years of production (see **Fig. 10**). From Fig. 10, it can also be observed that the produced fluid temperature drops to about 140°C in well GPK2, while in well GPK4, the produced fluid temperature remains high after the same period. The variation of produced fluid temperature from different wells is caused by several factors, namely, the number of hydraulically active flow paths between the injector and producer, the hydraulic length of these flow paths and the temperature difference between invading fluid and rock matrix along these flow paths. In general, a high number of flow paths originating from the injector, which span considerable distances before intersecting the producers, tends to delay the onset of thermal breakthrough (due a high heat-sweep efficiency). It may be noted from Fig. 10 that thermal breakthrough begins to occur at GPK4 at around 11 years.

Effect of thermally induced stresses on hot water production

In **Figs. 11a** and **11b**, the estimated reservoir impedances for two different degrees of stimulation are presented. Stage I stimulation (Fig. 11a) is over 26 weeks and stage II stimulation (Fig. 11b) over 42 weeks. As shown in Fig. 11b, the production rates at GPK2 increase rapidly for roughly one year and continue to increase but at a slower rate until about 8 years. Following this, a quasi steady state production with fluctuations is reached. The initial production period of one year is characterized by a steep increase in production rate as pressure builds up through the well connected network of stimulated fractures. The steady increase in production after one year can be attributed to the cooling of the rock matrix which induces thermal stresses (see **Figs. 12a** and **12b**). These thermal stresses consequently increase permeability of the fractured network, leading to changes in the pressure distribution and hence, the flow rates.

The effective stresses in the reservoir rock at early production time (3 years) and late production time (10 years) are presented in **Figs. 12a** (x direction) and **12b** (y direction). It should be noted again that a geomechanics sign convention is adopted for stresses (positive for compression). From both plots, it is apparent that the effective stresses in reservoir at late time (10 years) are significantly less compressive than those at early time. The decreases in effective stresses causes fracture dilation and therefore permeability enhancement. The continuous decrease in matrix temperature at an increasing rate can be observed in **Fig. 13**.

Effect of level of stimulation on reservoir impedance

The production flow rates at GPK2 were recorded for injector-producer pressure drops of 2000 psi and 1500 psi, for both stage I and II of stimulation. In Fig. 11a for the case of stage I stimulation, the production rates rise with time, until roughly 1.5 years, when a quasi-steady state pressure profile is attained. At this point, a 2000 psi pressure drop results in a production rate of roughly 30L/s while a 1500 psi pressure drop, roughly 16 L/s. Following this, the production rates continue to rise but at a much slower rate which was explained in the previous section. Peak production of 43 L/s is observed with a pressure drop of 2000 psi and 23 L/s with a pressure drop of 1500 psi.

In Fig. 11b, the production rate as a function of time after 42 weeks of stimulation is presented. It can be seen that the production rates with injector-producer pressure drops of 2000 psi and 1500 psi bear a similar trend to the case of stage I stimulation. The production rates begin to reach quasi-steady state (as observed in Fig. 11b) at around 1 year production time. Similarly, thermally induced stresses increase the production rates after this period for both cases of pressure drop. The production rate with a pressure drop of 2000 psi peaks around 100 L/s and around 63 L/s with a pressure drop of 1500 psi. The increased production rates were achieved by increasing the stimulation time from 26 weeks to 42 weeks.

Conclusions

In this paper, a poro-thermo-elastic reservoir model is developed and used to study the effects of induced fluid pressure and thermal stresses (cooling effect) on reservoir permeability and consequent increase in hot water production. The model is applied to the Soultz geothermal reservoir, France. The paper also investigates the effect of well placement on hot water production and thermal drawdown. From the results of this study, the following conclusions can be drawn.

It has been shown that for every geothermal system there exists an optimum injection schedule (injection pressure and duration). Further increases in stimulation effort, i.e. stimulation time for a given stimulation pressure, does not enhance any further reservoir permeability. In this study, for a bottomhole stimulation pressure of 10,000 psi, a stimulation time of 42 weeks has been found optimum.

Fracture connectivity has a significant bearing on thermal breakthrough, produced hot water temperature, temperature drawdown and the hot water production rate. Also demonstrated, was the non-uniform spatial distribution of shear event occurrences with time.

Thermal stresses induced during the circulation of cold water have a significant effect on the long term production rate. As thermal drawdown of the rock matrix takes place, tensile thermal stresses are induced which allow residing fractures to dilate and enhance permeability. This gradually increases the fluid velocities between the injector and producer, yielding increasing production rates with time.

References

- Baria, R., Baumgärtner, J., Gérard, A., Jung, R., Garnish, J., 1999. European HDR research programme at Soultz-sous-Forêts (France) 1987–1996. Geothermics 28, 655–669.
- Beeler, N. M., Wong, T. F. & Hickman, S. H., 2003. On the expected relationships among apparent stress, static stress drop, effective shear fracture energy, and efficiency. Bull. Seismol. Soc. Am. 93, 1381-1389.
- Beeler, N.M., Simpson, R.W., Hickman, S.H. and Lockner, D.A., 2000. Pore fluid pressure, apparent friction, and Coulomb failure, J. Geophys. Res. 105, 25533– 25542.
- Gentier, S., Rachez, X., Ngoc, T. D. T., Peter-Borie, M. and Souque, C. (2010). "3D Flow Modelling of the Medium-Term Circulation Test Performed in the Deep Geothermal Site of Soultz-Sous-forets (France). Proceedings World Geothermal Congress 2010 - Bali, Indonesia, 25-29 April 2010.

- Ghassemi, A. and G. Suresh Kumar (2007). "Changes in fracture aperture and fluid pressure due to thermal stress and silica dissolution/precipitation induced by heat extraction from subsurface rocks." Geothermics **36**(2): 115-140.
- Ghassemi, A., Nygren, A., Cheng, A., 2008. Effects of heat extraction on fracture aperture: A poro-thermoelastic analysis. Geothermics **37**, 525–539.
- Jing, Z., J. Willis-Richards, et al. (2000). "A three-dimensional stochastic rock mechanics model of engineered geothermal systems in fractured crystalline rock." J. Geophys. Res. **105**.
- Kumar, G.S. and Ghassemi, A., 2005. Numerical modeling of non-isothermal quartz dissolution/precipitation in a coupled fracture–matrix system. Geothermics **34** (2005) 411–439.
- McDermott, C.I. and Kolditz, O., 2006. Geomechanical model for fracture deformation under hydraulic, mechanical and thermal loads. Hydrogeol. J. **14**, 487–498.
- Muskat, M. (1937). The Flow of Homogeneous Fluids Through Porous Media, Edwards Publisher.
- Narayan, S. P., Z. Yang, et al. (1998). HDR reservoir development by fluid induced shear dilation: A numerical study of the Soultz and the Cooper Basin granite rock. International Hot Dry Rock - Forum, Strasbourg, France.
- O'Sullivan, M.J., Pruess, K., Lippmann, M.J., 2001. Geothermal reservoir simulation. The state of practice and emerging trends. Geothermics **30** (4), 395–429.
- Rahman, M. K., M. M. Hossain, et al. (2000). "An analytical method for mixed-mode propagation of pressurized fractures in remotely compressed rocks." International Journal of Fracture **103**(3): 243-258.
- Rahman, M. K., M. M. Hossain, et al. (2002). "A Shear-Dilation-Based Model for Evaluation of Hydraulically Stimulated Naturally Fractured Reservoirs." Int. J. for Numerical and Analytical Methods in Geomech. **26**(5).
- Sanyal, S. K., E. E. Granados, et al. (2005). An Alternative and Modular Approach to Enhanced Geothermal Systems. World Geothermal Congress 2005, Antalya, Turkey.
- Sausse, J., Desayes, C. and Genter, A. (2007). "From geological interpretation and 3D modelling to the characterization of the deep seated EGS reservoir of Soultz (France)." Proceedings European Geothermal Congress 2007, Unterhaching, Germany, May 30-June 1, 2007.
- Shaik, A. R., M. A. Aghighi, et al. (2008). "An Innovative reservoir simulator can Help Evaluate Hot Water Production for Economic Development of Australian Geothermal reservoirs." GRC Transactions **32**: 97-102.
- Shaik, A.R., Koh, J., Rahman, S. S., Aghighi, M. A. and Tran, N. H., 2009. Design and evaluation of well placement and hydraulic stimulation for economical heat recovery from enhanced geothermal systems. GRC Annual Meeting October 4–7, 2009, conference proceedings.
- Tran, N., Z. Chen, et al. (2007). "Characterizing and modelling of fractured reservoirs with object-oriented global optimization." Journal of Canadian Petroleum Technology **46**(3): 39-45.
- Willis-Richards, J., K. Watanabe, et al. (1996). "Progress toward a stochastic rock mechanics model of engineered geothermal systems." J. Geophys. Res. **101**.
- Zhou, X. X., Ghassemi, A. and Cheng, A. H.-D., 2009. A three-dimensional integral equation model for calculating poro- and thermoelastic stresses induced by cold water injection into a geothermal reservoir. Int. J. Numer. Anal. Meth. Geomech. 2009; **33**, 1613–1640

Figures and Tables

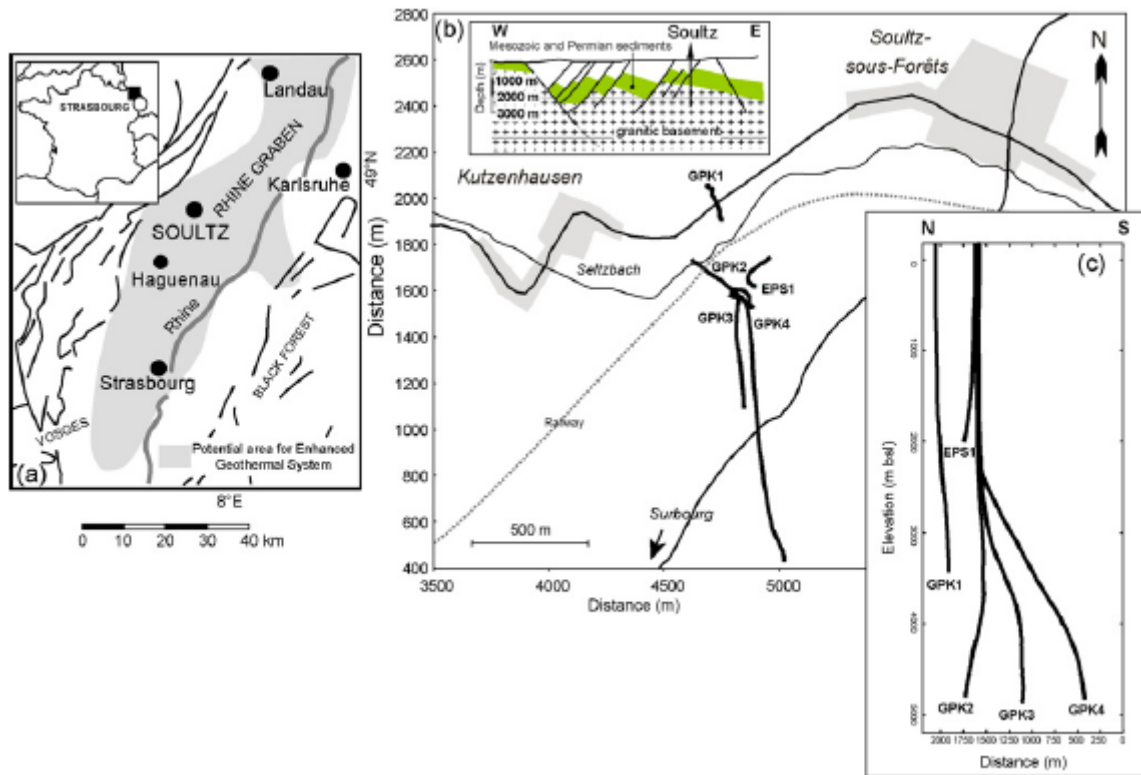


Fig. 1. Schematic geological map of the Rhine Graben and location of the Soultz-sous-Forêts EGS site (a and b). Location and traces of the Soultz deep geothermal wells; solid lines correspond to well traces (b and c). (Sausse et al., 2006)

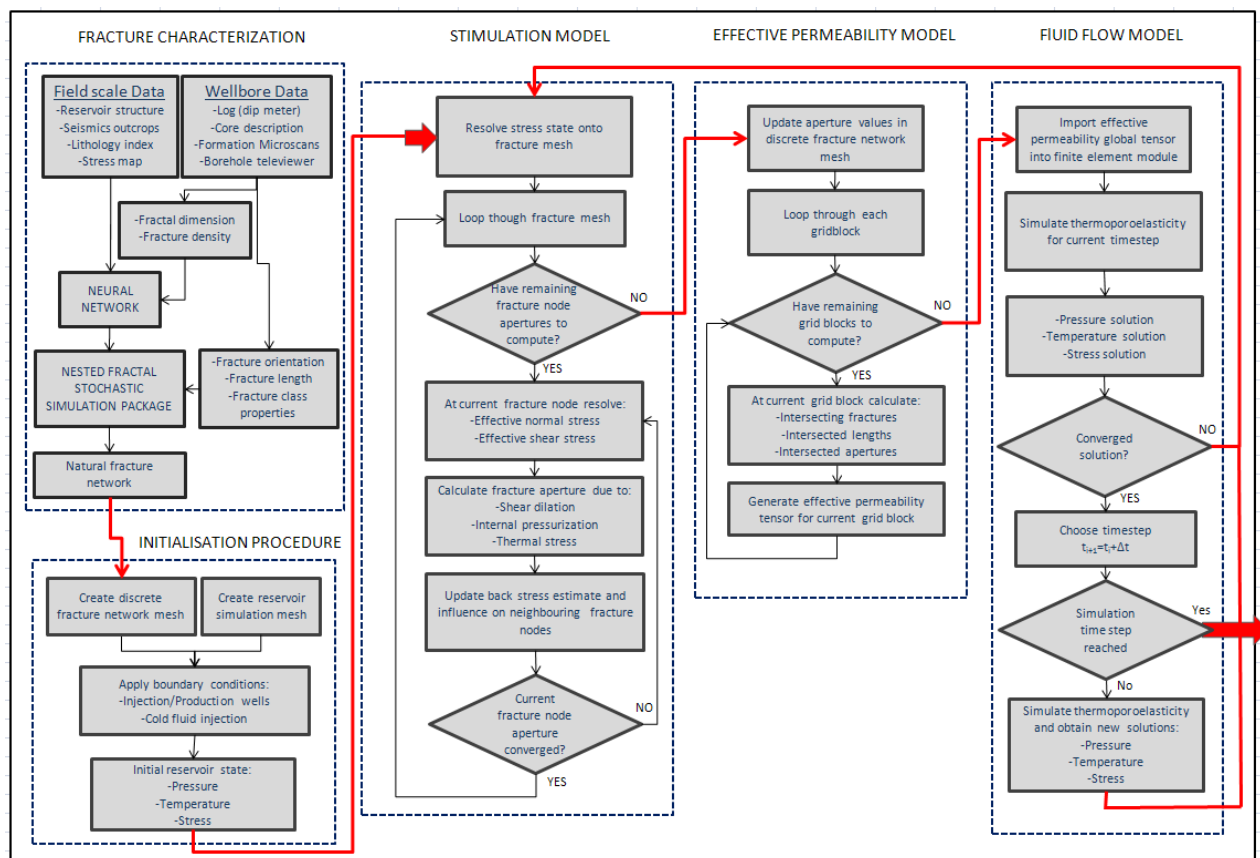


Fig 2. Flow chart describing the numerical procedure and integration between the various models.

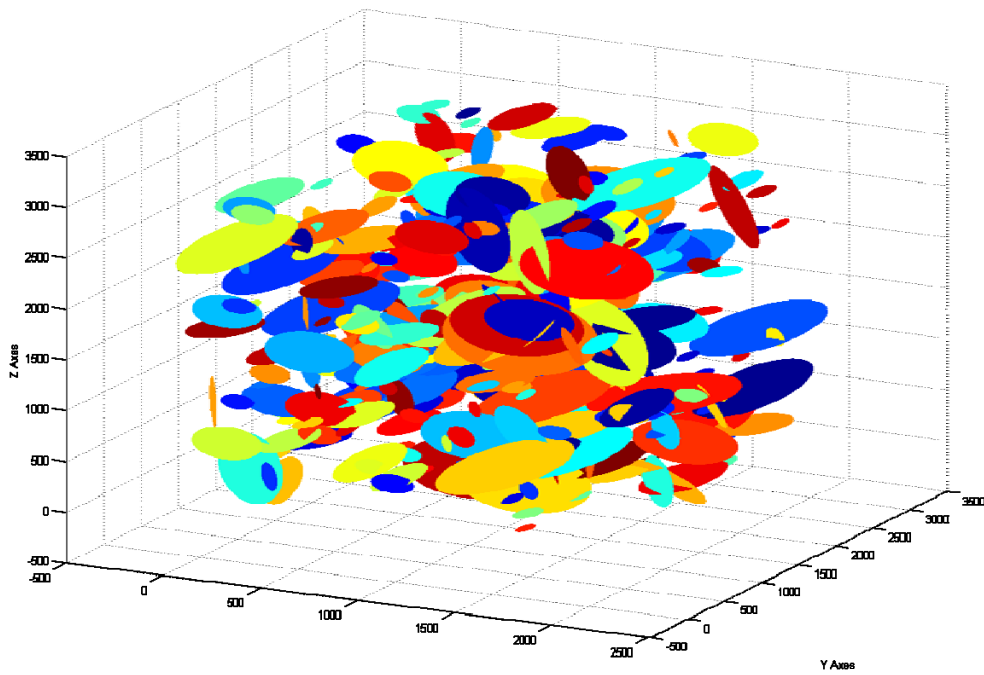


Fig. 3. Generated fracture network of the deep geothermal Soultz reservoir based on statistical data from Gentier et al. (2010).

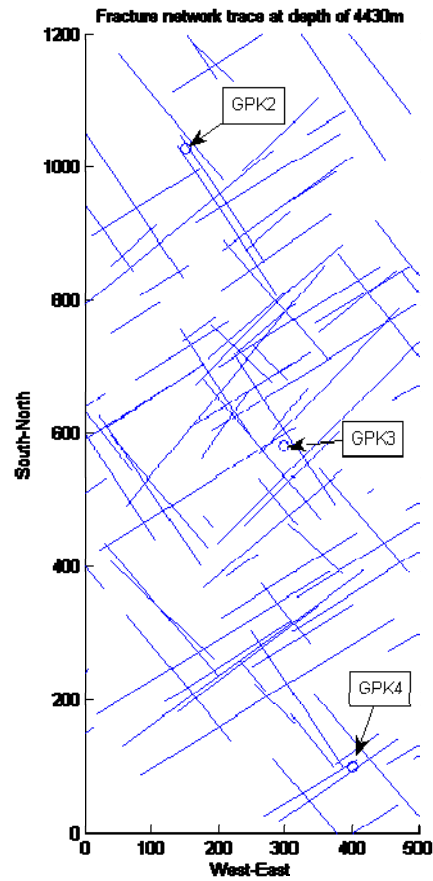


Fig. 4. A Soultz natural fracture network trace wells GPK2, GPK3 and GPK4 open holes at 4430 m. Trace plotted for fractures with radius greater than 60 m.

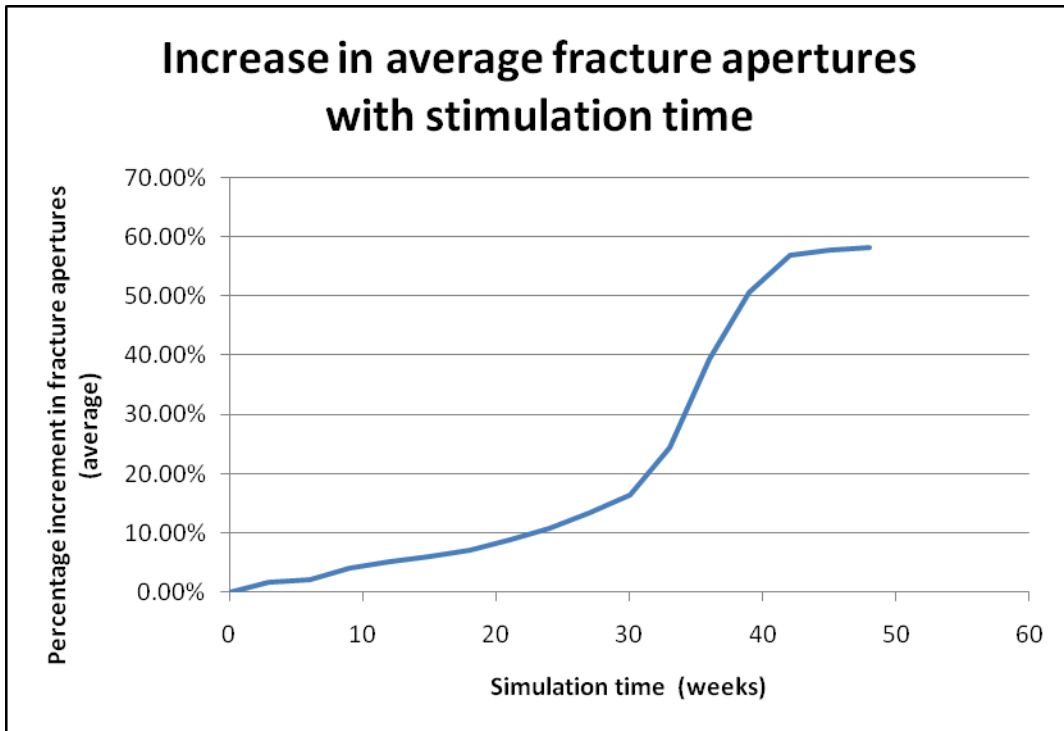


Fig. 5. Increase in average fracture aperture (retainable) with stimulation time. Injection pressure is 10,000 psi.

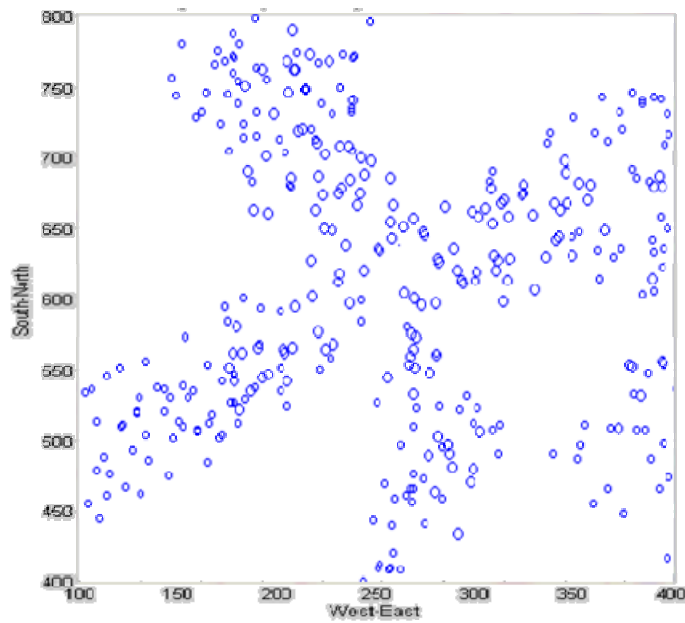


Fig. 6a. Cumulative shear dilation events in the fracture network after 8 weeks of stimulation (10,000 psi injection pressure) in a strike-slip stress regime. Marker sizes are proportional to the log of the event magnitudes.

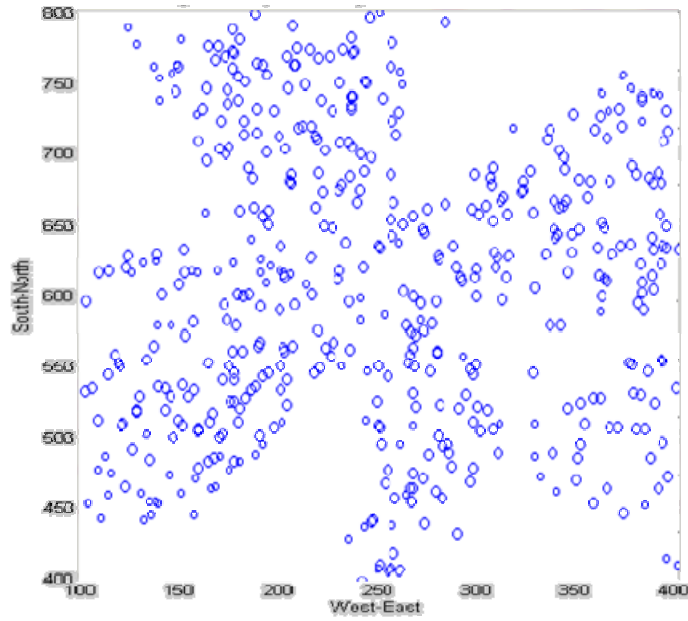


Fig. 6b. Cumulative shear dilation events in the fracture network after 24 weeks of stimulation (10,000 psi injection BHFP) in a strike-slip stress regime. Marker sizes are proportional to the log of the event magnitudes.

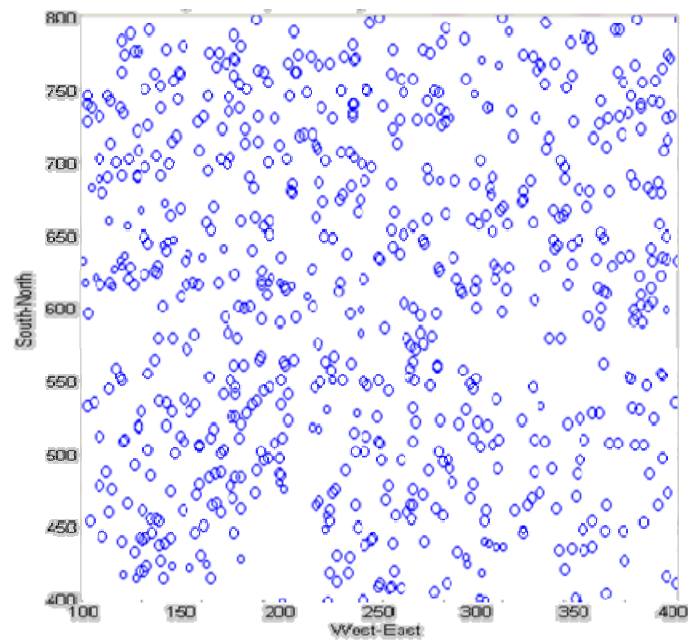


Fig. 6c. Cumulative shear dilation events in the fracture network after 40 weeks of stimulation (10,000 psi injection BHFP) in a strike-slip stress regime. Marker sizes are proportional to the log of the event magnitudes.

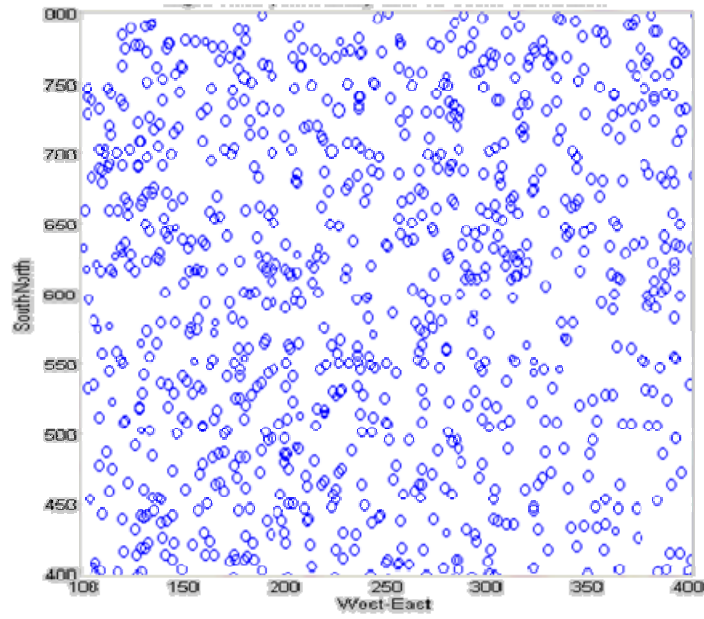


Fig. 6d. Cumulative shear dilation events in the fracture network after 52 weeks of stimulation (10,000 psi injection BHFP) in a strike-slip stress regime. Marker sizes are proportional to the log of the event magnitudes.

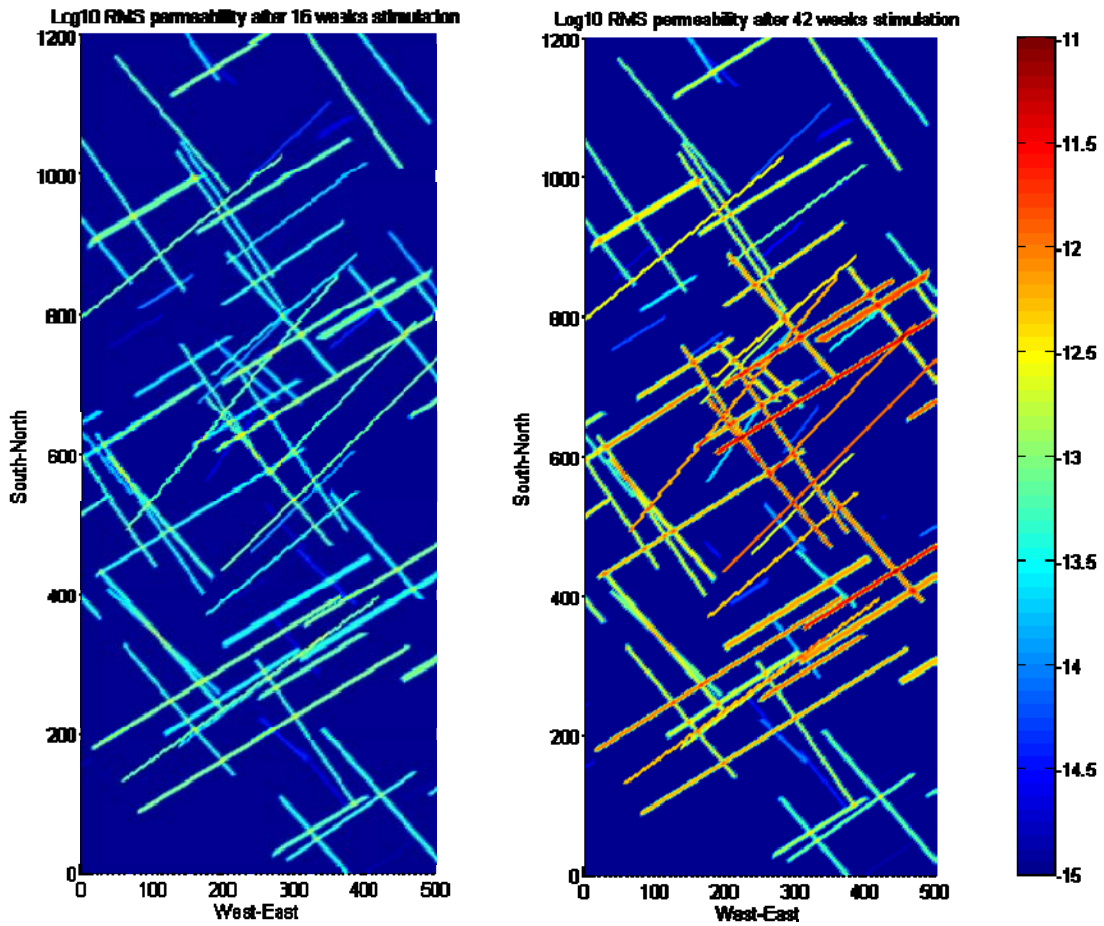


Fig. 7. Log₁₀ RMS effective permeability profile (magnitudes of diagonal terms) after 16 weeks (left) and 42 weeks (right) of stimulation with 10,000 psi injection pressure, pre-production phase.

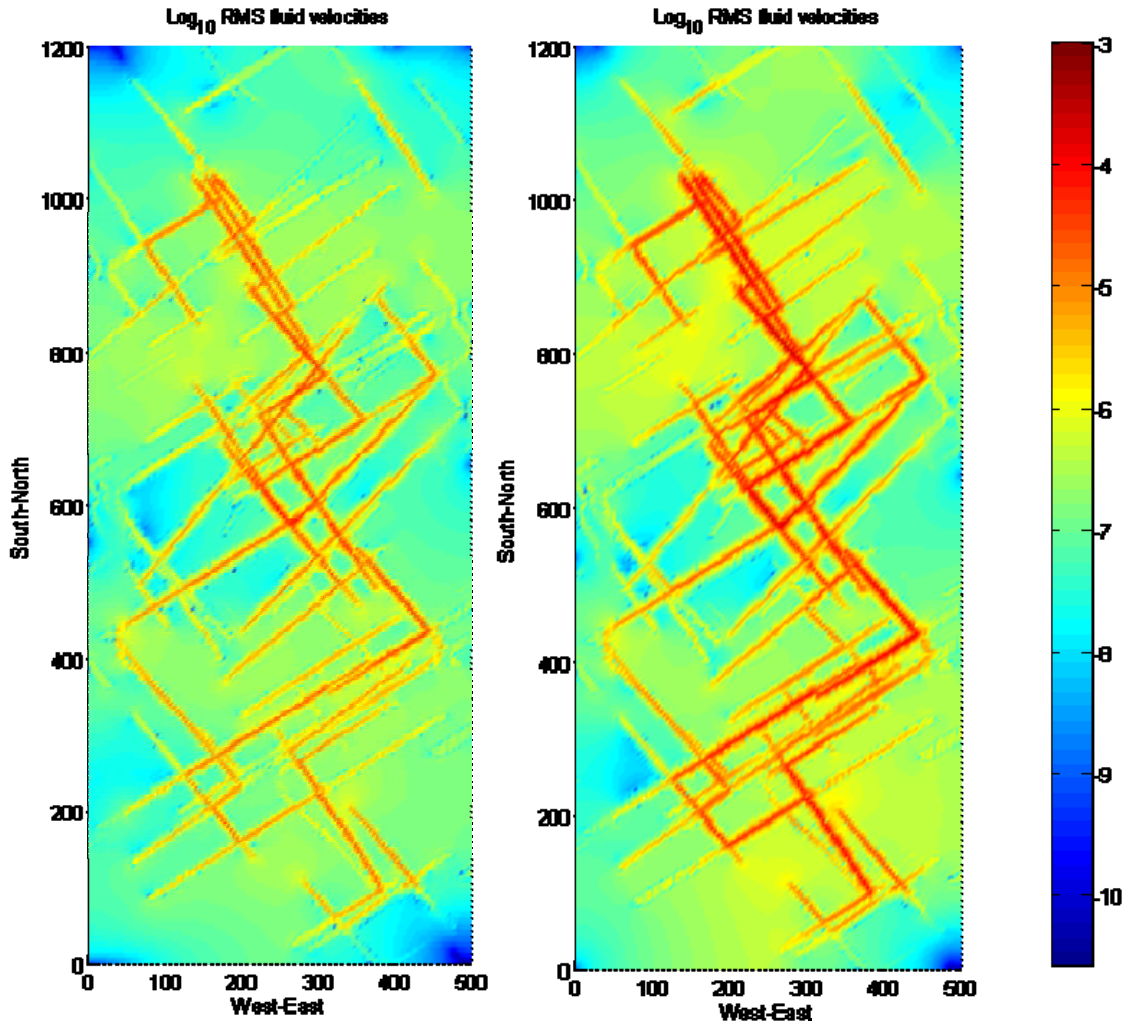


Fig. 8. Log₁₀ fluid RMS velocity profiles (magnitudes) after 10 years production for injector-producer pressure drops of 2000 psi, stimulation time prior to running the production case was 16 weeks (left) and 42 weeks (right).

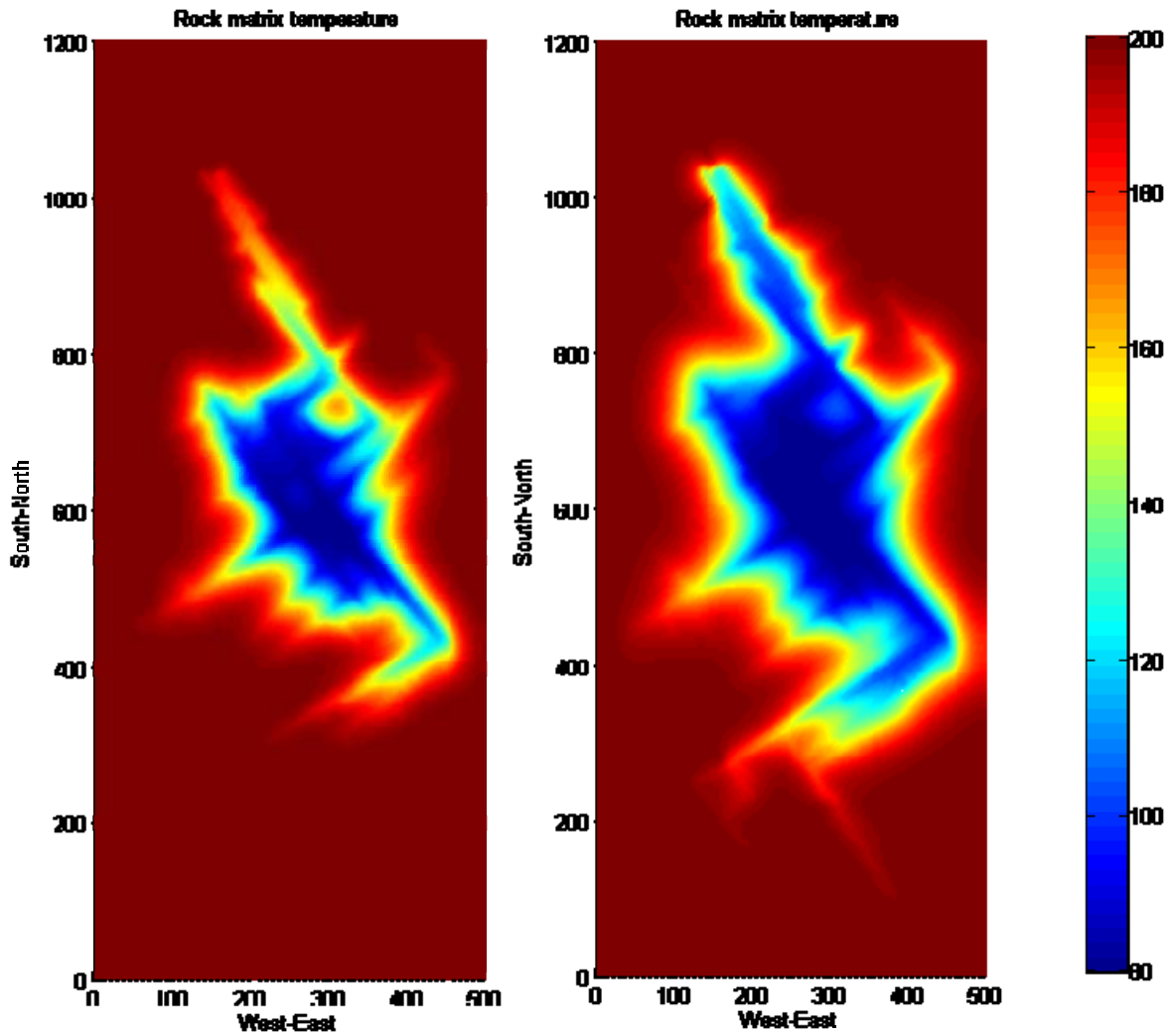


Fig. 9. Rock temperature profile after 10 years production for a injector-producer pressure drops of 2000 psi. Blue indicates rock at 80°C and red indicates rock at 200°C, stimulation time prior to running the production case was 16 weeks (left) and 42 weeks (right).

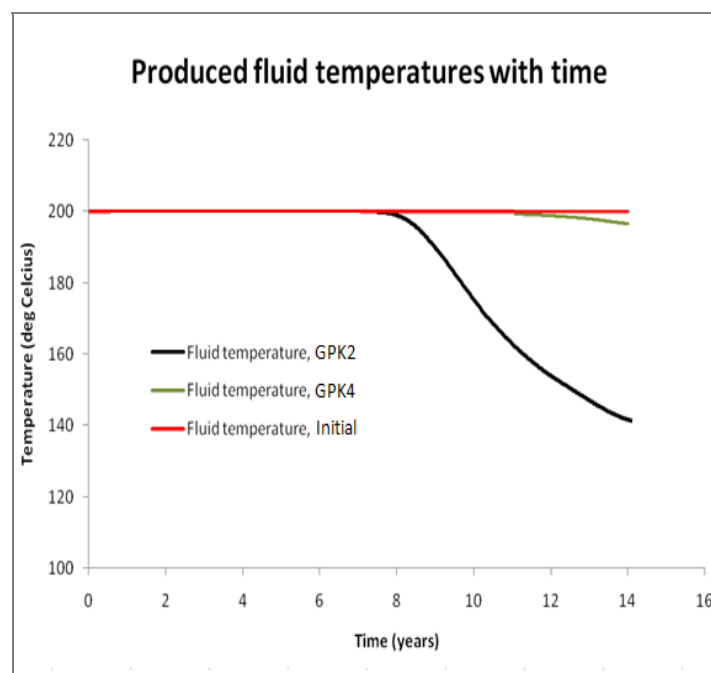


Fig. 10. Produced fluid temperatures vs. production time for GPK2 and GPK4. Stimulation time prior to running the production case was 42 weeks.

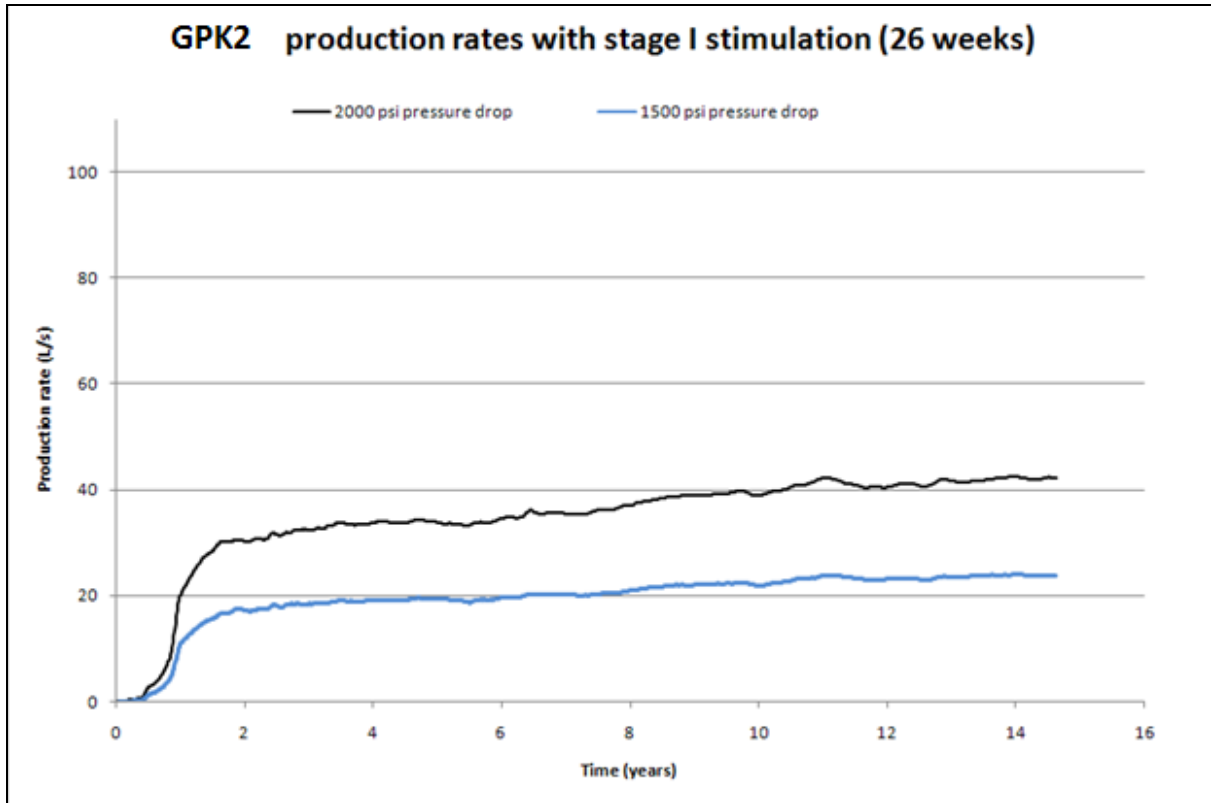


Fig. 11a. GPK2 production rates for injector-producer pressure drops of 2000 psi and 1500 psi over 15 years, with a reservoir stimulation time of 26 weeks.

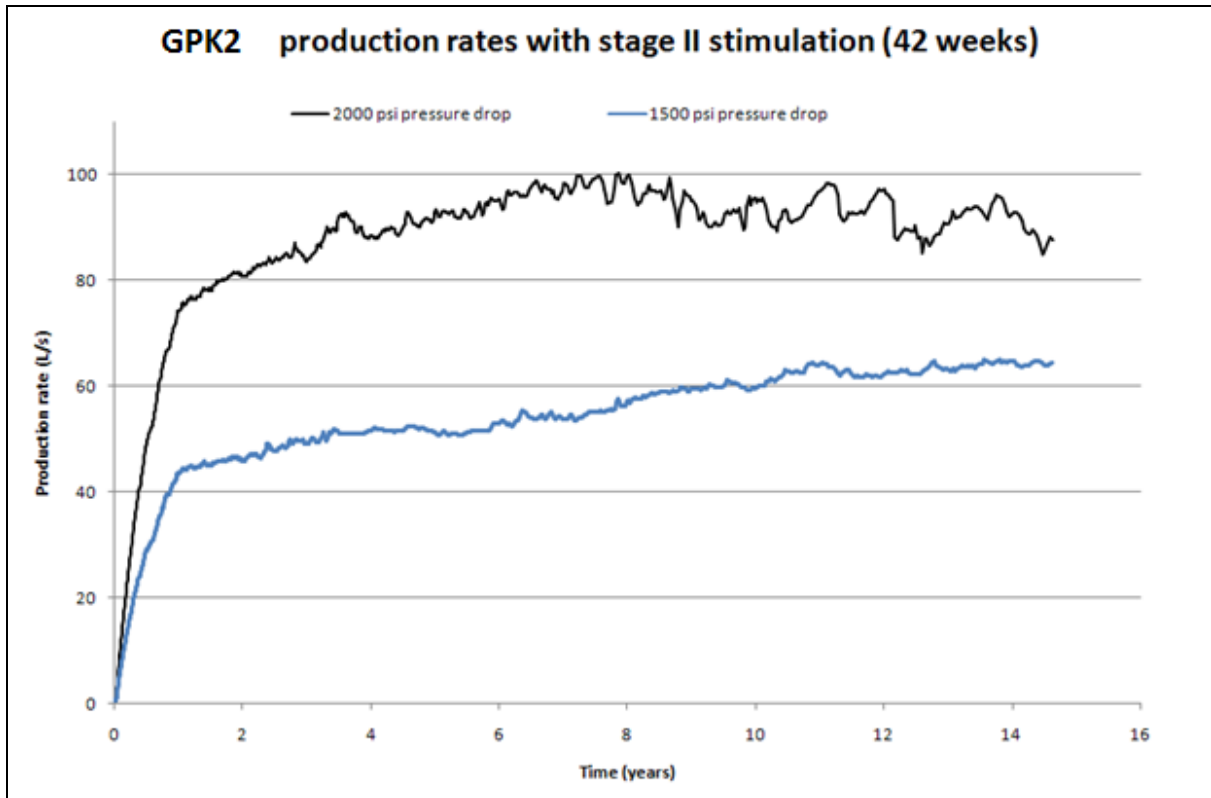


Fig. 11b. GPK2 production rates for injector-producer pressure drops of 2000 psi and 1500 psi over 15 years, with a reservoir stimulation time of 42 weeks.

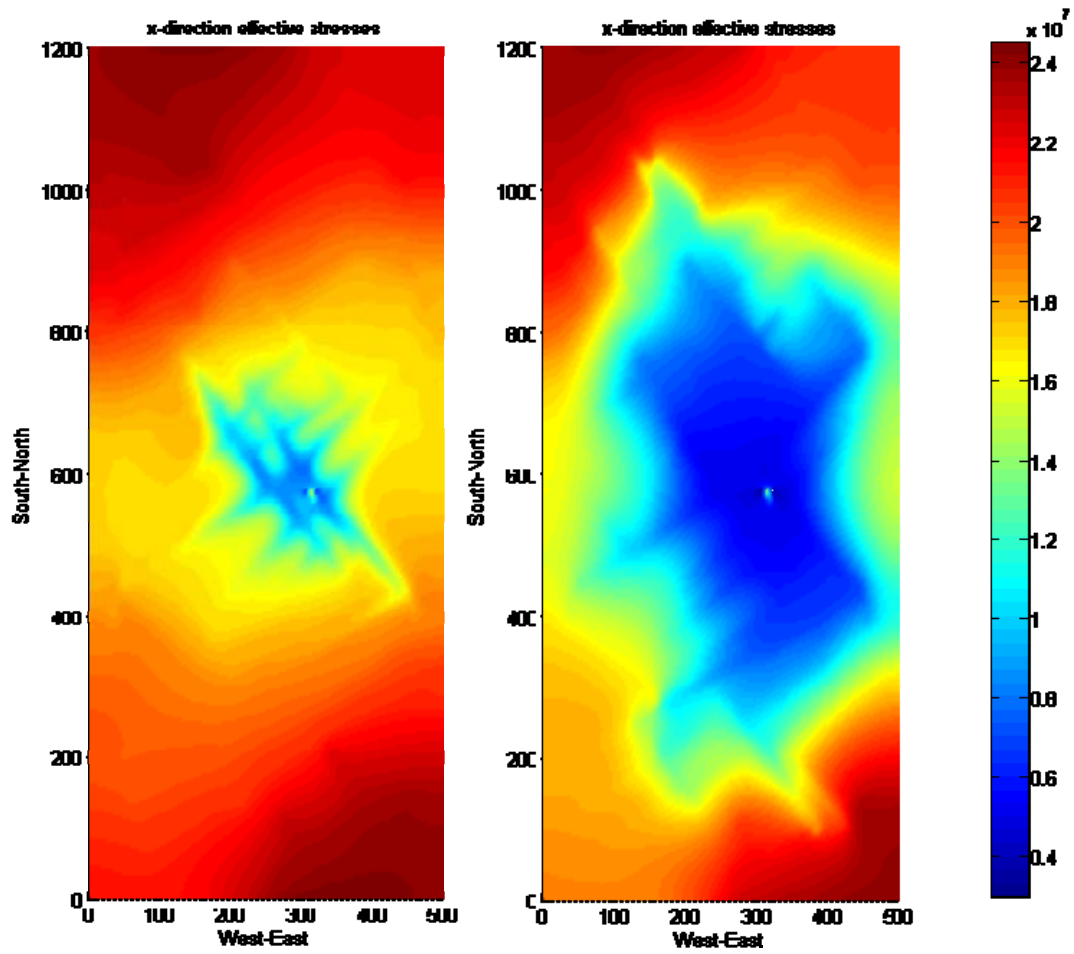


Fig. 12a. Effective stresses in the x direction at 3 years (left) and 10 years (right) injection time. Stimulation time prior to running the production case was 42 weeks.

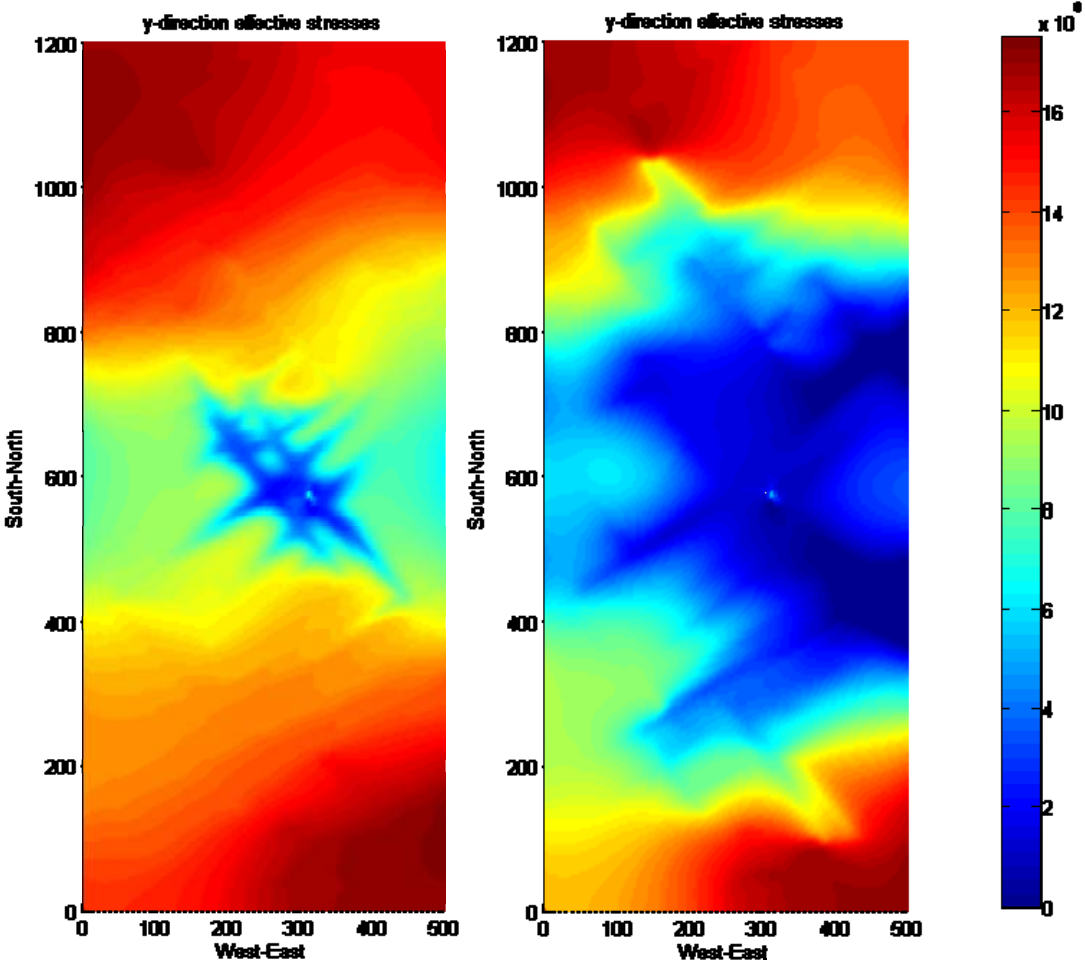


Fig. 12b. Effective stresses in the y direction at 3 years (left) and 10 years (right) injection time. Stimulation time prior to running the production case was 42 weeks.

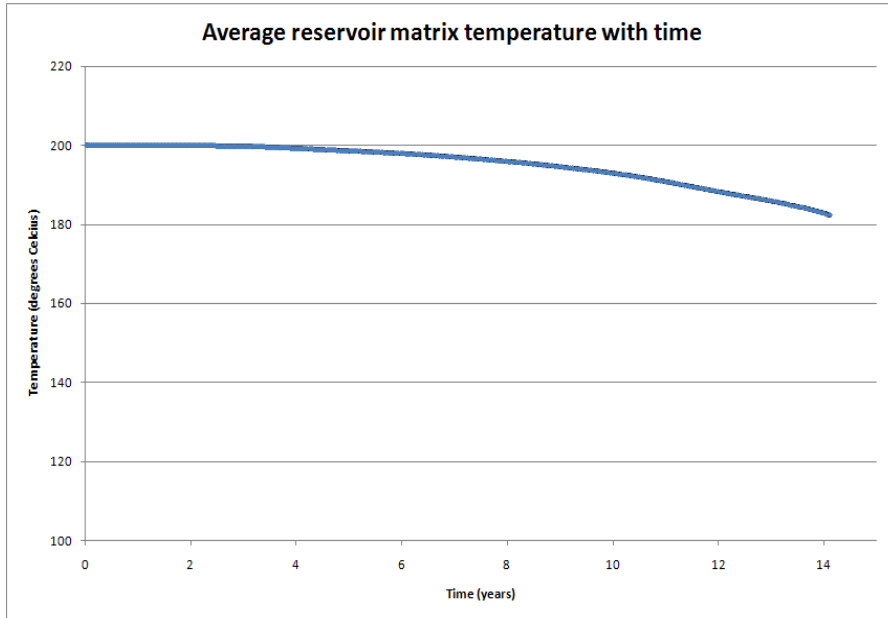


Fig. 13. Average matrix temperature vs. production time for 1.2 km (North-South) by 1.0 km (East-West) block enclosing wells GPK2, GPK3 and GPK4. Stimulation time prior to running the production case was 42 weeks.

Fracture set #	Plane direction			Dip				Number of fractures centers/m ³	Radius [m]	Transmissivity [m ² /s]
	Distribution law used	Mean	Half-width	Distribution law used	Mean	Half-width	Dip direction			
F1	Normal	2	16	Normal	70	7	NW	$1.30 \cdot 10^{-7}$	187	$6.0 \cdot 10^{-6}$
F2	Normal	162	19	Normal	70	7	NE	$3.00 \cdot 10^{-4}$	150	$6.0 \cdot 10^{-6}$
F3	Normal	42	6	Normal	74	3	NW	$1.76 \cdot 10^{-8}$	95	$4.0 \cdot 10^{-6}$
F4	Normal	129	6	Normal	68	3	SW	$3.30 \cdot 10^{-8}$	112	$2.0 \cdot 10^{-6}$
F5	Uniform	0	180	Normal	70	9	--	$1.00 \cdot 10^{-8}$	100	$5.0 \cdot 10^{-7}$

Table 1. Characteristics of statistical fracture sets obtained from Gentier et al. (2010). Plane direction is measured positive clockwise from North and dip positive downward from horizontal.

<i>Rock Properties</i>	
Young's modulus (GPa)	40
Poisson's ratio	0.25
Density (kg/m ³)	2700
Fracture basic friction angle (deg)	40
Shear dilation angle (deg)	2.8
90% closure stress (MPa)	20
<i>In situ</i> mean permeability (m ²)	9.0 x 10 ⁻¹⁷
<i>Fracture properties</i>	
Fractal Dimension, D	1.2
Fracture density (m ² /m ³)	0.12
Smallest fracture radius (m)	15
Largest fracture radius (m)	250
<i>Stress data</i>	
Maximum horizontal stress (MPa)	53.3
Minimum horizontal stress (MPa)	78.9
<i>Fluid properties</i>	
Density (kg/m ³)	1000
Viscosity (Pa s)	3 x 10 ⁻⁴
Hydrostatic fluid pressure (MPa)	34.5
Injector pressure, stimulation (MPa)	68.9
Injector pressure, production (MPa)	44.8
Producer pressure, stimulation	N/A
Producer pressure, production	31.0
<i>Other reservoir data</i>	
Well radius (m)	0.1
Number of injection wells	1
Number of production wells	2
Reservoir depth (m)	4430

Table 2. Stress and reservoir data for strike-slip stress regime.

Status of the Paralana 2 Hydraulic Stimulation Program

P. W. Reid *, L. McAllister * and M. Messeiller *

*Petratherm Limited, 129 Greenhill Rd, Unley 5061, South Australia

The Paralana Engineered Geothermal Project is located 600 km north of the city of Adelaide in South Australia (Figure 1). The project is testing for viable geothermal resources, within a sedimentary basin that lies immediately east of known high heat producing Mesoproterozoic basement rocks of the Mt Painter Region. In this area, 2D reflection seismic survey data and potential field geophysical (aeromagnetic, magneto-telluric and gravity) data delineate a major half graben informally termed the Poontana basin. Based on the interpreted geophysical data, Petratherm postulates that the high heat producing basement rocks observed in outcrop, continue under the insulating cover material, with the maximum thickness of the sedimentary cover in sections of the Poontana Sub-basin being modeled at greater than five kilometres. This favourable arrangement of thick sediments overlying anomalously radiogenic basement suggests that the Paralana area is an ideal location to test the development of an Engineered Geothermal System.

Petratherm Limited in joint venture with a major oil and gas (Beach Energy) and power industry energy utilities (TRUenergy) are initially seeking to build a 7.5 MW commercial power development to supply a local mine. In the second half of 2009 a deep geothermal well (Paralana 2) was drilled to 4012m. The well was designed as an injector, the first of an initial two well program to prove circulation between wells. An innovative strategy for development of the EGS reservoir is planned, involving massive hydraulic stimulation of multiple target zones within the sedimentary overburden. Multiple zone stimulation increases the chance of achieving a commercial flow rate which is the key commercial barrier for EGS developments around the world.

Keywords: EGS, Drilling, Fracture Stimulation

Paralana 2 Well Completion

The planned multizone stimulation of Paralana 2 involved the well being fully cased and cemented to allow better control on what intervals in the well would be stimulated in a cost effective manner. In the past, open hole hydraulic stimulations resulted in the main fracture developing at the zone of least resistance which is usually at the base of the casing shoe (lowest pressure point) or a locations where large natural fractures already occur. This in effect leaves much of the open hole unaffected by the stimulation program. Being the first well,

Paralana 2 was designed as an injector with the advantage of simplifying the well design and allowing learning from this well to be incorporated into the well design and planning of the production well (Paralana 3) to maximize the chances of achieving a commercial flow rate.

During drilling of the lower 8 1/2" section several fractures were encountered below 3400 m. High torques, drilling breaks, an increase in well-bore deviation followed by inflow of geothermal overpressurized brine provide strong indications for the presence of a natural and permeable fracture system between depths of about 3690 m and 3864 m. Increased rates of penetration during drilling through the fractured zones indicate a change in rock strength possibly related to open fractures. Shut in pressures indicated an overpressure of approximately 3,300 psi and the mud system required weighting up to 13.2 ppg to stop the inflow, and allow drilling to continue safely.

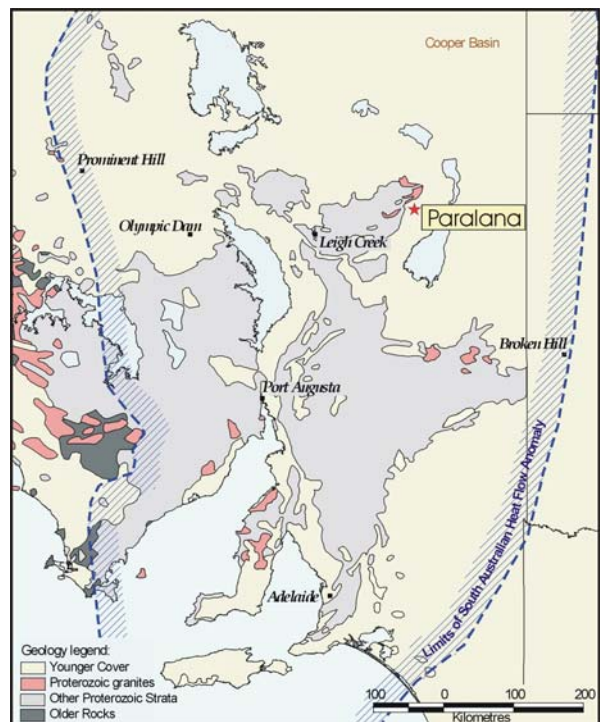


Figure 1: Regional Locality Map and extent of SAHFA (SAHFA modified from Neumann *et. al.* 2000)

Due to wellbore stability problems the characterization of this zone was limited to logging while drilling measurements down to 3740 m depth. The final 7" casing string was run to a depth of 3725 m as below this depth the well was too unstable to be able to set casing and cement in place (Figure 2).

Paralana 2 Geology

The litho- stratigraphic and structural environment of the Paralana Project area is complex and weakly constrained. The interpretation of the stratigraphic succession and lithology of the overlying Phanerozoic sequences and their contact with the underlying Adelaidean strata at Paralana-2 is based on the results of drilling Paralana-1B, drilled 1.5 km to west of Paralana-2. The Cambrian-Adelaidean unconformity is interpreted at 1115m and the sequence begins with the Amberoo Formation. The Tapley Hill Formation was entered at 1612m in Paralana2 and its contact with the underlying Sturtian Glacials has been interpreted at about 1803m. At 2855m, a 500metre thick haematic metaquartzose with siliceous cement underlies the tillite and grades to a litharenite with depth. Its age is ambiguous, but the metasediment is still considered as Adelaidean, within the Sturtian Tillite or the Callanna Beds.

At 3397m, a major change of lithology was observed during the drilling, associated with a key unconformity. It is related to a strong reflector observed on the seismic. Below the contact, the lithologies are mainly composed of dolomitic siltstones and sandstones, interbedded with numerous intervals of felsic tuffs. Several dolerite horizons are intercalated in the package, from a depth of 3450m to the bottom of the hole. Zircons extracted from the volcanic tuff returned a $^{207}\text{Pb}/^{208}\text{Pb}$ age of $1585 \pm 11\text{Ma}$ using a LA-ICPMS technique at the University of Adelaide. At 3910m, Paralana 2 entered a felsic intrusive, confirming high heat production rate of the basement of approximately 10 to $12 \mu\text{Wm}^{-3}$, and showing a similar Mesoproterozoic age of $1580 \pm 10\text{Ma}$.

Numerous intervals of fractures were encountered in the lower zone of the well based on interpretation of the logs and experienced during the drilling operation. A more complex tectonic history and the presence of dolerite in the sequence are indicated by a chaotic seismic signature below 3400m. The thick homogenous quartzite overlying the basal sequence is highly competent with rock strengths ranging between $16,000$ (110MPa) and $29,000$ psi (200MPa) as calculated from the sonic logs. This unit may be considered to act as a top seal to the fractured, overpressured unit below.

MEQ array

The Paralana Micro-seismic monitoring array has been operational since April 2008, recording the background seismicity at the Paralana Geothermal Project site. The array has recently been up-graded to a real-time monitoring network to enable Petratherm and the joint venture partners

to actively record, analyse and locate microseismic events during the stimulation of the geothermal reservoir. The growth of the fracture network during fracture stimulation will be monitored by seismologists from the Institute of Earth Science and Engineering, Auckland, New Zealand. The array combines sensitive downhole sondes with surface seismometers to enable the interpretation of a wide spectrum of seismic events. All events will be analysed, with auto-picking software, MIMO, developed by the Norwegian Seismic Array (NORSAR), providing data on the event location and magnitude.

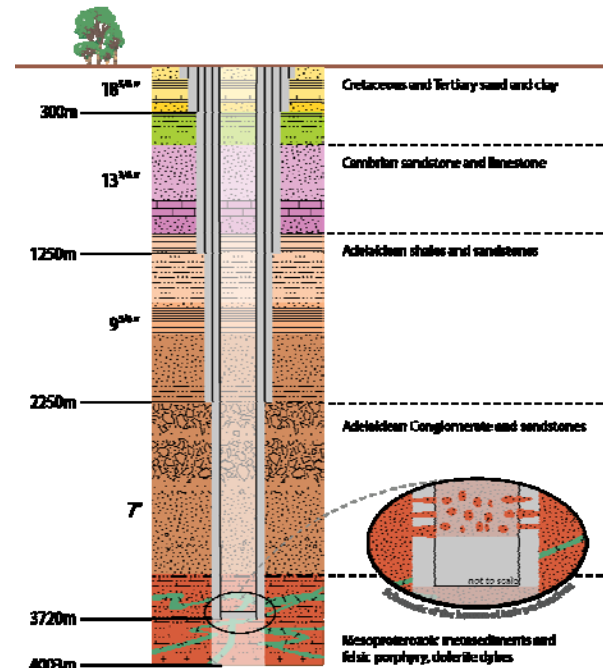


Figure 2: Paralana Well Completion and Geological log.

Stimulation Program

The initial stimulation program is to be undertaken in two stages. The Stage 1 Injectivity test involves perforation of the steel casing near the bottom of the Paralana 2 well and injection of a small volume of water to confirm fracture initiation and propagation. The test aims to derive information of the in-situ stress regime, reservoir properties and determine if the well is already connected to fractures of the natural overpressured zone encountered during drilling.

The Stage 2 fracture stimulation involves injection of large volume of water at higher rates. The stimulation aims to create a fracture network and connect to and enhance the existing natural fracture network intersected lower in the well. The stimulation also aims to generate significant micro seismic events, measured by the MEQ array, greater than 500 metres from the well bore. The volume and rate of the stimulation will be dependent on the micro-seismic response and adjusted to meet the objectives. A series of stepped injection rate tests are planned during

the stimulation to observe the development of the fracture network. Post the main water stimulation, tests will be performed to determine the injectivity flow rates. This will be followed by production testing if the well allows, to understand longer term reservoir performance. Acidizing and use of proppant with gel in the fracture stimulation is contingent on data obtained from the injectivity test. A second interval may be stimulated dependent on the results of the initial stimulation.

References

Neumann, N., Sandiford, M., & Foden, J. (2000) Regional geochemistry and continental heat flow: implications for the origin of the South Australian Heat Flow anomaly. *Earth and Planetary Science Letters*, 183, 107-120.

Three Dimensional Reservoir Simulations of Supercritical CO₂ EGS

Alvin I. Remoroza^{1*}, Behdad Moghtaderi¹, Elham Doroodchi¹

¹Priority Research Centre for Energy, School of Engineering (Chemical Eng.), Faculty of Engineering & Built Environment, University of Newcastle

University Drive, Callaghan, NSW 2308, Australia

*Corresponding author: remorozaair@yahoo.com

Following the work of Pruess (2008) on the production behaviour of CO₂ as a working fluid in EGS, a three dimensional (3D) reservoir sensitivity analysis of CO₂ mass flow and heat extraction rates on injection temperature, rock permeability, rock porosity and reservoir temperature were performed. The 3D reservoir simulations were performed using the TOUGH2 modelling code with the modified ECO2N module.

Keywords: CO₂-EGS, reservoir simulation, TOUGH2, ECO2N

Background of the study

The literature on the application of supercritical CO₂ for Engineered Geothermal System (EGS) is relatively scarce. Most of the available literature are 1D and 2D simulations of the thermodynamic and transport properties as well as exergy analysis (Atrens et al, 2008; Atrens et al, 2009; Atrens et al, 2009; Brown et al, 2000; Pruess et al, 2006; Reichman et al, 2008; Remoroza et al, 2009).

Pruess (2008) performed 2D and 3D reservoir simulations of injection/production behaviour of an EGS operated with CO₂ as working fluid using TOUGH2 with fluid property module "EOSM" which is not commercially available. His simulations examine production behaviour in 2D areal model at different reservoir pressures and then assessed 3D flow effects on energy recovery. Table 1 lists the reservoir and CO₂ injection parameters used by Pruess (2008) and in this study.

The equivalent permeabilities calculated from the Soultz granite inferred from geophysical and flow log analysis range from $5.2 \times 10^{-17} \text{ m}^2$ to $9.6 \times 10^{-16} \text{ m}^2$ (Sausse et al, 2006) while intact granite has 1.6 to $3.8 \times 10^{-19} \text{ m}^2$ permeabilities (Selvadurai, 2005). Soultz EGS average equivalent permeability is $5 \times 10^{-16} \text{ m}^2$.

Porosities of granite range from 0.2 to 4% (<http://www.granite-sandstone.com/granite-physical-properties.html>).

This study will expand the previous 3D reservoir simulations of Pruess (2008) by determining the impact of injection and reservoir parameters such as permeability, porosity, reservoir temperature and CO₂ injection temperature on the CO₂ mass flow and heat extraction rates. Also, the

applicability of the modified fluid property module ECO2N for EGS will be examined.

Table 1. Reservoir and CO₂ injection/production parameters.

	Pruess (2008)	This study
Formation		
Thickness, m	305 (5 layers)	305 (5 layers)
Fracture spacing, m	50	50
Permeable volume fraction	2%	2%
Permeability in fracture domain, $\times 10 \times 10^{-15} \text{ m}^2$	50	0.5, 5 and 50
Nos. of MINC	5	5
Porosity in fracture domain	50%	50%
Permeability in rock matrix, $\times 10 \times 10^{-15} \text{ m}^2$	50	0.5, 5 and 50
Porosity in rock matrix		0.2%, 2%
Rock grain density, kg/m^3	2650	2650
Rock specific heat, kJ/kg	1000	1000
Rock thermal conductivity, $\text{W/m}\cdot\text{°C}$	2.1	2.1
Initial conditions		
Reservoir fluid	CO ₂ , H ₂ O	CO ₂ , H ₂ O
Temperature, °C	200	200, 225
Pressure, bar	200	200
Production/Injection		
Production area, km^2	1	1
Fraction of the area modelled	1/8	1/4
Spatial resolution, m	32.14 and 70.1	20.83, 45.45
Injection Temperature, °C	20	20, 35
Injection pressure, bar	210 gravity equilibrated from top layer	210 gravity equilibrated from top layer
Production pressure, bar	190 gravity equilibrated from top layer	190 gravity equilibrated from top layer

Methodology

Because the fluid property module used in the only published 3D reservoir modelling of CO₂ flows in EGS is not publicly available; a modified ECO2N fluid property module is used in the present study. ECO2N is a fluid property module for the TOUGH2 simulator (Version 2.0) that was designed for applications to geologic sequestration of CO₂ in saline aquifers (Pruess, 2005). The temperature limitation of this module is $10^\circ\text{C} \leq T \leq 100^\circ\text{C}$. In the modified version of ECO2N the restriction on the upper temperature is removed with the provision that only pure

phases like CO₂ or H₂O are present (i.e. no mixture).

The 3D simulations in this study were conducted using TOUGH2 in conjunction with the pre and post-processing graphical interface PetraSim. Because of symmetry, only 1/4 of the calculation domain (1 km² five-spot well configuration) was simulated in this study (Figure 1). Also, a modified CO2TAB file was used so that wider ranges of pressure and temperature, which are more appropriate for EGS application, can be studied. CO2TAB lists thermodynamic properties of CO₂ at different temperature-pressure conditions which are then used by TOUGH2.

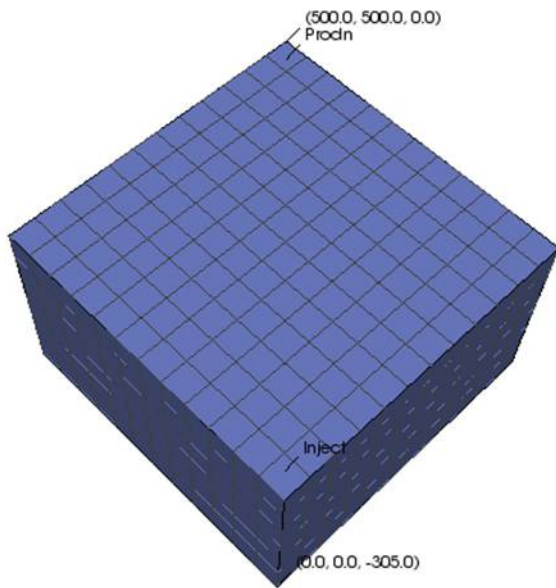


Figure 1: The 1/4 section of the five-spot well configuration showing an injection-production segment.

To validate the use of the modified ECO2N, the result of the previous 3D reservoir simulations were duplicated by finding the appropriate grid size equivalent to the previous model used by Pruess (2008). The previous study did not define rock wall specifications in the definition of fracture domain, i.e. permeability and porosity of the rock matrix. In the first attempt, different permeabilities were used for fracture domain and rock matrix (wall rock). A match was found for configuration where all layers of the production wells are open using a 12x12 areal grid (41.67 m side length) and rock matrix permeability of 1.9×10^{-14} m² and porosity of 0.2% (Figure 2). However, for configuration where only the top 50 m of the production well is open, the 12x12 areal grids of the 1/4 symmetric model gives higher mass and heat extraction rates (Figure 3).

Doubling the areal grid size to 24x24 (20.83 side length) and defining rock matrix permeability equal to fracture domain permeability (5×10^{-14} m²) and rock matrix porosity to 0.2% gave an almost perfect match both for CO₂ production well open

to all layers (Figure 4) and open only to topmost 50 m layer (Figure 5).

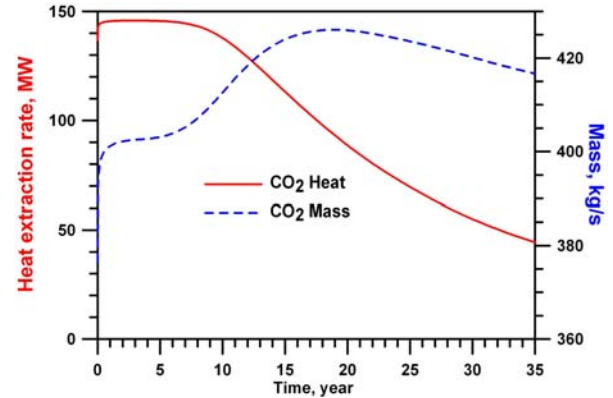


Figure 2: The CO₂ mass and heat extraction rates from this study match the previous study for a CO₂ production well open in all six layers using the 1/4 symmetric model having 12x12 areal grids and rock matrix permeability of 1.9×10^{-14} m² and porosity of 0.2%.

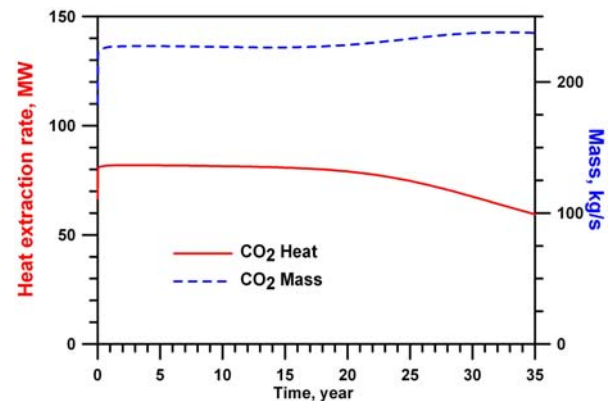


Figure 3: The CO₂ mass and heat extraction rates from this study are higher than the previous study for a CO₂ production well open only in topmost 50 m layer using a 1/4 symmetric model having 12x12 areal grids and rock matrix permeability of 1.9×10^{-14} m² and porosity of 0.2%.

The reservoir simulation results from the 1/4 symmetric model with 24x24 areal grid size was then used as the reference for sensitivity analysis. The result from this section of the study also proved the applicability of modified ECO2N for reservoir simulation of pure phase CO₂ reservoir flows.

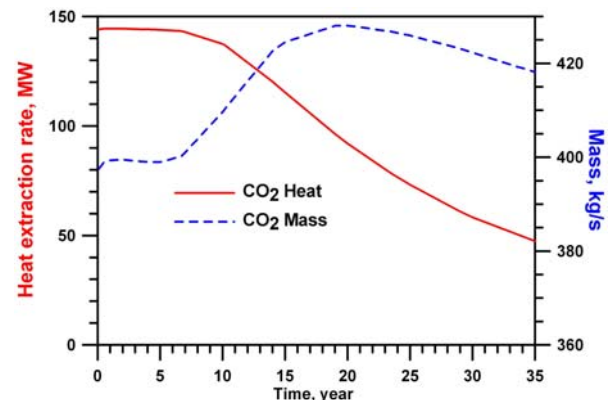


Figure 4: CO₂ mass and heat extraction rates from a 1/4 symmetric model having 24x24 areal grids and rock matrix

permeability of $5 \times 10^{-14} \text{ m}^2$ and porosity of 0.2% match the previous study from a CO₂ production well open in all six layers.

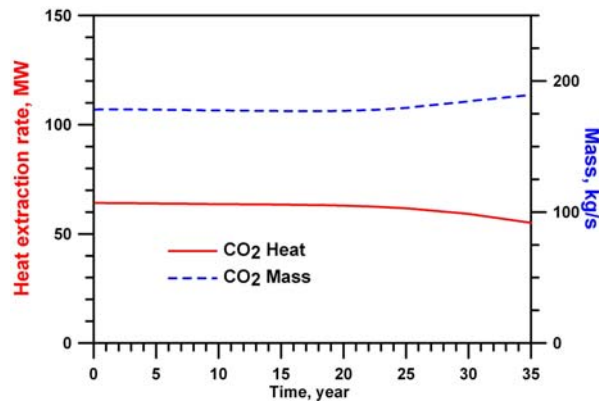


Figure 5: CO₂ mass and heat extraction rates using a 1/4 symmetric model having 24x24 areal grids and rock matrix permeability of $5 \times 10^{-14} \text{ m}^2$ and porosity of 0.2% match the previous study from a CO₂ production well open only in topmost 50 m layer.

Results and Discussion

The high CO₂ mass circulation at a reservoir temperature of 200°C for a production well open to all layers initially resulted in very high heat extraction rates and rapid decline of the reservoir thermal content (144 MW to 47 MW) due to thermal depletion of the reservoir. In contrast, H₂O mass circulation was found to be low with a relatively slow decline rates and consequently slow decline in heat extraction rates (24 MW to 16 MW, Figure 6). However, as the previous study recommended, for the case of CO₂ EGS when only the topmost 50 m layer configuration (Figure 5) was used in the analysis stable mass production and heat extraction rate of 64 MW after 2 years were resulted.

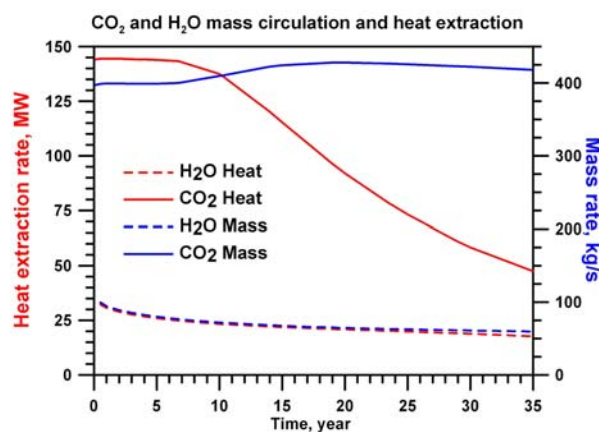


Figure 6: CO₂ and H₂O pure phase mass and heat extraction rates at 200°C reservoir.

The effect of injection temperature on CO₂ mass and heat extraction rates is shown in Figure 7. Increase in injection temperature above the critical temperature (31.4°C) resulted in higher mass production but lower heat extraction rates.

The 35°C injection temperature is more or less the appropriate value for regions with arid climate like Australia's EGS locations.

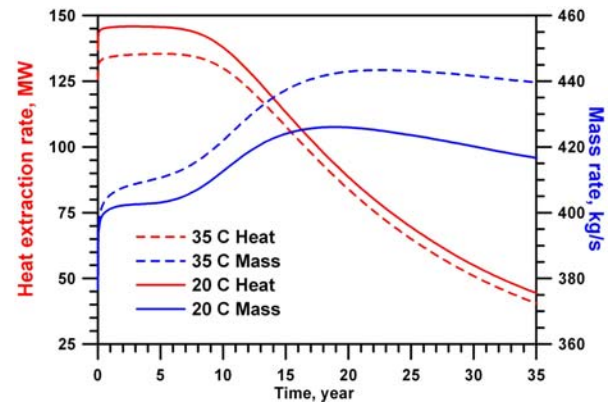


Figure 7: Effect of injection temperature on CO₂ mass and heat extraction rates in a 200°C EGS reservoir.

Rock matrix permeability has dramatic effect on CO₂ mass production. In our studies the mass production rates dropped from ~400 to 185 and 29 kg/s when one and two orders of magnitude decrease in permeability was implemented, respectively. Heat extraction rate, on the other hand, declined to 67 and 11 MW, respectively (Figure 8).

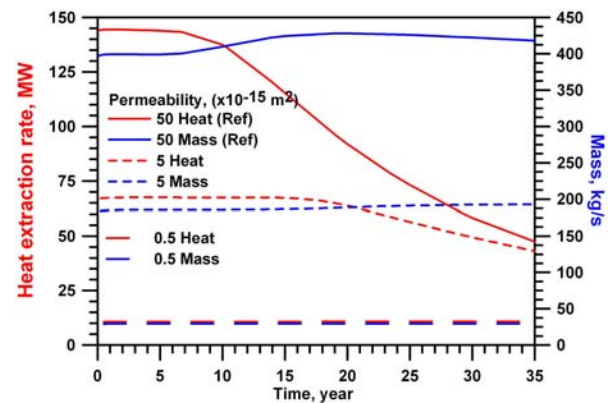


Figure 8: Effect of rock matrix permeabilities on CO₂ mass production and heat extraction rates.

Rock matrix porosity has no significant effect on the CO₂ mass production and heat extraction rates (Figure 9).

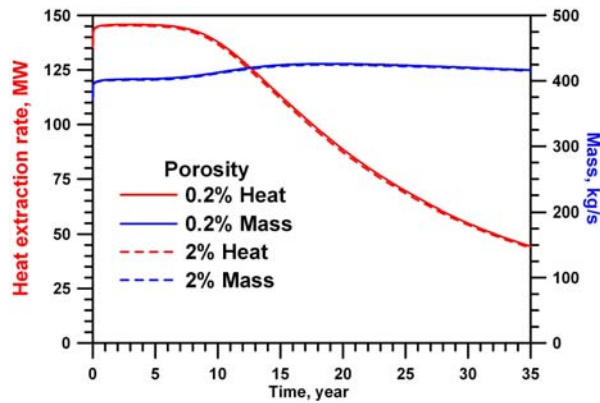


Figure 9: Effect of rock matrix porosity on CO₂ mass production and heat extraction rates.

The average CO₂ mass flow rates did not vary greatly with reservoir temperature (411 kg/s at 200°C, 398 kg/s at 225°C, and 395 kg/s at 175°C). Average heat extraction rates for the 200 and 225°C reservoir temperatures were found to be similar at 117 and 113 MW, respectively. However, at low reservoir temperature, the average heat extraction rate decreased to about 90 MW (Figure 10).

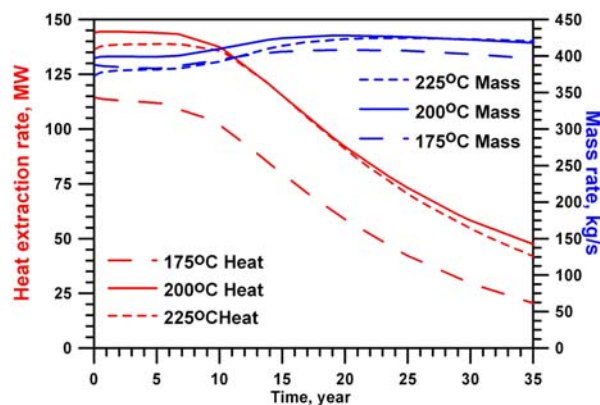


Figure 10: Effect of reservoir temperature on CO₂ mass production and heat extraction rates.

References

Somerville, M., Wyborn, D., Chopra, P., Rahman, S., Estrella, D. and Van der Meulen, T., 1994, Hot Dry Rocks Feasibility Study, Energy Research and Development Corporation, Report 243, 133pp.

Atrens, Al.D., Gurgenci, H., and Rudolph, V., 2008, *Carbon Dioxide Thermosiphon Optimisation*, Paper presented at the Proceedings of the Sir Mark Oliphant International Frontiers of Science and Technology Australian Geothermal Energy Conference, Rydges Hotel, Melbourne.

Atrens, Al.D., Gurgenci, H., and Rudolph, V., 2009a, CO₂ Thermosiphon for Competitive Geothermal Power Generation. *Energy & Fuels*, 23(1), 553-557.

Atrens, Al.D., Gurgenci, H., and Rudolph, V., 2009b, *Exergy Analysis Of A CO₂ Thermosiphon*, Paper presented at the PROCEEDINGS, Thirty-

Fourth Workshop on Geothermal Reservoir Engineering, Stanford University, Stanford, California.

Brown, D.W, 2000, *A Hot Dry Rock Geothermal Energy Concept Utilizing Supercritical CO₂ Instead Of Water*, Paper presented at the PROCEEDINGS, Twenty-Fifth Workshop on Geothermal Reservoir Engineering, Stanford University, Stanford, California.

Pruess, K., 2008, On production behavior of enhanced geothermal systems with CO₂ as working fluid, *Energy Conversion & Management*, 49(6), 1446-1454.

Pruess, K., and Azaroual, M., 2006, *On The Feasibility Of Using Supercritical CO₂ As Heat Transmission Fluid In An Engineered Hot Dry Rock Geothermal System*, Paper presented at the PROCEEDINGS, Thirty-First Workshop on Geothermal Reservoir Engineering, Stanford University, Stanford, California.

Pruess, K., 2005. ECO2N: A TOUGH2 Fluid Property Module for Mixtures of Water, NaCl, and CO₂. Report LBNL-57952. Earth Sciences Division, Lawrence Berkeley National Laboratory: Berkeley, University of California.

Reichman, J., Bresnehan, R., Evans, G., and Selin, C., 2008, *Electricity Generation using Enhanced Geothermal Systems with CO₂ as Heat Transmission Fluid*. 189. Paper presented at the Proceeding of the Sir Mark Oliphant International Frontiers of Science and Technology Australian Geothermal Energy Conference, Rydges Hotel, Melbourne.

Remoroza, A.I., Moghtaderi, B., and Doroodchi, E., 2009, *Power Generation Potential of SC-CO₂ Thermosiphon for Engineered Geothermal Systems*, Paper presented at the Australian Geothermal Energy Conference 2009, Hilton Hotel Brisbane.

Sausse, J., Fourar, M., and Genter, A. 2006 Permeability and alteration within the Soultz granite inferred from geophysical and flow log analysis. *Geothermics*, 35(5-6), 544-560.

Selvadurai, A. P. S., Boulon, M. J., and Nguyen, T. S., 2005, The Permeability of an Intact Granite. *Pure and Applied Geophysics*, 162(2), 373-407.

Measuring the Success of EGS Projects: An Historical to Present Day Perspective

Catherine E. Stafford*

Granite Power Ltd, Level 6, 9 Barrack Street, Sydney, NSW 2000.

*Corresponding author: cstafford@granitepwr.com

World wide, Enhanced Geothermal System (EGS) projects have been around for over 35 years, commencing with the Fenton Hill research and development project in New Mexico back in 1972. Many years of knowledge have been accumulated through various research and commercial projects.

As to be expected with an evolving industry, some significant development issues are still to be fully or properly overcome, such as a appropriate down-well technologies and management of induced seismicity. However, several factors indicate that this 'new' type of geothermal technology and its associated industry has moved beyond being just a research and development concept. Such factors include: the growth in the number of commercial projects, with some of these now in production; cementing of the industry through associations and government incentives; the development of geothermal reporting codes for commercial credibility (i.e. Australian and Canadian); and considerable progress in the resolution of ongoing development issues.

This paper provides a perspective on the success of EGS projects to date. This is very much a first-pass assessment as the technical and commercial data publicly available is currently too sparse and project specific to enable a rigorous quantitative study at this stage. However, it is intended to offer a snapshot take on the success and evolution to date of the EGS sector of the geothermal industry. It reveals that many projects have been successful at what they set out to achieve. It is also apparent that EGS development in Australia is likely to be more 'successful' than elsewhere because the continent's stress regime allows favourable sub-horizontal fracture development.

Keywords: Enhanced geothermal system, EGS, hot dry rock, HDR, success, industry, Hot Rock

Definition of EGS

Geothermal power has been generated from hydrothermal geothermal resources for many decades. However, such resources are limited to areas where accessible hydrothermal systems are found, such as the world's volcanic regions e.g. the Pacific Rim countries.

Geothermal exploration in all areas requires a balance of a accessible temperature, water supply and an adequate flow rate in order to produce

electricity economically. Water may have to be introduced to the system or may be present. In geothermal plays away from conventional geothermal terranes, required temperatures will likely be found at greater depth where permeability is often decreased (tight rocks), so reservoir enhancement by physical or chemical means is required to obtain flow rates that are considered economic.

Over the years the concept of enhanced geothermal reservoirs has been described with several acronyms e.g. Hot Dry Rocks (HDR), Hot Wet Rocks (HWR), Hot Fractured Rocks (HFR) and HR (Hot Rocks). Such projects have comprised the artificial creation of an underground heat exchanger by the drilling of a well into e.g. granite, the stimulation of that well to create a reservoir (usually by hydraulic stimulation and/or chemical stimulation), and the drilling of a producer well into the margin of the created reservoir.

In the last few years EGS has become the most accepted descriptor in the northern hemisphere. Recent definitions include:-

- *"EGS are a new type of geothermal power technologies that do not require natural convective hydrothermal resources."* (en.wikipedia.org/wiki/Enhanced_Geothermal_Systems)
- *"EGS are engineered reservoirs created to produce energy from geothermal resources that are otherwise not economical due to lack of water and/or permeability."* Department Of Energy, USA:
http://www1.eere.energy.gov/geothermal/enhanced_geothermal_systems.html)
- *"An Enhanced Geothermal System is an underground reservoir that has been created or improved artificially."* TP GEOELEC: the newly formed GEOELEC-Platform, was launched on 2nd of December 2009, and comprises more than 130 geothermal experts from the industry and the research sector who voted on the definition of EGS in March 2010. The secretariat of the panel is managed by the European Geothermal Energy Council.
(<http://www.egec.org/ETP%20Goelec/Conclusion%20EGS%20definition.pdf>)

This latest definition, would include all conventional geothermal wells that have been stimulated to improve reservoir performance.

During the development of the Geothermal Industry Technology Roadmap (DRET, 2008) the Australian community recognised that terms such as HFR, HDR and HWR were rather specific, and that EGS could be applied to geothermal resources with significant existing permeability. Therefore the term Hot Rock was adopted to encompass that end of the spectrum of geothermal resources that required significant permeability enhancement. The term Hot Sedimentary Aquifers is applied to that end of the spectrum where significant permeability exists naturally.

Here we consider the success of enhanced geothermal systems, with focus on the unconventional (non-volcanic related) systems.

The Rapid Growth of the EGS Sector

This preliminary (and non-exhaustive) review has found that to date there are in existence, or now terminated, some forty-seven EGS projects (to mid June 2010). These projects are listed in Table 1.

The data presented in this compilation is somewhat incomplete, has been variably sourced and as a result accuracy cannot be guaranteed. In the time-frame available for this preliminary study, project data was often difficult to acquire or was not acquired. It is recognised that such omissions impact on the results and hence, any interpretation of those results. For example, it may be more likely that there is non-publicity for unsuccessful projects or unsuccessful parts of projects. A more rigorous study is certainly needed but at this stage of the industry's development may not be possible due to the limited and site specific nature of the data.

The data show that over the last four decades, over 50% (27) of the EGS projects commenced in the last 5 years (Figure 1 and Table 1). Over the whole of the last decade 78% (37) of the total projects were commenced (Figure 1) with over half of these projects being commercially funded as opposed to demonstration or R&D projects (Table 1).

Conversely, during the 1970's, 80's and 90's projects were predominantly research-driven (Table 1).

The huge growth in the number of projects seen over the last five years indicates that confidence in this sector has grown rapidly. This can be attributed to the knowledge and acquired skills gained from the early projects, technology development e.g. drilling deeper being more

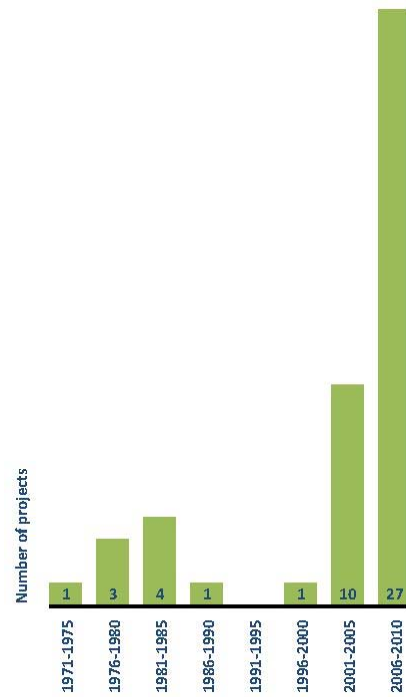


Figure 1: Bar chart showing the number of EGS projects commenced from 1970 to 2010.

easily attained and with less risk, government policy and to the perceived success of previous projects.

Indicators of Success

In a mature EGS industry, success would likely be measured by the amount of power produced i.e. in megawatts. However, relatively little data is yet available with only a modest number of projects well developed. Thus, measuring success is difficult at this stage. However, it is suggested that even a preliminary evaluation is useful as a tool for all concerned.

A broad-brush assessment is presented here looking at technical success and commercial success of projects, with these being defined below.

In terms of the development of the industry, there are many other factors, which are not discussed here, that can be indicative of the growth of the geothermal industry as a whole, as well as for the EGS sector. These include: acceptance of risk and risk management; wide application of the technology; government support via grants; geothermal studies; legislation; service industry support via dedicated groups and research and development; number of R&D/demonstration projects; number of commercial projects.

Table 1: EGS Projects Identified, as of Mid-June 2010

Start	Where	Region	Project	Who	Purpose	Status	Success		Reservoir rock	Depth	Temperature	Production temperature	Power output	Main source	Comment	
							Technical	Commercial								
1	1972	USA	NM	Fenton Hill		R	TE	Y	Y	Granite	3.5	195	158	3	1, 7	Producing power for >20 years. Ended 1996
2	1976	Germany	Bavaria	Falkenberg		R	TE	Y	N	Granite	0.3	85			1, 10	Successful fracturing, & short circ tests. Project finished 1985
3	1976	UK	Cornwall	Rosemanowes	Camborne School of Mines	R	TE	Y	N	Granite	2.7	79			1	Successful drill, frac & circulation for four yrs. Ended 1991
4	1977	France		Le Mayet de Montagne		R	TE	Y	N	Granite	0.8	33			1, 10	Granite from surface. Successful frac & circ tests. Project ended 1994
5	1982	Japan		Ogachi				Y	N		1.3	240			1	Volcanic. Poor connectivity (~90% water loss)
6	1983	Japan		Higashi-Hachimantai		R	TE	Y	N	Granite	0.4	60			10	
7	1985	Sweden		Fjalbacka		R	TE	Y	N	Granite	0.5	15			1	Successful 40 day circulation test. Ended 1989
8	1985	France		Soultz-en-Forêt	ENGINE	R	OP	Y	Y	Granite	4.2	200	155	1.5	1, 7, 8, 9	Prod. power for >15 years.
9	1988	Japan		Hijiori		R	TE	Y	N	Granodiorite	2.7	270	163		1, 4	A lot of short tests, with varied results; & water loss ~50%
10	1999	Australia	NSW	Hunter Valley	Pacific Power	D	TE			Granite					1	Elcom. Discontinued due to funding issue. Site later acquire by Geodynamics
11	2001	Australia	NSW	Jerry's Plain	Geodynamics	C				Granite						Inferred resource
12	2001	Switzerland		Basel		D	TE	Y		Granite	5	200			2	Fracturing caused 3.4R earthquake. Proj suspended.
13	2002	Germany		Bad Urach				Y		Mica-syenite	3.3	170			2	Series of successful short frac & circ tests
14	2002	Australia	SA	Cooper Basin	Geodynamics	C	DR	Y	Y	Granite	4.3	250	200		1, website	Proof of concept achieved 2009 (flow btw 2 wells)
15	2002	USA		Coso		R		Y							1	Stimulated same fracture via 2 wells. Second stimulation caused swarm of EQs
16	2002	USA	NV	Desert Peak	Ormat	C									1	Adjacent to conventional geothermal area.
17	2003	El Salvador		Berlin		C	OP	Y	Y		2					Stimulation of tight injection well for existing geothermal field
18	2003	Germany	Hanover	Horstberg (GeneSys)	GEOZENTRUM	R	TE	Y	N	Sandstone	3.8				2	Single well. Frac & circ was achieved, and inadequate circulation was proved.
19	2004	Australia	SA	Paralana	PetraTherm	C	DR			Metasediments	4.1				1	Have drilled injector well Paralana-2
20	2005	Australia	TAS	Charlton-Lemont	KUTH	C	FU			Granite					website	Inferred resource
21	2006	Australia	SA	Olympic Dam	Green Rock Energy Ltd	C	FU			Granite					website	Inferred resource
22	2006	Australia	SA	Parachilna	Torrens Energy	C	FU			Cryst Base/Sandst	<5				website	Inferred resource
23	2006	Australia	SA	Crower	Geothermal Resources	C	FU			Granite						Inferred resource
24	2006	USA	CA	Glass Mountain			TE									Cancelled due to political and environmental permitting issues.
25	2007	Germany		Landau		C	OP	Y	Y		3.4	150	2.5-2.9	2, 6		Commercial. Commissioned in Nov 2007. Expansion is reported planned.
26	2008	Germany		Bruchsal		C	OP	Y	Y		2.5	128		2		Operating. Commercial. Commissioned 2009
27	2008	Germany		Groß Schönebeck		R	DE	Y	Y	Sandstone	4.4			2		Following several stimulations, a well doublet is ready for planned power production.
28	2008	Australia	QLD	Nagoorin	Granite Power	C	FU			Meta-sediments	5				website	Inferred resource
29	2008	Australia	VIC	North Narracan	Granite Power	C	FU			Metasediments	5				website	Inferred resource
30	2008	USA	NV	Brady EGS	Ormat	C	DR			Meta-tuff					3	
31	2008	USA	NV	NW Geysers EGS	Geysers Power	D									3	Ptr: Lawrence Berkely Nat Lab
32	2008	USA	ID	Raft River Expansion	Uni Utah	D					1.8	149			3	
33	2008	USA	CA	Geysers	Altarock	D	SU	N								Suspended due to difficult drilling conditions (serpentinite)
34	2008	Germany		Insheim	HotRock Verwaltungs	C	DE	Y	Y		3.6?	>155			website	Power plant planned operational 2011
35	2009	Australia	SA	Roxby	Southern Gold	C	FU			Granite					website	Inferred resource
36	2009	Australia	WA	Jurien-Woodada	New World Energy	C	FU								website	Inferred resource
37	2009	Germany		Unterhaching		C	OP	Y	Y		3.4	122	3.4	2, 5		Commercial. Operating. Commissioned 2009
38	2009	Switzerland		St Gallen	Geowatt	C					4.1	150	(3-5)	8		
39	2009	UK	Cornwall	Eden Project	EGS Energy	C	FU			Granite	4			(3)	website	
40	2009	UK	Cornwall	United Downs	Geothermal Engineering Ltd	C	FU			Granite	4.5			(10)	website	
41	2009	USA	AK	Naknek Geo Project	Naknek electric	D					4.2				3	
42	2009	USA	NV	New York Canyon	TGP Development	D									3	
43	2009	USA	OR	Newberry Volcanic Bend	Altarock/Davenport	D	PE			Volcanics				(15)	3	
44	2009	Germany		Hannover (Genesys)	GEOZENTRUM	R	DR			Sandstone	3.9					
45	2010	Latvia		Riga EGS										(3-4)	8	
46	2010	Norway		Oslo EGS											8	
47	2010	Germany		Rulzheim	HotRock Verwaltungs	C					3				website	

KEY:-

Purpose

C Commercial
D Demonstration
R Research and development

Status

DR Drilling
OP Operational
TE Terminated
PE Permitting
FU Fundraising
DE Development

Technical success

Y indicates project was successful in stimulation and flow testing (if undertaken)

Commercial success

Y indicates project achieved flow rates and temperatures sufficient to enable a project to be commercially developed

References (see main text for full references)

- MIT Report 2006
- M Back (re current Germany, pers con, 27/4/09) or M Haring (re Basel, pers con, June 09)
- Jennejohn 2010
- Tezuka 2007
- Reif 2009
- Baumgartner et al 2007
- Brown 2009
- Holm et al 2010
- Cornet 2009
- Evans and Valley 2005

Note:

Blank cells indicate data not yet collected or available
Parentheses indicate expected power output
Projects in blue indicate assessment for technical success

Technical Success

At this stage of the industry's development, and in terms of 'technical success', a project could be deemed successful if circulation, or another specific technical goal was achieved e.g. creating a reservoir. This is particularly important when considering the early R&D projects. For example the Rosemanowes project, which did not set out to commercially produce power but to prove rock mechanics concepts behind EGS and achieve circulation. In that context, the project was a success, and as such has been valuable in driving the industry forward.

There are several environmental factors that can be said to affect the technical success of a project. Of these arguably the most important are water losses and induced seismicity. These risks have impacted on the identified projects to varying degrees, ranging from little to no impact to the suspension/cancellation of the project e.g. Basel.

These constitute risks to the project which need careful management and mitigation. Such management and mitigation strategies have been developed over the last few years (e.g. Majer *et al.* 2008, Moriella and Malavazos 2008) and continue to develop, with this having a huge impact on the public perception of the industry. However, for the purposes of this assessment they will not be considered to affect the technical success of a project.

Commercial Success

The 'commercial success' of a project can be measured with regard to the economics of that project at that particular site. It is dependent on drilling costs, temperatures, location relative to power infrastructure, markets, and feed-in tariffs as well as other factors. Several of these 'modifying' factors can change with time, as a result of a changing or uncertain regulatory environment e.g. emission trading schemes and power prices. This means that the economics of a project can change with time, all other factors being constant.

Several of the EGS projects to date did not set out to commercially produce power, but to explore the development of EGS. Hence, these projects cannot be assessed in terms of being a commercial success.

As a first-pass and broad-brush approach to assess commercial success, it is defined here as either production of power, or the project being advanced enough to have proven its potential to produce power via long-term circulation tests.

Environmental factors such as induced seismicity or unsustainable flow rates can be deemed to affect the commercial success of a project, as they can lead to the closure of the project. Hence, they are considered here.

Preliminary Assessment of the Success of EGS Projects

Twenty projects allowed a first-pass assessment of technical success, as defined above. Of these projects one was deemed not successful due to drilling difficulties (serpentinite) leading to a suspension of the project (Geysers). This represents a 95% technical success rate for EGS projects.

Stimulations were noted to be successful within a range of lithologies (Table 1).

With regard to the commercial success of the projects: many of the earlier (1970-2000) projects did not set out to be commercial, and of these nine projects (see Table 1, Rows 1 - 9) only two can be considered as commercially successful and produced/is producing power (Fenton Hill and Soutz, Table 1, Rows 1 and 8).

However, the seven technically successful projects commenced in this last decade, for which commercial success could be assessed (Cooper Basin, Berlin, Landau, Bruchsal, Grossschonebeck, Insheim and Unterhaching), all are producing power or have been proven capable of producing power and are planning development for power production.

Reservoir development in Australia has been shown (e.g. Geodynamics, Cooper Basin) to be aided by the prevailing continental compressive stress regime (Hillis and Reynolds 2000). Under these conditions, hydraulic reservoir stimulations likely result in sub-horizontal fracturing leading to enhanced well connectivity. Hence, in Australia, a greater level of success may be anticipated.

Conclusions

It is appropriate to be cautious about the concept of success here, which has necessarily been kept relatively simple. In the future, the geothermal industry could arguably better define success as achieving a typical cost of production for power delivered into the retail market that is less than or equal to coal (on a pre-carbon tax basis) and then prioritise its R&D objectives according to the prospective contributions of various potential technical advances to achieving that benchmark of success.

At this moment in time, the early indicators generated from this industry worldwide show:-

- An exponential growth in the number of EGS projects over the last 5 years
- A commercially dominated industry in 2010 as opposed to R&D dominated activity 10 years ago.
- Early indications that technical success is consistently being achieved with this

translating into commercial success (where this is an aim)

The next decade will likely be a period of consolidation and further growth for this part of the geothermal sector, with several more projects likely to be producing power at the end of this period. As part of that evolution, projects are likely to increase in size.

Regulatory frameworks and government policies are needed which encourage this momentum and help consolidate the industry over this period with government support continuing to be made available at appropriate levels to further growth and encourage investor interest.

References

Baumgärtner, J., Menzel, H., and Hauße, P., 2007, "The Geox GmbH Project in Landau - The first geothermal power project in Palatinate / Upper Rhine Valley", in Proceedings *First European Geothermal Review, Geothermal Energy for Electric Power Production*, p. 33, Mainz, Rhineland Palatinate, Germany.

Brown, D.W., 2009, Hot dry rock geothermal energy: Important lessons from Fenton Hill. Proc. Thirty-Fourth Workshop on Geothermal Reservoir Engineering Stanford University, Stanford, California, February 9–11.

Cornet, F.H., 2009, From hot dry rock to enhanced geothermal systems: the Soultz-sous-Forets project, AAPG European Region Annual Conference, Paris-Malmaison, France, 23–24 November 2009

DRET (Department of Resources, Energy and Tourism) 2008, Canberra, 64pp.

Australian Geothermal Conference 2010

Evans, K.F. and Valley, B., 2005, An overview of enhanced geothermal systems, www.geothermal.ethz.ch/.../Geothermal%20publications/EvansEtAl_2005_EGS-Overview.pdf

Hillis, R. R. and Reynolds, S.D., 2000. The Australian Stress Map. *Journal of the Geological Society, London*, 157, 915-921.

Holm, A., Blodgett, L., Jennejohn, D. and Gawall, K., 2010, Geothermal Energy: International Market Update, Geothermal Energy Association Report, May 2010.

Jennejohn, D., 2010, US Geothermal Power Production and Development Update, Geothermal Energy Association Report, April 2010

Majer, E., Baria, R. and Stark, M., 2008, Protocol for Induced Seismicity Associated with Enhanced Geothermal Systems. Report produced in Task D Annex I (9 April 2008), International Energy Agency-Geothermal Implementing Agreement (incorporating comments by: C. Bromley, W. Cumming, A. Jelacic and L. Rybach).

Morelli, C., and Malavazos, M. (2008), Analysis and Management of Seismic Risks Associated With Engineered Geothermal System Operations in South Australia, in Gurgenci, H. and Budd, A. R. (editors), Proceedings of the Sir Mark Oliphant International Frontiers of Science and Technology Australian Geothermal Energy Conference, Geoscience Australia, Record

Reif, T., 2009, Economic aspects of geothermal district heating and power generation, Presentation, Tallinn University of Technology, 17 April 2009/GeotIS, Geothermische Vereinigung

Tezuka, K., 2007, Japanese EGS Experience and modelling efforts - a Review of the Hijiori HDR project. ENGINE Workshop 2, Volterra, 1-4 April 2007.

Estimates of sustainable pumping in Hot Sedimentary Aquifers: Theoretical considerations, numerical simulations and their application to resource mapping

J. F. Wellmann*, F. G. Horowitz, L. P. Ricard, K. Regenauer-Lieb
 Western Australian Geothermal Centre of Excellence, The University of Western Australia, 35
 Stirling Hwy, WA-6009 Crawley, Australia

*Corresponding author: wellmann@cyllene.uwa.edu.au

A method for a spatial analysis of potential sustainability for the early stage of exploration in Hot Sedimentary Aquifers (HSA) is presented here. Our analyses are based on well established estimations for the thermal breakthrough in a doublet well setting. We consider two significantly different scenarios: the placement of a well doublet in an aquifer without significant natural flow, and the case where a natural groundwater flow exists.

We integrate these two analytical estimations into one workflow with geological modelling and geothermal simulation. As a result, we obtain spatial analyses of theoretical sustainable pumping rates for a whole resource area. These maps are specifically suitable for the early stage of exploration where a potential target area has to be determined based on limited information.

We present the application of our method to a geothermal resource area in the North Perth Basin, from geological modelling, to the simulation of fluid and heat flow, and finally to map the analysis of sustainable pumping rates for an aquifer. The results contain a high degree of uncertainty, but indicate the distribution of future prospective areas. These maps can be combined with other spatial datasets, e.g. infrastructure. Also, as they are integrated into one workflow, an update of the analyses is directly possible when new data become available.

Keywords: Hot Sedimentary Aquifer (HSA); Resource Analysis; Sustainable Pumping Rate s; Geothermal Simulation; Geological Modelling

Introduction

This paper presents a novel exploration method to identify geothermal prospects based on the thermal and hydraulic properties of the subsurface. We combine estimates of sustainable pumping rates with simulations of fluid and heat flow, and derive maps of estimations for sustainable pumping rates.

Our work regards estimates of sustainability for well doublet systems. After a certain time t_B , the reinjected cold water front may reach the extraction well and cool down the extracted temperature (Fig. 1, red curve). This will affect the geothermal application and, at some stage, rule out further effective usage of the site. An

estimation of this breakthrough time t_B is required to evaluate the sustainability of a project.

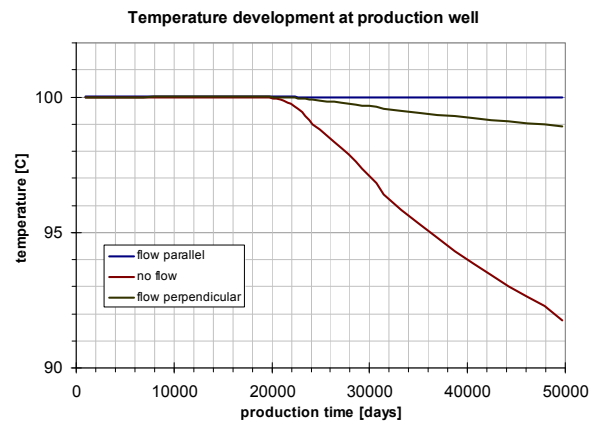


Figure 1: Comparison of temperature development at the extraction well for three different scenarios: i) If no advective flow is present, the cold reinjected water may reach the production/ extraction well (red curve) and the temperature of the pumped water will decrease; ii) For advective groundwater flow perpendicular to the wells, the temperature decrease is significantly slower (green curve); and iii) For the case that the reinjection well is directly downstream of the production well, no thermal breakthrough occurs (blue curve).

Analytical estimates of a sustainable long-term use for geothermal installations have been applied for many years (e.g. Gringarten, 1978, Lippmann and Tsang, 1980). Most of the approaches are based on many simplifications and assumptions. They nonetheless deliver an important insight into the distribution of promising areas for sustainable flow in the subsurface, especially in the early exploration phase, as not only available temperature and heat in place are considered, but also hydraulic parameters like permeability and porosity.

Another standard tool in geothermal exploration is numerical simulation of subsurface fluid and heat flow. (See e.g. O'Sullivan et al. 2001 for a detailed revision of applications.) A thoroughly performed study can deliver detailed insight into fluid and heat movement in the subsurface, within the usual limitations of data availability and model accuracy.

One problem with both estimations, analytical and numerical, is that they are usually only performed at one location, i.e. at a previously identified

target, to evaluate its long term behaviour. We propose here that it is useful to perform a raster analysis of sustainable pumping rates. This can be applied from the very first stages of geothermal exploration and subsequently refined during ongoing exploration, when more data become available.

We present here a method to perform the spatial analyses. Our approach is implemented in a complete framework covering geological modelling and fluid and heat flow simulations. The results we obtain have to be analysed critically as the many assumptions that go into the analysis prohibit an absolute interpretation of the results. For example, an estimated average pumping rate of 80 m³/s for a lifetime of 30 years may contain a high degree of uncertainty. But even if the total values might vary, we consider the general distribution of the analysis to be a valuable representation of potential target areas in a resource area.

Theoretical considerations and simulated examples

Here, we briefly review some of the commonly applied theoretical estimations of sustainability studies. All the presented estimations below are suitable for application in Hot Sedimentary Aquifer/porous media systems. The situation is much more complex in fractured systems (EGS) and special considerations are necessary. For more detailed information, see the recent review of Banks (2009).

Analytical estimations

The longevity of a doublet well can be defined as the time it takes for the reinjected cool water to reach the extraction well indicated at the point when the extracted temperature starts to decrease (e.g. Fig. 1). We are applying this definition here, but it should be noted that this time defines the lower end of the usability. After the thermal breakthrough, the extracted temperature will decrease but possibly the application will still be usable (e.g. Lippmann and Tsang, 1980, Banks, 2009).

In this paper, we consider two cases for the estimation of a sustainable pumping rate, with and without advective background flow.

Well doublet without advective background flow

We firstly consider the case of hydraulic breakthrough. This is the time t_{hyd} the reinjected water takes to reach the extraction well. For simple cases (flow along the shortest path, homogeneous aquifer, no dispersion) the hydraulic breakthrough time (e.g. Hoopes and Harleman, 1967) can be evaluated for a pumping rate Q , an aquifer with porosity ϕ , a thickness h

and a spacing D between extraction and reinjection wells as:

$$t_{hyd} = \pi \phi h \frac{D^2}{3Q}$$

The hydraulic breakthrough (i.e. the time when the reinjected water reaches the extraction well) is not equal to the thermal breakthrough (the time when the cold temperature front reaches the extraction well). The temperature front is delayed by a retardation factor R_{th} (Bodvarsson, 1972) that depends on the thermal properties (specific heat c and density ρ) of the aquifer rock (a) and the water (w):

$$R_{th} = \frac{1}{\phi} \frac{\rho_a c_a}{\rho_w c_w}$$

Therefore, the time for the arrival of the thermal front at the extraction well can be calculated as:

$$t_{the} = \frac{\pi D^2 h}{3 Q} \frac{\rho_a c_a}{\rho_w c_w}$$

Interestingly, the thermal breakthrough time in this case does not depend on the hydraulic conductivity / permeability of the aquifer, but only on geometric and thermal properties.

This estimation is based on many assumptions; the most important are:

- 1) Fluid properties are constant and do not depend on temperature.
- 2) The flow itself is steady-state, injection rate and temperature are constant and there is no mixing between the reinjected fluid and the native water.
- 3) The geometry of the aquifer is very simple: constant thickness, constant porosity and it is assumed to be horizontal.
- 4) Cap rock and bedrock of the aquifer are impermeable.

(For a further detailed discussion see e.g., Gringarten and Sauty, 1975.)

Apart from these conditions, another common assumption is that there is no heat transport from the aquifer into the surrounding rocks by conduction. This assumption is reasonable in many cases (see Gringarten and Sauty, 1975, for accurate criteria) and we will adopt it here as well.

Well doublet with advective background flow

If a native hydraulic gradient is present in the aquifer, the situation is more complex. It is now important to consider the well placement with respect to the natural advective groundwater flow

v_0 (Fig. 2). An analytical estimation for the thermal breakthrough can be derived for the case that the reinjection well is placed downstream of the extraction well (Lippmann and Tsang, 1980):

$$t_{the} = (D/v_0) \frac{1}{\phi} \frac{\rho_a c_a}{\rho_w c_w} \left[1 + \frac{4A}{\sqrt{-1-4A}} \arctan \frac{4A}{\sqrt{-1-4A}} \right]$$

where

$$A = \frac{Q}{2\pi h D v_0}$$

This equation does not have a real solution when the natural groundwater velocity is above a critical value

$$v_0 > \frac{2Q}{\pi \phi h D}$$

In this case, no thermal breakthrough will occur and the system is, in principle, completely sustainable and can be operated without time limitations.

Validity of the analytical solution

The analytical estimations of hydraulic and thermal breakthrough depend on many assumptions (see above). In a realistic setting, some effects might reduce the breakthrough time (hydraulic dispersion, heat conduction in the fluid phase) while others might lead to longer breakthrough times (heat re-supply from surrounding beds, stratification). A careful examination of these effects is possible with numerical simulations of pumping and reinjection.

Consideration of pressure drawdown

In both cases presented above, with and without natural groundwater flow, we can consider a maximum pressure drawdowns at the extraction well as another criterion for the determination of a sustainable pumping rate. Gringarten (1978) presented a relationship obtained from potential theory:

$$s = \frac{Q}{2\pi T} \ln \frac{D}{r_w}$$

We can see from this equation that the pressure drawdowns depends on pumping rate Q , aquifer transmissivity T and well diameter r_w , as can be expected, but also on the well spacing D , as the two wells interact and a smaller spacing leads to less drawdown.

Combined analysis

For a complete sustainability analysis for the well doublet, we might consider the thermal breakthrough time and a maximum pressure

drawdown in the reservoir. Concerning the temperature breakthrough time, we want to have a large well spacing D , but if we consider the pressure drawdown, a smaller spacing is more beneficial. The optimal value of D can not be determined analytically, but numerical solutions can be applied (e.g. Kohl et al., 2003, Wellman et al., 2009).

Numerical simulations

The theoretical estimations described above deliver a very useful estimation about potential geothermal targets. We therefore consider them as ideal for the early exploration stage. But as they depend on many assumptions and simplifications, numerical simulations of subsurface fluid and heat flow have to be applied to derive a more realistic insight into the sustainability of the system.

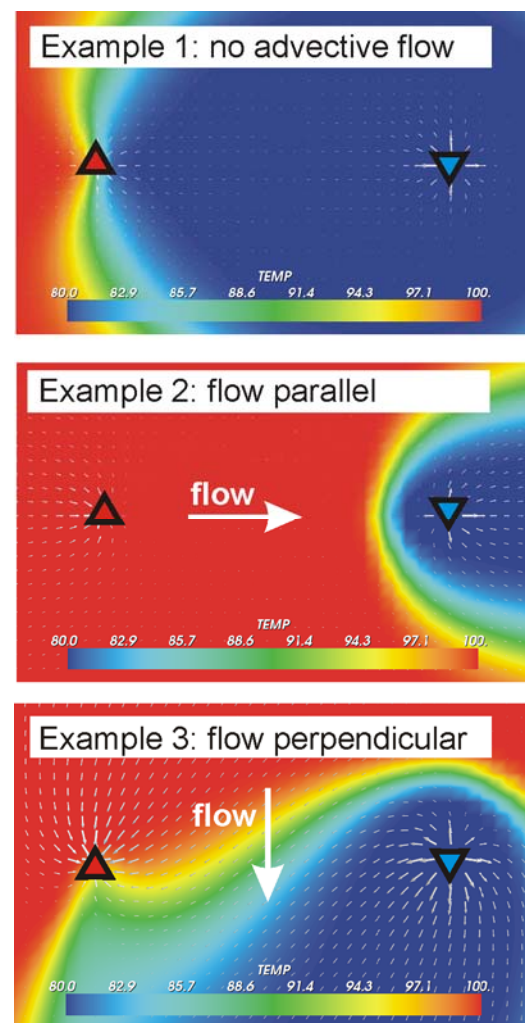


Figure 2: Fluid and heat flow representations for the three example scenarios described below, and presented in Fig. 1. In the first example, without advective flow, we can see that the reinjected cold water (re injection well: blue triangle) reaches the extraction well (red triangle) after a certain time, and the produced temperature decreases. Example 2: for natural advective flow in the direction of the injection well, the cold temperature fan does not reach the extraction well, and the system is completely sustainable. Example 3: for flow

perpendicular to the wells, less cold water reaches the extraction well, and the temperature decrease is reduced.

A variety of software codes exist to perform these simulations (see O'Sullivan et al., 2001). We used SHEMAT (Simulator of HEat and MAss Transfer, Clauser and Bartels, 2003) for the resource scale simulations presented in this paper (e.g. Fig. 3). To test the validity of the analytical estimation of breakthrough times, we simulated a well doublet (extraction and reinjection well) with SHEMAT and, additionally, with the petroleum reservoir engineering software Tempest/More from Roxar.

The plots in Fig. 2 show the temperature distribution (colour map) and fluid flow vectors (grey arrows) in the subsurface. The three examples given relate to temperature decrease at the extraction well for three different scenarios, as given in Fig. 1.

In summary:

- 1) Well doublet in an aquifer without groundwater flow, after thermal breakthrough occurred. We can see that the flow field affects a wide area perpendicular to the direct connection between the wells.
- 2) Natural groundwater flow, the reinjection well is in the downstream direction of the extraction well. The temperature field is now disturbed by the natural groundwater flow. For the same pumping rate, well spacing, and simulation time, the cold temperature field does not reach the extraction well. No thermal breakthrough occurs.
- 3) Natural groundwater flow perpendicular to the connection line of the well doublet. The temperature field is again clearly affected by the groundwater flow field and the temperature decrease at the extraction well is slowed down.

Example: North Perth Basin

Geological model

We applied the analytical estimations presented above to exploration-scale simulations of fluid and heat flow. For the first stage of exploration, we consider these analytical assumptions as a valuable indication of potential geothermal target areas.

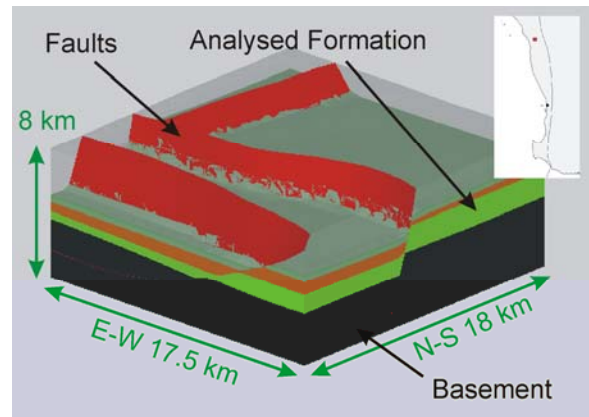


Figure 3: 3-D Geological model for a part of the North Perth Basin (In inset picture: model location=red square; black circle=Perth). Sedimentary formations are overlying basement which is offset by normal faults.

As an example here, we show the application of the method to an area in the North Perth Basin. The geology is characterised by thick sedimentary formations cut by normal faults in a graben setting (Fig. 3). The geological model was created with an implicit potential-field approach (Lajaunie, et. al. 1997), implemented in the GeoModeller software (Calcagno et al., 2008). The model is a simplified version of a more complex regional model.

Geothermal simulation

The geological model is directly processed to an input file for fluid and heat flow simulation with SHEMAT (see Clauser and Bartels, 2003). Rock properties (permeability, porosity, thermal conductivity and heat capacity) were assigned according to samples in this region where available. A strong anisotropy (horizontal / vertical = 10) was applied to all permeability values to achieve a more realistic model.

Figure 4 is a representation of the simulated fluid and heat flow field for the North Perth Basin model. The effect of fluid flow on the temperature distribution is clearly visible. The resulting temperature gradients appear reasonable and qualitatively in accordance with measured values in the area.

For a quantitative analysis of the results, the model has to be refined and adjusted further, especially at the borders (boundary conditions, see discussion). Respecting these current limitations to model verification, we next apply our resource analysis methods to this model. As all steps are integrated into one workflow, it is easily possible to update the model and all analyses later, when more data become available.

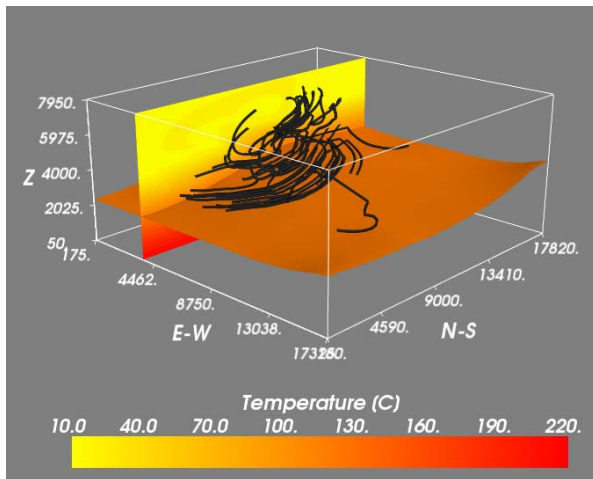


Figure 4: Visualisation of the temperature and fluid flow field simulated for the 3-D geological model of the North Perth Basin. The orange isosurface shows the depth to 120°C. The black lines indicate fluid flow pathways. General flow direction is N-S.

Novel resource analysis methods

Next we use the simulated fluid and heat flow field to estimate different aspects of geothermal resource sustainability. All the examples here are performed for the oldest sedimentary formation (see Fig. 3, light green unit). The minimum lifetime to consider a geothermal project site as “sustainable” is assumed to be 30 years for the following analyses.

Key novel aspects of all our analyses are:

- 1) We perform the analyses directly on the basis of the simulated fluid and heat flow field for the resource area, linked to the 3-D geological model.
- 2) All aspects (maximum sustainable pumping rate, heat in place, pressure drawdown) are evaluated on a spatial basis, i.e. we derive 2-D maps of these properties showing their distribution.
- 3) All relevant steps are integrated into one workflow, it is therefore readily possible to update the geological model and the geothermal simulation when more data become available.

Maximum sustainable pumping rate, without consideration of advective flow

Following the definition of the theoretical breakthrough time for the thermal front given above, we estimate a maximum pumping rate that could be expected for a doublet system. Spatial analysis is performed step-by-step at every point in space (Fig. 5).

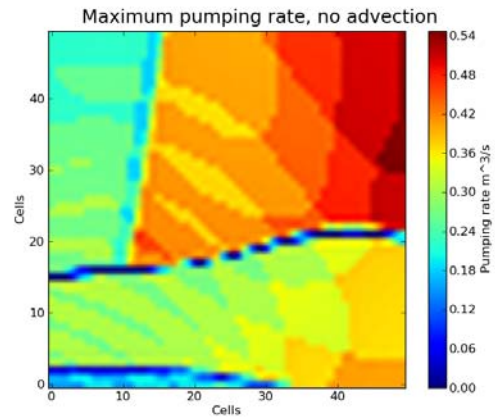


Figure 5: Maximum pumping rates for a doublet system with 800 m spacing and a lifetime of 30 years. All other properties required for the estimation of the pumping rate (see equations above) are directly taken from the simulation (e.g. density) and the model (e.g. formation thickness).

Consideration of natural groundwater flow

In Fig. 4 we can see from the distribution of the streamlines that groundwater flow is present at the regional scale for this specific model. So, if we hypothetically intelligibly place a well doublet in one of the flow areas, it is possible to determine a pumping rate where a thermal breakthrough will, theoretically, never occur (see Example 2 in Fig. 2). If we then apply this analysis again at every point in our model, we can derive a spatial analysis of these pumping values (Fig. 6) for which thermal breakthrough will never occur.

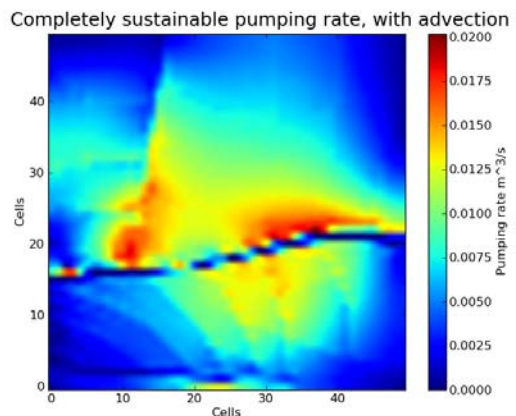


Figure 6: Estimation of a maximal pumping rate for the theoretical case of no thermal breakthrough (Example 2 in Fig. 2), in the presence of advection. This is of practical significance as areas with a high value can also be expected to allow a higher sustainable pumping rate (for a project duration less than infinity).

Combination with other important factors

These spatial analyses can now be used in combination with other relevant factors for geothermal exploration, e.g. mean temperature at depth for a target formation, or maps of local heat in place (Wellmann et al., 2009). Heat in place is referred to as one absolute number characterising

the geothermal potential of a geothermal reservoir volume. We define the local heat in place as the heat in place of a tiny subdivision of the reservoir. A local heat in place map gives crucial information on the connectivity of the geothermal reservoir and therefore is of high interests for reservoir engineering studies. As all results are in map view, they can easily be included in a GeoinformationSystem (GIS) and combined with, for example, infrastructure considerations.

Discussion

We have shown that it is possible to combine analytical considerations of resource sustainability, with geothermal fluid and heat flow simulations. Our approach enables a direct spatial analysis of relevant factors for geothermal exploration in Hot Sedimentary Aquifers. The major advantage is that geothermal prospects can be identified based on physical reasoning (in the context of geological modelling), geothermal simulation, and ideally, all available data. We propose that this method is a step forward for the identification of geothermal target areas from a regional analysis.

The example presented above for the North Perth Basin is performed for a resource-scale model, representative for an early stage of geothermal exploration. It contains a high degree of uncertainty and the determined numbers for sustainable pumping rate are probably not quantitatively correct. But as they are based on a full 3-D integration with geological knowledge, physical simulation and all available data, we can interpret the results spatially, i.e. identify areas which should be analysed more carefully. This is a major advantage to stand ard resource estimation methods, e.g. heat in place, where only one value for the whole resource area is determined.

In a realistic project scenario, the next steps would be to refine the model and adjust boundary conditions carefully to the local setting. But as we have integrated all relevant modelling, simulation and resource analysis steps into one workflow, an update at every stage is easily possible.

We recognise that the results are subject to a large degree of uncertainty. Two ways we will address this in future work, will be to combine this workflow with an uncertainty simulation of geological modelling (Wellmann et al., 2010), and with sensitivity studies of the geothermal simulation to derive a quantitative evaluation of the sustainability map quality.

Acknowledgements

This work was enabled by an Australian International Postgraduate Research Scholarship (IPRS) and a Top-up Scholarship from Green

Rock Energy Ltd. The Western Australian Geothermal Centre of Excellence (WAGCoE) is a joint centre of Curtin University, The University of Western Australia and the CSIRO and funded by the State Government of Western Australia. We are very thankful for the comments of an anonymous reviewer. We thank Roxar and Intrepid Geophysics for providing academic licenses of, respectively, TempEst/More and Geomodeller software.

References

- Banks, David, 2009, Thermogeological assessment of open-loop well-doublet schemes: a review and synthesis of analytical approaches: *Hydrogeology Journal*, v. 17, no. 5, p. 1149–1155.
- Bodvarsson, G., 1972, Thermal problems in the siting of reinjection wells: *Geothermics*, v. 1, no. 2, p. 63–66.
- Calcagno, Philippe; Chilès, Jean-Paul; Courrioux, Gabriel; Guillen, Antonio, 2008, Geological modelling from field data and geological knowledge: Part I. Modelling method coupling 3D potential-field interpolation and geological rules. *Recent Advances in Computational Geodynamics: Theory, Numerics and Applications: Physics of the Earth and Planetary Interiors*, v. 171, no. 1-4, p. 147–157.
- Clauser, Christoph; Bartels, Jörn, 2003, Numerical simulation of reactive flow in hot aquifers. *SHEMAT and processing SHEMAT*: Berlin, Springer.
- Gringarten, A. C.; Sauty, J. P., 1975, A theoretical study of heat extraction from aquifers with uniform regional flow: *Journal of Geophysical Research-Solid Earth*, v. 80, no. 35.
- Gringarten, Alain C., 1978, Reservoir lifetime and heat recovery factor in geothermal aquifers used for urban heating: *Pure and Applied Geophysics*, v. 117, no. 1, p. 297–308.
- Hoopes, J. A.; Harleman, D. R.F., 1967, Waste water recharge and discharge in porous media: *J. Hydraulics Div., Am. Soc. Civ. Eng.*, v. 93, p. 51-71.
- Kohl, Thomas; Andenmatten, Nathalie; Rybach, Ladislaus, 2003, Geothermal resource mapping-example from northern Switzerland. *Selected Papers from the European Geothermal Conference 2003: Geothermics*, v. 32, no. 4-6, p. 721–732.
- Lajaunie, Christian; Courrioux, Gabriel; Manuel, Laurent, 1997, Foliation fields and 3D cartography in geology: Principles of a method based on potential interpolation: *Mathematical Geology*, v. 29, no. 4, p. 571–584.
- Lippmann, M. J.; Tsang, C. F. (1980): Ground-water use for cooling: associated aquifer

temperature changes: *Ground Water*, v. 18, no. 5, p. 452–458.

O'Sullivan, M. J.; Pruess, K.; Lippmann, M. J., 2001, State of the art of geothermal reservoir simulation: *Geothermics*, v. 30, no. 4, p. 395–429.

Wellmann, J. F., Horowitz, F. G., Regenauer-Lieb, K., 2009, Concept of an integrated workflow for geothermal exploration in Hot Sedimentary Aquifers; Australian Geothermal Energy Conference (AGEC), Brisbane, Abstracts.

Wellmann, J. F.; Horowitz, F. G.; Schill, E.; Regenauer-Lieb, K., 2010, Towards incorporating uncertainty of structural data in 3D geological inversion: *Tectonophysics*, v. 490, no. 3-4, p. 141–151.

Hydrothermal Spallation for the Treatment of Hydrothermal and EGS Wells: A Cost-Effective Method for Substantially Increasing Reservoir Production Flow Rates

Thomas W. Wideman¹, Jared M. Potter^{1*}, Brett O'Leary², Adrian Williams²,

¹Potter Drilling, Inc. 599 Seaport Blvd., Redwood City, CA 94063

²Geodynamics Limited, Suite 1A Level 5 South Shore Centre, 85 The Esplanade SOUTH PERTH WA 6151

*Corresponding author: jared@potterdrilling.com

There is a need in many geothermal projects to greatly increase the productivity and/or injectivity of wells, with a direct impact on project economics. Flow testing in wells and associated modelling of EGS reservoirs has suggested that low productivity from EGS reservoirs can result from near-wellbore impedance, a restriction of fluid flow within the immediate vicinity of the borehole walls. Further modelling suggested that altering the geometry of an existing wellbore by longitudinally slotting the borehole wall could significantly decrease near-wellbore impedance. Hydrothermal spallation is an ideal technology to create slots in the hard rock found in these reservoirs. This paper describes the results of tests of hydrothermal spallation well enhancement technology in the laboratory and initial field trials as well as its application to increase production from geothermal wells.

Keywords: thermal spallation, hydrothermal spallation, well enhancement, Engineered Geothermal Systems, EGS

Background

Enhanced Geothermal Systems (EGS) have the potential to generate clean, renewable, base load electricity using heated fluid produced from engineered reservoirs. These reservoirs are created by enhancing natural fractures in hot basement rock using hydraulic fracturing technology. Once the stimulation process is completed, injection wells deliver fluid from the surface into the reservoir where the fluid is heated, and production wells drilled into the fractured rock extract the heated fluid to drive a surface-based power plant.

This EGS technology is on the verge of reaching its tremendous potential. Projects around the world are achieving their temperature objectives, but face the challenge of low circulation rates after the hydraulic stimulation. Most models suggest that EGS wells must produce 80-100 kg/sec of fluid at 200 °C per well to be economically viable. However, such rates have proven difficult to achieve in EGS projects to date. The potential to create additional fracture zones within a reservoir exists, but adds considerable cost and risk to a project and has not been accomplished at this point. Meeting the productivity targets in EGS

wells is critical to realizing the full potential of this promising renewable energy technology.

Geodynamics Limited ("Geodynamics"), a leading Australia-based developer of EGS projects worldwide, in collaboration with Australia's Commonwealth Scientific and Research Organisation (CSIRO), has conducted extensive field testing and associated modelling of EGS reservoirs. These studies suggest that low productivity from some EGS reservoirs primarily results from near-wellbore impedance, the restriction of fluid flow within the immediate vicinity (several inches or a few feet) of the borehole walls. This could be due to reduction in fracture permeability from drilling muds or other particulates, but the most influential factor is likely fluid turbulence due to rapidly increasing fluid velocities near the wellbore. To enter the production well, fluids must pass through pores and fractures in the walls of the borehole. Fluid velocities in the vicinity of the borehole are much higher than in the rest of the reservoir because of the limited surface area of the borehole walls and are estimated to exceed 55 km per hour near the entry into the wellbore in some cases. This near-wellbore impedance can limit both the output of production wells and, to a lesser extent, the input capacity of injection wells. A simple representation of this near wellbore effect is shown in Figure 1.

By altering the geometry of an existing wellbore through increasing the effective diameter, it is possible to reduce the near wellbore effect. This can be accomplished by slotting the borehole wall, as illustrated in Figure 2.

Spallation has been proposed as a simple means of expanding the diameter of a wellbore or a way to create underground caverns. For example, in Pedernal, New Mexico, Bob Potter and Ed Williams, from Los Alamos National Laboratory, demonstrated the ability to create 60-cm diameter holes in hard rock using only a 10-cm diameter axially-oriented flame jet. An illustration of this process is shown in Figure 3.

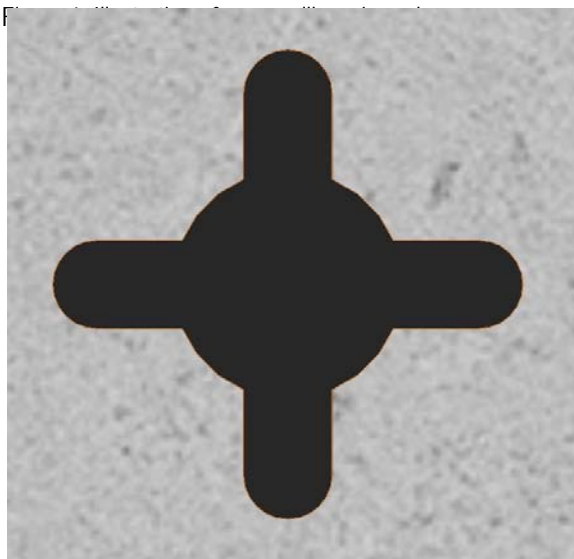
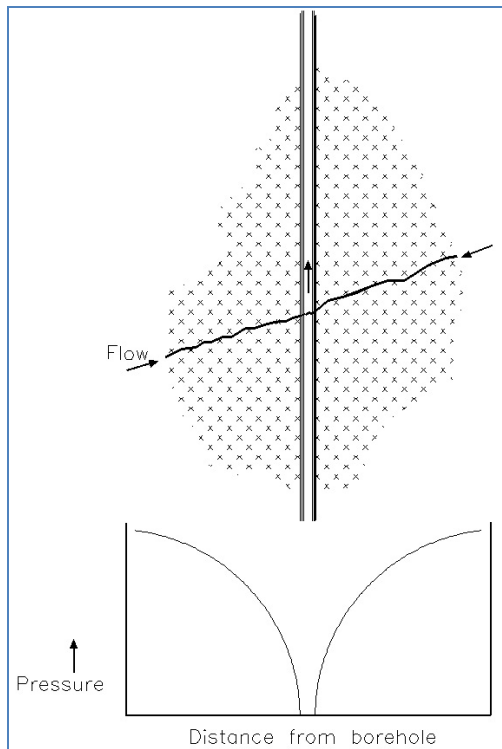


Figure 2: Borehole geometry for reduced wellbore impedance

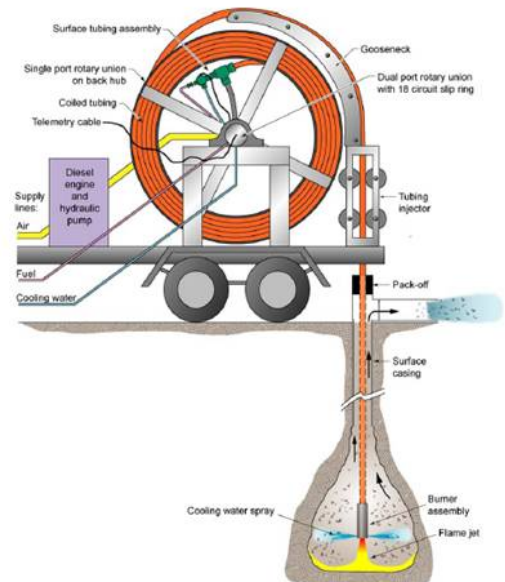


Figure 3: Flame spallation cavity maker

Flame jet spallation processes continue to be used commercially. For example, in Canada, thermal fragmentation mining employs a variation of this excavation technique to extract precious metals in thin, near-surface ore deposits. In a typical operation, a small pilot hole is drilled into the ore zone and an 8cm diameter flame jet drill is used to cut larger caverns up to about one meter in diameter. The spalls are then processed for their precious metals.

However, this air-based technology can only be used near the surface and to moderate depths in regions where air drilling is feasible. At the depths required for EGS, the wellbore will very likely need to be filled with fluid to prevent excessive water/oil/gas flows and maintain circulation and hole stability. For flame jet spallation, a fluid-filled wellbore poses serious challenges for both the transport of chemicals from the surface and for down-hole combustion.

As a result, hydrothermal spallation has been investigated as a viable means for the enhancement of deep, water-filled EGS wellbores.

Experimental Application

A hydrothermal spallation test apparatus was used for proof-of-concept tests on the laboratory scale. The test system shown in Figure 4 is capable of independently applying controlled hydrostatic, confining, and axial loads on 10 cm rock cores to simulate varying wellbore conditions to 2400 m.



Figure 4: Hydrothermal spallation deep well test rig
This system which uses superheated steam to spall the rock was used to create single axial slots of the desired depth in holes and investigate their interactions with induced fractures.

The process was then further scaled to cut the axial slots 10 cm wide and more than 25 cm deep in open-hole sections of granite blocks, as shown in Figure 5, using a full-scale well enhancement test rig.



Figure 5: Axial slots cut into 10 cm open hole section of Sierra White Granite using a full scale tool



Figure 6: Full scale well enhancement test rig

Geothermal Energy Conference, November 16-19 in Adelaide.

A 8.8 cm iteration of the slotting drill head was designed and fabricated for field trials. The drill head interfaces with a dynamic seal to isolate the working fluid from the cooling water, followed by instrumentation and controls, tension release, and connector subassemblies, as shown in Figure 7.

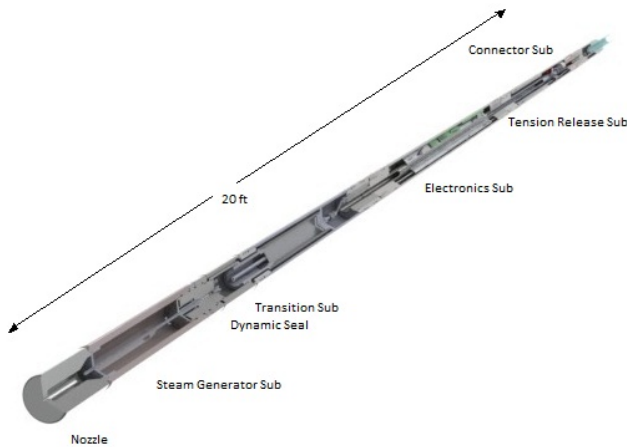


Figure 7: Cutaway rendering of field prototype bottom hole assembly

A coiled tubing string was assembled for purpose by nesting a 9.5 mm OD stainless steel capillary and 7-conductor wireline cable inside of a 50 mm OD, 3.40 wall, HS-90 steel coiled tubing string. The string was mounted on a tracked coiled tubing unit, shown in Figure 8. Rotating swivels and slip rings added to the reel allowed for transmission of the cooling water, electrical, and reactants through the hub.



Figure 8: Coiled tubing unit for field testing of hydrothermal spallation well enhancement.

A field location was chosen in the foot hills of the Sierra Mountains in northern California, where competent granite could be found close to the surface.

At the time of publication, the results from the field drilling tests were not yet available. The results will be presented orally at the 2010 Australian

References

Calaman, J. and Rolseth, H.C., 1961, Technical Advances Expand Use of Jet-Piercing Process in Taconite Industry: International Symposium on Mining Resources, University of Missouri.

Dreesen, D. and Betz, R., Coiled-Tubing Deployed Thermal Spallation Hard Rock Cavity Maker, FWP-02FE15.

O'Leary, B., 2010, Longitudinal Slotting for Wellbore Enhancement Purposes: Quantified Cost Benefit: Geodynamics Report.

Potter, R. M., Potter, J. M., and Wideman, T.W., 2010, Laboratory Study and Field Demonstration of Hydrothermal Spallation Drilling: GRC Meeting, Sacramento, California.

Williams, E., 1986, Thermal Spallation Excavation of Rock: U.S. Symposium on Rock Mechanics (USRMS), 27th annual meeting.

An Evaluation of Enhanced Geothermal Systems Technology: Geothermal Technologies Program, U.S. Department of Energy, Energy Efficiency and Renewable Energy; IPGT Workshop, August 27-28, 2010. Reykjavik, Iceland.

Flow Test Update: Geodynamics ASX Announcement, released April 22, 2008.

The Future of Geothermal Energy: Impact of enhanced geothermal systems (EGS) on the United States in the 21st century, Massachusetts Institute of Technology and Department of Energy Report, 2006: Idaho National Laboratory INL/EXT-06-11746.

Thermal effects on the wellbore stability

Bisheng Wu, Bailin Wu, Xi Zhang and Rob Jeffrey*

CSIRO Earth Science and Resource Engineering, Clayton, VIC 3168, Australia

*Tel: 03-95458354, E-mail: rob.jeffrey@csiro.au

Abstract

Thermal-mechanical behaviour plays an important role in wellbore stability of enhanced geothermal systems (EGS). Based on the thermo-poro-elastic model proposed by Coussy (1989) and by using Laplace transformation methods, analytical solutions for the temperature, pore pressure and stresses around a vertical well are obtained in the Laplace space. Then the solutions in the time domain are obtained via numerical Laplace inverse transformation. The results show that the cooling of the wellbore has a considerable effect not only on the pressure, in-plane radial and hoop stresses, but also on the vertical stress. It reduces the compressive radial and hoop stresses along the maximum horizontal stress direction. When the wellbore temperature is low enough, the hoop stress has a tendency to become tensile leading to the wellbore breakdown and the lower vertical stress implies the generation of an in-plane fracture. The possibility of wellbore shear failure is found to exist at places with higher compressive hoop stress.

Keywords: thermal effects, wellbore stability, Laplace transformation, numerical simulation

Introduction

The mechanical behaviour of a wellbore in a fluid-saturated porous medium has attracted a great deal of attention during the past several decades (Rice and Cleary 1976; Detournay and Cheng 1988; Rajapakse 1993; Ekbote et al. 2004). Most of these studies focus on the pore pressure and stress distribution around the wellbore based on Biot's formulation of linear poroelasticity (Biot 1941). It is worthwhile to mention that Detournay and Cheng (1988) first provided the poroelastic transient and plane-strain analytical solutions under a non-hydrostatic stress field.

Thermal effects should be considered in geothermal reservoir stimulation and production. Cold fluid is generally injected into the wellbore and the surrounding rock is at a higher temperature. Due to different thermal coefficients for fluid and rock matrix, the pore space in the rock will deform much less than the fluid in the pore when subject to a temperature variation. Obviously, this will lead to a higher (or lower) pore pressure that affects fluid diffusion. On the other hand, pervasive flow can carry low-temperature

water into a pore and thus the local temperature equilibrium is broken. To account for the thermal effects, many theories have been developed (McTigue 1986; Kurashige 1989). However, a general thermo-poro-elastic theory proposed by Coussy (1989) appears more suitable for the loss of local temperature equilibrium, which may be important to consider for a geothermal system. In this theory, a latent heat associated with the increase of fluid mass content is introduced with a different meaning from the conventional terminology.

For thermo-poro-elastic solids, Wang et al. (1994) and Li et al. (1998) obtained analytical solutions for stress distributions around a borehole. In their models, the temperature is decoupled from pore pressure. In this paper, the fully-coupled solutions are obtained based on the linear thermo-poro-elastic model proposed by Coussy (1989). As the borehole is much longer compared to its diameter, we consider the problem by assuming plane strain conditions for cross sections orthogonal to the borehole axis.

Problem Formulation

Figure 1 shows a vertical wellbore subjected to a vertical tectonic stress σ_v , a maximum and a minimum horizontal stresses, σ_{\max} and σ_{\min} . The initial pore pressure and temperature are P_R and T_R , respectively. When time $t > 0$, the wellbore temperature and pressure are kept constants, i.e. maintained at T_w and P_w .

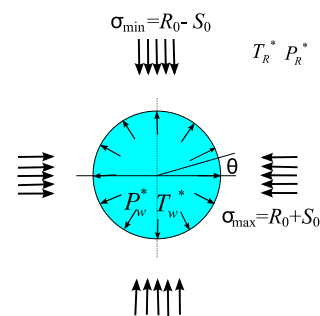


Figure 1: Problem geometry

Governing equations

The equations to be solved and initial and boundary conditions for this problem are listed as follows:

1. Linear thermo-poro-elastic constitutive law:

$$\begin{aligned}\sigma_r &= (K_B - 2G/3)\varepsilon_v + 2G\varepsilon_r - B_i P - 3\alpha_B K_B T \\ \sigma_\theta &= (K_B - 2G/3)\varepsilon_v + 2G\varepsilon_\theta - B_i P - 3\alpha_B K_B T \\ \sigma_{r\theta} &= 2G\varepsilon_{r\theta} \\ \sigma_z &= (K_B - 2G/3)\varepsilon_v - B_i P - 3\alpha_B K_B T.\end{aligned}$$

2. Compatibility equations

$$\varepsilon_r = \frac{\partial u_r}{\partial r}, \quad \varepsilon_\theta = \frac{u_r}{r} + \frac{1}{r} \frac{\partial u_\theta}{\partial \theta}, \quad \varepsilon_{r\theta} = \frac{1}{2} \left(\frac{1}{r} \frac{\partial u_r}{\partial \theta} + \frac{\partial u_\theta}{\partial r} - \frac{u_\theta}{r} \right).$$

3. Equilibrium equations:

$$\frac{\partial \sigma_r}{\partial r} + \frac{1}{r} \frac{\partial \sigma_{r\theta}}{\partial \theta} + \frac{\sigma_r - \sigma_\theta}{r} = 0, \quad \frac{\partial \sigma_{r\theta}}{\partial r} + \frac{1}{r} \frac{\partial \sigma_\theta}{\partial \theta} + 2 \frac{\sigma_{r\theta}}{r} = 0.$$

4. Governing equations for pore pressure and temperature

$$\begin{aligned}\frac{k}{\mu} \nabla^2 P &= \frac{1}{M} \frac{\partial P}{\partial t} + B_i \frac{\partial \varepsilon_v}{\partial t} - \frac{\rho_w L}{MT_R^*} \frac{\partial T}{\partial t}, \\ \lambda_A \nabla^2 T &= -\frac{\rho_w L}{M} \frac{\partial P}{\partial t} + 3\alpha_B K_B T_R^* \frac{\partial \varepsilon_v}{\partial t} + (C_v + \frac{\rho_w^2 L^2}{MT_R^*}) \frac{\partial T}{\partial t},\end{aligned}$$

where σ_{ij} are effective stresses, latent heat for fluids is defined as $L = T_R^* (3\alpha_u K_u - 3\alpha_B K_B) / \rho_w / B_i$, $P = P^* - P_R^*$ and $T = T^* - T_R^*$, $\lambda_A = \lambda_w + (1 - \Phi) \lambda_r$ and $C_v = \Phi \rho_w c_w + (1 - \Phi) \rho_r c_r$. We use the sign convention that stresses are positive if in tension.

The initial and boundary conditions for the problem are given as

$$\begin{aligned}P(r, 0) &= 0, \quad T(r, 0) = 0, \\ \sigma_r &= -P_w^* \quad \text{at } r=r_w, \\ \sigma_r &= R_0 + S_0 \cos 2\theta \quad \text{when } r \rightarrow \infty, \\ \sigma_\theta &= R_0 - S_0 \cos 2\theta \quad \text{when } r \rightarrow \infty, \\ \sigma_{r\theta} &= -S_0 \sin 2\theta \quad \text{when } r \rightarrow \infty, \\ P &= P_w^* - P_R^* \quad \text{at } r=r_w, \quad P = 0 \quad \text{when } r \rightarrow \infty, \\ T &= T_w^* - T_R^* \quad \text{at } r=r_w, \quad T = 0 \quad \text{when } r \rightarrow \infty.\end{aligned}$$

Method for solution

In order to make the problem tractable, the in-plane principal stresses are expressed in terms of equivalent isotropic (or mean) and deviatoric stresses defined as follows

$$R_0 = (\sigma_{\max} + \sigma_{\min}) / 2, \quad S_0 = (\sigma_{\max} - \sigma_{\min}) / 2.$$

The problem can then be decomposed into two modes: axi-symmetric (mode I) and deviatoric loading (mode II) (Detournay and Cheng 1988). For the first mode, the well is subjected to an isotropic far-field mean stress R_0 , borehole pressure P_w^* and temperature T_w^* at the wellbore wall. The second mode is associated with a borehole subject to a remote far-field pure shear stress. Moreover, the borehole boundary conditions are all included in the first mode, so that the boundary conditions for the second mode are homogeneous. Taking the stresses induced by mode I as $\sigma_r^1, \sigma_\theta^1, \sigma_{r\theta}^1$, and the stress induced

by mode II as $\sigma_r^2, \sigma_\theta^2, \sigma_{r\theta}^2$, the final stresses for the complete thermo-poro-elastic problem are found by superposition of the above solutions in Laplace space (Wu et al., 2009).

Numerical results

By using the numerical Stehfest method (Detournay and Cheng 1988), the solution in the time domain is obtained. The parameters used for the example calculations are listed in Table 1, and are for the particular case of a granite-water system. In the following figures, the black, red and blue curves are for the pure elastic, poro-elastic (Detournay and Cheng 1988) and thermo-poro-elastic solutions (the present solution), respectively. And, their difference in time is discerned by line types, solid curves for $t=0.9$ s, medium dashed curves for $t=1.5$ mins, short dashed curves for $t=2.5$ hrs, dotted curves for $t=10.4$ days, dash-dotted curves for $t=2.85$ years.

Table 1 Parameters for calculation

Parameter	Values
Fluid, rock mass density ρ_w, ρ_r (Kg/m ³)	1000, 2700
Fluid, rock specific heat c_w, c_r (J/Kg/K)	4200, 1000
Fluid, rock thermal conductivity λ_w, λ_r (W/m/K)	0.6, 2.4
Rock permeability k (mD)	4.0×10^{-5}
Fluid viscosity μ (Pa·s)	0.0004
Drained thermal expansion coeff. α_B (1/K)	5.0×10^{-6}
Undrained thermal expansion coeff. α_u (1/K)	1.0×10^{-5}
Biot coefficient B_i	0.47
Max principal stress σ_{\max} (Pa)	-1.7×10^8
Min principal stress σ_{\min} (Pa)	-1.3×10^8
Vertical principal stress σ_v (Pa)	-1.1×10^8
Initial pore pressure P_R^* (Pa)	7.0×10^7
Wellbore pressure P_w^* (Pa)	7.8×10^7
Wellbore temperature T_w^* (K)	323, 423
Initial temperature T_R^* (K)	523
Shear modulus G (Pa)	1.5×10^{10}
Drained and undrained poisson ratio ν, ν_u	0.25, 0.34
Porosity Φ	0.09

Thermal effects on pore pressure

From Figure 2(a) it is clear that the pore pressure obtained from the poro-elastic model for mode II loading decreases monotonically with radial distance and time to the reservoir pressure. However, for the thermo-poro-elastic solutions, the pore pressure in the region near the wellbore can decrease to below the reservoir pressure at small times if the far-field stresses are isotropic. When the cold fluid is injected into the wellbore, from Figure 3(a), we see that the temperature gradient near the wellbore is very high, although it decreases with time. This may lead to a reduction in pore pressure to below the reservoir pressure since the contraction of cooling water results in a

volume decrease of the pore fluid.

The pore pressure and temperature induced by the anti-symmetrical loading is displayed in Figure 2(b) and Figure 3(b). We see that, even though the thermal effect has been taken into account, the pore pressure curves from the thermo-poro-elastic solutions show little difference compared to the poro-elastic solutions. This confirms, as expected, that the shear deformation induced by the anti-symmetric loading does not cause significant temperature change, as shown in Figure 3(b). For the present case, the anti-symmetric stress S_0 is 20 MPa, from Figure 3(b) the temperature change is in the order of 1°C.

Figure 2(c) is superposition of Figure 2(a) and (b), where the thermal effect on the pore pressure can be strongly offset by the pressure change from shear loading.

Thermal effect on stresses

In mode II, the radial stress is not sensitive to the temperature difference between the well and the far field, as show Figure 4(b). But the radial stress depends on the wellbore temperature, since the thermal responses and volumetric change are both significant. At a certain distance to the wall of the well, the radial stress level is elevated by a cooler injection fluid as indicated in Fig. 4(c). However, the radial stress on the well wall is imposed by the boundary condition.

Figures 5(a)-(d) display the hoop stress evolution for two different well temperatures. Figure 5(b) shows that the hoop stresses induced by mode II loading follow the poroelastic solutions closely except at early time and near the wellbore. Figures 5(c) and 5(d) indicate that the cooler the well, the higher the hoop stress in tension. Moreover, the hoop stress at the wall, although it does not change with time, can be increased by imposing a cooler well condition. The hoop stress contours at different wellbore temperatures ($T_w^*=373$ K and 423 K) are shown in Figure 6. These plots clearly demonstrate the position along the maximum tectonic stress direction experiences the lowest compressive hoop stress.

In Figure 7, the vertical stress evolution is provided. When the wellbore temperature is equal to the far-field rock temperature shown in Figure 7(A), the vertical stress contours appear unchanged because of the very small temperature gradient in the whole domain.

However, when the wellbore is at a lower temperature (Figure 7(B)), the vertical stress change is also enhanced. The maximum tensile stress change in the vertical direction also exists at the position along the maximum tectonic stress. Moreover, if the vertical stress becomes less than the borehole pressure, a horizontal opening

fracture may well be formed at this corner. The plane strain assumption adopted here is expected to produce the strongest estimate for change in the vertical stress because of the built-in assumption of zero strain in the axial direction.

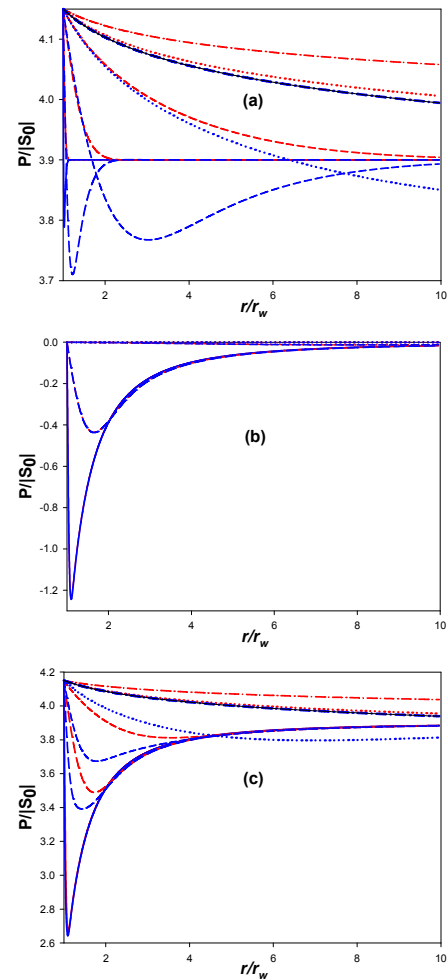


Figure 2: Pore pressure for (a) mode I, (b) mode II and (c) mode I+II for $\theta=0$.

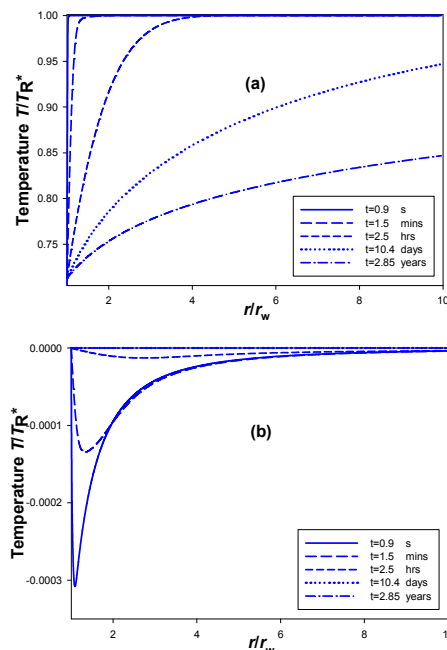


Figure 3: Temperature for (a) mode I and (b) mode II at $\theta=0$

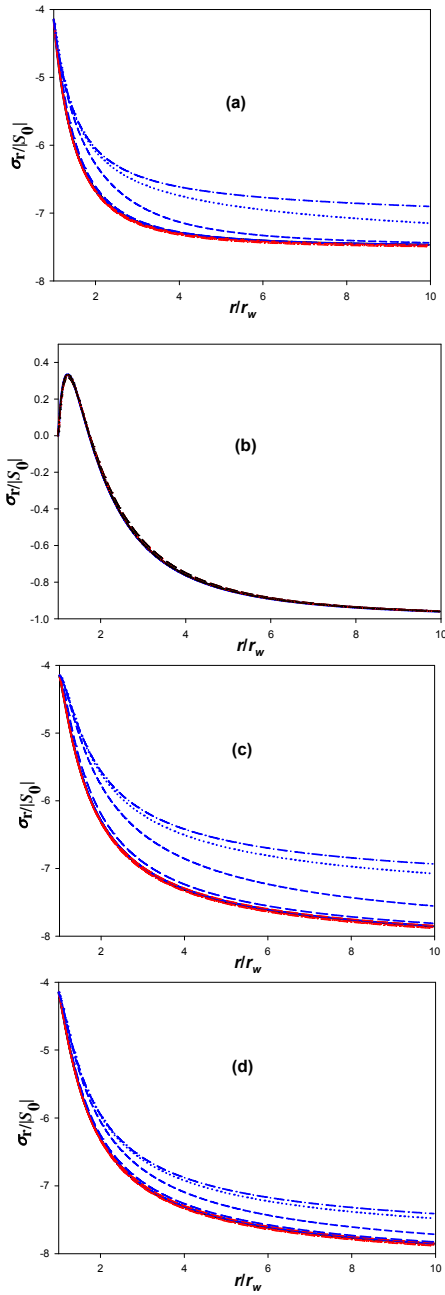


Figure 4: Radial stresses at $\theta=0$ for (a) mode I, (b) mode II and (c) mode I+II at $T_w^*=373$ K; (d) mode I+II at $T_w^*=423$ K.

Thermal effects on wellbore stability

Wellbore breakdown

The hoop stress on the wall of the well can be calculated theoretically. Based on rock strength theory, the breakdown pressure is obtained as follows (Wu et al. 2009)

$$p_b = \frac{\sigma_T - 2R_0 - 2\eta P_R^* - 4S_0 + \frac{6\alpha_B G K_B (T_R^* - T_W^*)}{K_B + 4G/3}}{2(1-\eta)},$$

where σ_T is the tensile strength. When $S_0 < 0$ the angle θ is taken as 0 to obtain the minimum pressure and when $S_0 > 0$, θ is taken as $\pi/2$ to obtain the minimum pressure.

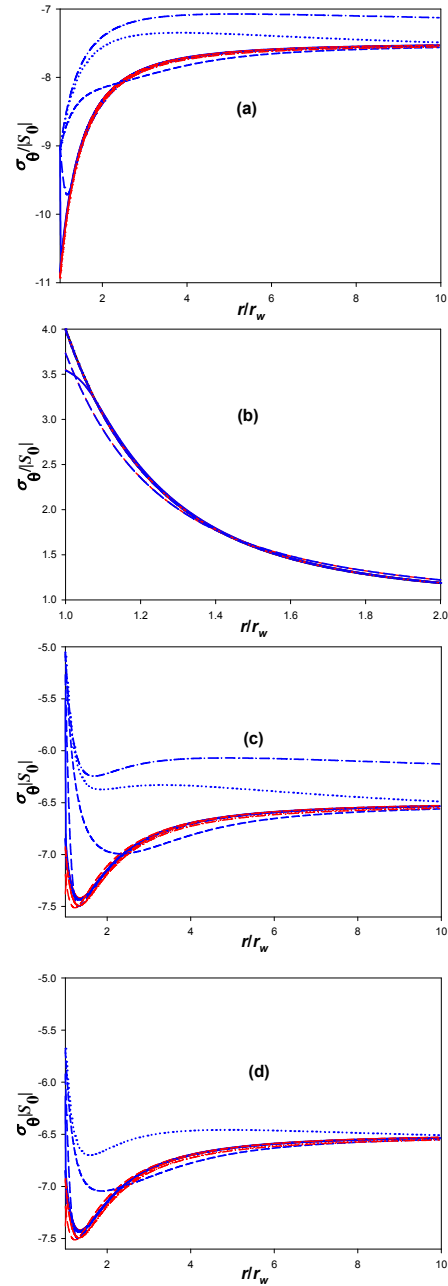


Figure 5: Hoop stresses at $\theta=0$ for (a) mode I, (b) mode II and (c) mode I+II at $T_w=373$ K; (d) mode I+II at $T_w=423$ K.

Wellbore shear failure

The Mohr Coulomb strength criterion is used to assess wellbore shear failure risk based on the solutions for σ_r , σ_θ , $\sigma_{r\theta}$ and σ_z . In terms of principal effective stresses, the criterion may be written as:

$$\sigma_1' = \sigma_s + (1 + \sin \varphi) / (1 - \sin \varphi) \sigma_3'$$

where σ_s and φ are the unconfined compressive strength and the internal friction angle respectively. The stresses σ_1' and σ_3' are the maximum and minimum principal effective stresses based on Terzaghi's definition. A safety factor for shear failure is defined based on the Mohr-Coulomb strength criterion as

$$SF = \left[\sigma_s + (1 + \sin \varphi) / (1 - \sin \varphi) \sigma_3' \right] / \sigma_1'$$

SF>1 indicates that the effective stress state is below the shear strength envelope and therefore safe from shear failure, whilst SF<=0 means the stress state is higher or on the strength envelop with an associated potential shear failure risk.

Figure 8 shows contour plots for the safety factor at different times for two wellbore temperatures in the near wellbore region. When the wellbore temperature is equal to the initial rock temperature (Figure 8(A)), the thermal effects on the stress distribution can neglected as expected and the safety factor does not change with time.

As shown in Figure 8(A), shear failure (blue) occurs at $\theta=\pi/2$ and $3\pi/2$ positions and is driven by the hoop and radial effective stresses. This type of shear failure is called breakout and has been widely used to infer in-situ stress orientation and magnitude.

However, when the wellbore temperature is decreased, the thermal effect on rock deformation becomes evident through changes in the distribution of the radial, hoop and vertical stresses.

Figure 8(B) shows the safety factor contour plot at different times with a wellbore temperature of 323K. Interestingly, in addition to the breakout type shear failure, shear failure (blue) occurs at $\theta = 0$ and π locations and the area of shear failure increases with time until the temperature in the near wellbore region stabilises. A close examination of the result indicates that the shear failure at these locations is induced by the hoop stress and the axial stress, which is the minimum effective principal stress because of the cooling effect. This is consistent with the low angle shear failure traces in the σ_{max} direction occasionally

observed from image logs of conventional oil and gas wells.

It should be pointed out that the axial stress calculation and, therefore the prediction of shear failure in the maximum horizontal stress direction, depends on the assumption of plane strain in the axial direction. Although intuitively reasonable for a deep vertical well, the plane strain assumption could be readily violated due to local geological conditions, such as natural fractures, formation inhomogeneity and dipping rock layers. Therefore, whether the low angle shear failure traces can be observed will very much be dependent on what extent the plane strain assumption is valid.

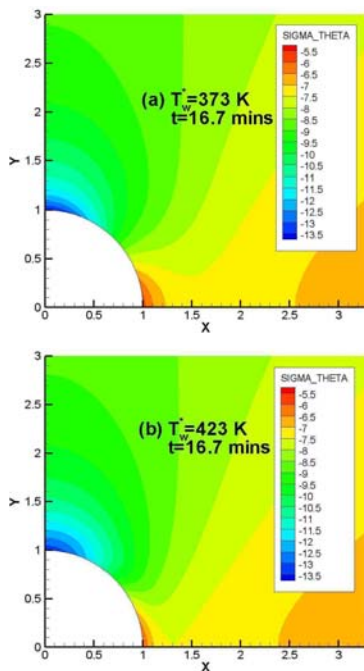


Figure 6: Hoop stress for different wellbore.

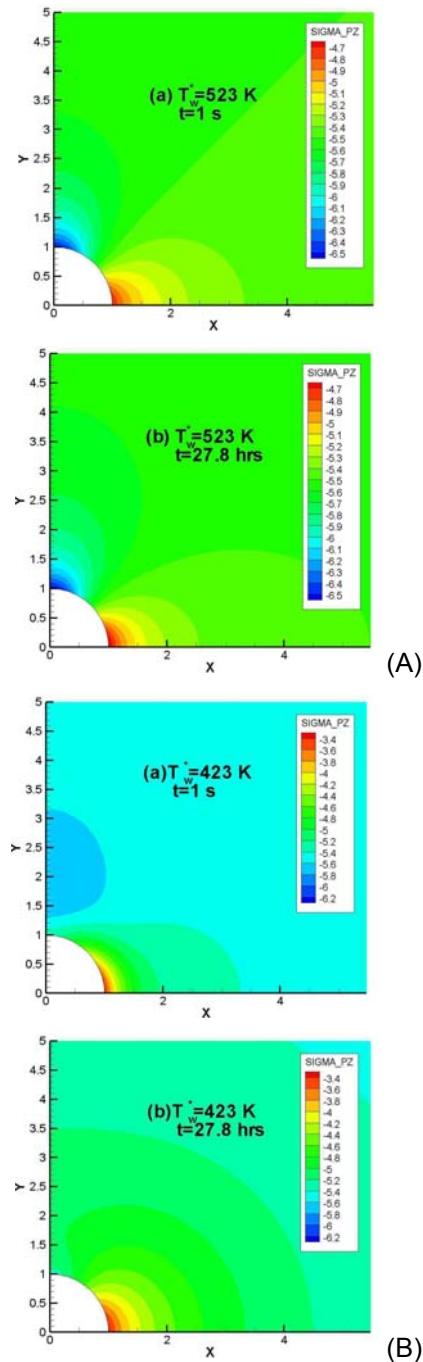


Figure 7: Vertical stress at different wellbore temperature.

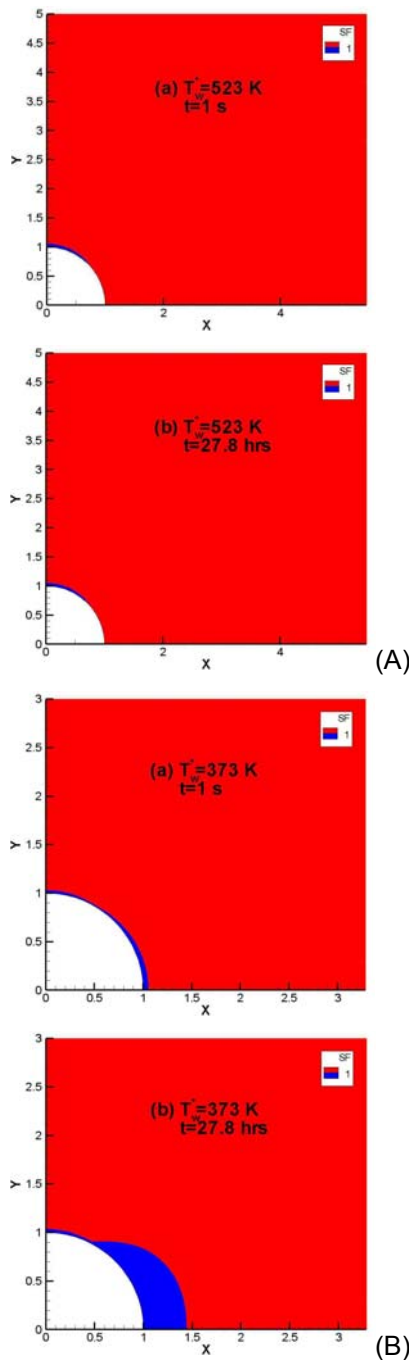


Figure 8: Safety factor for different wellbore temperature.

Conclusions

In this paper, the semi-analytical solutions for the temperature, pore pressure and stress around a wellbore are obtained. By comparing the results with those from the poroelastic solutions, the following interesting results are drawn:

1. The thermal effect can affect the pore pressure at small times and in the near-well region, but this influence decays with time.
2. The thermal effects can elevate not only the radial stress but also the hoop stress. This effect becomes more important with time and for a cooler well. It is also found that the vertical stress

can be reduced in magnitude if the well becomes cooler. This may lead to the formation of opening fracture from the borehole.

3. The breakdown pressure is reformulated to include the thermal effect.

4. In addition to the shear failure in the minimum horizontal stress direction often observed as wide breakout, shear failure can also occur in the maximum horizontal stress direction due to the wellbore cooling effect. However, the later is dependent on the plane strain assumption.

References

Rice, J.R. and Cleary, M.P., 1976, Some basic stress diffusion solutions for fluid saturated elastic porous media with compressible constituents, *Rev. Geophys and Space Physics*, v.14, no.2, p.227-241.

Detournay, E. and Cheng, A. H-D., 1988, Poroelastic response of a borehole in a non-hydrostatic stress field, *Int. J. Rock Mech. Min. Sci. & Geomech. Abstr.*, v.25, no.3, p.171-182.

Ekbote, S., Abousleiman, Y., Cui, L. and Zaman, M., 2004, Analyses of inclined boreholes in poroelastic media, *Int. J. Geomech.*, v.4, no.3, p.178-190.

Rajakpase, R.D., 1993, Stress analysis of borehole in poroelastic medium, *J. of Eng. Mech.* v.119, no.6, p.1205-1227.

Biot, M.A., 1941, General theory of three-dimensional consolidation, *J. Appl. Phys.*, v.12, no.2, p.154-164.

McTigue, D.F., 1986, Thermoelastic reponse of fluid-saturated porous rock, *J. Geophys. Res.*, v.91 (B9), p.9533-9542.

Kurashige, M., 1989, A thermoelastic theory of fluid-filled porous materials, *Int. J. Solids Struct.*, v.25, no.9, p.1039-1052.

Coussy, O. 1989, A general theory of thermoporoelastoplasticity for saturated porous materials, *Journal Transport in Porous Media*, v.4, no.3, p.281-293.

Wang, Y. L. and Papamichos, E., 1994, Conductive heat flow and thermally induced fluid flow around a wellbore in a poroelastic medium, *Water Resour. Res.*, v.30, p.3375-3384.

Li, X., Cui, L., and Roegiers, J.C., 1998, Thermoporoelastic analyses of inclined boreholes, In *SPE/ISRM Rock Mechanics in Petroleum Engineering*, Trondheim, Norway, p.443-451.

Wu, B., Zhang, X. and Jeffrey, R. G., 2009, CSIRO internal report.

3D Geological Modelling for Geothermal Exploration in the Torrens Hinge Zone

Matthew Zengerer^{1*}, Chris Matthews², Jerome Randabel³.

¹ 10 Holland St, Thebarton, SA, 5031.

² 6 Hollywood Way, Glenalta, SA, 5052.

³ Torrens Energy Limited. PO Box 506, Unley, SA, 5035.

* Corresponding author: mzengerer@hotmail.com

This paper describes 2D/3D Geophysical/Geological Modelling undertaken by the author for Torrens Energy in 2009, for the purpose of establishing 3D Geological Models of the upper crust within their Torrens Hinge Zone tenements in South Australia. Geological Models are a requirement for any Geothermal Energy explorer searching for Hot Dry Rock or Hot Sedimentary Aquifer targets. These Geological Models are assigned thermal parameters determined by field and laboratory measurements based on the lithologies included in the model. Heat resources may then be computed for the given volume based on the geological model and thermal rock properties. Whilst the studies were carried out for the purpose of creating temperature models and geothermal resource estimates, this document will discuss the geological models, geophysical investigations and tectonic implications generated by the study. Examples of Geological Models are shown from the Torrens Energy Port Augusta, Yadlamalka and Panchilina Geothermal Prospects, based over their GELs 230, 234, 235, 285 and 501.

Keywords: South Australia, 3D Geological Modelling, Geophysical Modelling, Heat Flow, Stratigraphy, Torrens Hinge Zone, Adelaide Geosyncline, Magnetics, Euler Deconvolution, Geothermal Energy.

Introduction and Geological Setting

The principle behind 3D Geological Modelling is to integrate existing geological and drilling information with geophysical data such as seismic, gravity and magnetics, in a 3D environment which will simulate the 3D geology of the region of interest by creating a 3D geological model which can then be used as an input for thermal modelling.

The Torrens Hinge Zone is a long but narrow (up to 40 km wide) geological transition zone between the relatively stable Eastern Gawler Craton

“Olympic Domain” to the west and the folded sedimentary basin known as the Adelaide Geosyncline to the east (Drexel et al., 1993). The THZ is essentially a region of overlap between the Gawler Craton and Adelaide Geosyncline (Figure 1). In the study areas of the THZ, the Adelaidean and Cambrian sedimentary sequences are underlain at depths between 2,000 and 7,000m by Paleoproterozoic to Mesoproterozoic Gawler Craton Olympic Domain rocks (Matthews and Godsmark, 2009).

Heat flow values of over 90 mW/m² have been recorded in several wells drilled in the THZ. With several kilometres thickness of moderate conductivity sediments overlying the crystalline basement in this region, predicted temperatures at 5000 m are up to 300°C in some areas (Matthews and Godsmark, 2009).

Data and Methodology

Available geological data included historic and Torrens Energy drillholes and South Australian (SA) geological mapping. Geophysical data comprised SA magnetic and Bouguer Gravity data along with recently acquired Torrens Energy and Geoscience Australia 2D depth-converted Seismic. Rock thermal properties were derived from laboratory measurements performed by Torrens Energy and top and downhole temperatures measured from drilling.

The Intrepid 3D Geomodeller suite was used to build the 3D Geological Model. The 3D Geomodeller software interpolates between geological boundaries, orientation data and drillholes to generate a 3D geological model that is flexible and readily adaptable with additional geological information. Geomodeller also supports faults and fold information into its interpolation. The final output can be discretised into a 3D “voxel” model of desired resolution to use in 3D Geothermal Modelling.

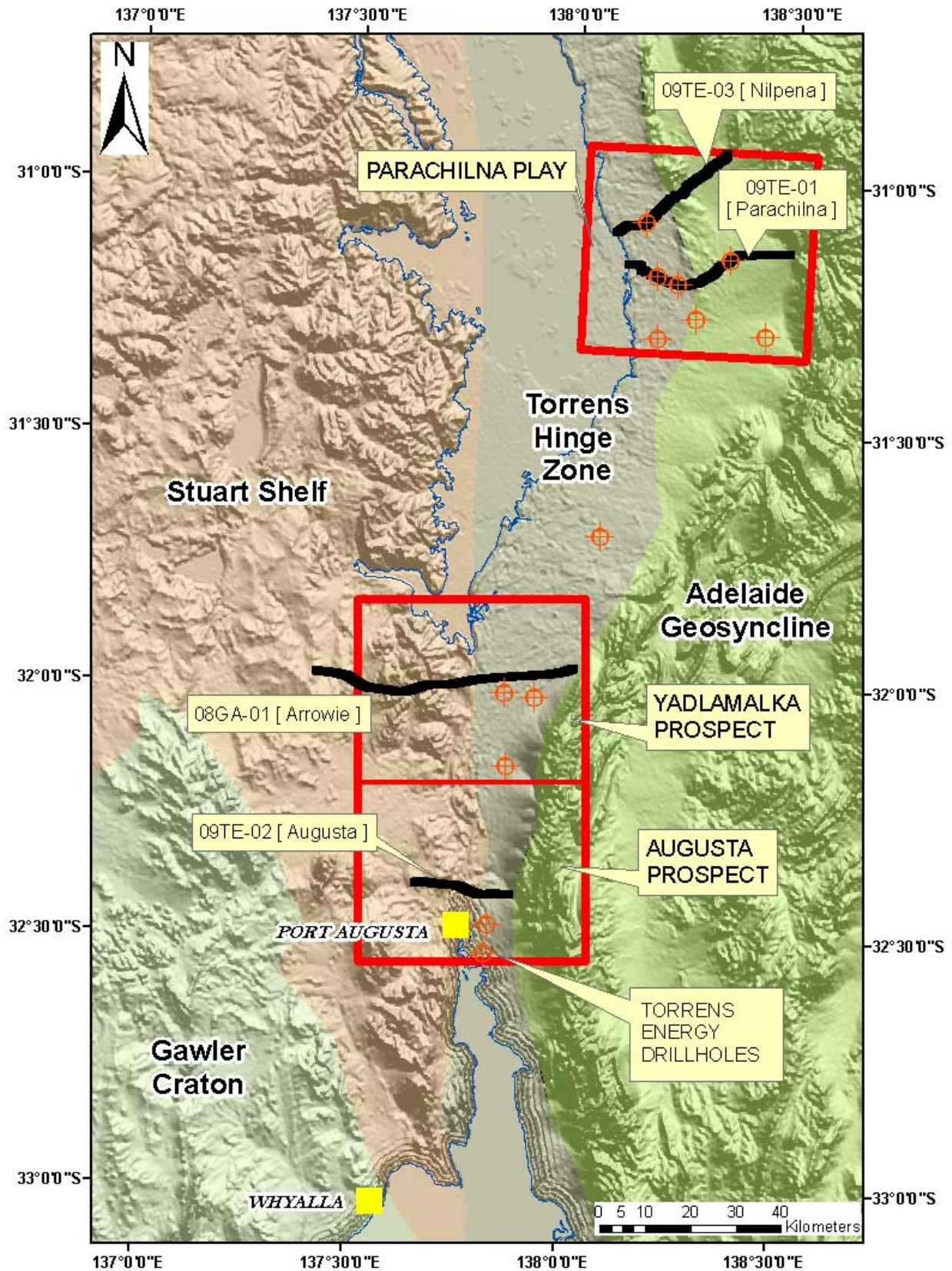


Figure 1. Map of Central South Australia showing tectonic elements and study areas together with Torrens Energy wells, seismic lines and prospects

Basic Modelling requirements

The following methodology was applied to construct a 3D Geological model. It relies heavily on interpretation and integration of many data types, as well as some creative thinking and intuition. All 3D geological models built by Geomodeller begin with 4 pieces of information. The first is a defined 3D volume of interest, set by rectangular coordinates of the target area, and a suitable depth dimension which will encompass (preferably) the heat source, basin thickness and topography. For both Parachilna and Port Augusta a depth below Mean Sea Level of 7km and a maximum of 1.5km above MSL to clear the range topography was deemed sufficient, giving an 8.5km thick model. They are covered in the Parachilna model was 50x45 km, and 50x80km over Port Augusta/Yadlamalka.

A surface topography is required for the model to compute the intersections of the geological interfaces at surface, i.e. to have an initial 2D section at which to input geological information and have it reproduced by the model computation for validation. Topography was imported into the models from SRTM DEM grids at 90 m resolution clipped to the Area Of Interest (AOI), Figure 1.

The third and fourth requirements are the defined geology in the form of lithological interfaces and associated structural orientations, and a stratigraphic pile which defines the relationships between the lithologies. The latter is particularly important as contacts need to have relationships defined as either Onlapping or Erosional, as this determines whether interface isolines intersect or remain apart with respect to one another. Sequences of geological units such as found in sedimentary basins may also be grouped in onlapping series, whereas intrusives are always erosional and appear where required in the stratigraphic pile to best satisfy contact relationships. In strongly deformed regions, structural requirements may imply that lithologies must obey onlapping rather than erosional rules. A simplification of the stratigraphy was also created for ease of modelling (Figure 2), which essentially has grouped the Cambrian and Neoproterozoic sequences into their major tectono-stratigraphic units.



Figure 2. Simplified Parachilna Stratigraphy.

Geological information at surface came from importing simplified or grouped shapefiles derived from State 100k geology polygons, and assigning these to the simplified stratigraphic formations. Likewise orientation data, where known from mapping, have been supplied where possible and assigned to specific formations. Torrens Energy and historic diamond drillhole data have provided constraint in the 3rd dimension. Once again the geological logs of these drillholes were simplified to the stratigraphy and the drillholes imported using the import tools in Geomodeller (figure 3).

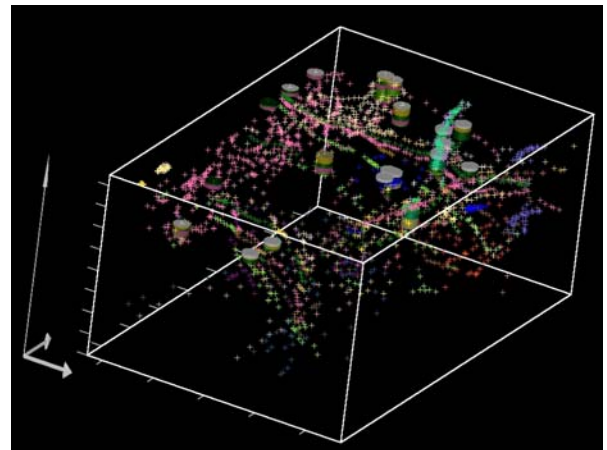


Figure 3. Port Augusta 3D Interface Points and Drillholes in Geomodeller project.

Supplementing Geology with Geophysics

Unless there is a complete coverage of mapped geological information at surface, it is unlikely that reliable models may be derived from surface mapping alone. To supplement the existing geological information, interpretation of four 2D depth-converted seismic lines, (two from the Parachilna area and two from the Port

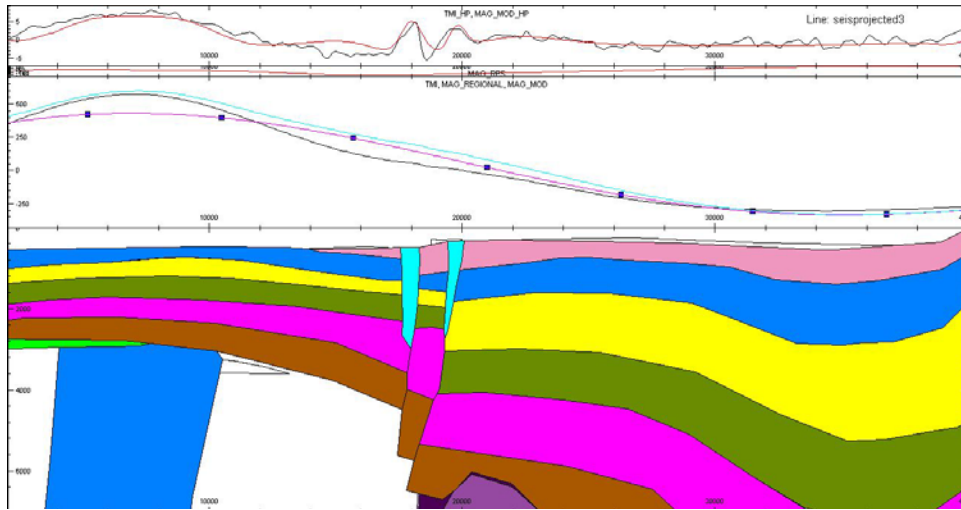


Figure 4. 2D Magnetics Model across Parachilna , showing main basin elements, possible magnetic intrusives and shallow fault-related magnetic bodies

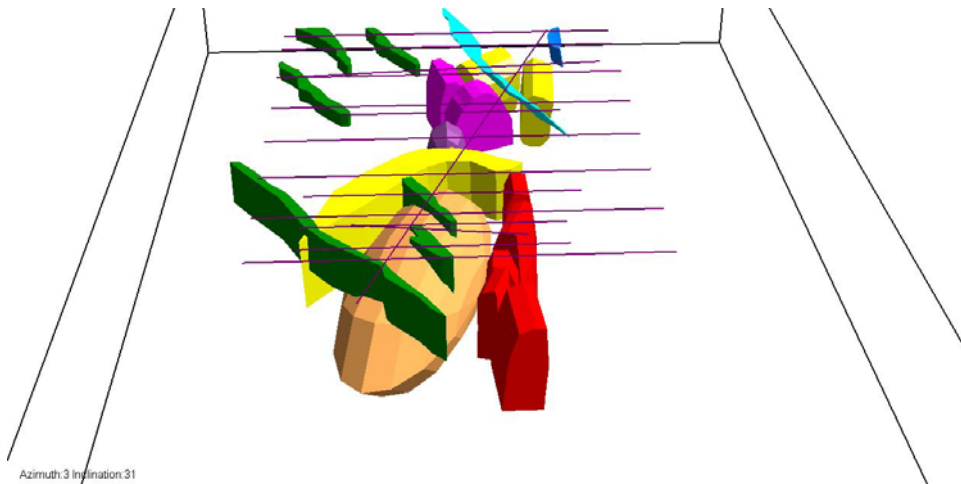


Figure 5. Persepective view of 3D Bodies derived from 2.5D Magnetic modelling within Augusta/Yadlamalka across Parachilna , including dykes, possible magnetic intrusives and sheet-like layers, probably thrustured Beda Volcanics.

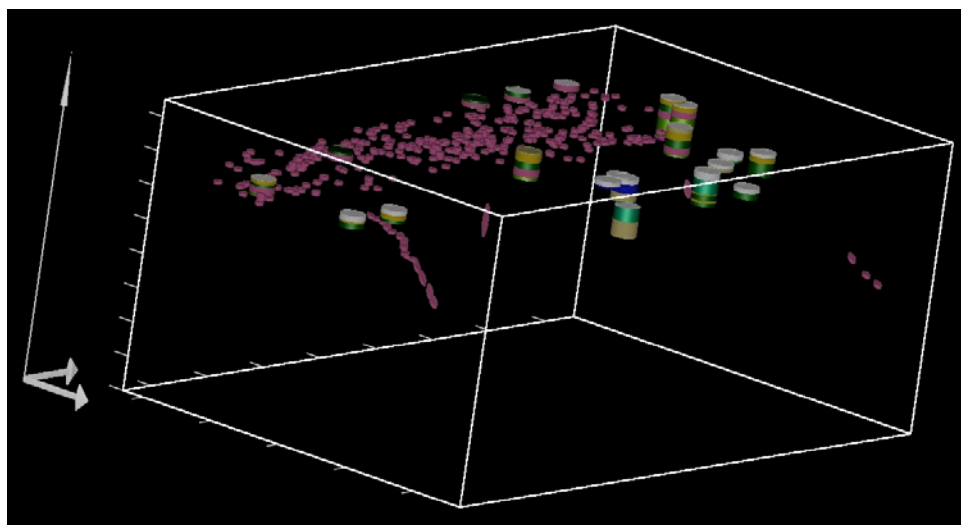


Figure 6. Depths to Base Sturtian, ie top Beda Volcanics, derived from Euler Deconvolution of Magnetics. Shown together with drillholes from Augusta/Yadlamalka prospects.

Augusta/Yadlamalka area), was performed (see Appendix 1). These were constrained wherever possible by drilling and outcrop information. These seismic sections were imported into Geomodeller as image backdrops along vertical sections through the model and the interpretation transformed into interfaces within these vertical sections.

The interpretation along these sections was augmented further in the Parachilna AOI by 2D modelling of state magnetic data along two lines adjacent to the 09TE-01 seismic line (figure 4). In the Port Augusta region, 2D magnetic modelling was also performed in order to obtain estimates of basement depth and magnetic body shapes and locations (figure 5). In each case images or actual 3D data points from the results were imported back into Geomodeller.

Euler Deconvolution of magnetic data was also used in this area to provide spot estimates of depth to shallow-dipping volcanic units, implying local estimates to the top of Willouran -age Beda Volcanics (figure 6). Additional scans using a larger window size revealed information about the shape and size of deeper magnetic bodies which correlate well with 2D magnetic modelling results. Finally, structural interpretation of both gravity and magnetic data was used to define fault traces in Geomodeller (see Appendix 2).

3D Geological Models

Computation time of the two 3D Geological models is dependent on the amount of data supplied. Results which are strongly biased to orientation data were treated with caution. Some additional inference of contacts and orientations was required to ensure geological consistency, especially near faults. Additional sections linking drillholes provided stronger cross-correlation of geological interfaces, especially in the Port Augusta/Yadlamalka area where data was widely spaced. Although in some cases actual outcrop geology was further from the area of interest than required, it was included to provide geological reality and well-defined constraints on modelling.

As faults also require orientation information to be computed in the modelling, their direction, dip and apparent movement was estimated either from seismic images or geological and geophysical images.

Parachilna

Emphasis on interpretation and modelling in the Parachilna area focused on areas west of the Ediacara fault (Figure 7a, 7b, Appendix 2) where there is simpler geology according to the seismic data. In this area we see from modelling that the Early Cambrian to Adelaidean rocks transition

relatively flat-lying in the west to moderately east-dipping at the Ediacara fault contact.

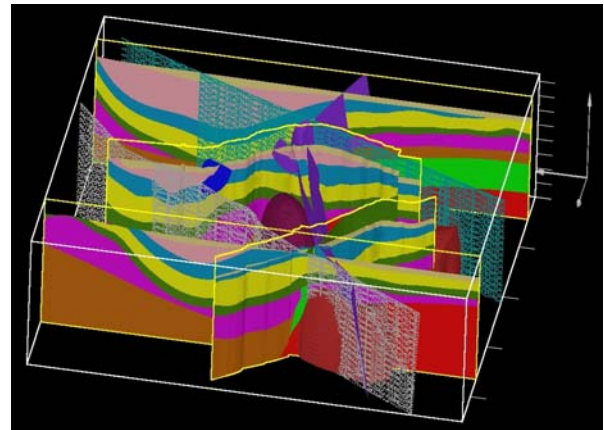


Figure 7a. Projected section view of Parachilna 3D Geology Model, view SE. Vertical. exaggeration= 2:1

The Ediacara fault zone changes in character from south to north. Our modelling shows it to be a steeply west-dipping feature, upthrown on the eastern side, which evolves in the south from a relatively simple antiform, to a complex horst structure involving several faults and possibly basement or diapiric material from the centre of the Parachilna AOI to its northern edge. Basement depths in the far west are predicted to range from 2km depth in the north to 5 km in the south. In the vicinity of the Ediacara Fault footwall basement depth reaches 6km, but this decreases to 2.5-3km in the far north. In the faulted horst blocks of the Ediacara Fault region basement or diapiric material may reach depths of 2km. East of the Ediacara Fault in the central and southern areas is a moderately folded disturbed region leading eastward into a very deep synclinal basin within the Cambrian – Adelaidean sequences adjacent to the range front fault. To the north of this area the model predicts less intense folding with flatter basin sequences, but still basin thicknesses of > 7km.

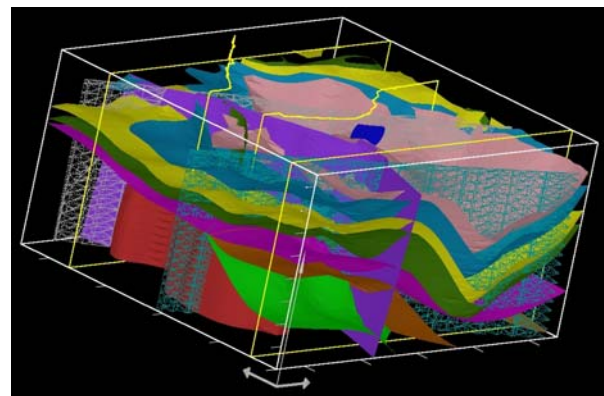


Figure 7b. Interfaces and Faults, Parachilna 3D. View NE, VE=3:1

Cainozoic erosional units tend to range in thickness from 300–400m and thin out in the vicinity of the Ediacara Fault hanging wall. Early to Middle Cambrian units of the Lake Frome, Unnamed, and Hawker Groups have been confirmed by deep drilling, whilst Adelaidean rocks of Mari noan to Sturtian ages are expected to lie beneath the sequence based on their presence in the Ediacara Hills to the north in the fault zone and outcrops of the sequence units to the west on the Stuart Shelf. Inference of Torrensi an to Willouran rocks is based on the apparent presence of diapirs to the south and east, although these rocks are expected to thin out somewhere in this region. Torrensi an rocks in particular may not appear anywhere west of the Ediacara Fault system. Basement has been largely undifferentiated in the Parachilna 3D model with the exception of what are inferred to be two large magnetic intrusives in the central parts and northwest.

Port Augusta/Yadlamalka

A very large area has been modelled in this study, which naturally implies a greater amount of both inference and uncertainty. To complement this is more complex geology and more drilling data, as well as much more diverse magnetic signatures and seismic imagery.

The interpretation on the seismic lines 09TE-02 (Augusta) and 08GA-01 (Arrowie) is still the subject of some debate, until such time as some specific drilling is performed along the lines and stratigraphic correlations are performed. The interpretation has been made through careful cross-comparison of nearby drillholes using Geomodeller as a guide, using logged depths to specific units and comparing how they are distributed across the area, and existing geological mapping.

Inferences have been made on the nature and distribution of the Willouran and Torrensi an age rocks in a fashion similar to the interpretation at Parachilna, as well as deeper Proterozoic basement units. These inferences will be discussed in the next section.

The final 3D model is shown as sections and surfaces in Figures 8a and 8b. In general the stratigraphy is identical to that used at Parachilna, with the addition of several intrusive basement units of varying magnetic signature and a split of the Willouran-age rocks into Beda Volcanics/Backy Point Formation, general Willouran – age rocks and several thrust Willouran – age slices. The overall trends modelled show an eastward – thickening wedge of sediments toward the range front, with possible down-thrown rift basins evolving closer to the range. To the northeast thrust faults occur sub-

parallel to the Gairdner Dyke Swarm before the range front and are possibly facilitated by Callanna group evaporitic units and/or diapirism. To the east of these significant thrusts, closer to the range fault, sediments begin to dip more strongly or are deformed. Some deformation is also present immediately west of the thrusts on the footwall side, but this tapers out as sediments become more flat-lying to the west.

In the south and south central areas in the vicinity of Port Augusta, the model predicts gently dipping Adelaidean rocks of 800 – 1200m thickness, overlying granitic or metamorphic basement, crossing a significant north-northeast trending basin-defining fault approximately 10km northwest of Port Augusta, coincident with the onset of a significant gravity low and a step in the magnetics and seismic images. Here the basin thickness increases to at least 2000m, dropping away gradually to 3000m approximately 9km west of the range front, before dipping away more steeply to 4500m at the base of the range fault. Deeper reflectors in the Augusta seismic section are enigmatic but their pattern is suggestive of rifting, the timing of which should be investigated further, if proven (see Discussion). Modelling results based on historical drilling near Wilkatana (central southern Yadlamalka prospect) demonstrate localised basins containing Cambrian sediments.

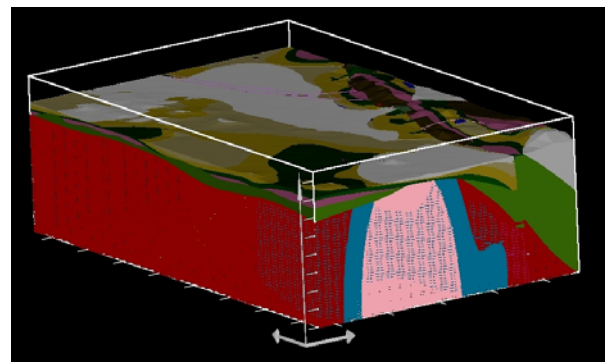


Figure 8a 3D volume model of Augusta/Yadlamalka. View NE, VE=3:1.

The northern parts of the model, described as Yadlamalka after the name of the station southeast of Lake Torrens near a major thrust zone, has similar gently dipping Adelaidean stratigraphy ranging from 600m thickness in the far west to 2300m before encountering a significant thrust fault which displaces Willouran volcanics close to surface, as evidenced by the Arrowie seismic section, drilling and magnetics. Unlike the more obvious extensional faulting regime exhibited farther south, basin units appear less disturbed, but a very marked angular unconformity exists between the sedimentary/volcanic pile and the basement, which comprises a series of west-dipping reflectors. East of the Yadlamalka thrust the

sedimentary pile is moderately folded and of unclear composition and thickness. What is clear is that thrusting and compressional deformation has disturbed the Adelaidean sequences in more than one location. It is also speculated that Willouran/Callanna Group salt formations may again be principally involved.

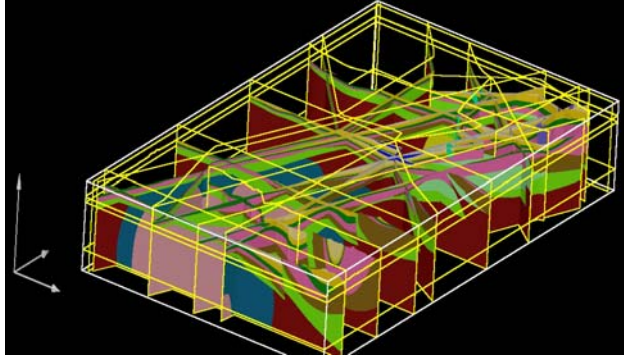


Figure 8b 3D section view of Augusta/Yadlamalka. View NW, VE=3:1.

In the northern part of the model magnetic modelling has suggested that a number of magnetic intrusives are present, along with slices of Willouran age volcanics. These have been emplaced into the model where most likely, but the remainder of the basement has been undifferentiated.

Partial modelling of the range to the east has been included to add both stratigraphic and structural control, but has been performed at a representative level only. Cainozoic strata also appear relatively thin in this region but have been included as a thin uppermost layer where evident.

Overall, the Early Cambrian to Neoproterozoic basin succession throughout the area remains relatively simple. Sequences dip gently eastward and thicken before the onset of thrusting, folding, or extensional faulting. Roughly midway across the model Torrensian lithologies are inferred to appear (see Discussion).

Discussion

Results and some of the methodology used in the Port Augusta/Yadlamalka area require some discussion due to inferences being made and the tectonic consequences of the modelled relationships

These inferences particularly concern the nature of the rocks within the basin sequences west of the range front fault. Torrensian/Burra Group rocks are not known to occur west of this structure or anywhere on the Stuart Shelf, however we have inferred from the seismic that Torrensian rocks pinch out or fault out fairly consistently 20-30km west of the range front, mainly at depths

deeper than what has been currently encountered in drill holes. The implication from this is that Torrensian sedimentation is controlled by a second onset of strong rift-related extension closer to the Central Flinders Zone.

Willouran age/Callanna Group rocks have long been enigmatic in terms of their relationship to other rocks of the Adelaide Fold Belt and the Gawler Craton, but inferences on their distribution and geology have implications for understanding the early evolution of the rift zone and later deformation. Basaltic rocks of the Beda Volcanics have been encountered in many drillholes on the Stuart Shelf, mostly at shallow depths, but also may have been confused with older Gawler Range Volcanics (GRV) in some holes. These rocks and associated intertonguing sediments of the Backy Point Formation are thought to form the basal units of the Adelaide Fold Belt rift sequence. Exactly how thick these units are, and whether additional sediments lie beneath the volcanics, is unknown, however drillhole information suggests that the Beda Volcanics are probably only a few hundred metres thick, and their flat-lying nature suggests that they should form a good reflector in seismic data.

Both seismic lines in the area show good deep continuous reflectors just above or not far above the basement, but in places drillholes appear to have intersected Beda Volcanics well above the suspected top basement horizon, at another reflector. The Port Augusta seismic line even appears to show what may be another rift graben well beneath what is interpreted as Willouran, but until this is confirmed by further studies we have assumed it to be basement, or at least GRV or similar age sediments. Elsewhere we have inferred that the Beda Volcanics are reasonably thick or probably have much larger proportions of Backy Point Formation beneath them for the purpose of modelling. The unmodelled other possibilities are that beneath the Beda/Backy Point rocks lie reasonable thicknesses of Mesoproterozoic rocks such as the Pandurra Formation and Gawler Range Volcanics (GRV), or that Torrensian and Sturtian rocks increase dramatically in thickness midway across the model, or both.

Further information was derived from the magnetics. Petrophysically, the Beda Volcanics are known to be moderately magnetic, but their flat-lying nature and probable magnetisation pattern means that unless they are tipped on their sides, the net effect is only to add a regional dc shift to the overall magnetic signal. High pass and analytic signal filtering of the state magnetics, however, has revealed where Beda Volcanics have been tipped on their sides and thrust to surface at the Yadlamalka thrust and Depot Creek on the range front, where they have been

intersected at surface or in drillholes, with the thrust also visible in the Arrowie seismic section.

Euler Deconvolution of magnetics is based around automated scanning of changes in the magnetic signal in windows across a grid, with depth estimates to magnetic sources dependent on the size, intensity, and shape of bodies, and window size. Two different window sizes were used, the first scanning to depths of 2km and the other to 8km. The results of the shallower window targeted mainly the tops of the Gairdner Dyke Swarm, which are known to be Beda Volcanic equivalent ages. These are therefore by implication minimum depths to the base of Sturtian Adelaidean rocks in the west, where Torrensian rocks are not present, and base of Torrensian rocks in the east where the method detected thrust Beda Volcanics. These results were statistically culled for reasonableness and proximity to dykes, thrust volcanics or closeness to interception in drillholes.

The remarkable consistency of Euler depth trends in the west for the shallow scan gives credence to the notion that Beda Volcanics overlie deeper sediments and/or volcanics. The idea that Gawler Range Volcanics lie below the obvious basement unconformity seen in the Arrowie seismic is not supported by this model, unless east of the major volcanic flows on the Gawler Craton the GRV were deformed along with Hiltaba suite and eroded prior to either Mesoproterozoic clastic deposition or Willouran rifting. Similar notions apply in the Port Augusta area.

The deeper window targeted magnetic intrusions, by implication a maximum depth to basement across the area. Again these results were statistically culled and sorted by proximity to the inferred "tops" of magnetic body depths. These results, along with results of 2D magnetic modelling were interpreted to be from deep magnetic intrusives, possibly even Iron Oxide Copper Gold – bearing intrusives lying in the centre of the region (though perhaps too deep for drilling), rather than belonging to metasediments, GRV or younger volcanics. Further support for this notion came from examination of filtered magnetic grid images as described above.

Values from the deeper Euler and 2D magnetic modelling were input back into Geomodeller as the basis for intrusive 3D body shapes.

Results of 3D modelling in the Parachilna area are currently considered less contentious. The principal features for discussion are the nature of the magnetic anomalies, whether they indeed correspond to deep intrusives, or are related to diapirism bringing basement magnetic material to closer to surface, or a combination. The strong gravity anomaly running through the centre of the region suggests it is more likely to be basement reactivated along the Ediacara Fault. Once again the other major issue for consideration is the presence and distribution of Torrensian and Willouran rocks.

Conclusion

Two large 3D Geological models have been made of sections of the Torrens Hinge Zone in South Australia. The northern model near Parachilna shows moderately dipping Cambrian to Adelaidean sediments of thicknesses between 2000 and 4000m overlying unknown basement in the west. A modern active fault system, the Ediacara Fault, has uplifted basement locally and forms the boundary of a deep, moderately deformed north-south basin adjacent to the Flinders Range front.

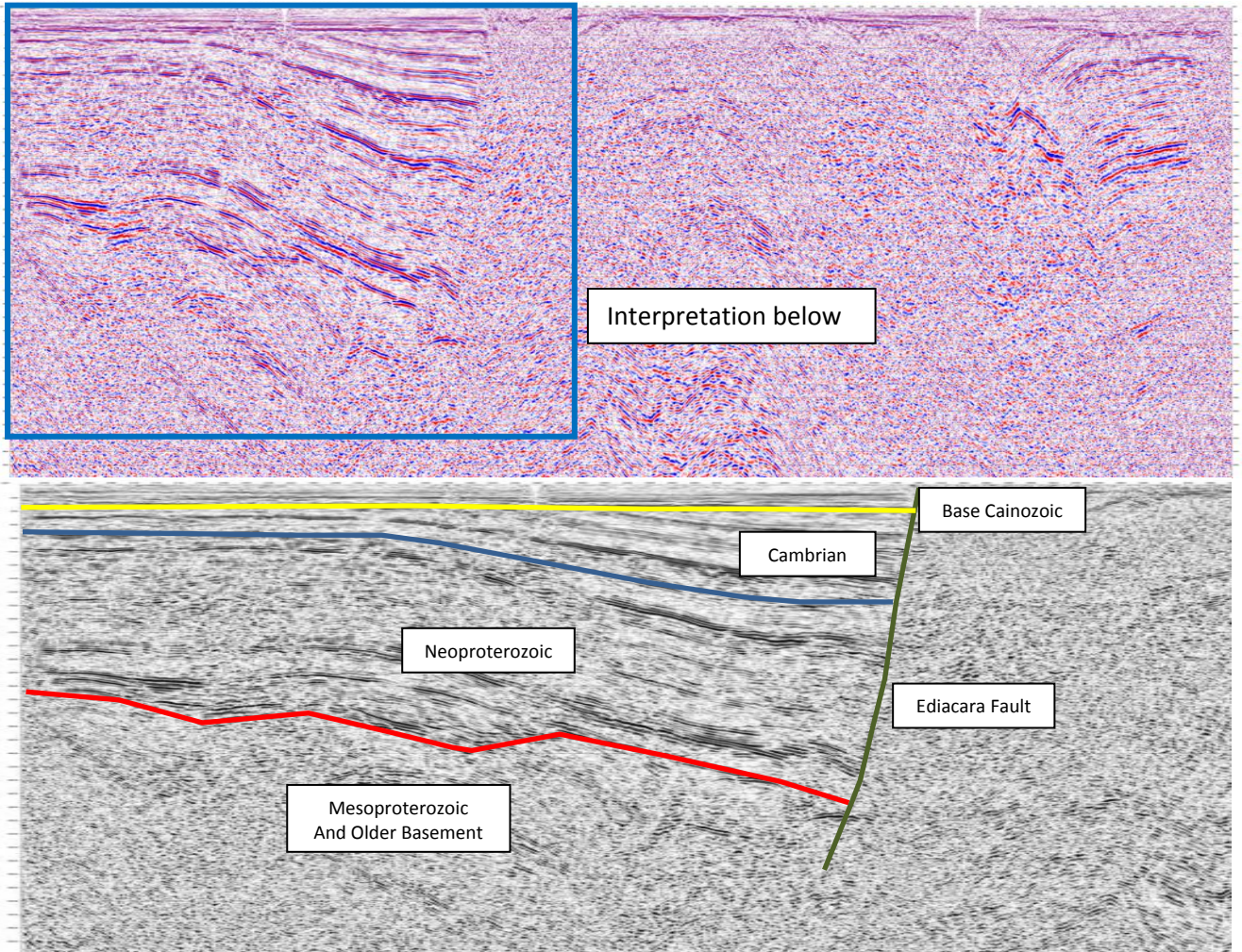
The southern model between Lake Torrens and Port Augusta shows transitions between gently dipping Adelaidean sequences of up to 2300 m thickness with thrust, deformed basins to the north and deeper rifted basins to the south. Evidence from seismic and magnetics suggests the presence of substantial sedimentary or volcanic sequences lying beneath Willouran Beda Volcanics and overlying deformed metamorphic or granitic basement with sharp unconformity.

References

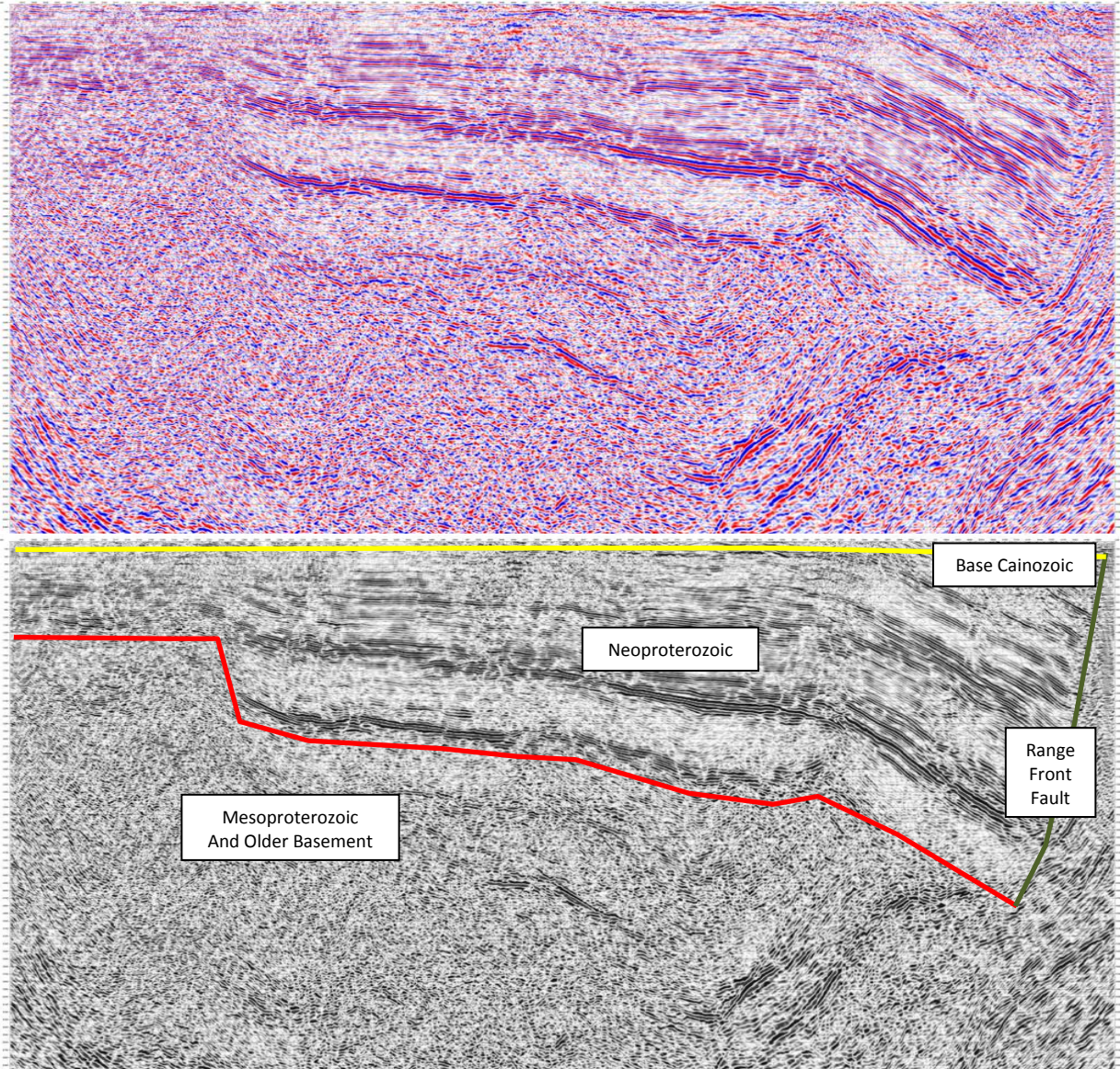
- Matthews, C. G. & Godsmark, B., 2009. Geothermal Energy Prospectivity of the Torrens Hinge Zone: Evidence from New Heat Flow Data. AGE 2009 Conference Extended Abstracts.
- Drexel J. F. Preiss W. V. & Parker A. J. eds. 1993. The Geology of South Australia, Geological Survey of South Australia Bulletin 54

Appendix 1: Seismic Surveys and Results (after Matthews and Godsmark, 2009)

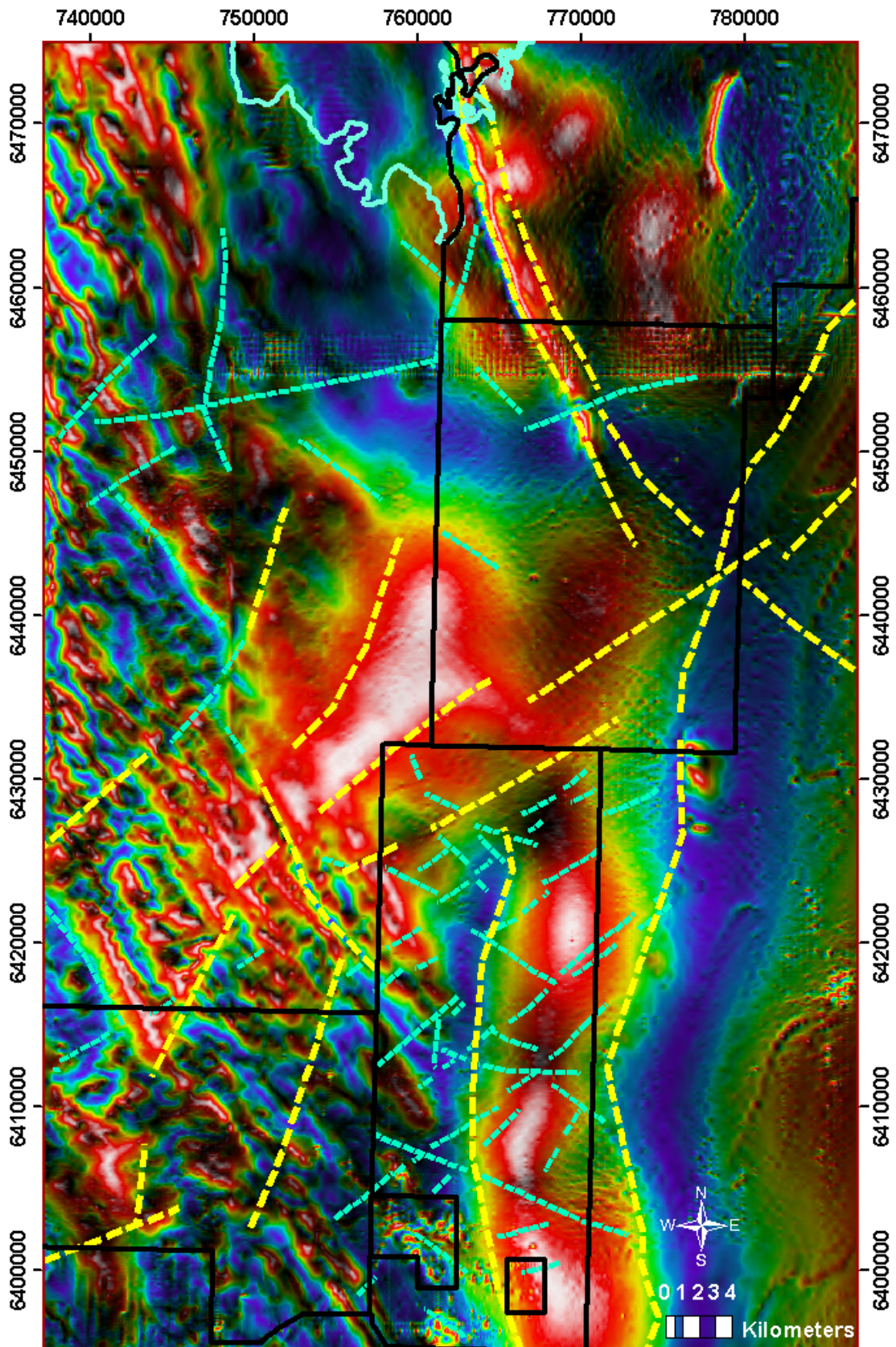
Parachilna Seismic Survey, completed January 2009



Port Augusta Seismic Survey, completed May 2009



Appendix 2: Fault Interpretation from Magnetics



Fault Interpretation (blue and yellow lines) of SA Magnetics in the Port Augusta/Yadlamalka area. Image is a Tilt Angle filter draped over Analytical Signal Amplitude. Torrens Energy GELs in black. MGA Zone 53.

Numerical simulation of geothermal reservoir systems with multiphase fluids

Zhang, J.^{1*}, Xing, H.L.¹

¹ Earth Systems Science Computational Centre, School of Earth Sciences, The University of Queensland, QLD 4072

*Corresponding author: ji.zhang@uq.edu.au

This paper describes a modular framework for simulating geothermal well and reservoir performance. The numerical model is able to account for transient, three-dimensional, single- or two-phase fluid flow in normal heterogeneous or fractured-matrix formations. Both conductive and convective heat flow are accounted for and fluid states in the reservoir can range between liquid phase, two-phase steam-water mixtures to superheated steam. Both short term well reaction and long term reservoir performance can be monitored as dynamic mass/heat flow processes. Equations-of-state (EOS) for water and CO₂ are integrated as part of the fully-coupled nonlinear finite element simulator. In this paper, the code has been applied for use in geotechnical risk assessments for mine developments in geothermal areas. Comparison of EGS-CO₂ and EGS-water is demonstrated in the paper and results show that the simulator or PANDAS/ThermoFluid can be used for both conventional geothermal fields and enhanced geothermal systems.

Keywords: Numerical simulation, Enhanced geothermal system, EGS, Geotechnical risk assessment, Carbon dioxide

Introduction

Geothermal energy is regarded as a renewable, clean, cost effective energy source, which is becoming increasingly attractive, especially since the enhanced geothermal system (EGS) has been proposed and applied as a new type of geothermal power technology. Geothermal reservoir modeling has been played an important role as an integral part of reservoir assessment and management in the past few decades. Although computer modeling is routinely applied in hydrothermal reservoir engineering, there are several aspects that continually need improvement:

(1) Two-phase flow phenomenology. This includes the implementation and calibration of relative permeability and capillary pressure, two-phase flow in fractures and mass transfer between phases (evaporation and condensation);

(2) Non-equilibrium models. To relax assumptions of local thermodynamic equilibrium, several non-equilibrium models have been developed, including double porosity models (Warren & Root, 1963), explicit fracture treatment (for sparsely fractured systems) and statistical models

("MINC"-TYPE, Pruess & Narasimhan, 1985) (for densely fractured systems);

(3) Natural-state modeling. Further validation of the computed natural state against early exploration well data is required;

(4) Constitutive representations. Reservoir fluids with dissolved solids (i.e. NaCl) and non-condensable gases are now available in several simulators. Modeling of fluid under extremely high temperature and pressure (supercritical state) is already being conducted but not in the geothermal modeling arena;

(5) Coupled reservoir chemistry. There are a few calculations that have been reported incorporating reactive chemistry, coupled with fluid flow by dissolution and precipitation of solids (creation and destruction of porosity and permeability), however, this area still provides a challenge to geothermal modeling;

(6) Automatic inversion techniques. Inverse modeling uses an iterative inversion procedure to drive conventional forward reservoir models (treated as sub-routines). With the increase in model complexity and degrees of freedom, the computational cost is extremely high.

In conclusion, further computational modeling and code development is urgently needed to improve our understanding of geothermal reservoir and the relevant nature. It is also needed for the enhanced evolution such as of enhanced geothermal reservoir system, and achieves a more accurate and comprehensive representation of reservoir processes in more details. It also helps to reduce the uncertainties in models, and to enhance the practical utility and reliability of reservoir simulation as a basis for field development and management. This paper will focus on our research efforts towards the simulation of enhanced geothermal reservoir systems with multiphase fluids.

PANDAS/ThermoFluid

PANDAS (Parallel Adaptive Nonlinear Deformation Analysis Software) is a modular system of finite element method based modules. Currently, it includes the following four key components:

- ESyS_Crustal for the interacting fault system simulation;
- PANDAS/Fluid for simulating the fluid flow in fractured porous media;
- PANDAS/Thermo for the thermal analysis of metals and fractured porous media;

- PANDAS/Pre and PANDAS/Post for conceptual modeling, mesh generation and visualization.

All of the above modules can be used individually or together to simulate the phenomena such as interacting fault system dynamics, heat flow and fluid flow with or without coupling effects.

PANDAS/ThermoFluid (the fully coupled modules of PANDAS/Thermo and PANDAS/Fluid) is a finite element method based module for simulating the fluid and heat flow in a fractured porous media by solving the conservation equations of macroscopic properties numerically.

The mass and energy conservation equations for transient two-phase water/steam coupled heat/fluid flow in porous medium used in PANDAS are given in Equations (1) and (2):

$$\frac{\partial}{\partial t} [\phi(S_w \rho_w + S_s \rho_s)] = \nabla \cdot [\rho_w \frac{Kk_{rw}}{\mu_w} (\nabla P_w - \rho_w g \nabla Z)] + \nabla \cdot [\rho_s \frac{Kk_{rs}}{\mu_s} (\nabla P_s - \rho_s g \nabla Z)] + q_m \quad (1)$$

$$\frac{\partial}{\partial t} [\phi(S_w \rho_w u_w + S_s \rho_s u_s) + (1 - \phi) \rho_r c_r] = \nabla \cdot [\rho_w h_w \frac{Kk_{rw}}{\mu_w} (\nabla P_w - \rho_w g \nabla Z)] + \nabla \cdot [\rho_s h_s \frac{Kk_{rs}}{\mu_s} (\nabla P_s - \rho_s g \nabla Z)] + \nabla \cdot (\lambda \nabla T) + q_e \quad (2)$$

To complete the governing equations, it is assumed that Darcy's Law applies to the movement of each phase (momentum balance):

$$\mathbf{v}_w = \frac{Kk_{rw}}{\mu_w} (\nabla P_w - \rho_w g \nabla Z) \quad (3)$$

$$\mathbf{v}_s = \frac{Kk_{rs}}{\mu_s} (\nabla P_s - \rho_s g \nabla Z) \quad (4)$$

where P is fluid pressure [Pa]; ϕ is the porosity; S is the phase saturation, with $S_w + S_s = 1$; ρ is the density [kg/m^3]; K is the intrinsic permeability tensor of the porous medium [m^2], k_r is the relative permeability of the phase; μ is the dynamic viscosity [$\text{kg/m}\cdot\text{s}$]; g is gravity, Z is the depth; u and h are specific internal energy and specific enthalpy respectively [kJ/kg]; λ is the thermal conductivity tensor of the porous medium [$\text{W/m}\cdot\text{K}$]; T is temperature [$^\circ\text{C}$]; q_m and q_e are source/sink terms of the total mass and energy respectively [$\text{kg/m}^3\cdot\text{s}$, $\text{kJ/m}^3\cdot\text{s}$]; \mathbf{v} is the fluid velocity vector in [m/s]; the subscript w , s and r denote water, steam phase and rock matrix respectively.

Thermodynamic properties of reservoir fluid s (such as water and CO_2) are of vital importance to understand the subsurface physical-chemical and

geological processes. The most accepted IAPWS-95 formulation (Wagner & Prub, 2002) for water equation-of-state (EOS) is integrated in our simulator, which allows us to retrieve basic physical parameters such as density and dynamic viscosity, as well as the saturated properties for phase transition modeling. SWEOS, an EOS for CO_2 which was originally developed by Span and Wagner (1996) based on their algorithm of an empirical representation of the fundamental equation of Helmholtz energy, has also been implemented into our simulator to model EGS- CO_2 processes.

For more details of PANDAS, please refer to Xing & Makinouchi (2002), Xing et al. (2006a, b, 2007, 2008, 2010). Model validation of PANDAS/ThermoFluid code is reported in Xing et al. (2008, 2009).

PANDAS/ThermoFluid application in Geotechnical risk assessments for mine developments in geothermal areas

To demonstrate the feasibility and value of multi-phase fluid flow modeling as a pit design tool and for risk analysis of geothermal hazards during mining in hot ground, a numerical model was developed for a gold mine site using the PANDAS/ThermoFluid model code. PANDAS/ThermoFluid was used for simulation of temperature, pressure and steam distribution in the seawall and foundation of the dam along a north-northeast to south-southwest oriented cross section.

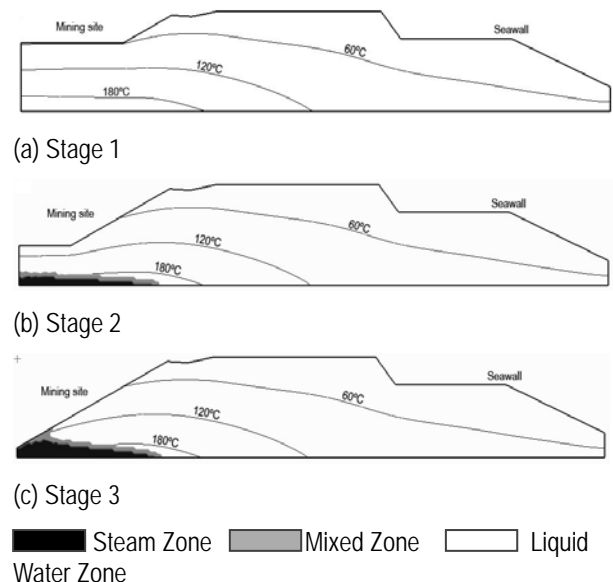


Figure 1: PANDAS/ThermoFluid results of the cross section model of pit excavation for three development stages.

For demonstration purpose, three pit excavation stages were simulated. The first to a depth of 90m, the second reaching the top of the boiling zone at 180m and the third down to 270m below surface.

It was found that after the first stage of excavation to 90m steam did not develop throughout the model domain despite temperatures computed to be partly significant above 100°C. This is due to high hydrostatic pressures preventing water from boiling at this stage. The simulation results for the second and third development stages predicted boiling to occur below the pit floor and in the lower benches of the seawall.

Short-term/long-term modeling of fracture dominated EGS-water and EGS-CO₂

Operating enhanced geothermal systems (EGS) with CO₂ instead of water as a heat transmission fluid is a new attractive concept with several benefits including: The lower viscosity of CO₂ would yield larger flow velocities for a given pressure gradient; less power consumption for fluid circulation systems due to buoyancy effects and geologic storage of greenhouse gases as an ancillary benefit (Brown, 2000, Pruess, 2006). The following section demonstrates simulations using EGS-water and EGS-CO₂ under typical geothermal field situations to compare the efficiency and longevity of both systems as well as the estimation amount of geologic storage of CO₂.

Pruess (2006) has compared the thermodynamic properties of CO₂ and water under typical reservoir conditions. A five-spot well pattern geothermal field was modeled by TOUGH2 (Pruess, 2006) and a series of comparisons between EGS-CO₂ and EGS-water has demonstrated the advantages of using EGS-CO₂ such as the long-term performance (up to 36 years) heat extraction rate, mass flow rate and pressure/temperature field.

In the development of enhanced geothermal systems, greater focus is shifted to the short-term dynamic response of well tests. A number of tests (with or without tracers) need to be run between the injection and production wells before power generation to assess the ability of production and circulation within an EGS. Here, a simplified 500x200m fracture dominated geothermal field (Figure 2) is modeled by PANDAS/ThermoFluid to compare both long-term and short-term performance of EGS-CO₂ and EGS-water.

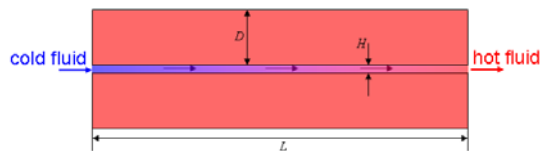


Figure 2: A fracture dominated geothermal field. L=500m, D=100m, H=0.1m. Permeability of the fracture zone is $5 \times 10^{-14} \text{m}^2$. Rock density is $2.65 \times 10^3 \text{kg/m}^3$, specific heat is 1kJ/(kgK) , thermal conductivity is 2.1W/(mK) . Initial temperature of entire region is 250°C , the Injection fluid is 90°C .

Figure 3 shows the fluid velocity evolution at an early stage of the well test. With the same pressure drop between injection well and production well, CO₂ has higher flow rates than water ($2.5 \times 10^{-3} \text{m/s}$ for CO₂ to $8.7 \times 10^{-4} \text{m/s}$ for water at its stable stage). It can also be seen that CO₂ takes about 81 hours to reach the stable state, while water takes less than 50 hours. The reason for the longer stabilization time for CO₂ is because it has a larger ratio of fluid density to viscosity (Pruess, 2006) and a larger compressibility (about 8 times of water) than water under reservoir pressure/temperatures.

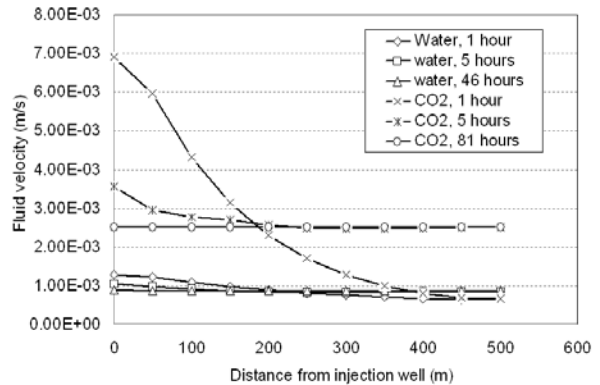


Figure 3: Fluid velocity evolution at early stage of well test. Injection well pressure is 44MPa, constant pressure drop of 10MPa is set between the injection well and production well.

Figure 4 shows a long term temperature distribution along the fracture zone. For this particular case, it takes less than 10 years for EGS-CO₂ to reduce temperature within the entire region to under 200°C, while EGS-water requires more than 20 years before temperature drops to 200°C. This is due to CO₂'s higher heat extraction rate which was suggested by Pruess (2006).

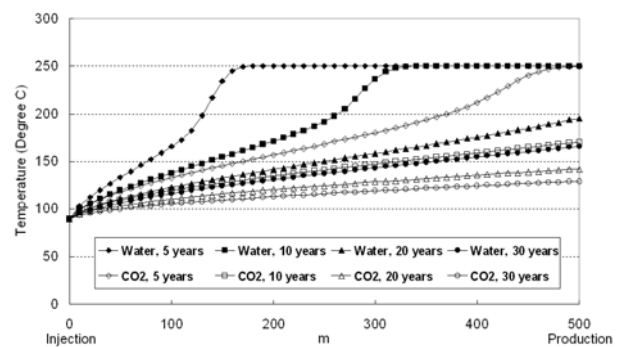


Figure 4: Comparison of fracture zone temperature at different years. Constant pressure drop of 10MPa is set between the injection well and production well. With the fracture space of 100m, flow rate for water and CO₂ are 7.3kg/s and 10.8kg/s, respectively.

Conclusions

Computer modeling of geothermal systems has been widely used in industry. Further computational modeling and code development is urgently needed to improve our understanding of

geothermal reservoir and the relevant nature. It is also needed for the enhanced evolution such as of enhanced geothermal reservoir system, and achieves a more accurate and comprehensive representation of reservoir processes in more details. It also helps to reduce the uncertainties in models, and to enhance the practical utility and reliability of reservoir simulation as a basis for field development and management. This paper introduced a simulator 'PANDAS/ThermoFluid' to model the transient, non-isothermal, multiphase fluid flow in heterogeneous fractured-matrix formations for simulating geothermal well and reservoir performance. It was applied for use in a geotechnical risk assessment of an open pit mining site situated in hot ground. As well as to look at short-term/long-term modeling of fracture dominated enhanced geothermal systems (EGS) with water and CO₂ as heat transmission fluids, PANDAS/ThermoFluid has proven to be a valuable tool to support the development and implementation of geothermal risk management strategies to combat geothermal hazards. Results also show its efficiency and usefulness in simulating both conventional geothermal fields and enhanced geothermal systems with multiphase fluids.

Acknowledgements

Support is gratefully acknowledged by the Australian Research Council and Geodynamics Limited through the ARC Linkage project LP0560932.

References

Brown, D.W., 2000, A Hot Dry Rock geothermal energy concept utilizing supercritical CO₂ instead of water: Proceedings of the Twenty-Fifth Workshop on Geothermal Reservoir Engineering, p. 233–238.

Pruess K., and Narasimhan T. N., 1985, A Practical Method for Modeling Fluid and Heat Flow in Fractured Porous Media: Society of Petroleum Engineers Journal, v. 25, no. 1, p. 14-26.

Pruess K., 2006, Enhanced geothermal systems (EGS) using CO₂ as working fluid - A novel approach for generating renewable energy with simultaneous sequestration of carbon:

Geothermics, v. 35, p. 351–367.

Span, R., and Wagner, W., 1996, A new equation of state for carbon dioxide covering the fluid region from the triple-point temperature to 1100K at pressures up to 800 MPa: Journal of Physical and Chemical Reference Data, v. 25, no. 6, p. 1509–1596.

Wagner W., and Pruett, A., 2002, The IAPWS for the thermodynamic properties of ordinary water substance for general and scientific use: Journal of Physical and Chemical Reference Data, v. 31, no. 2, p. 387–535.

Warren, J. E., and Root, P. J., 1963, The behavior of naturally fractured reservoirs: SPE J., v. 3, p. 245-255.

Xing, H.L., and Makinouchi, A., 2002, Three dimensional finite element modeling of thermomechanical frictional contact between finite deformation bodies using R-minimum strategy: Computer Methods in Applied Mechanics and Engineering, v. 191, p. 4193-4214.

Xing, H.L., Mora, P., and Makinouchi, A., 2006a, A unified frictional description and its application to the simulation of frictional instability using the finite element method: Philosophical Magazine, v. 86, no. 21-22, p. 3453-3475.

Xing, H.L., Mora, P., 2006b, Construction of an intraplate fault system model of South Australia, and simulation tool for the iSERVO institute seed project: Pure and Applied Geophysics, v. 163, p. 2297-2316. DOI 10.1007/s00024-006-0127-x.

Xing, H.L., Makinouchi, A. and Mora, P., 2007, Finite element modeling of interacting fault system: Physics of the Earth and Planetary Interiors, v. 163, p. 106-121. doi:10.1016/j.pepi.2007.05.006.

Xing, H.L. 2008, Progress Report: Supercomputer Simulation of Hot Fractured Rock Geothermal Reservoir Systems: ESSCC/ACCeSS Technical Report, The University of Queensland, p.1-48.

Xing, H.L., Gao J., Zhang J. and Liu Y., 2010, Towards An Integrated Simulator For Enhanced Geothermal Reservoirs: Proceedings World Geothermal Congress 2010. Bali, Indonesia, 25-29 April 2010.

Development of Hydraulic Fractures and Conductivity near a Wellbore

Xi Zhang and Robert G. Jeffrey*

CSIRO Earth Science and Resource Engineering, Melbourne VIC, Australia

ABSTRACT

Hydraulic fractures play an important role in establishing a high conductive pathway connecting the wellbore and reservoir. The near-wellbore fracture development is crucial to the efficiency of a fracture treatment as a smooth fracture path will reduce the flow impedance. A numerical model is used to simulate the propagation pathways followed by hydraulic fractures, in the presence of a pressurised well and natural fractures. By including the coupling of viscous fluid flow and rock deformation in the analysis, we find that the non-uniform pressure distribution along the fractures and the removal of near-well fracture closure result in growth of a fracture with less curvature (a measure of tortuosity) in its path. Moreover, the fracture curvature can be characterised by two dimensionless parameters. If multiple fracture sets coexist, fracture linkage is possible due to mechanical interaction between fractures, pre-existing natural fractures and the wellbore. Natural fractures can alter the hydraulic fracture propagation direction, can offset the fracture path and can provide sites for new fracture growth. In the case of two hydraulic fractures initially growing in opposite directions from the wellbore, the interaction with a natural fracture on one side of the well will result in the other fracture wing propagating faster. The complexity of the near-wellbore fracture geometry can be studied with the aid of our numerical model.

Keywords: Near-well fracture tortuosity, coupling mechanisms, naturally fractured reservoir, numerical modelling

INTRODUCTION

Multiple sub-parallel fractures can be generated near the wellbore because of fracture initiation from perforations spaced along and phased around the wellbore or from natural fractures and flaws that are usually not aligned with the far-field stress direction. Fractures initiated from these defects will reorient themselves to a plane perpendicular to the minimum far-field stress direction as they grow away from the wellbore. The overall result of such a fracture initiation process produces near-wellbore fracture tortuosity. As a consequence, the net pressure required to extend the fractures is increased considerably. Because of its importance to optimisation of fracture treatments, the study on this subject has continued for several decades

(Hamison and Fairhurst, 1970; Daneshy, 1973; Weng, 1993; Soliman et al. 2008; Cherny et al. 2009).

Geomechanical models are of significant value in treating the sorts of problems that relate to competing fracture growth, including local width restrictions and increased viscous frictional pressure loss. Based on such geomechanical analyses, various operational remedial techniques have been proposed to overcome or avoid the near-wellbore effects, such as using higher injection rates, higher viscosity fluids and orienting slots or perforations for fracture reinitiation (Manrique and Venkitaraman, 2001; Abass, et al., 2009). However, most studies were based on the uniform pressurization assumption so that the fracture problem can be treated by conventional fracture mechanics methods. In particular, the fracture turning processes, during which the fracture reorients as it grows from a wellbore to become perpendicular to the minimum principal stress direction, involves viscous fluid flow and frictional slip. In addition, a moving boundary exists associated with both the fluid flow and the fracture tip. These aspects of the problem increase its complexity, but must be included in any realistic model.

In this paper, we will employ a 2D numerical method that can model hydraulic fracture growth from a borehole. The 2D plane strain assumption is justified if the height of a slot or natural flaw is large compared to the well radius. Moreover, the method can directly cope with the fracture interaction with the wellbore and natural fractures. Although the thermal effect is not yet considered, the results provide insights into fracture development around the wellbore in a hot dry rock reservoir.

PROBLEM STATEMENTS

The properties used in the model for the rock, fluid and fractures are as follows. The elastic properties for the intact rock are Young's modulus (E), Poisson's ratio (ν) and the Mode I fracture toughness is K_{IC} . The injected fluid is incompressible and has a Newtonian viscosity given by μ . The sum of all injection rates of fracture branches growing from the well is assumed to be constant and is denoted as Q_{in} . It must be noted that the injected fluid rate into each fracture varies in time because of the different growth rates of each fracture. The total rate

injected, Q_{in} , is specified as constant and represents the rate fluid is injected into the well. In addition, the volume change (compressibility) of the borehole fluid and rock system is not accounted for in determining the injection rate.

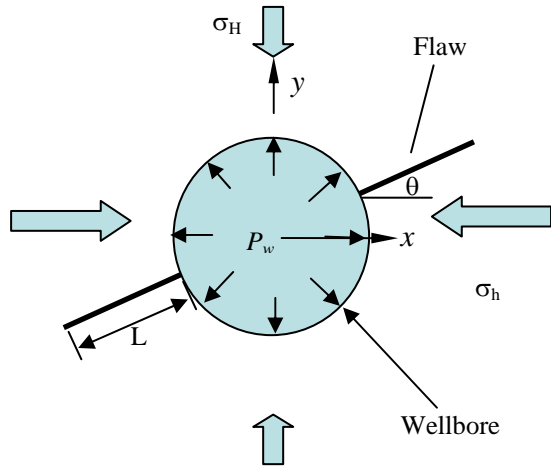


Figure 1 Fractures around a wellbore, in-situ stress and coordinate system. The origin of the coordinate system is at the wellbore centre.

The two sides of a fracture may come into contact, especially near the wellbore. The model allows for contact stresses to develop and uses a cohesionless Coulomb friction criterion for slip on surfaces in contact

$$|\tau| \leq \lambda(\sigma_n - p_f) \quad (1)$$

where τ is the shear stress along the closed fractures, σ_n is the normal stress acting across them, p_f is the fluid pressure and λ is the coefficient of friction.

In addition to the tangential displacement discontinuity (DD), v , associated with slip along the closed fracture segments, there exists opening displacement w along the opened hydraulic fractures, which contributes to fracture conductivity. All of these elastic displacements give rise to changes in the rock stress or changes in the tractions acting along the fracture surfaces. The governing equations for stresses, fluid pressure and displacements are given in Zhang et al. (2007, 2009), and are given in terms of Green's functions. We employ the displacement discontinuity method (DDM) for the simulation of rock deformation in a 2D homogeneous and isotropic elastic material, on which a uniform stress is applied at infinity.

The governing equations for fluid flow in the fracture channel are given by Zhang et al. (2009). There are two type of fluid migration along fractures. The fluid not only can diffuse along the closed fractures without any mechanical opening of the fracture, but also can flow through an open channel as a result of opening mode hydraulic

fracturing processes. In the latter case, the fluid pressure is balanced by the compressive stress caused by rock elastic deformation, that is, $\sigma_n = p_f$. We use Reynolds' equation to describe fluid movement inside the opened hydraulic fractures:

$$\frac{\partial(w + \varpi)}{\partial t} = \frac{\partial}{\partial s} \left[\frac{(w + \varpi)^3}{\mu'} \frac{\partial p_f}{\partial s} \right] \quad (2)$$

where w is the mechanical opening and vanishes for the closed segments, ϖ is the pre-existing hydraulic aperture arising from surface roughness and microstructures and $\mu' = 12\mu$.

However, it must be mentioned that effective stress changes in the fluid-infiltrated and pressurised fracture portion can produce changes of the hydraulic aperture without fully opening a fracture. The dilatation can slightly affect the internal pressure distributions since the resulting fluid conductivity varies in location and time. As stated above, the hydraulic aperture at the beginning is assigned an initial value w_0 for each closed fracture segment. The evolution of w_0 obeys a nonlinear spring model in response to any increments of the internal pressure. In particular, an equation governing the hydraulic aperture change associated with pressure change is given as follows,

$$d\varpi / dP_f = \chi\varpi \quad (3)$$

where χ is a small constant with a value of 10^{-8} per Pa in the model. A pressure diffusion equation is applied to calculate the fluid flow inside a closed natural fracture (Zhang et al., 2009)

$$\frac{\partial p_f}{\partial t} - c \frac{\partial}{\partial s} \left(\varpi^2 \frac{\partial p_f}{\partial s} \right) = 0 \quad (4)$$

where $c = 1/(12\chi\mu)$. This calculation applies to all closed portions of fractures, whether they are undergoing or have undergone slip or not.

To complete the problem formulation, we need boundary and initial conditions for the above governing equations. Initially, all fracture segments are assumed to be evacuated and the rock mass is stationary. Rock failure criterion will be given below, as well as the method used for handling fracture intersection and associated flux redistribution. For the fractures connected to the borehole, the sum of the fluid flux entering them is equal to the injection rate, that is,

$$\sum_{i=1}^N q_i(0, t) = Q_{in} \quad (5)$$

where N is the number of fractures and q_i the

fluid volumetric flux into fracture i .

At the fracture tip, the opening and shearing DDs are zero, that is,

$$w(l) = v(l) = 0 \quad (6)$$

and the fracture opening profile near the crack tip possesses a square root shape with distance from the tip as predicted by Linear Elastic Fracture Mechanics (LEFM) theory.

When the stress intensity factor at the fracture tip reaches the fracture toughness of the rock, fracture growth occurs. In general, the fracture propagation direction may change as dictated by the near-tip stress field characterised by the Stress Intensity Factors (SIFs). In particular, the mixed-mode fracture criterion is used for determining fracture growth in the model. This same approach has been used by a number of researchers (e.g. Mogilevskaya et al., 2000).

The coupled fluid flow (to obtain pressure) and rock deformation (to obtain fracture opening) problem is solved in an implicit manner by incorporating the elasticity equation into the Reynolds' equation. The responses obtained are history dependent because of the irreversible fluid flow and frictional sliding processes. Additionally, there are three moving fronts inherent in the problem, namely the slip front, the fluid front and the fracture opening (crack tip) front. The reader is referred to Zhang et al. (2007, 2009) for a detailed description of the numerical solution methods applied in modelling these processes. At the borehole, the fracture entry pressures must be equal to the borehole pressure. This condition is enforced through an iteration scheme. The fracture entry and borehole pressures are constrained to be equal by enforcing Eq. (5). The injection rate into each fracture is found based on the specified current borehole pressure, using the method described in our previous work applied to fracture junctions (Zhang et al., 2007). In the calculation, the convergence of the solution is very sensitive to the time step and the convergence error tolerance. To rapidly find a converged wellbore pressure, a relaxation factor is used in updating the borehole pressure at each iteration step. A tolerance ($< 10^{-4}$) is set for the relative error between the wellbore and fracture entry pressures. Therefore, in the program, a new iteration loop is introduced for obtaining a converged borehole and fracture entry pressure solution.

The numerical method has been verified, in our previous papers, by comparison to published solutions to a range of problems; see Zhang et al. (2009). However, to treat problems that include a borehole, the program was modified to allow correct treatment of the interior and exterior problems generated when the borehole is discretised using the DD (Displacement

Discontinuity) method. Discretising the well bore using conventional DD elements results in the formation of a disc of rock inside the wellbore, which can move rigidly. It must be mentioned that the resulting DDs along the wellbore boundary are fictitious although they are necessary for calculating pressure and displacement at the borehole wall and along the fractures. The fictitious DDs do not have a literal physical interpretation as DDs, but rather are needed to obtain the stress and displacement everywhere in the exterior part of the problem. Moreover, since the interior disc is free to move as a rigid body, the direct use of a conventional DDM is not possible without suppressing the rigid-body motion of this disc.

A simple method to suppress the rigid-body motions is as follows. Two additional elements are defined inside the borehole and assigned fictitious DDs. Then we calculate the displacement on the negative side of an element based on the fundamental elastic solutions. After that the four displacements at these two additional elements are set to zero, in order to construct a closed, well-posed problem for all DDs. The displacements on the negative side of the elements are given as Eq. (5.6.1) in Crouch and Starfield (1983) for both normal and tangential displacement components.

The elasticity equations for the normal and tangential DDs (Δu_k includes w and v .) at the middle of each element along the borehole and the fractures and for the two additional elements are, respectively,

$$K_{ijk} \Delta u_k = P_f \delta_{ij} - \sigma_{ij}^{\infty} \quad k = n, s \quad (7)$$

$$M_{ijk} \Delta u_k = 0 \quad k = n, s \quad (8)$$

where K_{ijk} and M_{ijk} are the coefficient matrices derived from the fundamental elastic solution as is done in conventional boundary element methods (see details in Crouch and Starfield, 1983); and σ_{ij}^{∞} are the resultant stresses along the fracture surface arising from far-field (in situ) stresses.

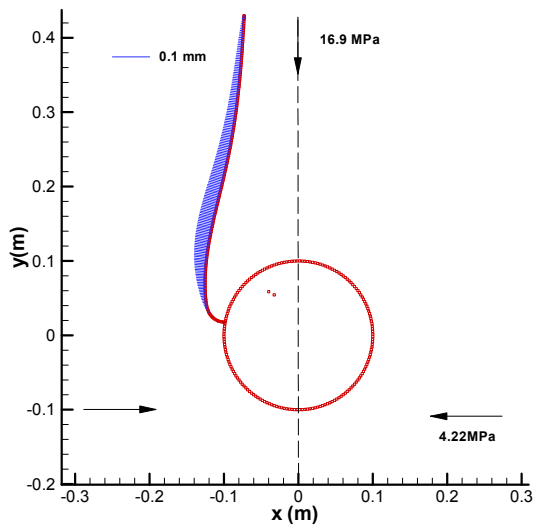
The above first equation enforces equilibrium at DD elements along the fractures and the wellbore, and the second one enforces the constraint that eliminates rigid body motion of the interior disc by requiring zero displacements at two additional interior elements. The above simultaneous equations (Eqns (7) and (8)) are solved for normal and shear DDs of all elements along the borehole, the fractures and of the two additional elements, once the fluid pressure is known. The DDs that are obtained can then be used to calculate stress or displacement at any other point inside the rock mass.

NUMERICAL RESULTS

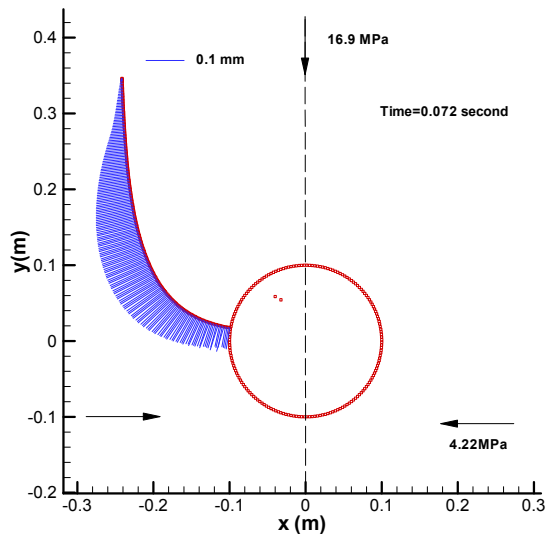
Single hydraulic fracture

We first compare the opening and path for a hydraulic fracture driven by a uniform pressure or by injection of a viscous fluid. A uniform pressure condition in a hydraulic fracture is equivalent to using an inviscid fluid (Detournay, 2004). The pressure magnitude is adjusted at each fracture growth step to satisfy the fracture extension criterion at the fracture tip. Fracture reorientation is clearly shown in Fig. 2 for both uniformly pressurised and viscous fluid flow cases. For zero viscosity fluids as shown in Fig. 2(a), the portion adjacent to the well wall is in contact. In this region, fluid flow will be restricted and frictional slip condition must be imposed. For generality of results, Mogil evskaya et al. (2000) showed that the fracture path is controlled by the following dimensionless parameter,

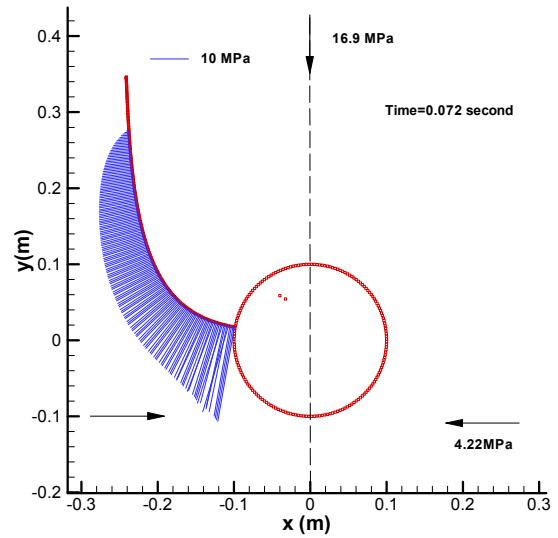
$$\beta = \frac{(\sigma_H - \sigma_h)\sqrt{R}}{K_{IC}} \quad (9)$$



(a)



(b)



(c)

Figure 2 Fracture trajectory, opening DD for uniformly pressurised fractures (a); opening DD (b) and internal fluid pressure (c) for fluid-driven fracture growth in the case of the borehole radius =0.1 m and crack starting angle of 170 degree.

If the fluid viscosity is 0.01 Pa s and the injection rate is specified as 0.0004 m²/s, the fracture pathway and associated opening DD and pressure distributions are given in Figs. 2(b) and (c). The fracture closure does not appear in this case, but a high fluid pressure results as the fluid enters the narrow fracture and opens it again at the higher normal stresses acting along its near well extent Fig. 2(c). Moreover, a fluid lag zone develops when viscous dissipation cannot be neglected and is represented in Fig. 2(c) as the unpressurised region of the fracture near the tip. This is one manifestation of the coupled flow and deformation process interacting with a moving boundary.

To characterize the effect of fluid viscous dissipation on fracture paths, we introduce another parameter which provides an apparent fracture toughness arising from viscous dissipation, as given in Jeffrey(1989), based on an earlier somewhat different formulation given by Settari and Price (1984), and as given by Detournay (2004) in the case of zero lag. This apparent toughness, when substituted for the rock fracture toughness in Eqn. 9 provides a dimensionless parameter, given by Eqn. 10, that we hypothesize will control the curving of a viscosity dominated hydraulic fracture growing from a wellbore (Zhang et al. 2010),

$$\chi_F = \frac{(\sigma_H - \sigma_h)\sqrt{R}}{(\mu' Q_{in} E'^3)^{1/4}} \quad (10)$$

where E' is the plane-strain modulus. In this formula, the product of injection rate Q_{in} and fluid

viscosity μ are parameters that can be controlled by a fracturing engineer.

The above two parameters given by Eqs. (9) and (10) can fully characterise the fracture path and related pressure evolution for a single hydraulic fracture growing from a wellbore. Zhang et al. (2010) provide numerical examples demonstrating that these parameters control the curvature in the hydraulic fracture path as it grows from an uncased wellbore.

Two winged hydraulic fractures

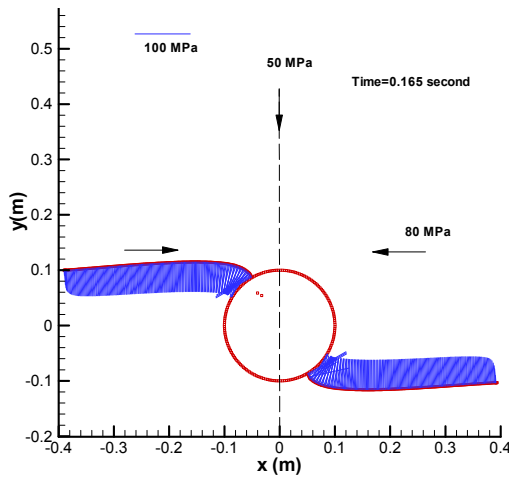


Figure 3 A pair of fractures growing from a wellbore: fracture trajectory and internal fluid pressure for high-angle fracture initiation. The fluid viscosity is 0.01 Pa s and the injection rate is specified as 0.0004 m²/s.

We next consider two fractures that grow simultaneously to form a single bi-wing fracture geometry as shown in Fig. 3. The pressure loss near the wellbore wall is less evident and fracture rotation to align with the maximum principal stress occurs in a very smooth way. This symmetric geometry is found in many field observations as described by Wen g (199 3) and Cherny et al. (2009).

Multiple hydraulic fractures

The more complicated initial condition consisting of six starter fractures that are arranged around the wellbore is considered next. The starter fractures have an uneven angular distribution to the x-axis of 30°, 120°, 150°, 210°, 240° and 330°, as shown in Fig. 4. The fractures at angles of 120° and 240° are in a more compressive initial stress state, which causes their growth to be completely suppressed compared with other four fractures. The remaining four starter fractures are all subjected to the same stress levels, except for the shear stress directions. The fracture at angle 150° is can extend more easily because it has a slightly longer initial fracture length. As the fractures grow and turn to align with the horizontal x direction, the fractures at the angle of 150° and 330° become more dominant and form a bi-wing fracture configuration. However, the other two

fractures at angle 30° and 210°, do extend but to a shorter distance. These two fractures propagate towards the longer fractures after leaving the influence region around the borehole and a sharp kink is evident in Fig. 4. The tendency for fracture linkage is also clear. The slowly growing and partially suppressed fractures propagate towards the dominant growing fractures and may link-up with them as previously found by Wen g (199 3). These results suggest that initiation of several fractures from a wellbore subject to a larger stress ratio favours interactions leading to link-ups as argued by Daneshy (1973).

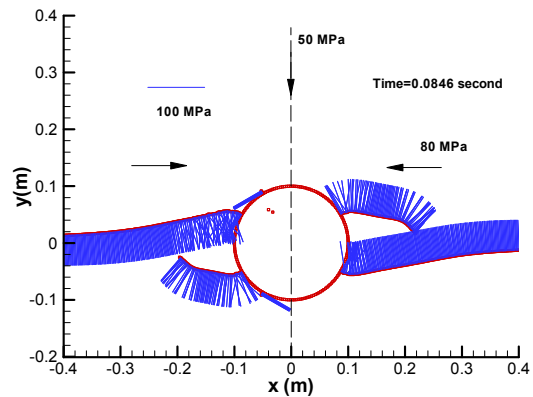
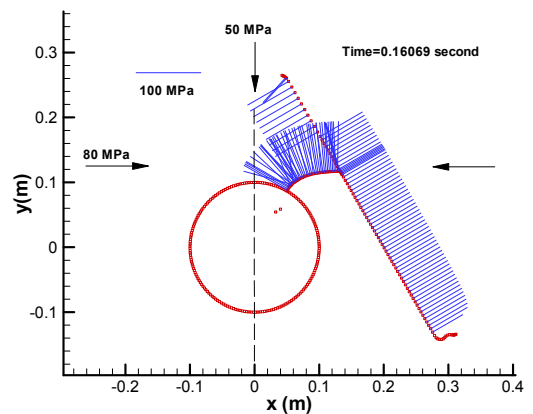


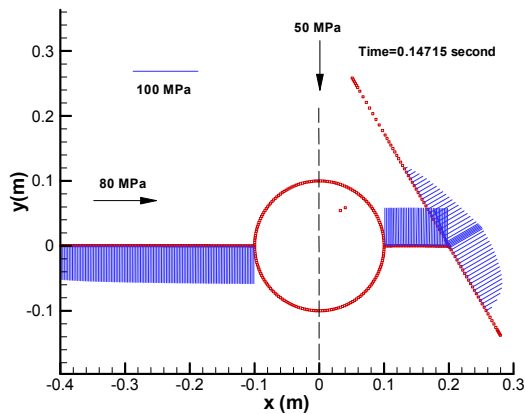
Figure 4 Fracture trajectory and internal fluid pressure in the presence of six initial flaws around the wellbore, where the fluid viscosity is 0.005 Pa s and the injection rate is specified as 0.0012 m²/s. The flaw alignment angles are 30°, 120°, 150°, 210°, 240° and 330°.

Effects of natural fractures

If there is a natural fracture in the fracture propagation pathway, fluid will enter it after a hydraulic fracture intersects it. The existence of natural fracture will affect the growth of the hydraulic fracture and the inflation of the natural fracture caused by the fluid pressure can induce slip along the natural fracture and fracture reinitiation from the ends of a finite-size natural fracture. The example fracture geometry is given in Fig. 5(a).



(a)



(b)

Figure 5 Fracture trajectory and internal fluid pressure in the presence of a natural fracture that has finite length and an inclination angle of 135 degree with respect to the x-axis. The coefficient of friction of the natural fracture is 0.3. The fluid viscosity is 0.01 Pa s and the injection rate is specified as 0.0004 m²/s.

The arrest of one fracture will facilitate the propagation of a second wing of a two-winged fracture, as shown in Fig. 5(b). The left-hand side fracture propagates at a lower pressure, taking most of injected fluid and growing much faster.

References

- Abass, H. H., Soliman, M. Y., Tahini, A. M., Surjaatmadja, J., Meadows, D. L., Sierra, L., 2009, Oriented fracturing: A new technology to hydraulically fracture openhole horizontal well, SPE 124483, Proceedings of the 2009 SPE Annual Technical Conference and Exhibition, New Orleans, Louisiana, October 4-7 2009
- Cherny, S., Chirkov, D., Lapin, V., Muranov, A., Bannkov, D., Miller, M., Willberg, D., Medvedev, O. and Alekseev, O., 2009, Two-dimensional modelling of the near-well bore fracture tortuosity effect, *Int. J. Rock Mech. & Mining Sci.* 46, p. 992-1000.
- Crouch, S. L. and Starfield, A. M., 1990, *Boundary Element Method in Solid Mechanics*, Unwin Hyman, Boston
- Daneshy, A. A., 1973, A study of inclined hydraulic fractures, *SPE J* 13: p. 61-68.
- Detournay, E., 2004, Propagation regime of fluid-driven fractures in impermeable rocks, *Int. J. Geomechanics* 4, p. 35-45.
- Detournay, E. and Jeffrey, R., 1986, Stress conditions for initiation of secondary fractures from a fractured borehole, proceedings of the international symposium on rock stress and rock stress measurements, Stockholm, Sweden, 1-3, September, 1986.
- Hamison, B. and Fairhurst C., 1970 In-situ stress determination at great depth by means of hydraulic fracturing, in *Rock Mechanics—Theory and Practice*, (ed.) W. H. Somerton, Am. Inst. Mining Engrg., 559–584, 1970
- Jeffrey, R. G., 1989 The combined effect of fluid lag and fracture toughness on hydraulic fracture propagation, SPE 18957, Proceedings of SPE Joint Rocky Mountain Regional/ Low Permeability Reservoirs Symposium and Exhibition, Denver, Colorado, March 6-8, 1989.
- Manrique, J. F. and Venkataraman, A., 2001, Oriented fracturing – A practical technique for production optimization, Proceedings of the 2001 SPE Annual Technical Conference and Exhibition held in New Orleans, Louisiana, 30 September–3 October 2001
- Mogilevskaya, S. G., Rothenburg, L. and Dusseault, M. B., 2000, Growth of pressure-reduced fractures in the vicinity of a wellbore, *International Journal of Fracture* 104, p. L25-L30.
- Settari, A. and H. S. Prince., 1984, Simulation of hydraulic fracturing in low-permeability reservoirs, *SPEJ* April 1984, p. 141-152.
- Soliman, M. Y., East, L. and Adams, D., 2008, Geomechanics aspects of multiple fracturing of horizontal and vertical wells, SPE 86889, *SPE Drilling and Completion*, Sept. 2008, 217-228.
- Weng, X., 1993, Fracture Initiation and Propagation from Deviated Wellbores, SPE 26597, presented at the 1993 ATCE, Houston, TX, 3-6 October, 1993.
- Zhang, X. Jeffrey, R. G. and Thiercelin, M., 2007, Deflection of fluid-driven fractures at bedding interfaces: A numerical investigation, *J. Structural Geology* 29, p. 396-410.
- Zhang, X. Jeffrey, R. G. and Thiercelin, M., 2009, Mechanics of fluid-driven fracture growth in naturally fractured reservoirs with simple network geometries, *J. Geophysical Research -Solid Earth*, 114, B12406.
- Zhang, X. Jeffrey, R.G., Bunger, A.P. and Thiercelin, M., 2010 Initiation and growth of a hydraulic fracture from a borehole under toughness- or viscosity-dominated conditions, 44th US Rock Mechanics Symposium and 5th U.S.-Canada Rock Mechanics Symposium, Salt Lake City, UT June 27–30, 2010.

Economics of geothermal feedwater heating for steam Rankine cycles

David L. Battye*, Peter J. Ashman, Gus J. Nathan
 Centre for Energy Technology
 University of Adelaide, SA 5005.

* Corresponding author: david.battye@adelaide.edu.au

We have investigated the economics of geothermal feedwater heating (GFWH) in a steam Rankine cycle with base capacity of 583 MW (gross). The capital cost per kW geothermal power (before geofluid pumping) is compared with those of stand-alone geothermal plants of equal power. The economic benefits of GFWH over stand-alone plants for enhanced geothermal systems are, in order of importance:

- 67% less operating and maintenance cost
- 28% less capital cost
- 30-35% less geofluid pumping loads

The reduction in levelised geothermal energy cost is estimated to be 48%.

Keywords: geothermal power, cost, economics, hybrid.

Introduction

In steam Rankine cycles, boiler feedwater must be heated from a low temperature at the condenser outlet (typically ~40 °C) to temperatures of typically 250 °C before entering the boiler. In “regenerative” steam cycles, this is accomplished in a series of feedwater heaters, which use steam extracted from various stages in the turbine. One feedwater heater is a deaerator, in which extracted steam and feedwater are in direct contact, liberating oxygen and other gases in the feedwater for venting to atmosphere. The other feedwater heaters are shell-and-tube heat exchangers where feedwater flows in the tubes and steam condenses on the outside.

If feedwater heating can be accomplished using geothermal heat, the steam normally extracted for feedwater heating can instead generate power in the turbine. The extra power generated by geothermal feedwater heating (GFWH) offers the following potential benefits:

- Existing plants may be retrofitted to accommodate a proportion of geothermal power
- Geothermal power may be generated more cheaply than in a stand-alone plant
- Steam cycles may be adapted for GFWH with no novel technology required.

GFWH is suitable for coal, gas, solar-thermal and nuclear-fuelled boiler plants, but not combined-cycle gas turbine plants. The latter plants use hot exhaust gas for feedwater heating in the Rankine cycle section.

Interest in geothermal feedwater heating has existed since the 1970s, when it was investigated for application at sites in California and Utah (Parsons, 1978). It has been recently studied by Bruhn (2002), Buchta (2009) and Borsukiewicz-Gozdur (2010). All studies agree that geothermal power generation by GFWH is significantly more efficient thermodynamically than in conventional stand-alone plants. However, to the authors' knowledge, no previous comparison has been reported of the economic benefits of GFWH over stand alone geothermal power generation. We seek to provide such a comparison, specifically with respect to power generation from enhanced geothermal systems.

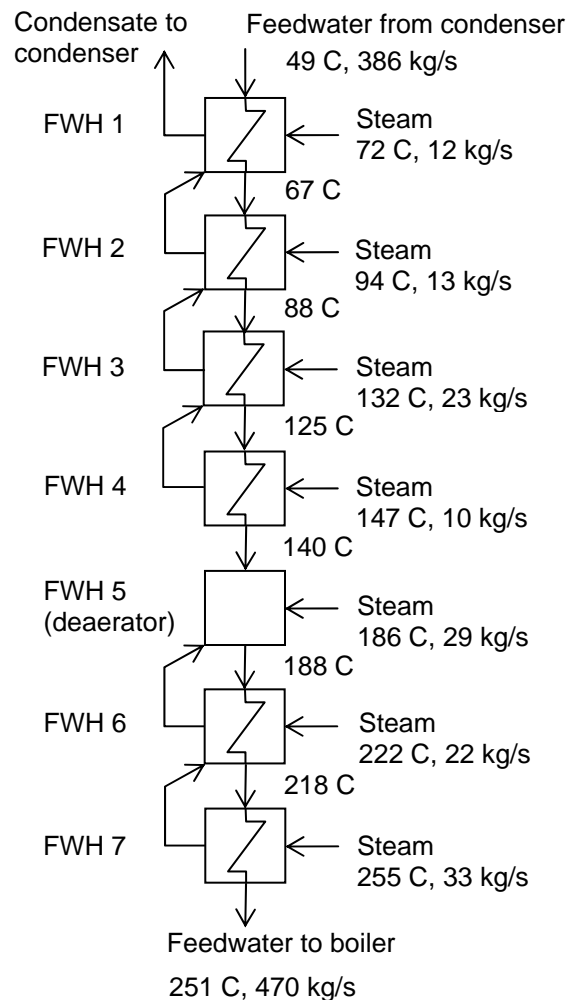


Figure 1: Feedwater heating section in a conventional 583 MW (gross) steam Rankine cycle. Steam flows extracted from turbine stages are shown at right. These steam flows may be replaced by a single flow of hot water from a geothermal reservoir.

Methodology

For our economic analysis we consider the case that GFWH is being used to provide extra capacity for a new Rankine steam cycle plant. This scenario is in contrast to the retrofit of an existing plant, where the capacity is typically fixed.

The basis for analysis is a 583 MW (gross) subcritical steam cycle with single reheat, for which design specifications and cost estimates have been reported (NETL, 2007). A process flow diagram of the feedwater heating section is shown in Figure 1. In the proposed GFWH scenario, feedwater is heated by geofluid instead of steam extracted from turbine stages. The otherwise extracted steam flows are then available for power generation in the turbine.

The temperature to which the feedwater is heated by the geofluid, T_{GFWH} , is a variable in the analysis. Above this temperature, we assume that feedwater heating is achieved by conventional heaters as per normal. However, the deaerator must be retained in the cycle, and may have to operate at higher temperatures than normal. We assume that the upper limit of GFWH input is one where feedwater is heated to 220 °C by geofluid, and a deaerator heats feedwater from 220 °C to 251 °C.

To estimate the increased costs of equipment in GFWH cases, the reported costs of components are increased in proportion to turbine exhaust steam flow (turbine, condenser, steam piping, and cooling system) or gross power (generator, accessory electrical plant, instrumentation and control).

The cost of feedwater heaters (apart from the deaerator) is proportional to the heat transfer surface area, which varies with the overall heat transfer coefficient, U, and mean temperature difference between geofluid and feedwater streams, MTD. We estimate that U is decreased by ~30% in GFWH, since the high film coefficients associated with condensing steam are absent. MTD is about 15 K on average in conventional feedwater heaters. In GFWH cases MTD is a variable. The resulting multiplier applied to the conventional feedwater heater train cost is:

$$f = 1 + \left(\frac{T_{GFWH} - 38}{213} \right) \left(\frac{21}{MTD} - 1 \right)$$

Geofluid costs are estimated assuming:

- Flow of 80 kg/s per well drilled
- Drilling costs vary exponentially with depth according to:

$$C_{drill} = 0.5e^{0.0001491d} \text{ \$M, 2000 US}$$

(Entingh, 2006), where d is depth in feet.

- Other costs (stimulation, geofluid pumps and piping) are 20 % of drilling costs.

Geofluid costs (2009 US dollars) versus geofluid temperature are shown in Figure 2 for thermal gradients of 40 and 50 K/km.

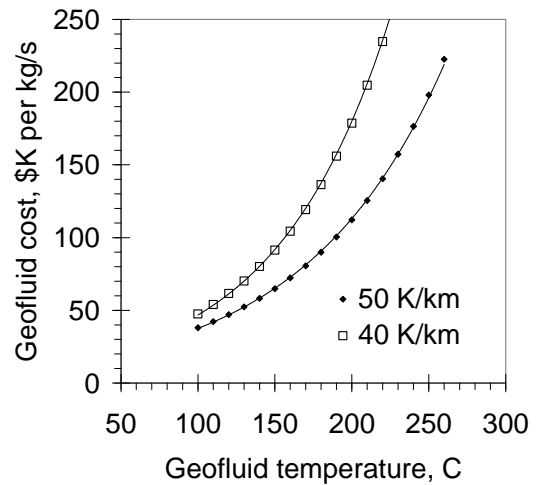


Figure 2: Geofluid cost versus geofluid temperature for thermal gradients of 40 and 50 K/km.

Estimates of the cost and performance of stand-alone geothermal power plants are based on data in the Next Generation Geothermal Power Plants report (Brugman et al., 1995 and CE Holt, 2006) and documentation for the Geothermal Electric Technologies Evaluation Model (GETEM) (Entingh, 2006).

All plants in the analysis are water-cooled and use a cooling tower.

The costs determined from the literature have been updated to 2009 US dollars using the Chemical Engineering Plant Cost Index.

Results and discussion

Figure 3 shows percentage extra gross power and exhaust steam flow versus T_{GFWH} . The effective geothermal power output (before geofluid pumping) ranges from 9.6 MW at 100 °C to 61 MW at 220 °C.

Figure 4 shows the consumption of geofluid per unit geothermal energy generated (net before geofluid pumping) versus geofluid temperature. The GFWH plants require significantly less geofluid than the stand-alone plants, typically 30-35% less above 200 °C. The explanation for this lies in the fact that the GFWH plants minimise thermodynamic inefficiency associated with heat transfer from the geofluid. The lower the MTD, the greater the thermodynamic benefit, but at the expense of higher heat exchanger costs.

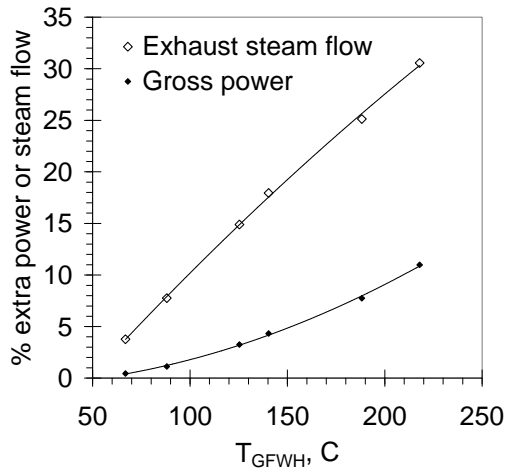


Figure 3: Percentage extra gross power and turbine exhaust steam flow versus geothermal feedwater heating temperature.

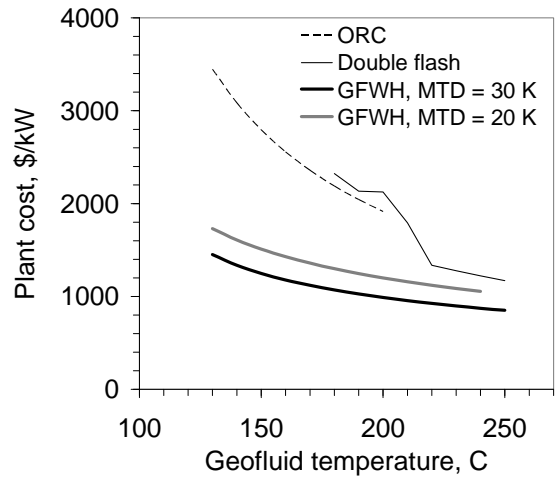


Figure 5: Plant cost versus geofluid temperature for equal power outputs. GFWH plant costs correspond to the increment on base plant cost.

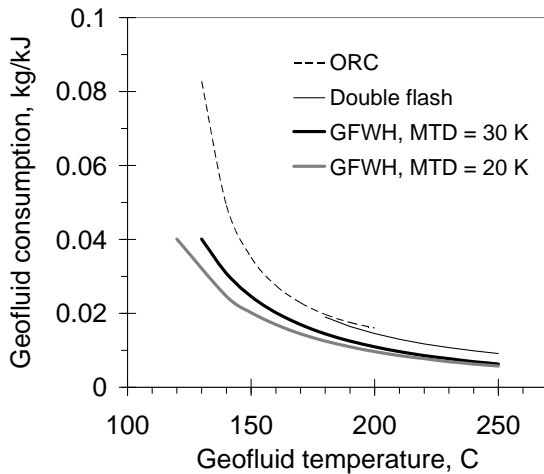


Figure 4: Geofluid consumption per unit geothermal energy generated (net before geofluid pumping) versus geofluid temperature.

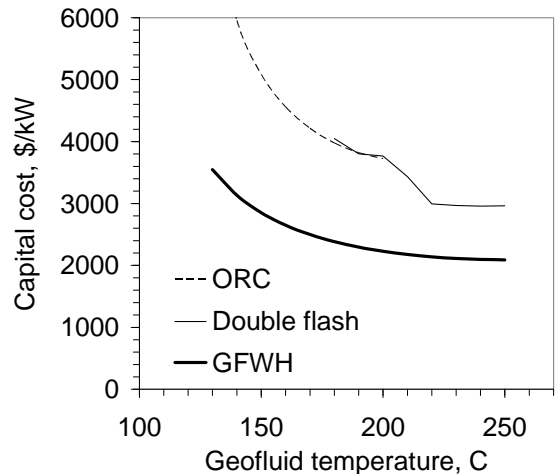


Figure 6: Capital cost versus geofluid temperature for thermal gradient of 50 K/km.

Figure 5 compares plant costs for GFWH and stand-alone plants, ie. Organic Rankine Cycles (ORC) and double flash steam plants. Increasing geofluid temperature reduces the cost of all plants due to improving thermal efficiency. However, the stand-alone plant cost also decreases due to economies of scale. GFWH plant costs correspond to the increment on base plant cost. Since the base plant capacity is already many times greater than for the stand-alone plants, GFWH plant costs are much lower on average over the geofluid temperature range. At the upper geofluid temperatures in Figure 5, the GFWH plant costs are 15-25 % lower than for a double flash plant.

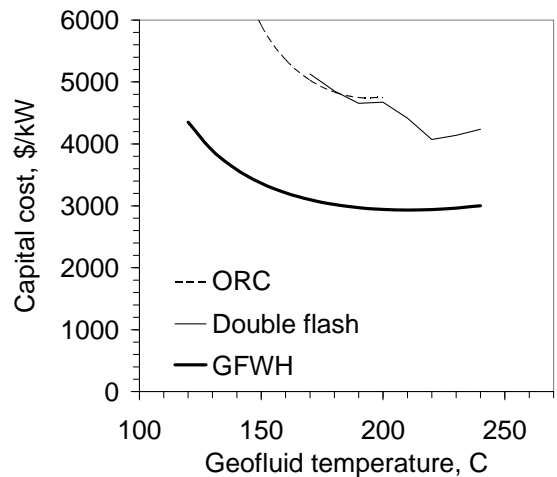


Figure 7: Capital cost versus geofluid temperature for thermal gradient of 40 K/km.

Total capital costs are shown in Figures 6 and 7 for thermal gradients of 50 K/m and 40 K/m respectively. Note that the \$/kW value is for geothermal power before geofluid pumping. The

value of MTD is optimised in each case: 30 K for 50 K/km and 20 K for 40 K/km. The following is observed:

- Optimal geofluid temperatures are 220 °C or greater.
- Optimal GFHW plants reduce total cost by 28% relative to optimal stand-alone plants in both cases.
- GFHW with a 40 K/km thermal gradient can generate power at the same cost as a stand-alone plant with a 50 K/km gradient.
- GFHW can generate power at the same cost as optimal stand-alone plants, but at geofluid temperatures of only 120-150 °C as opposed to 220 °C.

Relative to stand-alone plants, GFHW has the additional benefit of incurring less geofluid pumping power loads, which are not accounted for in the preceding analysis. Since GFHW consumes 30-35 % less geofluid above 200 °C, pumping loads are reduced by the same amount relative to stand-alone plants.

Another economic benefit is that geothermal operating and maintenance costs are drastically reduced by GFHW. For example, O&M costs in a 61 MW stand-alone geothermal plant are estimated at 7.3 \$/M/year (Sanyal, 2004) whereas 61 MW generated by GFHW only incurs 10 % of the annual O&M costs of the whole plant, ie. 2.4 \$/M/year (NETL, 2007), a saving of 67%.

A simple estimate of the reduction in the levelised cost of geothermal energy can be made using figures reported by Sanyal (2007) for EGS power. Table 1 illustrates how the estimate is made and suggests a reduction in total levelised cost approximating 48%.

Table 1: Estimate of reduction in levelised cost of geothermal energy by GFHW, based on estimates of Sanyal (2007) and preceding analysis.

	Levelised cost for stand-alone plant, ¢/kWh (US, 2007)	Reduction by GFHW	GFHW levelised cost, ¢/kWh (US, 2007)
O&M	2.75	1.84 (67%)	0.91
Capital and cost of money	2.68	0.75 (28%)	1.93
Total	5.43	2.59 (48%)	2.84

Concluding remarks

The economic analysis has shown geothermal feedwater heating in a purpose-built steam Rankine cycle to have economic merit. Given that good solar and EGS resources in Australia are generally co-located, solar-geothermal hybrids using GFHW are possible. Further work will investigate the economics of retrofitting existing steam Rankine cycle plants for GFHW.

References

Borsukiewicz-Gozdur, A., 2010, Dual-fluid-hybrid power plant co-powered by low-temperature geothermal water, *Geothermics*, 39, 170-176.

Brugman, J., Hattar, M., Nichols, K. and Esaki, Y., 1995, Next Generation Geothermal Power Plants, Electric Power Research Institute (EPRI) Report No. EPRI/RP 3657-01.

Bruhn, M., 2002, Hybrid geothermal–fossil electricity generation from low enthalpy geothermal resources: geothermal feedwater preheating in conventional power plants, *Energy*, 27, 329–346

Buchta, J., 2009, Green power from conventional steam power plant combined with geothermal well, *Proceedings of the IEEE International Conference on Industrial Technology*, Article No. 4939553.

CE Holt Consulting Firm, 2006, NGGPP process data for binary cycle plants, Document for U.S. Dept. of Energy.

Entingh, D.J., 2006, US Dept. of Energy (DOE) Geothermal Electricity Technology Evaluation Model (GETEM): Volume I – Technical Reference Manual.

National Energy Technology Laboratory (NETL), 2007, Cost and Performance Baseline for Fossil Energy Plants, Volume 1: Bituminous Coal and Natural Gas to Electricity Final Report, Report No. DOE/NETL-2007/1281.

Parsons, R.M., 1978, System design verification of a hybrid geothermal/coal fired power plant, City of Burbank and Ralph M. Parsons Company; US Dept. of Energy (DOE), Report No. SAN-1572-T2.

Sanyal, S.K., 2004, Cost of geothermal power and factors that affect it, *Proceedings of the Twenty-Ninth Workshop on Geothermal Reservoir Engineering*, Stanford University, Stanford, California, Jan. 26-28, SGP-TR-175.

Sanyal, S.K., 2007, Cost of electricity from enhanced geothermal systems, *Proceedings of the Thirty-Second Workshop on Geothermal Reservoir Engineering*, Stanford University, Stanford, California, Jan. 22-24, SGP-TR-175.

A Protocol for Estimating and Mapping Global EGS Potential

Graeme Beardsmore^{1*}, Ladislaus Rybach², David Blackwell³ and Charles Baron⁴

1. Hot Dry Rocks PL, PO Box 251, South Yarra VIC 3141, Australia

2. Geowatt AG, Dohlenweg 28, CH-8050 Zürich, Switzerland

3. Southern Methodist University, Dallas, TX 75275, USA

4. Google.org, 1600 Amphitheatre Parkway, Mountain View, CA 94043, USA

* Corresponding author: graeme.beardsmore@hotdryrocks.com

Abstract

We present a Protocol to estimate and map the Theoretical and Technical potential for Engineered Geothermal Systems (EGS) in a globally self-consistent manner compatible with current public geothermal Reporting Codes. The goal of the Protocol is to standardise the production of regional estimates and maps of EGS potential so that they are directly comparable to one another globally.

The Protocol is divided into five stages:

1. Model the temperature, heat flow and available heat of the Earth's crust to a depth of 10,000 m
2. Estimate the Theoretical Potential for EGS power in the crust to a depth of 10,000 m
3. Estimate the Technical Potential that can be realized with current technology, and considering geographic, ecologic, legal and regulatory restrictions
4. Define a level of confidence in the estimated Technical Potential at each location, consistent with public Reporting Codes
5. Present results using KML visualization and data architecture

The maps, estimates and source data underpinning the estimates and maps will be made freely available for public use and presented in the Keyhole Markup Language (KML) for Google Earth.

Keywords:

Engineered Geothermal Systems; EGS resource estimation; Global geothermal resource inventory; Google Earth; Keyhole Markup Language; KML

Introduction

Engineered Geothermal Systems

'Engineered Geothermal Systems (EGS)' is a generic term for the process whereby heat is extracted from the Earth's crust by circulating water through an artificially engineered set of permeable fractures in hot rocks (Figure 1). Although significant engineering and financial hurdles remain, EGS plants hold the promise of nearly ubiquitous, low to zero CO₂ emission, secure, base-load power for millennia to come. In theory, EGS plants may be constructed anywhere that the mechanical limits of drilling and fracture

engineering allow. Furthermore, geothermal systems have the second lowest land footprint of all electrical generating technologies (McDonald *et al.*, 2009). These attributes make EGS an attractive potential major contributor to world energy supplies.

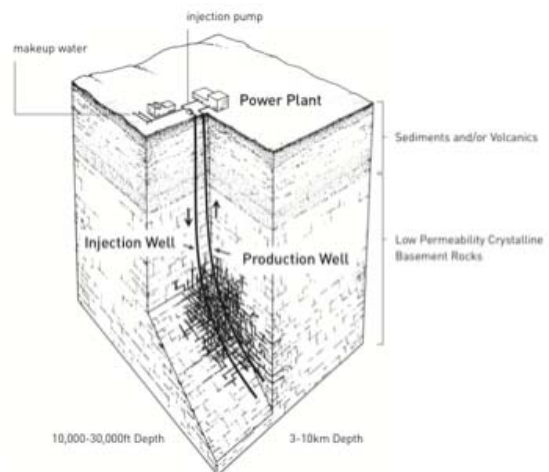


Figure 1. Conceptual EGS power plant design (from MIT, 2006)

For EGS to play a material role in the global energy mix, improving public awareness and dispersing knowledge of the global potential and its regional distribution is a vital precursor to informed R&D, energy policy making, and broad-scale commercial deployment.

A Protocol for estimating and mapping global EGS potential

This paper summarises a Protocol to estimate and map the Theoretical Potential and Technical Potential (as defined by Rybach, 2010) for EGS in a globally self-consistent manner. Any estimate or map of EGS potential in a region involves a number of inputs about geology, thermal properties, recovery factors, power conversion efficiencies, ambient temperatures and so on. It follows that an inventory of the global EGS potential requires a globally consistent methodology and a globally consistent set of assumptions to fall back on when real data are not available.

The Protocol does not seek to provide a unique picture of the magnitude and distribution of the world's EGS potential. Alternative approaches to estimating EGS potential may be more relevant in particular locations and more robust analyses will

certainly be required to assess the commercial viability of EGS at specific sites. The Protocol will, however, provide consistent methodologies and assumptions that will ultimately allow a self-consistent inventory and map of EGS potential around the world.

The Protocol will provide utility for academia, policy makers and commercial entities by standardizing technical language, improving understanding of EGS generation potential, providing a consistent visualization platform, and facilitating international commercialization efforts.

The basis for the Protocol

The Protocol closely follows the methods underpinning a report by the Massachusetts Institute of Technology, which concluded in 2006 that EGS could provide 100,000 MW of electrical generating capacity to the United States by 2050 (MIT, 2006). An integral component of that study was a review of the heat resource within the top 10,000 m of the crust by Professor David Blackwell and his team at Southern Methodist University (SMU; Blackwell *et al.*, 2007). SMU assumed that conduction is the primary heat transfer mechanism in the crust, and that the upper crust can be broadly divided into sections of 'sediment' and 'basement', each with its own physical properties of thermal conductivity and internal heat generation.

In 2008, the SMU team and Google.org converted the MIT findings into KML format for visualization on the Google Earth platform (Figure 2). The layers are available for free download and viewing from www.google.org/egs/.

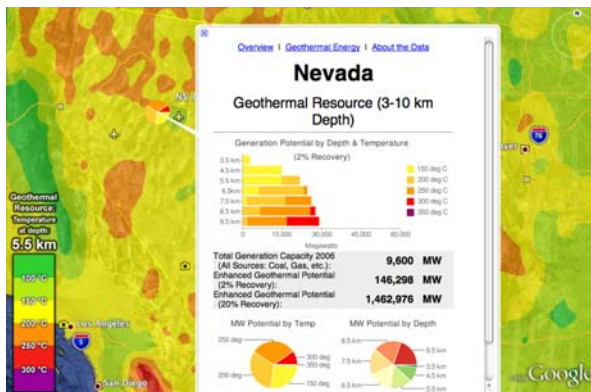


Figure 2. Screen capture of a Google Earth layer depicting the predicted temperature at 5.5 km and the EGS Potential base for Nevada, USA.

Theoretical and Technical Potential

The Protocol calls for an initial estimate of the 'Theoretical Potential' for EGS across a region, following the terminology of Rybach (2010). Theoretical Potential is "defined solely by the physical limits of use and thus marks the upper limit of the theoretically realizable energy supply contribution." From the Theoretical Potential, the

Protocol provides guidelines to estimate the 'Technical Potential', or "the fraction of the theoretical potential that can be used under the existing technical restrictions...structural and ecologic restrictions as well as legal and regulatory allowances" (Rybach, 2010). These restrictions vary greatly with geology, location and time, providing some flexibility to modify Technical Potential based on current local conditions.

Geothermal Resource reporting codes

Codes for the reporting of Geothermal Resource estimates exist for Australia and Canada. The Protocol aims to conform to those reporting Codes in so far as respecting their underlying principles of 'transparency', 'materiality' and 'competence'. These principles will be honoured through the inclusion of all relevant information (generally as metadata) with each set of maps and tables produced, and by including the personal endorsement of one or more 'Competent' or 'Qualified' Persons. The Protocol proposes the following minimum level of information to comply with these principles:

1. A statement that the data should not be relied on to inform commercial investment decisions
2. Sources of all data utilized for the estimates of EGS potential
3. A brief description of the modelling technique
4. Assumed ambient temperatures, recovery factors, and conversion efficiencies
5. Assumed lifespan of power generation
6. Statement of relative accuracy / confidence
7. The name(s) of the Competent or Qualified Person(s) who accept(s) responsibility for the Resource estimate.

Methodology

The Protocol assumes that pure vertical conduction dominates heat transport through the crust, and that a simple two-layer geological model ('sediment' on 'basement') approximates the top 10,000 m of crust in all continental areas. A region is divided into a grid-work of 'cells', and the simple two-layer model is used to estimate the local thermal structure in each cell. The EGS Theoretical Potential (relative to a defined 'base temperature') is then tallied over different depth/volume intervals by assuming density and specific heat values for the rocks in question, and assuming a uniform heat-electricity conversion pathway. The discrete estimates of each cell may be summed to estimate the total EGS potential over the region or depth interval.

In practice, the process is divided into five stages:

1. Model temperature, heat flow and heat in the Earth's crust down to a depth of 10,000 m

2. Estimate the Theoretical Potential of EGS power in the crust down to a depth of 10,000 m
3. Estimate the Technical Potential given current technology, geographic, ecologic, legal and regulatory restrictions
4. Define a level of confidence in the estimated Technical Potential at each location, consistent with public Reporting Codes
5. Present results using common visualization and data architecture

Model temperature, heat flow and heat in the Earth's crust down to a depth of 10,000 m

The temperature in the crust can be estimated using a 'top down' approach, where surface heat flow (Q_0) is assumed to extend downwards, gradually decreasing with increasing depth due to the distribution of heat generation in the rocks. Average thermal gradient can be estimated over any depth interval from the heat flow and thermal properties of the rocks. The Protocol recommends estimating the temperature profile through the top 10,000 m of crust using a 'top down' approach. Figure 3 provides a flow chart for a process that can be applied for any location.

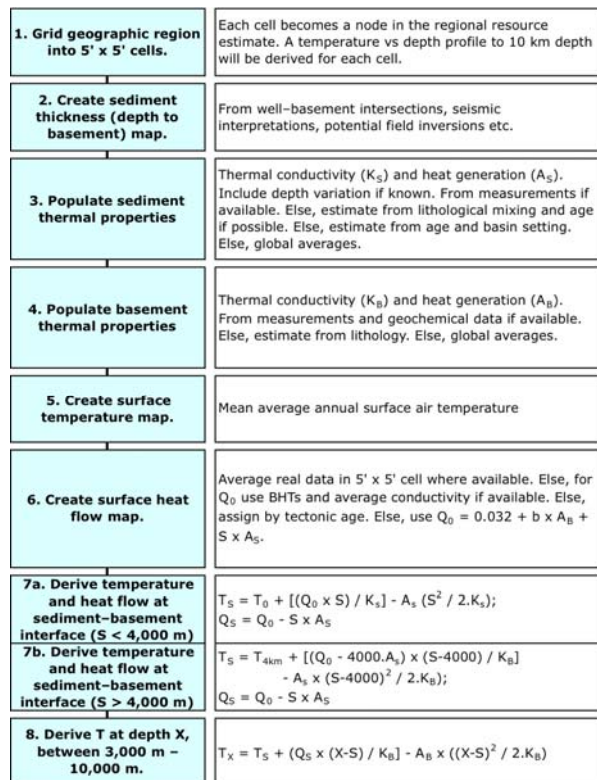


Figure 3. General process for estimating the temperature profile of the crust to 10,000 m depth. See Glossary for symbol definitions.

The region under investigation is first divided into a regular grid. 5' x 5' graticules are recommended as the basic 'cell' size. A region such as Australia (7.6 million square kilometres at an average latitude of around 25°S) requires ~100,000 cells.

The next step is to chart the average thickness of 'sediment' overlying 'basement' in each 5' x 5' cell—in effect, develop a 'depth to basement' map for the region of interest. For Australia, the SEEBASE™ database provides a first pass estimate of the thickness of Phanerozoic basins across the continent (Figure 4), and can be freely downloaded over the Internet. SEEBASE™ is a registered trademark of FrOG Tech Pty Limited in Australia, and stands for Structurally Enhanced view of Economic BASEment.

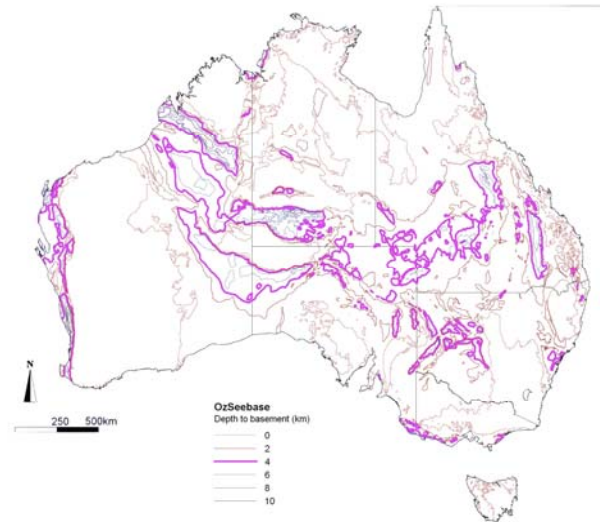


Figure 4. A visualization of the SEEBASE™ database.

Temperature can be predicted at any arbitrary depth for a given surface heat flow (Q_0), thermal conductivity and heat generation (A) structure. The temperature prediction process requires that the sediment and basement sections of each cell be individually characterised with values of thermal conductivity (K_s and K_b for sediment and basement, respectively) and heat generation (A_s and A_b , respectively). To maintain consistency with Blackwell *et al.* (2007), the Protocol assumes that the thermal conductivity of sediment deeper than 4,000 m is the same as the basement (K_b).

Mean surface temperature (T_0) is an important boundary condition for models of underground temperature and for estimates of EGS potential. The Protocol assumes that mean surface rock temperature is approximately equal to mean surface air temperature.

Temperatures at depth are estimated in two steps. The first step is to estimate the temperature at the sediment-basement interface (T_s). T_s is derived using one or both of the following formulae, depending on whether sediment thickness (S) is greater than or less than 4,000 m.

If $S < 4,000$ m:

$$T_s = T_0 + [(Q_0 \times S) / K_s] - A_s \times [S^2 / (2 \times K_s)] \quad \text{Eq 1}$$

If $S > 4,000$ m, the conductivity of that portion of sediment deeper than 4,000 m is K_B . In this case, first calculate T_{4km} using $S = 4000$ in Eq 1, then:

$$T_S = T_{4km} + [(Q_0 - 4000.A_S) \times (S - 4000) / K_B] - A_S \times [(S - 4000)^2 / (2 \times K_B)] \quad \text{Eq 2}$$

Heat flow at the sediment–basement interface (Q_S) becomes the ‘surface heat flow’ for estimation of temperature at deeper levels. Q_S is derived by subtracting the total contribution of sedimentary heat from Q_0 :

$$Q_S = Q_0 - S \times A_S \quad \text{Eq 3}$$

The second step is to estimate temperature at depth (X) in the basement (T_X):

$$T_X = T_S + [(Q_S \times (X-S)) / K_B] - A_B \times [(X-S)^2 / (2 \times K_B)] \quad \text{Eq 4}$$

At the completion of this step, a mean predicted temperature profile to 10,000 m depth should be available for each 5' x 5' cell.

Estimate the Theoretical Potential of EGS power in the crust down to a depth of 10,000 m

The heat stored within a volume of rock is proportional to the temperature, heat capacity, density and volume of the rock. In addition, it can only be estimated relative to a ‘base temperature’. Estimates of EGS potential, therefore, require values for each of these parameters. Figure 5 provides a flow chart of the recommended five-step process for estimating the Theoretical Potential for EGS in the top 10,000 m of crust in any location.

1. Derive average T for each 1000 m depth interval	Approximate by calculating temperature at mid-point of depth interval
2. Assign density, ρ , and specific heat, C_p , of interval.	Generally for basement: $\rho = 2,550 \text{ kg/m}^3$; $C_p = 1,000 \text{ J/kgK}$
3. Derive volume of each 5' x 5' x 1,000 m cell, V_c	This volume will vary slightly with latitude. Expressed in m^3 .
4. Calculate available heat for each depth interval in each cell, H	Heat energy expressed in Exajoules: $H = \rho \times C_p \times V_c \times (T_X - T_r) \times 10^{-18}$
5. Derive Theoretical Potential power	Electrical power expressed in Megawatts: $P = H \times 10^{12} \times \eta_{th} / 9.46 \times 10^8$

Figure 5. General process for estimating stored heat energy and theoretical power generation potential. See Glossary for symbol definitions.

Crustal temperature is the key determinant of Theoretical Potential for EGS at any specific location. Equation 4 provides this value for any specific depth. To relate temperature to heat content in a particular volume of crust, we need to assign a density (ρ) and specific heat (C_p) value for the volume of interest.

Each depth interval beneath a surface cell will contain a different amount of thermal energy. The total available heat in exajoules (H) in a volume of

crust (V_c) is a function of the temperature, density, specific heat, and a ‘base temperature’ (T_r):

$$H = \rho \times C_p \times V_c \times (T_X - T_r) \times 10^{-18} \quad \text{Eq 5}$$

The base temperature is the temperature to which the crust can theoretically be reduced through utilization of geothermal heat. The Protocol proposes following the lead of the USGS in a recent assessment of geothermal potential in the USA (Williams *et al.*, 2008), in which the USGS assumed approximately $T_r = T_0 + 80^\circ\text{C}$.

Again following the lead of the USGS (Williams *et al.*, 2008), Theoretical Potential power generation is derived using the following assumptions:

1. All heat (H) above the base temperature is theoretically recoverable in all locations
2. 30 years life span of power generation
3. Cycle thermal efficiency, η_{th} , is a function of resource temperature as per MIT (2006):

$$\eta_{th} = 0.00052 \times T + 0.032 \quad \text{Eq 6}$$

Note that the temperature appropriate for Eq 6 is the average of the initial rock temperature and the base temperature:

$$T = (T_X + T_r) / 2 \quad \text{Eq 7}$$

The potential power generation, P (MW_e), from a volume of rock with available heat, H, is:

$$P = H \times 10^{12} \times \eta_{th} / 9.46 \times 10^8 \quad \text{Eq 8}$$

Theoretical Potential power generation can be collated and tabulated for specific depth and temperature intervals.

Estimate the Technical Potential given current technology, geographic, ecologic, legal and regulatory restrictions

It is impossible to realize the entire Theoretical Potential for EGS power in any location. Following the terminology of Rybach (2010), the ‘Technical Potential’ is that part of the Theoretical Potential that can be extracted after consideration of currently ‘insurmountable’ technical limitations. ‘Technical’ is defined in its broadest sense, including factors such as land access, rock type, drilling technology, fracture density, stress orientation, regulatory framework, power conversion technology and availability of water.

Rybach (2010) argues that “the EGS potential cannot yet be termed ‘technical’”, but the Protocol proposes a set of assumptions for deriving an estimate of Technical Potential. The steps are illustrated in Figure 6.

National parks, conservation areas, densely populated areas, mountains, large lakes and swamps, militarized zones, deserts with no available water resources, and other areas may be excluded from EGS development. The proportion of each cell that is accessible and available for EGS (R_{av}) is a value between 0–1.

Define a level of confidence in the estimated Technical Potential at each location, consistent with public Reporting Codes

1. Exclude parts of cells for which land access limits EGS potential	Remove environmentally sensitive areas, major cities, major topographic features, lakes, and other land areas judged inaccessible or unavailable for EGS development. Weight each cell for proportion of 'available' area, R_{av} .
2. Limit volume to technically accessible depth	6,500 m is proposed as the current practical limit for drilling and engineering a reservoir.
3. Assign recoverability factor, R, according to rock type	Following USGS—crystalline rocks, mean $R = 0.14$. Proposed min-max range is 0.02–0.20. Assume the same for meta-sediments until experience dictates otherwise.
4. Assume a limit to the allowable temperature drawdown	Following MIT (2006), assume it is only technically feasible to reduce resource temperature by 10°C.
5. Calculate Technical Potential for each depth interval in each cell, P_T	Power expressed in Megawatts: $P_T = P \times R_{av} \times R \times R_{TD}$
6. Collate total Technical Potential at each location	$= \sum P_T$

Figure 6. General process for estimating Technical Potential of EGS from the Theoretical Potential. See Glossary for symbol definitions.

The Protocol recommends limiting estimates of Technical Potential for EGS to the top 6,500 m. This may change if there are significant advances in hard-rock drilling technology.

Recoverability factor (R) is the proportion of heat that can ultimately be recovered from a volume of rock. The Protocol suggests estimates of potential be based on a range of R values representing the expected minimum, maximum and mean values. This Protocol proposes 0.02 as the minimum R, following the precedent of MIT (2006), and 0.14 and 0.20 as the mean and maximum R, respectively, following the findings of Williams *et al.* (2008). These values are based on the results of numerical modelling. While they fulfil the aim of the Protocol to provide a globally consistent set of assumptions, estimates of Technical Potential using this Protocol should only be viewed as preliminary until such time as practical experience provides real data on recoverability.

There is a practical limit to the temperature drawdown a power plant can withstand before it will no longer operate effectively. This Protocol recommends following the methodology of MIT (2006) by assuming a maximum allowable temperature drawdown of 10°C. This effectively introduces a 'temperature drawdown' recoverability factor (R_{TD}) defined by:

$$R_{TD} = 10 / (T_X - T_r) \quad \text{Eq 9}$$

The Technical Potential (P_T) is that part of the Theoretical Potential accessible from the surface, shallower than 6,500 m, accessible via fracture networks, and available with <10°C drawdown:

$$P_T = P \times R_{av} \times R \times R_{TD} \quad \text{Eq 10}$$

Technical Potential power generation can be collated and tabulated for specific depth and temperature intervals.

The Protocol avoids using the terms 'Resource' or 'Reserve' to describe estimates of potential EGS heat or power. Those terms have specific meanings under the Australian and Canadian Geothermal Reporting Codes relating to the commerciality of the heat energy. The Protocol makes no claims for or against the commerciality of areas identified with EGS potential.

In areas where the Protocol derives EGS potential using real data, the resulting estimates of thermal energy might meet the definition of 'Resources' under the Codes (so long as other Code requirements are met). In areas where EGS potential is derived entirely from assumed values, or using data of low confidence, the results are best described as 'Exploration Results' in the terminology of the Reporting Codes.

In addition to the qualitative assessment of confidence described above, the Protocol also lends itself to a robust quantitative assessment of uncertainty. All parameters in this Protocol could be assigned numerical uncertainty values, which could then be propagated through the calculations to determine the uncertainty of the estimated Potential at each cell location and depth. Such an approach is allowable under the Reporting Codes, and could be added to a future version of the Protocol. It would provide an additional valuable layer of information.

Present results using common visualization and data architecture

Assessments of EGS potential generated as a result of the Protocol are intended to be public data, freely and conveniently accessible to all interested parties. All results will therefore be tabulated in a format compatible with popular data viewing and manipulation platforms such as Google Earth, utilizing Keyhole Markup Language (KML). Google.org's 'U.S. Geothermal Resources (3–10 km)' layer is a reference for visualization architecture (available at www.google.org/egs).

Differences from the MIT report

The intention of the Protocol is to conform closely to the methodology utilized by MIT (2006) to assess the EGS potential of the United States. However, the Protocol departs from that methodology in some key ways.

Firstly, the Protocol explicitly differentiates between Theoretical Potential and Technical Potential.

Secondly, the Protocol aims to conform to the tenets and terminology of public Geothermal Reporting Codes, with results at different locations and depths classified according to different confidence levels.

Thirdly, the Protocol extends the methodology described by MIT (2006) and Blackwell *et al.* (2007) to apply in areas where real data are scarce or non-existent.

Fourthly, the Protocol recommends assessing EGS potential relative to a base temperature of $T_0 + 80^\circ\text{C}$, rather than relative to T_0 .

Conclusions

Estimates of EGS potential derived using the Protocol will not be 'final'. They will continue to be refined as more relevant data become available. Theoretical Potential will be refined as new geological and geophysical data improve our understanding of the thermal structure of the crust. Refinements here are expected to be gradual. Technical Potential will be refined as technological advancements in drilling, power conversion and legal regimes allow greater amounts of the Theoretical Potential to be realized. Changes here are expected to be sudden and dramatic.

Application of the Protocol will undoubtedly reveal gaps and uncertainties that will require the Protocol itself to be refined through time. The Protocol will, therefore, be a 'living document'.

The authors hope that the EGS potential of most of the world's continental surface will eventually be assessed and charted following the guidelines of the Protocol, allowing for the first time a coherent view of the size and distribution of the 'hidden' energy stored in the rocks of the top 10,000 m of the Earth's crust.

Acknowledgements

The development of the Protocol was made possible by the financial support of Google.org through its 'Renewable Energy Cheaper than Coal' initiative (RE<C). The details of the Protocol have been widely reviewed and the result is due in no small part to constructive criticism by Colin Williams (USGS), Anthony Budd (Geoscience Australia), Susan Petty (AltaRock Inc), Christoph Clauser (RWTH Aachen University), Dan Yang (Borealis GeoPower Inc), Arner Hjartarson (Manvitt Engineering), Wendy Calvin (Great Basin Center for Geothermal Energy) and others.

References

Blackwell, D.D., Negraru, P.T. and Richards, M.C., 2007, Assessment of the Enhanced Geothermal System Resource Base of the United States. Natural Resources Research. DOI: 10.1007/s11053-007-9028-7.

MIT (Massachusetts Institute of Technology), 2006, The Future of Geothermal Energy—Impact of enhanced geothermal systems (EGS) on the United States in the 21st century. MIT Press.

McDonald, R.I., Fargione, J., Kiesecker, J., Miller, W.M. and Powell, J., 2009, Energy sprawl or energy efficiency: climate policy impacts on natural habitat for the United States of America. PLoS ONE 4(8): e6802. doi:10.1371/journal.pone.0006802.

Rybach, L., 2010, "The future of geothermal energy" and its challenges. Proceedings World Geothermal Congress 2010 Bali, Indonesia, 25–29 April 2010.

Williams, C.F., Reed, M.J. and Mariner, R.H., 2008, A review of methods applied by the U.S. Geological Survey in the assessment of identified geothermal resources. USGS Open File Report 2008-1296. 27pp.

Glossary of symbols

- η_{th} : thermal efficiency for power conversion (0–1)
- ρ : density (kg/m^3)
- $A_{\text{S,B}}$: heat generation: sediment, basement (W/m^3)
- b : thickness of heat generating basement (10000 if $S < 3000$ m, else $[13000 - S]$) (m)
- C_p : specific heat capacity (J/kgK)
- H : total available thermal energy (EJ)
- $K_{\text{S,B}}$: thermal conductivity: sediment, basement (W/mK)
- P : Theoretical Potential EGS power (MW_e)
- P_T : Technical Potential EGS power (MW_e)
- $Q_{0,S}$: heat flow: surface, base of sediment (W/m^2)
- R : recoverability factor (0–1)
- R_{av} : proportion of cell available for EGS (0–1)
- R_{TD} : 'temperature drawdown' recoverability factor (0–1)
- S : thickness of sediment (m)
- $T_{0,S,X}$: crustal temperature: surface, sediment base, depth X ($^\circ\text{C}$)
- T_r : base, rejection, or re-injection temperature ($^\circ\text{C}$)
- V_c : volume of section of crust (m^3)
- X : arbitrary depth in crust (m)

Changes to Geothermal Reporting Code and Guidelines on Company Reporting

Beardsmore, G.¹, Budd, A.², Goldstein, B.³, Holgate, F.⁴, Jeffress, G.⁵, Larking, A.⁶, Lawless, J.⁷, Libby J.⁸, Middleton, M.⁹, Reid, P.^{10*}, Stafford, C.¹¹, Ward, M.¹², Williams, A.¹³

¹ Hot Dry Rocks Pty Ltd, PO Box 251, South Yarra, VIC 3141; ² Geoscience Australia, GPO Box 378, Canberra ACT 2601; ³ Primary Industries and Resources, PO Box 277, Adelaide SA; ⁴ KUTh Energy Ltd, 35 Smith Street, North Hobart, TAS 7000; ⁵ CSA Global, PO Box 139, Burswood, WA 6100; ⁶ Green Rock Energy, PO Box 1177, West Perth, WA 6872; ⁷ Sinclair Knight Merz, PO Box 9806, Newmarket, Auckland NZ; ⁸ New World Energy, Level 3, 46 Ord St, West Perth, WA 6005; ⁹ WA Department of Mines and Petroleum, 100 Plain Street, East Perth, WA 6004; ¹⁰ Petratherm Limited, 129 Greenhill Rd, Unley 5061, South Australia; ¹¹ Granite Power Limited, Level 6, 9 Barrack St, Sydney NSW 2000; ¹² Geothermal Advisory Pty Ltd, PO Box 150, Richmond Tas 7025; ¹³ Geodynamics Limited, PO Box 2046, Milton, Qld 4064

* Corresponding Author: preid@petratherm.com.au

With the launch of the First Edition of the Geothermal Reporting Code in August 2008, Members of the Australian Geothermal Energy Association (AGEA) agreed to report their Exploration Results, Geothermal Resources and Geothermal Reserves in accordance with the Geothermal Reporting Code. In its first year of operation, a number of issues became apparent in the use and interpretation of the Geothermal Reporting Code. Most significant amongst these were:

- That the definition of an Inferred Geothermal Resource was allowing large estimates of stored heat to be reported. Whilst derived by legitimate methodologies, it was perceived that these large figures may not be properly understood by non-technical people and may result in a diminution of credibility of the industry;
- The units of energy described in the First Edition were not always consistent or practical; and
- Companies were misunderstanding the circumstances requiring a Competent

Person sign-off on public reports and other company announcements.

The Geothermal Reporting Code Committee consulted with industry and received feedback from companies and practitioners both in Australia and overseas. The Second Edition of the Geothermal Reporting Code addresses the issues identified above. In some cases definitions and meanings have been changed (for example, the re-defining of Geothermal Resources as *recoverable* energy, rather than energy in place) whilst in others, aspects of the Geothermal Reporting Code that were already in place have been made more explicit (for example, the obligations in respect of Competent Person sign-offs). This presentation outlines the key changes to the Second Edition of the Australian Geothermal Reporting Code, and provides clarification on the public reporting requirements of Companies.

Keywords: Geothermal Energy, Resource Estimation, Australia

References

The Australian Geothermal Code Committee, 2008. "Australian Code for Reporting of Exploration Results, Geothermal Resources and Geothermal Reserves; The Geothermal Reporting

Code 2008 Edition” Australian Geothermal Energy Group and the Australian Geothermal Energy Association.

The Australian Geothermal Code Committee, 2010. “Australian Code for Reporting of Exploration Results, Geothermal Resources and Geothermal Reserves; The Geothermal Reporting Code 2010 Edition” Australian Geothermal Energy Group and the Australian Geothermal Energy Association.

3D analysis of induced micro-seismic event records compared with geology and structure: Preliminary results of a Cooper Basin project

Chloé Bonet^{1,2}, Stewart Hore¹, Desmond FitzGerald¹, Michel Rosener³,
Helen J. Gibson¹ and David Jepsen⁴

¹ Intrepid Geophysics, Unit 2, 1 Male Street, Brighton, Victoria, 3186, Australia.

² Institut de Physique du Globe de Paris of Earth's Geophysics, Paris, France.

³ Geodynamics Limited, Level 2, 23 Graham Street, Milton, Queensland, 4064, Australia.

⁴ Geoscience Australia, Cnr Jerrabomberra Avenue & Hindmarsh Drive, Symonston, ACT, 2609, Australia.

* Corresponding author: chloe@intrepid-geophysics.com

Abstract

The concept of an EGS geothermal prospect is based on fracture network permeability enhanced by hydraulic stimulation. Characterisation of fracture/fault mechanisms and geometries are therefore an important part of prospect development.

In this study, building a prospect-scale 3D geology and structure model of the Cooper Basin geothermal field has assisted prospect exploration and evaluation, but even greater advantage will come from the ability to integrate (in the same workspace) information from induced seismic events records such as location, magnitude, timing, focal mechanism, and shear plane orientation.

Keywords: Induced seismicity, fracture/fault networks, clustering, focal mechanisms, 3D geology models.

Introduction

The Cooper Basin geothermal field is located near the common borders of Queensland and South Australia. Since geothermal exploration began in 2002, 4 wells have been drilled into the underlying granite, with final depths around 4300 metres. Of these, the designated injection well, Habanero-1 was hydraulically stimulated in 2003 and again in 2005. Both stimulations induced detectable micro-seismicity centred on TD of Habanero-1 (4421 m).

Detailed studies by Geodynamics, Geoscience Australia, and Q-Con (Baisch et al, 2006) concluded that the hydraulic stimulations successfully enhanced hydraulic permeability between the injection well (Habanero-1) and one of the production wells (Habanero-2). Compared with the earlier stimulations, those in 2005 extended the previous stimulated reservoir, as well as further enhancing permeability.

Beyond the goal of increased permeability, hydraulic stimulations also provide an opportunity to gather induced seismicity event records which enable studies on:

- Fracture / fault mechanism and geometry characterization, and
- likelihood of seismic risk to infrastructure from geothermal reservoir activities.

Joint R&D project outline

Since March 1st 2010, Intrepid Geophysics and Geodynamics have been engaged in a collaborative project with the following goals:

1. Develop a 3D micro-seismic time records viewer so that new knowledge about fault geometries and fault mechanisms can evolve and be integrated in the context of all available geology and geoscience observations.
2. Investigate clustering or condensing of the event records in a manner that is coherent with geological and geomechanical principals, with the aid of filtering capabilities.
3. Characterize focal mechanisms in a suitable viewing format, e.g., triangular state diagram.
4. Synthesize and integrate other disparate observations of the geothermal field in a 3D workspace, such as: tectonic stress, well fracture records, and rock velocity data. The aim here is to facilitate creation of workable 3D velocity models, and hence to improve the accuracy of locating the hypocenters of micro-seismic events.

Induced Seismicity Database

The primary database underpinning this project is the induced seismicity events records from the mid-September 2005 hydraulic re-stimulation of Habanero-1. Over a period of 13 days 22,500m³ of water was injected into 4421 m. (For details of the injection flow rate and wellhead pressure, see Baisch et al., 2009.)

In April 2005 a continuous seismic monitoring system was installed at the Cooper Basin geothermal field, and this captured the events of the September 2005 re-stimulation. The seismic station network includes instruments at depths varying from surface, to shallow depths (80-370m)

and one deep station at 1780m. (See Baisch 2009 for details.)

During the mid-September 2005 injection of Habanero-1, approximately 16,000 detectable seismic events were recorded. From this total, Q-Con determined absolute hypocentre locations for 8886 events, that is, events for which at least five P-phase and three S-phase onsets could be identified (Baisch et al. 2009).

The data processed by Q-con (containing hypocenter locations, magnitudes and focal mechanism data for 8886 micro-seismic events) was selected for use in the joint R&D project, ahead of an alternative dataset available from a Japanese processing team.

3D model of the Copper Basin geothermal field

A preliminary 3D geology model of the Cooper Basin geothermal field site has been constructed in 3D GeoModeller software (e.g., see Calcagno et al, 2008) using formation tops data from the three Habanero wells, and McLeod-1 drilled in 1983 on a site approximately 440 m east-north-east of Habanero-1 (Table 1).

Wells names	Latitude	Longitude	Depths (m)	Dip	Date
Habanero 1	27°48'57.0"	140°45'15.9"	4420.82	90°	14/10/03
Habanero 2	27°49'9.7"	140°45'4.9"	4357.73	90°	31/03/05
Habanero 3	27°48'43.3"	140°45'28.9"	4221.48	90°	05/02/08
McLeod 1	27°48'53.2"	140°45'31.3"	3806.34	-	08/10/83

Table 1. Location and description of the Habanero-1, -2, -3, and McLeod-1 wells.

The geological model was also constrained by formation tops data derived from interpreted conventional seismic lines.

The preliminary geological model has extents of 10 x 10 x 6.5 km, and incorporates the stratigraphic successions of the Cooper and overlying Eromanga Basin (Fig 1). The mainly Triassic-aged basin fill, has an average bedding angle around horizontal, and top of the granitic bedrock lies between 3500 and 4200 m (Fig 2).

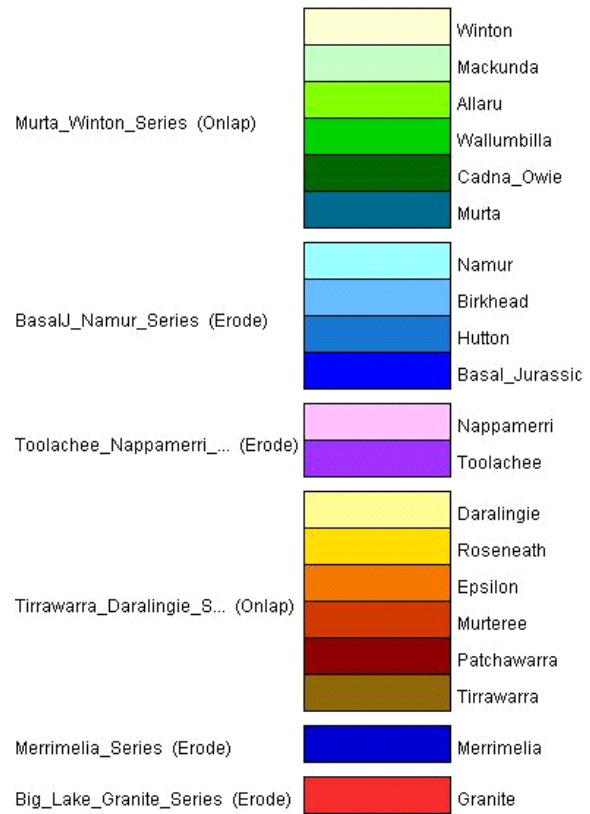


Figure 1. Stratigraphic pile for the Cooper and Eromanga Basins, within the geothermal field (excluding Cainozoic Eyre Fm), as used in the geology model shown in Figure 2, below.

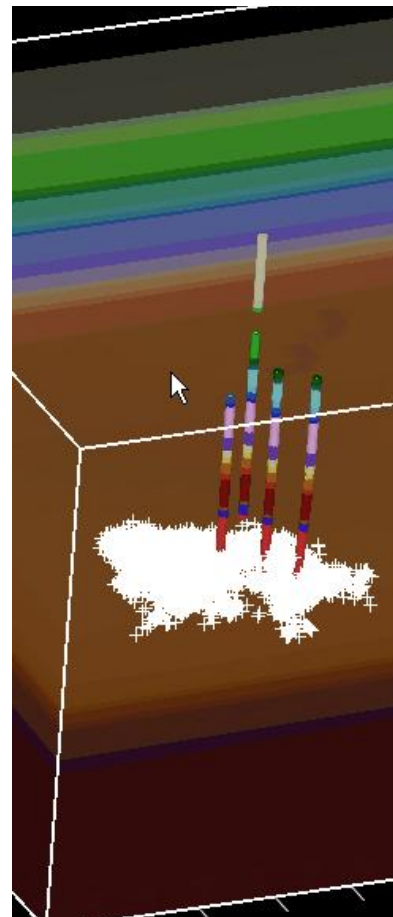


Figure 2. Preliminary geological model for the Cooper Basin geothermal field (view to the northeast). Exaggerated drill hole intersects are highlighted for Habanero-1, -2 and -3, and for McLeod-1 (at the rear). Hypocentre locations estimated by Q-Con for 8886 micro-seismic events induced during the September 2005 hydraulic simulation of Habanero-1 are shown by the cloud of white symbols.

Interpreted basement fault characterization

As viewed in Figure 2, the hypocentre locations estimated by Q-Con for 8886 micro-seismic events induced during the September 2005 hydraulic stimulation of Habanero-1 are localised in a zone approximately 3200 m x 1800 m horizontally (long-axis oriented NNE) and within 600 m vertically, centred on TD of Habanero-1 (4421 m).

Analysis of these event locations by Q-Con suggests induced seismicity aligns along a single, reactivated sub-horizontal fracture system (Baisch et al, 2009; Rothert & Baisch, 2010). Indeed, a best-fit plane to the seismic cloud supports this interpretation.

Pre-existence of this sub-horizontal fracture and it's primary tectonic origin, is evidenced by logging data acquired before any reservoir tests began (D. Wyborn unpublished data, in: Baisch et al, 2009).

Viewing focal mechanism information

Goal number 3 of the joint R&D project being undertaken by Geodynamics and Intrepid Geophysics is the ability to visualize focal mechanism information about faults at the hypocentres of induced seismicity. Plots created on-the-fly from a whole or filtered database are required in order to differentiate discrete faults / fractures activated during hydraulic stimulation, and to determine their stress state, orientation, and slip direction, etc. This requires a pre-processed dataset to be loaded, and demands sophisticated plotting and visualization options.

Plotting of triangular state diagrams is likely to be implemented. These will allow groups of seismic events representing similar focal mechanisms, to be identified, and conclusions about the presence of single or multiple structures to be made. For each diagram, the 3 poles will represent an end-member sense of movement on a fault: normal, thrust, or strike-slip. Two complete triangular state diagrams are required: one each containing dextral strike-slip and sinistral strike-slip sense.

Fracture orientations in the Cooper Basin geothermal field

As above, focal mechanism information for 8886 micro-seismic events recorded during the September 2005 stimulation of Habanero-1 was processed by Q-con, and provided for this R&D project by Geodynamics. From this information, we imported the fracture orientations of all seismic events, noting (on a first-pass) the existence of two distinct populations of fracture orientations:

- a) 96% of fractures orientations are similarly oriented, with a mean dip of 9° towards 247° (pale blue discs in Fig 3)

- b) 3% of fractures orientations are similarly oriented with a mean dip of 20° towards 164° (red discs in Fig 3)
- c) 1% of fracture orientations are not defined as belonging to any population.

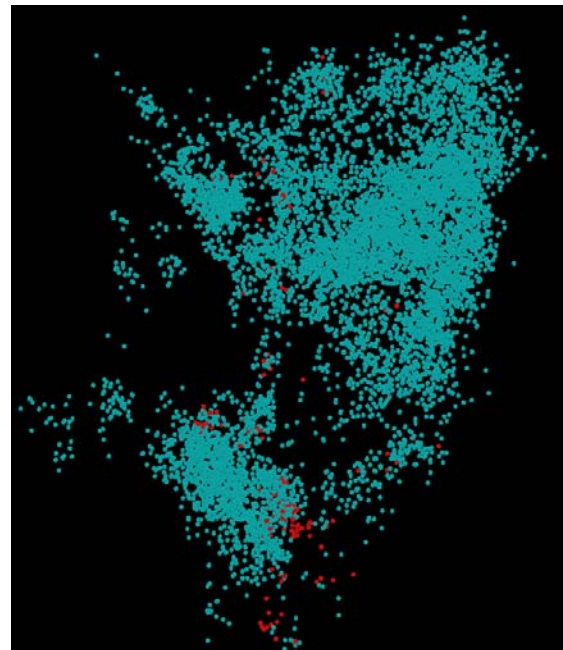


Figure 3. Visualisation in 3D GeoModeller of fracture orientations of the seismic cloud captured during the 2005 hydraulic stimulation of Habanero-1. One dominant and one minor population constitute the dataset. (See text.)

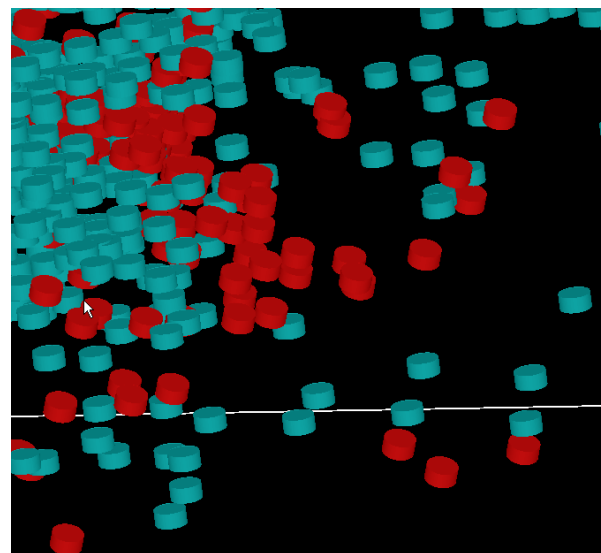


Figure 4 Enlargement of part of the seismic cloud from Fig 3, to highlight the variations in orientations.

Compared with the simple analysis visualised in Figs 3 and 4, the ability to further filter and sort the fracture orientation dataset is required, so that individual faults and fault-families can be tagged, assisting the interpreter to trial scenarios of possible fault network interpretations – while working with superimposed representations of prior knowledge of geology and structure, and other independent data.

Micro-seismic event magnitude

Additionally, for the Cooper Basin geothermal field we have facilitated visualization of variable magnitudes of micro-seismic event records from the 2005 stimulation of Habanero-1 (Fig 5). Again these data were made available through the processed dataset of Q-con which includes focal mechanism information.

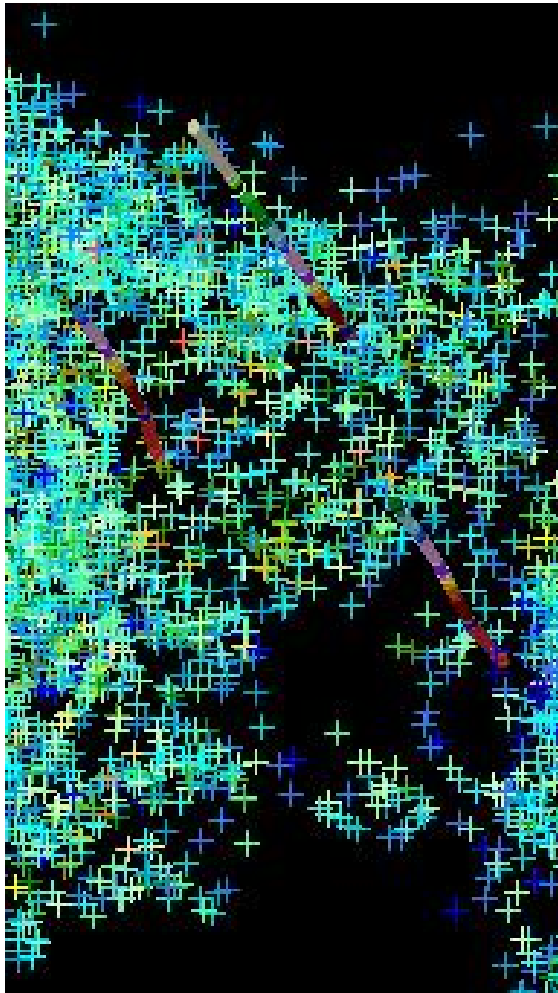


Figure 5. Oblique view to the northeast, through hypocentre locations for micro-seismic events of the 2005 stimulation of Habanero-1, including enlarged well traces for Habanero-1 (lower), Habanero-3 (middle) and McLeod-1 (upper). The variations of event magnitude range from +2.9 to -1.0 (Moment Magnitude Scale), with highest magnitudes in red, mid-scale in yellow, and lowest in blue.

Concluding Note

Beyond customised objectives and early access to the project results for Geodynamics Ltd, a key objective of this joint R&D project is to develop a micro-seismic time records viewer capability in ¹3D GeoModeller. As described above, the viewer will also have the ability to filter and sort records based on attributes such as timing, magnitude and focal mechanism.

These improvements will give reservoir engineers a tool to directly interpret the micro-seismic event record against the background of the prior

geological and geoscientific knowledge. In turn, improved knowledge on fault / fracture locations, orientations and connectivity will lead to a better understanding of the overall behaviour of a reservoir in terms of mechanics, and also hydraulics.

Acknowledgements

¹3D GeoModeller is a commercial software developed by BRGM and Intrepid Geophysics.

References

- Baisch S, Vörös R, Weidler R And Wyborn D (2009). Investigation of fault mechanisms during geothermal reservoir stimulation experiments in the cooper basin, Australia, *Bulletin of the Seismological Society of America*, 99, 148-158
- Baisch, S.; Weidler, R; Voros, R; Wyborn, D. And de Graaf, L. (2006). Induced seismicity during the stimulation of a geothermal HFR reservoir in the Cooper Basin, Australia. *Bulletin of the Seismological Society of America*, 96, 2242-2256
- Calcagno, P., Chiles J., Courrioux, G. and Guillen, A. (2008) Geological modelling from field data and geological knowledge. *Phys. Earth Planet. Interiors*, doi: 10.1016 / j.pepi.2008.06.013
- Rothert E And Baisch S (2010). Passive seismic monitoring: Mapping enhanced permeability, *Proceeding world geothermal congress 2010*.

Geothermal Energy's Transition from Resource to Power: Legal Challenges

Anna Collyer*, Nadia Harrison and Natasha McNamara

Allens Arthur Robinson.

Level 27, 530 Collins Street, Melbourne, 3000.

* Corresponding author: Anna.Collyer@aar.com.au

Growth and development in the geothermal energy sector will require the industry to understand and comply with several forms of regulation. The geothermal energy sector has much in common with mining of petroleum and minerals, and is regulated as such. However, because geothermal will ultimately serve as a source of electricity, it is equally important to understand the legal regime that governs the national electricity market and the sector's entry into the electricity market. Differences in State and Territory regulation of geothermal projects mean that the sector will have different obligations with which to comply in different jurisdictions. Different approaches to allocating priority among holders of overlapping tenements are taken under the various State and Territory regimes. The geothermal energy sector's engagement with the Scale Efficient Network Extension (**SENE**) framework and the National Electricity Market established by the National Electricity Law will be crucial if it is to have a significant role in electricity production.

Keywords: geothermal; regulation; overlapping tenements; National Electricity Market; Scale Efficient Network Extensions

Regulation of geothermal resources

State and Territory Regulatory Regimes

The geothermal sector must come to terms with the different systems regulating geothermal projects in each State and the Northern Territory. Each legislative scheme imposes different obligations, and the differing classifications of geothermal resources have implications that will affect project development. In South Australia and Western Australia, petroleum legislation was amended so that it now regulates both petroleum and geothermal energy. In Queensland, Victoria and the Northern Territory, geothermal energy is regulated by a dedicated Act. In New South Wales and Tasmania, a geothermal resource is defined as a mineral and is regulated under mining legislation.

In the Australian Geothermal Industry Development Framework, which was published by the Federal Department of Resources, Energy and Tourism in 2008, concern was expressed that that differences in legislative schemes have the

potential to affect investment decision-making. Investment decisions may be influenced by the number of hurdles to exploration and exploitation a particular legislative scheme imposes and the degree of certainty it provides. Thus, decisions that should be based on the potential of the geothermal resource may be influenced by differences in regulation of the industry. One of the objectives outlined in the framework is to 'harmonise the framework governing the industry across Australia.' Given the existence of seven different schemes for the regulation of geothermal energy, this objective will be difficult to achieve.

The practical implications of the differing legislative regimes must be understood. Two examples serve to illustrate this. First, in South Australia activity may only be conducted if the region or land concerned is covered by a Statement of Environmental Objectives that has been approved by the Minister. Geothermal and petroleum activities are governed by the same Act in South Australia, so Statements of Environmental Objectives developed for petroleum activities can be adopted for geothermal operations.

Second, native title negotiations must be approached based on the different regulatory treatment of geothermal energy in each jurisdiction. In South Australia, the Government has made a determination that geothermal activities are not mining activities. This means that holders of South Australian geothermal licenses are not subject to the additional criteria under the right to negotiate process associated with holding mining leases. In Queensland and Western Australia, holders of geothermal tenements are subject to the more stringent right to negotiate procedure. In Victoria and the Northern Territory, native title is dealt with explicitly under geothermal legislation. In Victoria, native title holders must be compensated for any loss or damage sustained in relation to their interests as a result of geothermal activity. In the Northern Territory, the Minister must be satisfied the native title holder's consent has been obtained and the federal *Native Title Act* procedures followed before granting the geothermal authority applied for.

Overlapping tenements

Tenements granted for the purpose of development of geothermal resources may overlap with other mineral or petroleum

tenements. For example, the Cooper Basin is the site of a geothermal resource and significant gas and oil reserves. The legislative regimes resolve the question of prioritisation of interests in different ways. The approach to overlapping tenements taken in each jurisdiction is linked to classification of geothermal energy and the mode of regulation of geothermal energy adopted in each state.

In South Australia and Western Australia, geothermal tenements and petroleum tenements may subsist in the same area. Governed under the same legislation in these states, geothermal and petroleum resources are treated equally. However, prior to the grant of the second tenement (geothermal or petroleum), the Minister must consult the existing tenement holder. Thus, in both of these jurisdictions, the Minister has a responsibility to hear and take into account the concerns of the existing tenement holder.

In Queensland, a more prescriptive approach is taken. Geothermal exploration cannot be undertaken to the extent that it adversely affects activity under a mineral or petroleum tenement that has already started. Conversely, activity on tenements granted under the mineral and petroleum legislation cannot be undertaken to the extent that it adversely affects activity under a geothermal tenement that is already under development. This approach clearly gives priority to the holder of the tenement that was obtained first, whereas in Western Australia and South Australia the existing tenement holder need only be consulted before the Minister grants the second interest. Although one of the purposes of the Queensland Act is to facilitate consultation with and compensation for persons adversely affected by geothermal exploration, the Act provides no guidance as to how to determine whether a project is 'adversely affected' by a geothermal project. The Queensland legislation dictates that a project that is first in time and adversely affected by a second proposed activity on the same land has priority. However, discretion in relation to what constitutes an 'adverse effect' remains. The question of whether the first activity will be 'adversely affected' by the second is a matter that will require resolution in each case of overlapping tenements.

In New South Wales and Tasmania, geothermal resources have the same status as other minerals. In New South Wales, an overlapping tenement may not be granted without the consent of the existing tenement holder. As in South Australia and Western Australia, the Minister has a role to play: disputes between the overlapping tenement holders are referred to the Minister for determination. In Tasmania, an exploration license or mining lease cannot be granted over land that is already the subject of a tenement. Because geothermal resources are not

distinguished from other minerals in these states, the approach taken to overlapping tenements is more rigid.

The Victorian Act is silent on the question of overlapping tenements. However, the Operation Plan that is submitted to the Minister prior to the carrying out of the geothermal operation must detail the risk of injury to land users in the vicinity of the operation.

As well as describing these differing regulatory regimes in the abstract, analysis of the practicalities associated with attempts to comply with them will also be provided.

In the Northern Territory, the holder of a geothermal tenement must consult the holder of an existing mining right or petroleum interest about the proposed geothermal activities. Unlike the Queensland legislation, the Northern Territory's *Geothermal Energy Act* does not provide that holders of mining rights and petroleum interests must consult with holders of existing geothermal tenements. Unlike the South Australian and Western Australian requirement that existing tenement holders be consulted prior to the grant of an overlapping tenement, geothermal tenement holders need only consult the holder of an existing right or petroleum interest before conducting geothermal activities.

The resolution of issues associated with overlapping tenements often rely on the exercise of Ministerial jurisdiction, either at the time when the tenement is granted, or in the event of a dispute. The exercise of Ministerial discretion may be influenced by political considerations. Holders of overlapping tenements may benefit from using contract to overcome uncertainty as to how their interests will be prioritised. Another situation in which contractual negotiation and agreement may also benefit the development of the project is where tenements over a single geothermal resource are granted to different parties. In some jurisdictions, cooperation can be mandated. In Western Australia, license holders can be required to enter into an agreement if the Minister is of the view that unit development of the geothermal resources area would secure more effective recovery of geothermal energy. Similarly in Victoria, the Minister may require holders of extraction licences that cover adjacent areas to enter into cooperative agreements for the extraction of geothermal energy. Further insights will be provided into how contracts are likely to operate as a practical tool. Our analysis will draw from contexts which share important characteristics with the geothermal energy sector, including experiences of the wind power sector.

Regulation of geothermal energy

While geothermal remains a young and underdeveloped industry in Australia, there will be

a tendency for industry participants to focus on regulatory systems governing preliminary issues such as exploration, prospecting and valuation. As geothermal resources are developed to become sources of power, parties with an interest in geothermal projects will need to become familiar with the requirements and peculiarities of the National Electricity Market (**NEM**) and the rules which apply to it.

The NEM: an overview

An outline of how the NEM operates and some of the key principles underpinning the National Electricity Law and the NEM will be provided. This will be distinguished from the system which operates in the Northern Territory and Western Australia. A brief description of the rules and standards likely to be particularly important for geothermal projects will also be provided.

Entry into the NEM and Contracting

Electricity prices in respect of base load power are determined according to bids placed by generators at five minute intervals. In this competitive environment, the capacity to sell electricity at a specified price cannot be taken for granted.

Contracting

The production of geothermal energy requires significant capital investment when compared with other electricity generation methods. The Massachusetts Institute of Technology cites Californian research indicating that capital reimbursement and interest charges account for 65% of the total cost of geothermal power. This can be compared to combined-cycle natural gas plants for example, for which equivalent costs account for approximately 22%. In each case the remaining costs cover items including fuel (eg water), labour and access charges.

There will therefore be an understandable desire among industry participants to obtain some security regarding electricity sales and prices.

Generators may seek to negotiate longer term underlying contracts to give themselves, their financiers and their investors certainty. Such contracts are commonly relied upon within the current market. The NEM structure means that derivatives are often used for this purpose, although a PPA may also be appropriate in certain circumstances.

As RECs will support the economic viability of geothermal projects under the Renewable Energy (Electricity) Act 2000 (Cth), it is likely that proponents will sell a bundled product comprising electricity ('black') and RECs ('green').

An outline of the operation of such contracts within the electricity market currently, including

some practical tips on contract drafting, negotiation and key risks will be provided.

Scale Efficient Network Extensions (SENE)

In order to promote development of the infrastructure needed to transfer electricity from (often remote) energy generation sites to the electricity grid, the Australian Energy Market Commission has drafted proposed amendments to the National Electricity Rules which would facilitate the construction of SENEs between new electricity generators and existing infrastructure. While the extensions will be available to various types of energy producers, they are likely to be particularly important for the renewable energy sector.

According to the current proposal, SENEs would be developed by Network Service Providers with Generators paying for the right to transmit energy through an SENE and the cost of any shortfall being passed through to customers. Customers here are those registered with AEMO as customers and therefore would include retailers rather than end use customers. Customers are however expected to benefit from the prevention of costly duplication which could result if companies were left to each construct their own infrastructure in order to connect to the network.

Outlined below is a sample of some of the issues raised by the draft amendment which are likely to present challenges.

Capacity

The fact that geothermal sites in any particular region are likely to develop in a staggered manner makes the determination of suitable capacity for SENEs particularly difficult. Clearly, there should be enough to enable geothermal and other generators to transmit electricity to the market. At the same time, a potential over-sizing or 'asset stranding' would be paid for by electricity customers and would likely be passed through to their end-use consumers in the form of higher electricity costs.

As the Network Service Providers responsible for developing SENEs will be able to recover their costs entirely from generators and customers, the AEMC notes that the incentives may favour over-sizing (and excessive capacity) rather than under-sizing (and inadequate capacity).

Notwithstanding, geothermal industry participants considering investing in reliance on transmission services offered through an SENE should not consider this to constitute a capacity guarantee. The draft rules prescribe that the AER may disallow proposed SENE projects. Moreover, a Network Service Provider will only be required to commence the SENE planning procedure if there is a reasonable likelihood of other generators

connecting to the proposed SENE and its development is likely to offer material scale efficiencies. In the event that there is inadequate capacity, the draft rule provides that the generator whose requirements cannot be met is required to fund an augmentation to the SENE. If the generator does not agree to fund such an augmentation and its generation (in excess of its agreed power transfer capability) has 'constrained off' another generator connected to the SENE, the first generator will be required to pay the other compensation. Importantly, compensation is calculated with reference to a formula which will not necessarily result in recovery of the 'true economic cost of connection'.

Relationship with shared network

Depending on the way in which the SENE infrastructure develops, its interaction with the shared network could present challenges. Where the SENE generates benefits and/or costs for users of the shared network, there is limited allowance in the rules for their allocation. There may also be practical difficulties associated with the fact that the shared network operates through an open access system whereas after the introduction of the SENE, generators will be allocated a specific agreed power transfer capability.

Infrastructure development efficiency

The Clean Energy Council has noted that the Network System Operators responsible for developing SENEs have few incentives to avoid cost blow outs.

References

Australian Energy Market Commission, 2010, Consultation Paper National Electricity Amendment (Scale Efficient Network Extensions) Rule 2010.

Australian Energy Market Operator, 2010, AEMO's Submission to the AEMC's Consultation Paper on Scale Efficient Network Extensions, Ch. 1, 6, 7, 9, 10.

Bartlett, R. H., Native Title in Australia, 2004.

Blodgett, L., Holm, A., Jennejohn, D. and Gawell, K., May 2010, Geothermal Energy: International Market Update, p. 4-10, 51-52.

Department of Resources, Energy and Tourism, 2008, Australian Geothermal Industry Development Framework.

Geothermal Energy Resources Act 2005 (Vic).

Geothermal Exploration Act 2004 (NT).

Goldstein, B., Malavazos, M., Long, A., Bendall, B., Hill, T., and Alexander, E., 2010, The Regulator's Perspective – Best Practice Activity

Approval Process for EGS Projects (including Induced Seismicity), Workshop on Geothermal Reservoir Engineering, 35th, Stanford University, Abstract.

Gove-White, G., and Frederiks, P., June 2010, Geodynamics - The Opportunity.

Hedge, J., 2006, Recent Developments: Geothermal Energy Heating Up, AMPLA Limited 13th Annual Conference, Melbourne.

Lund, J. W., 2007, Characteristics, Development and Utilization of Geothermal Resources, p. 1-3, 7-9.

Massachusetts Institute of Technology, 2006, The Future of Geothermal Energy: Impact of Enhanced Geothermal Systems (EGS) on the United States in the 21st Century, Ch. 8-9.

Steol Rives LLP Attorneys at Law, McKinsey, J.A., 2009, The Law of Lava, p. 10-17.

Mineral Resources Development Act 1995 (Tas).

Mining Act 1992 (NSW).

Mining Regulation 2003 (NSW).

Native Title Act 1993 (Cth).

Petroleum and Geothermal Energy Act 2000 (SA).

Petroleum and Geothermal Energy Resources Act 1967 (WA).

Geothermal Exploration Act 2004 (Qld).

The authors have also relied on various internal research resources owned by Allens Arthur Robinson.

Trusted Regulation for Geothermal Resource Development (Including Induced Seismicity Associated with EGS Operations)

Barry Goldstein, Betina Bendall, Alexandra Long, Michael Malavazos, David Cockshell and David Love
 Primary Industries & Resources South Australia (PIRSA), GPO Box 1671, Adelaide, South Australia, 5001

Abstract

Operations need be managed to reduce material risks to acceptable levels and as low as reasonably practical to meet community expectations. Public trust in both industry and regulators to deliver safe outcomes fosters investment and enables efficient land access and activity approvals. These principles and practices are especially important for Engineered Geothermal System development which may pose uncertain risks from induced seismicity. The objective based, one-stop-shop, regulatory framework in South Australia (*Petroleum and Geothermal Energy Act 2000*) and the behaviour of the regulator, Primary Industries and Resources – South Australia (PIRSA) are recognized as “a relatively straightforward regulatory system, which could be considered a benchmark for other jurisdictions” (Australian Productivity Commission, 2009).

The regulatory instruments that deliver trust and efficiency in South Australia are: non-prescriptive; allow for innovation while ensuring that operators demonstrate their ability to manage all possible risks to an acceptable level; and entail extensive stakeholder consultation to set standards which are aligned with community expectations.

Operations in South Australia include internationally significant Enhanced Geothermal Systems (EGS) developments. Recognizing EGS is (at least to the public) a new technology with uncertain risks, PIRSA has taken account of international developments, commissioned research and is supporting national cooperation to increase certainty in relation to risk management for EGS operations.

This paper describes practices and technologies that can help to inform activity approvals for EGS operations anywhere.

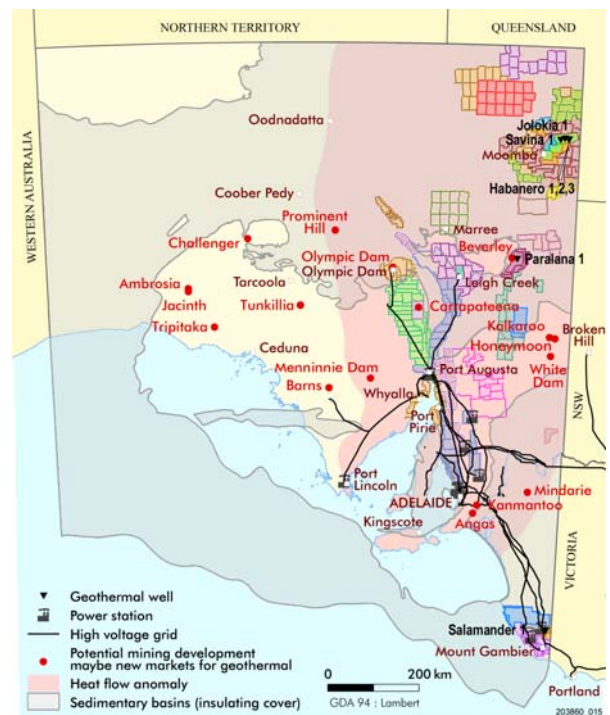
Efficient Co-regulation through Statements of Environmental Objectives (SEOs) and Environmental Impact Reports (EIRs)

The South Australian geothermal licenses shown in figure 1 are governed by the *Petroleum and Geothermal Energy Act 2000* (P&GE Act).

In the context of the P&GE Act, the legal standards set for the protection of natural, social, heritage and economic environments are agreed through a robust, open and transparent research and consultation process that culminates in P&GE Act license operators owning and abiding by SEOs and associated EIRs (Laws, et al, 2002). EIRs detail potential impacts of proposed operations and specify strategies to mitigate risks to as low as reasonably practical (ALARP).

SEOs set standards for area and operation specific compliance with co-regulatory objectives for the sustainability of natural, social, heritage and economic environments. Hence, SEOs enable PIRSA to act as a first-line, one-stop-shop for co-regulation for the full-cycle of geothermal, upstream petroleum, high pressure pipelines and gas storage operations in the State of South Australia.

Figure 1: Figure 1. Geothermal licenses in South Australia and the South Australian Heat Flow Anomaly (adapted from Neumann, et al 2000)



Trust Underpins Efficient Co-regulation

Embedding relevant local, State and Federal objectives and standards into SEOs make a breach of co-regulatory standards a breach of the P&GE Act.

Stakeholders are engaged during the development of EIRs and draft SEOs and usually in a staged process that entails face-to-face meetings. The process for SEO consultation with stakeholders can take 3 months or more depending on the level of impact of the activity, and stakeholder consultation requirements. Given potential for relatively low environmental impacts and sufficient prior publicly developed and disclosed criteria, the Minister (who is an elected Parliamentarian) may agree public consultation may be restricted to a time after a relevant SEO is fully developed for consideration. Public consultation is undertaken for the development of other EIRs and draft SEOs.

Final SEOs, final EIRs and annual statements of licensees' performance against SEOs and the Minister's determinations of the level of environmental impact of proposals are freely available to the public on PIRSA's website. PIRSA also proactively participates in public forums to enable well-informed consideration of risk management strategies put in place to protect natural, social and economic environments.

This openness and transparency underpins trust in PIRSA's roles as first-line regulator for: the integrity of plant and equipment; the protection of: water; air; flora; fauna; landscape; heritage; native (aboriginal) title; and as an interlocutor for disputes between P&GE Act licensees and stakeholders in multiple land use. In addition to the first-line roles listed above, PIRSA also works closely with South Australia's lead agency for the regulation of occupational health, safety and welfare (SafeWorkSA) matters.

Formal agreements and policies explicate mutual expectations and underpin both the efficiency and effectiveness of co-regulation. Hence, licensees have a one-stop-shop for regulation.

Australia's Productivity Commission (2009) review concludes that PIRSA "has a clear mandate, clear regulatory responsibilities, good processes to engage with other agencies, and checks and balances that apply in high risk situations" and "is widely seen as a model for other jurisdictions to emulate".

Geothermal SEOs and EIRs

The P&GE Act requires that any activity can only be conducted if it is covered by an approved SEO for the region and/or land system within which it will be carried out. Hence, geothermal operators must develop appropriate EIRs and SEOs or conclude a bridging assessment to make plain the practicality of adopting and then abiding by pre-existing SEOs for analogous operations in analogous areas. When adopting pre-existing SEOs, the bridging assessment must satisfy relevant co-regulators that location-specific risks are adequately covered in adopted SEOs. If location-specific risks are not already adequately covered, then a new relevant SEO is drafted by the operator for stakeholder consultation. In some instances, SEOs developed for petroleum license activities are adopted for analogous geothermal operations.

EIRs underpin the relevance and contents of SEOs. All licensed field activities must be covered by an SEO approved by relevant Minister(s).

When considering EIRs, PIRSA makes a determination whether proposed activities should be characterized as low-, medium or high-level environmental impact. For activities characterized as:

- Low-impact – PIRSA consults with relevant co-regulatory government agencies.
- Medium impact – PIRSA undertakes public consultation with support from the operator; and

- High impact – an Environmental Impact Statement process is instigated under South Australia's Development Act 1993.

In this way – final SEOs cover all material concerns raised by stakeholders.

Licensees are required to report annually and by exception on their performance against SEOs. Five-yearly reviews consider the efficacy of SEOs and, following the principle of transparency, these reports are available to the public from PIRSA's website.

Table 1 provides examples of EIRs and SEOs that illuminate potential risks, strategies to mitigate risks to as low as reasonably practical and standards for outcomes for geophysical survey and well operations (including drilling) used to date for deep geothermal well operations.

Table 1. Examples of Environmental Impact Reports and Statements of Environmental Objectives (SEOs)

Geophysical Surveys

- State-wide EIR for non-seismic geophysical surveys www.pir.sa.gov.au/_data/assets/pdf_file/0003/50844/EIR_GeoOps_NonSeis.pdf
- State-wide SEO for non-seismic geophysical surveys www.pir.sa.gov.au/_data/assets/pdf_file/0004/50845/SEO_GeoOps_NonSeis.pdf
- Cooper Basin EIR for geophysical operations www.pir.sa.gov.au/_data/assets/pdf_file/0011/27398/cooper_basin_geophysical_operations_eir.pdf
- Cooper Basin SEO for geophysical operations www.pir.sa.gov.au/_data/assets/pdf_file/0010/27397/cooper_basin_geophysical_operations_seo.pdf

Drilling and Well Operations

- Cooper Basin EIR for drilling and well operations www.pir.sa.gov.au/_data/assets/pdf_file/0004/27409/drilling_and_well_operations_eir_february_2003.pdf
- 5-Year Review of Operations, Addendum to Cooper Basin EIR for drilling and well operations www.pir.sa.gov.au/_data/assets/pdf_file/0009/123030/Santos_-_Drilling_and_Well_Ops_EIR_Addendum_-_November_2009_Final.pdf
- Cooper Basin SEO for drilling and well operations www.pir.sa.gov.au/_data/assets/pdf_file/0010/123031/Santos_-_Drilling_and_Well_Operations_SEO_-_November_2009_Final.pdf
- Habanero Well Operations EIR www.pir.sa.gov.au/_data/assets/pdf_file/0018/27441/habanero1_eir_sept2002.pdf
- Habanero EIR and SEO for circulation www.pir.sa.gov.au/_data/assets/pdf_file/0007/27439/habanero_circulation_eir_seo_oct2004.pdf
- Jacaranda Ridge 2 EIR www.pir.sa.gov.au/_data/assets/pdf_file/0010/52588/Adelaide_Energy_PEL_255_Region_EIR.pdf
- Jacaranda Ridge 2 SEO www.pir.sa.gov.au/_data/assets/pdf_file/0010/52597/Final_Adelaide_Energy_PEL_255_SEO.pdf

Geodynamics demonstrated the existing Cooper Basin SEO for drilling and well operations was relevant, and adopted that SEO for its operations in the Habanero, Jolokia and Savina wells.

Petratherm also adopted the Cooper Basin SEO for its Paralana 2 drilling and well operations.

Panax Geothermal has adopted the Otway Basin (Jacaranda Ridge) SEO for its Salamander 1 drilling and well operations.

Responsible Operator's Need to Know Best (Practice)

P&GE Act's non-prescriptive requirements for risk management enable experienced geothermal operators to easily deploy their existing corporate governance standards for risk management for use in South Australia. New entrants to geothermal operations do sometimes express a sense of uncertainty while documenting their own standard operating (including risk management) procedures. This uncertainty leads some relatively new entrants to ask to be told how to operate, as a perceived easier path to attaining competence in managing operational risks. In such cases, PIRSA willingly (and often does) 'hold-the-hand' of new entrant operators ascending learning curves that result in licence-holders adopting or developing their own activity- and area-specific SEOs and EIRs. Operator ownership of activity outcomes (and potential liabilities) also satisfies the government's policy objective that the public is protected from insufficiently managed risks. Additionally, South Australia's non-prescriptive approach allows operators to innovate and manage risks so efficiently as practical to attain standards set for outcomes. Sustainable operations and benign outcomes elicit community trust in both the regulator and industry. This is a virtuous cycle.

Activity Approvals

Local issues for particular field operations are addressed case-by-case during activity approval processes. In the activity approval process, PIRSA reviews: operator capabilities; fitness-for-purpose of plant and equipment; risk assessments concluded by licensees; and site specific environmental impacts. License operators who have demonstrated capabilities that consistently achieve regulatory compliance require low-level surveillance and only need to notify the regulator of activities, rather than seeking case-by-case activity approval.

Advance Notice of Entry

License operators must provide 21 days notice in writing to users of the land that may be affected by specific regulated activities to relevant stakeholders, including PIRSA. Land users have 14 days to raise access-related concerns with the license operator and have the option of raising the concern directly with the regulator, and the final dispute resolution is a Warden's Court proceeding.

Induced Micro-seismicity

The most advanced engineered geothermal system (EGS) projects in Australia are remote from population centers, so experience in Australia will be gained while potential risks of induced micro-seismicity are effectively managed. This experience will be of great value in showing the extent and magnitude of induced micro-seismicity, the reliability of pre-stimulation forecasts, and providing a logical basis for predicting safe distances from fracture stimulation operations in built-up areas.

Regulatory Research for EGS Operations

Many of the geothermal resources in South Australia are expected to be hydraulically fracture-stimulated to achieve optimum (high) rates of heat flow from well-bores. Fracture stimulation of reservoirs inevitably induces seismic events of some measurable magnitude. Proper planning and management of EGS operations can ensure that risks to people, buildings and infrastructure are reduced to as low as reasonably practical and acceptable levels.

To inform regulation, mitigate potential risks and address concerns raised by stakeholders, in 2005, PIRSA contracted University of Adelaide researchers to address a critical uncertainty shared by all geothermal licensees planning to demonstrate EGS in South Australia. That research (Hunt and Morelli, 2006) assessed induced seismicity within the context of local geologic conditions in the Innamincka area of the Cooper Basin, and concluded:

- Granite basement in the Cooper Basin in South Australia is ideally suited to EGS activities in terms of its compressive stress regime (prone to sub-horizontal fracture propagation), low levels of natural background seismicity and the availability of extensive high quality reflection seismic to illuminate faults and fracture trends;
- Reactivation of faults in the vicinity of the Habanero site is unlikely. This is due to the nearby faults being beyond the reach of the induced seismicity associated with EGS activity.
- Induced seismic events at the Habanero well site in the Cooper Basin could reasonably be expected to fall below a ground acceleration of 0.05 g, which is a safe level for the Habanero location and its surrounds.

These findings informed the regulator and stakeholders that the fracture stimulation of geothermal wells in the Innamincka area of the Cooper Basin could be safely managed so that micro-seismic events induced during the fracture stimulation:

- would be well below potentially damaging levels;
- were unlikely to induce slip and consequent, larger seismic events on larger geological faults; and
- were unlikely to create hydraulic communication between the stimulated granite (basement) zones below 4,000 metres and the overlying sedimentary Cooper Basin above 3,700 metres.

This last finding is based on:

- the prevailing, natural, highly compressive stress regime acting to constrain fracture propagation to sub-horizontal intervals;
- acceleration attenuation is at least one order of magnitude greater in soft rocks and soils than in crystalline rocks; and
- high frequency motion is attenuated more quickly with distance than low frequency

motion and the seismic events induced during fracture stimulation and pumping into Hot Fractured Rocks (HFR) are characteristically high frequency (100–500 Hz).

Indeed, fracture stimulation and injection programs in Geodynamics' Cooper Basin Habanero wells were both conducted safely and were successful in the enhancement and flow testing of EGS reservoirs.

Risk Management for Induced Seismicity

Given the results in the Cooper Basin, and looking forward to many additional EGS projects in Australia (and South Australia, in particular), PIRSA commissioned the development of risk management protocols for induced seismicity associated with EGS reservoir development in 2007. The findings (Morelli and Malavazos 2008) are fully consistent with the findings of Majer, Baria and Stark (2008) and are summarized in Table 2.

Running Ahead of the Frac Crew

An informed risk assessment for EGS operations starts with an analysis of:

- historical (monitored) earth movements magnitude and location; and
- geophysical survey data to relate earth movements to faults and fracture trends.

The adequacy of seismic monitoring arrays has a bearing of the certainty of seismic event magnitudes, locations and sense of motion, and hence the usefulness of recorded (historical) base-line information. Equipment capable of sensing seismicity (detectability) may only provide complete records of all movements at a higher level (completeness), because instrumentation maybe insufficient to detect many small events. The seismic monitoring stations in South Australia are depicted in Figure 2. Additional seismic monitoring stations are located in adjacent jurisdictions. The locations of four additional stations in South Australia have been agreed between State and Federal Government agencies (as shown in Figure 2) and the equipment to be deployed will enhance both the completeness and accuracy of measuring seismic events.

The detection limits of the existing seismograph network in and around South Australia is variable (as shown in Figure 2, based on Dent, 2009), and this array is reliably locating all events above Richter magnitudes of 3.5 (e.g. recording is complete for events >3.5) and is more resolute (complete for events above Richter magnitudes of 2.0) for settled areas. This is considered sufficient to manage public safety under current circumstances. If required, existing networks can be augmented to provide higher resolution of the location and depth of hypocentres.

Table 2 Information that can most help to inform activity approvals (or otherwise) for the fracture stimulation of geothermal reservoirs includes:

- Characterization of the local environment, infrastructure and population for vulnerability to ground movements and loss modeling (taking account of design standards)
- High-quality records of seismicity waveforms, magnitude and location;
- Thickness and shear velocity of soil and weathered cover over bedrock. Measuring shear velocities to 30 metres depth is a generalized suggestion;
- Reservoir data for characterization – including:
 - Orientation and magnitude of stress fields;
 - Location, extent of faults and fracture trends;
 - Mechanical, thermal and chemical rock properties, and
 - Hydrologic parameters (extent, pressure, chemistry and nature of confining aquitards)
- Conclude loss modeling (taking account of design standards and infrastructure that pre-dates design standards)

Non-exhaustive protocols for credible risk management for geothermal operations that may induce seismicity

- Apply national or international standards for risk management
- Proponent to demonstrate adequate assessment of potential consequence of induced seismicity for sites selected for hydraulic stimulation or large scale injection.
- Stakeholder engagement to start as soon as is practical
- If required, augment the existing seismic monitoring network to detect and gather seismic events of magnitudes (Richter scale) less than 3. It will be advantageous to deploy seismic monitoring stations to:
 - Continuous digital high sample frequency (≥ 100 htz) recording;
 - Attain adequate network to accurately locate seismic events and measure attenuation; and
 - Geophysical surveys to calibrate regolith response models at EGS locations.
- Maintain the seismic monitoring network for the life of the project.
- As practical, deploy at least one sub-surface seismic monitoring station (below regolith if possible) prior to hydraulic stimulation or large scale injection.
- Deploy down-hole and near surface monitoring stations to determine attenuation and regolith amplification.
- Sustain an evergreen watching brief so new information is assessed and considered for induced seismicity risk management.

The location and magnitude of historical, recorded earth movements in South Australia are depicted in Figure 3. This map does not express the uncertainty of epicenter locations, but this uncertainty is a factor considered when assessing potential risks posed by EGS operations.

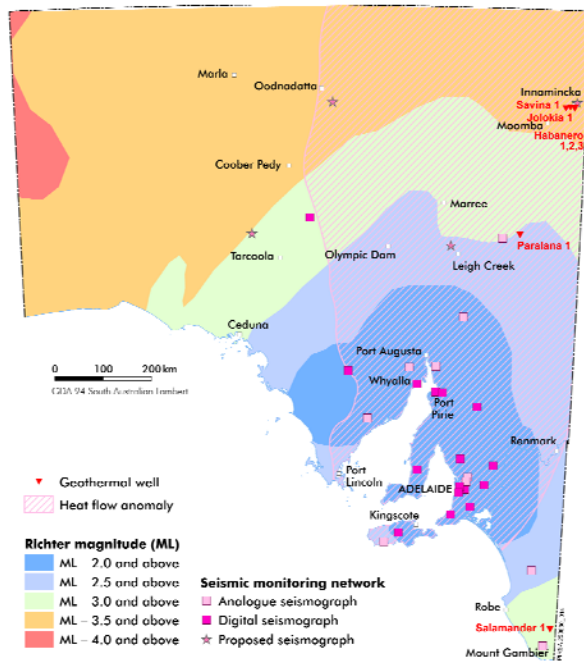
The most advanced EGS projects in Australia are those of Geodynamics (Habanero, Jolokia and Savina wells – see figure 1) and Petratherm (Paralana 2 – see figure 1). Only Habanero wells have been fracture stimulated by year-end 2009. High resolution seismic monitoring arrays have been installed at Habanero and Paralana to better measure both background seismicity and seismicity induced during stimulation, production and circulation operations. The array positioned at Habanero can detect and locate events as low as -2.5 (Richter scale) at a depth of 5 km, with a 3D

locational accuracy of about 30metres, but the completeness of accurately computing all events is probably limited to -1 (Richter scale). Networks can be augmented as required to provide greater resolution and completeness of the epicenter locations.

Hot Sedimentary Aquifer projects that do not require fracture stimulation and entail well operations largely analogous to petroleum well operations do not necessarily need to deploy seismic monitoring arrays.

Reflection seismic is useful to optimize drilling locations for EGS targets. Figure 4 depicts vast areas in the South Australian Heat Flow Anomaly that are remote from population centers, and covered with at least some modern reflection seismic information.

Figure 2. Locations and approximate capability of seismograph network in South Australia (including use of seismographs in adjacent States and the Northern Territory). Adapted from Dent, 2009. The South Australian Heat Flow Anomaly is also shown (adapted from Neumann, et al 2000).



Tools of Trade in Assessing Attenuation

Standards for attenuation for induced seismicity need be locally appropriate. The largest recorded magnitude seismic event associated with EGS operations at Habanero in the Cooper Basin determined to be of magnitude 3.7 on the Richter scale e.g. an event felt but one that would rarely cause damage, and which had no significant negative impacts on local social, natural or economic environments.

Analysis of natural and induced seismicity (associated with EGS operations in the term 2003-5) in the Innamincka region in the Cooper Basin, Hunt and Morelli (2006) found:

- natural seismicity can be expected to range between Richter magnitudes of 3.5 and 4.0 once every 50 to 167 years;
- the largest event in the area prior to 2003 was in 1979 with magnitude 2.9;

- the Australian Building Code AS 1170.4 - (1993) characterizes this region as having a 10% chance in 50 years of experiencing a peak ground acceleration of 0.05g, and
- the calculated maximum peak ground acceleration from EGS operations in the Habanero wells is 0.041g, which for this location.

Figure 3 Location and magnitude of historical earth movement epicenters in South Australia. The South Australian Heat Flow Anomaly is also shown (adapted from Neumann, et al 2000).

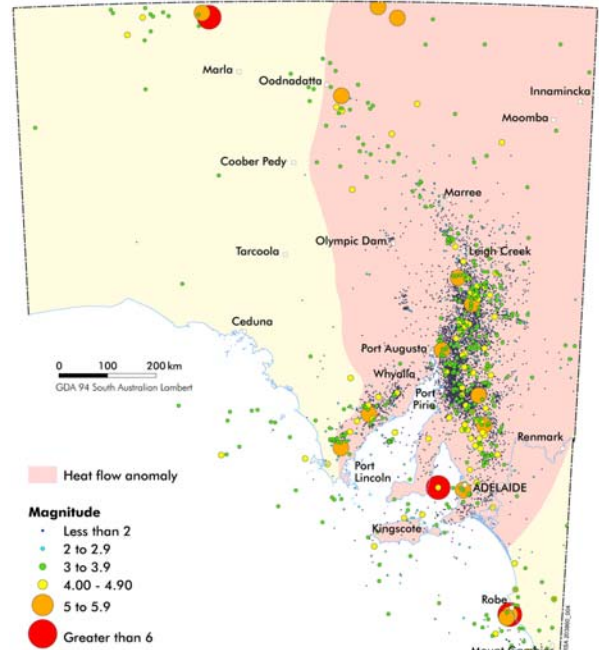
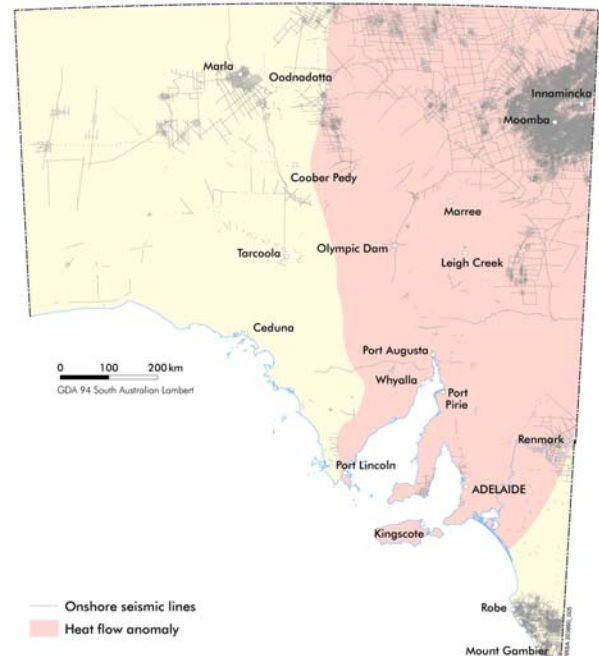


Figure 4. Reflection seismic lines (2D and 3D surveys) onshore South Australia. The South Australian Heat Flow Anomaly is also shown (adapted from Neumann, et al 2000)



Using Toro's (1997) relationships, Hunt and Morelli (2006) mapped the attenuation distance of peak ground acceleration in units of gravity (g) and distance (in kms) from the Habanero site as redisplayed here in figure 5.

Figure 5. Toro (1997) relationship calculation of attenuation distance of peak ground acceleration in units of gravity (g) and

distance (in kms) generated at the Habanero well locations near Innamincka in the Cooper Basin. From fig.8 in Hunt and Morelli, 2006)

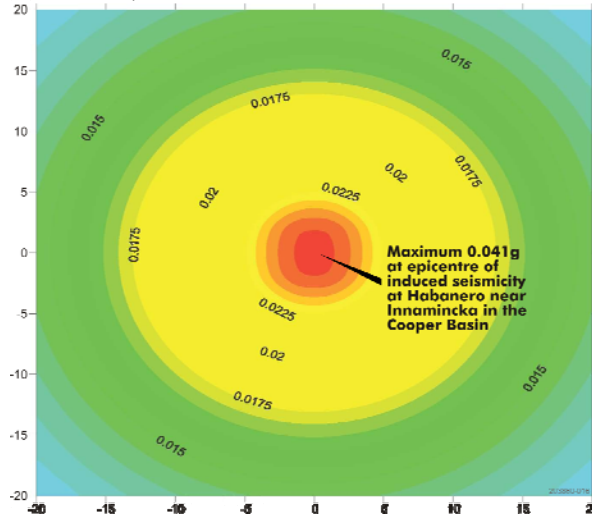
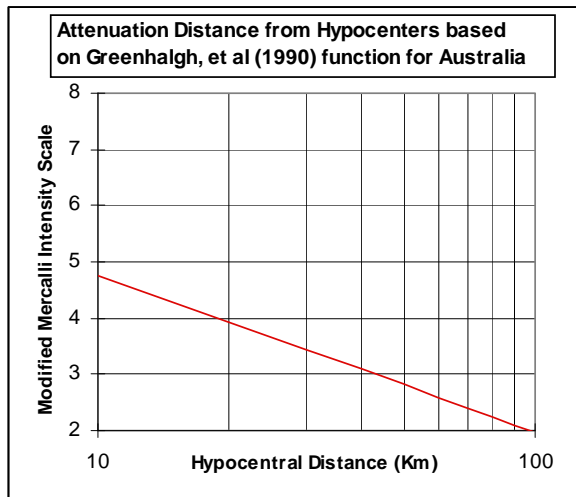


Figure 6. Estimated attenuation of earth movement intensity of a Richter scale 3.7 magnitude seismic event with distance from an event hypocenter in northeast South Australia.



Another approach is illustrated with Figure 6, which is output from a spreadsheet tool developed by PIRSA (Love, 2009) that uses estimates of earth movement (seismic wave) velocities to forecast modified Mercalli scale intensity attenuation with distance from hypocentres. This spreadsheet tool estimates intensity attenuation based on five functions published in: Bierbaum, et al, 1994; Gaull, et al 1990; Greenhalgh, et al, 1990; and Greenhalgh, et al 1994. The Greenhalgh, et al (1994) function for Australia is considered the best approximation of these five correlations to characterise seismicity induced during EGS operations in the Cooper Basin in South Australia. More detailed analyses (akin to the analysis illustrated in figure 5) are expected to be concluded by EGS operators to optimise fracture stimulation programs, assess potential hazards, and underpin consultation with stakeholders. Based on this correlation (figure 6), the maximum (3.7 on the Richter scale) recorded event at Habanero is characterised as having attenuated to a modified Mercalli scale intensity of 4.8 at 10 km distance from the hypocenter and diminished to a slight

intensity at a distance 20 km from the hypocenter e.g. <4 on the modified Mercalli scale, similar to vibration from the passing of a truck. Further experience in remote locations will provide calibration for predictive modeling of EGS operations.

Perfect predictions?

One of the best predictors of large seismic events (as geo-hazards) are Gutenberg-Richter plots of Richter scale magnitude (on a linear scale x-axis) versus the number of recorded events (for a given area) exceeding Richter scale magnitude (on a log scale y-axis). Gutenberg-Richter plots can be interpreted to define maximum magnitudes in a given area, but those interpreted maximum magnitudes are generally too high to be of much practical use. More usefully, Gutenberg-Richter plots define predictable potentially harmful events where not-so-harmful (moderately-sized) earth movements are relatively frequent, and are used to inform risk management standards. It seems intuitively obvious that low levels of modest magnitude natural seismicity corresponds to a lower probability of more harmful events, but there is not yet enough empirical calibration of this hypothesis to draw associated categorical conclusions.

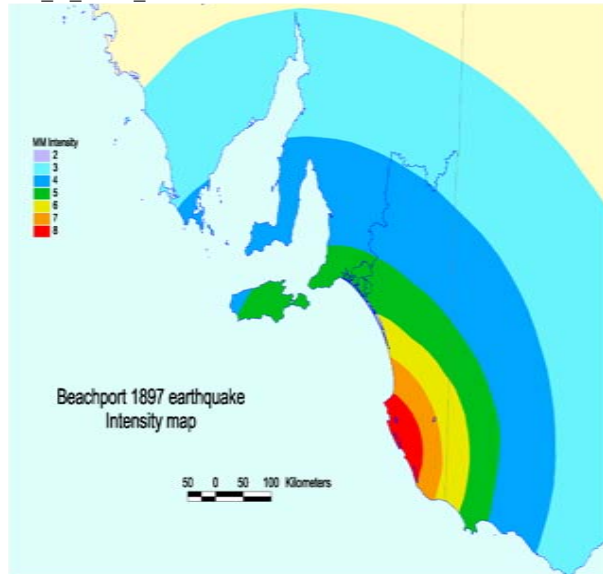
Acknowledging the need for further calibration, as proposed by Majer, et al (2006), real-time analysis of induced seismicity provides an opportunity to set thresholds and gain experience from 'traffic light' risk management during fracture stimulation (pumping) and production of geothermal reservoirs. Experience gained in geohazard risk management associated with dams and mine operations can also provide insights for EGS operations.

Pre-stress tested regions?

The extent of influence of seismic events can be mapped in terms of intensity (and also velocity and acceleration) to levels of accuracy enabled by monitoring systems. Figure 7 illustrates Modified Mercalli intensity based on newspaper reports of damage caused by the largest (6.5 Richter scale magnitude) earthquake documented in South Australia since 1837. This earthquake in southeast South Australia caused significant damage at Kingston, Robe and Beachport, and caused minor damage 312 kilometres to the north in Adelaide. It was felt as far away as Port Augusta (592 kilometres north from Beachport) and Melbourne (437 kilometres east from Beachport). Several cases of liquefaction were recorded and it is thought that the epicentre was offshore. No tsunami was reported, but aftershocks continued for months.

Trustworthy modeling methods and operational protocols to mitigate potential risks of induced seismicity remain high priority research objectives.

Figure 7. Intensity map of the Beachport (South Australia) earthquake of 10 May 1897 based on print media reports from http://www.pir.sa.gov.au/minerals/earthquakes/major_earthquakes_in_south_australia.



Better Baseline Data

A unique opportunity arises for cooperation to efficiently meet multiple objectives for public safety, and exploration for EGS, unconventional gas reservoir sweet-spots and geosequestration.

This would entail cooperation of: government agencies responsible for assessing geo-hazards associated with earth movements; proponents of developing fractured reservoirs for the production of heat energy (e.g. EGS); proponents of developing coal bed methane, shale gas and tight gas reservoirs; and proponents of subsurface greenhouse gas storage

In particular – it will be advantageous for companies exploring for reservoir sweet-spots related to tensile rock fabrics and seismically quiescent storage reservoirs and relevant government agencies to coordinate plans in the context of:

- publically managed seismic monitoring networks, so those networks are augmented with multiple objectives in mind;
- privately installed monitoring stations become public assets, post-decommissioning of industry's projects; and
- national and international forums to foster interoperability of databases and software applications (input and output).

Cooperation will advance both knowledge of induced seismicity risks and reservoir development opportunities.

Conclusions

1. Co-regulatory efficiency and effectiveness for geothermal operations can be delivered with an objective-based and transparent one-stop-shop approach as applied in South Australia.
2. PIRSA's research into potential risks posed by EGS operations has informed regulatory approvals for fracture stimulation operations in geothermal wells in areas that are remote from population centers.

3. The magnitude and extent of micro-movement induced by fracture stimulation and injection at Habanero in the Cooper Basin were largely as predicted e.g. EGS reservoirs were created and circulated without adverse impacts.
4. Calibration of predictive models for the risk management of induced seismicity in remote locations will provide benchmarks for the regulation of EGS projects nearer to populated locations.
5. Australia is becoming a globally important laboratory for EGS operations.
6. Given enough experience – risk management strategies for fracture stimulating and injecting into geothermal reservoirs are expected to evolve and EGS operations are expected to become predictably profitable and reliably safe. The outcome will be wide-spread community and investor trust in EGS development.

References

- Australian Building Code AS 1170.4 (1993), Minimum design loads on structures. Part 4 Earthquake Loads. The Australian Standard was prepared by Committee BD/6, Loading on Structures. It was approved on behalf of the Council of Standards Australia on 21 April 1993 and published on 16 August 1993. A 2007 update of this reference is available for purchase from the sales agent for Standards – Australia from: <http://infostore.saiglobal.com/store2/Details.aspx?ProductID=215710>.
- Bierbaum, S. J, 1994. Earthquake hazard and micro-tremor analysis, South Australia" Honours Thesis, Flinders University of South Australia, Australia. Quotes formula used in Love (2009) that was developed by K. Malpas.
- Dent, V. F., 2009. Seismic network capability and magnitude completeness maps, 1960 – 2005 for West Australia, South Australia and the Northern Territory, proceedings from the Australian Earthquake Engineering, Society Conference, Newcastle, NSW, Australia, 11-13 December 2009 (see: <http://www.aees.org.au/Proceedings/Proceedings.html>).
- Gaull, B. A., Michael-Leiba, M. O., and Ryan, J. M. W., 1990; Probabilistic earthquake risk maps of Australia, Australian Journal of Earth Sciences v 37 pp 169-187.
- Greenhalgh S. A., and McDougall, R. M. 1990. Earthquake Risk in South Australia, Australian Civil Engineering Transactions v 32 no 3.
- Greenhalgh S. A., Love, D., Malpas, K., and McDougall, R. M. 1994. South Australian earthquake, 1980-92, Australian Journal of Earth Sciences v 41 pp 483-495.
- Hunt, S.P. and Morelli, C., 2006. Cooper Basin HDR hazard evaluation: predictive modelling of local stress changes due to HFR geothermal energy operations in South Australia. South Australia Department of Primary, Industries and Resources. Report Book 2006/16.

Laws, R. A., Aust, T. and Malavazos, M., 2002. Environmental regulation of the upstream petroleum industry in South Australia. *The APPEA Journal*, 42 (1), 683–96.

Love, D., 2009. unpublished spreadsheet to calculate intensity attenuation with distance from hypocentres, Primary Industries & Resources – South Australia.

Majer, E., Baria, R., Stark, M., Smith, B., Oates, S., Bommer, J., and Asanuma, H. (2006). *Induced Seismicity Associated with Enhanced Geothermal Systems*. Available at: <http://www.iea-gia.org/documents/ISWPf1MajerWebsecure20Sep06.doc>

Majer, E., Baria, R. and Stark, M. (2008). Protocol for induced seismicity associated with enhanced geothermal systems. Report produced in Task D Annex I (9 April 2008), International Energy Agency-Geothermal Implementing Agreement (incorporating comments by: C. Bromley, W. Cumming, A. Jelacic and L. Rybach). Available at: <http://www.iea-gia.org/publications.asp>.

Morelli, C., and Malavazos, M. (2008), "Analysis and Management of Seismic Risks Associated With Engineered Geothermal System Operations in South Australia, in Gurgenci, H. and Budd, A. R. (editors), *Proceedings of the Sir Mark Oliphant International Frontiers of Science and Technology Australian Geothermal Energy Conference*, Geoscience Australia, Record 2008/18, pp 113-116. Download from

http://www.ga.gov.au/image_cache/GA11825.pdf
Neumann, N., M. Sandiford, J. Foden, 2000. Regional geochemistry and continental heat flow: implications for the origin of the South Australian heat flow anomaly *Earth and Planetary Science Letters*, 183 pp. 107-120.

Productivity Commission, 2009, *Review of Regulatory Burden on the Upstream Petroleum (Oil and Gas) Sector*, Research Report, April 2009, Melbourne, Australia. Published by the Commonwealth of Australia. Download from: http://www.pc.gov.au/__data/assets/pdf_file/0011/87923/upstream-petroleum.pdf

South Australian Government (2009), *Petroleum and Geothermal Energy Act 2000*, as amended in December 2009. Download from: <http://www.legislation.sa.gov.au/LZ/C/A/PETROLEUM%20AND%20GEOTHERMAL%20ENERGY%20ACT%202000.aspx>.

Toro, G.R., N.A. Abrahamson and J.F. Schneider (1997). A Model of Strong Ground Motions from Earthquakes in Central and Eastern North America: Best Estimates and Uncertainties. *Seismological Research Letters*, v.68, no. 1, pp. 41-57.

USGS, 2009. The Modified Mercalli Intensity Scale. Abridged from *The Severity of an Earthquake*, USGS General Interest Publication 1989-288-913. Webpage updated 27 October 2009 at: www.earthquake.usgs.gov/learn/topics/mercalli.php

p

Acknowledgments

The authors thank Ladsy Rybach (GeoWatt), Roy Baria (EGS-Energy) and PIRSA colleagues for their kind inputs, especially James Coda, Belinda Hayter Carice Holland, Peter Hough, and Shane Farrelly.

Keywords: geothermal, EGS, induced seismicity, attenuation distance, one-stop-shop regulation, geohazards

GREAT EXPECTATIONS FOR GEOTHERMAL ENERGY – FORECAST TO 2100

Goldstein, B.A., Hiriart, G., Tester, J., B., Bertani, R., Bromley, Gutierrez-Negrin, L., C.J Huenges, E., H, Ragnarsson, A., Mongillo, M.A. Muraoka, and V. I. Zui,

INTRODUCTION

Geothermal energy systems have: a modest environmental footprint; compared to many renewable and conventional alternatives ; will not be impacted by climate change; and have potential to become the world's lowest cost source of sustainable thermal fuel for zero-emission, base-load direct use and power generation. Displacement of more emissive fossil energy supplies with geothermal energy can also be expected to play a key role in climate change mitigation strategies. In this context, shared challenges on the road to a global portfolio of safe, secure, competitively priced energy supplies are drivers for international cooperation in research, exploration, pilot demonstration and pre-competitive development of geothermal energy resources and technologies.

The intellectual and financial inputs for international, pre-competitive initiatives are coming from public and private investors with aspirations for low emissions, affordable, and globally deployable 24/7 energy supplies. It is reasonable to conclude that the outcomes (improved technologies and methods) of these collective efforts over the next 20 years will underpin great expectations for widespread, profitable and environmentally sustainable use of geothermal energy for centuries to come. This paper provides a synopsis of recent findings and current objectives of notable international fora enabling cooperation to reduce impediments to widespread use of geothermal energy.

SHARING OF PRE-COMPETITIVE KNOWLEDGE

The co-authors of this paper have supported one or more of the international geothermal energy fora listed in Table 1.

Table 1. Names and websites of 10 key international geothermal energy fora

International Energy Agency's Geothermal Implementing Agreement (IEA GIA)	http://www.iea-gia.org/
International Geothermal Association (IGA) and its World Geothermal Congress (WGC) ^(a)	http://www.geothermal-energy.org/
International Partnership for Geothermal Technologies (IPGT) ^(a)	http://internationalgeothermal.org/
Geothermal Engineering Integrating Mitigation of Induced Seismicity in Reservoirs (GEISER)	http://www.geiser-fp7.eu/default.aspx
ENhanced Geothermal Innovative Network for Europe (ENGINE)	http://engine.brgm.fr/
European Energy Research Alliance Joint Programme on Geothermal Energy (EERA JPGE)	http://www.eera-set.eu/index.php?index=36
European Geothermal Energy Council (EGEC)	http://www.egec.org/
Geothermal Resource Council (GRC) and its annual conference in particular	http://www.geothermal.org/
Geothermal Resource Association (GEA)	http://www.geo-energy.org/
Stanford University Geothermal Workshops	http://pangea.stanford.edu/ERE/research/geoth/conference/workshop.html
International Panel for Climate Change (IPCC) Working Group III – Special Report on Renewable Energy (and in particular Chapter 4 – Geothermal)	http://www.ipcc-wg3.de/publications/special-reports/special-report-renewable-energy-sources

SHARED CHALLENGES BEGET COMPLEMENTARY ACTION

Improved, evermore reliable, cost-effective methods to enhance the productivity of geothermal systems will be essential to the competitiveness of geothermal resource in energy markets. In particular, the commercialisation of fracture and/or chemical stimulation methods to reliably create Engineered Geothermal Systems (EGS) will be one key milestone on the road to great expectations for widespread economic use of geothermal energy. A scan of the objectives of the international geothermal energy fora define the high priorities summarized in Table 2.

Table 2. Twenty key priorities for international geothermal energy fora. This is an update priorities presented in Goldstein et al., 2009.

1. Openness to cooperation to engender complementary research and the sharing of knowledge	2. Informing industry experts, government policy makers and the public at large through presentations, publications, websites, submissions to enquiries and the convening of conferences, workshops and courses
3. Creating effective standards for reporting geothermal operations, resources and reserves	4. For EGS, improved hard rock drill equipment
5. Predictive reservoir performance modelling	6. For EGS, improved multiple zone isolation
7. Predictive stress field characterisation	8. For deep EGS, reliable submersible pumps
9. For EGS, mitigate induced seismicity	10. Longevity of well cement and casing
11. Condensers for high ambient-surface temperatures	12. For EGS: Optimum fracture stimulation methods
13. Use of CO ₂ as a circulating fluid	14. High temperature logging tools and sensors
15. Improve power plant design	16. High temperature flow survey tools
17. Technologies & methods to minimise water use	18. High temperature fluid flow tracers
19. Predict heat flow and reservoirs ahead of the bit	20. Mitigation of formation damage, scale and corrosion

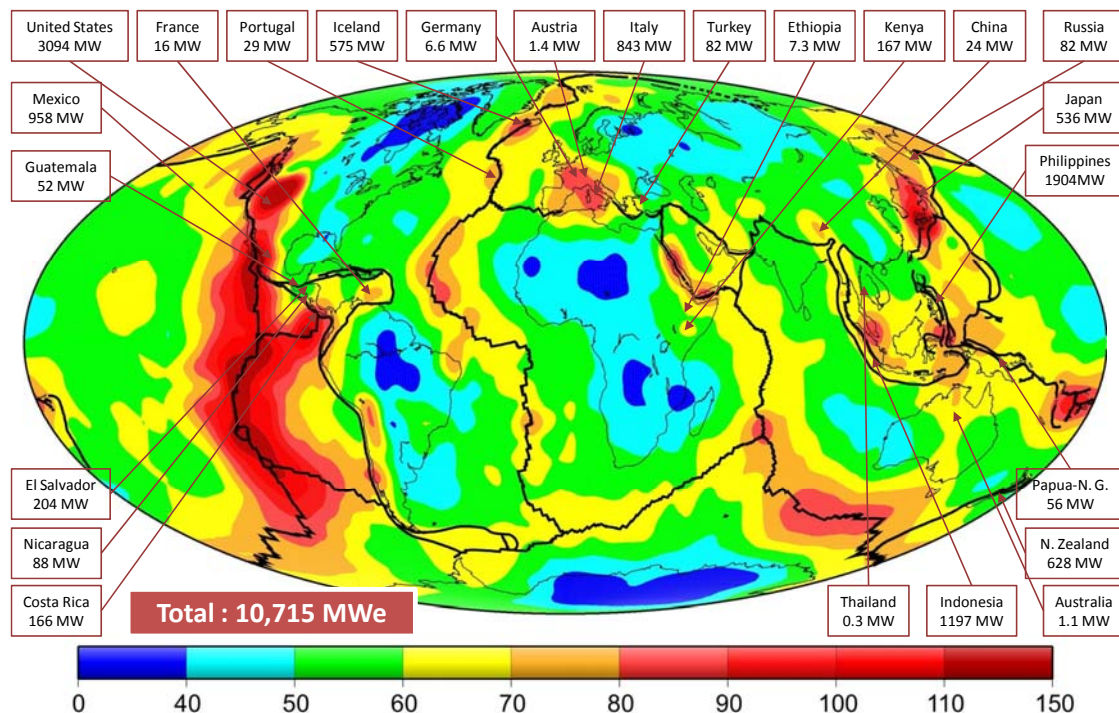


Figure 1 Geothermal-electric installed capacity by country in 2009. Figure shows worldwide average heat flow in mW/m² and tectonic plates boundaries (illustration adapted from a figure in Hamza et al., 2008 with data from Bertani, 2010). This map of heat flow does not reconcile all geothermal information. The delineation of geothermal resources will be improved by integrating temperature gradient, heat flow and reservoir data.

INFORMING POLICY MAKERS AND THE PUBLIC AT LARGE

WORLD REPORT - GEOTHERMAL ENERGY USE

Geothermal energy supplies are currently used to generate base-load electricity in 24 countries with an installed capacity of 11 gigawatts of electricity (GWe) and a global average capacity factor of 71%, with newer installations above 90%, providing 10% to 30% of their electricity demand in six countries (Bertani, 2010). Figure 1 is a map of estimated heat flow in milliwatts per square metre ($W \times 10^{-6} / m^2$) annotated with geothermal electricity generation capacity by country. Geothermal energy supplies are also used for direct use applications in 78 countries, accounting for 50 GW thermal including district (space) heating and cooling and ground-source (geothermal) heat pumps (GHPs), which have achieved significant market penetration worldwide (Lund et al., 2010).

BUILD (INNOVATE) AND MARKET BETTER MOUSE-TRAPS

The obvious generalised impediments to massive, global geothermal energy use are:

- currently insufficiently predictable reliability of geothermal reservoir performance (and in particular, the predicable reliability of engineered geothermal system reservoirs); and
- current costs of geothermal well deliverability (and in particular, fluid production levels from stimulated engineered geothermal systems and the high costs of drilling deep wells)

Hence, the over-arching common and well justified objectives of global government initiatives are to stimulate technologic and learn-while-doing breakthroughs that will lead to a point where the cost of geothermal energy use is reliably cost-competitive and comparatively advantageous within markets.

MARKET (COMMUNICATE!)

Geothermal resources contain thermal energy that can be produced, stored and exchanged (flowed) in rock, gas (steam) and liquids (mostly water) in the subsurface of the earth.

With proper management practice, geothermal resources are sustainable and renewable over reasonable time periods. As stored thermal energy is extracted from local regions in an active reservoir, it is continuously restored by natural conduction and convection from surrounding hotter regions, and the extracted geothermal fluids are replenished by natural recharge and by reinjection of the exhausted fluids. Additionally:

- geothermal plants have low- to emissions-free operations and relatively modest land footprints. The average direct emissions yield of partially open cycle, hydrothermal flash and direct steam electric power plants yield is about 120 g CO₂/kWh¹. Current binary cycle plants with total reinjection yield less than 1 g CO₂/kWh in direct emissions. Emissions from direct use applications are even lower (Fridleifsson et al., 2008). Over its full life-cycle (including the manufacture and transport of materials and equipment), CO₂-equivalent emissions range from 23-80 g/kWh for binary plants (based on Frick et al. 2010 and Nill, 2004) and 14-202 g/kWh for district heating systems and GHPs (based on Kaltschmitt, 2000). This means geothermal resources are environmentally advantageous and the net energy supplied more than offsets the environmental impacts of human, energy and material inputs;
- geothermal electric power plants have characteristically high capacity factors; the average for power generation in 2009 is 71% (67,246 GW_{electrical} used from installed capacity of 10.714 GW_{electrical} based on Bertani, 2010), and modern geothermal power plants exhibit capacity factors greater than 90%. This makes geothermal energy well suited for base-load (24/7), dispatchable energy use;
- the average estimated 27.5% capacity factor for direct use in 2009 (121.7 TWh_{thermal} used from installed capacity of 50.6 GW_{thermal} based on Lund, et al., 2010) can be improved with smart grids (as for domestic and industrial solar energy generation), by employing combined heat and power systems, by using geothermal heat absorptive and vapour compression cooling technology, and by expanding the distributed use of ground source heat pump energy generation; and
- properly managed geothermal reservoir systems are sustainable for very long term operation, comparable to or exceeding the foreseeable design-life of associated surface plant and equipment.

CHARACTERISING GEOTHERMAL RESOURCES, RESERVES AND SUPPLIES

The theoretical global geothermal resource base corresponds to the thermal energy stored in the Earth's crust. The technical (prospective) global geothermal resource is the fraction of the earth's stored heat that is accessible and extractable for use with foreseeable technologies, without regard to economics. Technical resources can be subdivided into three categories in order of increasing geological confidence: inferred, indicated and measured (AGEG-AGEA, 2009), with measured geothermal resources evidenced with subsurface information to demonstrate it is useable. Geothermal reserves are the portion of geothermal resources that can confidently be used for economic purposes. Geothermal reserves developed and connected to markets are energy supplies. Accessible geothermal resources are enormous as detailed in Figure 2. Resources size is clearly not a limiting factor for global geothermal energy development.

¹ This is the weighted average of 85% of the world power plant capacity, according to Bertani and Thain, 2002, and Bloomfield et al., 2003

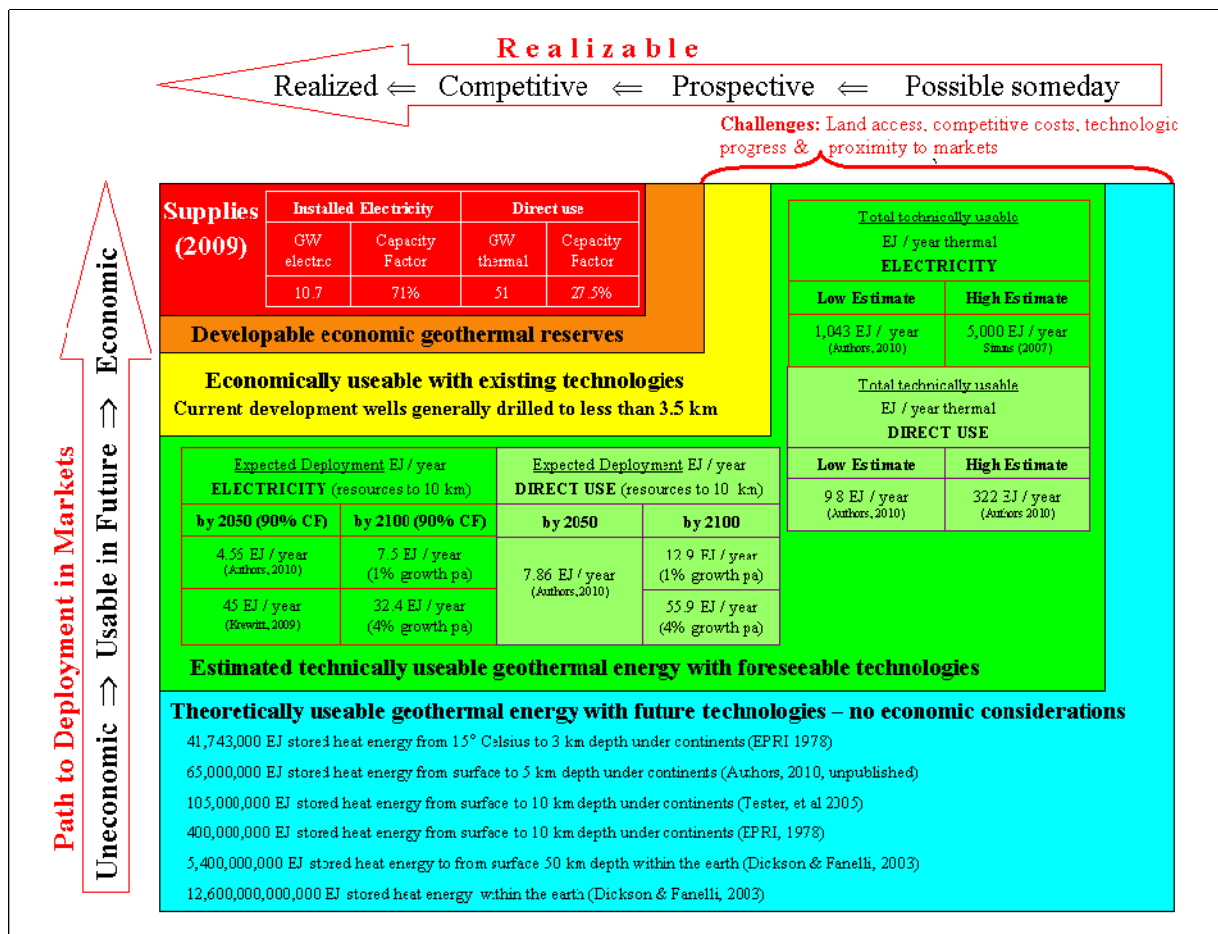


Figure 2. Potential geothermal energy resources split into categories e.g. theoretical, technical, economic, developable and existing supplies for power generation and direct use. All categories for power generation assume a 71% capacity factor and 8.1% average efficiency for converting thermal into electrical energy, though both factors will likely improve (increase) in future. All direct use estimates assume an average 31% capacity factor, somewhat higher than the average (27.5%) in 2009. Adapted from a figure developed by Ladsy Rybach and published in the Proceedings of the Joint IEA-GIA-IGA Workshop: Geothermal Energy Global Development Potential and Contribution to Mitigation of Climate Change, 5-6 May 2009, Madrid, Spain, edited by M.A. Mongillo, 20 March 2010

FAQ: WHAT IS GEOTHERMAL ENERGY AND HOW DOES IT WORK? (COMMUNICATE!)

Geothermal energy is the terrestrial heat stored in, or discharged from rocks and fluids (water, brines, gases) saturated pore space (including fractures), and is widely harnessed in two ways: for power (electricity) generation; and for direct use e.g. heating, cooling, aquaculture, horticulture, spas and a variety of industrial processes, including drying. The use of energy extracted from the constant temperatures of the earth at shallow depth by means of ground source heat pumps (GSHP) is a common form of geothermal energy use. The direct use of natural flows of geothermally heated waters to surface have been practised at least since the Middle Palaeolithic (Cataldi, 1999), and industrial utilisation began in Italy by exploiting boric acid from the geothermal zone of Larderello, where in 1904 the first kilowatts of electric energy (kWe) were generated and in 1913 the first 250-kWe commercial geothermal power plant was installed (Burgassi, 1999).

Where very high temperature fluids (> 180° C) flow naturally to surface (e.g. where heat transfer by conduction dominates), geothermal resources are the manifestation of two factors:

- a geologic heat source to replenish thermal energy; and
- a hydrothermal reservoir that can be tapped to flow geothermal fluids for its direct use and/or for generating electricity.

Elsewhere, a third geologic factor, the insulating capacity of rocks (acting thermal blankets) is an additional necessary natural ingredient in the process of accumulating usable, stored heat energy in geologic reservoirs that can be tapped to flow heat energy, and replenished by convective, conductive and radiated heat flow from sources of geothermal energy.

Usable geothermal systems occur in a variety of geological settings. These are frequently categorized as follows: **1.** High-temperature ($>180^{\circ}\text{C}$) systems at depths above (approximately) 3.5 km are generally associated with recent volcanic activity and mantle hot spot anomalies. Other high temperature geothermal systems below (approximately) 3.5 km are associated with anomalously high heat producing crustal rocks, mostly granites. **2.** Intermediate temperature systems ($100\text{-}180^{\circ}\text{C}$) and **3.** Low temperature ($<100^{\circ}\text{C}$) systems Both intermediate and low temperature systems are also found in continental settings, formed by above-normal heat production through radioactive isotope decay; they include aquifers charged by water heated through circulation along deeply penetrating fault zones. However, there are several notable exceptions to these temperature-defined categories, and under appropriate conditions, high, intermediate and low temperature geothermal fields can be utilised for both power generation and the direct use of heat. Also, solar energy absorbed at the surface is sometimes included as geothermal energy, irrespective of its different source of heat energy. Offshore geothermal resources are also sometimes included in lists of ocean energy systems (Hiriart, et al, 2010).

Geothermal systems can also be classified as: *convection-dominated systems*, which include liquid- and vapour-dominated hydrothermal systems; conduction-dominated systems which include hot rocks; and hybrid systems that are sourced from convection, conduction and high heat producing source rocks. Geologic aquifers that overlie radiating sources of heat, and gain heat via convection and/or conduction are sometimes called hot sedimentary aquifer systems.

The most widely recognised manifestations of geothermal energy are related to convective heat flow, including: hot springs and geysers (e.g. the movement of hot water to land surface); volcanoes (e.g. the movement of magma to land surface and sea floors); and certain forms of economically significant minerals deposits resulting from the injection of geothermally heated fluids into lower temperature levels where minerals crystallize and are accumulated.

Geothermal wells produce naturally hot fluids contained in hydrothermal reservoirs from a continuous spectrum of natural high to low permeability and porosity (including natural fractures). The capacity of geothermal reservoirs to flow hot fluids can be enhanced with hydraulic fracture stimulation and acidization, creating artificial fluid pathways in Enhanced or Engineered Geothermal Systems (EGS) as well described in detail in Tester, et al (2006). Once at surface, heated fluids can be used to generate electric energy in a thermal power plant, or used in other applications requiring heat, as heating and cooling of buildings, district heating systems, aquaculture, agriculture, balneology, industrial processes and mineral drying. Space heating and cooling can also be achieved with GHP systems.

The number, depth and diameter of geothermal energy production wells vary with local requirements for direct use and electricity power plants. Higher temperatures and higher flow rates result in more thermal energy production per well. Wells drilled to depths down to 3.5 km in volcanic areas frequently produce high temperature ($> 180^{\circ}\text{C}$) fluids to surface. Indeed, temperatures above 1000°C can occur at less than 10 km depth in areas of magma intrusion. Given the global average land area surface temperature of (about) 15°C and an approximate global geothermal temperature gradient for land areas outside volcanic settings of (about) 30°C , the same high temperature ($> 180^{\circ}\text{C}$) can be reached (on average) at a depth of about 5.5 km below ground level.

The main types of geothermal power plants use direct steam (often called dry steam), flashed steam and binary cycles.

Power plants that use dry and/or flashed steam to spin turbines are the most commonly deployed form of geothermal electricity generation. These plants use the heat energy contained in water and steam flowed from geothermal wells to spin turbines, converting thermal and kinetic energy to electrical energy.

Organic Rankine power plants employing secondary working fluids are increasingly being used for geothermal power generation. These so-called binary closed-loop power plants do not flow produced geothermal fluids directly into turbines. Thermal energy contained in water and/or steam produced from geothermal wells is transferred to a secondary working fluid using a heat exchanger (hence the term binary closed-loop). Organic compounds with lower boiling points than water (such as propane that boils at about 28 degrees C are often used as working fluids. The heat energy in the geothermal fluid boils the working fluid changing it from a liquid to a pressurized gas within the closed-loop, which can then be expanded in a turbine to spins a generator. The exhausted working fluid is cooled, condensed back into a liquid, pressurized and then recycled into the heat exchanger to complete the cycle.

Australian Geothermal Conference 2010

Table 1 Estimated global long term forecasts of installed capacity for geothermal power and direct uses (heat) and of electric and direct uses (heat) generation from Bertani, 2010 and Authors, 2010.

Expected World Use	2020		2030		2050		2100	
	Direct (GWt)	Electric (GWe)						
Capacity	160.5	25.9	380.1	51.0	831.1	160.6	1,367 to 5,906	264 to 1,141
Expected global use	TWh _t /y	TWh _e /y						
	421.9	181.8	998.8	380.0	2184.0	1266.4	3,592 to 15,521	2,083 to 9,000
	EJ/y							
	1.52	0.65	3.60	1.37	7.86	4.56	12.9 to 55.9	7.5 to 32.4

HOW BIG WILL GEOTHERMAL BE? (COMMUNICATE!)

The extent or accessibility of geothermal resources will not be a limiting factor for deployment. Tables 1 and 2 summarise the conclusions reached by the co-authors in 2010). These forecasts assume improvements in capacity factors power generation from the current average 71% to 90% by 2050, a level already attained in efficient, existing geothermal power generation plants. Earlier estimates for deployment beyond 2010 that were considered in developing forecasts in Table 1 include: IPCC, 2007; IEA, 2008; and EREC, 2008.

Table 2 World installed capacity, electricity production and capacity factor of geothermal power plants 1995-2010, forecasts for 2015-2050 (adapted from data from Bertani, 2010 and Authors, 2010) and forecasts for 2100 based on 1% and 4% average annual growth for 50 years from 2050.

Year	Installed Capacity (GWe) Actual or mean forecast	Electricity Production (GWh/y) Actual or mean forecast	Capacity Factor (%)
1995	6.8	38,035	64
2000	8.0	49,261	71
2005	8.9	56,786	73
2010	10.7	67,246	71
2015	18.5	121,600	75
2020	25.9	181,800	80
2030	51.0	380,000	85
2040	90.5	698,000	88
2050	160.6	1,266,400	90
2100	264 to 1,141	2,082,762 to 8,999,904	90+

NEXT STEPS IN GLOBAL RESOURCE ASSESSMENTS

A further global geothermal resource assessment is planned under an existing IEA GIA research annex. This will include a probabilistic range of estimates, for example, assuming that a log normal distribution adequately describes the range of recovery of stored heat from a minimum of 0.5% at a 99% probability to a maximum of 40% of stored heat at a 1% probability. This implies: a low-side recovery of 1.34% of stored (90% probability); a mid-range recovery of 4.47% of stored heat (50% probability); a Swanson's mean² recovery of 6.68% of stored heat; and a high-side recovery of 14.95% of stored heat (10% probability).

CONCLUSIONS REGARDING DEPLOYMENT BY 2100

Current global trends and regional research underpin credible expectations for great growth in the global use of geothermal energy over the next 90 years. Great expectations are:

- Power generation with binary plants and total re-injection will become common-place in countries without high-temperature resources.

² Swanson's mean is the weighted approximation for a log-normal distribution equal to the summation of 30% of the 90% probability value, 30% of the 10% probability value, and 40% of the 50% probability value e.g. (P90 x 0.3) + (P10 x 0.3) + (P50 x 0.4) equals the Swanson's mean value

- Geothermal energy utilization from conventional hydrothermal resources continues to accelerate and the advent of EGS is expected to rapidly increase growth after 10 to 15 years putting geothermal on the path to provide an expected generation global supply of 4.56 EJ per year (~160 GWe) by 2050, and between 7.5 EJ per year (with 1% growth per year) and 32.4 EJ per year (with 4% growth per year) by 2100.
- In addition to the widespread deployment of EGS, the practicality of using supercritical temperatures and offshore resources is expected to be tested with experimental deployment of one or both a possibility by 2100.
- Direct use of geothermal energy for heating and cooling, including geothermal heat pumps (GHPs) is expected to increase to 7.86 EJ /year (~815 GWt) by 2050 and between 12.9 EJ per year (with 1% growth per year) and 55.9 EJ per year (with 4% growth per year) by 2100. Marketing and multiple internationally competitive supply chains will underpin this growth. This expectation is supported information published by Rybach, 2005
- Geothermal energy is expected to meet between 2.5% and 4.1% of the total global demand for electricity by 2050 and potentially more than 10% by 2100. It is also expected to provide about 5% of the global demand for heating and cooling in by 2050 and potentially, more than 10% by 2100. Geothermal energy will be a dominant source of base-load renewable energy in many countries in the next century.
- With its natural thermal storage capacity, geothermal is especially suitable for supplying both base-load electric power generation and for fully dispatchable heating and cooling applications in buildings, and thus is uniquely positioned to play a key role in climate change mitigation strategies (Bromley, et al., 2010).

ACKNOWLEDGEMENTS

The authors thank their international colleagues who have contributed so much of their professional lives and time to provide improved understanding of geothermal systems. We are especially grateful to: John Lund, Ladsy Rybach, Mike Mongillo, Ken Williamson, David Newell, Trevor Demayo, Arthur Lee, Subir Sanyal, Roland Horne, David Blackwell, and Doone Wyborn.

REFERENCES

AGEG-AGEA, 2009, Australian Code for Reporting of Exploration Results, Geothermal Resources and Geothermal Reserves, prepared by the Prepared by: The Australian Geothermal Code Committee - a committee of the Australian Geothermal Energy Group (AGEG) and the Australian Geothermal Energy Association (AGEA). Download from http://www.pir.sa.gov.au/geothermal/ageg/geothermal_reporting_code

Authors (of this report), 2010. Unpublished correspondence leading to tabulations of expectations for geothermal energy deployment from resources below 3,500 metres in 2020, 2030 and 2050. Bertani, R. and Tester, J. were instrumental in developing these estimates.

Bertani, R., 2010. World Update on Geothermal Electric Power Generation 2005-2009. Proceedings World Geothermal Congress 2010, Bali, Indonesia, April 25-30, 2010.

Bertani, R., and I. Thain, 2002. Geothermal power generating plant CO₂ emission survey. IGA News, 49, pp. 1-3. (ISSN: 0160-7782)

Bloomfield, K.K., J.N. Moore, and R.N. Neilson, 2003. Geothermal energy reduces greenhouse gases. Geothermal Resources Council Bulletin, Vol. 32, No. 2, pp. 77-79. (ISSN 01607782)

Bromley, C.J., M.A. Mongillo, B. Goldstein, G. Hiriart, R. Bertani, E. Huenges, H. Muraoka, A. Ragnarsson, J. Tester, and V. Zui, 2010. IPCC Renewable Energy Report: the Potential Contribution of Geothermal Energy to Climate Change Mitigation. Proceedings World Geothermal Congress 2010, Bali, Indonesia, April 25-30, 2010.

Burgassi, P.D., 1999. Historical Outline of Geothermal Technology in the Larderello Region to the Middle of the 20th Century. In: *Stories from a Heated Earth*, R. Cataldi, S. Hodgson, J.W. Lund eds., Geothermal Resources Council, Sacramento, CA. pp. 195-219. (ISBN: 0934412197)

Cataldi, R., 1999. The Year Zero of Geothermics. In: *Stories from a Heated Earth*, R. Cataldi, S. Hodgson, J.W. Lund eds., Geothermal Resources Council, Sacramento, CA. pp. 7-17. (ISBN: 0934412197)

- Dickson, M.H., and M. Fanelli, 2003. Geothermal energy: Utilization and technology. Publication of UNESCO, New York, 205 pp. (ISBN: 9231039156)
- Electric Power Research Institute (EPRI), 1978. Geothermal energy prospects for the next 50 years. ER-611-SR, Special Report for the World Energy Conference 1978.
- Frick, S., G. Schröder, and M. Kaltschmitt, 2010. Life cycle analysis of geothermal binary power plants using enhanced low temperature reservoirs. *Energy*, Vol. 35, Issue 5, pp. 2281-2294. (ISSN: 0360-5442)
- Fridleifsson, I.B., R. Bertani, E. Huenges, J.W. Lund, A. Ragnarsson, and L. Rybach, 2008. The Possible Role and Contribution of Geothermal Energy to the Mitigation of Climate Change. IPCC Scoping Meeting on Renewable Energy Sources, Luebeck, Germany 21-25 January 2008. 36 p. Available at: <http://www.ipcc.ch/pdf/supporting-material/proc-renewables-luebeck.pdf>
- Hamza, V.1; Cardoso, R.; and Ponte Neto, C., 2008. Spherical harmonic analysis of earth's conductive heat flow, *International Journal of Earth Sciences*, Volume 97, Number 2, April 2008, pp. 205-226(22), Publisher: Springer
- IPCC 2007, Climate Change 2007, Fourth Assessment Report of the Intergovernmental Panel on Climate Change, Working Group III: Mitigation of Climate Change, Chapter 4 - Geothermal, Section 4.3.3.4
- International Energy Agency (IEA), 2008, World Energy Outlook 2008, download from <http://www.iea.org/textbase/nppdf/free/2008/weo2008.pdf>
- European Renewable Energy Council (EREC) and Greenpeace International (GPI), 2008, Energy [R]evolution – A sustainable Global Energy Outlook (EREC-GPI-08). Download from: <http://www.greenpeace.org/raw/content/international/press/reports/energyrevolutionreport.pdf>
- Goldstein, B.A., Hill, A.J., Long, A., Budd, A. R., Holgate, F., and Malavazos, M., 2009. Hot Rock Geothermal Energy Plays in Australia, Proceedings of the 34th Workshop on Geothermal Reservoir Engineering, Stanford University, Stanford, California, February 9-11, 2009, SGP-TR-187
- Hiriart, G., R.M. Prol-Ledesma, S. Alcocer and G. Espíndola, 2010. Submarine Geothermics: Hydrothermal Vents and Electricity Generation. Proceedings World Geothermal Congress 2010, Bali, Indonesia, 25-29 April, 2010.
- Kaltschmitt, M., 2000. Environmental effects of heat provision from geothermal energy in comparison to other resources of energy. Proceedings World Geothermal Congress 2000, Kyushu-Tohoku, Japan, May 28-June 10, 2000. (ISBN: 0473068117)
- Krewitt, W., K. Nienhaus, C. Klebmann, C. Capone, E. Stricker, W. Grauss, M. Hoggwijk, N. Supersberger, U. Von Winterfeld, and S. Samadi, 2009. Role and potential of renewable energy and energy efficiency for global energy supply. *Climate Change*, 18, December 2009, 344 pp. (ISSN: 1862-4359)
- Lund, J. W., Freeston, D.H. and Boyd, T.L 2010. Direct Utilization of Geothermal Energy 2010 Worldwide Review. Proceedings World Geothermal Congress 2010, Bali, Indonesia, 25-30 April 2010.
- Mongillo, M.A., 2010, Proceedings of the Joint GIA-IGA Workshop - Geothermal Energy Global Development Potential and Contribution to Mitigation of Climate Change, 5-6 May 2009, Madrid, Spain. Download from http://www.iea-gia.org/documents/ProcGIA_IGAWorkshopMadridFinalprepress22Mar10_000.pdf
- Nill, M., 2004. Die zukünftige Entwicklung von Stromerzeugungstechniken, Eine ökologische Analyse vor dem Hintergrund technischer und ökonomischer Zusammenhänge, Fortschritt-Berichte VDI Nr. 518. Düsseldorf, D: VDI-Verlag, 346 (in German). (ISSN: 0178-9414)
- Rybach, L., 2005. The advance of geothermal heat pumps world-wide. IEA Heat Pump Centre Newsletter, 23, pp. 13-18. (ISSN: 0724-7028)
- Sims, R.E.H., R.N. Schock, A. Adegbululgbé, J. Fenhann, I. Konstantinaviciute, W. Moomaw, H.B. Nimir, B. Schlamadinger, J. Torres-Martínez, C. Turner, Y. Uchiyama, S.J.V. Vuori, N. Wamukonya, X. Zhang, 2007. Energy supply. In *Climate Change 2007: Mitigation. Contribution of Working Group III to the Fourth Assessment Report of the Intergovernmental Panel on Climate Change* [B. Metz, O.R.

Australian Geothermal Conference 2010

Davidson, P.R. Bosch, R. Dave, L.A. Meyer (eds)], Cambridge University Press, Cambridge, United Kingdom and New York, NY, USA. (ISBN-13: 9780521705981)

Tester, J.W., E.M. Drake, M.W. Golay, M.J. Driscoll, and W.A. Peters, 2005. Sustainable Energy – Choosing Among Options, MIT Press, Cambridge, MA, 850 pp.

Tester, J.W., B.J. Anderson, A.S. Batchelor, D.D. Blackwell, R. DiPippo, and E.M. Drake (eds.), 2006. The Future of Geothermal Energy Impact of Enhanced Geothermal Systems on the United States in the 21st century. Prepared by the Massachusetts Institute of Technology, under Idaho National Laboratory Subcontract No. 63 00019 for the U.S. Department of Energy, Assistant Secretary for Energy Efficiency and Renewable Energy, Office of Geothermal Technologies. 358 p. (ISBN-10: 0486477711, ISBN-13: 978-0486477718)

New Design Concepts for Natural Draft Dry Cooling Towers

Hal Gurgenci* and Zhiqiang Guan

The Queensland Geothermal Energy Centre of Excellence (QGECE), the University of Queensland, St Lucia, Brisbane, Qld 4072

*Corresponding author: h.gurgenci@uq.edu.au

Design of efficient natural draft dry cooling system is essential for Australian geothermal power plant applications. In fact, dry cooling may be the only option for most geothermal power plants planned to be established in Australia since these areas have limited access to water resource.

Natural draft cooling towers in coal-fired and nuclear power plants have been mainly of concrete construction. It has been reported that the highest concrete cooling tower in the world of 200 meters high has been built at the RWE power station at Niederaussem (Busch et al, 2002). Due to the lower thermal efficiencies of geothermal power plants, the heat rejection per kWh(e) of net generation from these plants will be four or more times as great as from fossil fuelled plants (Kröger 2004), which will require a much larger cooling tower for a geothermal power plant of compared to a coal-fired power plant of similar capacity. The design and construction of such a large concrete cooling tower is extremely expensive and takes a long time to build. The tower structure is heavy and requires substantial foundation.

The Queensland Geothermal Energy Centre of Excellence (QGECE) is to explore new concepts for natural draft dry cooling technologies for geothermal power plants. The aims for the new design concepts are to increase the performance of the cooling tower and reduce the overall cost. Two alternative designs are proposed: low cost air-lift mobile cooling tower (Gurgenci and Guan, 2009) and solar cooling tower.

The design concept for air-lift mobile cooling tower is as follow: the tower is built as a flexible shroud and is held in place in tension by the buoyancy force provided by a lighter-than-air gas. One benefit for the air-lift cooling tower is that the industry can construct very tall cooling towers at an acceptable cost. Other benefits include constructing such towers with a minimum of time and expense, which are of relatively light weight and which are not subject to frequent repairs. The towers are mobile and can be disassembled and moved to a new geothermal plant site with a minimum of time and effort.

The design concept for solar cooling tower includes a solar energy system which is used to preheat the air inside the cooling tower to increase the buoyancy of the natural draft cooling tower. The enhanced buoyancy enable the cooling tower be constructed with either reduced size or with increased tower performance, which

is especially beneficial during hottest time period in a day.

Keywords: Geothermal energy, Cooling tower and heat exchanger, natural draft cooling technologies.

Natural Draft Dry Cooling Towers

A natural draft dry cooling tower is a heat rejection device that creates the flow of air through the bundles of finned tube heat exchangers by means of buoyancy effects. Buoyancy occurs due to a difference in air density before and after heat exchanger resulting from temperature and moisture differences. The greater the thermal difference and the height of the tower structure, the greater the buoyancy force. Therefore, the volume flow rate of air across the heat exchanger bundle is directly proportional to the height of the cooling tower.

Natural draft dry cooling towers are particularly attractive as a cost-saving solution for larger power plants where water resource is limited and expensive. The unique economic advantage of natural draft cooling towers lies in their very low electric energy requirement. Fan cost and substantial amount of fan power are saved in this system. The operating costs are minimal.

Natural cooling towers have been designed in various ways. However, reinforced concrete structures have become standard to handle the high cooling water flow rates in large power plants.

Fig.1 shows a configuration of natural draft dry cooling tower used by the thermal power plants.

Fig.2 is a photo taken from Yangchen power plant of China.

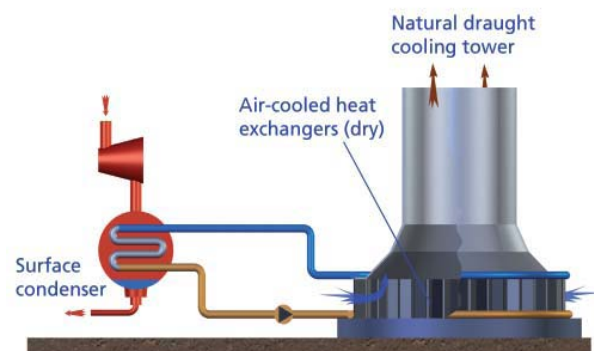


Fig.1 Natural draft dry cooling [GEA Aircooled Systems]

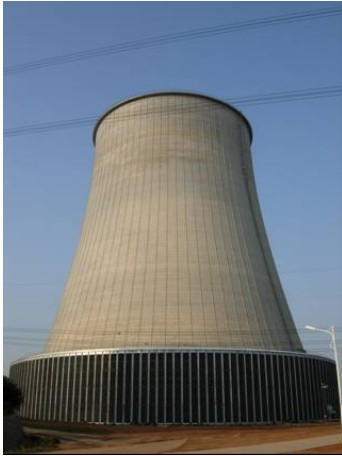


Fig.2 Yangchen Natural Draft Cooling Tower

New Design Concepts

Three design concepts are proposed in this paper. The first concept relies on a conventional steel construction design. The second concept, the air-lifted tower, is a radical invention that proposes the use of helium-filled toroidal rings to provide the tower structure. The third concept is a novel combination of the solar chimney idea with natural draft dry cooling towers.

Steel Towers with Advanced Heat Exchangers

One of the reasons behind the use of reinforced concrete construction as a method of building natural draft dry cooling towers in coal-fired power plants is the concern about corrosion caused by exposure to some of the elements in the flue gases in combination with the ambient effects. These concerns do not apply to a binary geothermal plant. Therefore, the use of steel towers is allowable in geothermal plants and this choice may offer new options that are not available to fossil fuel power plant designers. A combination of steel construction methods with some of the advanced heat exchanger options that deliver high heat exchange rate/ pressure drop ratios could then be a viable option. A steel tower design will be presented that will have the capability to power air-cooled condensers for a commercial geothermal power plant subject to ambient conditions typical of the Australian outback.

Air-lifted natural draft cooling tower

In this design, a flexible shroud is the main body of the tower structure and is held in place in tension by the buoyancy force. This flexible shroud includes stiffening rings, sealing skin and tensioning cables as shown in Figure 3. The shroud can be divided into several sections and prefabricated in factory and assembled/installed quickly in site.

The stiffening rings are made of different diameters and placed periodically to form the desired shape required (such as hyperbolic

concrete tower used in most coal-fired and nuclear power plants). The tension cables are connected to the stiffening rings to add strength and hold the shroud in place by tension. The sealing skin can be made of light materials and can be attached to the stiffening rings quickly and economically in site. The flexible shroud can have durability for wind load and weather resistance.

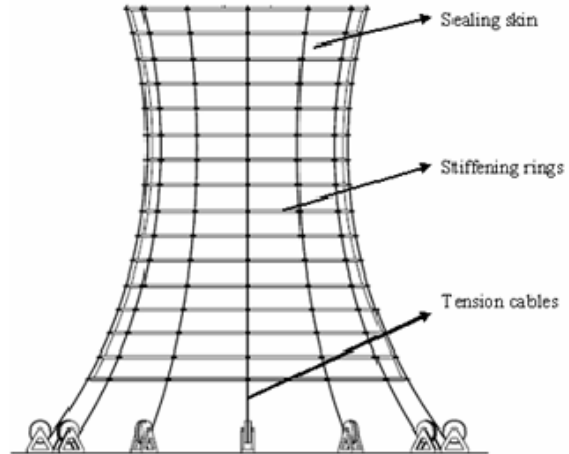


Fig.3 Proposed structure flexible shroud

To provide lifting force to the flexible shroud, stacked helium-filled toroidal vessels are connected directly to stiffening rings separately as indicated in Figure 4 to provide adequate lifting force. Each inflatable donut can pull either a single stiffening ring or several rings together. Each inflatable donut can have its own air inlet and can be pneumatically controlled. Redundancy is desirable in order to ensure that the tower integrity can be maintained during the maintenance and to facilitate repair of leaking donuts.

Not all donuts will need helium or lighter than air gas. Normal air can be pumped into some donuts, probably those towards the bottom, with predefined pressure to provide supporting force for the shroud. The donuts can be further divided into several sections vertically along the shroud (such as four or eight sections). Each vertical section can be individual controlled pneumatically.

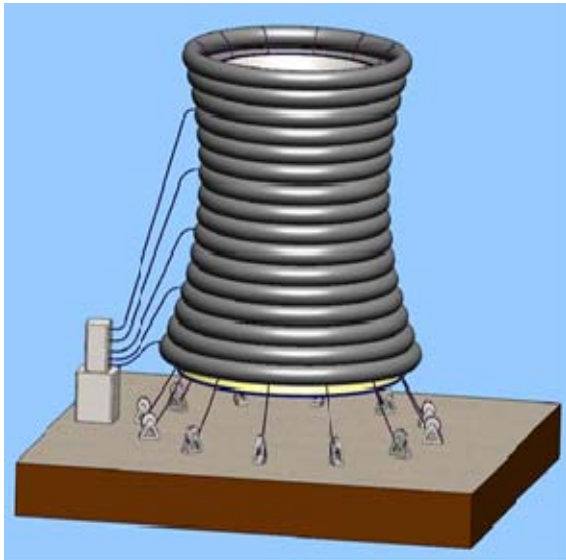


Fig.4 Design of donut-shaped air-lifted cooling tower

Solar enhanced natural draft cooling tower

In this design, based on the principal of solar chimney, a solar collector is placed at the base of a natural draft cooling tower between the tower and the vertically arranged heat exchanger. Heating of the air behind the heat exchanger (inside the tower) will enhance convection, and hence more airflow through the heat exchanger.

The cooling ability of this tower depends primarily on two factors: the size of the solar collector area and tower height. With a larger solar collector area, a greater volume of air is warmed to flow up the tower. With a larger tower height, the pressure difference increases the buoyancy effect.

Figure 5 shows schematic drawing of proposed design of solar enhanced natural draft cooling tower. In this design, heat exchanger bundles are placed circumferential at the base of the tower. A solar collector is added between the heat exchanger bundles and the cooling tower to heat the air below. Due to the upstream air temperature of the heat exchanger has been heated and much higher than the downstream air temperature, the flow rate of the air through the heat exchanger increase, which results either the tower size can be reduced (for fixed heat sink) or the performance of the tower increases (for fixed tower size).

The cooling tower structure can be a standard concrete tower used in power plant or it can be a chimney shape as shown in figure 5. The air-lift cooling tower can also be used in this design.

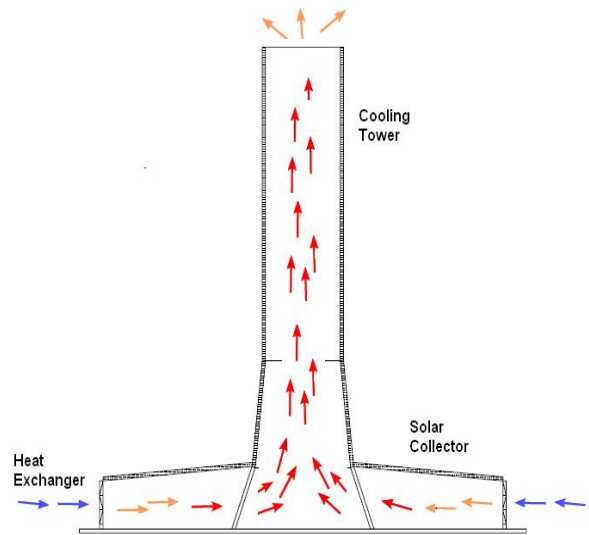


Fig.5 Schematic of solar natural draft cooling tower

Air-Lifted Tower Construction

To erect the air-lift cooling tower shown in Figure 4, the stiffening rings are placed first around the bases in order and the top stiffening ring is connected to the first donut shape vessel and the top end of the tension cables. Helium is then pumped into the top donut vessel which lifts the first stiffening ring and part of the tension cables. After the first ring has been raised to a desired position above the ground, the second top ring can be connected to the tension cables in the same way. The ascending height of the assembled rings is controlled by the release of tension cables. The sealing skin can be formed and fixed to the already assembled stiffening rings with various fixing mechanisms.

With the same process repeated as above, the controlled upward motion of the lifting donut vessels result in a corresponding advance of the cooling tower shroud. The intermediate advance of the installation of the cooling tower is shown in Figure 6.

Once the bottom ring has been assembled and raised to desired position, the tension cables are then secured to their respective anchors.

Conclusions

Air-lift cooling towers provide an alternative to the widely used concrete cooling tower used in power industries. This alternative will achieve a construction with minimum of time and expense.

Since materials of the tower can be made of nonferrous and light materials, the resulting tower will therefore be corrosion free and it will be lightweight allowing quick installation with the advantages of easy disassembly and mobilisation at a minimum of time and effort. The whole tower can be reused in a new site.

The inflatable donuts (cells) can be divided into portions which are so arranged that malfunction of one or more of them will not interfere with operation of the tower as a whole. Such redundancy provides reliable maintenance and repair.

The shroud is made of light material and can be factory manufactured in segments or as a whole. This provides for a quick and easy field installation. Since there is less material (weight) to be transported to the construction site, it will reduce the cost of transportation which may have significant impact when the site is located in a remote area.

The most serious concern on air-lift cooling tower is its deformation and stabilization under strong wind which could affect the performance of the tower. Mechanism for improving design and control will be identified.

By adding solar collector to preheat the upstream air temperature of the heat exchanger, it results a more air flow rate through the heat exchanger due to a much higher buoyancy effect. This can either reduce the tower size (for fixed heat sinking) or increase the performance of the tower (for fixed tower size).

A comparative life cycle cost analysis for both conventional and the new design concepts of natural draft dry cooling tower is necessary in future work.

References

- Busch D., Harte R., Kraitzig W.B. and Montag U. 2002, New natural draft cooling tower of 200 m of height, *Engineering Structures* 24 (2002) 1509–1521.
- Kröger, D.G. 2004, *Air-Cooled Heat Exchangers and Cooling Towers*, Penwell Corp., Tulsa, USA.
- Gurgenci, H., and Guan, Z. 2009, Dirigible natural draft cooling tower in geothermal and solar power plant applications, 14th IAHR Cooling Tower and Air-cooled Heat Exchanger Conference, 1 to 3 December 2009, Stellenbosch, South Africa.

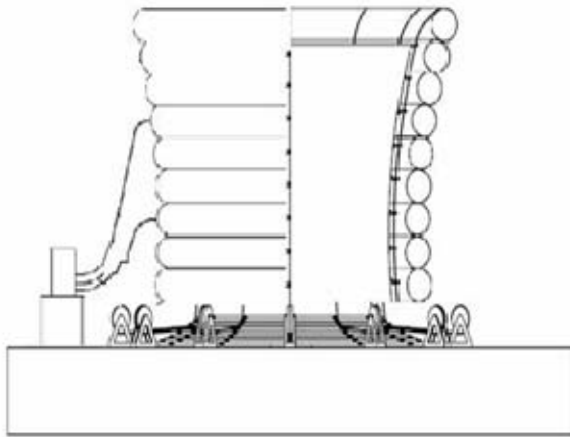


Fig.6 Intermediate position of installation

Future Work

An engineering feasibility study on the above new design concepts will be carried first based on the environmental conditions in the proposed geothermal power plant sites.

Should the feasibility study favour the air-lift cooling tower concepts, a detailed design of such cooling tower for a planned 50MW geothermal power plant will be conducted. A 3D model is to be built to predict tower deformation and its performance under various wind conditions.

Simulation and modelling of the solar natural draft cooling tower will be carried out by the PhD student Zeng Zhang who started his study in March 2010.

Full economic study needs to be performed for both conventional concrete cooling tower and the new design concepts as proposed in this paper. Once the study favours air-lift option, a scaled physical model will be built and tested in our mobile plant. Different wind loads will be simulated and the best stabilizing controlled mechanism will be identified. All modelling and simulating results will also be confirmed by the laboratory testing results.

Materials for the toroidal vessels, sealing skin and stiffening rings of the shroud play important roles in cost reduction and durability of the tower. It is therefore required to search, identify and test different materials suitable for the shroud and vessels.

Optimisation of the area of solar collector and size of the tower for solar enhanced natural cooling tower will be carried in future by a PhD student.

Stress analysis for tower structure for new design concepts will be done to determine the strength of the structure.

QGECE Research on Heat Exchangers and Air-Cooled Condensers

Kamel Hooman

Queensland Geothermal Energy Centre of Excellence,
The University of Queensland, Brisbane, Australia
k.hooman@uq.edu.au

Abstract

The aim of this paper is to give an overview of the research conducted at Queensland Geothermal Energy Centre of Excellence (QGECE) on air-cooled condensers for application in geothermal power plants. The application of metal foam heat exchangers in Natural Draft Dry Cooling Towers (NDDCTs) has also been studied in detail. Samples of the numerical and experimental results are presented. These findings are then backed up by theoretical modelling that enables us to run parametric studies which are sensible to different working/environmental conditions.

Keywords: Air-cooled condensers, NDDCT, heat exchangers, theoretical, experimental, CFD

Introduction

Australia's current policy targets an annual renewable energy generation of 45,000 GWh by 2020. Geothermal energy systems have the potential to produce a base load generation capacity capable of replacing existing coal-fired plants. However, there are some technical challenges to be overcome first. One of the major technical difficulties is the cooling system. Although wet cooling is more efficient than dry cooling, water shortages and harsh environmental conditions in areas such as the Australian desert have forced designers to consider less efficient and more expensive air-cooled systems, or dry-cooling as it is often termed.

Air-cooled plants offer potential economic advantages due to plant siting flexibility. Both natural draft and mechanical draft dry-cooling towers, equipped with air-cooled heat exchangers (almost always with extended airside surface area), are used. The fan-driven systems can be built quickly and at relatively low cost but their operating costs are higher due to their higher maintenance requirements and the parasitic losses associated with running the fans. The cooling system is a significant cost item in the power plant and affects the performance of the entire power cycle. If the cooling system does not provide adequate cooling, the overall plant efficiency plunges with serious economic consequences (e.g. decreased electricity production).

It has been reported that approximately 0.3 GWh (per year) of electricity generation in the United

States is lost because of cooling towers operating below their design efficiency. This corresponds to an economic penalty of around 20 million US dollars per year [1]. It is therefore, very important to design and analyse highly efficient dry cooling systems for power plants.

Though air-cooled condensers are not very popular, their application to power industry is not a new practice. Interestingly, a hyperboloid cooling tower was patented in 1918. The reason for the renewed interest in air-cooled condensers is scarcity of water or high humidity [2]. In either case fan-cooled systems can lead to high parasitic losses. This makes the NDDCT an ideal option for such cases. The reason for QGECE's interest in NDDCT is obvious. Most of our geothermal resources are located where there is no water. Besides, the thermal efficiency of our binary power plants is already so low that we cannot afford parasitic losses (fans).

Methodology

In view of the above, QGECE has been looking into applying efficient heat exchangers to reduce the cost of towers. This would have been impossible unless a proper test bed is provided. In doing so, a 2m height cooling tower is built and is operational at our QGECE lab, see Figure 1.



Figure 1: The QGECE lab scale model for a NDDCT.

The tower has a square cross-section with $1.4 \times 1.4 \text{ m}^2$ base area and $0.9167 \times 0.9167 \text{ m}^2$ tower exit area. The heating elements are four electrically heated copper bars of 10 mm diameter. At the same time, a numerical model is built, as depicted by Figure 2, so that parametric study of the problem is possible [3]

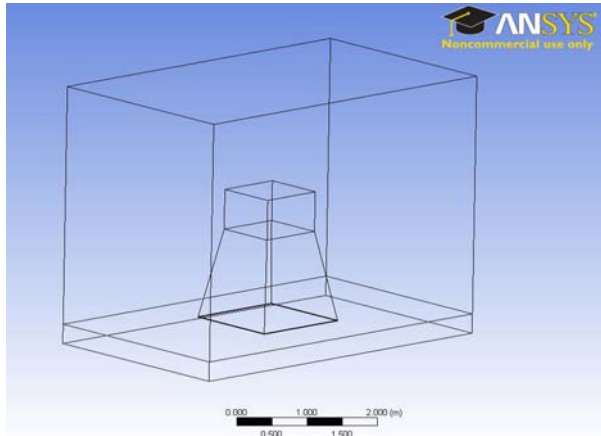


Figure 2: The computational QGECE lab scale model for a NDDCT.

Parallel to these tests and simulations a theoretical model is developed to shed some light on the scaling of such NDDCTs under no wind conditions [4].

A new design for tubes in air-cooled condensers is currently being examined at QGECE. The idea is to replace the fins by a layer of metal foams, see Figure 3, to increase the heat transfer area and, hence, reduce the total tube numbers and heat exchanger size/cost [2]. This can significantly reduce the cost as an efficient heat exchanger will lead to a less expensive (and shorter) cooling tower.



Figure 3: The metal foam-wrapped tube used in QGECE labs to conduct experiments on air-cooled condensers.

Theoretical and numerical analysis of such foam-wrapped tubes in air-cooled condensers have been reported in an earlier study [5]. Thus, experimental analysis followed initial high-level theoretical investigations. Figure 4 illustrates a photo of our test section where air is forced (by a suction fan) to flow over a heated metal foam-wrapped tube. The tube surface temperature is kept constant by using a circulation heater that pumps water (at adjustable flow rates) through the tube to keep the tube surface temperature uniform and constant similar to a condenser where the

fluid flowing in the tubes undergoes phase change. The same test section is used to collect data for a finned-tube of 30 mm OD with (197 fins of 0.6 mm thickness per meter). This is a typical design for an air-cooled condenser; similar to the ASPEN design one analysed in [3].



Figure 4: The low speed wind tunnel test facility; the hot water circulator and data acquisition system (sitting on the desk).

Results and discussion

Cooling tower results

Experiments are conducted to evaluate the tower frictional (shape) resistance, i.e. by excluding the heat exchanger resistances. A total of 25 data-points were used to measure the air temperature at the exit from the tower, as depicted by Figure 5. The results are then compared to numerical and theoretical predictions. The result from the temperature measurements involves the uncertainty of measurements which is estimated by using a basic uncertainty analysis [6]. The measured air velocity at the exit is $0.543 \pm 0.064 \text{ m/s}$ which is very close to both theoretical (0.515 m/s) and numerical (0.515 m/s) predictions.

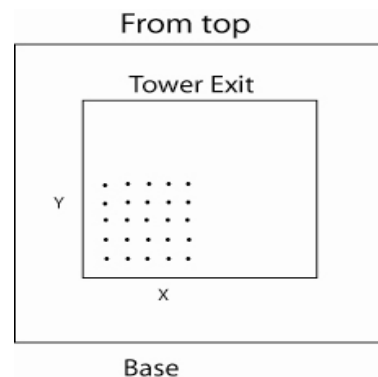


Figure 5: The location of the thermocouples to measure the air temperature at the exit from the tower.

The following formula [4] has been used to predict the tower inlet velocity, U , for the empty tower

$$U \sim \sqrt{\frac{2g\Delta\rho H}{K}} \tag{1}$$

and for the case where heat exchangers introduce a resistance to flow

$$U \sim \sqrt{\frac{K g H \Delta\rho}{t C_F}} \tag{2}$$

with k , g , K , H , t , C_F , and $\Delta\rho$ being the frictional loss coefficient, gravitational acceleration, bundle permeability, the tower height, the bundle thickness, form drag coefficient, the inlet-outlet air density difference, respectively.

Figure 6 illustrates the results of numerical simulations compared to theoretical predictions for taller cooling towers where the bundle velocity is plotted versus the tower height on a log-log scale. The 200m tower is designed to dump 283 MW of heat for a power plant that generates 50MWe [3]. The volumetric heat generation rates for shorter towers are then scaled down and implemented as inputs to our CFD simulations. As seen, the developed theory in [4] is capable of predicting the thermohydraulic performance of a NDDCT under no wind conditions. However, as wind can dramatically affect the performance of a NDDCT [7-12], QGECE is focusing on better understanding of the effects of cross-wind on scaling of the cooling towers.

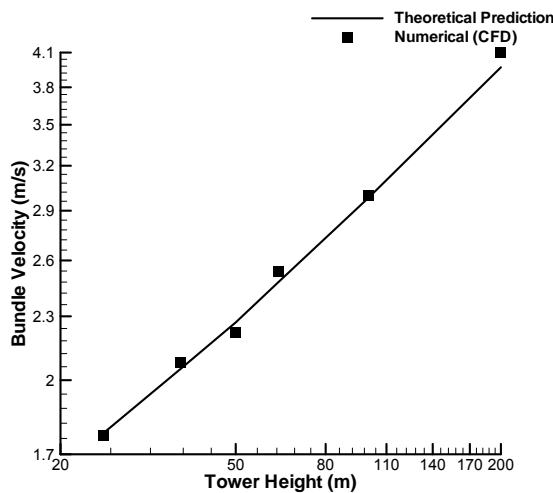


Figure 6: Numerical and theoretical prediction of bundle velocity for towers of different heights.

Metal foam results

In our last year report at Australian Geothermal Conference, it was numerically shown that the metal foams can be used in air-cooled condensers with a potential to reduce the size and cost of the condensers [13]. It has been argued that the area goodness factor (j/f ; dimensionless

heat transfer to pressure drop ratio) of the foam heat exchanger is higher than that of an ASPEN designed finned-tube one; see Figure 7.

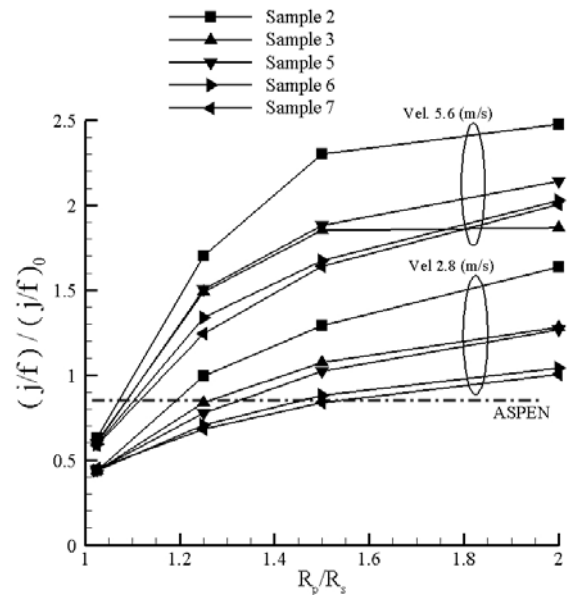


Figure 7: Normalized area goodness factor versus porous layer thickness for different samples and free stream velocities (samples 2-7 refer to commercially available ERG metal foam samples).[13]

Figure 8 illustrates a sample of our recently collected experimental data. This figure shows plot of heat transfer ratio versus the approaching air velocity.

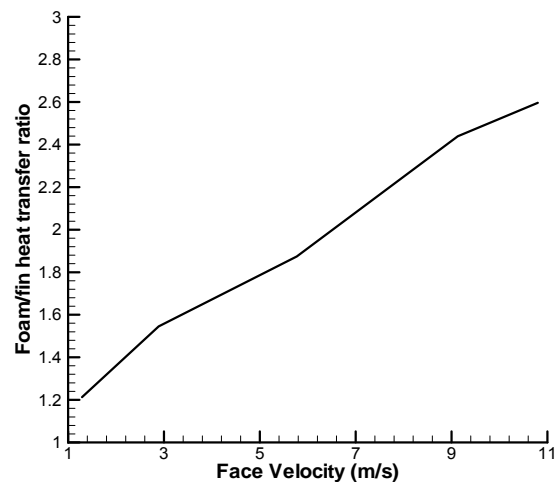


Figure 8: Heat transfer ratio (foam-wrapped tube divided by finned-tube) versus face velocity. Finned-tube is designed by ASPEN where tubes are 30 mm OD with 197 fins per meter. Fin diameter is 60 mm and the fin plate thickness is 0.6 mm; see [3] for more details.

Interestingly, with the same pressure drop, the heat transfer from a foam-wrapped tube is always

higher than that of a finned tube. The ratio can figure out at 2.6 at high velocities which can lead to more compact tube bundles and thus results in decreasing the capital cost. This gain for fan-cooled systems can lead to significantly reduced parasitic losses as with new design the number of bundles is almost halved (so are the parasitic losses). Furthermore, the pressure drop in the air cooled condenser is reduced as the number of the bundles is almost halved. Another point in favour of such compact systems is the lower tube-side pressure drops because of the elimination of a large number of the tubes in the condenser.

Concluding remarks

An accurate model, compared to experimental and CFD results, is developed to predict the heat and fluid flow through NDDCTs. Metal foam heat exchangers are tested and found to be superior to fins for air-cooled condensers. Further research is planned at QGECE to examine different working and environmental conditions.

References

- [1] North American Electric Reliability Council, Generating Availability Data System Report, Princeton, NJ, 1986.
- [2] Hooman K, Gurgenci H. Different heat exchanger options for natural draft cooling towers. World Geothermal Congress Nusa Dua, Bali, Indonesia 2010: Paper # 2633.
- [3] Hooman K, Gurgenci H. Porous medium modelling of air-cooled condensers. *Transport in Porous Media* 84 (2010): 257-273.
- [4] Hooman K. Dry cooling towers as condensers for geothermal power plants. *International Communications in Heat and Mass Transfer* 2010;in press.
- [5] Odabae M, Hooman K, Gurgenci H. Metal foam heat exchangers for heat transfer augmentation from a cylinder in cross-flow. *Transport in Porous Media* 2010;in press.
- [6] Mee DJ. Uncertainty analysis of Conditions in the test section of the T4 shock tunnel, Department Research Report # 1993/4, Division of Mechanical Engineering, The University of Queensland, Brisbane, Australia, 1993.
- [7] Kroger DG. Air-cooled heat exchangers and cooling towers. Pennwell Corp., 2004.
- [8] Al-Waked R, Behnia M. The Effect of Windbreak Walls on the Thermal Performance of Natural Draft Dry Cooling Towers. *Heat Transfer Engineering* 26(2005): 50-62.
- [9] Zhai Z, Fu S. Improving cooling efficiency of dry-cooling towers under cross-wind conditions by using wind-break methods. *Applied Thermal Engineering* 26 (2006): 1008-1017.
- [10] Sabbagh-Yazdi SR, Goudarzi MA, Mastorakis N. Solution of Internal and External Wind Induced Pressure for a Single Cooling Tower in Kazerun Power Plant (IRAN), in: S.H. Sohrab, H.J. Catrakis, N. Kobasko, S. Necasova, N. Markatos (Eds.), 6th IASME/WSEAS International Conference on Fluid Mechanics and Aerodynamics; 2008 Aug 20–22, World Scientific and Engineering Academy and Society, Rhodes, Greece.
- [11] Liu BM. Numerical Prediction for the Performance of a Natural Draft Cooling Tower with Comparison to the Field Test Data, in: G.F. Hewitt (Ed.), 10th International Heat Transfer Conference; 1994 Aug 14–18, Institute of Chemical Engineers, Brighton, England.
- [12] Iovino G, Mattoni H, Mazzocchi L, Senis R, Vanzan R. Optimal Sizing of Natural Draft, Dry Cooling Towers for ENEL Combined Cycle Power-Plants, in: S.S. Stecco, M.J. Moran (Eds.), *Florence World Energy Research Symp*; 1990 May 28–Jun 01, Pergamon Press Ltd, Florence, Italy.
- [13] Odabae M, Hooman K, Gurgenci H. Comparing the tube fin heat exchangers to metal foam heat exchangers. Australian Geothermal Energy Conference, Brisbane, Australia, November 11-13, 2009.

Equation-Free Summary of the 2010 Mathematics in Industry Study Group on Geothermal Data Analysis and Optimization

Robert McKibbin¹, *Franklin G. Horowitz^{2,3}, Neville Fowkes⁴, Brendan Florio⁴

¹Massey University Institute of Information & Mathematical Sciences

²Western Australian Geothermal Centre of Excellence,

The University of Western Australia ³School of Earth & Environment and ⁴School of Mathematics & Statistics,

Abstract

The Australia and New Zealand Industrial and Applied Mathematics (ANZIAM) division of the Australian Mathematical Society (AustMS) held its annual Mathematics and Statistics-in-Industry Study Group (MISG) both at RMIT in Melbourne, and via telepresence at UWA using the access grid from the 7th through the 12th of February 2010. The Geothermal Working Group attracted a total of 18 academic, professional, post-doctoral, and post-graduate applied mathematicians and others to study problems of potential interest to the geothermal projects in the Perth Basin Hot Sedimentary Aquifer plays. In the interests of attracting the wider AGECC community's attention to the annual MISG efforts, reproduced below is the "Equation Free Summary" of the week-long intensive effort. The detailed summary paper and several flow-on papers are currently being prepared for publication. The author list of this current document are comprised of the so-called "Industry Representative", the "Project Moderators", and "Student Moderator". A full list of the participants in the geothermal study group are found in Appendix 1.

Equation-Free Summary

The aim of this project was to assess the economic feasibility of extracting geothermal energy from the deep sedimentary Perth Basin in Western Australia. The WA Geothermal Centre of Excellence (WAGCoE), based in UWA, has been collecting data from (groundwater and oil) boreholes in the area as well as examining remotely-sensed observational data of ground surface temperatures. The question was how to interpret the available data to gain information on the modes of thermally-driven convective flows, if any, in the groundwater aquifers, thereby determining which parts of the system would be most economical to use for energy extraction.

The 2010 MISG "Geothermal" study group concentrated on problems of advective transport of heat in stratified geological units appropriate for the conditions found in the Perth Basin of Western Australia. The main hypothesis examined – for several different sub-problems – is that advective transport of heat is an important contribution to the overall heat transport. Measured temperatures in the system indicate an approximate temperature increase through the main aquifers from about 40 °C to 80 °C. Clearly, conductive heat transport is present (as elsewhere over the Earth's surface), but we

desired to find out whether the system is susceptible to "unforced" or natural convection.

There is a well-developed theory in the fluid mechanics/porous media literature about the conditions required for convective instability in non-homogeneous permeable systems that are heated from below. The criterion manifests itself in a dimensionless combination of thermodynamic and rock matrix parameters known as the Rayleigh number, denoted Ra . This was seen as relevant for our study, so we concentrated on using the available field data to determine whether or not conditions in the Perth Basin would be right or not.

It is likely there is also an advective transport component due to a hydraulic gradient from a recharge zone assumed to be at an elevated height in the Darling escarpment to the east, westwards to a discharge zone assumed to be offshore. However, for the purposes of most of our sub-problems, we neglected the hydraulic gradient effects.

The geological background

Rocks of the Perth Basin consist of multiple layers of sedimentary strata, where matrix (as opposed to fracture) hydraulic permeability is expected to be dominant. Immediately below the ground surface, there is an unconfined aquifer consisting of rocks geologically known as the "superficial" formations. These rocks are underlain by various shallow confined aquifers consisting of rocks of the Kings Park Formation (locally), the Leederville Formation, and the South Perth Formation. For the study group's convenience, since these rocks are not in hydraulic communication with the deeper and hotter aquifers, we lumped all of these aquifers together into a group we labelled (perhaps confusingly to people familiar with the stratigraphy) as the "superficial" units and basically ignored them (other than the boundary conditions they provide) in our models.

At a depth assumed for our purposes to be about 600 m we find the top of a confined aquifer consisting of rocks from the Gage Formation. Those rocks are assumed to be about 200 m thick, with uniform physical properties. Below the Gage, but in hydraulic communication with it, we find rocks of the Yarragadee Formation. The contact between the two formations is an erosional unconformity, so the thicknesses of the two units vary with map position. The rocks of the Yarragadee are assumed to be about 1000 m thick, also with uniform physical properties.

(These assumptions of uniform rock properties were relaxed in various ways in several of our sub-problems.) Below the Yarragadee lie the rocks of the Cadda Formation, about 600 m thick, also in hydraulic communication with the Yarragadee. Indeed, in the groundwater community, rocks of all three formations (Gage, Yarragadee, and Cadda) are often called the "Yarragadee Aquifer".

Below the Cadda Formation lie rocks of the Cattamarra Coal Measures. These rocks are dominantly shales, with interbedded sandstone layers. Hence, we treat the basal contact of the Cadda with the Cattamarra as being a hydraulic seal.

The result is our basic model of three stratified layers, with physical properties internally uniform, all participating in a single hydraulically connected system.

Well Log constraints

The closest deep borehole to the sites of WAGCoE's proposed exploitation systems is the Cockburn Number 1 oil well. Cockburn 1 was drilled in 1967, to a total depth of 10,020 feet (3054 m), with cores recovered from several discrete sites within the bore. Results of laboratory measurements of porosity, permeability and other physical parameters from these cores are found in the well completion report. Such well logs have been used to try to determine a relation between porosity and permeability from the core measurements; it yielded two different estimates of the vertical distribution of permeability. Statistics from these estimates were used in the sub-problem concerned with estimating Rayleigh numbers and critical values thereof for our Perth Basin problem.

Mathematical modelling

The usual modelling paradigm for such problems is to use a spatially averaged continuum approximation for the rock matrix and fluid components of the system. Standard fluid mass, fluid momentum (Darcy's law in this case) and thermal energy conservation laws enable a set of differential equations to be formulated. With appropriate geometric and thermal boundary conditions, the mathematical problem may be solved; usually this has to be completed using numerical techniques since the equations and the thermodynamic parameters are non-linear. However, with simplified geometry and certain assumptions, the mathematical problem is tractable using analytic methods.

Some numbers

To get an idea of the times and fluid speeds involved, we estimated that a water particle descending into the aquifer in the Darling Range would flow underground to the west at a speed of

about 3.5 m year^{-1} , and take about 8,500 years to complete the 30 km journey.

If "waste" fluid from a geothermal energy installation was pumped into the aquifer at a rate of 100 l s^{-1} , after 1 year the injected fluid would have penetrated to a radius of about 100 m, with the fluid speed at the cylindrical front being about 50 m year^{-1} at that time. This speed is significantly greater than the estimated natural flow above, so the injected fluid would be likely to penetrate the aquifers "upstream" against the natural slow current.

Convective instability

Some effort was spent in attempting to determine whether the system was prone to convective instability; this would, according to theory and experiment, result in large-scale convective "rolls" of fluid motion that sought to augment the conductive heat transport. A series of aligned rolls, each in counter-rotation to its neighbours, would induce hot spots or alignments near the ground surface, as well as cooler areas near the downflows. A consequent question was: Could the associated perturbed isotherm patterns and non-uniform surface heat flux actually be measured? Even if there was convection, how would we know the pattern?

Figure 1 shows a simple idealized model of a porous slab that has a base maintained at a uniform constant temperature that is higher than that at the top. The hotter fluid near the bottom is less dense than the cooler fluid near the top. Provided the net buoyancy force can overcome viscous resistance everywhere, convective motion is induced. The most unstable mode is a set of longitudinal "rolls".

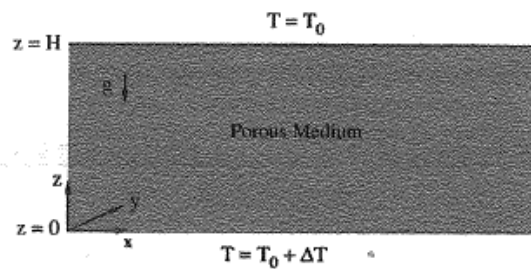


Figure 1: Idealized set-up for a permeable slab subjected to a vertical temperature gradient.

Linear perturbation theory for thermal convection in this idealized porous medium that is laterally unconfined determines that, for a uniform matrix, the critical value of the Rayleigh number is $Ra_{crit} = 4\pi^2$, with the most unstable mode being horizontal rolls with square cross-sectional boundaries. If the temperature gradient in the system is too small, so that Ra has a sub-critical value, then the heat transfer mechanism is conductive only. Above critical, heat transfer is by conduction and convection. The simplified theory assumes a

linearization of thermodynamic parameters around a certain temperature.

When the isothermal bounding surface above is at ground level some distance above the porous region, the above results are modified. The isotherms near the top of the convection region are then not horizontal. This is shown schematically in Figure 2, which also indicates the general form of the convective rolls.

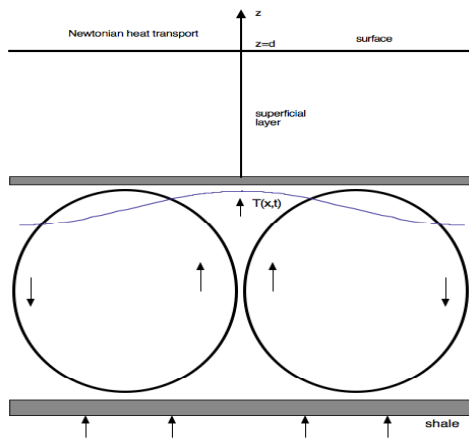


Figure 2: Schematic of longitudinal rolls in the permeable aquifer beneath a confining stratum, with an example perturbed isotherm near the top of the convection region.

Associated with supercritical conditions is an enhancement of the heat transfer. This increases with temperature gradient; the general trend of the so-called Nusselt number Nu , defined as the ratio of heat transferred by conduction plus convection to that transferred by conduction alone, is shown in Figure 3.

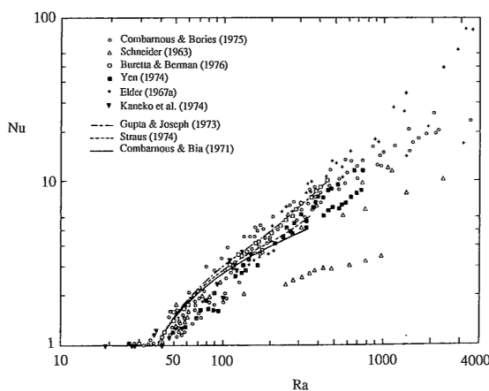


Figure 3: Trend of Nusselt number Nu with Rayleigh number Ra ; compilation of results from various theoretical and experimental studies (from Nield & Bejan, 2006).

First we considered a homogenized matrix system where the rock parameters were assumed uniform with somewhat arbitrarily-averaged values from the borehole core values. The

calculated values of Ra exceeded the critical value only for high enough (and perhaps unrealistic) values of the datum. However, the lack of euphoria was briefly tempered by the thought that the layering of the system may influence the calculation. It was further determined from the theory that anisotropy of thermal conductivity and permeability of the matrix produces an estimate of the critical Rayleigh number that is different from that for a homogeneous system.

Anisotropy in the thermal conductivity theoretically increases the critical Rayleigh number; however, the conductivity of rocks varies very little, so the anisotropy in that parameter is negligibly different from unity (measured data gave a value of around 1.06). Anisotropy in permeability is induced by material layering. Geological strata necessarily induce a permeability that is averagely greater in the bedding plane than perpendicular to it. What is more, such anisotropy generally reduces the (theoretical) critical Rayleigh number!

Amidst some excitement, an assessment of this anisotropy, from a rather complicated set of rock core measurements and well logs, was made as a stratum-thickness weighted average of intrinsic rock permeabilities, with the result that the horizontal value is about 4.6 times that in the vertical. These estimates reduced the critical Rayleigh number to 21.6, about half that computed from the homogenized parameters. Immediately, it became possible that conditions for convection may be met, even using the linearised theory with the lowest datum temperature (40 °C) for the linearised calculations.

Convective rolls and heat transfer

In optimistic anticipation of such a result, a small group had been working on how enhanced heat transfer in the Yaragadee Aquifer would manifest itself in the temperature distribution in the near-surface superficial formations. This is a fairly standard problem in heat transfer, and quick progress was made. However, it was shown that there would be a very small signature at ground surface level, and instrumentation would have to be sensitive and widespread to obtain significant measurements. So, this encapsulated the problem overall: Even if there was a convective process at work, how would measurements be able to be made to detect the upflow and downflow regions? So, how could advantage be taken of the convection even if the Ra estimates were correct?

The UWA Groupies

Over in WA, the small "at home" group was working; with the assumption that convection was occurring, they trawled the literature for information about theoretical work on layering effects on cell-size, and the stability of such convection cells. The idea was that significant

sub-layering caused by thick differently-permeable strata might produce vertically-aligned but largely separated co-rotating cells that, in tandem, would advect heat from the hot base to the surface. At the end of the week, no firm conclusions had been able to be made.

Simulation

Driven by concern that the thermodynamic properties of water were being approximated too severely in the linear stability theory, a numerical simulation of 2-D rolls was made using a commercial computer package. This allowed more accurate values for the water's temperature-dependent density, viscosity, etc. to be used. While the simulations were completed post-MISG, it turned out that there were only small qualitative differences in the flow patterns.

Slope-induced thermal convection

A late idea resulted from current work by one of the group members; it considers the possibility that longitudinal convection may be induced in a sloping aquifer by a near-vertical temperature gradient. The warmer fluid near the bottom would move up-slope (in this case, towards the east) while the returning cooler fluid near the top moves down-slope. It was not clear how this would affect the possible exploitation, because the temperature profile would remain conductive, and only be altered by convective rolls as were already considered above.

A small group of postgraduate students from the group seized upon some aspects of this, and their efforts will be rewarded by co-authorship of a paper to be submitted later in the year. A more general case will be considered, where induced convection in a layered sloping aquifer is investigated for optimal net convective heat transport by such a mechanism, as well as the stability of such motion to longitudinal rolls. The enthusiasm to participate in this way reinforces the benefits of MISG to engagement of postgrads in mathematical enquiry into useful applications.

Summary

The problem was tractable, but depended on suitable estimates of rock matrix properties from drill cores and well logs which were rather complex in structure. It also depended on good estimates of aquifer temperatures; the deeper values were elusive, and had to be deduced from extrapolations of shallow well measurements. However, by the end of the study week, there was a good increase of understanding of the problem, the issues to be resolved, and possible mechanisms at work in the Perth Basin.

Geothermal systems are complicated geological-geophysical-thermodynamical entities. A multi-disciplinary approach to understanding them is necessary. However, the quantification of their

attributes is well-handled by mathematically-able scientists and the MISG proved a suitable venue to tackle the WAGCoE problem.

Keywords: Convection, Hot Sedimentary Aquifers, Anisotropy

Reference

Nield, D. A., & Bejan, A. (2006). *Convection in Porous Media*. Springer, 3rd ed.

Appendix

Participants in the 2010 MISG Geothermal Study Group (alphabetically by surname):

Nurul Syaza Abdul Latif, Massey University NZ

Manarah Eraki, (Affiliation Missing)

Brendan Florio, University of Western Australia

Neville Fowkes, University of Western Australia

Luke Fullard, Massey University, NZ

Tony Gibb, Consultant, South Australia

Nick Hale, Oxford University, UK

Des Hill, University of Western Australia

Frank Horowitz, University of Western Australia

Grant Keady, University of Western Australia

Thiansiri (Pat) Luangwilai, ADFA, Australia

Fleur McDonald, Massey University, NZ

Robert McKibbin, Massey University, NZ

Melanie Roberts, University of Western Australia

Thomas Stemler, University of Western Australia

Rob Style, Oxford University, UK

Christian Thomas, University of Western Australia

Nicole Walters, Victoria University of Wellington, NZ

Status of Compliance With The Geothermal Reporting Code

Jim Lawless*, Graeme Beardsmore, Malcolm Ward, Fiona Holgate and Graham Jeffress

*SKM PO Box 9806 Newmarket, Auckland, NZ
JLawless@skm.co.nz

Abstract

The Australian Geothermal Reporting Code has now been in operation since late 2008. The Code currently operates on a voluntary basis and as yet has no legal status or sanctions. However, in late 2008 AGEA members agreed that its use in Public Reports would be mandatory for them and a Compliance Subcommittee (currently comprising the above authors) was established. The Subcommittee has since reviewed all Public Reports that we have become aware of to check for compliance. This paper presents an analysis of instances of non-compliance broken into several categories but without identification of the companies concerned. In each case the company concerned was informally notified about the issue. In general there has been a high level of willingness to comply with the Code and companies have responded positively to any issues raised. Most instances of non-compliance have been of a procedural nature such as omitting to include Competent Person statements in public presentations which include resource estimates. The experience gained has been valuable and has been taken into account in drawing up the Second Edition of the Code and its accompanying Lexicon. Other jurisdictions have been studying the Australian Code which has led to an almost identical Code being established in Canada. It is currently understood that consideration is also being given to equivalent Codes in the USA and Europe. The benefits of the Australian Code are being appreciated even in countries where it has no formal standing and Code compliant reports have recently been produced on resources in Chile and Indonesia.

Keywords: Geothermal, resources, reserves, compliance, Australia

Introduction

The Australian Geothermal Reporting Code has now been in operation since late 2008. The Code currently operates on a voluntary basis and as yet has no legal status. However, in late 2008 AGEA members agreed that its use in Public Reports would be mandatory for them and a Compliance Subcommittee (currently comprising the above authors) was established under the Joint Australian Geothermal Reporting Code Committee (JAGRCC). The Subcommittee has since reviewed all Public Reports that we have become aware of to check for compliance. This

paper presents an analysis of instances of non-compliance, broken into several categories, but without identification of the companies concerned.

Analysis

Most instances of non-compliance have been of a procedural nature such as omitting to include Competent Person (CP) statements in public presentations which include resource estimates. It is safe to say that there has been no case of an apparent intention to issue misleading information, though a few statements have verged on the over-enthusiastic at times.

Figure 1 shows the number of reports reviewed and number of companies concerned against time. As is to be expected, the number has increased with time but has fluctuated depending on the quarterly and annual reporting cycle as well as the frequency of reviews. The latest review has shown a drop in the number of reports and several companies which have previously reported have not done so, which perhaps reflects the generally static state of the industry at this time.

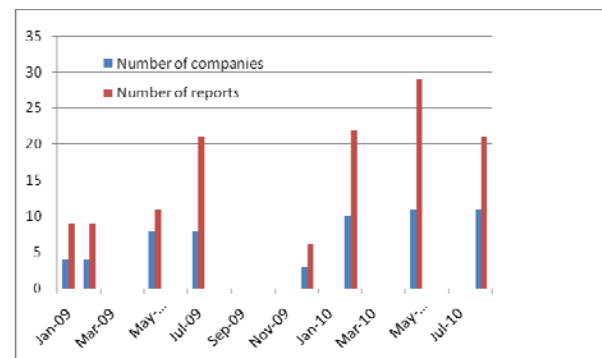


Figure 1: Reports reviewed and number of companies with time

Figure 2 show the percentage of reports which have been considered fully compliant. Although there is still significant room for improvement, it is pleasing to see this increasing with time. Furthermore, a simple percentage does not reflect that the initial instances of non-compliance were generally more significant and those recently have generally been of a less serious nature. The companies have clearly embraced the reporting process and learned from it. It would also be fair

Australian Geothermal Conference 2010

to say that the Compliance Sub-committee has also refined their understanding and criteria over time.



Figure 2: Percentage of fully compliant reports with time

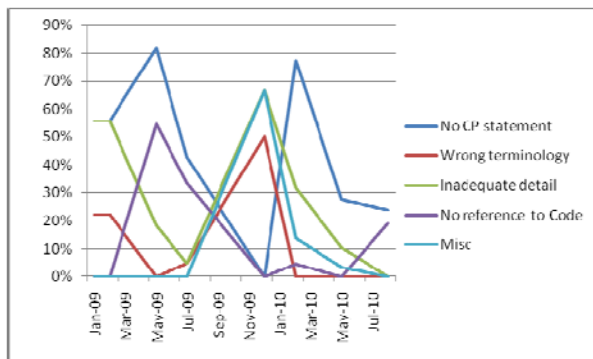


Figure 3: Break down of non-compliance by type

In Figure 3, the instance of non-compliance are broken down by category. Discussing each of these in turn:

No (or incorrect) Competent Person statement. This has generally speaking been the most common issue and one that has proven somewhat intractable with time in that instances are still occurring. The usual situation is that a compliant resource estimate has been prepared which includes a CP statement, but then that is summarised down to a brief ASX announcement, conference or shareholder presentation in which the CP statement is omitted.

It is noteworthy that in the Canadian geothermal reporting Code, which in most instances is based on and identical to the Australian Code, strict compliance in terms of including a CP statement in every Public Report is not required. However, this issue has been debated by the JAGRCC, and it is considered that every public announcement which refers to reserves or resources, and which could be deemed to provide information to

investors, is a Public Report under the Code, so the fundamental principle of requiring a CP statement has been adhered to. In reaching this conclusion the JAGRCC has adhered to a standing practice of consistency with the Joint Ore Reserve Committee (JORC) Code for minerals resource statements on which the Geothermal Code was originally modelled.

Wrong terminology. This has largely been a matter of companies coming to terms with the resource and reserve categories, and there are now few problems with the latest reports.

Inadequate detail. This has been a much-debated issue, as there is a tension between providing so much information as to make reports too complex for the average investor while at the same time fulfilling the requirements for materiality. The issue has been dealt with in part by allowing relatively brief Public Reports, but with more detailed back up being available. A number of example reports have also been produced to provide guidance.

No reference to Code. This is an issue that has decreased with time, although there has been a steady stream of new companies coming on to the market who have had to be informed about the Code. Responses have been positive.

Miscellaneous issues include items such as inappropriate aggregation of resources and conversion of heat-in-place to barrels of oil equivalent, delivered electricity or numbers of households that could potentially be supplied, without stating the assumptions involved. There has sometimes been a degree of over-enthusiasm in making such claims. The Code is not prescriptive as to methodology in such instances but they remain matters of concern.

Reaction

In each case on perceived non-compliance the company concerned has been informally notified about the issue. In general there has been a high level of willingness to comply with the Code and companies have responded positively to any issues raised.

The Way Forward

The experience gained in reviewing reports has been valuable and has been taken into account in drawing up the Second Edition of the Code and Lexicon which, at the time of writing, have been finalised and which should be released at this conference. Other jurisdictions have been studying the Australian Code which has led to an

almost identical Code being established in Canada, and it is understood that consideration is also being given to Codes in the USA and Europe. The benefits of the Australian Code are being appreciated even in countries where it has no formal standing and Code compliant reports have recently been produced on resources in Chile and Indonesia, as is described in a companion paper.

Application of the Australian Geothermal Reporting Code to “Conventional” Geothermal Projects

Jim Lawless*, Zim Aunzo and Jose Seastres, Jr

*SKM PO Box 9806 Newmarket, Auckland, NZ

JLawless@skm.co.nz

Abstract

The Geothermal Reserves and Resources Reporting Code was developed in Australia with the intention of it being principally applied to Australian geothermal projects, though it was framed in such a way as to apply to geothermal projects of all types. Recently, SKM has applied the Code to a number of “conventional” high temperature magmatic-related geothermal projects outside Australia. This paper describes how the Code principles and the underlying resource estimation methodology have been applied in those cases. Some of the major issues which had to be addressed included:

- What conversion efficiencies are applicable when the project is to include a flash steam cycle ?
- How are resources and reserves to be categorised when estimates are based on numerical simulation models ?
- How is energy already extracted to be dealt with in the case of project with an existing production history ?
- How is energy remaining after the assumed project life to be categorised ? Although these projects have been based on magmatic-related resources which do not occur in Australia, some of the insights gained in the process will have application as Australian projects move towards commercialisation, and as Australian listed companies develop this type of system elsewhere in the world.

Small Australian seismic events and their effects

David N. Love^{1*}, Gary Gibson², Russell Cuthbertson³ and Wayne Peck²

¹ PIRSA, GPO Box 1671, Adelaide SA 5001

² ES&S, 8 River St Richmond Vic 3121

³ ES&S, 81 Bishop St Kelvin Grove Qld 4059

* Corresponding author: david.love@sa.gov.au

We review four small earthquakes in Australia and highlight various seismological aspects that are relevant when considering induced seismicity. The four events are in the magnitude range 2.5 to 4.1, a range that is likely to be of interest for those investigating geothermally induced events.

Keywords: Australia, earthquake, induced event, intensity

Mt Barker (South Australia) event 16 April 2010 Magnitude 3.8

This earthquake occurred at 11:27pm on Friday night, about 25 km from the Adelaide CBD. It was widely felt, with a massive response to police and radio stations. There was no indication that the phone system failed, or that power outages occurred. The Primary Industries and Resources SA (PIRSA) earthquake network operated smoothly through the event, giving a very good location and magnitude estimate in less than 3 minutes. It took about 15 minutes to quickly review the event, and report it to the emergency services. The location was not entered on the PIRSA website until after the weekend. The first epicentre entry on the US Geological Survey website was about 100 km in error, but with a listed error estimate of 152 km. The first Geoscience Australia (GA) magnitude estimate was 3.2. While the internet remained operating, the GA and PIRSA websites were overloaded for a time. The PIRSA website received about 13,000 hits, a record. Hundreds of these emanated from overseas.

ABC radio Adelaide is normally run from Sydney late at night, but the Adelaide station was reopened in response to overwhelming public interest. Twitter and Facebook registered a huge amount of traffic. AdelaideNow website had about 1400 comments in short time; USGS Did You Feel It (DYFI) website plotted over 300 replies in less than one hour, and ES&S and GA had many replies to their website questionnaire. Management, particularly those associated with emergency response, expressed frustration at not knowing where to go for the best information at the early stages. In the following few weeks, a large number of insurance claims were lodged, with an estimate of 1,000 by one loss adjuster.

PIRSA circulated a questionnaire, but responses have not yet been analysed. Of the responses,

only the USGS Did You Feel It system was available within a short time frame. As the earthquake was not in the US, the location information was limited to 6 'city' locations, instead of postcode areas, rendering it of limited value.

There is a clear need for a DYFI system to be operated within Australia which can more effectively utilise location and intensity information, and disseminate it rapidly.

The depth of this earthquake was 25 km, with an uncertainty of about 2 km. This is quite deep for Australia. Normally depths of hypocentres are not available due to poor network coverage, however the new Adelaide network is producing accurate depths for a moderate number of events.

The magnitudes for stations of the Adelaide network ranged from 3.2 to 4.1, for stations of the GA network 3.5 to 4.2, and for stations of the ES&S network 3.4 to 4.0. These magnitudes were from peak amplitude measurements of seismographs, not moment magnitudes. Very little has been published on magnitudes in Australia in the last decade. Very few studies have been done to investigate corrections for individual sites on the basis of local geology, or to see how well magnitudes compare between networks.

The Eugowra (New South Wales) event 21 August 1994 Magnitude 4.1

This was the largest of a swarm of hundreds of events that occurred near the town of Eugowra, east of Orange, in country NSW. The swarm was very shallow, mostly less than 1 km deep. (Gibson *et al*, 1994)

The number of events, initially increasing in size resulted in public meetings being called. There was some concern, but generally not great. The main shock did stop the serious drinkers in the hotel for 5 minutes, but damage was limited to minor cracking and contents.

Portable instrumentation was installed close to the activity at an early stage in the swarm. From a beginning of one instrument, there was an increase eventually to 8 instruments, at moderately high sample rates of 200 to 400 sps. This resulted in probably the most accurately

recorded sequence of events in Australian seismological history. It was possible to demonstrate the fault plane that accounted for most of the events in the sequence (figure 1). This, in conjunction with the local topography, gave a convincing geological story. It was also possible to roughly estimate the size of the main shock at about 1 km square from the accurate location of the shocks in the following 9 days (figure 2). Aftershocks in the following 9 months were spread out still further. No other earthquake under magnitude 5.5 has been monitored well enough to show the size, dip and strike of the faulted area. No fault mechanism was produced for any of the events, but the geological conclusion is that it was mainly thrust.

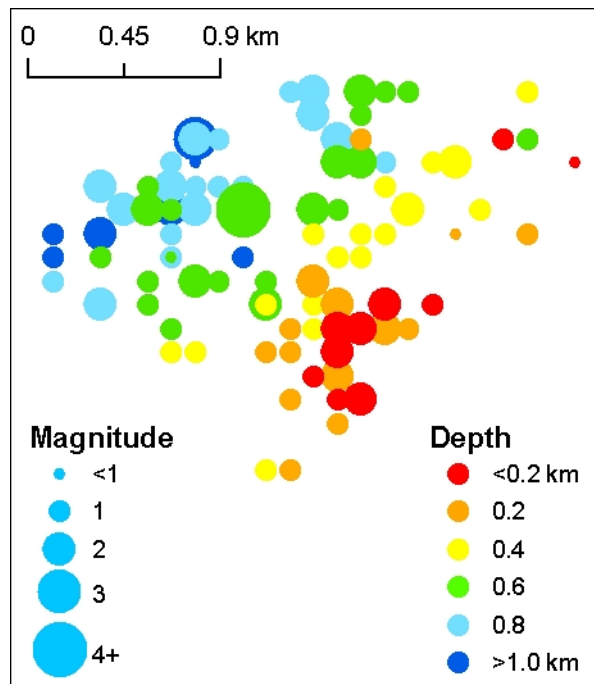


Figure 1: Hypocentres of the Eugowra earthquake swarm showing a shallow fault rupture clearly dipping to the north-west.

One accelerograph recorded a peak value of 0.97g. This is the largest acceleration recorded to date from an earthquake in Australia. The frequency of this peak was above 50 Hz. Unfortunately the sampling rate on the instrument was insufficient to calculate a velocity. The damage was very minor, demonstrating that acceleration is definitely not a good parameter to use when considering a management plan for induced events. Velocity is a much better predictor of damage, although it does not solve all problems. Detailed intensity information was not processed for this event, as a large effort was put into monitoring.

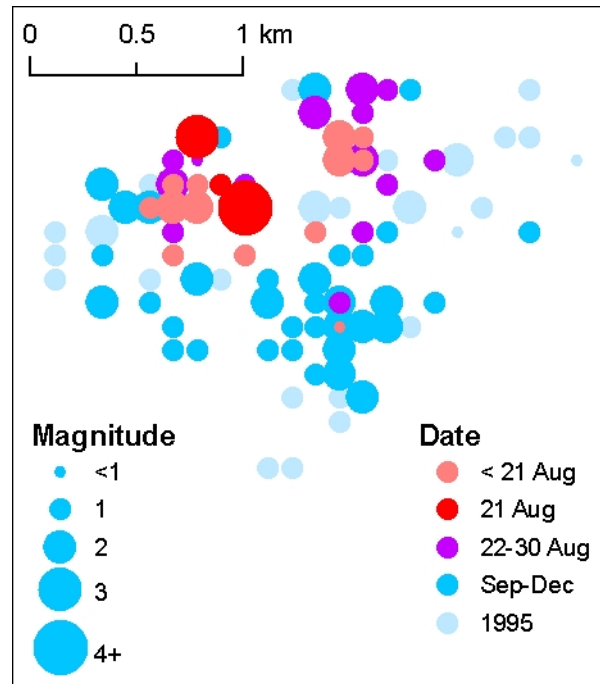


Figure 2: Hypocentres of the Eugowra earthquake swarm. The 22-30 August hypocentres outline an area of approximately 1 square km, which was probably the rupture surface of the largest event, magnitude 4.1.

Acacia Ridge (Queensland) event 18 July 1996 Magnitude 2.7

This earthquake shows that even small events, which often may not be felt in other countries, are still noticed in Australia. This earthquake occurred at 3:40pm in the suburbs of Brisbane, only 13km from the central business district. It initially produced only a small number of reports, however press reports and a phone survey collected over 150 intensity reports (Lynam and Cuthbertson 1997). The general radius of perceptibility of the main felt area was about 14 km with another felt area to the south-west and an isolated report as far as 70km away. Intensities assigned were low, with no reports reaching intensity 5 (figure 3).

The higher intensities were concentrated around the epicentre, and in a separate area to the south-west. The intervening area had lower intensities and even *not felt* replies. Variations in the intensities showed some correlation with surficial geology; lower intensities were associated with areas of Mesozoic sandstones and coal measures and Cainozoic sandstones and basalts, while higher intensities occurred on the Palaeozoic basement rocks. This observation, somewhat contrary to what is usually observed, is thought to be due to the high frequency nature of this relatively small magnitude event. Attenuation of the high frequency energy in the Mesozoic and Cainozoic rocks may have been more significant

than the amplifying effects normally associated with surface sediments and lower frequencies of larger events. Many smaller events are noticed more by the noise, emanating from very high frequencies, than the vibration.

While there were nine seismographs within 90 km, the distribution of these meant that there is an uncertainty of several kilometres in the epicentre (particularly in a NE-SW direction) and the depth is unknown. This is common for most events in Australia. This lack of hypocentral depths means that there are limited data available to compare intensities with hypocentral distances at the close distances that are of interest to the geothermal industry.

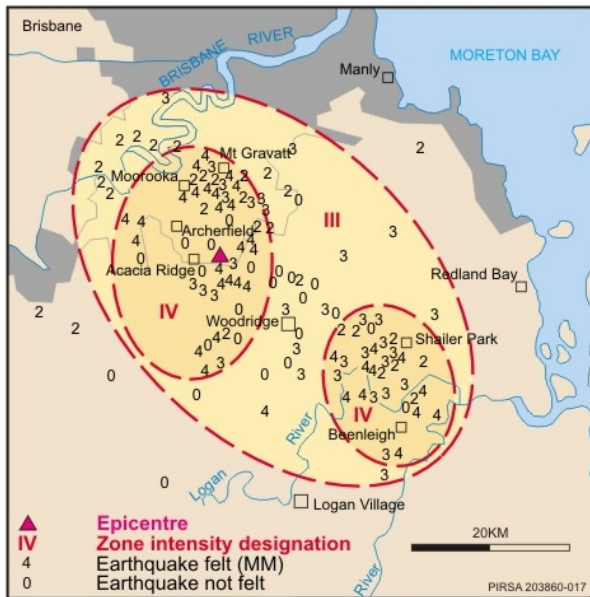


Figure 3: Isoseismal map of the Acacia Ridge earthquake. Source: Geoscience Australia

**Caulfield (Melbourne) event
22 October 2006 Magnitude 2.5**

An even smaller event was widely felt in Melbourne at 10:36pm while most people were quietly at home.

Information for this isoseismal map (figure 4) was collected by the intensity form on the ES&S website. As a result, in contrast to the Acacia Ridge earthquake, it has only one *not felt* reply. There are only two MM5 intensity reports listed, again showing the expected low intensities.

Despite the very low magnitude of the event, and the low intensities reported to the ES&S website, there were many insurance claims made, primarily for cracked plaster, cracked and lifted tiles and other cosmetic damage.

The good seismograph distribution meant that the epicentre and depth were known to within about 2 km. This is fairly unusual for Australia. It has the benefit that any measured velocities and estimated intensities can be included in more specific attenuation analyses for small earthquakes at close range. Peak amplitudes for the four closest seismographs were in the 10 to 25 Hz range. Individual station magnitudes varied from 2.0 to 3.4.

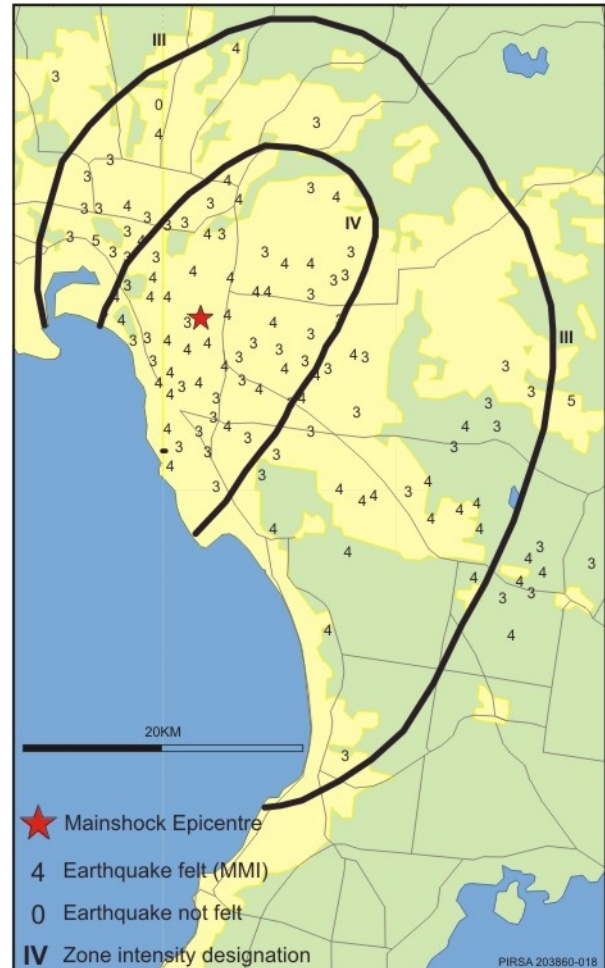


Figure 4: Isoseismal map of the Caulfield earthquake

Conclusions

Quite small events are felt, heard and newsworthy in Australia, even though the real damage consequences are minor or non-existent. While there is a considerable amount of information of interest and value available to the geothermal industry, some extra effort could improve the data collection and interpretation to more suitably address the needs of the industry.

Information that is accurate, and quickly available saves the difficulty and complaints that come later, from the inability of management and the public to find the information when desired.

Given the large public response, even for small events, there is clearly a need for a good community consultation program which addresses perceived risk as well as the risk of damage.

A 'Did You Feel It' intensity collection system, run in Australia would significantly improve the collection of intensity data, particularly over the important populated areas, and make it rapidly available in easily understood form. This will lead to improved attenuation formulae. The project should be easy and inexpensive. Improved intensity data will give a much clearer indication of the level of induced seismicity that may be tolerated, and the level of public response to vibrations.

There are currently New Generation Attenuation (NGA) formulae in use in earthquake hazard assessment. (Power *et al*, 2008) The development of modified NGA formulae to cover the magnitude range 3 to 5 would also provide valuable tools for use in induced seismicity risk assessments. The current NGA formulae are designed for higher magnitudes and lower frequencies, and not suitable to be extrapolated beyond these ranges. There is a vast amount of recorded information for smaller earthquakes. Unfortunately these are nearly all from overseas events. Events from stable continental areas, especially Australia would be needed, particularly for better handling of high frequencies.

More detailed monitoring, particularly active and populated areas would lead to improved source information, and more local data for modified NGA formulae. Unfortunately this is a more expensive exercise, and most populated areas are not monitored to this extent. More portable

deployments of larger scale to measure swarms or aftershocks at close range, and with higher sample rates, would provide valuable information on velocities, accelerations, rupture sizes and focal mechanisms of use to the industry. This is not done as often now as it was in the past.

The collection of intensity data in the same localities as velocity data will further improve the estimation of effects and damage in populated areas.

There is a need to compare magnitude data across Australia, review magnitude formulae currently in use, begin usage of moment magnitudes, and investigate seismograph site magnitude corrections. This is not difficult, but has not been happening over the last decade, with limited interaction between seismological observatories.

References

- Gibson, G., Wesson, V. and Jones, T., 1994, The Eugowra NSW Earthquake Swarm of 1994, Seminar Proceedings, Australian Earthquake Engineering Society pp71 - 80
- Lynam, C. and Cuthberton, R., 1997, The Acacia Ridge (Brisbane) earthquake of 18 July 1996, Queensland University Advanced Centre for Earthquake Studies, Report no 2, pp71 - 81.
- Power, M., Chiou, B., Abrahamson, N., Bozorgnia, Y., Shantz, T. and Roblee, C., 2008, An overview of the NGA Project 3, Earthquake Spectra v1 n4, pp 3 - 22

Community Consultation Best Practice Manual

Steve Kennedy², Chris Matthews^{1*}, Damia Ettakadoumi², Cynthia Crowe²

¹ Australian Geothermal Energy Association. PO Box 1048 Flagstaff Hill SA 5159

² Department of Primary Industries GPO Box 4440 Melbourne VIC 3001

The Australian Geothermal Energy Group Technical Interest Group 1 (AGEG TIG 1) and the Australian Geothermal Energy Association (AGEA) have collaborated on a project to produce a best practice manual (BPM) on community consultation for the development of geothermal projects in Australia.

There is a growing expectation from the community, government regulators and leading industry players that stakeholders and the wider community will be fully informed and encouraged to provide input to decision making about the industry activities that have the potential to affect their communities.

AGEG and AGEA undertook the project to create the BPM with the following objectives:

- Companies meet government regulations and expectations
- Companies meet community expectations and maintain the 'social licence to operate'
- All parties follow the Australian Ministerial Council for Minerals and Petroleum Resources (MCMPR) Principles for engagement with communities and stakeholders
- Give clear advice to developers on the intricacies (such as timing) of reporting to both the community and corporate regulators such as the ASX.

When scoping this project, AGEN and AGEA recognised that there is a significant body of work that already exists on best practice community engagement, both in the Australian resources industry and in the international community.

It is for this reason that AGEN and AGEA decided to create tailored "best practice notes" that draw on the existing body of knowledge and provide guidance in the context of the emerging geothermal energy sector in Australia.

The "notes" format (rather than a single manual) means that each theme of community engagement is a stand-alone document. Companies can pick and choose the topics that are useful or relevant to them at the time. As the geothermal industry matures and community engagement principles change over time, the notes can be individually modified without having to update an entire manual.

The best practice notes series is a precursor to a more complete BPM on community engagement, to be completed by AGEN and AGEA in the near future.

Keywords: Community and Stakeholder engagement, best practice manual, key messages, communicating risks, media management, outrage management, geothermal energy, Australia, South Australian Resources Industry Code of Practice for Stakeholder and Community Engagement, Australian Geothermal Energy Group, Australian Geothermal Energy Association.

Context: The need for community consultation

The emerging geothermal industry as a whole (including government regulators, developers and stakeholders) understands the need to establish community understanding and support, sometimes known as the "social licence to operate" (SLO). Variation in Australia's population density and land use across the country means that the SLO will be more difficult to obtain in densely populated areas such as Victoria and New South Wales, compared with sparsely populated areas such as far northern South Australia. Failure to achieve the SLO may lead to delays in approving the project, result in expensive or onerous conditions or, in some cases, may even lead to the rejection of a proposal by regulators.

The regulatory process is likely to proceed more smoothly and expeditiously if effective stakeholder and community engagement has, as far as practical, addressed stakeholder concerns prior to applying for the required approvals (SACOME 2009).

The best practice manual process

Several organisations have worked over the last few years to establish a standard of practice that meets the requirements of best practice community consultation in resource development.

A number of benchmarking documents already exist that outline standards for stakeholder and community engagement that communities can expect from geothermal developers. These include documents published by the Minerals Council of Australia (e.g. MCA 2005), the MCMPR (MCMPR 2005) and the International Association for Public Participation (e.g. IAP2 2007).

A number of state government departments also have manuals on community engagement. These include the Department of Primary Industries Victoria (DPI Victoria 2010) and the Western Australian Government (WA Department of Indigenous Affairs 2005).

Drawing on and complying with these and other documents, the South Australian Chamber of Minerals and Energy (SACOME), in collaboration with Community Engagement Group Australia (cega) and Primary Industry and Resources SA (PIRSA) produced a Code of Practice for Stakeholder and Community Engagement in the SA resources industry (SACOME 2009). A Supporting Document, also published in 2009, supplemented the Code, which included guidelines and a community engagement toolkit designed by cega.

Best practice notes

With the knowledge that several benchmark documents already exist that adequately meet nationally and internationally recognised standards, AGEG and AGEA decided to create tailored “best practice notes” that draw on the existing body of knowledge and provide guidance in the context of the emerging geothermal energy sector in Australia.

Each note covers one of the following topics:

- Existing resources and tools for community engagement
- Identifying and engaging stakeholders
- Key messages about geothermal energy
- How to communicate messages about risks
- Skills required for community engagement
- Media management
- Outrage management

The best practice notes series is a precursor to a more complete BPM on community engagement, to be completed by AGEG and AGEA in the near future.

AGEA Membership commitment to best practice

The final objective of the BPM process is that members of AGEA, the peak geothermal industry body, will sign up and agree to abide by best practice community engagement as a prerequisite for being members.

The undertaking of this commitment will give all stakeholders, whether they be government funding bodies, communities, regulators or any other stakeholder groups, comfort that world's best practice is being applied when Australian geothermal projects are being undertaken.

References

Department of Primary Industries, 2010, Geothermal Energy in Victoria Landholder Information.

International Association For Public Participation (IAP2), 2007, Core Values.

Minerals Council of Australia, 2005, Enduring Value, the Australian Minerals Industry Framework for Sustainable Development, Guidance for Implementation.

Ministerial Council for Mineral and Petroleum Resources, 2005, Principles for Engagement with Communities and Stakeholders.

SACOME, 2009, South Australian Resource Industry Code of Practice for Stakeholder and Community Engagement. Code and Supporting Document.

Western Australian Government Department of Indigenous Affairs, 2005, Engaging with Aboriginal Western Australians.

Optimising ORC use in Australian Geothermal Applications

Craig Morgan¹, David Paul²

¹ Pacific Heat and Power, Level 14, 500 Collins Street, Melbourne VIC 3000

² Pratt & Whitney Power Systems, 400 Main Street, East Hartford, Connecticut, USA

* Corresponding Author: craig.morgan@pacificheatandpower.com, +61 3 9013 4425

Introduction

Since Pratt & Whitney Power Systems acquired a majority stake in Turboden in 2009, many hot sedimentary aquifer geothermal power applications across the world have been assessed. A variety of power configurations have subsequently been developed and costed that have relevance for the future of the Australian geothermal industry.

This paper summarises the key considerations made in designing systems, as well as factors that affect overall performance.

Keywords: PureCycle®, Pratt & Whitney Power Systems, Turboden, Organic Rankine Cycle, Pacific Heat and Power

Input conditions

Input conditions for ORC use in geothermal applications across the world vary substantially:

- Geothermal brine input conditions vary such as 74C in shallow and small scale Alaskan wells, 98C in Birdsville, 130C from a hot sedimentary aquifer in the USA, 150C at the outlet of a high temperature separator in New Zealand, or as high as 240C+ in enhanced geothermal applications. These temperature conditions, including flow rate may also change over time.
- Air temperatures vary from -5 C to 50C+ during the day in desert regions of Australia.
- Water for cooling is sometimes available, but many times it is not.
- Energy prices vary between AUD 5c/kWh to 20 c/kWh, and is sometimes a market rate or government-regulated.
- Incentives include Renewable Energy Certificates equivalent to 2-4 c/kWh, or tax-incentive regimes.
- Well and steam field developments vary from free-flowing wells to 5km-deep wells.
- Noise restrictions vary from site to site depending on the location of the plant.
- Flammability and toxicity of ORC working fluids is subject to a variety of planning regulations.

- Atmospheric conditions can include H₂S which aggressively corrodes copper in plant and equipment.
- Some project developers wish to contract for supply and commission of the ORC only, whilst others wish for a fully packaged Engineer-Procure-Construct (EPC) solution.

Amongst this, the ORC supplier must optimise each individual application according to a specific client's requirement, generally for highest economic return on their project and not necessarily lowest specific cost of the power plant (\$/kW).

ORC design considerations

Apart from the input conditions, key considerations in the ORC system design include:

- Corrosion → special and costly materials for the heat exchangers influence the unit cost significantly increase lead time.
- Scaling → there may be limits to the minimum temperature of the geothermal brine due to deposition of silica or other products.
- Fouling → removable covers and straight cleanable tubes assist in cleaning and on-going efficiency.
- Cascade use and cogeneration (using the condensing heat for other purposes) can improve feasibility.
- Working fluid flammability can be an issue for urban areas / insurance cost.
- Vapour plume from cooling towers are unsightly and there is a need for makeup water in evaporative devices.
- There is a larger footprint required, and additional noise emissions from the fans in an air condenser or fin/fan cooler.

Water use is becoming a significant issue.

Evaporative cooling towers feature:

- Smaller footprint.
- Lower noise emissions.
- Fresh water consumption.
- Chemical water treatment requiring operation cost and environmental impacts.

Air condensers feature:

- Larger footprint.
- Higher noise emissions.
- No water needed.
- Virtually no environmental impact and low operating costs.

Other options include hybrid cooling systems that operate dry in winter and cooler ambient conditions, whilst using water in hotter conditions.

Critical issues we observe are:

- Investment costs need to take into consideration initial capital requirements, ongoing costs, and future water availability.
- The generated yearly power output is tightly linked to cooling conditions and parasitic loads, and is particularly significant for cooler resources.

The best solution is dependent on the application, but in the main we see Australian clients preferring dry or hybrid cooling systems of some sort.

ORC performance & practical systems

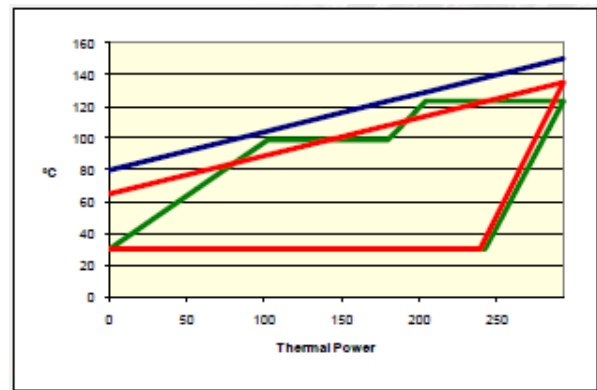
Availability of PWPS and Turboden ORC technologies in real world applications is at > 98%. Maintenance costs are very low relative to other power generation technologies such as engines, gas turbines or steam turbines.

The selection of working fluid is influenced by:

- Cost.
- Environmental impact.
- Pressure levels selected.
- Heat input curve.
- Enthalpy drop & flow rate.
- Flammability.
- Cooling system.

The optimal fluid, pressure levels, and turbine size varies from case to case.

In hot sedimentary aquifer applications the geothermal fluid normally stays in liquid phase. Currently the most proven and reliable ORC technology uses single-phase working fluids in 'normal' pressure cycles. These systems can be cascaded using multiple pressure levels to approach the ideal Lorentz cycle, minimising disadvantages whilst maximising the benefits of reliable systems.



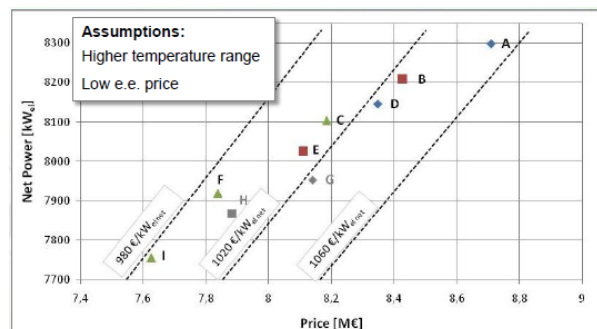
Technical innovations

The product development team continue to make system improvements that increase efficiency, broaden the variety of suitable applications, and provide the ability to operate in with zero water for cooling. Features available are:

- Air condenser for use in areas with limited access to water. The refrigerant is condensed directly in the air-condenser to maximise heat transfer.
- Coatings and equipment modifications such as those necessary for a high H2S environment in some international geothermal fields.
- High pressure evaporators may also be selected on a case by case basis for some applications.

Price vs Performance

A manufacturer is able to design for maximum efficiency, or minimum specific cost. It is critical that the client and equipment supplier work together to optimise the unit design for each specific application. The chart below illustrates this.



The table shows price/power ratios for different possible configurations of an air-cooled ORC unit (installed, BoP excluded) for the same Project.

Generally speaking the price/power ratio is influenced by the boundary conditions as follows:

- a colder(hotter) geothermal water will raise(decrease) the price/power ratio.
- a more aggressive and impure geothermal water will raise the price/power ratio.
- a higher(lower) average annual air temperature will raise(decrease) the price/power ratio.

But in the design phase the choice between a bigger or a smaller heat exchanger will influence performance and price, that means also the price/power ratio

The future and corporate update

PWPS and Turboden have recently been successful in winning orders for a 5 MW geothermal power plant in Germany (based on the Turboden technology), and a 500kW geothermal power plant in Taiwan (based on PureCycle®).

Conclusion

There is a wide variety of input conditions and design considerations that influence the final cost of an ORC power plant, and as such each project, whilst based on modular technology, will most likely be configured in a project-specific manner. It is therefore critical that you work closely with your equipment supplier to optimise the configuration to balance:

- Technical performance
- Efficiency
- Economic performance,
- Reliability and
- Operability

Mineral scaling in geothermal fields: A review

Yung Ngothai^{1*}, Norio Yanagisawa³, Allan Pring², Peter Rose⁴, Brian O'Neill¹, Joël Brugger²

¹ School of Chemical Engineering, The University of Adelaide, SA 5005

² South Australian Museum, North Terrace, Adelaide, SA, 5000

³ Institute for Geo-Resources and Environment, AIST, Tsukuba, 305-8567, JAPAN

⁴ Energy and Geoscience Institute, The University of Utah, Utah 84109, USA.

*Corresponding author: yung.ngothai@adelaide.edu.au

Abstract

Geothermal power is an established energy source in several countries, for example New Zealand and Iceland. However the proposed geothermal operations in South Australia occurs at a much greater depth (5 km) and the heat source is radioactive decay rather than volcanism. A number of issues relating to the geochemistry of geothermal fluids are required to be considered and explored to ensure safe, economic energy production from geothermal fields. Low pH and saline waters, at temperatures much greater than 200°C, are highly corrosive, and it is vital to prevent the generation of scales as the brines are transported to the surface. This paper provides a review on silica, calcite and metal sulphide scaling at various geothermal fields. The solubility of silica and calcite as a function of temperature and/or pressure were discussed and how it affects scaling at various locations in the geothermal plant.

Keywords: silica scaling, calcite scaling, metal sulphide scaling, EGS, HDR.

Introduction

In many developed geothermal fields in USA, New Zealand, Indonesia, Japan etc., mineral scales tend to precipitate with change of fluid temperature and/or pressure, leading to fluid flow problems. To overcome the operational problems associated with this scaling, several methods have been developed to eliminate and/or reduce the amount of mineral deposition. It is however important that we further investigate the mechanisms involved and the relation between mineral scaling and the physical and geochemical characteristics of the rocks and fluids in the geothermal system under exploitation.

For future geothermal systems, research and development of Enhanced Geothermal System (EGS) is required at a rapid pace, especially in Australia.

The outline of EGS (or Hot dry rock – HDR) system is described as follow; injected water is heated in artificial reservoir constructed using hydrofracturing technology by flowing through a high temperature granite. The heated fluid produced in reservoir, is used for power generation.

The first EGS project was carried out at Fenton Hill, New Mexico (USA), which ran from 1970. After that other EGS projects were established in a number of countries e.g., Japan (at Hijiori), Soultz, France, etc. Metal corrosion and mineral scaling were observed at these EGS systems. For example, in Soultz, metal corrosion occurred due to high Cl concentrations (Baticci et al, 2010) while in Hijiori, anhydrite and calcite scaling occurred in the lower production wells and pipelines at ground level due to dissolution of anhydrite in the reservoir by the injected low temperature water (Yanagisawa et al., 2008). These problems are common to the well-developed conventional geothermal power plants and likely to feature in EGS systems.

This paper presents a brief review of mineral scaling in geothermal fields and discussion for future EGS development.

Mineral scaling

The fluid in a natural geothermal system has a long residence time (thousands of years) at a relatively high temperature (> 150°C – 300°C) which therefore indicates a significant rock-water interaction. Since the system has had a long residence time, it is often assumed to be in a state of chemical equilibrium (Grigsby et al., 1989). Therefore, when fresh water is introduced into the system to extract heat, the system is no longer in equilibrium, which leads to precipitation and dissolution of different parts of the mineral assemblage. Precipitation, or scaling, is one of the major problems in geothermal energy extractions. Minerals may precipitate depending on the compositions of the granite and the injected brine.

In geothermal fields, it has been reported that silica, calcium carbonate, anhydrite, metal sulphides and iron minerals scales precipitated around production and injection wells and in the piping.

Silica scaling

Silica scaling is a well known problem in conventional geothermal systems, which occurs due to the presence of amorphous silica, during heat extraction or partial flashing (Robinson, 1982). Amorphous silica can contain several metals such as iron, magnesium, and calcium, etc.

Silica scale precipitated in many geothermal fields due to its high solubility at high temperature in the reservoir through water-rock interactions and the solubility rapidly decreases with decreasing temperature. The solubility of silica is also strongly dependant on pH. For example, iron-bearred amorphous silica tends to precipitated at fluid mixing points. At this point, temperature, pressure and pH of fluid change rapidly and leading to significant changes in solubility and chemical equilibrium leading to silica precipitation.

Furthermore, silica has several structural phases, for example, quartz and amorphous silica while silica exists in solution both as a polymer and a monomer form. This variety leads to a complex array of mechanisms for silica precipitation, especially in lower temperature environment such as at the injection well.

The dissolution of solid silica phases (SiO₂) in water has been extensively studied (Mackenzie and Gees, 1971; Owen, 1975; Robinson, 1982). The solubility data for various silica phases (Rimstidt, 1980 cited from Robinson, 1982) are shown in Figure 1 where the solubility of different silica phases is plotted versus temperature. Quartz is thermodynamically the most stable phase of silica thus its solubility at any given temperature is lower relative to other silica phases.

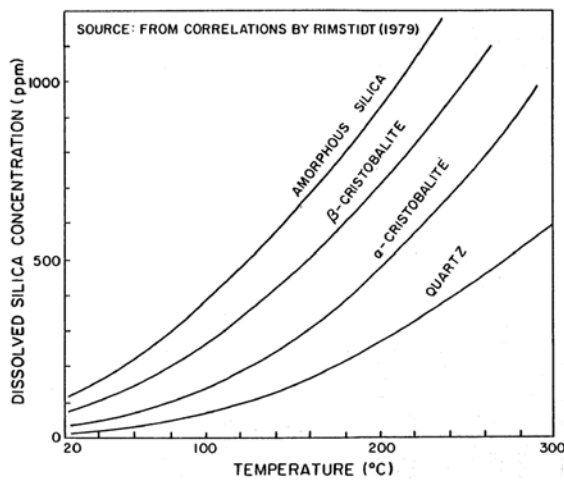


Figure 1: Equilibrium solubilities of silica phases

Silica concentrations in geothermal reservoir waters at 200-350°C are approximately 300-700 mg/kg SiO₂ (Gunnarsson & Arnórsson, 2005). Fournier and Rowe (1966) state that the silica content in geothermal waters is controlled by the solubility of quartz at depth and not the solubility of amorphous silica at and near the surface of the ground. When hot brine is brought to the surface it is either flashed or cooled while passing through a power plant system to release its available thermal energy. Chan (1989) states that the

dissolved silica in the brine may then become supersaturated. Depending on the degree of supersaturation the dissolved monomeric silica may nucleate and deposit as amorphous silica scale on equipment, such as heat exchanger surfaces (Chan, 1989). The factors which affect the solubility of amorphous silica in solution include temperature, pH, pressure and salt content (Chan, 1989). Gunnarsson & Arnórsson (2005) state that there are two processes involving aqueous silica that occur in an amorphous silica super-saturated solution. The first process is the direct precipitation of amorphous silica directly onto the surface of equipment. The second is the tendency for silica to polymerise and form colloids that remain in suspension for long periods of time. Polymeric silica has less tendency to precipitate from solution than monomeric silica.

Kinetics of silica dissolution needs to be established in order to evaluate the likelihood of silica scaling. Factors that control the rate of polymerization of dissolved silica are pH, salinity, degree of supersaturation, presence of solid substances, and temperature (Angcoy, 2010). Bethke (1996) compiled the rate constants for quartz and amorphous silica dissolution which were originally determined by Rimstidt and Barnes (1980), are shown in Table 1.

Table 1: Rate constants of quartz and amorphous silica dissolution

T(°C)	Quartz	α-Cristobalite	Amorphous silica
25	4.20×10 ⁻¹⁸	1.71×10 ⁻¹⁷	7.32×10 ⁻¹⁷
70	2.30×10 ⁻¹⁶	6.47×10 ⁻¹⁶	2.19×10 ⁻¹⁵
100	1.88×10 ⁻¹⁵	4.48×10 ⁻¹⁵	1.33×10 ⁻¹⁴
150	3.09×10 ⁻¹⁴	6.12×10 ⁻¹⁴	1.49×10 ⁻¹³
200	2.67×10 ⁻¹³	4.81×10 ⁻¹³	9.81×10 ⁻¹³
250	1.46×10 ⁻¹²	2.55×10 ⁻¹²	4.43×10 ⁻¹²
300	5.71×10 ⁻¹²	1.01×10 ⁻¹¹	1.51×10 ⁻¹¹

Calcite scaling

Calcite or aragonite (CaCO₃) scaling is also a well known problem in conventional geothermal systems, Calcite scale occurs near the flashing point in the production wells due to decrease in calcite solubility.

Calcium solubility varies with the pressure of CO₂ (P_{CO₂}) and temperature of the fluid. Figure 2 shows the calcium solubility curve as a function of P_{CO₂} and temperature by Fournier (1985). It is noted from this curve that under the same temperature condition, calcite solubility is higher with respected to increase of P_{CO₂}. This explains why it is common to observe scaling at the flashing point. During flashing, where vapour release occurs causes the P_{CO₂} to decrease,

calcite solubility therefore drops and calcite scale precipitates there. Furthermore, as calcite solubility is lower at high temperature conditions, calcite precipitation tends to occur at deep points in production wells and could be a serious problem. Many geothermal fields with high calcium or hydro-carbonate concentration experience calcite scale problems. In Japan, especially at the Mori and Oku-Aizu geothermal field calcite scaling is a serious problem.

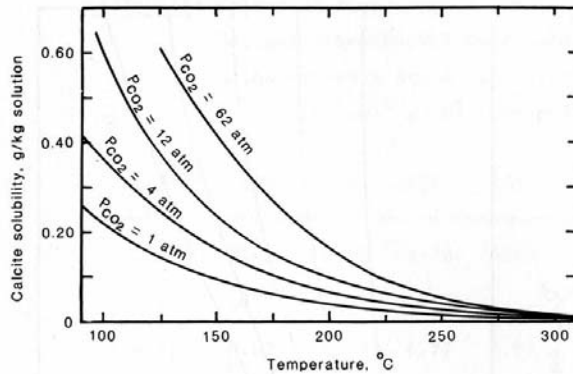


Figure 2: Solubilities of calcite as a function of temperature and pressure of CO₂

To prevent calcite scaling in wells, various chemical inhibitors have been used in many geothermal fields. For example, sodium polyacrylate, C₂H₃COONa, has been used for several Japanese geothermal fields and hot spas. Similar chemicals have been used around the world. At high fluid temperature, sodium polyacrylate reacts with calcium ion to make complex. Calcium complex cannot react with the bicarbonate ion (HCO₃⁻) to precipitate calcium carbonate. Thus, this sodium polyacrylate inhibitor is effective to prevent calcite scaling. For a production well, a capillary tube is inserted into well until it reaches the depth of the flashing point and the chemical inhibitor is then injected directly at this point and prevents scaling.

Similarly the solubility of anhydrite (CaSO₄) is lower at higher temperature and tends to precipitate deep in the production wells and at the peak temperature point. In this case, with the temperature of fluid from deeper parts increases anhydrite precipitate due to its decreasing solubility. It has been reported that in Japan, Mori and Sumikawa geothermal fields experience anhydrite scaling.

Metal sulphide scaling

Metal sulphide scaling is often occurred in volcanic or high Cl environment. For example, at Salton Sea geothermal field, the salinity (35% NaCl) and metal concentrations (around 20% copper) in the fluid are very high (Skinner et al., 1967), many sulphide minerals form scales, such as bonite (Cu₅FeS₄), chalcocite (Cu₂S) have been found.

In Japan, metal sulphide scaling is found in Oku-Aizu (Nitta et al., 1991) and Yamagawa (Akaku, 1988). At Oku-Aizu geothermal field, the sulphur removal system near power plant has been built to prevent sulphide scaling.

The sulphide mineral scaling indicate the conditions in the deep-seated reservoir, especially in granitic rocks. For example, at the Kakkonda geothermal area, in north-eastern Japan, there is a 80 MW geothermal power plant using high temperature fluid from the reservoir at the boundary between the Quaternary Kakkonda granite and the Pre-Tertiary formations at about 3km depth. Metal sulphide minerals deposit in the production wellhead and pipelines (Yanagisawa et al., 2000).

The metal sulphide scales are classified into two types, based on sulphide mineralogy. These are Pb-Zn rich type and Cu rich type. Pb-Zn rich scale is found in Well-19 located at the marginal part of the Kakkonda granite as shown in Figure 3. It is mainly composed of amorphous silica, galena (PbS), sphalerite (ZnS) and pyrite (FeS₂). The brine of WD-1a at 3.7km depth, in the Quaternary Kakkonda granite rock, underlied Well-19, is rich in Pb and Zn and the scale in Well-19 is of similar composition.. Cu-rich scale is found in Well-13, located at the central part of the Kakkonda granite. It is mainly composed of amorphous silica, chalcocite (Cu₂S), bornite (Cu₅FeS₄), loellingite (FeAs₂) and native antimony (Sb). It is also rich in Au, Ag, As, Cr, Ni and Mo compared to Pb-rich scale.

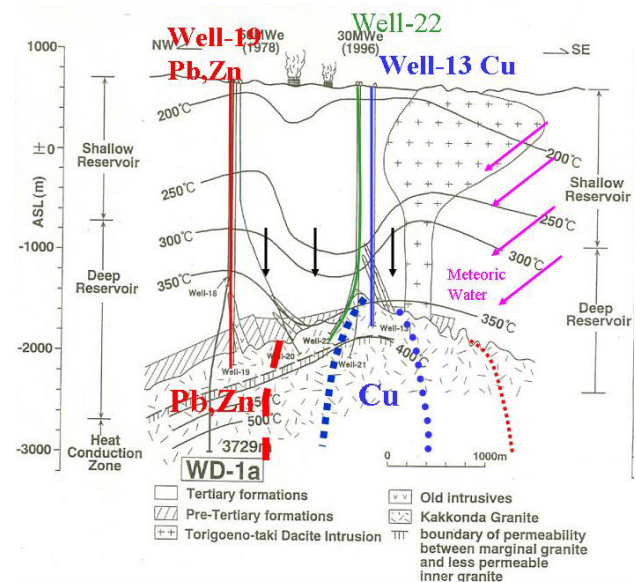


Figure 3: Schematic geothermal cross-section of the Kakkonda geothermal system including well name and metal in precipitated sulphide and brine in granite

Scaling in EGS system

In EGS system, several different types of scale mineral precipitated in the Hijiori system, located

Australian Geothermal Conference 2010

Nitta, T., Adachi, M., Takahashi, M., Inoue, K. and Abe, Y., 1991, Heavy metal precipitation from geothermal fluid of 87N-15T production well in the Okuaizu geothermal field, Tohoku district, Japan. *Resource Geology*, 41, p.231-242 (in Japanese).

Owen, L. B., 1975, Precipitation of Amorphous Silica from High-Temperature Hypersaline Geothermal Brine, California University, Livermore (USA), Lawrence Livermore Lab., Technical Report

Rimstidt J. D. and Barnes, H. L., 1980, The Kinetics of Silica-Water Reactions, *Geochimica et Cosmochimica Acta*, 44, pp. 1683-1700.

Robinson, B. A., 1982, Quartz Dissolution and Silica Deposition in Hot Dry Rock Geothermal systems, Thesis.

Skinner, B. J., White, D.E., Rose, H. J., Jr. and Mays R.E., 1967, Sulfides associated with the Salton Sea geothermal brine., *Economic Geology*, 62, p.316-330.

Yanagisawa, N., Fujimoto, K. and Hishi, Y., 2000, Sulfide scaling of deep-geothermal well at Kakkonda geothermal field in Japan, *Proceedings of World Geothermal Congress*, p.1969-1974.

Yanagisawa, N., Matsunaga, I., Sugita, H., Sato, M. and Okabe, T., 2008, Temperature dependent scale precipitation in the Hijiori Hot Dry Rock system., *Geothermics*, 37, p.1-18.

Direct GeoExchange Cooling for the Australian Square Kilometer Array Pathfinder – Field Trial

Donald J. B. Payne^{1,2*}, and Dezso Kiraly³

¹ School of Physics, University of Melbourne, Parkville, VIC, 3010.

² Direct Energy Pty. Ltd., 6 Alma Rd, St Kilda, VIC, 3182.

³ CSIRO Astronomy and Space Sciences, Corner Vimiera & Pembroke Rd, Marsfield, 2122.

* Corresponding author: djbpayne@unimelb.edu.au; 0414 990 310

Direct Geoechange Heat Pumps (DGHPs) provide chilling via refrigerant-carrying copper loops buried in the ground which act as a condenser and achieve higher efficiency than equivalent air source heat pumps because of the ground's constant heat capacity. DGHPs are particularly suited to desert environments with more extreme ambient temperatures. The Australian Square Kilometer Array Pathfinder (ASKAP) radio telescope will be an array of 36 x 12-m diameter parabolic dish antennae situated in Boolardy, WA each requiring 5 – 9 kW_{th} cooling for computer equipment and pedestal. Following successful tests of a prototype installation at Marsfield, NSW (ground temperature 17 C) a DGHP is installed at antenna site #29 (the first erected). The DGHP provides chilling to a variable test load (3.6, 4.8, 8.4, 9.6, 13.2 kW) via a 200 L water buffer. 6 x 30m bores containing copper loops deliver up to 14 kW of chilling to maintain 13 - 15 C water temperature in the buffer. 5 data bores monitor ground temperature variation in the centre of the 6 active bores and at 0.3, 0.6, 3.0, 6.0 m (outside the bore field). System pressures & power are also monitored. A higher-than-expected baseline ground temperature of 27 C is measured and verified by three methods. The nominal 14 kW DGHP can maintain 15 C water temperature at all loads including 13.2 kW. Note that 0.5 kW pump heating means the effective load is 13.7 kW. We describe the results from this field installation in detail and present an abridged set of data.

Keywords:

Direct Geoechange, Direct Use, Geothermal Heat Pump

Direct Geoechange

The emerging geothermal industry in Australia is focused on producing electricity ("indirect use") and should begin delivering substantial results over the next decade. *Direct Use* geothermal energy is more efficiently available as it entails only one energy conversion (absorption or radiation of heat), rather than the several that occur in electricity generation and usage, with each step losing a percentage on conversion. Geothermal Heat Pumps (GHPs) are a direct use of geothermal energy which involve circulating a fluid (water, brine or refrigerant) through earth

loops (poly pipe or copper) a few tens of metres deep (Fig. 1, Payne et al. 2008).

Direct Geoechange Heat Pumps (DGHPs) which circulate refrigerant through copper loops have greater efficiency than water-loop GHPs because:

- (i) copper is more thermally conductive than insulating plastic;
- (ii) latent heat transfers directly with the ground on evaporation or condensation; and
- (iii) an intermediate water-to-refrigerant heat exchanger between the ground loops and compressor is not required.

DGHPs transfer heat via 30-metre deep, 75-mm diameter bore holes compared with 100-metre deep, 150-mm diameter bores used for water-loop GHPs. A continuous, closed loop of copper piping is inserted and sealed with a thermally conductive grout (cement). Below 5 metres the Earth remains at a stable temperature all-year-round (27° C at Boolardy, WA). The smaller temperature difference between the heat source/sink and the building or water to be heated/cooled results in lower head pressure and energy requirement of the compressor compared to conventional heating and cooling systems. A "desuperheater" may be employed in chilling applications to further optimise the performance and produce hot water or air which can be used usefully elsewhere.

ASKAP

The Australian Square Kilometer Array Pathfinder (ASKAP) radio telescope is an array of 36 x 12-m diameter parabolic dish antennae situated in Boolardy WA (Fig. 2) whose construction commenced in early 2010 and is a precursor to the Square Kilometer Array (SKA) of several thousand 12-m dishes. A prototype of the Electronics Systems (ES) and Phased Array Feed (PAF) package to be cooled has been installed at the CSIRO Australian Telescope National Facility (ATNF) headquarters in Marsfield, NSW. These two components should not exceed 20 - 30° C under all operating and weather conditions and require an estimated heat dissipation of 5 – 7 kW_{th}. Various cooling methods have been considered and the extreme desert temperatures and high price of diesel generated power strongly favour a DGHP solution. The results of testing of a DGHP at Boolardy are summarised in this paper.

System Design

Cooling is provided by a 14 kW_{th} DGHP which circulates refrigerant (R407C) through 6 x 30-m copper earth loops to a refrigerant-to-water, coil-in-tank heat exchanger. Water in the 200 L buffer tank is chilled to 7 – 15° C. Water is circulated from this buffer tank to the PAF & ES to deliver the required cooling to the heating load (the “secondary” circuit). The design of the secondary circuit is beyond the scope of this paper – here the performance as a function of thermal load is explored by a test load. The test load is a 50 L water tank with three elements (3.6, 4.8, 4.8 kW) that can be switched on to produce 3.6, 4.8, 8.4, 9.6, 13.2 kW. A circulation pump continually circulates water through this test load and contributes circa 0.5 kW of heating. A controller achieves the specified water temperature.

Earth Loop Installation

The 14 kW_{th} system requires 6 x 30-m copper earth loops (½-inch vapour and ¼-inch liquid) with PVC insulation on the upper 15-m of the liquid line to minimise heat transfer between the two and stop flashing of the liquid refrigerant. 70-mm diameter holes are drilled vertically 30-m deep in a hexagonal configuration around a point 10m from the pedestal foundation edge with 3-m spacing between them to allow sufficient thermal diffusion through the ground. After insertion of the loops the holes are filled with a thermally conductive (geothermal) grout (e.g. 111-mix, Therm-Ex, IDP-357, Barotherm) ensuring that there are no air pockets. The liquid & vapour lines from the earth loops are brazed to their respective manifolds (½-inch liquid & 7/8-inch vapour) using a 15% silver brazing alloy. The liquid line is insulated with ½-inch non-corrosive insulation material (e.g. Armaflex, Insul-Lock) and run towards the heat pump (compressor) with a maximum length of 40-m. 5 data bores were also drilled. The location of all bores was logged by triangulation to GPS pegs on the foundation (as shown below).



Figure 1: Loops, liquid & vapour manifold and trenches.



Buffer Tank, Heat Exchanger & Test Load

Chilling is delivered through a submerged copper evaporator coil inside a 200 L buffer tank – this is in contrast to the brazed-plate heat exchanger used in the Marsfield installation. Water flows over the coils via a central perforated copper pipe to ensure effective heat transfer. A minimum flow rate of 0.6 L/s (36 L/min) is required to achieve this. A 50 L test tank equipped with three switchable heating coils (4.8, 4.8 & 3.6 kW) simulates the load. The test tank is connected to the buffer tank via 32mm polyethylene pipe.



Figure 4: Evaporator coil & load tank

Heat Pump Design & Refrigeration

The DGHP installed at Boolardy differs from that installed Marsfield in the following ways:

- The desuperheater coil is built into the unit
- The unit is cooling only having no reversing valve
- It has a nominal capacity of 14 kW_{th} (cf. 10.5 kW_{th}) to cater for pedestal cooling

The components are described in turn.

Compressor: A 3-phase Scroll compressor drives the heat pump with compression ratio of 4. Its efficiency is a function of the evaporating and condensing temperatures (pressures).

Active Charge Control (ACC): This:

- prevents liquid refrigerant from reaching the compressor by acting as a reservoir;
- evaporates refrigerant to keep the system properly charged and to eliminate superheat;
- improves volumetric efficiency, reduces power draw, and lets compressor run cooler;
- enables passage of oil entrained in refrigerant;
- indicates refrigerant level via 3 sight glasses.

Liquid Flow Control (LFC): This is an efficient Thermal Expansion Valve (TXV) which:

- Sets proper refrigerant flow rate based on condenser (upstream) operating conditions;
- Ensures zero sub-cooling so condenser is fully active;
- Reduces compressor discharge pressure and lowers power requirement;
- Prevents vapor from “blowing through”.

Oil Separator: Oil lubricates the compressor and the oil separator acts with the ACC to prevent oil from migrating down the earth loops.

Dryer: This filters and dries the refrigerant before it enters the LFC.

Refrigerant: R407C [HFC azeotrope: R32 (23%) + R125 (25%) + R134a (52%)]. Future work will explore other HFC and hydrocarbon refrigerants.

Expected Performance

The Air-Conditioning, Heating and Refrigeration Institute (AHRI) has a well-established standard for DGHPs: ANSI/ARI Standard 870, 2001. Also, DGHPs are EnergyStar rated, endorsed by the Environmental Protection Authority (EPA) and Electrical Testing Laboratories (ETL) tested. The DGHP manufacturer, EarthLinked, provides performance tables which are derived from both the Scroll compressor’s performance and field trials. For an earth temperature of 27° C and chilling water to 15° C, the expected Coefficient of Performance (COP = thermal energy removed/ electrical energy input) is 4.5 – 5.0 depending on load. The theoretical maximum (Carnot cycle) performance for cooling is given by $T_{evap} / (T_{cond} - T_{evap})$ where T_{cond} is the condensing temperature and T_{evap} the evaporating temperature (Kelvin) and is 7.7 for $T_{cond} = 42° C$ and $T_{evap} = 6° C$ which correspond to the above conditions. Select7 software from Emerson Climate Technologies (manufacturer of Copeland Scroll compressors) suggests 14 kW.

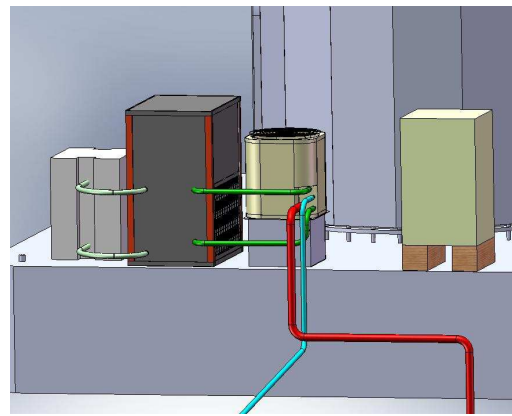


Figure 5: Final setup

Methodology

To find the most efficient means of cooling, the COP is measured as a function of the controllable aspects of the system. The key controllable variables are:

Buffer Set Point (T_{b-set}): the temperature to which the buffer tank is controlled to be chilled – it is measured inside the buffer tank.

Buffer Maximum (T_{b-max}): the buffer tank temperature at which the controller switches on the chilling DGHP.

Cabinet Set Point ($T_{cabinet}$): the temperature to which the cabinet is cooled.

Secondary Load (P_{load}): the thermal power which is simulated with a set of heaters.

Tank Load (P_{tank}): there are no elements in the tank.

Other input variables include:

Ambient Temperature: this includes both the wet (T_{wet}) and dry (T_{dry}) bulb temperatures.

Environmental Gain (P_{envt}): the tank & pipes are insulated but there is still environmental gain.

Tank Volume (V_{tank}): the buffer tank volume.

Water Volume (V_{water}): volume of water in the system: tank, primary & secondary pipes.

Output variables include:

Compressor Electrical Power (P_{comp}): the electrical power used by the compressor.

Cycle Time (t_{cycle}): the time between compressor start-ups.

Compressor Time (t_{comp}): the time the compressor is on during a cycle.

Duty Cycle (D): the percentage of time the compressor is on (t_{comp}/t_{cycle}).

Earth Loop Temperatures (T_{5-30m}): The temperatures measured at 5, 10, 15, 20, 25 & 30m.

Refrigerant liquid & vapour temperature (T_{liq} , T_{vap}): the temperatures to and from the earth loops

Suction, Head & Return Pressures (P_{head} , P_{suc} , P_{ret}): The pressures in & out of the compressor and returning from the earth loops.

Results

COP Calculation

The default input values are: $T_{b-set} = 13^{\circ} C$, $T_{b-max} = 15^{\circ} C$, $T_{cabinet} = 23^{\circ} C$, $P_{load} = 8.4 kW_{th}$, $P_{tank} = 0$, $V_{tank} = 200 L$, $V_{water} = 273 L$. The ambient temperature varies between 10 and 35° C during the test periods and future results will be calibrated against this. An estimate of the environmental gain was determined by cooling the buffer to 15° C, leaving the system off and measuring the time taken (t_{envt}) for the temperature to increase a known amount (ΔT_{test}). $P_{envt} = C_{pw} \cdot V_{water} \cdot \rho_w \cdot \Delta T_{test} / t_{envt}$ where $C_{pw} = 4.2 kJ/(kg \cdot K)$ is the specific heat of water, $\rho_w = 1 kg/L$ is the density of water. It was found that for $\Delta T_{test} = 2 K$, $t_{envt} = 135 min$ giving $P_{envt} = 208 W$.

Figure 5 shows the temperature and pressure outputs for the above input conditions. From these results, the COP can be derived. We find $t_{cycle} = 1160 sec$, $t_{comp} = 780 sec$, giving $D = 67.24\%$. There is a temperature overshoot of typically 0.3 – 0.5 K below T_{b-set} and above T_{b-max} giving $\Delta T = 2.8 K$. The power required to reduce the system water temperature is $P_{water} = C_{pw} \cdot V_{water} \cdot \rho_w \cdot \Delta T / t_{comp} = 4.12 kW_{th}$.

The electric power consumed by the compressor + pump + monitoring equipment is measured continuously along with the electric power required for the pump alone. This allows the total electrical energy consumed over a known number of cycles to be computed. For this run, $E = 3.081 MJ$ is consumed over $n_{cycle} = 3$ cycles (19.33 min) and the average power (directly monitored) $P_{comp} = E / (t_{comp} \cdot n_{cycle}) = 3.95 kW_{elec}$.

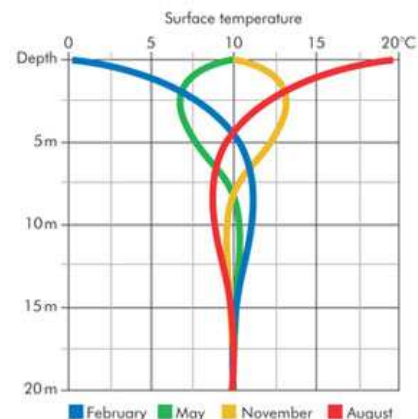
$COP = [P_{water} + (P_{load} + P_{envt}) / D] / P_{comp} = 4.46$. Note that D accounts for the fact that the load and environment are constantly delivering heat to the system which must be dissipated by the heat pump whilst on.

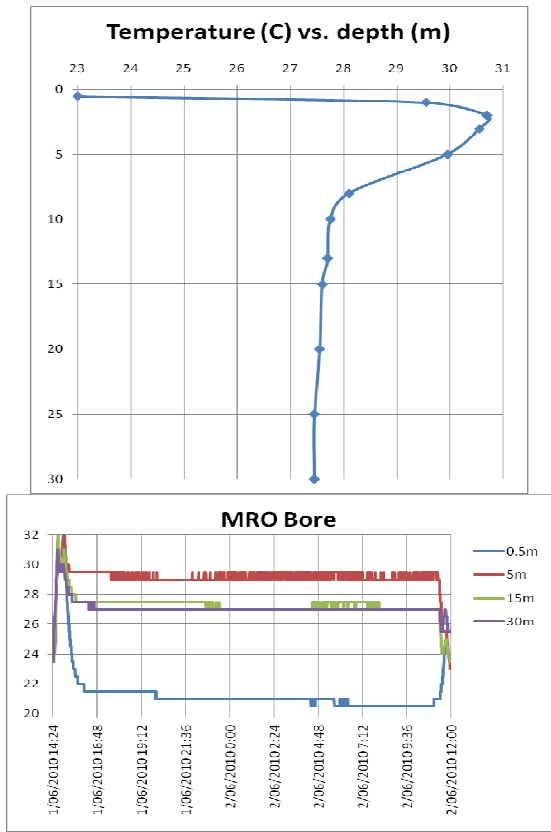
Using this method (see appendix), the COP is calculated as a function of load and DGHP configuration and plotted below. It is clear that the system should not be designed to run with a 100% duty cycle. An initial configuration of the system had the heat pump unit 30 m away from the earth loops. After moving the DGHP to within 4 m of the earth loops, the pressure drop across the earth loops was 5 – 15 PSI lower. Also, the manifold pit was initially exposed for testing and thus about 15 m of the copper earth loops was exposed to air and thus not efficiently dissipating heat. Backfilling the manifold pit boosted the performance.



Mean Earth Temperature

The undisturbed mean ground temperature was measured every 5m to 30m down six bore holes (two active and four data) via temperature sensors. One of the bore holes (B5) has sensors at 1, 2 and 3m also. Initial temperature readings were measured on 4th May 2010 and they were corroborated with data loggers (LASCAR EL-USB-2) on 2nd June 2010 (late Spring in Australia, equivalent to November in the Northern Hemisphere). The temperature is plotted as a function of depth below and corroborates with what is expected. Independent verification of temperature data has been important as the expected mean earth temperature was 23 C. A 120m test hole for water geoexchange was drilled at the Murchison Radio Observatory central site approximately 2 km away from the DGHP installation at antenna #29. Bore water inhabited this hole at a depth of 31.3m. The data loggers were hung down the hole to a depth of 30m on a rope at depths 0.5, 5, 15, 30 m and left for 20 hr with resultant mean earth temperatures of 21, 29.5, 27.5, 27 respectively (see figure). A sample of the bore water (jar down rope) was taken and its temperature upon extraction was just under 27 C measured with a probe thermometer. This provides a third means of verifying the bore temperature and corroborates.



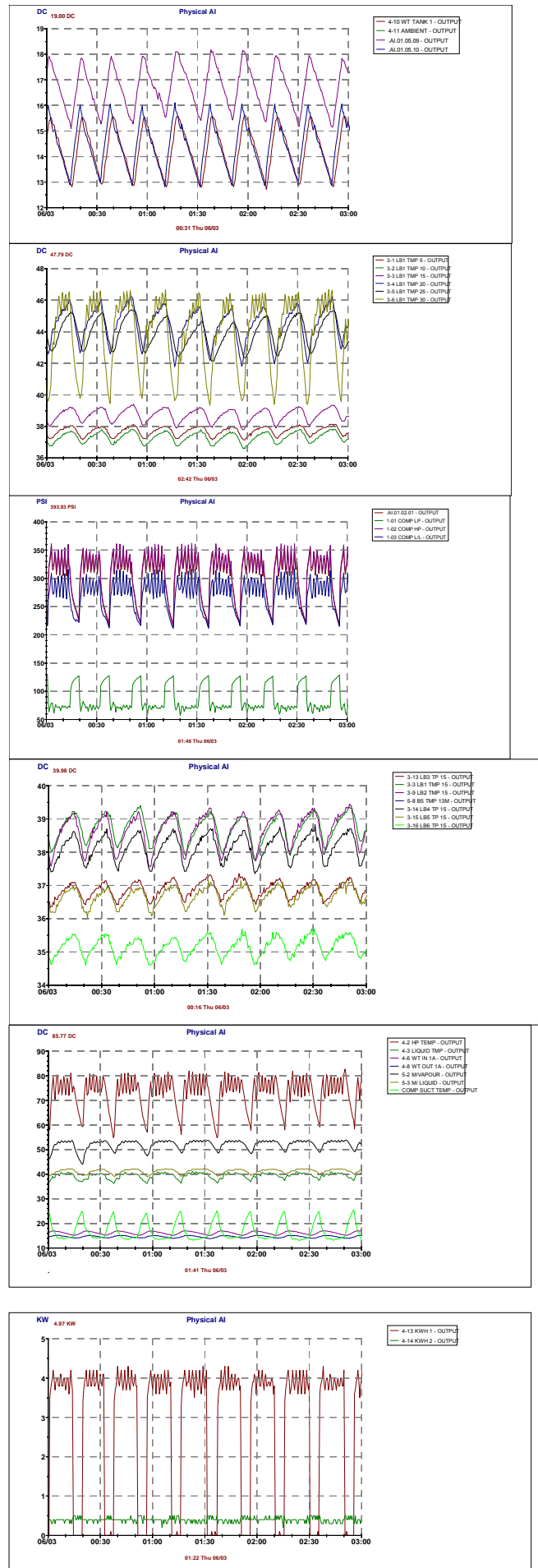


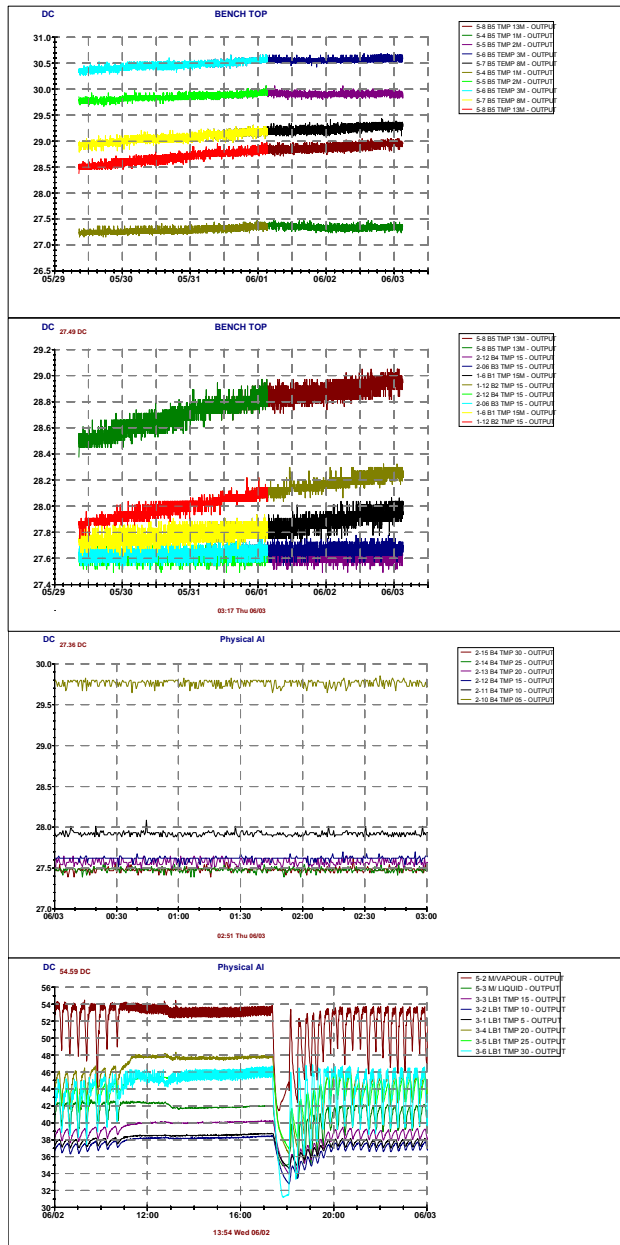
Ground pH & Bore water salinity

The pH and salinity of bore water used for the thermal grout was measured with testing strips. pH = 7.8 - 8.2 - acidity is thus not an issue for corrosion of the copper loops. The chloride levels are circa 850 mg/L. This is a borderline reading of the bore water. The aquifer was not penetrated by the site #29 bores and the ground is probably benign. Taking a conservative approach, a Cathodic Protection System will be installed for this system – a solar solution for its power is being exploring.

Abridged Results

For the presentation of data, a period from 12:00 – 3:00am on 3rd June 2010 was chosen. Below appear the water (buffer tank) temperatures, temperatures down LB1, pressures, 15m bore temperature for all active bores, refrigerant temperatures throughout the system, and electric power. Also initially available temperatures from the data bores are plotted: B5 0.3m data bore, 15m bore temperature for all data bores, B4 6m data bore.





Analytic derivation of the expected ground temperatures will be presented in a future paper. As seen above, after the compressor starts, the ground temperatures rise asymptotically towards saturation at which thermal output matches thermal dissipation in the ground. Maximum load (13.2 kW_{th}) was applied from 10:38am to 17:17 and the water temperature was held down to 15 C. After switching off the load, the ground recovers. At 18:11 a 3.6 kW load is applied, at 18:45, 4.8 kW and at 19:26:30, 8.4 kW.

Conclusions & Further Work

DGHPs are an efficient solution for heating and cooling and are particularly suitable for cooling in a desert environment with no power infrastructure. It has been shown that a DGHP is able to deliver 13-15 C chilled water despite high ground temperatures of 27.5 C. It does with a COP between 4 and 5 for the expected load range.

This corroborates with data obtained from Marsfield – it was expected that the higher ground temperature would slightly reduce output & performance. As in Marsfield, it has been demonstrated that COP decreases as a function of load in the secondary circuit (which determines the duty cycle) simulated by a test tank. Further results are being obtained for this configuration and additional experiments include the use of alternative refrigerants. The thermal conductivity & other properties of the ground will be calculated by comparison with analytic and numerical models.

Acknowledgements

This scientific work uses data obtained from the Murchison Radio-astronomy Observatory. We acknowledge the Wajarri Yamatji people as the traditional owners of the Observatory site. We acknowledge the CSIRO, CASS team including Grant Hampson, Evan Davis, Antony Schinckel, Graham Allen, Steve Broadhurst along with Robert Rechtman & Mike Francis of Direct Energy, David & Peter Manoni from Geothermal WA, Hugh Campbell & Nigel Foster of Dongara Drilling and Shannon Lovett, Nick Holt & Mark Alden of Emerson Climate Technologies.

References

Payne, D. J. B., Hampson, G., Kiraly, D. and Davis, E. Direct GeoExchange Cooling for the Australian Square Kilometer Array Pathfinder, Australian Geothermal Conference 2009

Payne, D. J. B., Ward, M. And King, R. L., Position Paper: Direct Use Geothermal Applications, Australian Geothermal Energy Association (AGEA), Feb 2008.

Yu MZ, Peng XF, Li XD, Fang ZH, A simplified model for measuring thermal properties of deep ground soil, Experimental Heat Transfer, 17(2): 119-130, 2004.

Cui, Ping, H. Yang and Z. Fang, Heat transfer analysis of ground heat exchangers with inclined boreholes, Applied Thermal Engineering, Vol.26, 1169-1175

Marcotte, Denis and Philippe Pasquier, The effect of borehole inclination of fluid and ground temperature for GLHE systems, Geothermics, Volume 38, Issue 4, pp 392-398

Bristow, K. L., R. D. White, and G. J. Kluitenberg, Comparison of single and dual probes for measuring soil thermal properties with transient heating, Aust. J. Soil Res. 32, pp. 447-464

A Research Well for the Pawsey Geothermal Supercomputer Cooling Project

Klaus Regenauer-Lieb^{1,2} and the WAGCoE team^{1,2,3}, Peter Malin⁴ and the IESE team, Steve Harvey² and the CSIRO CESRE team, Edson Nakagawa² and CSIRO'S Geothermal & Petroleum Portfolio, Hal Gurgency⁵ and the QGECE team

^{1,2,3} Western Australian Geothermal Centre of Excellence, ¹The University of Western Australia, M004, 35 Stirling Av. 6009, Crawley

²CSIRO Earth Science & Resources Engineering, ARRC, 26 Dick Perry Avenue, Kensington, Western Australia 6151
³Curtin University, Kent Street, Bentley, Perth Western Australia, 6102

⁴Institute for Earth Science Engineering, University of Auckland, Auckland, NZ

⁵ Queensland Geothermal Centre of Excellence, The University of Queensland
Brisbane, Queensland, 4072 Australia

Abstract:

The Australian Government has funded the Pawsey supercomputer in Perth, providing computational infrastructure intended to support the future operations of the Australian Square Kilometre Array (SKA) and to boost next-generation computational geosciences in Australia. Supplementary Federal EIF funds have been directed to the development of a geothermal exploration well to research the potential for direct heat use applications at the Pawsey Centre site. Cooling the Pawsey supercomputer may be achieved by geothermal heat exchange rather than by conventional electrical power cooling, thus reducing the carbon footprint of the Pawsey Centre and demonstrating an innovative green technology that is widely applicable in industry and urban centres across the world. The exploration well is scheduled to be completed in 2013, with drilling due to commence in the third quarter of 2011. One year is allocated to finalizing the design of the exploration, monitoring and research well, and first concepts will be presented at AGEC for discussion and participation. Success in the geothermal exploration and research program will result in an industrial-scale geothermal cooling facility at the Pawsey Centre, and will provide a world-class student training environment in geothermal energy systems.

Keywords: Direct Heat, Absorption Chiller, Hot Sedimentary Aquifer, SKA, High Performance Computing

Introduction

June 9th, 2010 marks the first step to one of the largest direct heat demonstrators in Australia. A direct heat geothermal demonstration project, using hot sedimentary aquifers to provide cooling and ventilation to the Pawsey High-Performance Computing Centre and the co-located CSIRO facility the Australian Resources Research Centre secured funding through the Sustainability Round of the Education Investment Fund (EIF). The Pawsey Centre demonstrator is part of the

infrastructure of Australia and New Zealand's bid to host the SKA (square kilometre array) radio telescope. The Pawsey Centre (see Figure 1) supports the enormous data requirements for deep space research and is also planned to be a prime enabling platform for Australia's computational geoscience and nanoscience communities. The supercomputer-cooling project will be the first of its kind and will demonstrate the feasibility for widespread use of the clean and sustainable geothermal energy source to power, for example, hospitals, shopping centres and other industrial scale applications.

The Pawsey Centre is to be situated on the deep sediments of the Perth Basin, where a vertical sequence of hot sedimentary aquifers suitable for direct heat geothermal applications is now being studied.

Construction on the exploration well project is scheduled to commence in November 2010, drilling of the exploration hole is scheduled for November 2011 and the project is to be completed in August 2013 (see table 1), the provisional timetable is coordinated with the international SKA decision-making process. Australia and New Zealand, together, are in competition with an African SKA bid, involving South Africa, Namibia, Botswana, Mozambique, Madagascar, Mauritius, Kenya and Ghana. A decision is expected to be made in 2012. The Pawsey Centre geothermal demonstrator is part of a portfolio of solar and geothermal technologies, notably an additional ground source heat pump design for radio antenna cooling. The overall goal is to supply a reliable and clean, sustainable energy solution for the Australian/NZ SKA bid.

This contribution gives a brief overview of the entire concept, its location, timing, and the above and below ground technology concepts planned to support the design of a production geothermally powered cooling system. Collaborations between Australian and NZ researchers on potential designs for the exploration well are discussed.

The Pawsey Supercomputer Cooling project, a brief overview

One of the strategic goals of the successful EIF Sustainability Round proposal is to form through demonstration projects a joint research focus for scientists and students from all over Australia and NZ in renewable energy, as well as in astronomy, computer science, engineering, geology and environmental management.

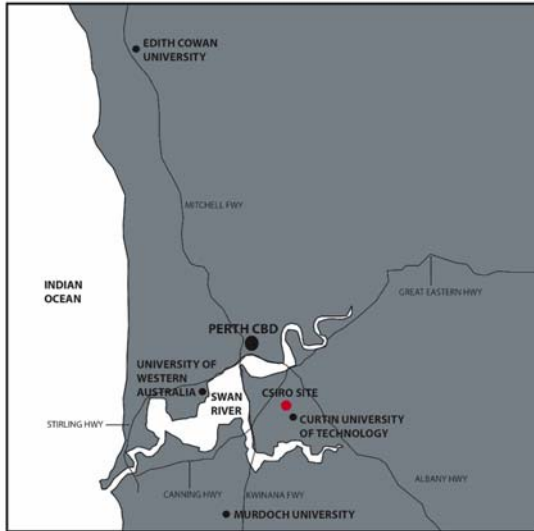


Figure 1. The Pawsey High-Performance Computing Centre cooling project will be located on the CSIRO Technology Park site near the Perth CBD close to Western Australian universities.

The Pawsey Supercomputer Cooling (PSC) project is located centrally in Perth (Figure 1) and its collaborations with Australian and NZ partners sets a sound basis for achieving this goal. The additional placement of a research well offers the

necessary infrastructure investment for research collaboration in the wider Australian and NZ geoscience community for testing, monitoring and exploitation of hot sedimentary aquifers.

The PSC direct heat geothermal demonstrator utilises a hot sedimentary aquifer under Perth with an estimated temperature of 100 °C at 3 km depth.

Based on the available information and extrapolation from a 3 km deep petroleum exploration well (Cockburn 1, see Figure 3) located 21 km away from the Pawsey site one possible scenario could be a 3 km deep extraction and injection well into the Cadda formation with a measured permeability of 632-732 mDarcy and a measured layer thickness of 350 m. Another optional target layer is the Yarragadee aquifer directly above the Cadda formation featuring permeabilities of up 1200 mDarcy according to the Cockburn 1 records. The advantage of this target is its expected lower salinity than the Cadda Formation. Shallower portions of the Yarragadee aquifer have been successfully used in ten different fully commercial low-temperature projects in Perth, mainly for swimming pool heating. The injection wells in such systems are much shallower than the extraction bores which implies minimal risk of thermal breakthrough. The selection of injection depth is governed by local permeability, net formation water balance and water quality. Choice of the lower Yarragadee over the Cadda will depend on the trade off between flow rates and temperatures encountered in the exploration well.

The first design of the above ground infrastructure comprises two absorption chillers (Figure 4) at a

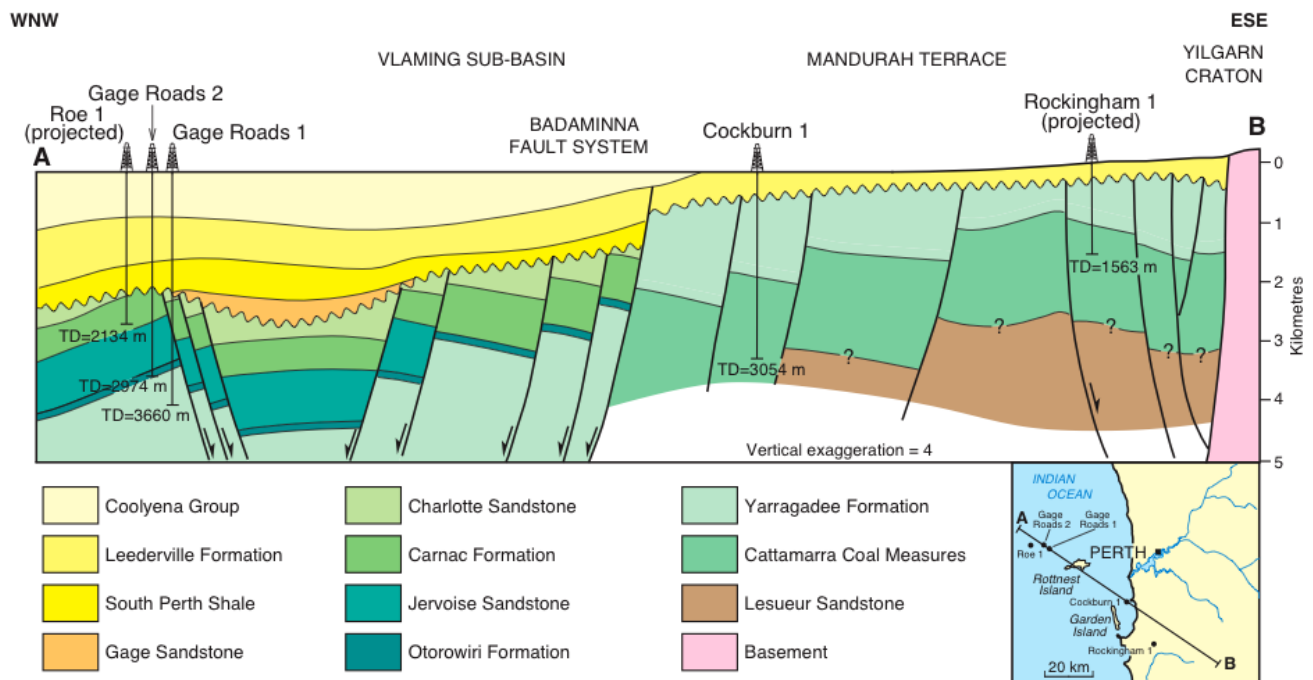


Figure 2. Stratigraphy along a section through Cockburn 1 deep petroleum exploration well, passing ~20 km to the south-west of the Pawsey Centre. Section from Crostella and Backhouse (2000).

maximum capacity 5 MW_{th} each, one unit is implemented as a backup unit. The dimension for each chiller is around 9.38m(L) x 2.2m (W) x 3.6m (H). The absorption chillers require heat rejection with an approximate maximum capacity of 25 MW_{th}. The preliminary design will be adjusted once the actual cooling requirement of the PSC is known.

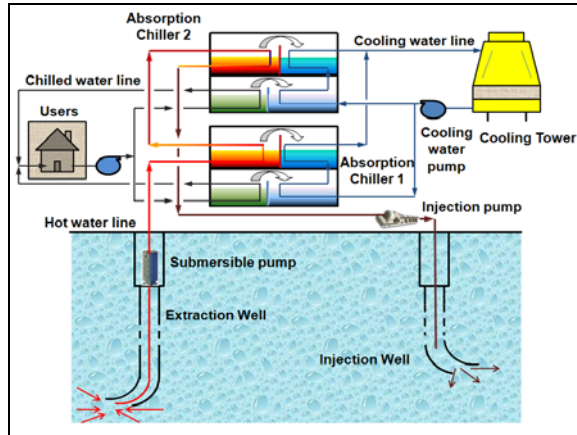


Figure 3. The Pawsey High Performance Computer cooling demonstrator design scheme consists of absorption chiller technology driven by heat from the hot sedimentary aquifer.

Table1 Preliminary Timetable*

Planned Project Milestone	Planned Completion Date
Project start	October 2010
Perth geothermal drilling program commences	August 2011
Perth geothermal drilling completed	November 2011
Project completion	December 2013

* timings are tentative only and subject to revision

The Dual Purpose of the Exploration/Research Well

The exploration/research well is designed for a dual purpose: (1) it breaks the ground and obtains the first direct samples of the chosen site prior to installation of the geothermal production wells; and (2) it offers the unique opportunity for implementing purpose-designed downhole-sensors, long term monitoring and active testing.

An additional attraction for research may be a small flux of geothermal waters from the aquifer,

which could be abstracted for testing small scale above ground demonstrators. Key aspects of the sampling include water quality analyses that provide important indicators for heat exchange plant and reinjection sustainability. Given, the long lead-up time for commencement of drilling (Table 1) the design of the exploration well and the above and below ground research components are fully open for discussion. In the spirit of the EIF funding we call here for active research collaborations that can complement the funded infrastructure with the best available expertise and interpretation.

Preliminary design scenarios of the Exploration well

There is no hard data indicating water temperature (and chemistry) at depths of ~3 km in the Perth Basin – the proposed depth of the geothermal production wells. Data acquired from the drilling program associated with the UWA geothermal demonstration site will provide a better indication of water temperature at depth in the Perth Basin, but will not obviate the need for the ARRC geothermal exploration/research well.

This depth of drilling is based on data sourced from a ~800m Water Corporation bore adjacent to the ARRC site. Data recently acquired from re-logging this bore by the WA Geothermal Centre of Excellence suggests water temperatures of ~100 °C at a depth of 3 km. Temperature, (fluid and sediment) chemistry and permeability data will be acquired through the proposed geothermal exploration/research well. Data on the advective regimes operating at depth in the stratigraphic sequence will also be sought in order to facilitate the construction of a geothermal reservoir model for the Pawsey Centre.

The reservoir model will include hydrothermal flow processes necessary to describe circulation phenomena in moderate-permeability HSA geothermal plays. The reservoir model will inform the design specifications of the subsequent production and injection well infrastructure.

In preparation to the EIF bid IPS Australasia has been tasked to prepare potential design scenarios for the exploration well which are here laid open for discussion. A number of scenarios have been considered for the drilling, evaluation, testing and completion of the exploration well with proposed schematics shown in Figure 4.

Scenario 1 (Base Case)

Scenario 1 (Base Case) is designed with a three-string casing program with final hole section cased with 178mm (7") casing to 3000 m True Vertical Depth from Rotary Table (TVD RT) (Figure 5). This design places the 244 mm (9-

5/8”) surface casing at 1000 m TVD RT in the Yarragadee Formation and contains the above Leederville and South Perth Shale behind casing (Figure 2). This design offers a 216 mm (8½”) open hole to conduct straddle testing of the proposed target intervals to 3000 m TVD RT.

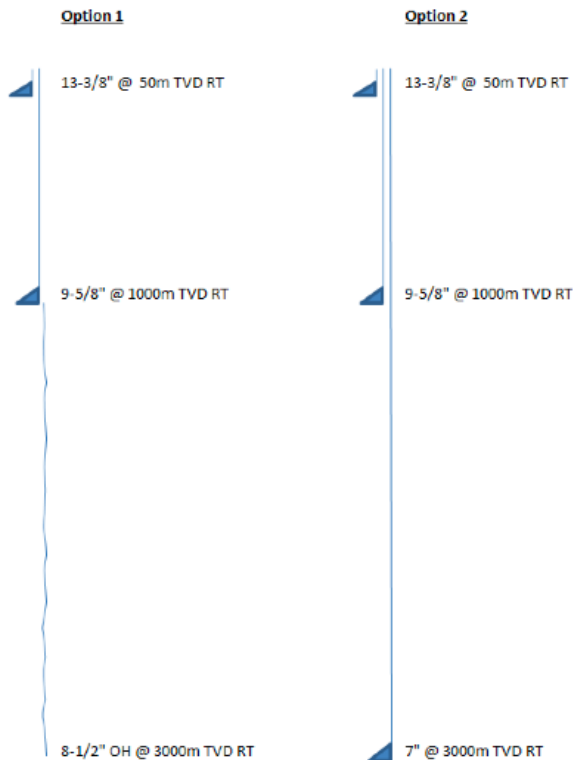


Figure 4. Wellbore schematics of the exploration well according to a Desk Study of IPS Australasia

The casing configuration is summarized as follows:

- The 340 mm (13½”) conductor shoe is set at a depth between 50 and 100 m TVD RT.
- The 244 mm (9½”) casing shoe is set at a depth of approximately 1000 m TVD RT.
- At well TD of 3000 m TVD RT following open hole testing of target intervals, a 178 mm (7”) casing string will be set.

Scenario 2

Scenario 2 is of a similar design to Scenario 1 with a three-string casing program to 3000 m TVD RT with the addition of a 152 mm (6”) hole section drilled to 3500 m TVD RT. This design places the 244 mm (9½”) surface casing at 1000 m TVD RT in the Yarragadee Formation and contains the above Leederville Formation and South Perth Shale behind casing. This design offers a 216 mm (8½”) open hole to conduct straddle

testing of the proposed target intervals to 3000 m TVD RT. The 152 mm (6”) hole section drilled to 3500 m TVD RT will allow formation evaluation of deeper target intervals with the option of testing and casing with a 5” liner.

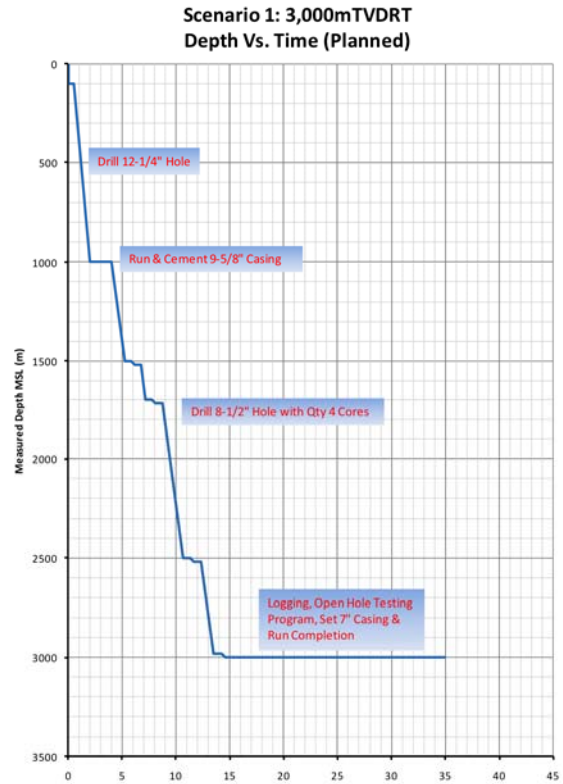


Figure 5. Wellbore schematics of Scenario 1 exploration well suggested by IPS Australasia (2009).

The casing configuration is summarized as follows:

- The 340 mm (13½”) conductor shoe is set at a depth between 50 and 100 m TVD RT.
- The 244 mm (9½”) casing shoe is set at a depth of approximately 1000 m TVD RT.
- Following open hole testing of target intervals to 3000 m TVD RT, a 178 mm (7”) casing string will be set.

Preliminary Design of the Research Equipment

The preliminary list of research equipment for deployment in the exploration well includes:

Along-Casing Sensors: Optical fibre temperature monitoring system (Raman scattering based), Optical fibre pressure, temperature, acoustic, EM (Bragg grating/cladding based), Surface optical system, electromagnetic/magneto-telluric-receiver-station.

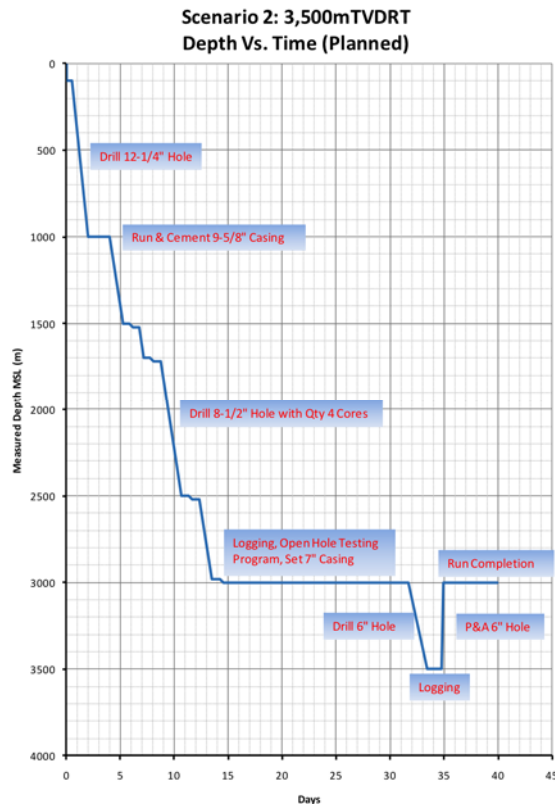


Figure 6. Wellbore schematics of Scenario 2 exploration well suggested by IPS Australasia (2009)

Inside Hole: Water pressure tube, mechanical packers, banding standoffs (cable protectors between pipes), pressure transducer, geochemical / environmental monitoring sampling system

Downhole Sonde: Deep sonde (seismometer) thermistor, fluxmeters (desorption method which need to be deployed in packed zones to isolate from in-well gradients).

Redeployable Wireline Exploration System: Wire / data cable and winch system flow meter downhole formation imager, spectral gamma tool, electrical conductivity, caliper log.

This equipment will allow us to monitor the pressure, temperature and acoustics of the aquifer along time and depth, collect fluid samples at a range of depths for geochemistry analyses, seismic, flow rate and temperature data to monitor the impact of the production plant.

Above Ground Engineering Research

While this project is demonstrating the direct use of the geothermal heat in space cooling, another objective for the Australian geothermal energy sector is the generation of electricity using geothermal heat. Additional targets are proof of technology for geothermal desalination of seawater, saline aquifer water and industrial process water. Both Australian based inventions

are currently being built with support from different Centres of Excellence in Australia.

The Queensland Geothermal Energy Centre of Excellence (QGECE) is developing new supercritical cycle technologies to increase electricity production from a given geothermal resource by up to 25% for low temperature geothermal resources and by up to 50% for high temperature geothermal resources. One of the current research projects at the QGECE is aiming to develop a 100-kWe portable power plant to demonstrate a supercritical power generation capability for a sub-150°C geothermal resource. Using this plant as a test bed, optimum design and operating conditions can be ascertained for electricity generation using the geothermal fluid produced by a Perth Basin hot sedimentary aquifer in local ambient conditions.

The Western Australian Geothermal Centre of Excellence (WAGCoE) in collaboration with the National Centre of Excellence for Desalination intends to use the extracted geothermal water both as a heat source and feedstock to develop a WAGCoE’s protected distillation based desalination technology by constructing a containerized 4 m³/day desalination plant, as schematically suggested in Figure 7. This technology is expected to boost the freshwater yield of conventional technology by 30%.

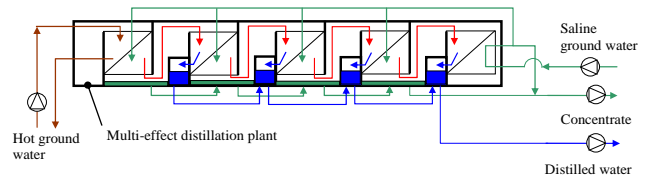


Figure 7. A geothermal distillation desalination plant

References

Crostella and Backhouse (2000) Geology and Petroleum Exploration of the Central and Southern Perth Basin, Western Australia, Geological Survey of Western Australia, DMP Report 57

IPS Australasia (2009) A Desk Study: Proposed Geothermal Project at the Australian Resources Research Centre.

Fracture Stimulation – legal risks and liabilities

Kyra Reznikov, Senior Associate, Finlaysons

Abstract

Fracture stimulation (also known as hydraulic stimulation) involves pumping water at high pressure into a well, which causes fracturing of the rock. This additional fracturing enhances the permeability of the hot dry rock in order to create an efficient hydraulic loop for the purposes of harnessing geothermal energy.

The process of fracturing the rock can also give rise to seismicity events – that is, it can induce small earthquakes which have the potential to damage property and infrastructure not only within the exploration licence area but also on adjacent land and further afield.

The paper will examine the legal risks and potential consequences of fracture stimulation, including:

- damage caused by seismicity events could result in the commission of an offence under environment protection legislation (which prohibits the causing of harm to the environment, property and the health, safety and amenity of people) or under resources legislation (which for instance prohibits interference with mining operations);
- landowners or operators of infrastructure that suffer damage to their property may also seek compensation for losses caused by the seismicity events;
- if concerned about the potential impacts on the environment and property, regulators could issue orders preventing fracture stimulation, or allowing it only after precautionary measures are put in place.

The paper will discuss the legal risk management measures that geothermal operators should include in project planning to

seek to mitigate their potential liabilities where fracture stimulation is proposed.

QGECE Mobile Geothermal Test Plant & ORC Cycle Challenges

Andrew S. Rowlands and Jason Czaplá

The Queensland Geothermal Energy Centre of Excellence (QGECE),
The University of Queensland, St Lucia, Brisbane, Qld 4072

*Corresponding author: a.rowlands@uq.edu.au

Geothermal energy reserves in Australia have the potential to provide electrical energy for hundreds of years. However, due to the variety of temperatures in geothermal resources a one-size-fits-all approach to surface power infrastructure is not appropriate. Furthermore, the use of traditional steam as a working fluid is rarely a feasible option because resource temperatures lie in the range of 100-200°C. To overcome this, organic fluids with lower boiling points than steam may be utilised as working fluids in organic rankine cycles (ORC) in binary power plants. Due to differences in thermodynamic properties, certain fluids are able to extract more heat from a given resource than others over certain temperature and pressure ranges. This phenomenon enables the tailoring of power cycle infrastructure to best match the geothermal resource through careful selection of the working fluid and turbine design optimisation to yield the optimum overall cycle performance. Here we look at a selection of promising ORC cycles using a range of high-density working fluids operating at sub-, or trans-critical conditions that are being studied by QGECE as potential binary cycle systems; discuss the challenges facing design of ORC cycles and how some of these challenges are being addressed in the QGECE Mobile Geothermal Test Plant.

Keywords: Geothermal energy, Organic Rankine Cycle, Working fluids.

Modelling Binary Power Cycles

In this investigation, the thermodynamic cycle of an ORC was simulated for conditions representative of a geothermal power station. The ORC was modelled as (1) pump work in, (2) heat addition in (i.e. pre-heater, evaporator, superheater), (3) turbine work out, (4) heat rejection out (i.e. pre-cooler, condenser) and (6) regeneration (when the temperatures allow). Figure 1 illustrates the basic layout of an ORC and denotes the state points for calculating thermodynamic properties.

The fluids database employed was the NIST's REFPROP (NIST 2007). REFPROP offers equations of state for 84 pure fluids as well as user defined mixtures. However, only pure fluids

were used in this analysis (Mixtures may be the focus of future work).

To allow for ranking results of the various cycles, the critical metric used for comparing fluids and cycles is Brine Consumption (β) (Franco, 2009) defined as follows:

$$\beta = W_{net} / mf_{geo} \text{ (kJ/kg)}$$

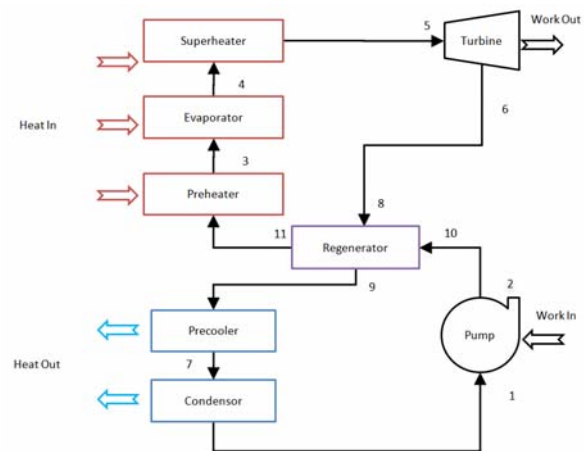


Figure 1: General ORC Layout

Where W_{net} (kW) is the net work produced by the cycle and the mf_{geo} (kg/s) is the mass flow rate of the geothermal brine. Greater β values indicate a greater yield of energy production per unit mass of brine. This can be a good metric for geothermal energy because it focuses on optimising the energy produced for the geothermal brine produced.

The cycle analysis performed indicates that the pinch point in an evaporator has a significant impact on β . This is in agreement with what others have stated previously in other publications (i.e. Saleh 2007). The pinch point is a product of the working fluid's latent heat of evaporation (which is pressure dependent). Minimising pinch point effects will allow the cycle to make more efficient use of the brine flow rate in the evaporator.

In an ideal scenario the brine would cool to the inlet temperature of the working fluid and the working fluid would heat up to the inlet temperature of the brine, transferring all the heat from the brine to the working fluid. However, there will always be a temperature differential between the brine and working fluid because some temperature difference is required to drive

heat through the walls of the heat exchanger. The aim then, is to minimise the temperature differential and extract as much heat as possible from the brine flow.

Figure 2 shows an example of a T-s diagram and associated pinch point plot. The cycle represents a subcritical cycle with superheating.

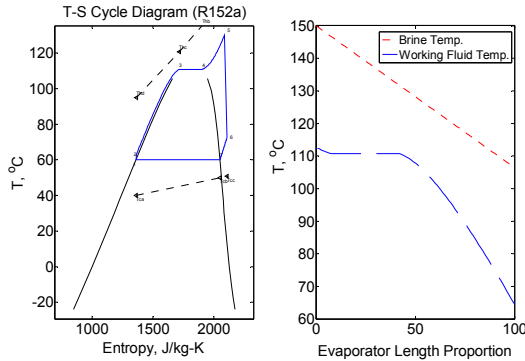


Figure 2: T-s diagram and pinch point plot for R152a (T_{geo} 150°C and T_{amb} 40°C).

Figure 3 shows an example of a T-s diagram and associated pinch point plot. The cycle represents a supercritical cycle. It can be seen that at supercritical conditions the effect of pinch point is gone.

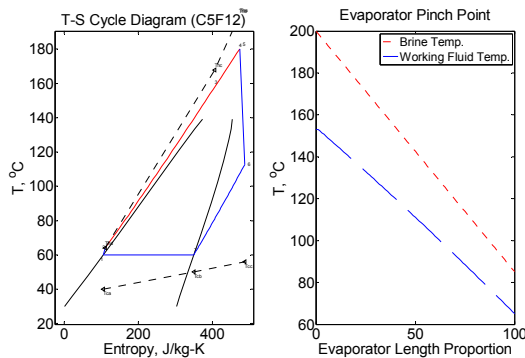


Figure 3: T-s diagram and pinch point plot for C_5F_{12} (T_{geo} – 200°C and T_{amb} 40°C).

Supercritical cycles have the potential to yield efficient cycles because they minimise pinch point effects in the evaporator and there tends to be a large enthalpy differential available across the turbine in the cycle analysis. However, a thorough turbine analysis must be undertaken in conjunction with the cycle analysis to validate the calculated turbine work out from the cycle analysis.

Fluid Performance

Three general categories of geothermal temperature ranges were focused on to see how different fluids performed at different operating conditions. The ranges were labelled as low, mid and high at temperatures of 100, 150 and 200°C, respectively. The ambient temperature was set at 40°C to represent high temperatures that can be seen in central Queensland where our research is

focused. For each temperature range the fluids were ranked in ascending order of their calculated β . An abbreviated summary of the results is shown below in Tables 1-3.

An obvious trend in the results tabulated above is that haloalkanes perform well at temperature conditions associated with geothermal resources.

Table 1: Top 5 Fluids (T_{geo} = 100°C)

Fluid	β (kJ/kg)	Evap. Case
C4F10	2.07	Subcritical
C5F12	2.06	Subcritical
RC318	2.04	Subcritical
R227ea	2.04	Subcritical
R236FA	2.03	Subcritical

Table 2: Top 5 Fluids (T_{geo} = 150°C)

Fluid	β (kJ/kg)	Evap. Case
R152a	18.55	Superheated
R134A	18.40	Superheated
RC318	18.28	Superheated
COS	18.14	Superheated
R236FA	17.78	Superheated

Table 3: Top 5 Fluids (T_{geo} = 200°C)

Fluid	β (kJ/kg)	Evap. Case
C5F12	57.91	Supercritical
R236EA	55.67	Supercritical
ISOBUTAN	54.61	Supercritical
R152a	52.06	Supercritical
DME	51.35	Supercritical

Performance maps were also generated for each fluid for a range of temperature conditions (T_{geo} and T_{amb}). This allows for visualisation of how cycle performance can vary with changing inlet brine temperatures (i.e. a geothermal source may cool over its operating life) and ambient air temperature (i.e. for air cooled systems this represents shifts in temperature throughout the day/night and seasonal change). This can be useful in ensuring that the fluid and cycle selected will operate effectively at all anticipated operating conditions. Figure 5 shows an example performance plot for R245fa. The top plot in the figure shows T_{geo} and T_{amb} on the x and y-axes while β is on the z-axis. It is intuitive that when T_{amb} is at a minimum and T_{geo} is at a maximum β would be at its peak value. It is perhaps not so intuitive to see that evaporator pressure associated with the optimum β for a given set of T_{geo} and T_{amb} varies as it does. This can be an

important factor in plants performance. If temperatures vary, then so should the pressure (along with other parameters that can be optimised similarly) to achieve the best performance.

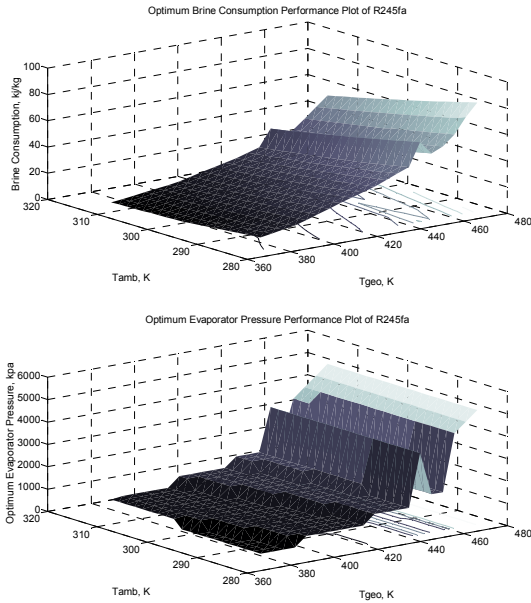


Figure 4: Performance plots for R245fa, optimum brine consumption (top) and associated evaporator pressure (bottom)

Haloalkanes as Working Fluids

Many haloalkanes, especially the hydrofluorocarbons, such as 1,1,1,3,3-Pentafluoropropane (HFC-245fa) and 1,1,1,2-Tetrafluoroethane (HFC-134a), which is in widespread use as a refrigerant, are inflammable, non-toxic and relatively inert. These properties make them highly attractive to use as working fluids in binary power cycles.

One of the drawbacks of these fluids is thermal stability, which, in most cases, is less than the non-halogenated hydrocarbon equivalent and may limit the maximum temperature for which they can be used in power cycles. This is an area of significant uncertainty for ORC technology based on current generation fluids.

Some of the decomposition products can not only cause system performance to degrade but are also toxic and/or strong acids that may negatively impact plant. While some degradation of the cycle fluid to a static level may be tolerable in certain situations, gross scale degradation over time of the working fluid is not acceptable.

While there have been a number of studies (Angelino, 2003; Calderazzi, 1997) looking at the stability of these fluids, existing data does not necessarily agree on exact degradation temperatures and have, in general, looked only at the stability when in contact with stainless steel,

which has negligible catalytic interaction. However, in real-world applications the working fluid may come into contact with a number of different materials, all of which may interact differently with the working fluid and may further reduce the reported degradation temperature. Further effects, including atmospheric contamination (e.g. the presence of small amounts of water, which may accelerate decomposition) have not been thoroughly investigated to the best of our knowledge.

This is of concern when designing a plant as the presence of materials that may act as catalysts for degradation must be avoided in all parts of the system that come into contact with the working fluid. Even common materials used in heat exchangers may be cause for concern.

Optimising the Operating Pressure

Not only do certain fluids perform better than others at certain temperatures, but there exists an optimum pressure for cycle performance.

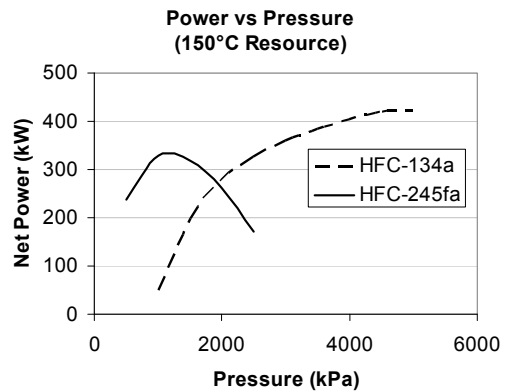


Figure 5: Optimum cycle pressures at 150°C for HFC-134a and HFC-245fa.

The general assumption that higher pressure directly translates to higher work output does not necessarily hold true at pressures both below and above the critical pressure, depending on the fluid in question. Figure 5 shows the calculated power output over a range of pressures for HFC-134a and HFC-245fa at operating temperatures of 150°C. As can be seen, at this temperature the optimum system pressure for these two fluids is different and produces significantly different net power outputs.

Optimising the Turbine

Working fluid properties, resource temperature, flow rate and condensing pressure are all variables that dictate turbine design. In most instances, the goal is to generate the highest output power possible. Therefore design optimisation centres around generating the highest efficiency turbine. Generally, this results in turbine designs that need to operate at high rotational speeds that are not suitable for direct

coupling to grid synchronous generators. QGECE is focussing on optimising turbines that have operational speeds of 24,000 RPM (400 Hz). This results in high operating efficiencies and is compatible with existing power electronics, such as that found in aircraft. To date, current QGECE preliminary turbine design has not indicated dramatic differences in turbine efficiencies for various ORC cycles operating with pressure ratios of between 2 and 6.

Optimising the Cycle

So far we have touched on a number of considerations of various key cycle components including the working fluid, system operating pressure and turbine design. When combined, a different picture may begin to emerge as to the composition of elements that yields optimum power output for a given resource temperature. For instance, depending on the design conditions assumed in the thermodynamic cycle analysis, the pressure ratio calculated that gives an optimum theoretical cycle performance may result in a suboptimal turbine efficiency, which may affect the initial ranking of working fluid selection.

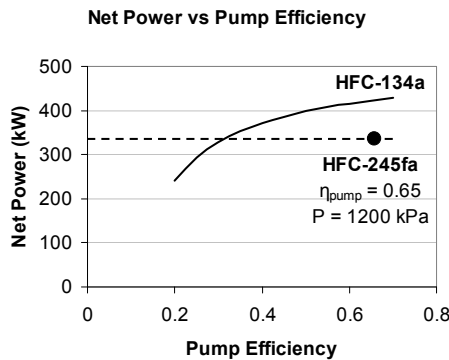


Figure 6: Effect of η_{pump} on net power.

Furthermore, variations in efficiencies of other components in the system are often neglected in theoretical studies for ease of comparison, but can have a large impact on overall system performance. For instance, the benefits of trans- and supercritical cycles can be harnessed only if high performance pumps or compressors exist for the required conditions, otherwise a subcritical cycle may become increasingly attractive due to lower pump work and reduced operating pressures. Figure 6 shows the impact on net power for a supercritical HFC-134a cycle operating at 5 MPa compared to an optimised subcritical HFC-245fa cycle operating at 1.2 MPa at the same temperature.

QGECE Mobile Test Plant (Terragen)

The Terragen Project is a QGECE initiative to develop a modular portable transcritical power plant able to generate approx. 75 kW of power from geothermal or waste heat sources. One of

the primary goals is to demonstrate that useful amounts of energy can be produced even from low-grade resources using transcritical fluids.

Terragen consists of three containerised modules: a control module, power-plant module and an air condenser module. The system is being designed around two working fluids HFC-134a and HFC-245fa using oil-free technologies.

Terragen will be a real-world demonstration and validation of cycles and technologies being developed at QGECE and will primarily be an experimental rig based at The University of Queensland’s rural Pinjarra campus. The portable nature of Terragen means that it will also be available for companies to carry out well-testing and help prove the electricity-generation capability of resources to assist with attracting public and private sector funding.

Terragen is currently under development in collaboration with our project partner, Verdicorp, and is expected to be completed mid-late 2011.

Conclusions

The general assumption that higher pressure directly translates to higher work output does not necessarily hold true at pressures both below and above the critical pressure, depending on the fluid in question. Figure 5 above shows the calculated power output over a range of pressures for HFC-134a and HFC-245fa at operating temperatures of 150°C.

In developing an ORC that generates optimum cycle power output from a given resource there are a number of critical considerations including, but not limited to, selection of best-suited fluid for operating temperature; selecting optimised operating pressures for chosen fluid; optimised turbine design and selection of auxiliary cycle components that complement these major cycle elements.

Future work will work towards verifying the predicted performances experimentally both in the lab at small power scales and at larger scale using the QGECE Mobile Plant. Furthermore, future work will address the life cycle analysis of implementing various sub- and transcritical cycles to verify that the cycles that give the best performance theoretically still out-perform the other cycles on an economic and feasibility basis.

References

Angelino G, Invernizzi C, 2003, *Int J. Refrig.* 26(1)
 Calderazzi L, di Paliano PC, 1997, *Int J. Refrig.* 20(1).
 Villani M. Franco, A., 2009, “Optimal design of binary cycle power plants for water-dominated, medium-temperature geothermal fields”. *Geothermics*, 38(4): 379 – 391
 Lemmon, E.W., H. M. M. M. NIST Standard Reference Database 23: Reference Fluid Thermodynamic and Transport Properties-REFPROP 2007

Saleh, B., Koglbauer, G., Wendland, M., Fischer, J., "Working Fluids For Low Temperature Organic Rankine Cycle" Energy, 2007, 32, 1210–1221

Australian geothermal Industry working with Investors - Defining the key parameters contributing to the long run marginal cost of geothermal and providing a comparison benchmark on the key unknowns

Jonathan Teubner*,

* Business Development Manager, Petratherm Ltd, 1/129 Greenhill Road Unley SA 5061,
jteubner@petratherm.com.au

Abstract

The development of the Australian geothermal industry is unique as, especially in the early exploratory phases, the industry is driven by capital investment raised via equity markets. This equity is supported in some instances by grants provided by the Commonwealth Government through its Geothermal Drilling Program (GDP) and, in the case of the commercial demonstration of the technology, via the Renewable Energy Development program (REDP).

The costs involved in the deep exploration phase are significant, as are those involved in the commercial demonstration of the technology. It is understood by the industry that until it has been able to prove the commercial reality of its projects, all funding is required to come from equity markets or government grants.

Australian geothermal companies are therefore, in essence, competing for a limited pool of risk capital from the equity markets and grant monies from the Commonwealth government. This money will be provided to those projects and companies which are expected to deliver a commercial project and this provide the best returns.

A number of reviews by Equity brokerage firms have been provided recently (Morgan Stanley, RBS Morgans and Goldman Sachs JB Were) reviewing the prospects of the industry and commenting on each of the companies within the sector. It is not the purpose of this paper to review individual companies' prospects, however these papers have provided a summary of the key parameters for company attractiveness:

- Experience of the board and management;
- Presence of project partners, and the experience and size of such;
- Development options of the company (effectively the breadth of the project portfolio to diversify risk);
- Funding capability through access to government grants and large partners at either the project or equity level;
- Project quality assessed in respect of location, quality and risk

The ability to attract the capital (human as well as financial) to develop a project is ultimately a

function of the project quality. The project quality in turn is a function of a number of competing factors which will be discussed in more detail below, but is ultimately determined by the expected cost of production of geothermal energy arising from the project.

Australian geothermal companies therefore are competing for limited capital allocations on the basis of their project's forecast cost of production. This cost of production is typically evidenced by a calculated Levelized Cost of Electricity (LCoE) or Long Run Marginal Cost (LRMC).

Recognizing the importance of this figure in the allocation of capital within the industry, the Australian Geothermal Energy Association (AGEA) formed an Economics Committee to develop a framework for the reporting of Economic parameters to the public to ensure consistency across releases.

This paper represents that framework which defines the key parameters in the economic assessment of the project, and thus which assumptions need to be released to support any economic releases. Further, it also provides data sets where available of what has been achievable in respect of these assumptions elsewhere in the world to give interested parties an independent benchmark of what has been previously achieved and prompting explanations from companies as to where their assumptions sit on this frequency distribution curve and why.

The paper highlights the close cooperation that exists between the investment community and the geothermal industry and is an example of how the informational needs of investors can be met by a cooperative industry approach. It is an excellent guide to how companies can work with investors in other emerging technology markets.

$$u = u^\theta + u^* = [4\alpha\Theta(x, t)] + \left[\frac{\bar{u}_l^*}{l} x + \bar{u}_0^* \right]$$

COMMUNITY TRUST Engagement & Communication

O. Boushel, *T.Hazou, C. Scott & Roger Winders
SINCLAIR KNIGHT MERZ 590 Orrong Road, Armadale, 3143, VIC

*Corresponding author: thazou@skm.com.au

Effective community engagement from the start of any project is critical to gaining public support. The geothermal industry in Australia faces particular challenges in consulting with the community because its technology is relatively unknown. The challenge includes:

1. a process of public education;
2. a process of managing public perceptions of risk.

Add to these the range of views about climate change and confusion around the role of renewable energy in general and the community engagement task can seem daunting.

Local community concern about geothermal projects in their vicinity should therefore come as no surprise.

Planning for community concern and taking an approach that prioritises long-term relationship building with the community is critical to successful project management. This presentation will provide a practical introduction to community relations and consultation management drawing on lessons both from the geothermal and the broader renewables sector. The presentation will provide a brief outline of the context of community consultation, a consultation framework, as well as some practical Do's and Don'ts.

Keywords:

Stakeholder relations, community relations, consultation and engagement; outrage mitigation; action research; public relations, Strategic communications; risk; consultation tools and methods; program evaluation.

Introduction

Stakeholder and community relations (SCR) is a complex and demanding aspect of corporate management and design and construct project delivery. SCR is now very much part of the industry and business landscape and is seen as an integral aspect to Corporate Social Responsibility (CSR) and Public Relations (PR). In the coming pages, an introduction to PR, CSR and SCR and their differences will be provided, followed by an overview of community consultation practice. This will include an illustration of the distinct aspects of SCR and what differentiates it from PR and reputation management. This will be followed by an

explanation of community consultation principles, frameworks, and tools. Finally, an illustration of how SCR is used in a practical context will be provided with an explanation of some 'rules of engagement' or practice Do's and Don'ts. This will provide an ability to identify the practices and skills required to perform in the field of stakeholder and community relations.

Stakeholders and communities

Stakeholder and community relations (SCR) is a field of practice that demands expertise, and professionalism. It has emerged from a range of industries and professions and covers a wide variety of work practices and organisational functions. Understanding this diversity and intersections will assist in grasping the competing expectations of the field.

Public relations (PR) can be defined as "the ethical and strategic management of communication and relationships in order to build and develop coalitions and policy, identify and manage issues and create and direct messages to achieve sound outcomes within a socially responsible framework" (Johnston & Zawawi, 2004). Through this definition the PR profession is often seen as 'the custodian of reputation management.' As such PR often overlaps many aspects of organisational management such as marketing, media and crisis management, investor and community relations, internal communications, ethical conduct and strategic planning.

If PR generally (in all its forms) is about communicating a message and "staying on message" then SCR is the ability to adapt and change the message in order to prioritise relationships. SCR is about 'winning trust' and understanding the community in a manner that impacts on actions and words for the long-term. SCR professionals are ideally the first to identify issues and challenges and must then manage the discussion on behalf of the organisation (Moore, 1996).

Corporate Social Responsibility (CSR) has also emerged as an important corporate function in recent years. CSR is recognition by corporations and organisations that they exist in a social environment. It is a reflection of the 'triple bottom line' and the need for organisations to address public concerns of 'accountability and responsibility' (Regeister, 2001). In fact, CSR has

developed to the point where it is no longer “Do no harm” and it is “Do good beyond the narrow limits of making profit” (Argenti and Forman, 2002). With this has come a sophisticated understanding of public communications on CSR matters. Aside from issues of ethical conduct communities have grown to understand that PR is the outward sign of an organisations inward character (Moore, 1996), resulting in a growing paradigm shift towards social responsibility.

CSR has growing recognition by management of its importance and influence in creating positive outcomes for organisations and achieving long-term goals. As a result of CSR expectations governments, organisations, and companies are now investing time and energy into SCR. Typically SCR exists on two levels (Tymson and Lazar, 2002). 1. The local level: to help an organisation communicate with local leaders, residents and organisations to facilitate positive relations and good outcomes. 2. The corporate level: to acknowledge an organisation as a citizen within a wider social framework.

As a result, SCR has developed as a distinct area for four important reasons. First, it is concerned with outcomes and impacts rather than image and message. That is it is concerned less with how something will look in the media and more with what will happen as a result (Fletcher, 1999). Second, SCR emphasises ‘outside-in’ thinking and the ability to see an organisation from the outside point of view inwards (Regester, 2001). Third, SCR is crucially distinguished by “two-way communication”. Communication is an interactive process between parties rather than a process of ‘delivering on message’; it requires a dynamic ability to listen, reflect and respond to concerns and desires (Forrest and Mayes, 1997). Finally, SCR is about developing and maintaining positive long-term relationships (Forrest and Mayes, 1997).

Changing socio-political environment

Communities are increasingly active and informed. We live in a media environment where information is more accessible than it has ever been, and an increasing number of technologies assist communities to network and (if necessary) mobilise against projects. Both new technology and changes in legislation are creating more opportunities for communities to engage in and influence individual project proposals.

Globalisation described as a process by which regional economies, societies, and cultures have become integrated and shrinking through a global network of communication, transportation, and trade (Appadurai, 1996) has had an acute impact on community, government and corporate expectations.

Social media, mobile phones and the internet enables social networks to activate with a speed

that was unthinkable until recently. The expense of media access no longer impedes community participation in the public sphere as new media is widely accessible for minimal cost, and reaches broad audiences. Evolution of Web 2.0 through applications that facilitate interactive sharing, inter-operability, user-centred design, and collaboration on the World Wide Web is also key (Tim O'Reilly 2005. retrieved 2006-08-06).

Traditional modes of PR communication using static and mass communication channels are becoming less relevant and proving less effective as people rely on alternative sources of information (represented below). One-way channels of connecting with the target are “a typical monologue model with little if any open exchange of ideas, thoughts, or information. The one-way arrows represent one way information flows, as opposed to dialogue.” (Mark Parker. retrieved 2010-09-04).

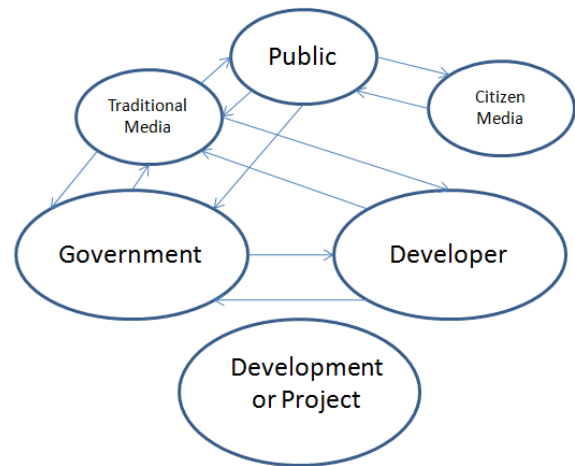


Figure 1: <http://smartselling.wordpress.com/tag/web-20/>

In this context, and the growth of the ‘information age’ there is a higher demand on corporations “to manage the establishment and maintenance of credibility and trust” (Tymson and Lazar, 2002).

Johnston and Zawawi (2004) also point out that a reflexive and socially conscious management of communications within a socially aware and informed environment is critical. People today want to and do know more about organisations generally. “More people want to know more about the organisation they are working for, the organisation they are buying from, and the organisations they are investing in” (Tymson and Lazar, 2002).

In recent years, community engagement has become part of business as usual for capital intensive projects and their proponents. While stakeholder engagement has always been required to some extent, the geothermal industry (along with others) is now being asked to formalise and improve its approach.

Community expectations

The increase in community activism and awareness has been facilitated by changes in legislation that reflect the public's desire to be involved in helping guide how their communities grow and adapt to projects. Often projects now have federal, state and council triggers in planning processes that require public consultation to be included in any planning process. Importantly these triggers mean that the support of key stakeholders such as government for a project, hinges on what benefit the project has for the wider public.

At the most basic level these new technologies may be restricted to email, blogs or basic websites. However, improvements in communications technologies have allowed even the smallest groups to advocate for or express their concerns about projects in very polished, convincing campaigns using technologies such as interactive websites such as, Facebook, YouTube or Twitter.

These technologies are not only being utilised by the public, but increasingly by developers and project proponents to effectively engage a wider range of people, improve the effectiveness of communication strategies and gather critical information from the public that may affect the community. For example, VicRoads is undertaking a consultation process for its Hoddle Street Study by using an online tool called "Bang the Table" to gather feedback from the wider community about key considerations in their planning study such as existing operations, the role of public transport and bicycle access.

The wider public is also becoming better educated, improving their ability and desire to engage in policy and planning processes in increasingly sophisticated ways. Further, there are increasing expectations for companies to measure up to community expectations of social responsibility and to earn their 'social license to operate'. These expectations are often shared by the bodies responsible for approving projects.

This can translate into unexpected and unforeseen demands on companies to deliver in areas that were previously viewed as outside their area of responsibility. Relevant recent examples of this include the \$5 million Regional Benefits Program undertaken as part of the Sugarloaf Pipeline Project (Melbourne Water. retrieved 2010-09-02) or the AGL Hallett Wind Farm Community Fund with total annual total grants \$22,000 available for communities and communities in the Northern Areas Council (NAC. retrieved 2010-09-02).

Government expectations

Governments also expect an in-depth level of community consultation as part of corporate and industry performance.

Directions to proponents for the preparation of development approvals often include specific elements relating either to community consultation and/or social impact assessment.

Local government in particular is establishing consultation requirements as part of approvals processes above and beyond regular public exhibitions and notices.

Funding and tender requirements now emphasise community consultation obligations forcing industry to respond to contractual and approvals requirements.

Industry expectations

There is a growing awareness by industry that effective community engagement rather than being a regulatory burden, provides opportunities to improve project delivery through the early identification of issues, contribute to social wellbeing, and to deliver on CSR and sustainability agendas.

Corporations (venture partners, banks and financiers) now have high expectations that companies will manage community relations in a proactive and responsible manner.

For these reasons, community expectations of companies to deliver open and accountable consultation processes are now, as great as they have ever been. Community engagement strategies for geothermal projects must acknowledge and navigate through this environment.

Effective engagement

Geothermal energy, like many renewable energy sources, is a relatively new industry in some regions. In these cases communities are unlikely to have an understanding of what potential development projects involve. As a result, any community engagement will also need to play an educative role with the public, shaping community perceptions of the industry.

Consultation methodology

A number of effective consultation methodologies are available to guide public engagement. The two major approaches utilised in Australia are the Organisation for Economic Co-operation and Development (OECD) model and International Association of Public Participation (IAP2) spectrum of engagement.

The OECD model provides three different approaches to consultation depending on the context in which it occurs:

- Notification
- Consultation
- Participation

Notification in itself is not consultation as it is a one way process in which the organisation informs the public. This is often the first step in consultation where people are notified about the project;

Consultation involves the two-way flow of information between the project and the wider community. This process may be used to allow groups to voice their concerns about the project, ask questions or provide feedback.

Participation involves the public in the decision making process.

The IAP2 spectrum, which shares a lot in common with the OECD model, is fast becoming accepted as a baseline by a range of stakeholders in Australia and internationally.

The IAP2 spectrum has five engagement approaches:

1. Inform
2. Consult
3. Involve
4. Collaborate
5. Empower

Each type of engagement is tailored to desired engagement goals as shown in the table below.

Approach	Goal
Inform	Provide the public with information about a project, plan or action
Consult	Obtain feedback from the public about a project, plan or action
Involve	Continually obtain feedback and consideration from the public at several stages throughout the project
Collaborate	Work with the public on the project, involving them in the planning and decision making
Empower	Providing the public with decision making power on a project.

Figure 2: IAP2 Approaches and Engagement Goals

These approaches are not mutually exclusive. Often, several different approaches are used with differing aspects of a project. For example, a proponent may inform the public about a project, consult landholders about land access, involve local government in traffic management plans during construction, and empower landholders in the reinstatement process.

In the context of a single project, the project team needs to continually assess the tools and approaches used for their efficacy with the public. Where appropriate, tools should be adapted to

accommodate differences in the public and the socio-political environment.

Importantly, where a community engagement program has worked well for a project, it is critical to review and reassess before reapplying it. Different communities, environments and technologies will require a different approach.

Planned and structured approaches to community consultation not only produce the best results but also leave a lasting impression and community confidence in corporate processes.

Action research

A good practical approach to evaluating SCR methods and tools is to adopt an Action Research Methodology (ARM). Action research is simply a form of self-reflective enquiry undertaken by participants in social situations in order to improve the rationality and basis of their own practices, their understanding of these practices and the situations in which the practices are carried out. (Carr & Kemmis, 1986).

Action Research does not set out to answer a hypothesis or find a single 'objective truth'. It focuses on a development process that engages individuals and enables change and improved performance.

Action research can be done through a range of 'typical' survey and interview research methods. A crucial aspect is that each method should inform a circular model of inquiry. This allows for the building of improvements into practice. To do this it involves participants in a collaborative approach to investigation in order to resolve specific problems or create systematic (change) actions (Stringer, 1999).

The action research cycle, involves four key steps; planning, action, observation, reflection:

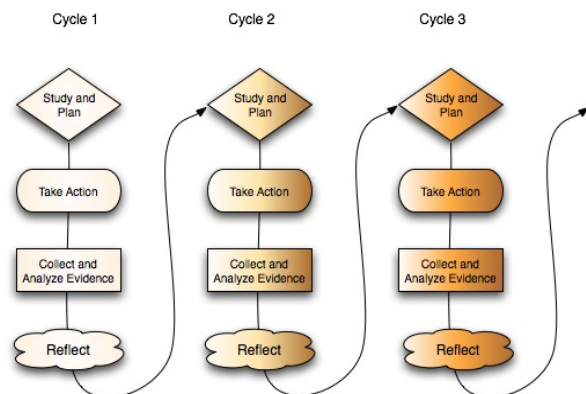


Figure 3: <http://cadres.pepperdine.edu/ccar/define.html>

Action research is particularly well suited to SCR as its intent is not only to 'get the job done' but to facilitate improvements. It does this by taking an 'organisational change' approach based on participation and involvement.

Consultation tools

There are a number of tools available for use to engage the community. As shown in the IAP2 spectrum below, these can be grouped according to the engagement approach used. Typical examples include:

- Information sheets / community bulletins
- Web sites, blogs and email
- Community Information sessions
- Focus groups, surveys
- Public meetings and public comment
- Workshops and advisory committees
- Community reference groups
- Citizen juries and community ballots

IAP2 Public Participation Spectrum

Developed by the International Association for Public Participation

INCREASING LEVEL OF PUBLIC IMPACT				
INFORM	CONSULT	INVOLVE	COLLABORATE	EMPOWER
Public Participation Goal: To provide the public with balanced and objective information to assist them in understanding the problem, alternatives, opportunities and/or solutions.	Public Participation Goal: To obtain public feedback on analysis, alternatives and/or decisions.	Public Participation Goal: To work directly with the public throughout the process to ensure that public concerns and aspirations are consistently understood and considered.	Public Participation Goal: To partner with the public in each aspect of the decision including the development of alternatives and the identification of the preferred solution.	Public Participation Goal: To place final decision-making in the hands of the public.
Promise to the Public: We will keep you informed.	Promise to the Public: We will keep you informed, listen to and acknowledge concerns and aspirations, and provide feedback on how public input influenced the decision.	Promise to the Public: We will work with you to ensure that your concerns and aspirations are directly reflected in the alternatives developed and provide feedback on how public input influenced the decision.	Promise to the Public: We will look to you for direct advice and innovation in formulating solutions and incorporate your advice and recommendations into the decisions to the maximum extent possible.	Promise to the Public: We will implement what you decide.
Example Techniques to Consider: ● Fact sheets ● Web sites ● Open houses	Example Techniques to Consider: ● Public comment ● Focus groups ● Surveys ● Public meetings	Example Techniques to Consider: ● Workshops ● Deliberate polling	Example Techniques to Consider: ● Citizen Advisory Committees ● Consensus-building ● Participatory decision-making	Example Techniques to Consider: ● Citizen juries ● Ballots ● Delegated decisions

Figure 4: <http://iap2.org.au>

These tools need to be selected on the basis of the engagement goals of the project. Engagement goals should be determined by a number of factors, most importantly the possible risks to the project, the organisation and its reputation.

While risks are best determined in terms of specific issues relative to a project, they are often a product of a number of factors, as follows:

- The number and type of stakeholders
- The characteristics of the community
- Potential issues associated with the project (perceived or real)
- The potential benefits of the project for the community (perceived or real)
- Stage of the project

For example, undertaking a number of upgrades to an existing plant that may have short term construction noise impacts in a sparsely populated during the day may be determined to be a low risk activity from a community consultation perspective. Therefore it may be

decided to not undertaken any engagement or to use an inform approach to let any adjoining landholders know. As such, a letter to local households about the project may be all that is required.

However, a greenfield development that will occur in close proximity to adjoining properties may require a different approach. The possibility of community concerns about issues such as property acquisition, noise, vibration and amenity issues may mean that failure to consult the public may result in community outrage, confusion and misinformation. To avoid this, a consulting approach may be deemed most appropriate with adjoining landholders. This may involve in person meetings, a public information session or other tools that are appropriate in this context.

Advantages/Disadvantages

Different engagement approaches create different levels of expectations within the public. These engagement approaches carry implicit undertakings. These are described as follows:

Goal	Undertaking
Inform	We will keep you informed.
Consult	We will keep you informed, listen to and acknowledge concerns and provide feedback on how public input influenced the decision.
Involve	We will work with you to ensure that your concerns and aspirations are directly reflected in the alternatives developed and provide feedback on how public input influenced the decision.
Collaborate	We will look to you for direct advice and innovation in formulating solutions and incorporate your advice and recommendations into the decisions to the maximum extent possible.
Empower	We will implement what you decide.

Figure 5: Source: <http://iap2.org.au>

The tools used often vary according to the engagement goals. Using the right tools allows for targeted community engagement that is cost effective, timely and addresses risks posed by potential public outrage.

Each approach has a number of advantages and disadvantages when they are used with different communities or in a particular context.

Consideration of these aspects when determining which tools to use is a worthwhile exercise. This

should not deter taking a certain approach, but rather allow strategic consideration and planning for some of the challenges that may face a particular project.

The following table contrasts the advantages and disadvantages of each public participation goal and will help in evaluating program planning and decisions.

Goal	Advantage	Disadvantage
Inform	<ul style="list-style-type: none"> ■ Inexpensive ■ Allows control of information ■ Wide dissemination of information 	<ul style="list-style-type: none"> ■ Limited information can be meaningfully communicated ■ Community concerns can be ignored
Consult	<ul style="list-style-type: none"> ■ Allows for community feedback ■ Inexpensive ■ can reach large numbers of people ■ Improved decision making 	<ul style="list-style-type: none"> ■ Can be difficult to manage public expectations ■ Superficial issues can be raised ■ Potential for small vocal groups to dominate public consultation
Involve	<ul style="list-style-type: none"> ■ Provides greater insight into public issues and perspectives and how these were formed ■ Creates community ownership of the project 	<ul style="list-style-type: none"> ■ Can be resource intensive ■ Smaller cross section of the public engaged ■ Can lead to direct conflict with the community about project goals
Collaborate	<ul style="list-style-type: none"> ■ Creates community ownership of the project ■ Increase public trust in the organisation ■ Can foster innovative local solutions ■ Well suited to smaller issues 	<ul style="list-style-type: none"> ■ Can be resource intensive ■ Smaller cross section of the public engaged ■ Public decisions not always feasible, leading to conflict between proponents and the community
Empower	<ul style="list-style-type: none"> ■ Creates ownership in the community over the project ■ Can increase community support of a project ■ can increase public trust in the organisation ■ Can create innovative local solutions ■ Well suited to small localised issues 	<ul style="list-style-type: none"> ■ Can be resource intensive ■ Smaller cross section of the public engaged ■ Public decisions not always feasible, leading to conflict between proponents and the community ■ Not suited to technical solutions

Figure 6: Advantages and Disadvantage of IAP2 Goals

Do's and Don'ts

While each consultation program must be tailor-made to particular project circumstances, it is possible to draw out a number of 'consultation do's and don'ts' from past experiences; including:

Trust and transparency

- Following through on what is promised. If you can't commit to a date, action or event, then don't promise you will.
- It's never enough to say 'trust me' to the public, be prepared with evidence to support any claims made.
- Inform the community where and to what extent they can influence a decision and where they cannot.

Timeliness and planning

- Provide the opportunity for the public to participate as fully as possible within the timeframe established
- Ensure that Community engagement is an integral part of the project planning process

New technology

- Don't be afraid to use new technologies, particularly where they can help you engage
- Don't assume that everyone has access to or is comfortable with the internet

Integrated design processes

- Community engagement needs to be integrated into the design process. Involving it at this stage allows for the identification of likely issues early in the process where they can be addressed in a cost effective manner. Failure to do this can result in costly revisions and risks of project delays during the construction stage.

Evaluating Choices

- Don't be afraid to ask for help from within the industry or outside of it. If you're not sure you are better off getting some specialist advice.
- Do take a systematic approach to considering tools, methods and consultation approaches.

Respect and Recognition

- Do acknowledge that local communities have an interest in your project and will want a say and input.
- Don't treat communities as 'stupid' or unable to grasp technology; if you do they may go elsewhere and get the 'wrong' information.
- Do try to simplify things and use common 'spoken' language to explain difficult concepts or technology.
- Do involve the community early and establish a 'bank of goodwill' that you can draw on if something goes wrong or a future presents itself.

Summary

As a fledgling industry in Australia, geothermal energy developers have an opportunity to 'stand on the shoulders of others', drawing on lessons learnt by other industries and sharing experiences from within the geothermal sector. This presentation aims to pool that knowledge and link it to the engagement challenges faced by the industry today.

Stakeholder and community relations is clearly about communicating 'early and often' establishing associations, mutual worth and investment in publics (Forrest and Mayes, 1997). Investing in a long-term relationship to understand community views, predict issues, reflect concerns, communicate on target, and maintain credibility can only be done with pro-active and comprehensive relations (Ledingham and Bruning, 2000). If SCR is about establishing credibility and trust then maintaining positive enduring relationships becomes the cornerstone of SCR practice.

This puts the industry in a unique position. Geothermal power doesn't have a legacy of negative community perceptions based on noise, amenity or other factors and has the opportunity to create an enduring positive image made possible by clear communication and a 'mature', and sensible approach to community engagement.

References

- Appadurai, A. (1996) *Modernity at Large: cultural dimensions of globalization*. Minneapolis: University of Minnesota Press.
- Argenti, P and J Forman (2002) *The Power of Corporate Communication, crafting the voice and image of your business*, Boston: McGraw-Hill Pty. Ltd.
- Brackertz, N., Zwart, Meredyth, D. and Liss Ralston (2005) *Community Consultation and hard to reach concepts and practice in Victoria local government*. Hawthorn: Institute for Social Research, Swinburne University of Technology.
- Riel, M. (2010) *Center for Collaborative Action Research*
<http://cadres.pepperdine.edu/ccar/define.html> (CFCAR. retrieved 2010-08-04).
- Fletcher, M (1999) *Managing Communication in Local Government*, London: Kogan Page Ltd.
- Forrest, C and R Mayes, (1997) *The Practical Guide to Environmental Community Relations*, New York, John Wiley and Sons Inc.
- Globalization. (2010)
<http://en.wikipedia.org/wiki/Globalisation> (Wikipedia. retrieved 2010-09-17).
- Johnston, J and C Zawawi (2004) *Public Relations: Theory and Practice*, 2nd Edition, NSW: Allen and Unwin.
- Ledingham and Bruning, (2000) *Public Relations as Relationship Management*, Mahwah, NJ: Lawrence Erlbaum Associates Inc.
- Melbourne Water Sugarloaf Pipeline Alliance (2008)
http://www.sugarloafpipeline.com.au/content/about_the_project/regional_benefits.asp (Melbourne Water. retrieved 2010-09-02)
- Moore, S (1996) *An Invitation to Public Relations*, London: Cassell Pty. Ltd.
- Northern Areas Council and AGL (2010)
http://www.nacouncil.sa.gov.au/webdata/resources/files/AGL_HWF_Community_Fund_Application_NAC_10.pdf (NAC. retrieved 2010-09-02).
- Parker, M. (2010)
<http://smartselling.wordpress.com/tag/web-20/> (Mark Parker. Retrieved 2010-09-04).
- Regester, M. *Managing Corporate Reputation Through Crisis in Jolly, A (Ed), (2001) Managing Corporate Reputations*, London: Kogan Page Ltd.
- Sandman, P. (1993) *Responding to community outrage: strategies for effective risk*. American Industrial Hygiene Association, Fairfax.
- Stringer, T. (1999) *Action Research 2nd Ed*. Thousand Oaks: SAGE Publications Inc.
- Tymson, C, Lazar, P and R Lazar (2002) *The New Australian and New Zealand Public Relations Manual*, Chatswood: Tymson Communications.
- O'Reilly, T. (2005) "What Is Web 2.0". O'Reilly Network.
<http://www.oreillynet.com/pub/a/oreilly/tim/news/2005/09/30/what-is-web-20.html>. Retrieved 2006-09-17

Geothermal energy legislation developments in Queensland

Melissa Zillmann* and Myria Makras

Energy Industry Policy Division, Department of Employment, Economic Development and Innovation, 61 Mary Street, Brisbane Qld 4000

Corresponding author: melissa.zillmann@deedi.qld.gov.au

The *Geothermal Energy Act 2010* (the Act) was passed by the Queensland Parliament in August 2010. The Act has been primarily established to provide a regulatory framework for the production of geothermal energy.

On commencement, the Act will repeal the current *Geothermal Exploration Act 2004* (the Exploration Act) which solely regulates geothermal exploration. The new Act largely duplicates the current exploration legislation, however experience and feedback gained from operation of the Exploration Act has led to some beneficial changes to the exploration regime.

Importantly the Act introduces a regulatory regime for geothermal production which will enable geothermal exploration permit holders to progress to a production tenure when a suitable geothermal resource has been identified.

This paper outlines the key changes to the exploration regime and the framework for geothermal production included in the Act.

Keywords: Queensland, geothermal energy legislation, geothermal production, production threshold, geothermal exploration, *Geothermal Energy Act 2010*, *Geothermal Exploration Act 2004*.

Geothermal Energy Act 2010

The Queensland Government recognises the importance of geothermal energy as a valuable energy resource that has the potential to contribute significantly towards reducing the State's carbon footprint. The *Queensland Renewable Energy Plan* launched in June 2009 outlined a roadmap for the expansion of the renewable energy sector in Queensland. The Plan forecasts 250 megawatts of generation capacity based on geothermal energy in Queensland's generation capacity mix by 2020. Development of this Act is a key milestone that will support development of the geothermal industry in Queensland and enable this forecast to be met.

The objectives of the Act are to encourage and facilitate the safe exploration for, and production of, geothermal energy. This will be achieved by providing for the grant of geothermal exploration permits to explore for sources of geothermal energy across the State and for the grant of geothermal production leases for large-scale geothermal production.

Where possible, the Act aims to ensure maximum consistency with Queensland's existing resource-based legislation and geothermal legislation of other jurisdictions.

Changes to geothermal energy exploration in Queensland

Land available for geothermal exploration

Under the current Exploration Act, an exploration permit can only be obtained when the State has facilitated a land release for competitive tender. This means the timing of exploration, and the land made available, is at the discretion of the State.

Under the new Act, applications for exploration permits will be available via two processes. Firstly, the tender process provided in the Exploration Act has been modified and is referred to as a 'released area' process. This will provide an 'application period' where applications may be made. Any applications within this period will be considered competitively after the period ends. Secondly, a new process which enables eligible persons to apply for exploration permits over land of their choice and at a time appropriate to them is introduced by the Act. This process is referred to as an 'over the counter application'. The introduction of this new application process will provide greater flexibility in gaining access to land for geothermal exploration activities and support increased geothermal exploration in Queensland.

In addition to making more land available for exploration, the exploration regime under the new Act increases the maximum area that can be applied for under an exploration permit. The area will be increased from 200 sub blocks (600 km²) to 50 blocks (3,750 km²) which brings the exploration permit area into line with other States and increases the chances of identifying a commercially viable geothermal energy resource. The term of an exploration tenure has also been increased under the Act from 12 to 15 years.

Exploration Exemption

To encourage use of geothermal energy for the purposes of geothermal heat pumps for heating and cooling buildings, the Act does not regulate exploration for these purposes. Exploration of this nature will generally depend on shallower operations within the relevant property boundary, which will not have the same impact on the environment and landholders as other exploration activities.

Retention Status

It is recognised that there may be delays between the discovery of a geothermal resource and its commercialisation. These delays could be related to factors such as investment attraction, development of infrastructure or securing supply contracts.

To address these issues, the Act introduces a retention status by way of a 'Potential Geothermal Commercial Area'. This is similar to the retention status provided for under the *Petroleum and Gas (Production and Safety) Act 2004*. The 'Potential Geothermal Commercial Area' can be granted for up to 5 years but it can not extend beyond the maximum term allowed for in the underlying exploration permit.

The grant of a 'Potential Geothermal Commercial Area' may provide an exemption from relinquishment provisions and may enable suspension of the exploration permit's work program where appropriate. However, an evaluation program will be required to ensure that the exploration permit continues to be actively developed and brought to production.

Production Testing

The Act provides clarity that restricted production testing can be carried out under an exploration permit to determine whether a geothermal resource is suitable for commercial development. The commercial grade of the geothermal energy resource will need to be quantified before an application for a production lease can be made. Before testing can commence, a test plan must be provided and any relevant authorities will need to be obtained.

Transitional provisions for Exploration Act permit holders

The Act provides existing exploration permit holders a period of 12 months to transition to the new geothermal energy framework after the commencement of the Act. Whilst the Act contains extensive provisions that automatically transfer tenures, decisions and processes to the Act, current exploration permit holders will need to comply with the requirement to obtain an environmental authority. A period of 12 months from commencement of the Act has been deemed a sufficient timeframe to comply with this requirement.

Geothermal production regime

The primary purpose of the Act is to introduce a framework for geothermal production. The principal means for allocating geothermal resources for production are via a production lease.

Under the Act, a production lease can only be applied for on the basis of an existing exploration

permit. A person who is not an exploration permit holder can only apply for a production lease if it is done jointly with an exploration permit holder or with the consent of the exploration permit holder. These provisions give priority production rights to exploration permit holders provided they comply with the requirements of the Act.

Scope of the Act (for production)

The proposed geothermal energy regime provides for a sliding scale of regulation of geothermal energy production under several Queensland Acts, according to the scale of production. Activities that are small or medium scale production will not be regulated by the Act.

Furthermore, the Act is not intended to regulate any associated use of the geothermal energy produced, such as in power stations or industrial activities. To minimise regulatory duplication, the use of geothermal energy will be regulated when it triggers existing legislation such as the *Electricity Act 1994* and the *Sustainable Planning Act 2009*. For example, a production lease holder may be granted rights to extract geothermal energy which may be used to produce electricity, but approvals to supply electricity must be obtained under the *Electricity Act 1994* and the building of any necessary infrastructure must be authorised under the *Sustainable Planning Act 2009*.

Small to medium scale production threshold

The use of heat pumps (considered as small scale production) will be encouraged under this framework since their use is not regulated by the Act and its requirements to obtain a production lease and provide development plans.

Under the *Plumbing and Drainage Act 2002*, installation of pipes for the purpose of conveying water within premises may only be undertaken by a licensed plumber. It is proposed to amend the *Plumbing and Drainage Regulation 2003* to allow the Queensland Plumbing and Wastewater Code to provide a framework for the regulation of the installation of geothermal heat pumps

Geothermal energy production below the large scale production threshold that is not via heat pump technology is considered to be medium scale production and it will not be regulated by the Act. Instead it will be regulated if the geothermal energy use triggers requirements under existing legislation such as the:

- *Sustainable Planning Act 2009* (material change of use provisions)
- *Water Act 2000* (taking or interfering with water provisions)
- *Environmental Protection Act 1994* (environmentally relevant activities provisions)

Large scale production threshold

The Act only regulates the large-scale production of geothermal energy. The Act provides that the threshold for large scale production will be prescribed in the supporting geothermal regulation.

Currently a power threshold which is not technology-specific and is flexible enough to apply to a variety of geothermal production applications is being considered to define the large-scale production threshold. A power threshold provides a direct measure of the rate of production of the geothermal resource that does not depend on how the resource is being utilised, thus avoiding the need to consider conversion efficiency.

A primary policy consideration for setting the threshold is that it should be set at a level low enough to enable commercial geothermal production activities of potential importance to be monitored by the Government. However, this needs to be balanced so that the threshold is set high enough to ensure that the uptake of smaller-scale geothermal activities which may offset carbon emissions are not unnecessarily captured or stifled by a requirement to have a production lease. Further consultation will be undertaken during preparation of the supporting regulation about how the large-scale production threshold will be defined.

Geothermal production leases

A geothermal production lease must be applied for if the proposed activities will trigger the threshold for large scale production. Geothermal energy production is defined in the Act as the recovery of geothermal energy from beneath or on the surface of the land in which it is contained.

The area required for geothermal production is not as large as the area required for geothermal exploration. Hence the Act allows for a maximum production lease area of 25 blocks (1, 875km²).

A production lease applicant must prepare a development plan setting out how the geothermal energy resource will be developed, and the proposed rate of energy production. The grant of a production lease requires the holder to commence commercial production within 2 years of its grant. To allow the ongoing monitoring of resource development, the holder will be required to submit further development plans during the term of the lease.

A geothermal production lease has an initial maximum term of 30 years. Subsequent renewals of the lease are limited to a maximum of 20 years, with no limit on the number of renewals that can be made.

Sub-lease of geothermal production lease

A holder of a geothermal production lease may sublease an area of the lease to a third party. The sublease is subject to approval by the Minister. Where a sublease has been approved and registered, the holder of the geothermal production lease must continue to comply with any terms and conditions of the lease including the area of the sublease.

Royalty

The Act provides that a royalty is payable on the use of geothermal energy. The royalty rate will be specified in the supporting regulation.

The Queensland Government recognises that the geothermal industry is in its infancy and faces technological and financial barriers to development. Key features of the royalty provisions include a royalty holiday and royalty free threshold that are aimed at reducing costs to geothermal production during the early start-up stages.

A royalty holiday that provides a full exemption from the payment of any royalties will be provided until 2020. Whilst the first half of the next decade is expected to be characterised by increased exploration activity, the later part of the decade should see geothermal projects coming into production and benefiting from this initiative.

After 2020, a royalty-free threshold will ensure that in the early years of production when financial margins may be low, a royalty is not payable if the wellhead value is below the royalty-free threshold.

General authority provisions

A number of key provisions apply to both exploration permits and production leases. These provisions are outlined below.

Environmental management

Persons proposing to carry out geothermal activities are required to obtain the relevant environmental authority under the *Environmental Protection Act 1994* before an exploration permit or a production lease can be granted.

Exploration activities conducted under an exploration permit will be classified as level 2 environmentally relevant activities under the *Environmental Protection Regulation 2008* (environmental regulation), unless these activities operate in an environmentally sensitive area or are associated with an environmentally relevant activity stated in schedule 2 of the environmental regulation.

Production activities conducted under a production lease will be classified as level 1 or level 2 environmentally relevant activities, depending upon the scale of production and associated environmental harm. This approach

largely ensures consistency with existing Queensland resource-based legislation in relation to environmental management requirements.

Where the geothermal energy produced is used for another activity that is an environmentally relevant activity under the environmental regulation e.g. aquaculture, that activity will require the relevant authority under the *Environmental Protection Act 2009* and the environmental regulation.

Water Management

The Act does not create any rights to water. Any relevant authorisations under the *Water Act 2000* must be obtained before an exploration permit or a production lease can be granted. The water authority will ensure that the taking of water for geothermal energy exploration or production is managed within a whole-of-catchment plan that ensures environmental flows are maintained.

The grant of a geothermal tenure will not create any preference or priority for the grant of a water entitlement. Geothermal tenure holders will be treated the same way as any other potential water users and may need to pay the market price for a water entitlement in order to consume water in the process of exploring for or producing geothermal energy.

The Act also mandates that an exploration permit or production lease applicant must assess any potential structural or other impacts on aquifers of the carrying out of the proposed activities. The Minister must consider this issue when deciding whether to grant the exploration permit or production lease.

Safety

Geothermal drilling and related activities are similar to those for petroleum and gas activities. Therefore, the safety and health aspects of geothermal energy exploration and production will primarily be regulated under Queensland's *Petroleum and Gas (Production and Safety) Act 2004* (P&G Act).

Currently, the definitions of operating plant under section 670 of the P&G Act only apply to certain authorised activities carried out in a geothermal tenure area.

In practice this would mean that other authorised activities on the tenure are regulated under the *Workplace Health and Safety Act 1995* (WH&S Act). The P&G Act and the WH&S Act have been amended to clarify the different responsibilities of the Department of Employment, Economic Development and Innovation and Workplace Health and Safety Queensland in relation to safety management on a geothermal tenure.

The construction of new operating plant will continue to be covered by the WH&S Act.

Geothermal exploration activities that involve, for example, seismic testing and drilling, will continue to be regulated under the P&G Act. Other activities associated with geothermal exploration (for example, construction activities) will continue to be regulated under the WH&S Act.

Petroleum type drilling does not occur in the production of Hot Sedimentary Aquifer (HSA) sources of geothermal energy. As such, the Act will not apply the safety provisions contained in the P&G Act to HSA geothermal production, regardless of the scale of the operation. These operations will continue to be covered by the WH&S Act.

Overlapping authorities

The Act includes provisions about overlapping authorities under different Acts. For example, a proponent may apply for a geothermal production lease over an area where another resource tenure exists under the P&G Act, the *Greenhouse Gas Storage Act 2009* or the *Mineral Resources Act 1989*.

The purpose of allowing overlapping authorities is to ensure the optimum use and appropriate management of the area's resources and is enshrined in all Queensland resource-based legislation.

The decision as to which resource authority gets priority rests with the Minister, who must consider specific criteria, including submissions made by each authority holder who would be affected by the grant of a geothermal tenure over the shared area, as well as the public interest.

The Act does not allow for an overlapping authority to be provided for two geothermal energy tenures. However, the Act allows a geothermal production lease holder to sub-lease a part of the land within the lease to any party that is an eligible person, as defined by the Act.

Land Access

The Act contains landmark changes to the way a number of Queensland resource tenure and authority holders may access private land and how compensation arrangements are arrived at. Under the changes, geothermal tenure applicants and holders will have new responsibilities in relation to land access.

The Act introduces a requirement for all geothermal authority holders to comply with a Land Access Code as a condition of the authority. The Land Access Code is structured in two parts: Part 1 which outlines non-statutory best practice guidance for communication between authority holders; and Part 2 which describes mandatory conduct conditions that must be complied with by authority holders.

The Act introduces activity thresholds that increase the level of regulation as the intensity or

impact of the proposed activity increases. This is a sensible measure that balances the level of regulation with the level of impact.

Early exploration activities may have minimal impact on private or public landholders. The Act defines these as 'preliminary activities' which might include taking rock, water or soil samples and walking the land.

For preliminary activities, a geothermal tenure holder will be required to give each owner or occupier of land within the tenure area an entry notice and copy of the Land Access Code at least 10 days prior to entry. Access for these activities does not require a Conduct and Compensation Agreement.

When the impacts of proposed activities on the private landholder or occupier are more significant, a higher level of accord is required. These activities are referred to as "advanced activities".

To access land to conduct advanced activities, geothermal tenure holders must either be party to a conduct and compensation agreement or a deferral agreement with each 'eligible claimant' for the land or have made an application to the Land Court to determine compensation. As defined in the Act, an 'eligible claimant' is each owner or occupier of private land or public land that is in the area of, or is access land for, the tenure. Where agreement is not reached, the framework provides for conferences or independent alternative dispute resolution (ADR) to be held.

To assist in the negotiation process, standard conduct and compensation and deferral agreements have been developed in consultation with resource and agriculture industry peak bodies, along with a negotiation tip sheet for landholders.

Conferences or ADR will become a legislative requirement if agreement negotiations break down. Matters cannot be referred to the Land Court for determination until a conference or ADR process has occurred. This requirement is aimed at resolving disputes early at the local level, without the expense of legal resolution.

A detailed compliance and enforcement strategy is currently being developed to ensure that these new land access provisions achieve their full effect on the ground, particularly with respect to the Land Access Code.

Development of geothermal energy subordinate legislation

The Act will commence by proclamation. It is anticipated that the Act will commence in the later part of 2011. During the intervening period, supporting subordinate legislation, guidelines and training will be developed and systems upgrades will be carried out in preparation for the Act

coming into force. There will be opportunities for industry involvement in the development of the subordinate legislation in late 2010/early 2011.